Theoretical and methodological approaches to studying recurrent processing in the human brain using transcranial magnetic stimulation

Rory Cutler

PhD Thesis

School of Psychology

Cardiff University

2017

Acknowledgements

First and foremost I must thank Chris Chambers and Chris Allen for their encouragement, support, guidance and patience throughout the past four years. I am incredibly grateful.

I am also grateful to Petroc Sumner for theoretical and methodological discussions.

I must also thank the School of Psychology for funding and all of my participants for making all of this happen.

I must also acknowledge Val Cutler, Andy Cutler and Barney Cutler for all their encouragement and support; without it, none of this would have been possible.

I also thank Anand Wills for mathematical and programming-related discussions, encouragement and support.

I am also grateful to Leah Maizey, Jemma Sedgmond, Rachel Adams, Karis Vaughan, Craig Hedge, Aimee Challenger, Sinead Morrison, Georgie Powell and Loukia Tzavella for supporting me and being kind throughout a difficult time.

DECLARATION

This work has not been submitted in substance for any other degree or award at this or any other university or place of learning, nor is being submitted concurrently in candidature for any degree or other award.

Signed …… (candidate) Date ……

STATEMENT 1

This thesis is being submitted in partial fulfillment of the requirements for the degree of PhD

Signed …… (candidate) Date ……

STATEMENT 2

This thesis is the result of my own independent work/investigation, except where otherwise stated, and the thesis has not been edited by a third party beyond what is permitted by Cardiff University's Policy on the Use of Third Party Editors by Research Degree Students. Other sources are acknowledged by explicit references. The views expressed are my own.

Signed …… (candidate) Date ……

STATEMENT 3

I hereby give consent for my thesis, if accepted, to be available online in the University's Open Access repository and for inter-library loan, and for the title and summary to be made available to outside organisations.

Signed …… (candidate) Date ……

STATEMENT 4: PREVIOUSLY APPROVED BAR ON ACCESS

I hereby give consent for my thesis, if accepted, to be available online in the University's Open Access repository and for inter-library loans **after expiry of a bar on access previously approved by the Academic Standards & Quality Committee.**

Signed …… (candidate) Date ……

Contents

Thesis summary

The experiments presented in thesis aimed to investigate how communication takes between and within different brain regions. A particular focus was on predictive coding frameworks, which may explain how information is fed forward and backward within the human brain (Rao & Ballard, 1999; Friston, 2005; Lamme & Roelfsema, 2000). Early visual cortex (EVC) and dorsolateral prefrontal cortex (DLPFC) were subjected to transcranial magnetic stimulation (TMS) in order to reveal when, and under what cognitive contexts, these two sites accomplish fundamental visual processes. Behavioural paradigms that manipulate and measure constituent cognitive functions were developed in order to test the critical premises of predictive coding. Since the main experiments were publicly pre-registered, a new approach for simulating data for *a priori* planning of statistical analyses in TMS studies was also developed. Results indicate that the temporal positions of EVC-and DLPFC-TMS induced effects occur at the same time. Results also indicate that the familiarity (or frequency) at which a target appears could be a determined of the duration of processing within EVC. The results also reveal a series of methodological considerations that should be taken into account when relying on a probabilistic experimental manipulation to probe the existence of predictive coding.

Chapter 1: General Introduction

A neurophysiological introduction to feedforward and feedback processes in the brain

Human brain function appears to be characterized by patterns of information transmission fed forward and backward through interconnected networks (Lamme & Roelfsema, 2000). The co-existence of feedforward and feedback-based mechanisms has led to the idea that they make distinct contributions to simple processes to such vision (Lamme & Roelfsema, 2000). There are a number of ways that brain regions can exchange information within a hierarchically organized system. One approach is unidirectional where information is fed forward from lower levels in the hierarchy to higher levels in the hierarchy via intermediate levels. Another, more complex method is bidirectional whereby information is exchanged by feeding forward information from lower levels in the hierarchy to higher levels *and* by feeding back information from the higher levels to the lower levels. The latter bidirectional exchange between different areas is becoming an influential idea of how the brain operates (Lamme & Roelfsema, 2000). It has been proposed that functions such as detecting the presence of an object are accomplished using the connections that feed information forward and feedback pathways that send information backwards (Lamme & Roelfsema, 2000; Felleman & Van Essen, 1991). However, the functional significance and the exact contributions of these ascending and descending pathways remains unclear, even in (relatively) simple processing such as visual perception (Lamme & Roelfsema, 2000; Kafaligonul, Breitmeyer & Öğmen, 2015). Computational approaches are beginning to offer potential functions for feedforward and recurrent processes, which explains how the structure and function of the brain enables processes like visual perception to be completed (Rao & Ballard, 1999; Friston, 2005).

The study of how vision is accomplished is a particularly useful approach because visual stimuli can be manipulated by the experimenter and the consequences on neurons and/or behaviour can be observed. Moreover, it is also possible to manipulate neurons in visually responsive areas in humans and animals, which enables causal inferences to be made about

particular neural responses and their relevance to behaviour. Measuring the response evoked within a neuron or a population of neurons by visual stimulation and how such responses change a function of time enables the existence of feedforward or recurrent places to be revealed (Lamme & Roelfsema, 2000; Super, Speikreijse & Lamme, 2001). Feedforward processes tend to take place early following the onset of visual stimulation whereas the recurrent processes tend to take place later on (Lamme & Roelfsema, 2000). The use of visual stimuli to evoke such processes is particularly useful because the progression of feedforward and recurrent processes can be monitored within a neural population relative to the onset of visual stimulation. Now, the following section will explain how such neural responses have been characterized in visually responsive areas and how feedforward responses can be altered by recurrent processes originating from different brain areas.

Visual representation within early visual cortices, which represent the earliest stages where incoming sensory information is processed by the brain were initially characterized by *simple cells* whose feedforward responses – or their *receptive field* - were determined by the position of stimuli of a particular shape and size within the visual field (Hubel & Wiesel, 1962). Such receptive fields are of interest here as they characterize how visual representation could take place based on the use of a feedforward exchange. In an experiment which presented cats with rectangular shaped stimuli which varied in terms of length, position where they were presented to the retina and their orientation. The overall response of one neuron within a set of visual cortical neurons was determined by the response of its neighbours (Hubel & Wiesel, 1962). An example of the stimuli used and some of the configurations of neurons discovered by Hubel & Wiesel (1962) can be found in figure 1. The overall response of one neuron was determined by the relative number of excitatory neurons relative to the number neighbouring inhibitory neurons responding to the bar stimulus. This phenomena is referred to as the classical receptive field (CRF). The relative number of inhibitory and excitatory neurons that were activated was altered by changing the size and orientation of a bar stimulus, which is illustrated in figure 1. Additional neurons were discovered called complex cells, which appeared to have receptive fields based on inputs from a configuration of simple cells which

have receptive fields tuned to the same orientation but occupy different retinal positions (Hubel & Wiesel, 1962). Remarkably, the two types of cell were rarely found in close proximity to one another, suggesting a segregation of function between the two. If such a feedforward framework existed, visual cortical neurons with small receptive fields that respond primarily to retinal location and stimulus orientation provide inputs feeding forward to complex cells, which respond based on the receptive fields of the simple cells below it in the hierarchy.

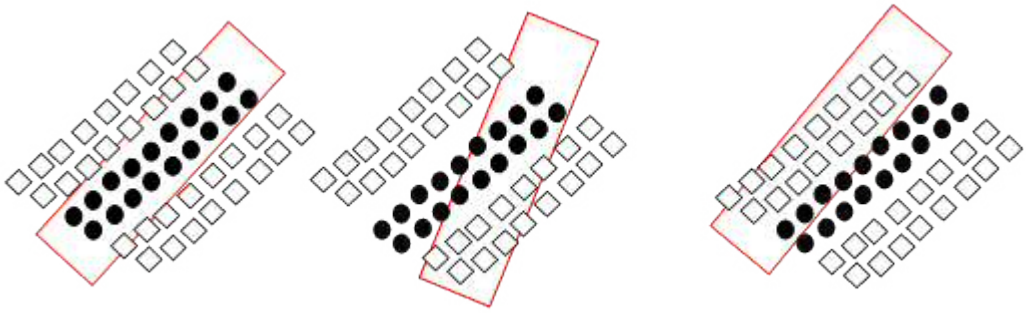

Figure 1. Examples of some of the different types of classical receptive field revealed by Hubel & Wiesel (1962). Black circles represent excitatory neurons. White diamonds represent inhibitory neurons. Red rectangles represent the bar stimuli used to discover the receptive field of individual neurons. Left: Bar stimulus covers more excitatory neurons than inhibitory neurons, which means that individual excitatory neurons will have larger responses.. Middle: Bar stimulus covers more excitatory neurons than inhibitory neurons, but slightly more inhibitory interneurons are covered, leading to a moderate response of the excitatory neuron. Right: More inhibitory neurons are covered than excitatory neurons leading to a small response of excitatory neurons. Reproduced with reference to Hubel & Wiesel (1962).

A serial approach to visual representation, like the approach outlined above, has turned out to offer a partial explanation of how visual representation is achieved in the human brain. However, the discovery of events in addition to the classical receptive field have had profound consequences for how feedforward and feedback connections contribute to visual representation. The source of such modulation could come from feedback, where higher-order sites modulate activity at the level below; or from lateral connections, where sites situated within the same level modulate other sites in the same level (Lamme & Roelfsema, 2000). The term feedback connection will be used to describe when a higher level site, such as V2, modulates the response of a lower level site such as V1 (Felleman & Van Essen, 1991). The term horizontal connection will be used describe when one site

modulated by responses within itself, such as one part of V1 modulating the response of a different part of V1 (Felleman & Van Essen, 1991).

The modulation of the classical receptive field appears to arise from both horizontal and feedback connections, although feedback connections appear to contribute more to a global visual representation (Angelucci & Bullier, 2003). One experiment revealed the classical receptive field of V1 neurons using a similar method to Hubel & Wiesel (1962) by altering the size, spatial frequency and orientation of a moving grating (Angelucci, Levitt, Walton, Hupe, Bullier & Lund, 2002). Once the classical receptive field of a V1 neuron was successfully discovered, the grating used to reveal the classical receptive field was presented in conjunction a surrounding grating. The diameter and orientation of the surrounding grating was then altered whilst the effect on V1 neurons response was observed. When the orientation of the surrounding grating was the same as the orientation of CRF grating, the response of the CRF neuron was reduced. However, when an blank annulus was introduced in between the CRF grating and the surround grating, and the size of surround grating was increased, the response of the V1 CRF neuron increased. Thus, it appears that the CRF is subjected to different influences, which can increase or decrease the response of a V1 neuron depending on the physical characteristics of visual inputs. Effects of increasing the size of the surrounding grating extended up to 13 visual degrees. The injection of tracers into V1, V2, V3 and V5 was then used to determine the spatial extent of horizontal connections and feedback connections within and between each of these sites in visual degrees. Horizontal connections covered an average of 2.47 visual degrees whereas feedback connections cover as little as 2.6^{o} in V2 up to 26.6^{o} visual degrees in MT. It appears that the influence of feedback relative to horizontal connections increases with the size of a stimulus but both of these influences are important when considering how the CRF can change. These different types of connection – horizontal or feedback – are the critical basis for recurrent processes, which can be distinguished from basic feedforward processes (Lamme & Roelfsema, 2000).

Theories that offer different functional roles for feedforward and feedback during visual representation have also emerged. Lamme (2006) proposed that the recurrent feedback creates a representation that can be consciously perceived. In contrast, feedforward inputs are necessary for recurrent processes to take place but feedforward inputs do not create representations that are themselves consciously perceived. One example of the extra-classical receptive field is figure-ground segregation. Super, Spekreijse & Lamme (2001) demonstrated that a recurrent interaction alters a V1 neurons response depending on whether a visual stimulus is reported as seen or not seen. Super et al. (2001) trained monkeys to make a saccade towards a figure that differed orthogonally in its orientation from a background when it was present and to remain fixated when such a figure was absent. Responses for the figure were greater than responses to r the ground *after* 90ms. Such responses in V1 were only observed when a saccade was made to indicate figure presence; these responses were not observed when the figure was absent, which suggests that seeing the ground was accompanied by a later increase in the V1 response. What is critical here is a later modulation of V1 response was not determined by the presence or absence of a texture that differed orthogonally in its orientation from the background; it was whether the texture was reported as *seen*. The later modulation that accompanies visual stimuli that are reported as seen suggests that a recurrent interaction underlies the process of creating a visual representation that can be consciously reported (Lamme, 2006). In contrast, the earlier feedforward phase may need to take place prior to the recurrent aspect, but these processes may take place outside of awareness (Lamme, 2006b). In order for the contents of earlier feedforward processes to reach awareness, they must be accompanied by a later stage of recurrent processing. The later stage of recurrent processing is accomplished by horizontal and/or feedback based recurrent processes (Lamme & Roelfsema, 2000). The finding of Super et al., (2001) provides neurophysiological evidence for the distinct roles of feedforward and recurrent processes during unconscious and conscious processing, respectively. Moreover, these findings provide evidence that can be used to support a definition of recurrent processing. It appears that the existence of a recurrent process can be defined by processes that

occur *later* on, which are accompanied by responses that are distinct from earlier feedforward processes (Lamme & Roelfsema, 2000).

Responses in regions outside of V1 and recurrent processing

Thus far, it has been established that the creation of visual representation relies on early feedforward processes, such as the CRF. However, the CRF does not appear to be determined by the physical properties of the stimulus itself but the greater visual context in which a stimulus appears (Angelucci et al., 2002). Modulation of the CRF appears to occur after an earlier phase of feedforward processing whereby recurrent processes take place, which can occur via horizontal or feedback connections (Lamme & Roelfsema, 2000; Felleman & Van Essen, 1991). Interestingly, a functional dissociation between feedforward and recurrent processes has been proposed, whereby feedforward processes occur outside awareness which are conditional for later recurrent processes which occur within awareness (Lamme, 2006), which could modulate the initial feedforward response within V1 itself (Super et al., 2001). Potential sources of this feedback to V1 will now be discussed, along with other areas that appear to engage in the process of global or local recurrent processing.

In particular, feedback from sites elsewhere in visual cortex appear to have a strong role in modulating what takes place within V1. There are a number of potential sources of feedback to V1. Direct evidence has revealed that V5 can alter the response of single neurons within V1. V5 was cooled whilst recordings took place in V1, V2 and V3. Whilst V5 was cooled, V1, V2 and V3 responses increased when a high contrast bar moved across the centre of their receptive fields whilst the background remained stationary (Hupe, James, Payne, Lomber, Girard & Bullier, 2001). V5 inactivation reduced V3 responses when a bar moved through the centre of a V3 neurons receptive field and responses were reduced when the bar and the background moved in the same direction when salience was low (Hupe et al., 1998). In light of this evidence, it appears that judgments of

target presence are accompanied by an effect of recurrent feedback within V1; this difference between judgments of target presence and target absence is observed *after* 90ms (Super et al., 2001). Yet the consequences of inactivating V5 are observed within *20ms* of the onset of visual stimulation within V1, V2 and V3 (Hupe et al., 2001), which is consistent with the idea that recurrent feedback can modulate subsequent early responses. However, the critical difference between these studies is that Super et al. (2001) integrated the process of making a decision into their experiment: when a target was present, a saccade was made to a target whereas when it was absent, the monkey remained fixated. In contrast, with Hupe et al. (1998, 2001) is it difficult to identify how recurrent feedback fits within the process of reporting a visual target as present or absent.

As highlighted by Lamme (2006), it is also important to identify *how* recurrent processes contribute to a visual representation that can be reported consciously rather than demonstrating the neurophysiological consequences of preventing feedback from elsewhere. In light of this criticism, it is important to demonstrate the feedforward and recurrent events that need to take place in order for a decision about a particular stimulus to be made. Studying the feedforward and recurrent processing when a decision is also madeoffers the potential to tease apart their relative contributions to visual representation. Lamme (2006) introduced two different types of recurrent processing which follow on from the feedforward sweep. Local recurrent processing which takes place when visual cortex exchanges information within itself can be distinguished from global recurrent processing whereby visual cortex exchanges information with frontal and parietal sites. During global recurrent processing, frontal and parietal sites also have the opportunity to exchange information with one another. The study of frontal and parietal sites has been particularly fruitful in identifying the functional significance of recurrent processes. A number of studies have successfully made electrophysiological recordings in sites outside of visual cortex, which elaborates on the responses that need to accompany the feedforward sweep.

A number of studies have carried out electrophysiological recordings in primates to characterize the responses that take place outside of V1. Responses within parietal cortex and the motion sensitive area V5 appear to be critical when forming a visual representation. In particular, the feedforward sweep within V5 appears to be translated into a sustained response within parietal cortex, which enables to enable a decision to be made about a visual representation. These responses are critical determinants as to whether a visual stimulus or a characteristic of a visual stimulus are reported as present. Salzman, Britten & Newsome (1990) identified how microsimulation of direction sensitive V5 neurons during the presentation of moving stimuli affects the decision making process. Direction sensitive V5 neurons were identified by recording their responses when a number of directions of motion were presented. When a neuron direction responded to the direction of motion that was used in the experiment, the neuron qualified for microstimulation while the primate made decisions about motion direction. The monkeys were presented with dots that moved within a circular aperture; a certain percentage of these dots moved in the same direction and the remaining dots moved in a random direction. The proportion of dots moving in the same direction reveals the *coherence* of the motion stimulus. As motion coherence increases, it becomes easier to successfully report the dominant direction of the motion. Microstimulating these direction sensitive neurons had an effect that was equivalent to increasing the number of coherently movingdots (Salzman, Britten & Newsome, 1990; Salzman, Murasagi, Britten & Newsome, 1992).

Such processes within V5 are important when considering the decision process and its implications for the functional importance of feedforward and recurrent processing. When primates viewed motion stimuli that were identical to those used by Salzman, Newsome and colleagues (1990, 1992) but lateral intraparietal area (LIP) was microstimulated (Hanks, Ditterich & Shadlen, 2006), a picture of how such processes may work emerges. Hanks et al. (2006) trained primates to make a saccade to parts of their visual field to indicate the direction of visual motion. LIP neurons were identified which exhibited an elevation in their responses when a saccade had to be made

towards a target in a specific part of their visual field. This part of their visual field corresponded to where a saccade had to be made in order to indicate a direction of motion. When microstimulation of these LIP neurons took place, the monkey was more likely to move its gaze to the response target associated with the motion direction (Hanks et al., 2006). Microstimulation of LIP neurons was also quivalent to increasing the coherence of motion, making it easier to 'discriminate' the direction associated with response target (Hanks et al., 2006). This suggests that LIP, in addition to V5, may be contributing to the process of visual representation.

To make an interim conclusion, it appears that V5 is involved in the creation of a visual representation that directly corresponds to the physical characteristics of visual stimuli (Salzman, Britten & Newsome, 1990; Salzman et al., 1992). Moreover, inactivation of V5 alters responses within V1, V2 and V3, which suggests that a feedforward and a recurrent exchange needs to take place in order for such a visual representation to be created (Hupe et al., 1998). Moreover, the consequences of V5 inactivation are observed within 20ms of visual stimulation when electrophysiological recordings are made throughout V1, V2 and V3 (Hupe et al., 2001). The conjunction of events within V5 corresponding to physical stimuli *and* potential for V5 to modulate responses within lower levels (V1, V2 and V3), suggests that there feedforward *and* recurrent processes that enable the bidirectional exchange of information during visual representation. In addition to these processes within visual cortex, there also appear to processes taking place in parietal cortex which require a sustained response to visual stimulation in order to successfully make a decision based on a visual representation. This neurophysiological evidence provides evidence for the idea of local recurrent processes within V1, V2, V3 and V5 (Hupe et al., 1998; Hupe et al., 2001; Salzman & Newsome, 1991; Salzman et al, 1992), whereby feedback from V5 can modulate responses in V1, V2 and V3. . However, local recurrent processing between V5 and V1, V2 and V3 (Lamme, 2006) does not appear to be the only condition that needs to be fulfilled. A response also appears to be necessary within LIP in parietal cortex, in which microstimulation of this site appears to be comparable with the process of visual representation itself (Hanks et al., 2006). The

conjunction of V5 and LIP in visual processing suggests that global recurrent processing is also taking place, which requires the exchange of information between visual cortex and parietal cortex (Lamme, 2006). Now that the bidirectional exchange of information between higher-order and lower-order sites has been illustrated, computational models which propose different functional roles for feedforward and recurrent processes will be illustrated as a potential explanation for the phenomena presented here.

An introduction to a computational theory that proposes distinct roles for feedforward and recurrent processes.

It has been illustrated that higher-order sites can modulate the response of lower order sites during visual stimulation (Angelucci et al., 2002; Hupe et al., 1998; Hupe et al., 2001). It has also been illustrated that higher order sites also need to be modulated by lower order sites to successfully create a visual representation (Salzman & Newsome, 1991; Salzman et al., 1992). Lower-order responses appear to be conditional for, but also modulated by, later recurrent processes which are instigated by higher-order sites (Hupe et al., 2001; Super et al., 2001). The distinction between feedforward processes (lower→ higher) and recurrent processes (higher → lower) has led to some researchers proposing that they are functionally distinct from one another (Lamme & Roelfsema, 2000) and that feedforward processes that occur outside awareness (Lamme, 2006). Recent theories have emerged that ascribe functional roles for feedforward and recurrent processes. These theories explain how feedforward processes trigger recurrent processes and how each of these processes make distinct contributions to visual representational.

Rao & Ballard (1999) proposed a model of the extra-classical receptive field called predictive coding. Under predictive coding, higher level cortical areas generate predictions which are conveyed to lower levels. The aim of these predictions is to successfully represent sensory inputs. Lower levels indicate whether a discrepancy exists between sensory inputs and these top-down predictions. Rao & Ballard (1999) proposed that such a framework is implemented by dividing a neural networks into

two different populations. One population represents a *top-down prediction*, which is formed based on the statistical regularities of the environment. The top-down prediction is fed back from higher levels, such as V2, to lower levels, such as V1, in order to represent sensory inputs. Another population represents the discrepancy between the top-down prediction and sensory inputs, which is called a prediction error. The prediction error is conveyed forwards in order to trigger a revision of the top-down prediction. The revised top-down prediction then needs to be fed back to V1 in order to represent sensory inputs. Thus, prediction errors are fed forwards from lower levels to higher levels to signal that the top-down prediction needs to be altered in order to successfully represent sensory inputs. The mismatch or prediction error may be all that is conveyed forward to the higher-level prediction neurons by the lower-level neurons. When the top-down prediction is successful, less prediction error is fed forward reflecting that the top-down prediction has successfully encoded the statistical properties of the environment.

In its initial form, predictive codingwas proposed to test whether feedback projections from V2 to V1 are predictions of incoming sensory inputs to V1 whereas feedforward projections from V1 to V2 carry the mismatch between the top-down prediction and the incoming sensory input and was implemented on a neural net representation of these regions (Rao & Ballard, 1999). This predictive coding model was trained by exposure to thousands of natural images. Following exposure, the first level of the network represented basic edges or bars, whereas the second level of the network represented the conjunction of features which were likely to co-occur within level 1 (Rao & Ballard, 1999). In short, level 1 represented basic orientations whereas level 2 represented the basic orientations that were likely to occur together. In doing so, level 2 generated top-down predictions of what was most likely to co-occur within level 1. Such a model was able to account for extra-classical receptive field effects, such as end stopping, which refers to the diminution of a V1 neuron's response when the size of a bar increases in size beyond its classical receptive field (Rao & Ballard, 1999). According to predictive coding, a V1 neuron's response falls when its size increases beyond its receptive field because lines tend not to occur on their own in natural images ; lines tend to

constitute part of a larger object, such as a tree. When a line increases beyond the size of a V1 receptive field in level 1, it forms part of a greater object, enabling level 2 to successfully predict the greater object based on the conjunctions of features that are most likely to occur based on previous exposure to natural images (Rao & Ballard, 1999). This framework can now be used as a potential explanation for interactions between higher-order sites, such as V5 and LIP, and lower-order sites, such as V1, V2 and V3.

Albeit circumstantial, such evidence demonstrates that the elimination of feedback can have two roles: it can be excitatory or inhibitory depending on the properties of the visual stimulus. Cortical responses must be able to exhibit these two properties in order for predictive coding to be a feasible model of cortical function. When top-down predictions successfully capture the statistical regularities of the visual environment, responses in V1, V2 and V3 would be reduced, reflecting the suppression of prediction error (Rao & Ballard, 1999). In contrast, when top-down predictions unsuccessfully capture sensory inputs, V1, V2 and V3 responses were enhanced. Hupe et al. (1998) demonstrate that these two criteria can be met by reducing V5 capacity to provide such feedback via cooling. Hupe et al. (1998) revealed that inactivation of a higher-order site (V5) can have an excitatory or an inhibitory effect on the responses of V1, V2 or V3. When a high contrast stimuli were used, the responses of V3 neurons were excited whereas V3 responses were inhibited when a low contrast image moved in the same direction as a background (Hupe et al., 1998). However, it was not possible to work out how these inhibitory and excitatory effects synergize to contribute to perception as the monkeys were under the influence of anaesthesia.

However, an additional criteria for the predictive coding account has been met circumstantially. Top-down predictions determine what is fed forward as a prediction error. In order for top-down predictions to determine what is fed back and included in a revised top-down prediction, the effects of feedback must be able to modulate the early responses of lower-level cortical areas. Such a prediction has also been confirmed. Effects of V5 inactivation on V1, V2 and V3

responses when moving or stationary flashed stimuli are presented against a background were observed within 20ms of motion onset and were observed up until the end of visual stimulation (Hupe et al., 2001), which suggests that the segregation of background motion from target motion is affected by V5 feedback very early on. Moreover, this also suggests that top-down predictions- if such top-down predictions exist within V5 – could determine what is fed forward from V1, V2 and V3, which is precisely what would be expected under predictive coding. Feedforward inputs from these sites would be affected early on because the top-down prediction, which is conveyed via feedback, determines what is fed forward as a prediction error (Rao & Ballard, 1999). What is fed forward as a prediction error is determined by the extent of the discrepancy between the top-down prediction and sensory inputs. When the discrepancy is low, less will be fed forward as a prediction error compared to when the discrepancy is low (Rao & Ballard, 1999).

Interestingly, the revised top-down prediction which is fed back to V1 following a prediction error could close correspond to the later phase of V1 responses reported by Super et al. (2001). Even more interesting is how the dissociation between feedforward and recurrent processes under predictive coding could correspond to unconscious and conscious processing as proposed by Lamme (2006b; Friston, 2005; Clark, 2013). Super et al. (2001) revealed that the initial responses of V1 neurons do not distinguish between stimuli reported as seen as those that are not whereas the late responses of V1 neurons do. Correspondingly, predictive coding models propose that a revised top-down prediction is sent to V1 *later on* following a prediction error (Rao & Ballard, 1999). One interepretation is that the top-down prediction, not the prediction error, may be what represents sensory inputs, which means that predictive coding models also propose that late V1 responses will determine what is reported as seen, as reported by Super et al. (2001). This interesting correspondence also has implications for the distinction between unconscious feedforward processes and conscious recurrent processes proposed by Lamme (2006).

Interim summary

So far, it has been established that there is potential for a discrete role for feedforward and recurrent processes in the brain. This has been established by examining predictive coding models (Rao & Ballard, 1999) as a potential explanation for electrophysiological phenomena in primates, whereby higher-level cortical sites convey top-down predictions via feedback connections to represent sensory inputs. Prediction errors signal when a discrepancy exists between the top-down prediction error via feedforward connections, which in turn triggers a revision of top-down predictions. The revised top-down prediction then needs to be fed back to early sensory areas such as V1 to represent sensory inputs. The process of feedforward and recurrent processes presented here may also correspond to the distinction between unconscious feedforward and conscious recurrent processes proposed by Lamme (2006).

Part of the remainder of the general introduction will now focus on the idea of how recurrent processes are accomplished in the human brain, and how recurrent processes within the frontal and occipital lobes contribute towards visual representation. A particularly useful experimental tool that can be used to probe the existence of a feedforward or a recurrent process is called transcranial magnetic stimulation (TMS). The use of TMS as an experimental tool will be explained with a particular focus on early visual cortex (EVC), which refers to the sites V1, V2 and V3 in TMS research (Thielscher, Reichenbach, Ugurbil & Uludag, 2010). The use of TMS as means of elaborating on the involvement of frontal regions will then take place in addition to studying recurrent processes within EVC. The remainder of the general introduction will explore how the hypotheses testing the critical premises of predictive coding models can be developed using humans as participants. Two complemtary approaches to predictive coding will be investigated. One of the approaches will investigate a particular variant of predictive coding, which proposes that the revision of top-down predictions in response to prediction errors can be explained using the principles of Bayes theorem (Friston, 2005; Clark, 2013). Another approach will test a fundamental proposition of

predictive coding models: that more processes need to be accomplished when a discrepancy exists between a top-down prediction and sensory inputs compared to when such a discrepancy does not exist (Rao & Ballard, 1999; Friston, 2005).

Using transcranial magnetic stimulation to probe feedforward and recurrent visual processes in humans

One limitation of using primate electrophysiology when studying visual processes is the state of the primate whilst viewing visual stimuli. Although Super et al. (2001) demonstrated that recurrent feedback accompanies stimuli reported as seen whilst the monkey was awake, the use of a saccade to indicate target presence is problematic. This is because it is not possible to verbally ask a monkey whether or not something is present or not; instead, they have to be trained to complete a task in order to retrieve a food-based reward. One more direct approach to studying recurrent processing, which has relatively high spatial and temporal resolution relative to electrophysiological recordings is transcranial magnetic stimulation (TMS), which can 'add noise' to neural processes via Faraday's law of electromagnetic transduction in the human brain (Walsh & Cowey, 2000). TMS works by sending an electric current through copper wire that rapidly changes in direction to produces a magnetic field that travels through the skull and alters neural activity within the underlying cortex, which enables a reversible interference with processing to take place (Walsh & Cowey, 2000). Moreover, altering the stimulus onset asynchrony, which refers to the onset of a TMS pulse relative to the appearance of a visual target can be used to reveal the chronometry of processes related to visual perception (Amassian, Cracco, Maccabee, Cracco, Rudell & Eberle, 1989)

The first demonstration of time locked TMS being able to affect performance in the visual domain presented participants with 3 randomly selected letters in their fovea (Amassian et al., 1989). During or immediately after presentation of these letters, single pulses of TMS were applied whilst the coil was placed 2cm above the inion at a tangent from the scalp. After the administration of TMS, participants had to report the identity of the letters (Amassian et al., 1989). Participants

could successfully identify the letters when TMS was administered at SOAs of 0 – 60ms and 120 – 200ms. However, participants ability to successfully identify all the letters was abolished when TMS was administered at 80 – 100ms (Amassian et al., 1989), suggesting that TMS could isolate a time period when occipital cortex is critical for accurate performance. Moreover, performance on this task gradually recovered when TMS pulses were delivered as the TMS was incrementally moved caudally from the inion (Amassian et al., 1989), suggesting that moving the coil away from occipital cortex causes the suppression of successful discrimination to cease. Amassian et al. (1989) note that TMS caused eye blinks but not eye movements, which may influence the ability to successfully discriminate the letters. However, other studies have since found that the effect of applying TMS to visual cortex at 80-120ms remains even when trials where eye blinks take place after the administration of TMS where removed from the analysis (Jacobs, de Graaf & Sack, 2012; Allen, Sumner & Chambers, 2014).

The application of TMS pulses to visual cortex at ~100ms producing a decrement in performance has become one of the most reliable effects in the TMS literature with almost all published accounts producing it with a range of stimuli (see de Graaf, Koivisto, Jacobs & Sack, 2014 for a review). The consequence of delivering TMS pulses at ~100ms to visual cortex produces an elevation in a participants threshold, which refers to the minimum stimulus intensity that is necessary for an observer to make a correct response (Kammer & Nussek, 1998; Kammer, Puls, Strasburger, Hill & Wichmann, 2005). Such an effect emerges regardless of colour (Paulus et al., 1999; Allen et al., 2014) and is so reliable that some studies investigating this phenomena only apply TMS pulses at 100ms to produce a decrement in performance (Kastner, Demmer & Ziemann, 1998; Rahnev, Maniscalo, Luber, Lau & Lisanby, 2010). Based on modelling of magnetic field and their interaction with the cortex, the site within visual cortex that is most affected by TMS pulses delivered at ~100ms which cause suppression of visual stimuli is estimated to be the dorsal part of V2 (Thielscher et al. , 2010; Salminen-Vaparanta, Noreika, Revonsuo, Koivisto & Vanni, 2011; Salminen-Vaparanta, Koivisto, Noreika, Vanni & Revonsuo, 2012) but areas V1 and V3 are also

affected to a lesser extent (Thielscher et al., 2010). In light of this methodological issue, the term early visual cortex (EVC) will be used to describe the cortical location where occipital TMS pulses affect performance in visual based tasks. This issue also illustrates an important practical limitation in used TMS to investigate horizontal and feedback connections. Although feedback connections between V1 and V2, V3 and V2 and V3 and V1 are of theoretical interest to how feedforward and recurrent processes operate, it is challenging to distinguish between these sites using TMS (Thielsher et al., 2010). However, TMS can still be used to demonstrate that recurrent processes are taking place within these sites. Moreover, TMS can also be used to compare processes within EVC to processes taking place elsewhere in the brain.

When assuming that an intact signal from V1 is necessary for awareness and V1, V2 and V3 visual evoked latencies occur as early as 34ms, 84ms and 55ms, respectively (Schmolesky, Wang, Hanes, Thompson, Leutgeb, Schall & Leventhal, 1998), why does TMS produce a reliable effect after a slightly later delay at ~100ms when applied to EVC? Of relevance here is the finding of Super et al. (2001) which revealed that the difference in V1 responses when a texture that differs orthogonally from a background is seen emerges at ~90ms, which suggests that visual stimuli evoking a response *per se* is not a critical determinant of whether it is consciously seen. Instead, it is whether the visual stimulus is accompanied by recurrent processing which enables, = or is consequence of , a recurrent process enabling a new visual representation to be created. Recurrent processes do not take place immediately, instead they appear to emerge ~90ms after the onset of visual stimuli when electrophysiogical recording take place in primate (Super et al., 2001). Interestingly, the effect of TMS at an SOA of ~100ms (de Graaf et al., 2014) closely corresponds to point in time that successfully distinguish between stimuli reported and seen and stimuli reported as not seen reported by Super et al. (2001). This correspondence suggests that the application of TMS to EVC interferes with recurrent processes when used to affect human vision at an SOA of ~100ms.

A number of TMS studies have also demonstrated a role for recurrent processes within EVC that are critical for visual awareness in humans. Some TMS studies produce impairments in performance at more than one SOA and such impairments can be separated by SOAs where TMS has *not* produced an impairment. Usually, earlier effects of TMS on performance are attributed to the feedforward sweep and later effects of TMS on performance are attributed to feedback from higher-level cortical sites (de Graaf et al., 2014). The delivery of TMS pulses to EVC at SOAs of 100ms and 220ms significantly reduces the ability to categorize animals as birds or mammals (Camprodon, Zohary, Brodbeck & Pascual-Leone, 2010). In this experiment two discrete effects of TMS were discovered with a return to baseline situated at SOAs in between 100ms and 220ms, which was interpreted as the early 100ms effect affecting a feedforward process and the later 220ms affect a feedback-based recurrent process. However, the ability to categorize animals is a higher-order ability, which implies TMS effects on recurrent feedback in humans are obtained under conditions where higher-order categorical information is required to complete a visual task. Evidence for this proposal comes from studies that found that later effects of EVC-TMS occur between 200 – 400ms for complex but not simple stimuli (Juan & Walsh, 2003; Dugue, Marque & VanRullen, 2011). However, later significant effects ranging from 236 – 320ms also emerge when reporting the presence or absence of visual stimuli such as a figure within ground and the direction or presence of an arrow have also been revealed (Wokke, Sligte, Scholte & Lamme, 2012; Heinen, Jolij & Lamme, 2005; Allen, Sumner & Chambers, 2014). Taken together, these studies show that feedback based recurrent activity defined as an additional, later time window in which EVC TMS pulses can produce visual suppression could affectvisual awareness. However, these experiments only demonstrate that the receipt of feedback in EVC has behavioural consequences; it does not demonstrate the *action* of a feedback mechanism whereby one site in the cortex begins to modulate the function of another site as a function of time. This well-established effect at ~100ms has recently been proposed to reflect feedforward *and* recurrent processes (de Graaf, Goebel & Sack, 2012; de Graaf et al., 2014; Koivisto, Lahteenmaki, Kaasinen, Parkkola & Railo, 2014).

Evidence for different kinds of recurrent interaction taking place within EVC at ~100ms were revealed by an experiment which presented participants with grating or faces and required them to indicate whether the gratings were horizontal or vertical or whether the face was male or female, respectively (de Graaf, Goebel & Sack, 2012). Performance recovered quicker for the gratings judgment than the faces judgment despite both stimuli having similar subjective visibility and the onset of EVC-TMS effects occurring at the same latency for both faces (de Graaf et al., 2012). This difference in the recovery of performance suggests that the early parts of the TMS-induced decrement on performance reflect feedforward processing and the later parts of the TMS-induced decrement on performance reflect a recurrent interaction. However, this experiment averaged performance at TMS-SOAs ranging from 60ms – 130ms (de Graaf et al., 2012) meaning that their statistical analysis could only quantify the *magnitude* of the TMS-induced effect on the faces and gratings judgments. The time course of the recovery of the masking curve (or the magnitude of recurrent processing) for each type of stimulus was not quantified, which means that it cannot be firmly concluded that these different kinds of stimuli are accompanied by a different magnitude of recurrent processing. However, this evidence suggests that the application of TMS to EVC at ~100ms is promising candidate to investigate the existence of feedforward *and* recurrent processes in the human brain.

The application of single pulses of TMS to EVC in a metacontrast masking paradigm revealed direct evidence for the existence of a feedback-based recurrent interaction within EVC at ~100ms (Ro, Breitmeyer, Burton, Singhal & Lane, 2003). Metacontrast masking refers to when a mask is presented after the onset of a target at different SOA.s The mask suppresses detection of the target at SOAs ranging from 10ms to 90ms (Di Lollo, Enns & Rensink, 2000; Tapia & Beck, 2014). In Ro et al. (2003), the target was a disk presented laterally from fixation and the mask was an annulus was centred on the same position as the disk but without any contours that overlapped with the disk. On the 50% of trials the disk was present and on 50% of the trials the disk was absent. Evidence for a recurrent process, whereby EVC was the recipient of feedback, was revealed by more TMS-induced

suppression of the *annulus* when the disk preceded it compared to when the disk was absent at TMS SOAs ranging from 100ms – 143ms (Ro et al., 2003). It appears that the devotion of feedback to disk processing within EVC comes at the expense of feedback-based processing of the annulus. The administration of TMS precludes processing of the annulus and enables more feedback to be subjected to the disk than the annulus, which in turn leads to more judgments of disk presence. There was also an additional effect on performance: effects of TMS-induced suppression of the annulus on detection of the *disk*. When TMS-induced suppression of the annulus took place, participants were *better* at detecting the presence of the disk at SOAs ranging from 86ms – 157ms (Ro et al., 2003). Recall that the annulus was presented after the disk, which means that TMS-induced suppression of the annulus enables more feedback to be devoted to the disk. The devotion of more feedback to be disk compared to the annulus led to more judgements of disk presence to take place. This combination of results suggests that there events which need to take place *within* EVC (in addition to events elsewhere in the cortex) after the onset of target that are critical for it to be reported as present.

Evidence that TMS can reveal the duration of recurrent processes in EVC by simply applying TMS at different SOAs for different types of stimuli has also been revealed. de Graaf et al. (2012) stimulated the *same* site and compared performance across TMS SOAs with two different stimuli. It may be possible to demonstrate the existence and temporal structure of a feedforward and feedback based exchange between two cortical sites using TMS, by revealing a temporal dissociation between two cortical sites whilst task demands and visual presentation are kept constant. The application of TMS to EVC reveals that effects of EVC-TMS arise at SOAs of 60-80ms and 100-120ms when participants have to report the direction of motion (Silvanto, Lavie & Walsh, 2005). However, an effect of V5 emerged in between these EVC-TMS effects at SOAs of 80 – 100ms (Silvanto, Lavie & Walsh, 2005). The temporal dissociation suggests that TMS can successfully distinguish between feedforward and recurrent processes between EVC and V5, which was indicated by the first EVC-TMS taking place prior to V5-TMS effect. This temporal dissociation also suggests that TMS can also

distinguish between feedback processes, which was indicated by the V5-TMS effect occurring *before* the second, later EVC-TMS effect. The temporal order of these effects suggests that there are indeed feedforward and recurrent processes that contribute to the creation of a visual representation (Lamme & Roelfsema, 2000). Feedforward processes could be defined as early TMS-induced effects that arise at earlier SOAs whereas recurrent processed could be defined at TMS-induced effects that arise at later SOAs. Some studies have managed to go further to provide evidence for the proposition that recurrent processes breach awareness but feedforward processes do not (Lamme, 2006).

Within TMS research there is a phenomena known as a phosphene, referring to a perceptual distortion of a participant's visual field following stimulation of EVC, usually while the participant is blindfolded (Kammer, Beck, Erb & Grodd, 2001). Walsh & Pascual-Leone (2001) that application of TMS to V5 reveals a moving phosphene whereas the application of TMS to EVC produces a static phosphene. However, when a V5 TMS pulse is delivered *before* an EVC-TMS pulse, a phosphene is reported as moving (Pascual-Leone & Walsh, 2001). However, the phosphene remains static when a V5-TMS pulse is delivered after an EVC-TMS pulse. The production of a moving phosphene when a V5-TMS pulse is delivered before an EVC-TMS pulse suggests that feedback from V5 to EVC is critical for moving stimuli to breach awareness and not the other way round (Lamme, 2006). These findings suggest that despite V5 occupying a higher point in the processing hierarchy (Felleman & Van Essen, 1991), feedback to V1 from V5 needs to take place in order for motion to be seen.

Further involvement of a critical role for the EVC in the awareness of motion comes from a study that stimulated EVC with TMS and compared its effect across SOAs on objective and subjective measures of performance (Koivisto, Mantyla & Silvanto, 2010). The objective measure of performance was whether participants successfully discriminated leftward or rightward motion. The subjective measure of performance was a rating of visibility of a scale from 1 – 4. Despite the fact that the same site was being stimulated across all SOAs, an effect of TMS on subjective visibility was

revealed earlier on at 20 – 60ms than the effect on objective discrimination which occurred slightly later at 20 – 80ms. Consistent with an account that a recurrent interaction characterizes the interaction between V5 and EVC, an effect of V5 TMS was observed at 40ms, which falls between the early 20 – 60ms effects and the late effects observed as a result of TMS on subjective and objective discrimination, respectively (Koivisto et al., 2010). However, it was also revealed that a later EVC TMS effect at 60ms, affected force choice performance on trials when the participants reported being aware *and* unaware of the motion direction in a subjective visibility task (Koivisto et al., 2010). The implication of is that recurrent processing clearly characterizes the interaction between extrastriate regions such as V5 and striate regions such as V1/V2 but such a striate-extrastriate recurrent interaction may not be essential for visual stimuli to reach awareness. It may be that the presence of motion on the retina triggers a process whereby recurrent feedback is delivered to V1 from V5 regardless of whether the motion is consciously perceived. For example, the presence of sufficient motion on the retina may lead to recurrent feedback from V5 being sent to V1 regarding the direction of motion, but such an interaction also occurs outside of awareness.

In order to identify candidate sites for recurrent interactions, it may be necessary to look beyond V5, such as parietal cortex, which may form part of a recurrent network that enables visual stimuli to reach awareness. When TMS pulses are applied to the intraparietal sulcus (IPS) at an SOA of 90ms conscious, but not non-conscious, perception is impaired (Koivisto et al., 2014) suggesting that IPS supports processes involved in awareness. Evidence that a feedback-based recurrent interaction characterizes conscious awareness can be found in the fact the EVC stimulation also affected conscious perception at SOAs of 60, 90 and 120ms where the IPS effect falls directly in between the range of SOAs were EVC TMS had an effect (Koivisto et al., 2014). It can be speculated that the 60ms EVC TMS effect that is followed by a 90ms IPS effects reflects a feedforward volley from EVC to IPS and the 120ms EVC effect that occurs after the 90ms IPS effect could reflect a recurrent feedback from IPS to V1 that is essential for stimuli to be consciously reported.

It can only be speculated that a recurrent interaction characterized by feedback is being reported by Koivisto et al. (2014). If a recurrent interaction between IPS and EVC took place, it would be expected that an EVC TMS effect would remain *after* the onset of the IPS TMS effect. In contrast, if feedforward rather than recurrent processing was taking place between the two sites, the an EVC-TMS effect would occur before an IPS-TMS effect, but a EVC-TMS effect would not. Thus, the *temporal order* of the effects are consistent with a feedback-based recurrent account (Lamme, 2006b; Lamme & Roelfsema, 2000). However, it does not provide direct evidence for EVC being the recipient of feedback from IPS. The experiments that were conducted here adopted the logic of Silvanto et al. (2005a) and Koivisto et al. (2014) in determining whether feedforward or recurrent processes are taking place. It becomes apparent that early and late effects of EVC-TMS can arise when TMS is applied at SOAs ranging from 60ms to 330ms (de Graaf et al., 2014). By applying TMS to sites in addition to EVC and comparing when these effects emerge relative to early and late EVC effects, it may be possible to identify sites that provide feedback to EVC in order to create a visual representation. This chapter will now pursue two separate objectives. The first objective will be to discover if an additional cortical site that could provide feedback to EVC in a recurrent based interaction can be identified. The site where single pulses of TMS will be applied at different SOAs will be dorsolateral prefrontal cortex (DLPFC), which could be of interest in recurrent interactions with EVC. In order to determine whether DLPFC is partaking in such interactions, the onset of DLPFC-induced TMS effects will be compared to onset of one or more EVC-TMS induced effects, if such effects arise.

The second objective will be to identify whether the predictive coding account can explain how TMS can differentially affect recurrent processes and feedforward processes within EVC. The investigation of predictive coding will be split into two parts. The first part will involve the development of paradigms to test the premises of a particular kind of predictive coding within EVC – Bayesian predictive coding (Friston, 2005). The second part of this section will aim to investigate a fundamental assumption of predictive coding – whether or not the mismatch between a top-down

prediction leads to more recurrent processing within EVC (Rao & Ballard, 1999). An increase in recurrent processing would reflect the process of revising a top-down prediction in response to prediction error.

Frontal regions in perceptual decision making: Implications for feedback-based recurrent interactions with early visual cortex

Interim summary

The evidence presented above suggests that parietal cortex and sites within visual cortex itself, such as V5, engage in recurrent processing with EVC in order to create a visual representation (Silvanto et al., 2005; Koivisto et al., 2014). These different sources of feedback are consistent with idea of local recurrent processing between V5 and EVC and global recurrent processing between visual cortex and parietal cortex (Lamme & Roelfsema, 2000; Lamme, 2006). TMS has been successful in demonstrating the existence of these different mechanisms (de Graaf et al., 2014). Here, the aim was to demonstrate whether global recurrent processes can extend to the frontal lobes in humans (Lamme, 2006). Like EVC, frontal sites such as DLPFC have been implicated in studies of visual awareness (Lau & Passingham 2006), which suggests there is potential for DLPFC involvement in recurrent processes (Lamme, 2006; Lamme & Roelfsema, 2000).

The frontal lobes and feeback-based recurrent interactions: Initial support

In addition sites in parietal cortex, which appear to engage in recurrent processing with EVC, there is also evidence that frontal sites can also modulate EVC responses. One source of feedback to EVC is frontal eye field (FEF). There is support for the proposition from primate electrophysiological stimulation(Moore & Armstrong, 2003) and functional neuroimaging in humans (Ruff, Blankenburg, Bjoertomt, Bestmann, Weiskopf & Driver, 2006). However, FEF will only be used to illustrate the potential for additional sites within the frontal lobe to engage in recurrent based

interactions. Instead, the focus will be on DLPFC and how this site can engage in recurrent processing with EVC.

Microstimulation of FEF at an intensity *below* the threshold required to produce a saccade to a retinotopic location corresponding to the receptive field of a V4 neuron increases the firing rate of the V4 neuron when a visual stimulus falls inside but not outside of its receptive field (Moore & Armstrong, 2003). This sets out the exact conditions for a feedback-based recurrent processing between the FEF and visual cortices: the V4 neuron needs sufficient drive by having a stimulus placed within its receptive field for FEF to amplify its response. The finding also emphasizes that the source of the change of the firing rate of a neuron within visual cortex is within the frontal lobes, suggesting that a recurrent interaction between the frontal and visual cortices could have a causal involvement in visual perception. Concurrent TMS-fMRI combined with psychophysics have confirmed that such interactions can take place between frontal and occipital cortex in humans. The application of TMS pulses to the right FEF during fMRI increased BOLD responses throughout V1, V2, V3 and V4 that register the peripheral visual field and *decreased* BOLD responses with the parts of these sites that register the central visual field (Ruff, Blankenbug, Bjoertomt, Bestmann, Freeman, Haynes, Rees, Josephs, Deichmann & Driver, 2006). Left FEF TMS also produces decreases in the BOLD response in sites within visual cortex that register the centre of a participants visual field (Ruff, Blankenburg, Bjoermont, Bestmann, Weiskopf & Driver, 2009), suggesting that the left FEF TMS and right FEF TMS may have different effects on visual cortex. Critically, pulses to right FEF, not vertex, caused these changes in BOLD throughout visual cortex (Ruff et al., 2006; Ruff et al., 2009). The increase in BOLD for peripheral but not central sites led to the test that right FEF TMS would improve judgments of perceived contrast for peripheral stimuli. This prediction was confirmed by 5 TMS pulses at 10Hz right FEF TMS shifting psychometric functions to the right, indicating that participants were able to detect finer differences in the contrast of Gabor patches (Ruff et al., 2006). Similar evidence for right FEF having a causal involvement in what participants report seeing was revealed in a double pulse TMS study that produced a statistically significant reduction in perceptual sensitivity

when applied 40-80ms after the onset of a search array containing a target to be detected (O'Shea, Muggleton, Cowey & Walsh, 2004).The application of TMS to FEF also facilitates awareness of targets when applied 40ms before the onset of a target (Grosbras & Paus, 2002), which suggests that there are pre-stimulus and post stimulus mechanisms whereby the frontal lobe can contribute to visual awareness.

Thus, the study of FEF has revealed there is potential for the frontal lobe to modulate what occurs. However, there is also recent evidence that DLPFC is also involved in the process of visual representation. The demonstration of DLPFC in visual representation has been revealed using functional MRI with stimuli where the influences of visual stimulus driven influences and the process of perceiving the visual stimuli can be dissociated (Lau & Passingham 2006; Rounis, Maniscalo, Rothwell, Passingham & Lau, 2010; Imamoglu, Kahnt, Koch & Haynes, 2012; Vernet, Brem, Farzan & Pascual-Leone, 2015; de Graaf, de Jong, Goebel, van Ee & Sack, 2011).

The frontal lobes and recurrent interactions: Dorsolateral prefrontal cortex

Functional MRI has revealed that there is potential for a causal influence for DLPFC in the creation of a visual representation. The role of DLPFC has been implicated in the process of *knowing* a particular stimulus has been present (Lau & Passingham 2006; Rounis et al., 2010). Moreover, tentative support for a global recurrent interaction between DLPFC and EVC (Lamme, 2006) has been revealed using Mooney figures and bistable stimuli (Imamoglu et al., 2012; Vernet et al., 2015; de Graaf et al., 2011). The use of Mooney figures, which initially appear as black and grey patches until they are eventually recognized as real stimuli, revealed that this process of recognition is associated with an increased feedforward drive from EVC to DLPFC using functional MRI (Imamoglu et al., 2011). Moreover, the perception of stimuli which can be perceived in two ways – bistable stimuli – can be altered by the application of repetitive TMS (rTMS) and paired-pulses of TMS to DLPFC (de Graaf et al., 2011; Vernet al., 2015). The effects of TMS on the perception of bistable images can be on voluntary switches, when the participant actively tries to perceive changes (de

Graaf et al., 2011) and when the participant does not (Vernet al., 2015). Taken together, this evidence suggests that DLPFC could be involved in the process of visual representation, and such a process may involve a global recurrent interaction between DLPFC and EVC (Lamme, 2006). Here, the potential for applying single pulses of TMS to modulate such a process within DLPFC will be introduced as a means of providing causal evidence for DLPFC in global recurrent processing (de Graaf & Sack, 2011; Lamme, 2006b; Lamme & Roelfsema, 2000).

The role of DLPFC in recurrent processing is particularly interesting because recent evidence suggest that the relationship between DLPFC and posterior sites, such as EVC, may be bidirectional. Imamoglu et al. (2012) demonstrated that recognizing images was associated with increased feedforward drive from EVC to DLPFC. Vernet et al. (2015) revealed that applying a pulse of DLPFC-TMS 10ms after an IPS-TMS pulse reduced the likelihood of a participant of a participant reported a change in a bistable stimulus. It is interesting to note here that evidence already exists for a recurrent process occurring between EVC and IPS, as highlighted by an overlap between IPS-TMS and EVC-TMS induced effects on performance (Koivisto et al., 2014). The application of TMS to DLPFC during functional MRI has also revealed that an effect of DLPFC-TMS emerges on BOLD within the 'house sensitive', parrahippocamoal place area (PPA) and face sensitive fusiform face area (FFA) depending what needs to be retained in working memory during distraction (Feredoes, Heinen, Weiskopf, Ruff & Driver, 2011). Although this experiment was not investigating perceptual processes during visual representation, it does illustrate that DLPFC could be capable of modulating the responses of posterior sites via feedback during a recurrent interaction. The experiments investigating the role of DLPFC in global recurrent processing presented here applied single pulses of TMS to DLPFC and EVC after the onset of a visual stimulus. The statistical analyses then sought to reveal whether an effect of DLPFC-TMS emerged at a particular SOA. If such an effect was identified, the onset of the DLPFC-TMS effect would then be compared to the onset of the EVC-TMS effect to understand how recurrent processing is accomplished between these two sites. Now, the findings of

studies which have applied TMS to DLPFC and assessed its influence on visual representation will be considered.

Functional MRI studies have shown the left DLPFC activation as measured by the BOLD signal has been implicated in the subjective aspects of vision such as *knowing* that a visual stimulus has just been presented (Lau & Passingham, 2006). This experiment used a backwards masking paradigm to dissociate proportion correct (PC) from participant's awareness of a target being present. Participants were presented with a square or a diamond which was followed by a metacontrast mask, which occurred at a different SOA on each trial. On each trial, participants were asked to indicate whether the target was a square or a diamond and whether they saw the target or whether they had guessed whether it was present. A dissociation between PC (whether the participant judged correctly) and reports of whether they had guessed or saw the target (whether the participant knew they were correct) emerged when the mask was presented 33ms after the onset of the target compared to when the mask was presented 100ms afterwards (Lau & Passingham, 2006). Participants reported they were guessing when the mask was presented at an SOA of 33ms but they did not report guessing when the mask was presented at 100ms. The higher level of awareness of having seen the target when the mask was presented at an SOA of 100ms was associated with significantly more BOLD in the left mid DLPFC (Lau & Passingham, 2006).The greater BOLD response in the left mid DLPFC raises an interesting question regarding the nature of recurrent processing that needs to take place in order for a stimulus to be reported as seen. It suggests that a response within EVC and DLPFC needs to take place in order for a target to be reported as seen whereby EVC neurons trigger a response within DLPFC neurons. Moreover, when the clarity of perceptual inputs (either faces or houses) is gradually increased, left DLPFC is sensitive to the stimulus visibility (Heekeren, Marret, Bandettini & Ungerleider, 2004) regardless of whether a hand or eye movement needs to be used to make the response (Heekeren, Marret, Ruff, Bandettini & Ungerleider, 2006). The application of theta burst TMS to the left DLPFC impairs the detection of change, reduces accuracy and increases reaction time in perceptual categorization tasks and impairs featural

processing (Turrato, Sandrini & Miniussi, 2004; Philiastides, Aucsztulewicz, Heekeren & Blankenburg, 2011; Renzi, Schiavi, Carbon, Vecchi, Silvanto & Cattaneo, 2013). Interestingly, the application of continuous theta burst TMS, thought to be a suppressive TMS protocol, to the right DLPFC reduces perceptual sensitivity in the search for an item characterized by a conjunction of visual featues but not a single feature (Kalla, Muggleton, Cowey & Walsh, 2009). Taken together, these studies provide causal evidence that a critical exchange needs to take place between stimulus selective brain regions and DLPFC in order for performance in the visual domain to be accurate.

Two studies have applied theta burst TMS bilaterally or to the right DLPFC and have made participants *less* aware that they are making accurate responses (Rounis, Maniscalo, Rothwell, Passingham & Lau, 2010; Chiang, Lu, Hsieh, Chang & Yang, 2015), similar to the metacontrast masking paradigm employed by Lau and Passingham (2006). Critically, comparing accuracy as a function of right DLPFC rTMS to a number of control conditions such as a vertex TMS, no TMS and sham TMS demonstrated that accuracy was similar across all conditions; the only change observed was an increase in the number of guessed responses compared to the number of confident responses linking the effects to metacognition (Chiang et al., 2015). These experiments demonstrate that there is potential for DLPFC involvement in a recurrent interaction. A hint at the temporal structure of DLPFC relative to posterior brain sites was an electroencephalography (EEG) study that investigated when the frontal cortex is 'activated' by visual stimulation (Foxe & Simpson, 2002). The dorsolateral frontal cortex was found to show changes in scalp measured potentials as early as 30ms and peaking as early as 80ms, suggesting that there is potential for dorsolateral prefrontal modulation of posterior sites very shortly after the onset of visual stimulation (Foxe & Simpson, 2002). The onset of such potentials within the frontal cortex are early enough to suggest that such responses could reflect the latency of DLPFC responses during the feedforward sweep (Lamme & Roeflsema, 2000). However, such an early latency is necessary for the initiation of a recurrent interactions whereby DLPFC engages in potentially bidirectional exchanges with posterior sites, such as EVC.

Rahnev, Nee, Liddle & D'Esposito (2016) combined fMRI, theta burst TMS and computational modelling to reveal that the right DLPFC is involved at an intermediate stage of the perceptual decision making process. Theta burst TMS was applied to right FEF, right DLPFC and right anterior prefrontal cortex based on the BOLD peak functional MRI co-ordinates in a task where a cue indicated where participants must attend and whether or not speed or accuracy must be emphasized whilst making their responses (Rahnev et al., 2016). The effects of theta burst TMS on reaction time were modelled using an evidence accumulation process where two separate accumulators gather evidence for one of two choices over time (Rahnev et al., 2016). When the evidence for one of these accumulators reaches a boundary, the decision is made (Rahnev et al., 2016). Applying theta burst TMS to the DLPFC increased RTs relative to sham TMS, which was found to produce a change in the boundary, which according to the model suggests that the right DLPFC is involved in the intermediate processes of gauging how much sensory evidence is necessary before a decision can be made. Interestingly, an additional study has modelled the effects of rTMS to the *left* DLPFC during a face-car categorization task. This indicated an effect on *drift rate*, not the boundary, which suggests that unlike the right DLPFC, the left DLPFC may be involved in the process of evidence accumulation, which is then used to guide subsequent responses (Philiastides et al., 2011). The fact that right DLPFC and left DLPFC theta burst TMS produce different effects on similar decision models suggests that functional heterogeneity exists between these sites in each hemisphere. However, the effects of right and left DLPFC TMS on these parameters suggest that DLPFC is involved in the *later* and/or intermediate stages of perceptual decision making, which involves translating representations in stimulus selective cortex into representations that can subsequently be used to make a decision (Rahnev et al., 2016; Philiastides et al., 2011). When considering the role of DLPFC in a recurrent interaction, this evidence would suggest that posterior sites such as early visual cortex would alter the responses of DLPFC as a function of time and that feedback from DLPFC to posterior sites is not an essential component of the perceptual decision making process.

In light of this evidence it becomes apparent that there is potential for an exchange between EVC and DLPFC during visual representation. Evidence from fMRI and theta-burst TMS combined with computation modelling suggests that DLPFC responses are driven by and sensitive to changes within early visual cortex or stimulus selective cortex within posterior brain sites (Heekeren et al., 2004, Heekeren et al., 2006; Imamoglu et al., 2012; Philiastides et al., 2011; Rahnev et al., 2016). However, the use of theta-burst TMS (de Graaf et al., 2011) and paired pulse TMS (Vernet et al., 2015) in conjunction with a bistable perceptual stimulus suggest that there is potential for feedback from DLPFC to modulate the responses of the IPS (Vernet et al., 2015). Moreover, studies found evidence for DLPFC accumulates evidence (Philiastides et al., 2011) based on the difference in BOLD between the house and face stimulus selective regions, the PPA and FFA, respectively, may be subjected to feedback from right DLPFC under particular conditions as revealed by TMS-fMRI (Feredoes et al., 2011). In order for evidence of feedback from DLPFC modulating the response of posterior sites in the brain, such as EVC, techniques with relatively high spatial and temporal resolution must be also utilized.

Chapter 3 will explore the temporal structure of recurrent processing in left DLPFC and EVC to identify whether any recurrent interactions are taking place g, and, when DLPFC-induced TMS effects arise relative to EVC-TMS effects. If a recurrent interaction is taking place, it would expected for one site to become critical for visual processing before the other. This is because it will be expected that stimulus driven activity will need to trigger a response within DLPFC and potentially trigger an additional response within EVC, if a feedback-based recurrent interaction is taking place. In contrast, if a recurrent interaction between left DLPFC and EVC is not taking place, it would be expected only one of these sites would be critical. This experiment was pre-registered.

Evidence for predictive coding: the use of Bayes theorem to integrate prediction errors and top-down predictions

The idea of feedforward and feedback based - or recurrent - interactions is becoming an influential notion of how the human brain operates (Lamme & Roelfsema, 2000). Predictive coding models offer a theoretical framework that can characterize when feedforward and recurrent processes are taking place and have implications of our understanding of visual cognition (e.g. Rao & Ballard, 1999; Friston, 2005; Spratling, 2008; Clark, 2013). Predictive coding models argue that feedback from a higher level cortical site to a lower level cortical site below convey a top-down prediction of what is going on whereas feedforward processes from a lower-level site to the higher level cortical site indicate a discrepancy between a top-down prediction and sensory input (Rao & Ballard, 1999; Friston, 2005). The key premise of predictive coding models is that the feedback represents sensory inputs and the feedforward processes merely signal that a change has occurred in the environment which requires the top-down prediction to be revised (Friston, 2005). A Bayesian computational framework that has been proposed to explain the how these top-down predictions and prediction errors operate and contribute to visual perception. Some researchers have proposed that such an explanation is difficult to falsify (Bowers & Davis, 2012). In chapter 4, behavioural and TMS paradigms are explored in order to utilize TMS to test the critical premises of predictive coding to identify whether if it offers a feasible model of brain function.

Another variant of predictive coding was proposed by Karl Friston, which proposed predictive coding as a general principle that characterizes cortical responses (Friston, 2005). Instead of characterizing the exchange between V1 and V2, this approach proposed that superficial pyramidal cells convey prediction error and deep pyramidal cells convey top-down predictions, which characterizes how the brain responds to sensory inputs. The exchange of top-down predictions and prediction errors was also proposed to be carried out according to Bayes theorem. According to Bayes theorem, two sources of information are combined: a prior-probability, which represents what is most likely occur given exposure to natural statistics in the past; and the prediction error, which represents the mismatch between the prior-probability and what has currently being presented. The prior-probability aims to successfully predict what occurs within the

lowest cortical site – V1 (Friston, 2005). This top-down prediction is applied to incoming sensory inputs, which in turn, determines the extent to which prediction error is fed forward. The more successful the top-down prediction is at 'explaining away' sensory inputs, the lesser the amount that is fed forward by the level below.

There are temporally discrete events that need to occur for Bayesian predictive coding to take place (Friston, 2005; Clark, 2013). The first event is the establishment of the prior-probability, which is a top-down prediction representing the most likely cause of sensory inputs given prior-experience at the bottom of the processing hierarchy. The second temporal event that can take place once the prior-probability is established and there is sensory input is a prediction error that is fed forward. The prediction error is only fed forward if the prior-probability fails to successfully represent the most likely cause of sensory inputs. Once a prediction error has been generated, the prediction error is conveyed forwards in the processing hierarchy and enters a process of integration with the prior-probability, which is the third discrete events under Bayesian predictive coding. Finally, a revised top-down prediction, called the posterior, is the product of this integration which is fed back to V1 in response to the prediction error.

Bayesian predictive coding offers an explanation of the function of feedforward and recurrent processes in the human brain. Feed forward events relate to a prediction error and recurrent activities relate to the process of integrating a prediction error with the prior-probability to produce a posterior. Additional recurrent activities then include the feedback of the posterior to V1 as a new top-down prediction to represent the most likely causes of sensory inputs. The EVC-TMS effect at ~100ms is a good candidate to investigate such processes, which is thought to reflect feedforward *and* recurrent processes (de Graaf et al., 2014; de Graaf et al., 2012) andcould be affected by feedback from higher-order sites such as IPS (Koivisto et al., 2014). Feedforward processes are prediction errors and recurrent processes are the revision of a top-down prediction (Friston, 2005). TMS can potentially isolate these two processes within EVC by applying pulses at

different SOAs. In order to test the premises of the Bayesian predictive coding account is important to account for the temporal order of the discrete events that need to take place, and to identify whether Bayes theorem can explain the relationship between prediction errors and top-down predictions that are conveyed forwards and backwards in the processing hierarchy, respectively. When considering how Bayes theorem operates, the idea of the *precision* of the prior-probability distribution and the prediction error becomes critical. The term precision is the inverse of variance and can explained by referring to the standard deviation of a mean. A precise distribution would have a low standard error whereas an imprecise distribution would have a large standard error (Feldman & Friston, 2010).

Precision and Bayesian processes in behavioural and neural events.

Investigating the precision of the prior-probability and how precision affects behavioural judgments appears to be important. If single pulse TMS is to be used to investigate Bayesian predictive coding, it is important to consider evidence that the precision of a prior-probability *and* of the prediction error can be reflected in behavioural judgments and neural events within the brain itself.

Evidence for the precision of a prior-probability distribution having a greater impact on perceptual judgments comes from an experiment investigating the perceived velocity of a target with and without eye movements (Freeman, Champion & Warren, 2010). Participants decided which set of moving dots moved fastest whilst fixating or pursuing (with their eyes) a fixation cross (Freeman et al., 2010). Participants required a greater difference in the speed of the two motion stimuli when pursuing compared to when they were fixating, meaning that their threshold was greater for pursuit relative to fixation (Freeman et al., 2010). The prior-probability used in this experiment was a zero motion prior, a naturally occurring prior based on the assumption that most visual stimuli in the environment are not moving. (Freeman et al., 2010). The application of a Bayesian model to participant's data whilst fixating and pursuing revealed that the influence of a

zero-motion prior was greater during pursuit compared to fixation (Freeman et al., 2010). The influence of such a prior was due to the *precision* of the sensory signals being greater during fixation compared to pursuit (Freeman et al., 2010). When the motion signals were imprecise during pursuit, the relative influence of prior was greater than the sensory signal, leading to a greater influence of the prior on performance. In contrast, when the motion signals were more precise during fixation, the relative influence of the prior was reduced compared to the sensory signal, leading to a smaller influence of the prior-probability on performance. This experiment demonstrates that the most likely cause of sensory inputs can influence perceptual judgments and that the precision of a sensory signal, determines the influence of such a probability on performance..

Evidence for the precision of prediction errors and prior-probability influencing haemodynamic responses comes from an fMRI study which presented participants with targets that were attended or unattended under conditions where a target was expected or not expected to appear in the attended location (Kok, Rahnev, Jehee, Lau & de Lange, 2011). In these circumstances, attention enhances the precision of sensory inputs by improving the spatial resolution of visual stimuli, which means that prediction error would be have greater precision than the prior-probability (Yeshurun & Carrasco, 1998; Feldman & Friston, 2010). The BOLD response in V1 was reduced when a target was expected in an *unattended* hemifield compared to when the target was not expected to appear in the unattended hemifield (Kok et al., 2011), suggesting that unexpected, unattended inputs trigger greater responses than expected inputs. Critically, the effect of expecting a target to appear in an *attended* hemifield was in the opposite direction: V1 BOLD was greater when an expected input was attended and expected compared to when it was attended but *not* expected (Kok et al., 2011). What is interesting here is that the combination of the expected the location of the target and the actual location of the target, and their respective effects on precision, can be observed at the earliest stage of processing – V1 (Felleman & Van Essen, 1991). There is evidence from fMRI that suggests that a prior-expectation (evoked by an auditory tone) of upcoming motion direction influences behavioural responses and the BOLD response (Kok, Brouwer, van

Gerven & de Lange, 2013), which suggests that a prior-probability determines *how* visual inputs are represented within the brain itself. For example, when a tone indicating an upcoming rightward direction was presented, behavioural responses were slightly biased to the right and visual cortex (V1, V2, V3, V4, V3A & MT+) showed a greater BOLD response in voxels sensitive to rightward motion compared to the voxels in these sites which were sensitive to upward motion (Kok et al., 2013).

When a prior-probability is integrated with a prediction error using Bayes theorem, the relative influence of the prior-probability and the prediction error is determined by the precision of the one relative to the other (Feldman & Friston, 2010). When sensory input is noisy it is *imprecise,* which means that the influence of the prior-probability will be greater when the two are integrated to produce a posterior (Feldman & Friston, 2010). In contrast, when the precision of the sensory input is greater than the precision of the prior-probability, for example with clear stimuli, the influence of the sensory input will be greater than the influence of the prior-probability (Feldman & Friston, 2010). Here, the initial aim was to utilize the ability of TMS to add noise to neural processes (Walsh & Cowey, 2000) to identify whether the addition of TMS-induced noise can reduce the precision of the prediction error and/or the prior-probability. When TMS-induced noise reduces the precision of the prior-probability, performance could be improved by increasing the precision of the prediction error relative to the prior-probability. In contrast, performance should be impaired *and* influenced by a prior-probability when TMS-induced noise reduces the precision of the prediction error relative to the prior-probability. Depending on when a TMS pulse is delivered relative to the onset of sensory signals, it may be possible to tease apart feedforward processes relating to prediction and error and recurrent processes related to the integration of the prediction error to produce a posterior.

Precision, TMS and the experiments presented here.

The experiments presented here initially aimed to develop a paradigm that can be used to probe for the representation of a prior-probability, a prediction error and a posterior within EVC. Predictive coding proposes that a prior-expectation – a prior-probability according to the Bayesian approach - should be in place within V1 before a prediction error can take place (Rao & Ballard, 1999). Once a prior-probability has been established, a prediction error can subsequently be triggered or not triggered in the event of violation or confirmation of the prior-probability, respectively (Friston, 2005). In the event of prior-probability violation, a posterior, which is a revised prior-probability, is produced by integrating the prediction error with the prior-probability (Friston, 2005). Thus, according for Bayesian predictive coding framework to be correct, the first temporal event must affect the prior-probability, otherwise no prediction errors can be generated. The second temporal event must be the prediction error, which occurs when the prior-probability is incorrect. Finally, the final temporal event must be the posterior, which reflects the integration of the prior-probability with the prediction error to complete perceptual inference.

These temporal events provide discrete periods of time whereby EVC-TMS can affect performance. The nature of the TMS effects during these discrete time periods can be used to identify whether such an effects are compatible or incompatible with the Bayesian predictive coding framework. According to predictive coding, the earliest process that EVC-TMS can disrupt is the establishment of the prior-probability within EVC. Without the prior-probability being established, V1 can deliver not feedforward inputs to the rest of the brain in the form of prediction errors. Despite early controversy (e.g. Corthout et al., 2000) regarding pre-stimulus EVC-TMS effects being due to TMS-induced blinks, there is growing evidence that EVC-TMS eapplied 20ms - 50ms before the onset of simple orientation stimuli prevents such stimuli from breaching awareness, evenwhen trials where blinks occurred are excluded from the analysis (Jacobs, de Graaf & Sack, 2014). Interestingly, pre-stimulus effects at 80ms, 50ms, 20ms and 10ms have been obtained when TMS

was applied to the same retinotopic location as the visual stimuli (Jacobs, Goebel & Sack, 2012; Jacobs et al., 2014). However, an effect of pre-stimulus EVC-TMS have been also obtained 60ms, 50ms and 40ms before visual stimulus onset and such effects were *not* retinotopic (Jacobs et al., 2014; de Graaf et al., 2014), which suggests that this event is relevant to perceptual representation outside of the classical receptive field.

Such effects occurred when there is no target stimulus-related input within EVC, so it is feasible that predict the non-retinotopic effects could reflect the anticipation of stimulus identity rather than an event related to representation in a certain part of the visual field. For the initial aims of the proposed experiments, it is feasible to also make predictions regarding the direction of the TMS-induced effects, if such TMS-induced effects are related to a prior-probability that aims to successfully predict and represent a visual stimulus. For example, pre-stimulus EVC-TMS effects at 50-60ms could influence stimulus representation by ialteringing the relative influence of the prior-probability by reducing its precision. The critical points here is that 50-60ms pre-stimulus TMS effects could occur on a similar timescale and affect the same network that is responsible for prior-expectation biasing sensory representation in visual cortex, which in turn, guides behavioural responses (Kok et al.; 2013; Freeman et al., 2010). If a prior-probability is integrated with a prediction error according to Bayes theorem under predictive coding, pre-stimulus TMS effects should alter the precision of the prior-probability distribution, *not* the precision of prediction error, which is what these experiments initially aimed to investigate. Freeman et al. (2010) stated that there are circumstances where a precise prior-probability can make performance worse. Thus, reducing the precision of the prior-probability could promote the influence of prediction error. Interestingly, Allen et al. (2014) revealed an improvement in performance when EVC-TMS was applied at early SOAs. Whether such an improvement is due to reducing the precision of a prior-probability in circumstances where a prior-probability could impair performance will be under investigation in chapter 3.

The robust and reproducible effect of EVC-TMS when applied at an SOA of approximately 100ms (de Graaf et al., 2014) will be expected to affect the prediction error being fed forward from EVC. What remains to be revealed about such an effect is whether it exclusively reflects feedforward processes or whether the effect is interfering with feedforward *and* recurrent processesThe predictions of the Bayesian framework are perhaps too flexible here: if the EVC-TMS at ~100ms reflects feedforward processing alone, then it could be concluded that EVC-TMS is affecting the precision of prediction error. In contrast, if EVC-TMS is disrupting feedforward *and* recurrent processes then it could be concluded that TMS is disrupting the integration of the prior-probability with prediction error and/or the feedback of a posterior. In this regard, it could be argued that Bayesian predictive coding approach is difficult to falsify (Bowers & Davis, 2012). However, a testable prediction is to investigate *when* effects on the a prior-probability emerge relative to effects on the prediction error. For Bayesian predictive coding tobe feasible, EVC-TMS should produce effects on the prior-probability *before* it produces effects on the prediction error. This is because the prior-probability must be established in EVC before feedforward inputs to the rest of the brain are generated in the form of prediction errors. If EVC-TMS is interfering with the precision of a prediction error, then participants should get the judgment wrong. Critically, the direction of such mistakes will be influenced by the prior-probability. EVC-TMS would reduce the precision of the prediction error, which would lead to the relative precision of the prior-probability being greater, leading to a greater influence of the prior-probability on perceptual judgments.

There have also been a number of experiments which have produced EVC-TMS induced effects on performance at SOAs beyond ~100ms (Heinen et al., 2005; Wokke et al., 2012; Allen et al., 2014; Chambers et al., 2014). All of these studies reproduced an effect of TMS at approximately 100ms. However, additional decrements in performance were also revealed later on at SOAs ranging from 236ms to 320ms in tasks requiring the detection of a target presented with noise (Heinen et al., 2005; Wokke et al., 2012; Allen et al., 2014) or the categorization of visual stimuli as a bird or a mammal (Camprodon et al., 2010). What is interesting about these effects at later SOAs is that they

may not be as intimately linked to feedforward processes within EVC as the robust effect at ~100ms, which may reflect feedforward *and* recurrent processing (de Graaf et al., 2011; de Graaf et al., 2014). Instead effects at SOAs from 200ms onwards may reflect *re-entrant* processing which is the output of higher-order cortical areas being fed back into EVC. Under the predictive coding framework, EVC-TMS effects on performance at SOAs of 200ms and beyond may be due to TMS interfering with the posterior, which is the product of integrating the prediction error with the prior-probability according to Bayes theorem. Regardless of whether the posterior is generated at ~100ms or after at 200ms, the order in which TMS affects a measure of a prior-probability, prediction error and a posterior is critical, and whether the direction such effects are consistent with Bayes theorem is also critical

Evidence for predictive coding: the mismatch between top-down prediction and bottom-up sensory input

The application of TMS pulses to EVC at ~100ms produces a robust and reproducible decrement in a participant's ability to report the characteristics or presence of a visual target (Amassian et al., 1989; de Graaf et al., 2014). Such an effect has been hypothesized to affect feedforward *and* recurrent processing within EVC (Lamme & Roelfsema, 2000; de Graaf et al., 2014; de Graaf et al., 2012). Predictive coding and single pulse TMS provide an opportunity to probe the temporal dynamics of processing within EVC. If EVC-TMS is affecting feedforward and recurrent processes, it could be possible to use TMS to test the predictions of predictive coding accounts.

According to predictive coding, a top-down prediction is generated first, which is applied to sensory inputs. Subsequently, the mismatch between the two is fed forward (Rao & Ballard, 1999). A revised top-down prediction is then fed back in order to reduce or eliminate prediction error. If the EVC-TMS induced effect at ~100ms is interfering with feedforward and recurrent processing, there could be discrete observable effects on a top-down prediction and a prediction error on performance. However, it would be challenging to test the model proposed by Rao & Ballard (1999)

which approximated processes that take place between V1 and V2 using single pulse TMS. Testing such a proposition would be challenging, if not impossible, as estimating which site in early visual cortex (V1, V2, V3) where the induced electric field is 14% greater in V2 than V1 and 21% than the induced electric field in V3 (Thielscher et al., 2010). In order to test this predictive coding account in humans, it has to be possible to isolate the cortical site where predictions originate from the cortical site where the prediction error is conveyed forward. Bayesian predictive coding offers a functional distinction between feedforward and recurrent process, which can be probed by single pulse TMS studies. Unlike Rao & Ballard's (1999) model, Bayesian predictive coding is not limited to V1 and V2: it is proposed as a general principle that explains how the cortex responds to its inputs. By extending the substrates for predictive coding beyond V2, it now becomes possible to test some predictions of the predictive coding account.

A key neural phenomena that led to the formulation of predictive coding is repetition suppression, which refers to when repeated presentation of the same visual stimulus leads to a reduction of a neural response (Desimone, 1996; Friston, 2005). The idea of a suppressed response when stimuli are repeated – or expected – has been interpreted as evidence for predictive coding (Friston, 2005). In particular, repetition suppression has been suggested to reflect the relationship between the top-down prediction and the sensory signal, which in turn, determines the extent of prediction error (Friston, 2005; Clark, 2013). According to predictive coding, repeated - or expected - inputs would be suppressed because they would be incorporated within top-down predictions, which suppress predicted inputs (Friston, 2005). Such a reduction could be also be due to a fall in the response of neurons that encode unnecessary features (Wiggs & Martin, 1998) and/or the fulfilment of a perceptual expectation (Summerfield et al., 2008). Functional MRI studies have revealed that repeated presentations of a unique face lead to repetition suppression in the fusiform face area (FFA) compared to when the presentation of one face alternated with presentation of another (Summerfield, Trittshuh, Monti, Mesulam & Egner, 2008; Grotheer, Hermann, Vidnyánszky & Kovács 2014). Moreover, the repetition of indoor and outdoor scenes followed by a novel scene yielded a

greater response in the parahippocampal place area (PPA), and old stimuli were given higher judgments of visibility compared to new stimuli (Muller, Strumpf, Scholz, Baier & Melloni, 2013). However, a caveat here is that the BOLD response in the FFA readily shows an effect of expectation when a face is followed by a cue that indicates it likelihood of appearing (Trapp, Lepsien, Kotz & Bar, 2016). The PPA, on the other hand, shows no such effects (Trapp et al., 2016). It appears that a reduction in the BOLD response is accompanied by a change in a participant's report of a visual image, which may be due to the revision of a top-down prediction. However, such phenomena may not be a general characteristic of cortical responses.

Although repetition suppression is widely reported, its occurrence is not always consistent with theory – if the response of category specific areas (such as FFA and PPA) are determined by the likelihood of a stimulus being in a certain category, then the BOLD response of both the FFA and the PPA should always be sensitive to the probability of target occurrence. Stronger evidence for an expectation based mechanism underlying cortical responses has been found in V1 – the first stage in the cortical processing hierarchy. Alink, Schwiedrzik, Kohler, Singer & Muckli (2010) devised a paradigm where a rectangle follows a 'zig zag' trajectory from the top to the bottom of the screen, which induces a phenomenon known as apparent motion. The motion is referred to as apparent because the participant is presented with a series of a static, disconnected images that are accompanied by an impression of movement (Alink et al., 2010). When the rectangle consistently follows a zig zag trajectory, a top-down prediction could be formed throughout presentation that the rectangle will continue to follow such a trajectory. Responses within V1 were reduced when the rectangle appeared in a position consistent with the zig zag trajectory compared to when the rectangle appeared in an inconsistent position (Alink et al., 2010). Unlike previous studies which revealed evidence further down the ventral stream (Summerfield et al., 2008; Grotheer et al., 2014), which revealed that the mismatch between what is presented and what is expected can be revealed within the earliest stage in cortical processing – V1.

Functional MRI revealed that V1 can reflect the mismatch between what is expected and what is observed. However, finer temporal resolution is required in order to garner evidence for predictive coding, or any other accounts that emphasize how neural responses change over time as a function of prior-expectation. A double-pulse TMS study, which applied two pulses of TMS at various stimulus onset asynchronies (SOAs) relative to the onset of a visual target, revealed that administering TMS pulses to V5 *before* the onset of apparent motion affected performance (Vetter et al., 2013). In this experiment, apparent motion was induced by presenting a series of spatially separated, stationary squares along a trajectory of a diagonal line (Vetter et al., 2013). Participants had to detect when a target appeared that was congruent or incongruent with the trajectory of a diagonal line. Without TMS, participants were better at detecting congruent targets than incongruent targets (Vetter et al., 2013). However, the administration of double pulse TMS 13ms – 53ms over left V5 before congruent target onset *reduced* the difference in RT between congruent targets and incongruent targets compared to when no TMS was applied (Vetter et al., 2016). According to predictive coding, a top-down prediction must be in place before the received sensory input can drive neural responses (Friston, 2005). In this case, disrupting the higher-level cortical site V5 *before* the onset of target occurrence reduces a detection advantage, which suggests that prior-expectations could be relayed from V5 to lower-level regions within visual cortex, such as V1, prior to target occurrence which in turn drive cortical responses.

Complementary evidence from functional MRI studies of apparent motion suggests that V1 appears to be a candidate recipient for such feedback. As mentioned previously, V1 responses are reduced when stimuli appear along a trajectory that is expected according to apparent motion (Alink et al., 2009). When considering effects of pre-target V5-TMS on performance, and the effects of prior-expectation violation on V1 responses, it appears that prior-expectations are relayed throughout visual cortex. Critically, top-down prediction in V5 occurs *before* target onset which could in turn, enhance or reduce V1 responses depending on whether target occurrence is congruent or incongruent with apparent motion (Vetter et al., 2014; Alink et al., 2009). Here, it

appears that within V1 is affected by prior-expectation, yet evidence for predictive coding comes from V5 TMS studies and V1 fMRI studies. In order to provide more well-rounded evidence (or lack thereof) for predictive coding, it would also be useful to apply TMS to EVC and identify whether effects of TMS are consistent or inconsistent with predictive coding.

The study presented here aimed to utilize single pulse TMS to test the key premises of predictive coding within EVC. The key premises of predictive coding initially explained feedforward and feedback processes within EVC (e.g. Rao & Ballard, 1999), which thenculminated with Friston (2005) proposing that top-down predictions about stimulus properties reflect the output from higher-level cortical sites beyond visual cortex that are sent to, and reflected by, the response of V1 neurons. The early responses of V1 neurons are affected by the prior-expectation and its relationship with current sensory inputs (Friston, 2005). If the prior-expectation successfully reflects current inputs, then the response will be suppressed and output from V1 to the rest of striate cortex and beyond will be reduced (Friston, 2005). However, when the prior-expectation unsuccessfully represents sensory inputs, a prediction error will be conveyed to the rest of striate cortex, and critically, an updated prior-expectation will then be fed back into V1 in response in order to suppress prediction error (Friston, 2005). In other words, more recurrent processing – or feedback to V1 – occurs when sensory inputs are unexpected. A study presented here aimed to capture the magnitude of recurrent processing for expected stimuli relative to unexpected stimuli by having participants complete a sensory discrimination task that is orthogonal to a manipulation of the frequency of occurrence of a visual stimulus. The visual stimulus frequency manipulation aims to alter the likelihood of one visual target appearing more than another, which could increase the duration by which TMS can interfere with recurrent processing for familiar, frequent stimuli compared to unfamiliar, infrequent stimuli.

Evidence suggests that the magnitude of rapid recurrent processes within EVC can be modulated by the type of visual stimulus that is used and the point in time at which TMS is applied.

The potential for a recurrent interaction that can be altered by the characteristics ofvisual stimuli was revealed by de Graaf et al. (2012), who showed that the duration of recurrent processes are reflected in the number of SOAs where a TMS-induced effect is present. Such an effect may be due to feedback from higher-order sites, such as IPS (Koivisto et al., 2014). Taken together, this suggests that TMS could be a tool that can be used to elucidate the fine grained temporal processes that enable a visual stimulus to be detected or discriminated, which may rely on the use of a prior expectation that is continuously updated to reflect the properties of the visual environment. If more recurrent processing does not accompany unfamiliar stimuli, then two possible outcomes can be anticipated. The first outcome is that the duration of TMS-induced effects for unfamiliar and familiar stimuli will be the same under the null hypothesis, which would suggest the mismatch between what is expected and what is presented is not encoded within EVC or that such a mismatch cannot be probed with a TMS paradigm. Alternatively, the opposite to the predictions of the predictive coding account could also be true: that more recurrent processing accompanies the familiar stimuli than the unfamiliar stimuli, which would suggest that familiar stimuli receive more recurrent processing than unfamiliar stimuli within EVC, which would also provide evidence against predictive coding.

Synopsis of experiments

Experiment 1 investigated the involvement of DLPFC in recurrent processes and the temporal relationship between recurrent processes in EVC and DLPFC. In this experiment, the temporal position of an EVC-TMS induced effect was compared to the temporal position of a DLPFC-TMS induced effect. In order to identify when such effects take place, single pulses of TMS were delivered to EVC and DLPFC after the onset a visual target. Participants had to indicate whether or not a target was present and to indicate the location of the target. It was hypothesized that the DLPFC-TMS induced effect would occur after the EVC-TMS induced effect. However, this hypothesis

was not confirmed. Instead, the temporal position of a EVC-TMS induced effect occurred at the same temporal position as the DLPFC-TMS induced effect.

Experiments 2 and 3 were concerned with the development of a behavioural paradigm which could isolate the influences of a prior-probability and prediction error on performance. A particular focus in these experiments was the precision of the prior-probability relative to the prediction error is a critical determinant of the prediction errors influence on the posterior (Feldman & Friston, 2010). The initial aim was to then isolate the influences of a prior-probability and the prediction error and their integration to produce the posterior as a function of time using single pulse TMS. Experiment 2 aimed to manipulate the prior-probability by informing participants of the likelihood of target occurrence in two different contexts: a high probability context and a low probability context. In order increase the precision of the prior-probability relative to the prediction error, target visibility was reduced . It was expected that reducing target visibility and explicitly informing participants of the likelihood of target occurrence would produce differences in performance between the high probability and low probability contexts. In the high probability context, it was expected that participants would make more judgments of target presence, regardless of whether the target was actually presented on each trial. In contrast, it was expected that participants would make more judgments of target absence in the low probability context, regardless of whether the target was present or not. These predictions were confirmed.

Experiment 3 involved a different approach to manipulate the precision of the prior-probability. Unlike experiment 2, which manipulated the prior-probability on a block-by-block basis, experiment 3 altered the prior-probability on a trial-to-trial basis. A modified version of the Posner cueing paradigm (Posner, 1980) was used whereby two arrows preceded the onset of a target. One of these arrows validly indicated the location of a target on the majority of trials. The other arrow did not indicate where the target would appear on valid trials. The relative difference in luminance between the cue arrow and the non-cue arrow was altered. On some trials, the relative difference

between the cue arrow and the non-cue arrow was high, where it was assumed that the precision of prior-probability indicated by the cue was high. The precision was high because the cue conveys information as to where the cue is most likely to appear. On other trials, there was no difference in luminance between the cue arrow and the non-cue arrow because their luminance was identical, which meant the precision of the prior-probability indicated by the cue was low. The precision was low because the cue conveys no information as to where the cue is most likely to appear. It was expected that proportion correct would differ as a function of the difference in luminance between the cue arrow and the non-cue arrow and the validity of the cue arrow. This would mean that proportion correct would be greater on valid trials than invalid trials when the difference in luminance between cue arrow was high but not when it was low. This hypothesis was also confirmed. However, a similar effect was not revealed on reaction time. An effect of increasing the precision of prior-probability was also found on the errors that participants made. Participants made more errors in the direction of the valid arrow cue when the precision of the prior-probability was high, but not when it was low.

Experiments 4 and 5 were not investigating the precision of the prior-probability and the prediction error and how they are integrated to produce a posterior estimate of sensory inputs (Friston, 2005; Feldman & Friston, 2010; Clark, 2013). Instead, a more fundamental assumption of predictive coding models was investigated: that a mismatch between a top-down prediction and sensory inputs triggers a prediction error (Rao & Ballard, 1999). A prediction error then triggers a period of recurrent processing whereby the top-down prediction is revised and subsequently fed back to EVC – ultimately V1 (Rao & Ballard, 1999; Friston, 2005). A number of behavioural experiments are presented which initially aimed to find an advantage in terms of proportion correct for familiar, frequently presented stimuli relative to unfamiliar, infrequently presented stimuli. Subsequently, a paradigm where participants indicated whether the upper or lower half of a familiar or unfamiliar shape is brighter in conjunction with single pulse EVC-TMS was employed. It was

hypothesized that EVC-TMS would affect performance over a larger number of SOAs for unfamiliar targets compared to familiar targets. Weak evidence for this hypothesis was obtained

Experiment 1 and experiment 5 included pre-registered statistical analyses which were uploaded to the Open Science Framework. All of the TMS based statistical analyses presented here involved the use of Gaussian models, which could quantify one or two TMS-induced effects as a function of TMS-SOA. Such models can also isolate the temporal position and duration of one or more TMS-induced effects. Chapter 1 explored how these models can be used to create simulated data sets, which can then be used to develop analysis pipelines and select the most appropriate choice of statistical tests. This simulation procedure was critical as Bayesian statistics were used here, which contain subjective parameters (Dienes, 2011; Rouder, Speckman, Sun, Morey & Iverson, 2009). Such parameters can drastically alter whether support is obtained for a hypothesis (Dienes, 2011). In order to ensure that the most sensitive choice of parameters were pre-registered, simulated data sets were used to compare different ways of producing evidence for or against a hypothesis using Bayesian statistics. In addition to these, simulated data sets are also useful when assessing whether it is feasible to produce evidence for or against a hypothesis when recruiting a feasible number of participants.

Chapter 2. The use of simulated data sets in conjunction with Bayesian statistics to assess the feasibility of TMS-based hypotheses prior to data collection.

Chapter 2: Summary

This chapter introduces a modelling procedure that simulates data that can be used to assess the feasibility of a proposed TMS experiment. The use of different kinds of statistics will be discussed and applied in conjunction with the modelling procedure to illustrate how it can be used to identify if it is feasible to produce evidence for or against a hypothesis in the context of a single pulse TMS experiment.

The creation of simulated data to assess the feasibility of hypotheses in TMS experimentsusing Bayesian statistics

One of the unique contributions of TMS to cognitive neuroscience is its ability to causally manipulate the cortex (and remotely connected areas) to identify which areas of the brain are implicated in cognitive processes and how these cognitive processes are accomplished (de Graaf & Sack, 2011). One of the cornerstones of TMS research was pioneered by Vahe Amassian and colleagues (1989) who administered single pulses of TMS at different SOAs after the onset of a visual target. The ability to report the identity of three letters was abolished when TMS was administered to EVC 60, 80 and 100ms after the onset of the letters (Amassian et al., 1989). This was one of the first demonstrations that a certain part of cortex is critical for a particular cognitive process at a certain SOAs, meaning that TMS achieves a relatively high degree of spatial *and* temporal resolution. Moreover, performance at SOAs ranging from 0ms – 40ms and from 140 – 200ms revealed that performance was unimpaired by EVC-TMS, suggesting that single pulse TMS can reveal when a site is and when a site is *not* critical for a particular process. However, when no effect on TMS is found across a range of SOAs, the absence of an effect is not considered important despite the fact that

TMS can reveal or not reveal causal evidence of a brain area being involved in a cognitive process with relatively high temporal resolution (de Graaf & Sack, 2011). This chapter will discuss different approaches that can be used to analyse data generated using single pulse TMS paradigms with a particular emphasis on simplifying analysis pipelines that detect when a critical time period emerges after applying single pulses of TMS to a cortical region. An additional goal, and a consequence of simplifying such analysis pipelines, was to develop a procedure that assesses whether it is feasible to produce evidence for or against a TMS-driven hypothesis using a realistic number of participants.

An introduction to basic hypothesis testing in TMS research

One of the principle objectives of single pulse TMS paradigms is to identify the SOA (or SOAs) where the largest difference exists between active TMS and a control condition, which is assumed to be the time point when a cortical site is critical for executing a particular process (Walsh & Cowey, 2000; Chambers & Mattingley, 2005). Usually, single pulses of active TMS and control TMS are applied at different SOAs throughout an experiment. Once the experiment has been completed, the mean level of performance for active TMS and control TMS is calculated separately at each SOA across participants. A two way (active/control x TMS SOA) within-subjects ANOVA is then applied to the data set. In order for TMS to reveal an effect of active TMS relative to control TMS at specific SOA, the two-way within-subjects ANOVA must reveal an interaction between TMS type (active or control) and TMS SOA. A two way interaction between TMS type (active or control) and TMS SOA would suggest that a difference between active TMS and sham TMS exists at a specific SOA. In order for this difference between active and sham TMS to be understood, post-hoc tests must be carried out. In the case of two-way within-subjects ANOVAs, this can involve applying a one-sample *t*-test on the subtracted difference between active TMS and sham TMS at each SOA. The SOA (or SOAs) where the one-sample *t*-test is significantly different from zero – usually by producing a *p* value less than 0.05 – are then assumed to be the points where the difference (or differences) exist between active TMS and a control condition. An issue with this approach is that TMS needs to be

administered at a large number of SOAs in order to a significant difference to be detected (e.g. Camprodon et al., 2010).

An alternative method of TMS hypothesis testing

The use of an ANOVA and post-hoc *t*-tests relies on an interaction between TMS type (active or control) and TMS SOA reaching statistical significance. It then relies on a number of post-hoc *t*-tests being applied to the difference between active TMS and a control condition at each SOA. A simpler method of identifying the time point where a cortical site is critical for executing a particular process involves the application of a Gaussian model to the TMS-induced difference between active TMS and sham TMS at each SOA (Stevens, McGraw, Ledgeway & Schluppeck, 2009; Chambers, Allen, Maizey & Bellgrove, 2013; Rusconi, Dervinis, Verbruggen & Chambers, 2013). Such a model is applied to the TMS-induced difference produced by subtracting control TMS scores at each SOA from corresponding active TMS scores for each participant's data. A single Gaussian model is as follows:

$$y = y_0 + a_1 e^{\left[-\left(\frac{x - x_1}{b_1}\right)^2\right]}$$

A single Gaussian model generates four coefficients, which are of interest when a single pulse TMS study aims to identify when the largest difference exists between active TMS and a control condition. Of particular interest is the peak amplitude coefficient, a_1, which quantifies the largest difference between active TMS and control TMS. For example, if the largest difference between active TMS and control TMS was positive, a_1 would indicate that the point where the difference between active TMS differs from control TMS is largest is a positive value. The production of a positive a_1 after this subtraction would suggest that active TMS has improved performance relative to sham TMS. In contrast, if the largest difference between active TMS and control TMS was negative, a_1 would be a negative value. This negative difference would indicate that active TMS has impaired performance. The temporal position coefficient, x_1, quantifies when a_1 arises as a function

of time, making it possible to identify when the largest difference between active TMS and sham TMS arises.

In contrast to ANOVA-based approaches, the use of Gaussian models can simplify the process of data analysis. An advantage of using a single Gaussian model is that the a_1 coefficient has already quantified the largest difference between active TMS and sham TMS within each participant's data set. As a result, the a_1 coefficient eliminates the need to rely on an interaction between TMS type (active or control) and TMS SOA to ascertain whether a difference between active TMS and sham TMS exists at a given SOA.This interaction can be bypassed as a result of relying on amplitude coefficients and a single one-sample *t*-test can be used to identify whether the mean of the a_1 coefficients differs significantly from zero. This simpler approach contrasts with relying on a two-way interaction following by the application of more than one one-sample *t*-tests to the mean difference between active TMS and sham TMS at each SOA.

The temporal position coefficient, x_1, is also useful as it can quantify when TMS-induced effect a_1 emerges, which can simplify the process of comparing the time course of two different cortical sites. The temporal order of one TMS-induced effect relative to another is particularly interesting when investigating feedforward processes and feedback-based recurrent interactions in the human brain. For example, a_1 coefficients can be used to determine whether the application of TMS to two distinct sites has affected performance. If an effect of TMS can be established on both sites, their respective x_1 coefficients can be used to determine whether the temporal position coefficient produced by applying TMS to one site differs from the temporal position coefficient produced by applying TMS to different site. For example, if temporal position coefficient, x_1, for site A occurs earlier in time than the temporal position coefficient for site A and site A is situated beneath site B in the processing hierarchy, it would indicate that a feedforward process from site A to site B is taking place. Conclusions about such an interaction taking place would be led by site A occurring earlier in the processing hierarchy than site B, meaning that TMS has captured the

temporal order of feedforward transmission between two separated sites in the brain. Such an interaction can then be subjected to further investigation. Statistics to test such an interaction are also straightforward. Similarly, conclusions can also be made about the potential for feedback-based recurrent processes taking place based on what is known about where sites are situated within processing hierarchy and the temporal positon of TMS-induced effects. For example, if a TMS-induced effect occurs for site B prior to site A and site B is situated at a higher level within the processing hierarchy than site A, there is potential for a feedback-based recurrent interaction taking place. All that needs to be applied is a one-sample *t*-test to the mean difference between the temporal position coefficients for site A and the temporal position coefficients for site B.

The use of temporal position coefficients in conjunction with amplitude coefficients also simplifies the process of determining the temporal order of processing throughout the brain. For example, Silvanto et al. (2005a) applied pulses of TMS to EVC and V5 and revealed three different effects of TMS, which depended on the site and SOA where TMS was administered. An initial effect of EVC TMS was revealed at 40 -60ms after the onset of motion, followed by a subsequent effect of V5 TMS 60 - 80ms after motion onset. The later effect of V5 TMS at an SOA at 60 – 80ms was followed by another EVC TMS effect at 80 – 100ms (Silvanto et al., 2005a). It was concluded that the early EVC TMS effect at 40 - 80ms was followed by the V5 TMS effect at 60 - 80ms, indicating effects on feedforward transmission from EVC to V5 (Silvanto et al., 2005a). The relationship between the V5 TMS at 60 - 80ms and the later EVC TMS effect at 80 - 100ms was concluded to represent a recurrent interaction between V5 and EVC in which EVC was the recipient of feedback from V5 (Silvanto et al., 2005a). Based on the fact that each of these effects arose at each a discrete, different SOA, it assumed that single pulse TMS could isolate feedforward (EVC → V5) and feedback based recurrent proceses (EVC ← V5) in the human brain. Applying a single Gaussian model enables the temporally distinct TMS-induced effects to be quantified in each participant prior to statistical analyses being carried out. The use of Gaussian models then incorporates individual differences in

when the largest difference between active TMS and sham TMS emerge as a function of TMS using temporal position coefficients when statistical analyses are applied to the entire data set.

Silvanto et al. (2005a) concluded that the existence of different temporal events responsible for feedforward or recurrent processes depended on the order that the effects took place *and* statistically significant effects being present for EVC and absent for V5 at the same SOA. The use of Gaussian models offers an alternative method of identifying whether the time course of one TMS site differs from the time course of another TMS site. Unlike the reliance on ANOVA, the use of a single Gaussian model identifies when a site is critical as consequence of identifying the temporal position (x_1) of the peak amplitude coefficient (a_1), the generation of x_1 coefficients can simplify the process of identifying whether time course of one cortical site differs from the time course of another cortical site. The use of a two-way ANOVA to identify when a significant difference between active TMS and control TMS exists at one SOA relies on variance on *y* axis, which represents performance. However, there is no source of variance on the *x* axis, which represents time as indicated by TMS SOA. The use of Gaussian models on the other hand enables the magnitude of a TMS-induced effect *and* the temporal position of such an effect to vary, which enables statistics to be used to identify whether the temporal position of TMS-induced effects differ between sites. Recall that the single Gaussian model is applied to each participant's data, which can capture individual differences in the magnitude of a TMS-induced effect on performance (a_1) *and* individual differences in when such an effect arises as a function of time (temporal positon - x_1). In short, the generation of x_1 coefficients simplifies the process of identifying the temporal order of critical events within different sites for a cognitive process. Analyses of this nature are useful at identifying the sites that could be involved in a feedback-based recurrent interaction. In order for such an interaction to take place, it must be demonstrated that the response within one site is being altered by the reception of feedback from another site.

Paradigms such as Silvanto et al. (2005a) identify the temporal order of processing between sites by applying TMS to EVC and V5 whilst keeping the task identical and then identifying when one site was critical for processing the direction of motion. The potential for a feedback-based recurrent interaction was outlined by the fact that a period where V5 was critical for TMS came in between two distinct epochs where EVC was critical for processing of motion. Another method which has demonstrated the potential for EVC being affected by recurrent interactions compared the effect of compared the duration of TMS-induced effects on two different tasks (de Graaf et al., 2012). de Graaf et al. (2012) compared how applying single pulse TMS to EVC affected performance in a face judgment compared to the effect on performance in a gratings judgment. EVC-TMS significantly impaired the gratings judgment at two SOAs: 90ms and 95ms whereas EVC-TMS significantly impaired the faces judgment at four SOAs: 50ms, 90ms, 95ms and 110ms (de Graaf et al., 2012). The latency of such effects were 88.9ms and 86.9ms for gratings and faces, respectively (de Graaf et al., 2012). Here, the latency of each effect was calculated by identified the earliest SOA where the largest difference between active and control TMS was found (de Graaf et al., 2012). Despite the same latency of such effects, the extension of the EVC-TMS effect into later SOAs for the faces judgment suggests that a recurrent interaction is being interfered with, which could be related to the reception of feedback within EVC. Critically, these results suggest that the magnitude of recurrent processing within EVC can be measured by the breadth of SOAs at which TMS interferes with behaviour under different conditions.

The application of Gaussian models to performance as a function EVC-TMS also provides an opportunity to quantify individual differences in the number of SOAs – or the duration – which TMS successfully produces a difference between active TMS and a control TMS. In addition to producing coefficients that quantify the maximum difference between active TMS and control TMS across SOAs and the temporal position of such an effect, a single Gaussian model also produces a bandwidth coefficient, b_1. The b_1 coefficient quantifies the duration of a TMS-induced effect on performance. When a TMS-induced effect is present for a larger number of SOAs for one condition compared to

another such as the two SOAs for a gratings judgment and the four SOAs for the faces judgment (de Graaf et al., 2012), the b_1 coefficient would be able to quantify differences in such an effect. In order to compare the duration of TMS-induced effects across different conditions, the mean difference in b_1 could be tested using a one-sample *t*-test. The use of b_1 coefficients is simpler than relying on a difference between TMS and a control condition, and the consequent interaction between TMS SOA and TMS type (active or control). In order for the ANOVA to reveal a difference in the duration of a critical epoch, it would have to show that the difference between active and control TMS exists at more SOAs under one condition than another. This approach usually relies on a number of one-sample *t*-tests demonstrating that a mean difference exists between control TMS and active TMS are more SOAs for one condition than another (e.g. de Graaf et al., 2012). In contrast, the use of the b_1 coefficients eliminates the need to carry out numerous *t*-tests in order to illustrate that differences between active and control TMS

The use of Gaussian models and the creation of simulated data sets

One of major strengths of TMS in cognitive neuroscience is its ability to provide causal evidence for the chronological involvement of a particular brain area in a particular cognitive process (Walsh & Cowey, 2000; de Graaf & Sack, 2011). In order to do so, a difference between active TMS and a control condition must be demonstrated at one SOA but not at others, thus demonstrating that a particular area becomes involved in processing at one time but not at another. One robust and reproducible example of such an effect is the effect that EVC-TMS produces on performance at ~100ms (de Graaf et al., 2014). Usually, the involvement of a particular cortical area at one time but another is revealed by demonstrating a significant difference between active TMS and control TMS at one SOA and the absence of such a difference at other SOAs, which involves applying a one-sample t-test between active TMS and control TMS at every SOA. As discussed, the use of a Gaussian model eliminates the need to apply numerous one-sample *t*-tests to demonstrate where differences between active TMS and control TMS. If a single Gaussian model is applied to the difference

between active TMS and control TMS when the control TMS score is subtracted from the active score at each SOA, the resulting a_1 coefficient isolates the largest difference between active TMS and control TMS. All that needs to be applied is a single one-sample *t*-test to the a_1 coefficients across participants, which is sufficient to demonstrate if a mean difference that is greater than zero exists across SOAs.

The use of Gaussian models not only simplifies questions that relate to the chronological order and duration of processing, it also provides the opportunity to create simulated data to assess the feasibility of experiments before data collection commences. As outlined previously, online TMS can be thought of as adding noise to neural processes, which can be used to infer whether or not a particular site is critical for a particular behavioural function. If such an effect is present, then there is potential for a particular brain area to be critical for the process of interest. However, if such an effect is absent, then there is potential for the brain area of interest to not be involved in the process that is under investigation. Despite the logic of the proposition that the absence of a TMS-induced effect enables the conclusion that site where TMS is administered is not critical for the process of interest, null results in TMS research are often underutilized (de Graaf & Sack, 2011). One of the reasons why null results are underutilized in TMS research has been coined the power argument (de Graaf & Sack, 2011). The power argument refers to the difficulty in concluding whether the absence of a TMS-induced effect is genuine or whether a TMS-induced effect is absent because insufficient participants were included within the analysis or whether participants completed an insufficient number of trials (de Graaf & Sack, 2011). The use of a Gaussian model provides an opportunity to simulate the data that could be expected from an experiment, and use such simulations to identify whether a TMS-induced effectcan feasibly be detected.

Simulated data created from single Gaussian models can be subjected to an analysis pipeline that can be used to assess whether it is feasible to provide evidence for or against an effect a TMS-induced effect using a particular paradigm. The question of feasibility becomes even more important

when an experiment is applying TMS to more than one site and the hypotheses are not just concerned with producing an effect of TMS but are concerned with the temporal order of TMS-induced effects between sites (e.g. Silvanto et al., 2005a). In order for an analysis to compare whether two sets of temporal positions differ one another, it is essential for more than one TMS-induced effect to be present. For example, it would not be possible to compare the onset of an EVC-TMS induced effect to the onset of a V5-TMS induced effect if a V5-TMS induced was *not* present or vice versa. In order for analyses to compare the temporal position of a TMS-induced effect for one site to the temporal position of a TMS-induced effect for another site to be feasible, it would be useful to identify if such effects can be identified before data collection begins. Even if it is feasible to expect TMS-induced effects upon more than one site, it may not be feasible to subsequently produce evidence for the temporal position coefficients (x_1) of one effect occurring at a different point to another TMS-induced effect. Gaussian models provide the means of simulating data that can identify whether it is feasible to expect TMS-induced effects *at all* and then establish whether it is feasible to expect x_1 coefficients to differ reliably between sites. Additionally, the b_1 coefficients provide a novel opportunity to probe the duration of TMS-induced epochs.

There are five different stages that go into the creation of simulated data. These five stages generate one set of simulated data for one simulated participant. If TMS is applied to more than one site, then these five stages would need to be repeated to generate simulated data as a function of applying TMS to each site. For example, if TMS was to be applied to EVC and V5 in the case of Silvanto et al. (2005a), then stages outlined here have to take place separately to generate simulated data for EVC and V5. The first stage involves the application of a single Gaussian model to pilot data. The second stage involves calculating the mean and standard deviation of the a_1, x_1, b_1 and *x0* coefficient within the pilot data set. The second stage provides the first means of creating simulated data for one simulated participant. The third stage uses the distributions created by calculating the mean and standard deviation of the Gaussian fits to the pilot data. The use of values drawn from the a_1, x_1, b_1 and *x0* distributions enables each simulated data set to reflect the magnitude of the TMS

effect relative the baseline (*x0*) that is most likely to occur (a_1) at a certain temporal position (x_1) for a certain duration (b_1) based on what has been obtained from pilot data. The fourth stage involves inserting these values into the equation for a single Gaussian across values of x, which are the SOAs where TMS will be administered. The fourth stage is where the simulated data across SOAs is created. The fifth stage involves fitting a single Gaussian model to simulated performance across SOAs, which generates coefficients that can be subjected to statistical analyses. The product of these stages 1 to 4 is illustrated in the top of figure 1. Stages 1 to 4 involve the creation of simulated data points across SOAs for each TMS site. Stage 5, on the other hand involves the fitting of Gaussian model to the simulated data. The product of stage 5 is a Gaussian curve that is fitted to a set of simulated data, which is illustrated on the bottom of figure 1. At stage 5, all the model constraints which are applied to the pilot data must be identical to the model constraints in the real experiment, which ensures that simulated Gaussian model fitting procedure is identical to Gaussian model fitting procedure that will take place in the real experiment.

Once these five stages have been completed, it is possible to start running prospective analyses upon the simulated data. For the purposes of the experiments that will be presented here, statistical analyses on simulated data sets will have the primary aim of identifying whether TMS-induced effects can be expected when TMS is applied to two different sites or whether TMS is applied under different conditions of visual stimulation. There are two different hypotheses that will be of interest here. The first hypothesis that can be assessed in terms of feasibility is whether evidence for the presence or absence of a difference in the temporal position of TMS-induced effects between two different sites can be obtained. The feasibility of a difference between the temporal position of two TMS-induced effects relies on the x_1 coefficients producing using the simulate data. The second type of hypothesis that can be assessed in terms of feasibility is whether the duration of one TMS-induced effect differs from the duration of another TMS-induced effect. The feasibility of a difference between the duration of two TMS-induced effects will be assessed

using the b_1 (bandwidth) coefficients generated from simulated data sets, which was used to develop experiment 5.

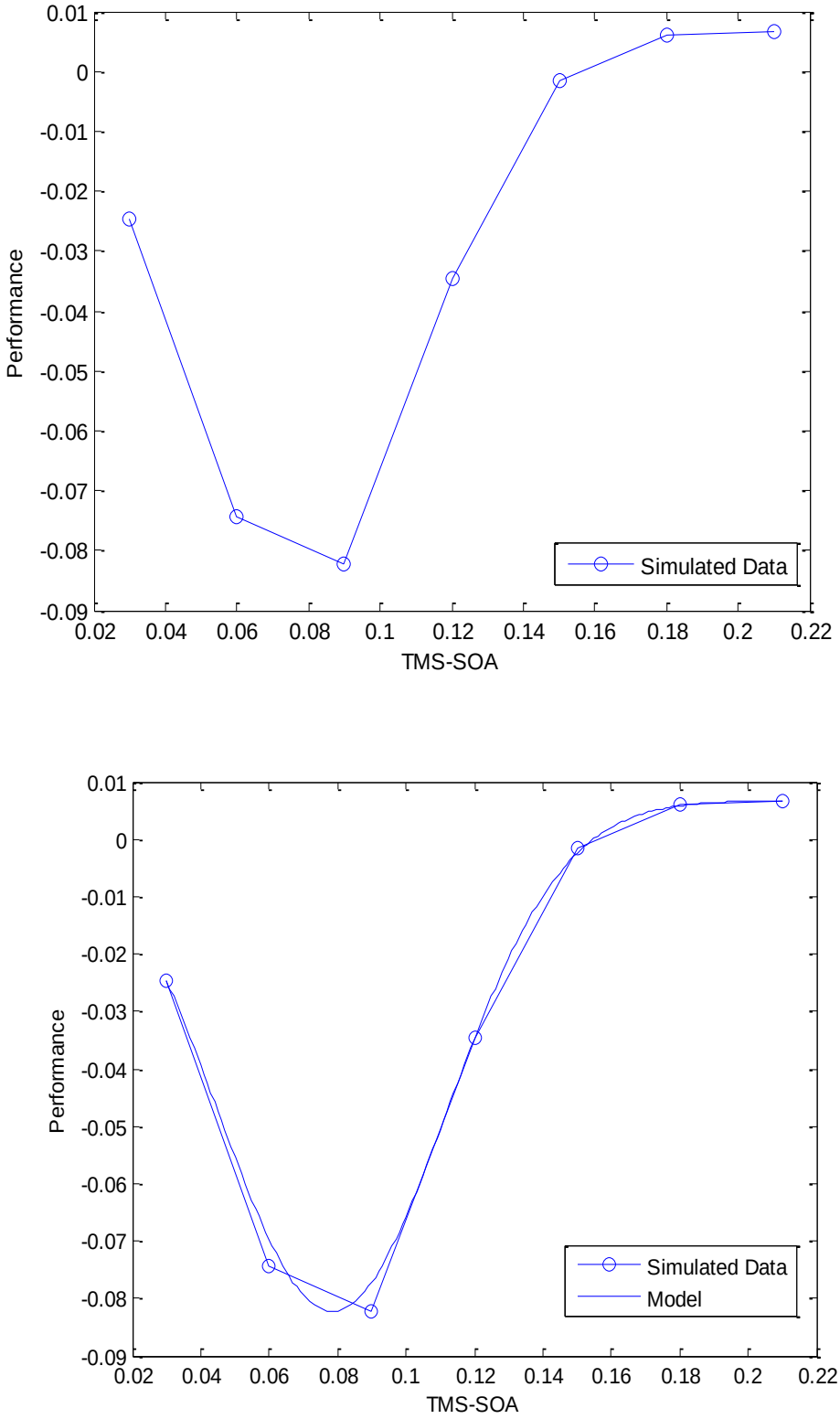

Figure 1. Top: Simulated data representing performance at each SOA for one simulated participant. Bottom: Simulated data representing performance at each SOA and corresponding Gaussian model fit for one participant.

The use of Gaussian models and the creation of simulated data sets to address the power argument (de Graaf & Sack, 2011) when assessing the feasibility of different TMS-based hypotheses

The power argument refers to the difficulty in concluding whether a null result is genuine or whether a null result would be absent if more participants were included within the analysis (de Graaf & Sack, 2011). The procedure which generates simulated data for simulated participants can generate coefficients that are produced from Gaussian model fits to simulated differences between active TMS and control TMS across SOAs. Any number of simulated coefficients can be created, which can be used to establish whether a null result persists beyond a certain number of participants or whether a null result is initially obtained with a small number of participants, which eventually reverses into a significant result once a sufficient number of participants have been included a. This latter outcome is of particular importance to addressing the power argument as it specifically refers to null results that are present due the inclusion of an insufficient number of participants (de Graaf & Sack, 2011).

Here, the use of simulated data will be introduced as a means of testing TMS-based hypotheses. The peak amplitude (a_1), temporal position (x_1) and bandwidth (b_1) coefficients can all be used to identify whether a particular effect of TMS or a difference between TMS conditions can be produced by an experiment. Three different TMS hypotheses will be discussed. The first is whether it is feasible to expect a difference between active TMS and control TMS. This is the most straightforward type of hypothesis that can be tested because it relies only on the peak amplitude (a_1) coefficients being significantly different from zero. If the a_1 coefficients are negative, this means that active TMS has impaired performance relative to control TMS. In contrast, if the a_1 coefficients are positive, this means that active TMS has improved performance relative to control TMS. In contrast, if the a_1 coefficients are approximately zero this suggests that no difference exists between active TMS and control TMS. The only condition that a simulated data set needs to fulfil to demonstrate the feasibility of a difference between active TMS and control TMS is whether the a_1 coefficient significantly differs from zero. A useful aspect of using simulated data sets is that the

presence or absence of a difference between active TMS and control TMS can be introduced by the experimenter.

Hypotheses that seek to identify whether the temporal position of a TMS-induced effect for one site differs from the temporal position (x_1) of a TMS-induced effect to another site rely on more than one condition being fulfilled. First of all, a difference between active TMS and control TMS must be present, which demonstrates a TMS-induced effect is present across SOAs. This condition must be fulfilled following the application of TMS to more than one site, otherwise it is not possible to compare the temporal position of one TMS-induced effect to the temporal position of another TMS-induced effect. If more than one TMS-induced effect is revealed, it is the necessary to fulfil another condition, which is whether a significant difference exists between the two sets of temporal position coefficients can be obtained. A simulation based approach to working out whether these conditions can or cannot be fulfilled in an experiment will also be presented here.

Finally, hypotheses that seek to identify whether the duration of processing in one site can differ when presented with different kinds of visual stimuli will be discussed. These hypotheses are similar to those tested by de Graaf et al. (2012) who revealed that face stimuli are affected by TMS by a greater number of SOAs compared to simpler grating stimuli. These hypotheses also require more than one condition to be fulfilled. First of all, a difference between active TMS and control TMS must be present, which demonstrates that a TMS-induced effect is present across SOAs. Moreover, more than one TMS-induced effect must be present, otherwise the duration of one TMS-induced effect cannot be compared to another. In order to demonstrate that the duration of TMS-induced effects differ from one another, a comparison of b_1 (bandwidth) coefficients must also be carried out. A simulation based approach to working out whether these conditions can or cannot be fulfilled in an experiment will also be presented here.

To summarize, a simulation based approach is about to be outlined, which reveals how the feasibility of different TMS hypotheses can be assessed. These range from simpler hypothesis, such

whether a difference between active TMS and control TMS exists across SOAs to more complex hypotheses which compare the temporal position or duration of two TMS-induced effects to one another. First of all, the coefficients of interest to each of these analyses will be demonstrated. Subsequently, the use of simulations to address the power argument will be shown.

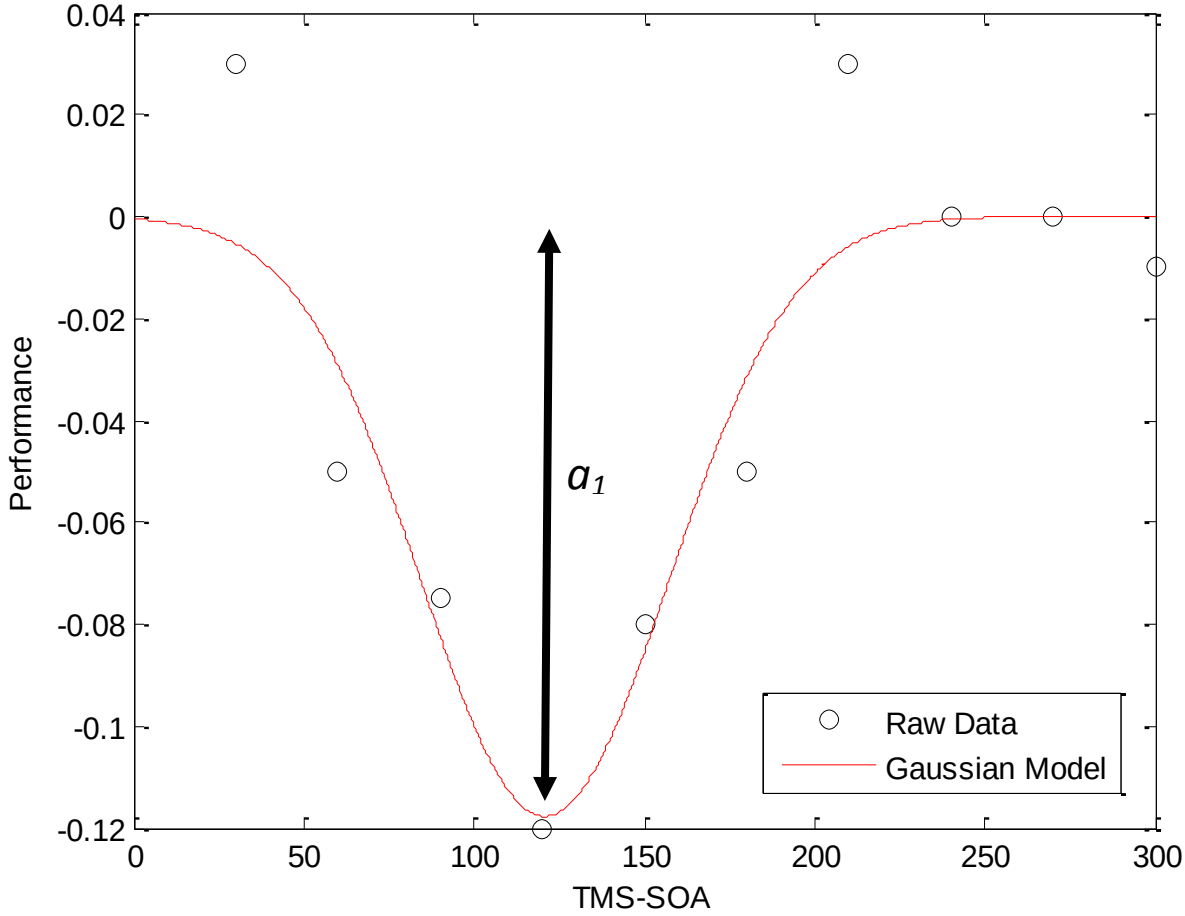

Figure 2. An illustration of the a_1 coefficients relevance when quantifying the difference between active TMS an sham TMS. The difference between active TMS and sham TMS is calculating by subtracting control TMS scores from the active scores.

<u>The use of simulated amplitude (a_1) coefficients to identify whether a difference exists between active TMS and sham TMS</u>

The first outcome of any analysis of a TMS experiment is to identify whether an effect of active TMS has emerged relative to control TMS at any SOA. As outlined previously, the use of a_1 coefficients simplifies the process of identifying whether an effect is present across SOAs by applying a single one-sample *t*-test to the mean a_1 coefficients as a function of a particular TMS condition. a_1 provides the opportunity to demonstrate where a time specific difference between active TMS and

sham TMS. This differs from the use of the interecept coefficient, *y0*, which refers to the baseline effect of TMS. Note TMS condition does not refer to control TMS versus active TMS here, it refers to the administration of TMS to a particular site or under a particular kind of visual stimulation. An illustration of the a_1 coefficients relevance to quantifying such a difference on a Gaussian model can be found in figure 2. Initially, the experimenter generates *n* sets of simulated coefficients as outlined in the procedure above. Once the *n* sets of simulated coefficients have been generated, a one-sample *t*-test can be applied in increments of 1, starting when 2 simulated participants are included in the analysis and adding one more simulated participant until the maximum *n* is reached. For example, if simulated data sets were created for 32 simulated participants, the first one-sample *t*-test would be applied would include the first 2 participants. The second one-sample *t*-test that would be applied would include the a_1 coefficients from the first 2 participants and an additional a_1 coefficient from a third participant. This incremental process of adding one a_1 coefficient from an additional simulated participant to the existing simulated data set can identify whether a null result persists or whether a significant result subsequently emerges e once a sufficient number of participants have been included within the analysis.

<u>The use of simulated data sets when testing whether the temporal positions of TMS-induced effects can differ from one another</u>

An effect of active TMS relative to control TMS is not the only question of interest to TMS research. The temporal order of a TMS-induced effect to one site, such as EVC, relative to another TMS-induced effect produced by applying TMS to another site , such as V5 (e.g. Silvanto et al., 2005) can also be of interest to TMS researchers. When these questions are of interest, identifying whether TMS –induced effects as measured by the a_1 coefficients is not sufficient. When temporal positions are of interest, it is also necessary to show that a difference in the temporal position of two TMS-induced effects is also present. In this instance, the x_1 coefficients generated by the Gaussian model are of interest, which simplifies the process of identifying the point in time (x_1) where the largest difference between active and control TMS (a_1) occurs. An illustration of how the a_1 and x_1 coefficients are of interest to these TMS designs is illustrated in figure 3.

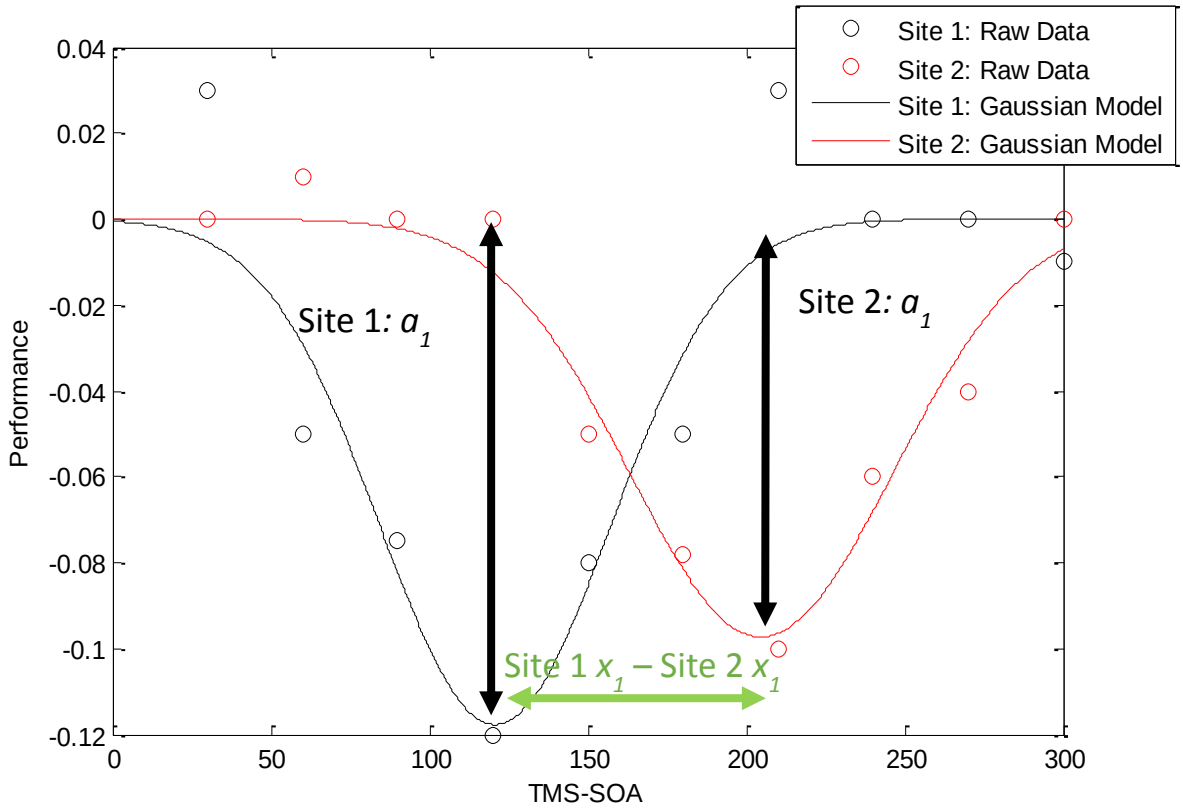

Figure 3. An illustration of how the a_1 coefficients from two separate curves are of interest in addition to the cor responding x_1 coefficients when the aim of an experiment is to reveal whether the temporal position of two TMS-induced effects differ from one another. First of all, a_1 for site 1 *and* site 2 need to significantly differ from zero using a one-sample t-test. Subsequently, an additional one-sample *t*-test is applied to the difference between the x_1 coefficients for each TMS site.

First of all, the procedure described above to identify whether a difference between active TMS and sham TMS needs to be completed. In this instance, however, the procedure is applied separately for two TMS sites. Although the hypothesis being tested differs in each simulated analysis, the procedure that identifies whether it is feasible to produce evidence will be the same in each one. Once again, a one-sample *t*-test can be applied to the difference between simulated x_1 coefficients under different TMS conditions are added incrementally to incorporate additional participants in the analysis. For example, if performance as a function of TMS-SOA was generated for 32 participants, the first one-sample *t*-test would be applied to the x_1 coefficient as a function of applied TMS to each site in a sample of two participants. Subsequently, simulated x_1 coefficients as a function of each TMS site from one participant would be added in to the sample and an additional one-sample *t*-test would be applied again. The process of adding one set of simulated x_1 coefficients

would be repeated until the full sample of 32 simulated x_1 coefficients were included within the statistical analysis.

The use of simulated data sets to address the power argument (de Graaf & Sack, 2011) when testing whether the duration of two TMS-induced effects differ from one another

An additional question of interest is whether the duration of processing within a cortical site differs as a function of different conditions of visual stimulation (e.g. de Graaf et al., 2012). When TMS is being applied under different conditions of visual stimulation, separate Gaussian models are applied to the performance as a function of TMS SOA for each condition of visual stimulation. To use de Graaf et al. (2012) as an example, this would involve fitting a Gaussian model to performance as a function of TMS for a gratings judgment and a separate model to performance as a function of EVC-TMS for the faces judgment. When these hypotheses are of interest, it is also not sufficient to demonstrate a TMS-induced effect on performance under different conditions of visual stimulation alone. As outlined previously, a difference between active TMS and control TMS of TMS under different conditions of visual stimulation would be revealed by a one-sample *t*-test indicating that the a_1 coefficients are significantly different from zero for both visual stimulation conditions. If such effects are obtained, the duration of each of the visual processes can be measured using the b_1 coefficients. Identifying whether it is feasible to test hypotheses measuring the duration of processing within a cortical site using b_1 coefficients can be approached in a similar way to the approach to identifying whether it is feasible to produce a difference in x_1 coefficients. An illustration of these coefficients in relation to separate Gaussian models can be found in figure 4.

In order to assess these hypotheses, Gaussian model coefficients would be generated by fitting separate models to each simulated condition of visual stimulation when a difference in b_1 is present or absent. In order to identify whether it is feasible to produce a difference in b_1 coefficients between two different conditions, a feasibility procedure similar to what has been outlined previously would be carried out. This would involve applied a one-sample *t*-test to an initial sample of two simulated participants with two simulated b_1 coefficients. Additional simulated b_1 coefficients

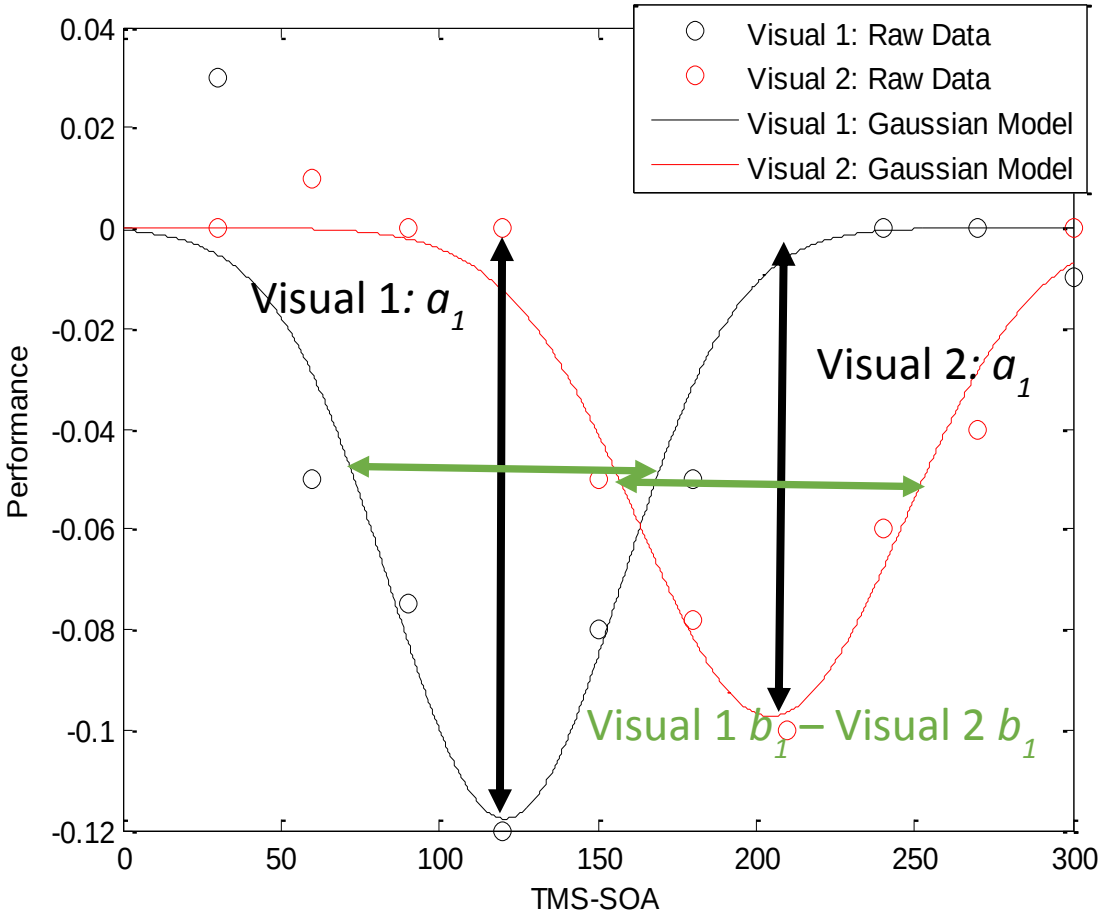

Figure 4. An illustration of how the a_1 coefficients from two separate curves are of interest in addition to the corresponding b_1 coefficients when the aim of an experiment is to identify whether the duration of one TMS-induced effect differs from another TMS-induced effect. First of all, a_1 under both conditions of visual stimulation needs to differ from significantly differ from zero using a one-sample *t*-test. Subsequently, an additional one-sample t-test is applied to the difference between b_1 coefficients for each condition of visual stimulation.

for the two different visual stimulation conditions would be added to the analysis in increments of 1 and a one-sample *t*-test would be applied again. This procedure would be repeated until a maximum number of simulated participants and simulated b_1 coefficients for each condition of visual stimulation has been reached. The outcome of such simulations would also be important to demonstrate the minimum number of participants that would need to be included within the statistical analysis the emergence and persistence of a difference in b_1 coefficients. Without these three distinct outcomes being addressed, it is not possible to identify whether it is feasible to test a hypothesis which aims to identify whether a difference in b_1 exists under different conditions.

How to use simulated data to assess whether evidence for or against a hypothesis using Bayesian statistics to address the power argument (de Graaf & Sack, 2011)?

A critical question that determines whether it is feasible or unfeasible to produce evidence for or against a hypothesis is the choice of statistical procedure which determines whether a hypothesis is true or false. A critical feature of the modelling procedure specified above is its ability to identify whether evidence for or against a hypothesis can be obtained after testing a certain number of participants. Such a question is critical as it outlines whether or not an experiment can achieve its aim *a priori.* de Graaf & Sack (2011) propose that one way of identifying whether an effect is in a predicted direction is by examining the effect size after testing each participant. If the effect size is in the predicted direction, the hypothesis can be said to be feasible and data collection can continue. In contrast, if the effect size is not in the predicted direction, the hypothesis could be unfeasible and data collection should not continue. In the modelling approach presented here, the basis for concluding whether or not it is feasible to test a hypothesis was a one-sample *t*-test. Rather than rely on the effect size aspect of the one-sample *t*-test, it was decided to rely another number that can be generated from a t-test – a Bayes factor (*BF*). The *BF* can be used to determine the strength of evidence for or against a hypothesis as a function of participant number. This contrasts with the use of an effect size alone which specifies that the mean difference is in the expected direction without specifying whether the effect size successfully quantifies evidence for or against a hypothesis.

This section will compare the conditions that determine whether the null or experimental hypothesis is true when applying Bayesian or orthodox statistics. Theoretically, but often not in practice, orthodox statistics require statistical power to be calculated *a priori*, which refers to the long term proportion of times the null hypothesis will be rejected when the null hypothesis is not true. In order to calculate power *a priori*, the researcher needs to know the minimum difference between conditions that would disconfirm the hypothesis, the number of participants that will be tested, and the level of significance to be used, which in turn yields the level of statistical power that

will be obtained (Dienes, 2011). In order to test whether the null hypothesis can be rejected, the researcher must gather data from the number of participants needed to obtain *x* statistical power before orthodox statistics can be applied. If the *p* value produce by the statistical test is less than 0.05, then the null hypothesis is rejected; in contrast, if the *p* value is more than 0.05 then the null hypothesis cannot be rejected.

To summarize, orthodox statistics state that data collection must terminate when *n* number of participants have been tested to obtain *x* power and the *p* value after testing *n* participants. The outcome of this procedure then determines whether the null hypothesis can or cannot be rejected. In contrast, Bayesian statistics allow data collection to terminate and enable a hypothesis to accepted or rejected under different conditions. Bayesian statistics require a hypothesis to be formulated as a distribution of outcomes that would be expected if a hypothesis is true relative to a null distribution, which in the case of a *t*-test are the mean differences that are most likely. For example, Dienes (2011) describes a probability distribution called a *uniform prior probability* which assumes that all mean differences between an upper (maximum expected mean difference) and lower limit (minimum expected mean difference) are equally likely. Such a prior is useful when the direction (positive or negative) of a mean difference can be predicted but the exact magnitude of the mean difference is uncertain (Dienes, 2011). The obtained mean difference within the data is known as the *likelihood*. The posterior – the likelihood of the prior (hypothesised mean difference) given the data (observed mean difference) – is calculated by integrating the prior-probability with the likelihood (Dienes, 2011). The Bayes factor (*BF*) then reveals whether the posterior supports the null hypothesis (mean difference = zero) or the experimental hypothesis (mean does not equal zero). If the *BF* is more than 1/3 but less than 3, then it is considered weak, inconclusive or anecdotal evidence whereas the if the BF is less than 1/3 or more than 3, it is considered to provide substantial evidence for the null or experimental hypothesis, respectively (Dienes, 2011).

In contrast to the orthodox stopping rule where data collection must terminate when *n* participants have been tested to obtain *x* power which has been decided prior to data collection, the Bayesian stopping rule is determined by whether the *BF* is *conclusive* after testing *n* participants. If the likelihood of the hypothesis being true or false being inconclusive (by convention, BF > 1/3 and BF < 3) given the mean difference in the data, the *BF* permits data collection to continue until the *BF* provides moderate evidence for (*BF* > 3) or against (*BF* < 1/3) the hypothesis. In short, Bayesian statistics enable a flexible stopping rule which enables data collection to continue until the evidence for the hypothesis being true or false is conclusive whereas orthodox statistics state that data collection *must* terminate when *n* participants for *x* power have been tested. The choice of Bayesian statistics and the corresponding stopping rule is of critical importance when the null hypothesis is true. When the null-hypothesis is true, all *p* values are *equally likely* to occur which means that the researcher can obtain a statistically significant *p* value if a flexible stopping rule is employed. Conversely, when a Bayesian *t*-test is applied a flexible stopping rule is permissible as the *BF* is driven towards zero when the null hypothesis is true unlike the *p* value which is not driven in any direction (Dienes, 2011).

The critical difference between orthodox and Bayesian statistics is illustrated by the following situation where two distributions are created by drawing values from the same distribution. Creating two distributions from an identical distribution creates a scenario where the null hypothesis is true. Creating two distributions which are different from one another creates a scenario where the null hypothesis is false. Each distribution contains 1000 subjects. Bayesian and orthodox two sample *t*-tests were then applied incrementally to samples of 2 to 1000 in one simulated participant increments under conditions where the null hypothesis was true or false. Figure 5 (top left) and figure 5 (bottom) reveal that *p* values and *BF*s are similar when the null hypothesis is false. Eventually, as illustrated in figure 5 (top left), *p* values fall below 0.05, which is regarded as the threshold the rejecting the null hypothesis. Similarly, the *BF* eventually rises above 3, which is regarded as the threshold for supporting that a mean difference exists (Dienes, 2011).

However, the critical difference between the *BF* and the *p* value emerges when the null hypothesis is *false*. Under these conditions, all *p* values are equally likely to occur which renders it meaningless at determining whether the null hypothesis is true or false, as illustrated in figure 5 (top right). In contrast, Figure 5 (bottom) reveals that the *BF* is also sensitive to the absence of a mean difference in a data set, which is quantified by the *BF* decreasing and eventually exceeding 1/3, the threshold for concluding the absence of a mean difference between two means (Dienes, 2011).

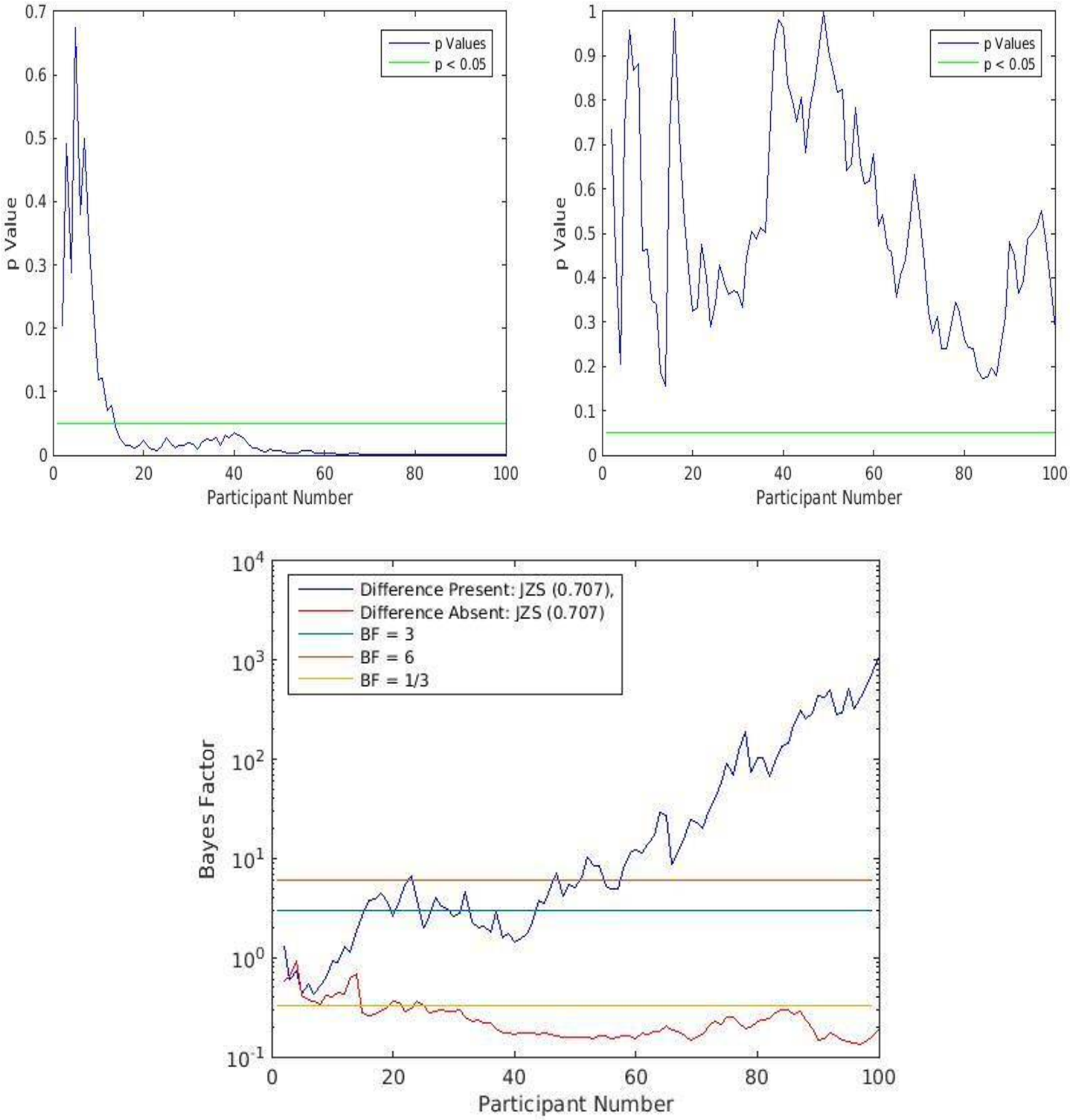

Figure 5. Top left: *p* value as a function of participant number when the null hypothesis is false. Top right: *p* value as a function of participant number when the null hypothesis is true. Bottom: *BF* as a function of participant number when the null hypothesis is true and false.

Using Bayesian statistics to address the power argument (de Graaf & Sack, 2011) using simulated data

As de Graaf & Sack (2011) point out, it is difficult to identify whether a TMS induced effect is truly absent or whether a TMS induced effect would be present if a sufficient number of participants were included within the experiment. As a potential solution, they suggest that researchers should examine whether the effect size is in the predicted direction; if so, data collection can continue; if not, data collection can be terminated. The use of Bayesian statistics complements this approach and provides a more principled criterion to decide whether or not to terminate or continue data collection. This approach is more principled as the prior-probability distribution enables the direction (positive or negative) and magnitude of the effect size to be formulated as a hypothesis to be tested. The likelihood and the *BF* would then inform the researcher as to whether TMS has produced an effect that supports or goes against a hypothesis. If the *BF* is inconclusive, then data collection can continue until moderate support the null ($BF < 1/3$) or experimental hypothesis ($BF > 3$) isobtained.

The use of Bayesian statistics in conjunction with simulated data will now be presented. Three different types of TMS-based hypothesis tests will be presented. The first will show how the *BF* is sensitive presence or absence the simulated presence and the simulated absence of a difference between active TMS and sham TMS. Subsequently, the sensitivity of the *BF* to the simulated presence and absence of a difference between x_1 and b_1 coefficients will also be shown. These approaches can be used to demonstrate whether or not it is feasible to produce evidence for or against different TMS-driven hypotheses. Such an approach is important because it is difficult to determine whether or not is feasible to produce evidence for or against a hypothesis based on the collection of pilot data alone. The use of simulations to create data can not only identify the number of participants that would be necessary to generate evidence for or against a hypothesis but whether such a participant number is *feasible* to obtain for the researcher. Here, the question of whether it is feasible to collect data from the participants is important. If the simulations suggest that 90 participants are required to provide conclusive evidence against a hypothesis, yet it is only

possible to obtain data from 30 participants, then it might not be feasible for the experiment to provide evidence against a hypothesis. The use of simulations to assess feasibility is important as it prevents the researcher from running experiments where it is not feasible to generate evidence for or against a hypothesis with a realistic number of participants. The rest of this chapter will now explore how the amplitude (*a*), bandwidth, (*b*) and temporal position (*x*) coefficients can be incorporated into simulations that can assess whether each of these coefficients are a feasible basis for testing a hypothesis using Bayesian statistics.

Using Bayesian statistics to identify if a difference between active TMS and sham TMS is present or absent as measured by a_1 coefficients

Now, some illustrations of how the modelling procedure can be utilized to produce evidence for or against hypotheses that are of interest to TMS research will be shown. The first analysis that will be illustrated will be essential for any TMS experiment that relies on a Gaussian model to measure performance, which requires evidence for or against a difference between active TMS and control TMS across SOAs. A single Gaussian model quantifies such an effect using an a_1 coefficient. Here, simulated data sets will be created where a TMS-induced effect is absent. This was accomplished by setting the amplitude of the single Gaussian model which was used to generate simulated data across SOAs to zero. Note, the single Gaussian model that is used to generate the difference between active and sham performance at each SOA is different from the single Gaussian model that is *fitted* to simulated performance at each SOA. The latter outcome where fitting takes place generates simulated coefficients which are subjected to statistical analysis. When a TMS-induced effect was absent, the sensitivity of the *BF* to the absence of a mean difference as produced by a Bayesian one-sample *t*-test with a JZS prior (Rouder et al., 2009) can be found in figure 6 (bottom). Figure 6 (bottom) illustrates that the *BF* decreases towards and beyond 1/3 when the absence of a TMS-induced effect is simulated, quantifying support for the null hypothesis. In contrast, figure 6 (bottom) illustrates the opposite outcome. The opposite outcome – when a TMS-induced effect is present – was simulated by having the single Gaussian model that creates the

simulated data at each SOA have an a_1 of -0.15. The use of such a coefficient emulates an outcome when the largest difference between active TMS and control TMS is ~-0.15 when the subtraction of control TMS performance takes place at each SOA. As illustrated by figure 6 (top) the *BF* increases beyond 3 as function of participant number when a simulated negative difference between control TMS and active TMS. Below, a similar comparison between different pairs of b_1 coefficients is also presented.

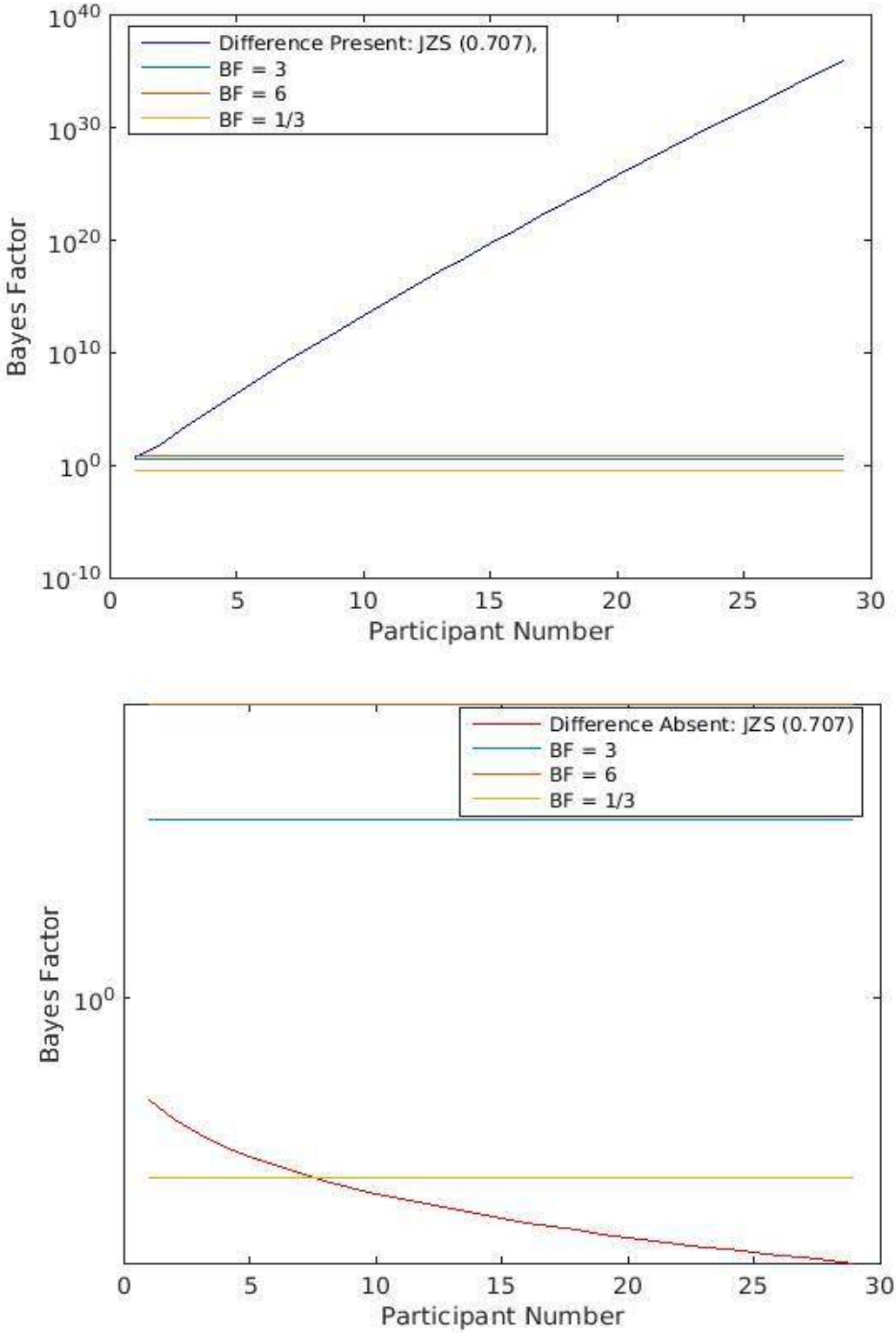

Figure 6. Top: Bayes factor as a function of participant number when amplitude coefficients are -0.15, which differs from zero. Bottom: *Bayes factor* as a function of participant number when amplitude coefficients are equal to zero.

Using Bayesian statistics to identify if a difference between the temporal position of two TMS-induced effects is present or absent as measured by x_1 coefficients

Now the sensitivity of *BF* to a difference in x_1 coefficients will be demonstrated. The x_1 coefficient is of interest when a TMS experiment is motivated by identifying the temporal order of critical events within different brain areas (e.g. Silvanto et al., 2005). Simulated data will be generated with the presence and absence of a difference in x_1 coefficients and the sensitivity of the *BF* to both of these outcomes as a function of participant number will be illustrated. A comparison where x_1 coefficients are identical will be emulated by creating simulated data where the point in time where the difference between active TMS and control TMS is largest occurs at the same point for each site. This outcome will be emulated by setting the x_1 coefficients to exactly the same value when a single Gaussian model is used to simulate the difference between active TMS and control TMS at each TMS SOA. Note, the single Gaussian model that is used to generate the difference between active and sham performance at each SOA is different from the single Gaussian model that is *fitted* to simulated performance at each SOA. The single Gaussian model that is fitted to simulated performance is then subjected to statistical analyses. Figure 7 illustrates that the *BF* produced by a one-sample Bayesian *t*-test with a JZS prior (Rouder et al., 2009) increases towards and beyond 3 when a difference in x_1 of ~100ms occurs when a_1 for one site occurs ~100ms later than a_1 for a different site. Figure 7 also illustrates that the *BF* produced by a one-sample *t*-test with a JZS prior can successfully quantify evidence for the absence of a difference in x_1 when the point where the difference between active TMS and control TMS is largest is at the same time point for the two simulated sites where TMS is administered. Such an outcome was simulated by setting the x_1 coefficient that was used to create differences between active TMS and control TMS at each SOA.

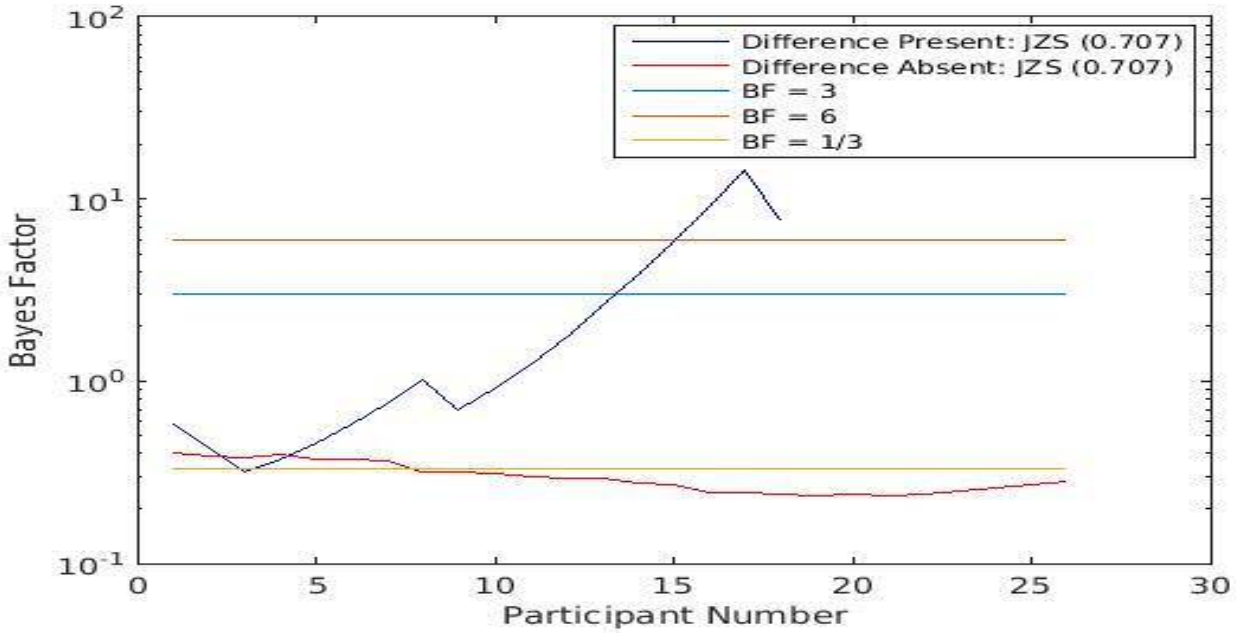

Figure 7. Bayes factor as a function of participant number one-sample Bayesian *t*-test is applied when a mean difference of 100ms exists between two sets of temporal position coefficients (blue line) and when no difference exists between two sets of temporal position coefficients (red line)

Using Bayesian statistics to identify if a difference between the temporal positions of two TMS-induced effect is present or absent as measured by b_1 coefficients

The second type of TMS analysis that will be illustrated with the modelling procedure here will be when an experiment is motivated by identifying how the duration of processing within one cortical site differs under different conditions of visual stimulation (e.g. de Graaf et al., 2012). Simulated data will be presented here when difference in b_1 coefficients is present or absent along with the sensitivity of the *BF* to these different outcomes. A difference in b_1 coefficients was simulated by introducing a 30ms difference in b_1 for one condition relative to another when a single Gaussian model is used to create simulated differences between active TMS and control TMS at each SOA. Subsequent fitting of a single Gaussian model to the simulated data at each SOA then produced the coefficients upon which statistical analysis were applied. The application of a Bayesian one-sample *t*-test with a JZS prior (Rouder et al., 2009) revealed that the *BF* increased towards and beyond 3 when a difference of 30ms was introduced between two sets of simulated b_1 coefficients. The *BF* as a function of participant number can be found in figure 8. . In contrast, model fits to the

simulated data when a difference in b_1 is absent revealed that the *BF* produced by a Bayesian one-sample *t*-test with a JZS prior produces a *BF* that decreases towards and beyond 1/3 as a function of participant number. Such a *BF* demonstrates that evidence can be garnered for the null hypothesis. A *BF* that increases towards and beyond 3 when an effect is present and towards and beyond 1/3 when an effect is absent suggests that it is feasible to use the modelling procedure in conjunction with Bayesian statistics to assess whether it is feasible to produce evidence for or against a hypothesis when testing whether the duration of a TMS-induced effect differs under different visual conditions.

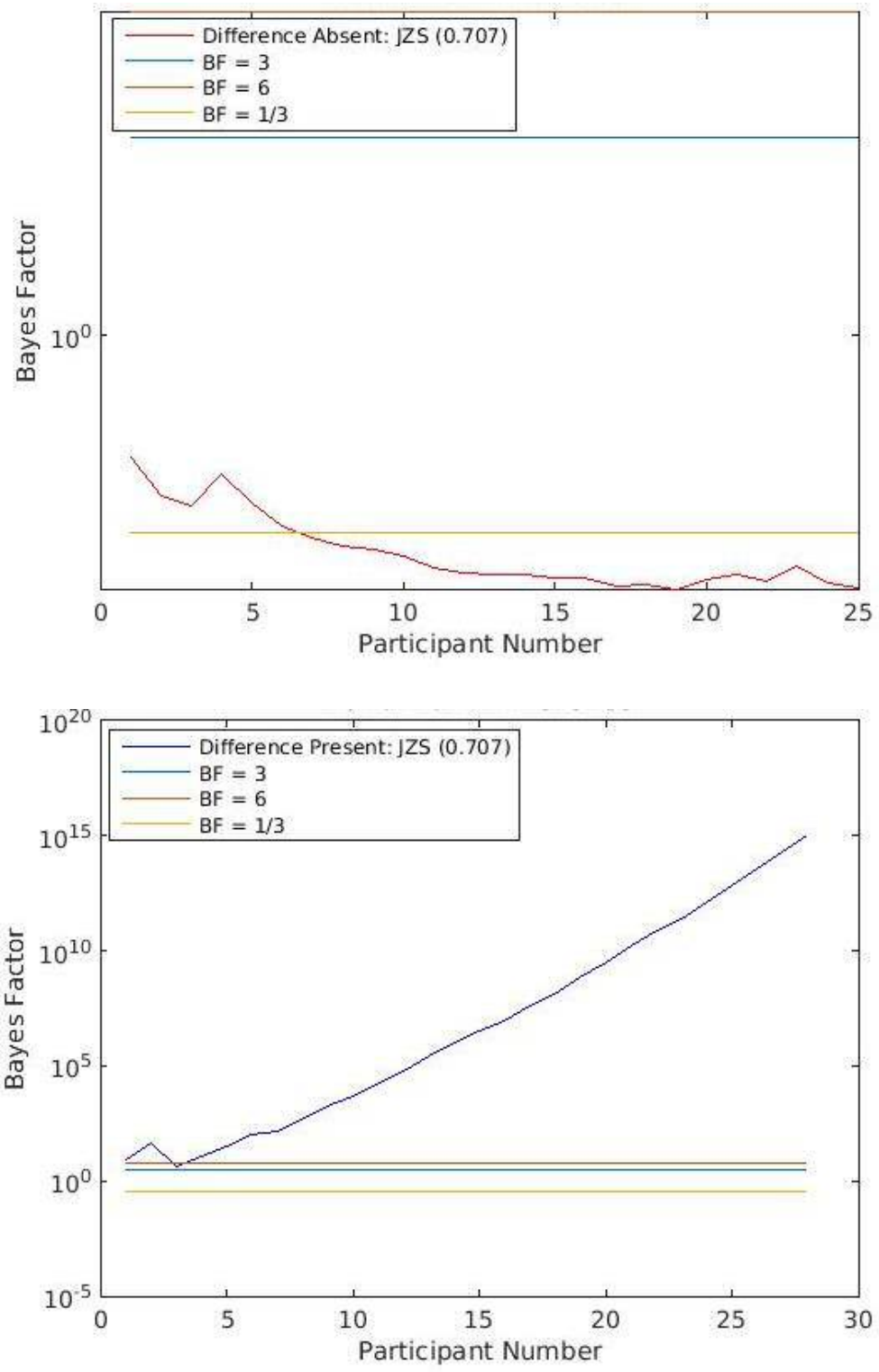

Figure 8.Top: Bayes factor produced by the absence of a difference in bandwidth between two sets of bandwidth coefficients as a function of participant number. Bottom: Bayes factor produced by the presence of a 30ms difference in bandwidth between two sets of bandwidth coefficients as a function of participant number.

Concluding remarks

This chapter has introduced how a modelling procedure can be used in conjunction with Bayesian statistics to assess whether it is feasibile to obtain evidence for or against hypotheses that are of interest to single-pulse TMS experiments. This modelling procedure revolves around the use of a Gaussian model to generate differences between active TMS and control TMS at SOAs where TMS will be administered in an experiment. Subsequently, a Gaussian model is then fitted in the simulated data across these SOAs, which produces coefficients that are used within statistical analyses. The use of coefficients based on simulated data can be used to demonstrate the presence or absence of differences in the temporal position (x_1 coefficient) of TMS-induced effects for one or more TMS sites using the *BF* produced by a Bayesian one-sample *t*-test. The use of coefficients based on simulated data can also be used to demonstrate the presence or absence in the duration of a TMS-induced effect (b_1) using the *BF* produced by a Bayesian one-sample *t*-test. The simulation of differences that are present or absent in data set can then be assessed as a function of participant number. These simulations will approximate the number of participants that could be required to provide evidence for or against a hypothesis. These simulations can also be used to qualify whether the number of participants required to produce such evidence is feasible to obtain within the temporal constraints often facing the researcher. If the number of participants that data can be gathered from is less than the number of participants indicated by the simulations, then it is unfeasible to generate conclusive evidence for or against a hypothesis.

Chapter 3. Are there temporally distinct frontal and occipital phases during visual perception?

Chapter 2: Overview

Chapter 2 aimed to investigate recurrent processes between the frontal and occipital lobes usihg single-pulse locked TMS. A basic visual detection paradigm was employed whereby participants had to indicate whether or not they saw a visual target and to indicate where this target appeared. Pre-registered and exploratory analyses were then completed which aimed to identify whether a DLPFC-TMS induced effect arises after a EVC-TMS effect. Exploratory analyses revealed evidence contrary to this hypothesis; instead, it appears that EVC and DLPFC are critical for visual processing at the same time.

1. Introduction

At discussed in Chapter 1, visual perception could be achieved by two phases: a feedforward sweep, which enables visual stimuli to enter the cortex, and recurrent processing whereby feedback appears to modulate this initial representation (Lamme & Roelfsema, 2000). The presence of recurrent processing involving prefrontal, parietal and early visual cortices is thought to be a critical determinant of whether a stimulus is seen (Bor & Seth, 2012; Lamme, 2006; Tapia & Beck, 2014). Evidence that recurrent processing accompanies stimuli that are reported as seen has been revealed within early visual cortex (e.g. Super et al., 2001). There is also evidence that recurrent processing within the frontal lobes could also accompany stimuli that are reported as seen (e.g. Lau & Passingham 2006; Rounis et al., 2010). This conclusion was revealed by an experiment which presented a shape, which had to be reported by the participants which was masked at different SOAs. Despite the physical characteristics of the shape remaining constant throughout the experiment, a dissociation between proportion correct and awareness of shape identity emerged when the target was masked at an SOA of 33ms (Lau & Passingham, 2006). The BOLD response within left mid-DLPFC was reduced when the target was masked at an SOA of 33ms (Lau & Passingham, 2006). It appears that there is potential for a s interaction between EVC and the frontal lobes yet it is unclear *when* recurrent processing emerges within the frontal lobes relative to the feedforward and recurrent processes within early visual cortex.

This experiment aimed to use two-coil single-pulse transcranial magnetic stimulation (TMS) to investigate when recurrent processing occurs within the frontal lobes relative to feedforward and recurrent processes within early visual cortex, and how these processes affect visual perception. The application of TMS pulses to early visual cortex (EVC) at different stimulus onset asynchronies (SOAs) has established the time course of visual perception (de Graaf et al., 2014). In such paradigms, EVC TMS produces a clear and reproducible effect on performance at an SOA of ~100ms (de Graaf et al., 2014). This outcome suggests that something critical is happening in EVC at ~100ms that determines whether or not a visual stimulus is reported as seen, which could be attributed to the feedforward

sweep or recurrent processing (de Graaf et al., 2014). Other effects on behaviour have been revealed at 200ms & 250ms (Camprodon et al., 2010; Heinen et al., 2005) and up to 300-400ms (Chambers et al., 2013; Allen et al., 2014), which may depend on the type of stimulus used, task demands and the shape and size of the TMS coil (de Graaf et al., 2014). The presence of later critical periods of processing within EVC suggest that visual perception relies on an *early* phases of processing at ~100ms and *later* phases of processing that occur beyond ~200ms. TMS effects on the later phases of processing could interfere with recurrent processing within EVC (Camprodon et al., 2010; Heinen et al., 2005; Chambers et al., 2013; Allen et al., 2014;), which could be affected by frontal recurrent processes. The segregation of early EVC-TMS at SOAs of ~100ms and at and beyond ~200ms as feedforward and recurrent processes, respectively, is far from conclusive. Recently, it has been proposed that the EVC-TMS effect at an SOA of ~100ms reflects feedforward *and* recurrent processing (de Graaf et al., 2014). However, this is a caveat of interpreting the ~100ms EVC-TMS effect does not hamper the interpretation of the effects of EVC-TMS at SOAs beyond as an effect on recurrent processing.

Evidence that the frontal lobes could be involved during visual perception has stemmed predominantly from functional magnetic resonance imaging (fMRI) studies. Imamoglu et al. (2012) revealed that functional connectivity between EVC and left dorsolateral prefrontal cortex (DLPFC) accompanied stimuli that were consciously recognized compared to those that were not. Moreover, left mid-DLPFC could be important consciously *knowing* a visual stimulus has been present (Lau & Passingham, 2006). Taken together, these two experiments suggest that DLPFC could play an importanrt role in conscious processing. Consistent with this, bilateral DLPFC-TMS reduces participants knowledge of a visual stimulus having been presented whilst preserving their ability to respond to its characteristics and repetitive right DLPFC-TMS impairs conscious detection of change (Rounis et al., 2010; Chiang et al., 2014; Turatto et al., 2004). Left DLPFC-TMS has also been found to have more immediate perceptual consequences by reducing accuracy and perceptual sensitivity and increasing reaction time (Philiastides et al., 2011; Kalla et al., 2008). Although some theories

emphasize the importance of recurrent processing within prefrontal cortex during visual perception (Bor & Seth, 2012), no studies that we are aware of have utilized the potential of single-pulse DLPFC-TMS to isolate *when* DLPFC is critical for visual perception. However, evidence from electroencephalography demonstrates that potential evoked by visual stimulation could occur within dorsolateral frontal cortex ~100ms after the onset of visual stimulation (Foxe & Simpson, 2002), suggesting that single-pulse DLPFC-TMS effects could be observed shortly after the onset of a visual stimulus.

Identifying when DLPFC TMS effects emerge relative to EVC TMS effects could reveal when feedforward and recurrent processes occur within EVC and DLPFC and how these processes affect visual perception. This experiment employed two-coil single-pulse TMS in conjunction with a simple visual detection paradigm. Active TMS wasl be applied to left DLPFC or EVC at 1 of 10 SOAs, from 60ms to 330ms in steps of 30ms. Sham TMS was also applied at each of these SOAs in order to provide a control measure of performance without electromagnetic induction within EVC or left DLPFC. Participants will be presented with a focal visual target (dot) that can appear in one of 360 different locations arranged in a circle. Their first response will be to report where the visual target appeared by moving a cursor using a mouse and their second response will be to indicate whether they saw the visual target with a yes or no response. Two main measures will be derived. The first response will provide the basis for ΔAcc (change in accuracy) measure, which is designed to quantify the TMS-induced difference in indicating target location. The second response will provide the basis for ΔPr measure, the TMS-induced difference in perceptual sensitivity based upon non parametric signal detection theory (Corwin, 1994). The TMS-induced difference (Δ) on each measure will be calculated by subtracting their performance during sham TMS from their performance on during active TMS at each of the SOA's.

The first reason for the use of these separate measures of performance is that the effect of TMS on the standard ΔPr measure can be used to validate the effect of TMS on the other novel ΔAcc measure. If a TMS disrupts a basic visual process, there should be evidence of it in both measures of

performance. Although dissociations between the two may be of interest (see Allen, 2012). The second reason is that ΔAcc can measure how accurate the participant is at indicating target location on *individual* trials at an SOA whereas ΔPr can measure how accurate the participant is at indicating target presence using *all* trials at an SOA. Additionally, ΔAcc reduces the likelihood of participants successfully guessing the correct response when they are unaware of its presence or location. In a standard 2 alternative forced choice paradigm, there is a 50% chance of participants successfully guessing the correct response. In contrast, the ΔAcc measure offers the participant a range of different locations distributed around the circumference of a circle; the target itself only appears in one of these locations. When the participant is unaware of where the target appeared, there is a lower, near zero probability of the participant successfully guessing the location of the target. The implication of this for TMS-based paradigms is that TMS-induced suppression of performance could be more likely in the ΔAcc task due to reduced likelihood of guessed responses being correct when left DLPFC or EVC TMS precludes awareness of the target itself or of its location.Like previous studies (Stevens et al., 2009; Chambers et al., 2013; Rusconi et al., 2013), a biphasic Gaussian model was used to analyse the effects of TMS on performance. Such models are capable of producing coefficients that represent the *peak amplitude* (the magnitude of a TMS-induced effect), the *temporal position* of the peak amplitude (when the TMS-induced effect arises), and the *bandwidth* (the overall duration of a TMS-induced effect on performance) (Stevens et al., 2009; Chambers et al., 2013; Rusconi et al., 2013). The use of a biphasic Gaussian model will enable both EVC and DLFFC TMS to isolate two phases that could be critical for visual perception as a function of time. Two phases were being investigated in this study because one phase could capture the feedforward sweep and the second phase could capture recurrent processing with a site. For example, a biphasic Gaussian could produce coefficients that capture the early EVC TMS effects at ~100ms *and* a later TMS effect that could occur beyond ~200ms. These coefficients will be used as the basis for two separate analyses. One analysis, the group analysis (GAn) will be applied to all participant data. Another analysis, the subgroup analysis (SGAn) will screen for the presence of TMS-induced effects

on each measure. The SGAn will only include data from participants that successfully passed a pre-specified criteria. Both the GAn and the SGAn will aim to identify whether a TMS-induced effect is present when applying TMS to EVC and left DLPFC. If this aim is met, both analyses also aimed to identify whether the temporal position of the EVC-TMS induced effect (EVC*x*) occurred earlier in time from the temporal position of the left DLPFC-TMS induced effect (DLPFC*x*). If later EVC TMS-induced effects are also produced, it will also be of interest whether the temporal position of a later EVC TMS effect occurs before or after the temporal position of left DLPFC TMS effects. Additional exploratory analyses were carried out which applied a single Gaussian model to performance as a function of EVC-TMS and left DLPFC-TMS, which can only detect one of the largest differences between active TMS and sham TMS across all SOAs.

This experiment tested two hypotheses. The first hypothesis was that the application of active TMS to EVC and left DLPFC will affect performance relative to sham TMS at a discrete time point, which was tested using the peak amplitude coefficients of the model applied to each site. If active TMS made performance worse relative to sham TMS, subtracting the sham score from the active score would l produce negative peak amplitude coefficients. In contrast, if performance on active trials is facilitated then subtracting the sham score from the active score would produce positive peak amplitude coefficients. However, subtracting the active scores from the sham scores across SOAs will produce peak amplitude coefficients of approximately 0 if TMS has *no effect.* If a Bayesian one-sample *t*-test reveals that *at least one* peak amplitude supports that active TMS has an effect relative to sham TMS *for both TMS sites*, it will be concluded that active EVC and left DLPFC TMS has affected performance, which will confirm the first hypothesis. If the first hypothesis is confirmed a second hypothesis would be tested. In order to identify the best way to represent the mean differences between EVC*x* and DLPFC*x* in order to test this hypothesis, a number of prior-probabilities were applied to the simulated presence and absence of a difference between EVC*x* and DLPFC*x*. These simulations were based on pilot data. These simulations also assessed the feasibility of these hypotheses *a priori*.

The second hypothesis was that the temporal position of each EVC TMS effect would occur earlier than the temporal position of the left DLPFC TMS effects. The second hypothesis was tested using the temporal position coefficients that correspond to the peak amplitude coefficients that reflect TMS-induced effects. A number will be generated by subtracting EVC*x* coefficient from the DLPFC*x* for each participant. If DLPFC*x* occurs later in time than EVC*x*, this difference will be positive. In contrast, if EVC*x* occurs later in time than DLPFC*x*, this difference will be negative. A Bayesian one-sample *t*-test with a uniform prior (Dienes, 2011) established whether the mean difference of all participants in each analysis supports whether EVC*x* occurs before DLPFC*x* or whether DLPFC*x* occurs before EVC*x*. A positive difference between EVC*x* and DLPFC*x* would support the idea that processes within EVC occur earlier in time than processes within left DLPFC. In contrast, a negative difference would support the idea that processes within left DLPFC occur earlier in time than initial critical processes within EVC. The Bayesian hypothesis tests which aimed to identify if TMS effects occur for each of these sites and the chronological order of such effects were pre-registered on the Open Science Framework. This was the first experiment to apply single pulses of TMS to EVC and left DLPFC and pre-register a number of analyses. All analyses that were not pre-registered will be highlighted as exploratory. This approach will enable the proposed study to identify whether EVC TMS effects arise before DLPFC TMS effects and whether later EVC TMS effects occur after DLPFC TMS effects. By identifying the chronological order of EVC TMS effects relative to DLPFC effects, it would be possible to identify whether a recurrent processing view of awareness is feasible. For example, if the first phase of EVC suppression is followed by an initial suppression of DLPFC, and the DLPFC suppression is followed by another phase of EVC suppression, the chronological order of these effects would fall within the feedforward (EVC→ DLPFC) and recurrent processing (DLPFC → EVC) framework outlined here.

2. Methods

2.1: Design

TMS was applied to EVC or left DLPFC at 10 SOAs relative to the presentation of a visual target. The paradigm involved the presentation of circular target that can appear in 1 of 360 locations arranged in a circle – each target will be presented at 1.5o eccentricity of visual angle. The visual target was present on 70% of trials. The experimental procedure is illustrated below in Figure 1. A 1000ms fixation period was followed by the target, presented for 10ms. After a brief 390ms interval, a cursor appeared and participants moved it using the mouse to where they thought the target appeared. Initially, the response dot appeared in red in the centre of screen. The response dot was then moved more than 0.75^{o} of visual angle from central fixation, at this point it will snap to 1.5^{o} eccentricity from fixation in exactly the same direction. Once the dot has snapped to this position, the participant can then move the dot to where they thought the target appeared around the circle and click the mouse when their judgment is complete. The participant was only able to indicate where they thought the target has appeared once the dot snapped to 1 .5^{o} of eccentricity from fixation. Once the participant has indicated where the target appeared, they indicated whether they saw the target with a yes or no response. The question of whether or not they saw the target was made explicit in the instructions given to the participant. Accuracy, not speed, was emphasized when participants make their responses.

On each trial the TMS coil delivered a single pulse of active or sham stimulation over either left DLPFC or EVC at one of 10 SOAs from 60ms to 330ms in 30ms increments (60ms, 90ms, 120ms, 150ms, 180ms, 210ms, 240ms, 270ms, 300ms, 330ms). 40 pulses of active TMS and 40 pulses of sham TMS were applied at each SOA at each site, which meant that 400 active and 400 sham pulses were applied to each site throughout the experiment. Each participant completed 16 blocks of TMS; each block contained 100 trials. Only one type of TMS (active or sham) was delivered to one site (EVC or left DLPFC) throughout each block. Each TMS-SOA occurred 10 times within each block; each

TMS-SOA contained 7 visual target-present trials and 3 visual target-absent trials presented in a randomized order.

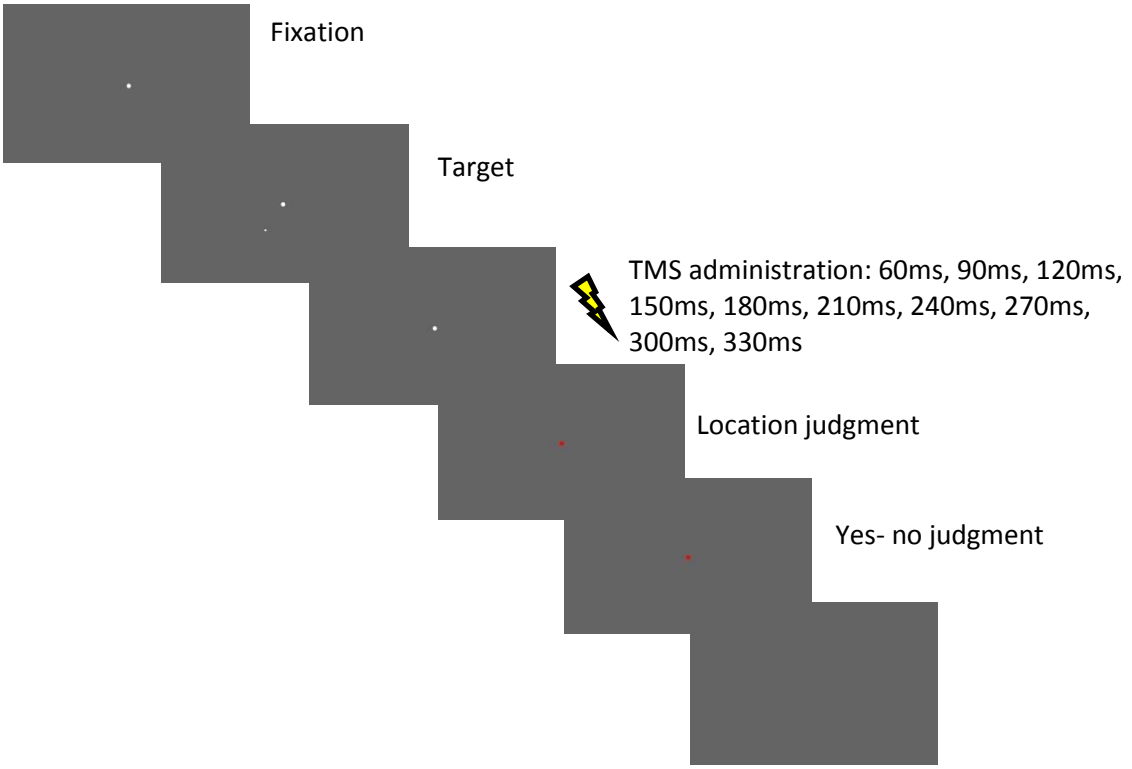

Figure 1. Schematic illustration of the experimental display sequence. The appearance of the fixation dots indicates the trial has begun. After this fixation period, a visual target dot appears off fixation for 10m. The administration of TMS will then occur at one of the 10 TMS SOAs displayed above. One type of TMS (active or sham) will be delivered to one site on each trial throughout a block of TMS. The occurrence of the central red dot instructs the participant to indicate whether they saw the target, using a left or right click. Two difference response mappings for the yes and no responses will be used in order to enable counterbalancing. One mapping will be left click: yes, right click: no, and the other mapping will be left

In terms of block order and counterbalancing, the 16 blocks were completed as 8 sets of active and sham simulation pairs. To avoid order confounds active EVC-TMS blocks were completed before *and* after sham EVC-TMS blocks *and* sham left DLPFC-TMS blocks. Conversely, it was also critical that active left DLPFC-TMS are completed before *and* after sham left DLPFC-TMS *and* sham EVC-TMS. To address this issue, a balanced Latin square design was employed (Edwards, 1951). A balanced Latin square produced a matrix which determined the order that participants underwent

active and sham stimulation from each TMS site. Eight different active and sham pairings were incorporated in the experiment (EVC-active followed by EVC-sham, left DLPFC-active followed by left DLPFC-sham, EVC-sham followed by EVC-sham, left DLPFC-sham followed by left DLPFC-active, EVC-active followed by left DLPFC-sham, leftDLPFC-active followed by EVC-sham, left DLPFC-sham followed by EVC-active and EVC-active followed by left DLPFC-active). A balanced Latin square counterbalanced the order that these pairs are experienced by participants by producing an 8x8 matrix. Within this matrix, the numbers 1 to 8 were used to identify each of the active and sham pairs described above. Each of these numbers occurred once in each row and column of the matrix. Moreover, each number appeared equally in each *position* within each row and column, which ensured that the order in which participants underwent each active and sham stimulation pair was counterbalanced. The rows of this matrix determined the sequence of active and sham stimulation experienced by the participant whereas the columns of this matrix determined whether active or sham stimulation (from EVC or left DLPFC) was experienced during each block, enabling counterbalancing to take place. To ensure that all active-sham sequences were experienced by an equal number of participants, participants were tested in batches of 8.

2.1.1: Calculation of ΔPr

ΔPr was calculated using non-parametric signal detection theory (Corwin, 1994). Pr subtracts a participants false alarm rate (FAR) from their hit rate (HR), which is the proportion of target present (yes) responses when the target is present (Corwin, 1994). A hit was defined when the participant made on a 'yes' response on a target present trial. A miss was defined when the participant made a 'no' response on a target present trial. A correct rejection was made when the participant made a 'no' response on a target absent trial. A false alarm was made when the participant made a 'yes' response on a target absent trial. Their HR was calculated by dividing the total number of hits and dividing it by the total number of target present trials. Their FAR was calculated by dividing the total number of false alarms by the total number of target absent trials.

ΔPr as a function of EVC TMS was calculated at each SOA by subtracting the sham EVC TMS score from the corresponding active EVC TMS score. ΔPr as a function of left DLPFC TMS will be calculated at each SOA by subtracting the sham left DLPFC TMS score from the corresponding active left DLPFC TMS score. Non-parametric signal detection theory was chosen instead of parametric signal detection theory (e.g. Macmillan & Creelman, 1991) for the following reasons. Recent experiments have highlighted potential issues with the use of parametric signal detection theory when participants have very low (< 0.05) or very high (> 0.95) hit (HR) and false alarm rates (FAR) (Bor, Schwartzmann, Barrett & Seth, 2017). Under circumstances where HR and FAR are this high or low, the *z* function which is applied to the difference between the HR – FAR approaches positive or negative infinity, respectively. When participants who exhibit HR or FAR that conform these high rates are excluded from the analysis, previous effects of DLPFC-TMS on awareness have not been reproduced (Rounis et al., 2010; Bor et al., 2017). Non-parametric signal detection theory does not rely on the application of a z function to the difference between HR and FAR, which bypasses the production of d' (perceptual sensitivity) values that approach positive or negative infinity when the HR or FAR is more than or less than 0.95 or 0.05, respectively.

2.1.2: Calculation of ΔAcc

ΔAcc was measured by calculating the circular difference between the presented angle of the target and the reported angle of the target in radians on each trial. First of all, Acc was calculated separately on each trial. Circular mean Acc was then calculated across all trials at each TMS SOA as a function of sham TMS and active TMS for each site. ΔAcc as a function of EVC TMS SOA was then calculated by subtracting the sham EVC TMS score from the corresponding active EVC TMS score at each SOA. ΔAcc as a function of left DLPFC-TMS SOA was calculated by subtracting the sham DLPFC TMS Acc score from the corresponding active left DLPFC-TMS Acc score at each SOA. The calculation of Acc is illustrated in figure 2.

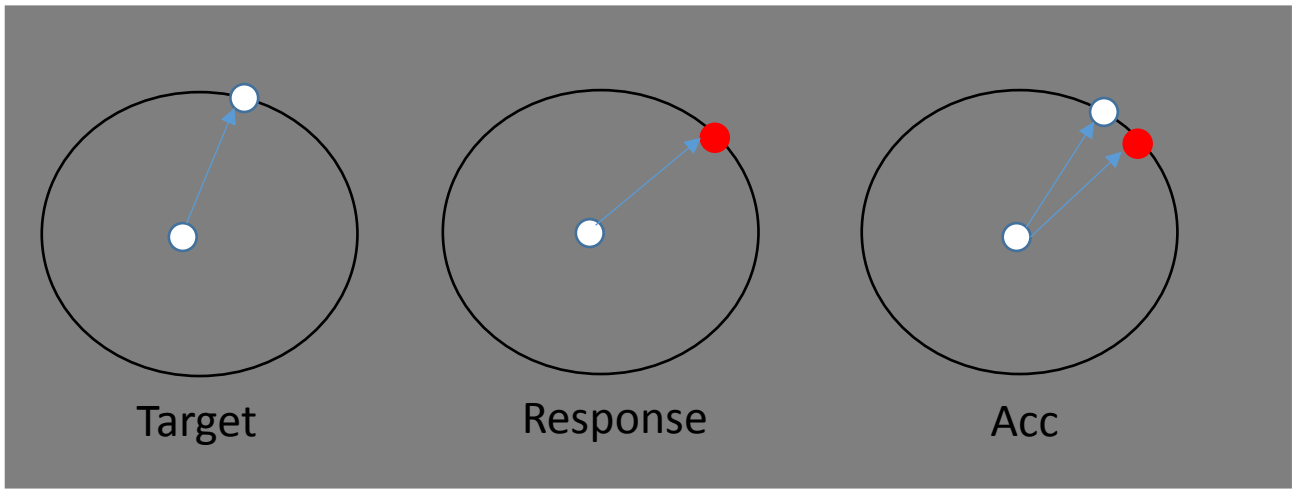

Figure 2. Illustration of the calculation of Acc. First, the target is presented at one of 360 angles from fixation. Secondly, the response is made, which can only be in one of these 360 locations. Acc is calculated by working out the circular difference between these two angles.

2.2 Calibration

2.2.1: Phosphene threshold

Firstly, a phosphene threshold (PT) was sought by identifying the stimulator output that produced a phosphene after 50% of TMS pulses, which was described to them as a brief distortion of their visual field as documented previously (Franca, Koch, Mochizuki, Huang, Rothwell, 2006; Stokes, Barker, Dervinis, Verbruggen, Maizey, Adams & Chambers, 2013). Prior to thresholding, the participant's head location was calibrated to an individual magnetic resonance image of their brain (obtained via a 3T whole-body General Electric scanner during a separate session) using a Brainsight System (Rogue Research Inc.). The Brainsight System was used to monitor the position of the coil relative to the participant's head. The coil was then placed 1cm above the inion with the handle pointing dorsally, whilst single pulses were initially delivered at 40% of stimulator output and increased in steps of 5% up to 180% of their motor threshold (obtained from a separate experiment or induction session) until a phosphene was produced. Participants were asked to close their eyes and say 'yes' in the presence of a phosphene, 'no' in the absence of a phosphene and 'no' if they were unsure. If a phosphene was not produced, the coil was relocated and the procedure was repeated. Once a phosphene was produced, a number of pulses were then delivered in order to

familiarize participants with phosphenes. The TMS coil location on the scalp that successfully produced a phosphene was thenmarked using the Brainsight system so it could be used to guide the location of the coil to induce subsequent phosphenes. A phosphene was then sought that was reasonably clear and, at least in part, and covered part of the centre of their visual field according to the participants report. Once a phosphene that meets this criterion was identified, it was also marked using the Brainsight software.

Once a clear phosphene covering part of the centre of the participant's visual field was identified, the minimum stimulator output required to produce a phosphene was sought using a staircase method. The coil was placed above a scalp location that successfully produced a clear phosphene that covered part of the centre of their visual field. Stimulator output was set at 50% and then increased in steps of 5% (up to 180% of their motor threshold) until a phosphene was reported on 5 out of 10 trials. Subsequently, stimulator output was decreased in steps of 2% until a phosphene was not reported on 5 out of 10 trials. Finally, stimulator output was increased in steps of 1% until a phosphene was reported on 5 out of 10 trials, which was used as an approximate PT (APT). A similar procedure to that described in Allen et al. (2014) was then completed. The APT was then be altered by 80%, 90%, 100%, 105%, 110% and 115% to generate 6 values for subsequent thresholding. The order of these intensities was randomized 3 times to create 3 separate blocks of TMS. Before each of these blocks, a clear phosphene that covered part of the centre of the participant's visual field was sought. Once identified, the coil location was marked using the Brainsight software. Within each block the participant completed 10 trials at each TMS intensity. Once all blocks were completed, the mean proportion of phosphenes reported across blocks at each TMS intensity was calculated. A linear or sigmoid function (depending on which produces the highest adjusted r^2 value) was then fitted to mean proportion of phosphenes as a function of TMS intensity. The function was solved to identify the TMS intensity that produces a phosphene on 50% of trials to produce a final phosphene threshold (FPT). 120% of the FPT was used as the basis for a comfort threshold to ensure they are comfortable with the intensity of stimulation. The comfort threshold

involved delivering a TMS pulse at 120% of their FPT to left DLPFC and EVC. If the participant did not report discomfort, 120% of their FPT was delivered to both sites throughout the experiment. If the participant reported discomfort, the TMS intensity was reduced to a stimulator output between 119% and 100% of their FPT. The intensity the participant is comfortable with was then delivered to both sites throughout the experiment. If discomfort was reported at 100% of their FPT, the participant was excluded from the experiment (see exclusion criteria, section 2.6). If 120% of their FPT was greater than 180% of their motor threshold, the stimulator output that was equal to 180% of their motor threshold was used as the basis for the comfort threshold (see section 2.3).

2.2.2: Detection threshold

Once the FPT was calculated, a detection threshold was sought. Where possible, this was carried out within the same session as the PT; otherwise, it was carried out at the beginning of their next session. First of all, participants were given task instructions and the experimenter engaged in discussion with them to ensure they understood them. Participants completed 10 trials with target brightness at its maximum to familiarize themselves with the experimental protocol, which continued until participants achieve a Pr of 1.

Subsequently, participants were presented with 10 target brightness levels in 3 separate blocks, each containing 100 trials with each brightness level occurring 10 times. The order of each brightness level was randomized. A sigmoid model was then fitted to mean Pr as a function of target brightness across all 3 blocks to generate a psychometric function. The psychophysical function was then used to identify the brightness level that produces a Pr value of 0.5. Prior to their first TMS block participants completed 40 trials with Pr set at this value. If Pr fell within ±0.1 of 0.5, the experiment proceeded further. If performance was beyond -0.1 or +0.1, target brightness was increased or decreased, respectively, and another 40 trials were completed. The increase or decrease in target brightness was determined by examining their individual psychophysical function obtained from the detection threshold. Once a brightness level produced a Pr value that fell within the range specified above, the first two active and sham TMS blocks commenced with target

brightness set at this level. If Pr fell below -0.1 or above +0.1 of 0.5 on a sham TMS block, target brightness was increased or decreased, respectively, before the next active and sham stimulation pair. The increase or decrease in target luminance was chosen with reference to their individual psychophysical function obtained from the detection threshold.

2.3 Equipment

TMS was delivered to each TMS site using a Magstim high-power 90mm round coil supported by a Magstim Rapid^2 biphasic stimulator. TMS pulse delivery and visual stimuli was produced by Matlab running the Psychophysics Toolbox 3 on a gamma-corrected 21" Mitsubishi CRT monitor (refresh rate: 100 Hz). A Cambridge Research Systems chin-rest mounted infrared eye tracker (refresh rate: 250 Hz) was used to identify trials where blinks occurred so these trials could be eliminated from the data analysis. Blink trials that were eliminated are defined as signal loss from the pupil across consecutive frames lasting between 50ms and 500ms (Caffier et al., 2005) that occur during the onset of the visual target.

The TMS coil was only be placed above one of the TMS sites (EVC or left DLPFC) throughout each block. Moreover, only one type of TMS (active or sham) was delivered throughout each block. Before the first EVC block in each session, regardless of whether active or sham TMS was being applied, a reasonably clear phosphene covering part of the centre of the participant's visual field was identified. Once discovered, the coil location that produced such a phosphene was marked using the Brainsight software (Rogue Research Inc.) so the coil could be placed above this location during active EVC TMS blocks for the rest of the session. During active EVC blocks, the coil was placed with the handle pointing dorsally with side B facing the participant.

During active left DLPFC TMS blocks, the coil was positioned above the nearest scalp coordinate to the left DLPFC based on the mean MNI co-ordinates from 4 fMRI studies on visual consciousness and perceptual decision-making (Heekeren et al., 2004, 2006; Lau & Passingham, 2006; Imamoglu et al., 2012). These mean MNI co-ordinates are -35, 31 and 30 and are presented in

Table 1 and are presented in the coronal, axial and sagittal planes on a Montreal Neurological Institute (MNI) standard brain in Figure 3. The nearest scalp co-ordinates were identified by finding the closest scalp co-ordinate to the centre of left DLPFC using a participant's magnetic resonance image of their head using Matlab and FSL. This process was completed as follows: Left DLPFC target was found by creating a mask in standard space using FSL (version 4.1.4) using the mean MNI co-ordinates displayed above. This mask was then transformed for standard space into native space using FSL's FLIRT. The three-dimensional Euclidean distance between the mask and each scalp location on the top of the participants head was then be identified. The scalp location that was s closest to the mask was then marked using Matlab and subsequently marked using the Brainsight software so the TMS coil can be placed at this scalp location during active left DLPFC TMS blocks. During active left DLPFC TMS blocks, the coil handle was placed tangentially on the nearest left DLPFC scalp location with side B facing the participant with the coil handle pointing upwards.

Before active EVC and left DLPFC TMS blocks, the position of the coil on the participant's scalp was marked using the Brainsight software. If the coil moved more than 10mm from this scalp location, the block was terminated and the participant started it again. The stimulator output of TMS delivered to each location throughout all blocks was the stimulator output that was identified during the comfort threshold (100% - 120% of their FPT or 100% of their FPT – 180% of their motor threshold). During sham EVC and left DLPFC blocks, the coil was placed perpendicular to the scalp in an approximate position to the coil location during active blocks with 10.6mm plastic spacer inserted between the coil and the scalp.

Authors	***MNI co-ordinates***
Heekeren et al. (2004).	x = -24, y = 24, z = 36
Heekeren et al. (2006).	x = -23, y = 29, z = 37
Lau & Passingham (2006).	x = -46, y = 48, z = 14
Imamoglu et al. (2012).	x = -45, y = 23, z = 34

Table 1. Individual MNI co ordinates used to calculate the mean MNI co-ordinates for left DLPFC. These were taken from four studies from the visual consciousness and perceptual decision-making literature.

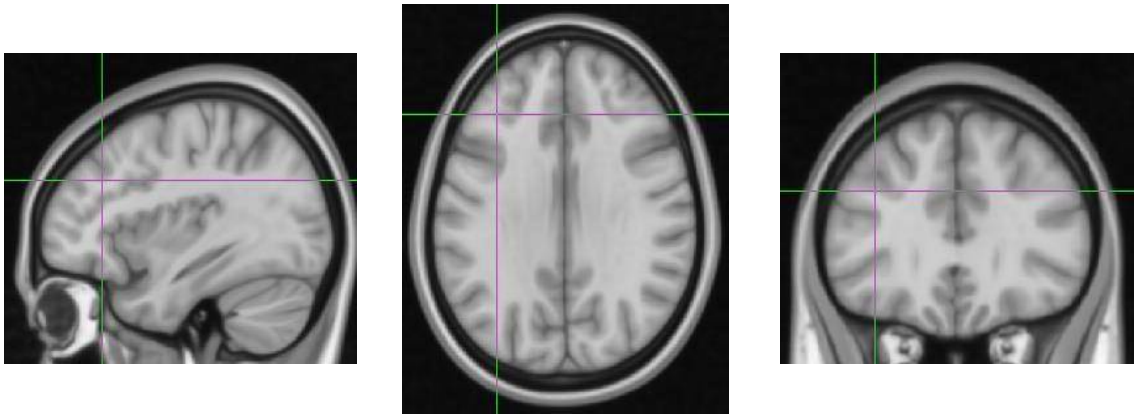

Figure 3.Mean MNI co-ordinates presented on an MNI template brain which will be used to target the left DLPFC in the coronal (left), axial (middle) and sagittal (right) planes.

2.4 Statistical analyses

A biphasic Gaussian model was applied to each participant's ΔPr and ΔAcc data separately as a function of each TMS site to identify whether the temporal position of EVC and left DLPFC TMS-induced effects differ from one another. Such a model has been shown to detect whether TMS-induced effects have taken place at two *phases* (e.g. Stevens et al., 2008; Rusconi et al., 2013; Chambers et al., 2013), which can then be separated as a function of time. A biphasic Gaussian model is the sum of two Gaussian functions:

$$y = y_0 + a_1 e^{\left[-\left(\frac{x - x_1}{b_1}\right)^2\right]} + a_2 e^{\left[-\left(\frac{x - x_2}{b_2}\right)^2\right]}$$

Each model produces 7 coefficients which were used to understand the data. a_1 and a_2 refer to the peak amplitude of the first and second phase of the Gaussian, respectively. Amplitude coefficients can be used to understand the *magnitude* of a TMS-induced effect on ΔPr and ΔAcc, which can be used to establish if TMS has affected performance. If the amplitude coefficients support that a TMS-induced effect has taken place. x_1 and x_2, refer to the temporal position of *a1* and *a2,* respectively, reveal when these effects arise as a function of time. b_1 and b_2, refer the bandwidth of the first and second phase of the Gaussian, respectively, which can be used to understand the *duration* of the

TMS-induced effect *a* at time *x. y0* refers to the intercept of the model, which refers to the effect of overall effect of TMS on performance across all SOAs. The term *first phase* will denote a_1 or b_1 that occurs with at the *earliest* temporal position, x_1, whereas the term *second phase* will denote a_2 or b_2 that occurs at the *latest* temporal position, x_2. The presence of two phases within each model will mean that a minimum of one and a maximum of two TMS-induced effects on ΔPr or ΔAcc can be detected as a function of applying TMS to each site. The biphasic Gaussian model was fitted to ΔPr and ΔAcc as a function of EVC and left DLPFC TMS SOA with the following constraints:

1. $a_{1\&2}$ > the absolute difference between the first and second smallest ΔPr or ΔAcc scores obtained across all 10 TMS-SOAs.
2. $a_{1\&2}$ < the absolute difference between the first and second largest ΔPr or ΔAcc scores obtained across all 10 TMS-SOAs.
3. $x_1 < x_2$, which prevented the temporal position of the second Gaussian peak from occurring earlier in time to the temporal position of the first Gaussian peak.
4. $b_{1\&2}$ > 10ms, which prevented the bandwidth of the first and second Gaussian phases falling below 10ms.
5. $b_{1\&2}$ < 380ms, which prevented the bandwidth of first and second Gaussian phases exceeding 380ms.
6. *y0* > lowest ΔPr or ΔAcc score & *y0* < highest ΔPr or ΔAcc score, which prevented the intercept of the model falling below the lowest ΔPr or ΔAcc score or exceeding the highest ΔPr or ΔAcc score, respectively.

The following starting points were used for each of the coefficients of the biphasic Gaussian model:

1. $a_{1\&2:}$ --0.5, 0 and 0.5.
2. $x_{1\&2}$: 0.07, 0.13, 0.19, 0.25 and 0.31.
3. $b_{\&2}$: 0.1, 0.19 and 0.28.
4. *y0: 0*

All combinations of these starting parameters for each of these coefficients were applied to ΔPr and ΔAcc as a function of EVC-TMS and left DLPFC-TMS. These coefficients formed the basis for two analyses: a group analysis (GAn) and a subgroup analysis (SGAn), which were applied to ΔPr and ΔAcc separately. Both the GAn and SGAn had the same aim: to identify whether the temporal position of an EVC TMS induced effect on performance differs from the temporal position of a left DLPFC TMS induced effect on performance. The GAn was split into two parts: GAn-1, which assessed whether the peak amplitude coefficients reflected TMS-induced effects at *the group level*; and GAn-2, which had the aim of identifying whether the temporal position of the EVC TMS effects occured earlier or later in time than the timing of the left DLPFC TMS effects *at the group level*. GAn-2 only proceeded if GAn-1 identified at least one set of peak amplitude coefficients *for each TMS site* provide support for a TMS-induced effect on performance.

The SGAn was also applied to ΔPr and ΔAcc separately as a function of TMS site. The first stage of the SGAn screened whether *individual participant's* peak amplitude coefficients reflect TMS-induced effects on ΔPr and ΔAcc*.* Previous research has revealed that splitting data sets from brain stimulation experiments into subgroups, such as 'responders' and 'non-responders' (Fregni, Marcondes, Boggio, Marcolin, Rigonatti, Sanchez, Nitsche & Pascual-Leone, 2008), is a useful method when determining whether an effect of brain stimulation is present. The division of data into subgroups where response is present is particularly useful when inter-subject variability is present within a data set (Tremblay, Larochelle-Brunet, Lafleur, Mouderrib, Lepage & Theoret, 2016). In this experiment, inter-subject variability may manifest itself in terms of the presence of a TMS-induced effect on performance. The division of participants into subgroups may enable 'responders' who exhibit EVC and DLPFC-TMS induced to be segregated from 'non-responders', who do not exhibit such effects. Such division could reduce inter-subject variability and enable the temporal onset of an EVC-TMS effect to be distinguished from the temporal onset of a DLPFC-TMS effect. Pre-registration of such a procedure also prevents 'cherry picking' of results that meet a *post-hoc* criteria, which may produce a false positive significant result. If at least one TMS induced effect

was present at the individual participant level *for both sites*, the participant will qualified for inclusion within the SGAn. The SGAnl then identified whether the temporal position of an EVC TMS-induced effect differed from the temporal position of a left DLPFC TMS-induced effect in a subgroup of participants who qualified for the SGAn. The pre-registered SGAn then compared those who had EVCx_1 a_1 coefficients and DLPFCx_1 a_1 coefficients that qualified for inclusion and an additional, separate comparison of EVCx_1 a_1 coefficients to DLPFCx_2 a_2 coefficients that qualified for inclusion.

2.4.1: Group analyses

The GAn contained ΔPr and ΔAcc coefficients from all participants who completed the experiment. The GAn will was carried out once completed once groups of 8 participants had completed a balanced Latin square, which ensured that all participants had undergone counterbalancing. Thus, the GAn was applied after 8, 16, 24 and 32 participants had been tested. The GAn was applied to ΔPr and ΔAcc separately. A flowchart illustration of the GAn can be found in Figure 4. The first stage of the GAn (GAn-1) applied a Bayesian one-sample t-test with a JZS prior with the default scaling factor of 0.707 (Rouder et al., 2009) to the first and second phase amplitude coefficients for ΔPr and ΔAcc as a function of EVC and left DLPFC TMS. The GAn-1 identified whether the Bayes factor (*BF)* provided evidence for a TMS-induced effect on performance (*BF* > 3, supporting the experimental hypothesis) or evidence for no TMS-induced effect on performance (*BF* < 1/3, supporting the null hypothesis) for the ΔPr *or* ΔAcc peak amplitude coefficients. The *BF* from GAn-1 established whether active TMS has produced an effect on performance relative to sham TMS for either measure, which determined whether the GAn proceeded further.

The second stage of GAn (GAn-2) only proceeded if GAn-1 established that a TMS-induced effect was present as a function of EVC *and* left DLPFC TMS for at least one of the measures. The aim of GAn-2 was to establish whether EVCx_1 occurs earlier in time than DLPFC$x_{1\&2.}$ The GAn-2 only contained the temporal position coefficients (x_1 or x_2) that corresponded to the peak amplitude coefficients (a_1 or a_2) that produced a *BF* that is more than 3. If both measures indicated that a TMS-induced effect was present, the GAn-2 was carried out separately on both measures. If one measure

provided evidence for an EVC-TMS effect and the other measure provided evidence for a left DLPFC-TMS effect, GAn-2 did not proceed. However, if an effect was present as a function of EVC and left DLPFC TMS on the same measure, the GAn-2 proceeded. A Bayesian one-sample *t*-test with a uniform prior (Dienes, 2011) was used to identify whether DLPFC*x* occurs after EVC*x* when ΔPr is used as a measure. In the document that was pre-registered on the Open Science Framework, a Bayesian one-sample *t*-test with a JZS prior with a scaling factor of 0.707 was proposed to compare EVC*x* to DLPFC*x* when ΔAcc is used as a measure whereas a Bayesian one-sample *t*-test with a JZS prior (Rouder et al., 2009) will be used when ΔPr is used as a measure . However, an amendment was made here whereby the same uniform prior that was used for GAn-2 for was applied to ΔPr as a function of EVC-TMS and left DLPFC-TMS. The uniform prior will be a distribution of mean differences between EVC*x* and DLPFC*x* that could be obtained when applying TMS to both sites at SOAs ranging from 60ms to 330ms. Previous TMS research has revealed a well-established EVC TMS effect at an SOA of ~100ms (Kammer, 2007; de Graaf et al., 2014). In contrast, it is difficult to predict when a left DLPFC TMS effect will arise as a function of time because few single-pulse left DLPFC TMS studies have been conducted. As a result, a uniform prior distribution (Dienes, 2011) was used to establish the temporal position of a left DLPFC TMS effect arises before or after the well-established EVC TMS effect at ~100ms. A uniform prior was chosen because it assumes that all mean differences between EVC*x* and DLPFC*x* are equally likely, as it is not known when a left DLPFC TMS effect will emerge in this experiment.

The hypothesis testing that EVC*x* differs from DLPFC*x* involved subtracting each participant's temporal position of the EVC TMS effect from their corresponding temporal position of the left DLPFC TMS effect. The temporal position coefficients that were selected corresponded to the phase that was supported as a TMS-induced effect by the GAn-1. There are two analyses that could be carried out in the GAn-2. If EVC TMS α_1 and DLPFC α_2 were supported as TMS-induced effects by the *BF*, EVC x_1 will be subtracted from DLPFC x_2. Also, if the *BF* supports that EVC α_1 and DLPFC α_1 were affected by TMS, EVC x_1 will be subtracted from DLPFC x_1.The outcome of the subtractions was used

to identify whether EVC*x* occurs before, after or at the same time as DLPFC*x* with a one-sample *t*-test with a uniform prior (Dienes, 2011). If the outcome is positive, the *BF* will support that DLPFC*x* occurs after EVC*x* and if the outcome is negative, the *BF* will support that DLPFC*x* occurs before or at the same time as EVC*x*. One of the advantages of using Bayesian statistics here is that the *BF* can also support whether EVC*x* and DLPFC*x* occur at the same time. GAn-2 will be applied to all the temporal position coefficients that accompany significant peak amplitude coefficients in GAn-1.

The prior distribution had pre-registered lower and upper limits, which described the plausible differences between EVC*x* and DLPFC*x* that could be obtained when applying TMS across the SOAs that were used in the proposed study (Dienes, 2011). These limits were influenced by the well-established EVC TMS effect that can be expected at ~100ms and the latest TMS-SOA that was used in the proposed study. The upper limit was the maximum difference between EVC*x* and DLPFC*x* that could be obtained if DLPFC*x* occurs *after* the well-established EVC TMS effect at an SOA of ~100ms (de Graaf et al., 2014). The latest time point where DLPFC*x* could be produced is 330ms, which was the latest TMS SOA in the experiment. The upper limit – the highest plausible difference between EVC*x* and DLPFC*x* - is 230ms (330ms – 100ms), which is the product of subtracting the expected temporal position of an EVC-TMS effect subtracted from the latest temporal position where a left DLPFC-TMS effect can be produced. The upper limit of 230ms specified the maximum mean difference that can be expected with a uniform prior (Dienes, 2011). The lower limit of the prior, on the other hand, was 0ms, because it is possible for EVC*x* and DLPFC*x* to occur at the same time. If EVC*x* and DLPFC*x* occur at the same time, the mean difference between the two sets of temporal position coefficients will be distributed around zero.

2.4.2: Subgroup analyses

The SGAn was carried out on a subgroup of participants who exhibited at least one *a* coefficient from each measure for *both* sites that could be considered a TMS-induced effect. The SGAn was carried out after groups of 8 participants had completed a balanced Latin square, which ensured that all participants have undergone counterbalancing. Thus, the SGAn was applied after 8,

16, 24 and 32 participants had been tested. A flowchart illustration of how the SGAn proceeded can be found in Figure 5. The first stage of the SGAn, SGAn-1, began by screening each participant's ΔPr or ΔAcc data for EVC and left DLPFC TMS-induced effects. Screening involved a *z* score between their individual ΔPr or ΔAcc *a* coefficients and a *z* distribution based on their performance during sham trials (see Allen, 2013, for a similar application). For ΔPr or ΔAcc as a function of EVC TMS, the *z* distribution was formed using their ΔPr or ΔAcc data, respectively, as a function of sham EVC TMS. For ΔPr or ΔAcc as a function of left DLPFC TMS, the *z* distribution was formed using their ΔPr or ΔAcc data, respectively, as a function of sham left DLPFC TMS.

The aim of the SGAn was to identify whether the a_1 and a_2 coefficients quantified effects of EVC or DLPFC TMS on ΔPr. For the SGAn on ΔPr, a sham *z* distribution was created for each participant by subtracting 0.5 from the mean of their sham data across SOAs. A value of 0.5 was chosen because Pr was calibrated to 0.5 throughout the experiment based on Pr on EVC and left DLPFC sham blocks. This subtraction took place to create a distribution of scores that would be expected if performance as a function of active TMS SOA was approximately equal to performance as a function of sham TMS-SOA for each site. If such an outcome took place, Pr as a function of active TMS and sham TMS should both equal ~0.5 (due to luminance calibration) and should be distributed in a similar way. When sham TMS is subtracted from active TMS and both scores are ~0.5, the difference between them at each SOA would be approximately zero. Correspondingly, the a_1 and a_2 coefficients would also be approximately zero to quantify such an effect. Calculating a *z* score using a distribution that would be expected if ΔPr was approximately zero and the a_1 and a_2 coefficients reveals whether the coefficients differ from what would be expected if no difference between active and sham TMS existed across SOAs. If no difference between active and sham TMS exists across SOAs, a_1 and a_2 would be approximately zero, suggesting that an active TMS effect of the largest magnitude at a given SOA is negligible. Moreover, if performance as a function of active TMS is no different to performance as function of sham TMS, performance across all active TMS SOAs should be distributed in a similar way to performance across all sham TMS SOAs. However, if a

TMS effect is present at a discrete temporal position, performance as a function of active TMS will differ from performance as a function of active TMS. An active TMS-induced effect is most likely to occur due to a decrease in performance relative to sham TMS which peaks at a particular SOA (de Graaf et al., 2014). Under these conditions, the a_1 and a_2 coefficients of the biphasic Gaussian models will differ from the distribution of scores produced as a function of sham TMS. Moreover, under these conditions a *z* score between the peak amplitude of the Gaussian model and the distribution of scores as a function of sham TMS should reach statistical significance by the *z* score producing a *p* value that is less than 0.05

A participant's data qualified for the SGAn if the *z* score between their at least one of their a_1 or a_2 coefficients as a function of EVC and left DLPFC TMS significantly differ from their respective sham *z* distributions by producing a *p* value that is less than 0.05. A participant qualified for the SGAn if they exhibited significant a *z* score for at least one measure as a function of TMS for both sites. If this screening procedure supported an effect of EVC TMS on one of the measures and supports an effect of left DLPFC-TMS on the other, the participant did not qualify for inclusion in the SGAn. In contrast, if this screening procedure supported an effect of EVC-TMS and left DLPFC-TMS on the *same* measure, the participant qualified for inclusion in the SGAn. Subsequently, the second stage of the SGAn, SGAn-2, was carried out. The SGAn-2 on ΔPr involved a Bayesian one-sample *t*-test with a uniform prior (Dienes, 2011) with the same upper and lower prior limits as the GAn. It was pre-registered that the comparison of EVC*x* and DLPFC*x* in the SGAn-2 on ΔAcc would involve a Bayesian one-sample *t*-test with a JZS prior with a scaling factor of 0.707 (Rouder et al., 2009). However, an amendment was made and a Bayesian one-sample *t*-test with a uniform prior was applied. The upper and lower limits of the uniform prior were identical to the upper and lower limits that were applied to the pre-registered uniform prior in the GAn-2and SGAn-2.on ΔPr. There were two different comparisons that could take place in the SGAn-2 based on the a_1 or a_2 coefficients that qualified for inclusion. The first comparison compared EVCx_1 to DLPFCx_1 and the second compared EVCx_1 to DLPFCx_2.

2.4.3: The GAn, SGAn and the decision to terminate data collection

A number of different outcomes were pre-registered which could terminate data collection. It was pre-registered that data collection would continue until the GAn-1 produces moderate support for the presence of a TMS-induced effect for one site but moderate support for the absence of a TMS-induced effect for another. If such an outcome took place, it would mean that the GAn-2 could not be carried out because an effect of TMS would only have been obtained for one site. Data collection would also have terminated if a *BF* that is less than 1/3 or a *BF* that is more than 3 was obtained for the Bayesian one-sample *t*-test in the GAn-2 on ΔPr, which would quantify moderate evidence for or against the hypothesis that DLPFCx_1 or DLPFCx_2. A final stopping rule was determined by 32 participants being tested, which was feasible according to our simulations.However, Bayesian one-sample *t*-test with a JZS prior were also applied to the α_1 and α_2 coefficients as a function of EVC- and DLPFC-TMS after 8, 16, 24 and 32 participants were included within the analysis. A Bayesian one-sample test was completed incrementally after increasing the number of participants to enable data collection to terminate if one of *BF*s produced evidence for the absence of a TMS effect. For example, it is feasible that the *BF* could be inconclusive after testing 8 and 16 participants but then subsequently producd conclusive evidence for the absence of an effect after testing 24 participants. This procedure would enable data collection to continue until conclusive evidence for the absence of an effect is found and subsequently enable the experiment to terminate. The experiment would terminate because the later analyses on x_1 and x_2 coefficients were contingent on EVC and DLPFC-TMS effects being present. Data collection in this experiment terminated because 32 participants were tested. It must also be noted that an amendment to the stopping rule took place. Initially, it was pre-registered that the outcome of the SGAn could also influence the decision to terminate data collection. However, throughout the course of data collection it was decide to consider the SGAn as exploratory and base the decision to terminate data collection prior to reaching 32 participants based on the GAn alone. This amendment was made to guarantee that as many participants as possible were included in the first comparison of the critical time course of EVC and left DLPFC.

2.5: Exclusion criteria

Any participants whose screening procedure indicated an elevated risk of seizure or other mild or major adverse effects as a result of TMS were excluded from the experiment, which meets the ethical approval standards set out by the ethics committee at the School of Psychology, Cardiff University (also see Maizey, Allen, Dervinis, Verbruggen, Varnava, Kozlov, Adams, Stokes, Klemen, Bungert, Hounselkl & Chambers, 2013; Wassermann, 1998). Participants who exhibited any of the following were also excluded:

1. Participants who do not report phosphenes.
2. Participants who have experienced an adverse reaction to TMS that warrants exclusion (see Maizey et al., 2013)
3. Participants whose FPT is greater than 180% of their motor threshold.
4. Participants who do not find the application their FPT to left DLPFC or EVC uncomfortable or exhibit uncomfortable facial twitches throughout active TMS blocks .
5. Participants blink after the offset of an active TMS pulse on 40% or more of trials, then the participant's data was not included into the GAn and SGAn.
6. Participants whose movement requires coil repositioning (see section 2.3) on 50% or more of active TMS blocks
7. If any technical difficulties are encountered which lead to a participants data set becoming compromised, their data will not be included in the GAn and SGAn.
8. Any participant data that has been collected will be excluded from the GAn and SGAn once one of these analyses produces support for the null or experimental hypothesis.

Four participants were excluded from the experiment in total. One of these participants was unable to report the presence of phosphenes throughout the PT procedure and the remaining four were excluded because participants blinked on 40% or more of trials

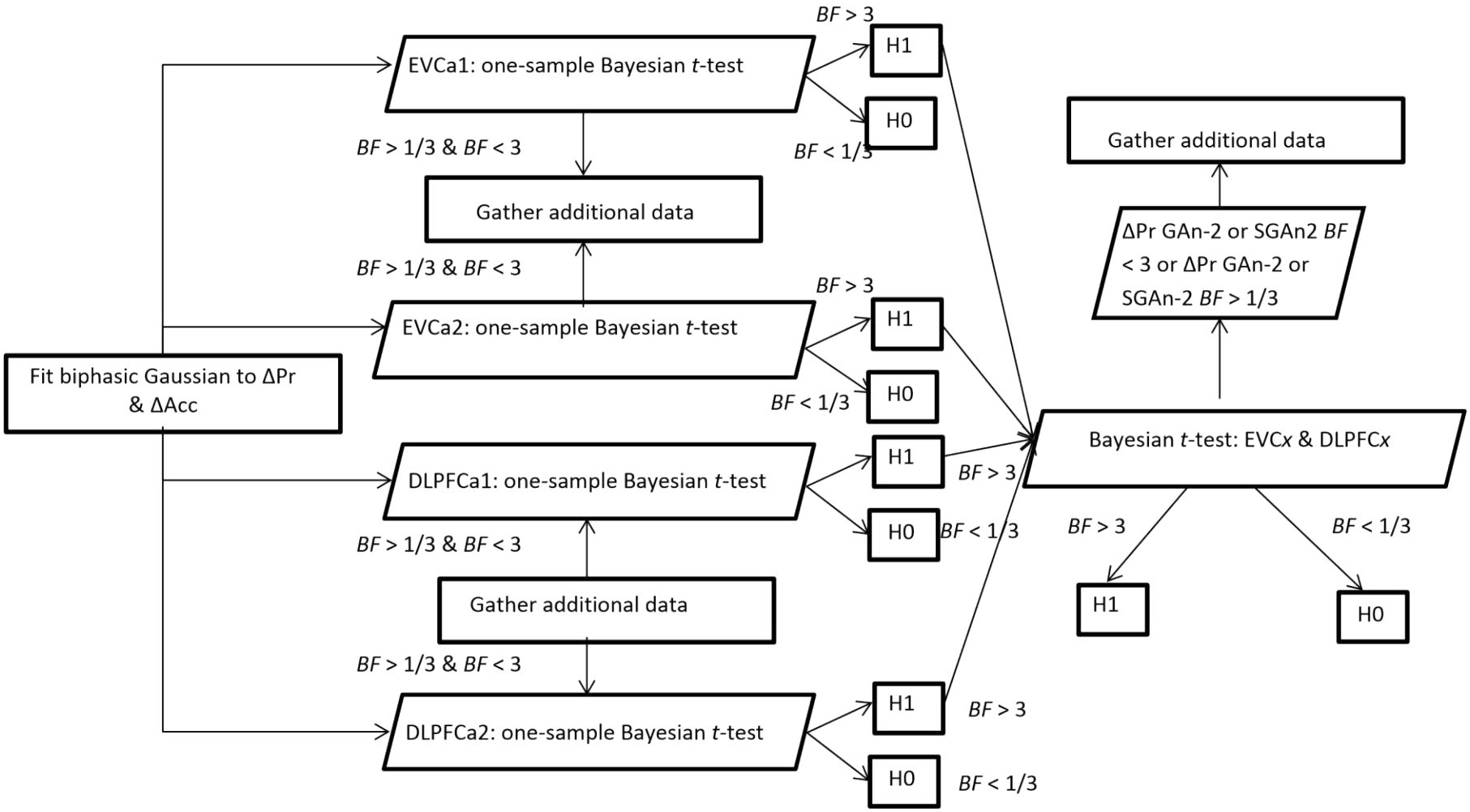

Figure 4. Flowchart illustration of how the group analysis (GAn) will proceed. Firstly, a biphasic Gaussian was separately fitted to each participant's ΔPr and ΔAcc data. The first stage of the GAn applied a Bayesian one-sample *t*-test with a JZS prior (Rouder et al., 2009) to the peak amplitude coefficients belonging to each phase of the biphasic Gaussian obtained from all participants. The first stage of GAn was applied separately to ΔPr and ΔAcc as a function of TMS to each site. This Bayesian *t*-test assessed whether the peak amplitude of a TMS-induced effect significantly differed from zero. A value of zero means that TMS has produced no effect on ΔPr or ΔAcc. Data collection aimed to obtain a Bayes factor *(BF)* that moderately supports the null (*BF* < 1/3) or experimental hypotheses (*BF* > 3) for an effect of TMS on ΔPr. If the *BF* moderately supported an effect of TMS on at least one phase for both sites *on the same measure*, the GAn proceeded to the second stage. If the *BF* moderately supported that no effect of TMS is present on both phases for one site and substantially supported an effect for at least one phase for the other site, the GAn did not proceed any further. The second stage in the GAn, GAn-2, on ΔPr and ΔAcc involved a Bayesian one-sample t-test with a uniform prior (Dienes, 2011). Both Bayesian tests were applied to the temporal positions of the statistically significant peak amplitude coefficients from EVC TMS and DLPFC TMS obtained from all participants. Data collection would have continued until a *BF* that moderately supports the null (*BF* < 1/3) or experimental hypotheses (*BF* > 3) is produced by the GAn or SGAn on ΔPr. Data collection terminated once a feasibility limit of testing (32 participants) has been reached due to the expiration of PhD funding.

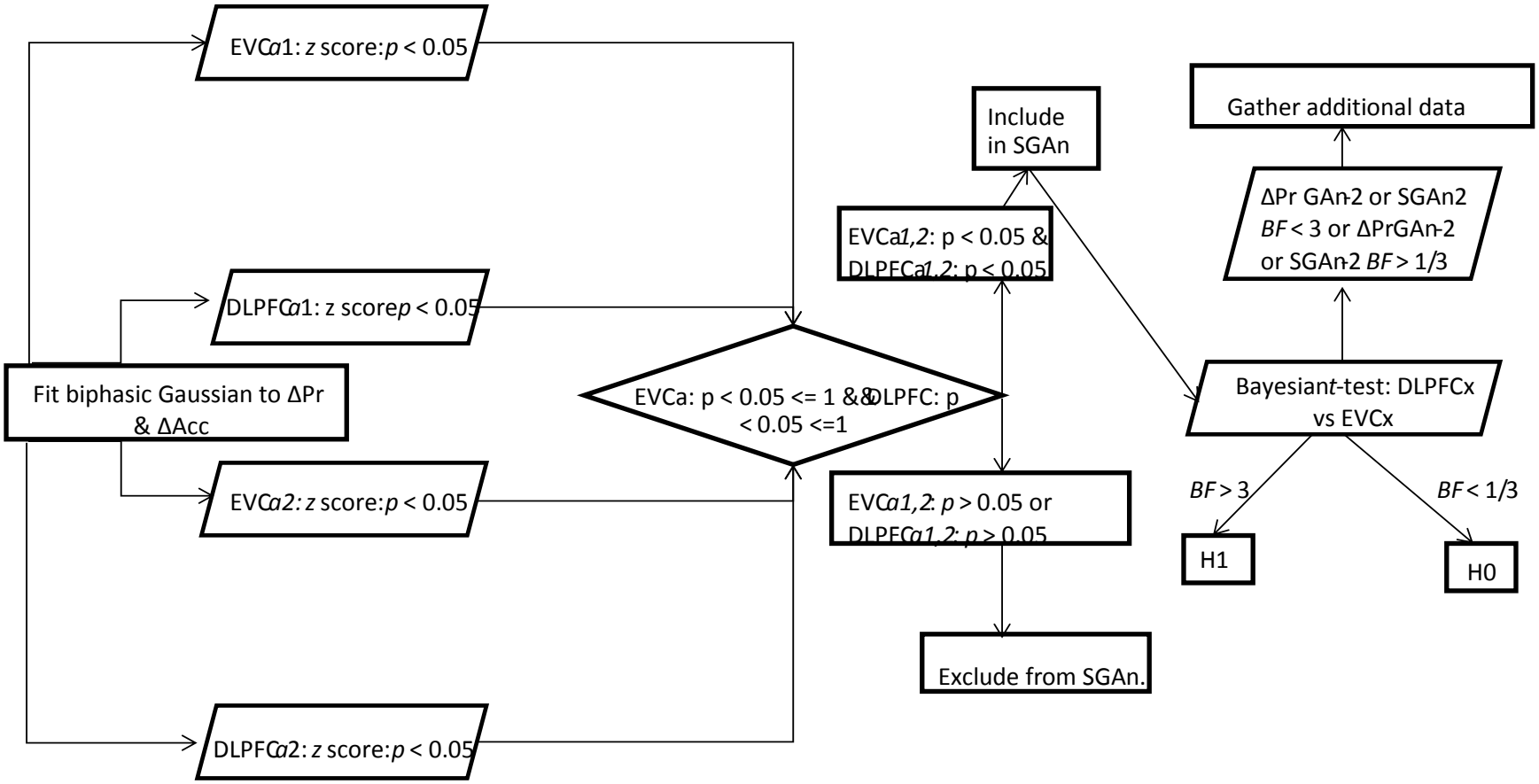

Figure 5 Subgroup analysis (SGAn): Firstly, a biphasic Gaussian was separately fitted to each participant's ΔPr and ΔAcc data. The first stage of the SGAn, SGAn-1, calculated a *z* score between each peak amplitude coefficient from each site and a sham *z* distribution for each site. The variance of these values at each SOA was the same as the participant's individual variance exhibited during sham EVC and sham DLPFC TMS, respectively. If the *z* score produced a *p* value that was less than 0.05 for at least one phase *for both sites with the same measure*, the participants phases that contaiedn the significant peak amplitude coefficients qualified for inclusion within the next stage of the SGAn. This screening procedure was completed separately for ΔPr and ΔAcc. In doing so, SGAn-1 created a subgroup of participants whose ΔPr and ΔAcc data contained evidence for EVC *and* DLPFC TMS-induced effects. The next stage, SGAn-2, was also applied to ΔPr and ΔAcc separately and it was only be applied to the participants who pass GAn-1. If their ΔPr data was successfully screened, it did not mean that their ΔAcc also successfully passed the screening procedure and vice versa. The SGAn-2, on ΔPr dentified whether the temporal position of the successfully screened EVC and DLPFC TMS-induced effects within this subgroup significantly differ from one another using a Bayesian one-sample t-test with a uniform prior (Dienes, 2011). The SGAn-2 on ΔAcc applied a Bayesian two-sample t-test with a JZS prior (Rouder et al., 2009). Data collection continued until a feasibility limit oif testing 32 paticipants was reached.

3. Pilot Data

3.1: Overview

The first part of this section contains pilot data produced by for the TMS experiment. The second part of this section contains pilot data which is behavioural only with no TMS, which was gathered prior to the TMS pilot experiment. The aim of this section was to compare Acc and Pr as measures of performance and to determine the number of trials that would be required at each TMS-SOA. ΔPr and ΔAcc data and the corresponding biphasic Gaussian models as a function of EVC- and left DLPFC-TMS SOA at the individual participant and at the group level are presented. These plots aimed to illustrate how the biphasic Gaussian model may capture performance across the range of TMS-SOAs that will be used in the proposed study. This pilot data is being shown because it was also used to generate simulated data to investigate the likely outcomes of the experiment and to identify the Bayesian prior distributions that would be most sensitive to the predicted outcomes. The selection of a prior for the proposed study was not straightforward because no single pulse left DLPFC TMS studies have revealed the critical time course of left DLPFC in a basic visual detection task. For this reason, we identified which of two priors, a JZS prior (Rouder et al., 2009) and a uniform prior (Dienes, 2011), produced a *BF* that was most sensitive to the presence and absence of simulated difference between EVC*x* and DLPFC*x* as measured by ΔPr and ΔAcc. Carrying out this procedure enabled the structure of the analysis and the Bayesian statistical tests that will be applied to be decided upon, verified and pre-registered before data collection commences. Not only did the use of simulations enable selection of an appropriate prior-probability distribution, it also enabled the feasibility of such a prior-probability distribution to provide evidence for or against a hypothesis with a feasible number of participants. This is critical, as no experiment that we were aware of had applied single pulses of TMS to left DLPFC so it is uncertain whether it is feasible to test hypotheses related to effects of left DLPFC-TMS on performance. It is also uncertain whether it is also feasible to assess how the temporal onset of left DLPFC-TMS effects relate to the temporal onset of EVC-TMS effects. The pre-registered hypotheses required both of these conditions to be met, yet is is

uncertain whether it feasible to expect both of these conditions to be met. Thus, simulations were carried out to assess whether it is feasible to expect these conditions to be met *a priori* with a feasible number of participants.

Additionally, the second part of this section contains pilot data which was used to assess the use of Pr and Acc as measures of a participant's ability to indicate the presence or absence of a target. This took place *before* data collection began for the pilot data revealed in this section. These two measures are distinct from one another. Pr is calculated by subtracting a participant's false alarm rate from their hit rate. Each of these rates are calculated by combining the proportion of yes and no responses on *all* target present and target absent trials. In contrast, Acc provides an alternative measure which measures performance on a trial-to-trial basis on target present trials. Psychophysical functions are displayed which were obtained from a pilot sample to compare how each of these measures characterize performance. Simulations were also completed in order to identify how many trials each of these different measures require in order to provide an accurate measure of performance at each TMS-SOA. These simulations involved separate calculations of the standard error as a function of trial number for Pr and Acc and identifying the point where the standard error decreases and asymptotes. Identifying the point where the standard error asymptotes before data collection begins increases the likelihood of stable data points being collected at each SOA, which would improve the quality of data being simulated in this section and the quality of data collected in the experiment itself.

3.2: TMS pilot data

This section illustrates individual participant and group mean ΔPr and ΔAcc data as a function of TMS-SOA along with the corresponding biphasic Gaussian models. Figure 6 displays the ΔPr (left column) ΔAcc (right column) and the corresponding biphasic Gaussian model fits from all 3 participants. The mean biphasic Gaussian fits for ΔPr and ΔAcc as a function of EVC and left DLPFC TMS can be found in Figure 7. These plots were generated by calculating the mean of each coefficient that generated each mode across participant, which were then placed into the equation

fora biphasic Gaussian. This process was completed for both ΔPr and ΔAcc. These mean first phase coefficients– the peak amplitude that occurs at the earliest temporal position – for ΔPr and ΔAcc were then used to inform the simulations presented in the next section. The correspondence between the raw ΔPr and ΔAcc and modelled ΔPr and ΔAcc across TMS SOAs can be found in Figure 6 for EVC-TMS and left DLPFC-TMS. The correspondence between the raw mean and modelled mean ΔPr and ΔAcc across TMS SOAs can be found in Figure7. .

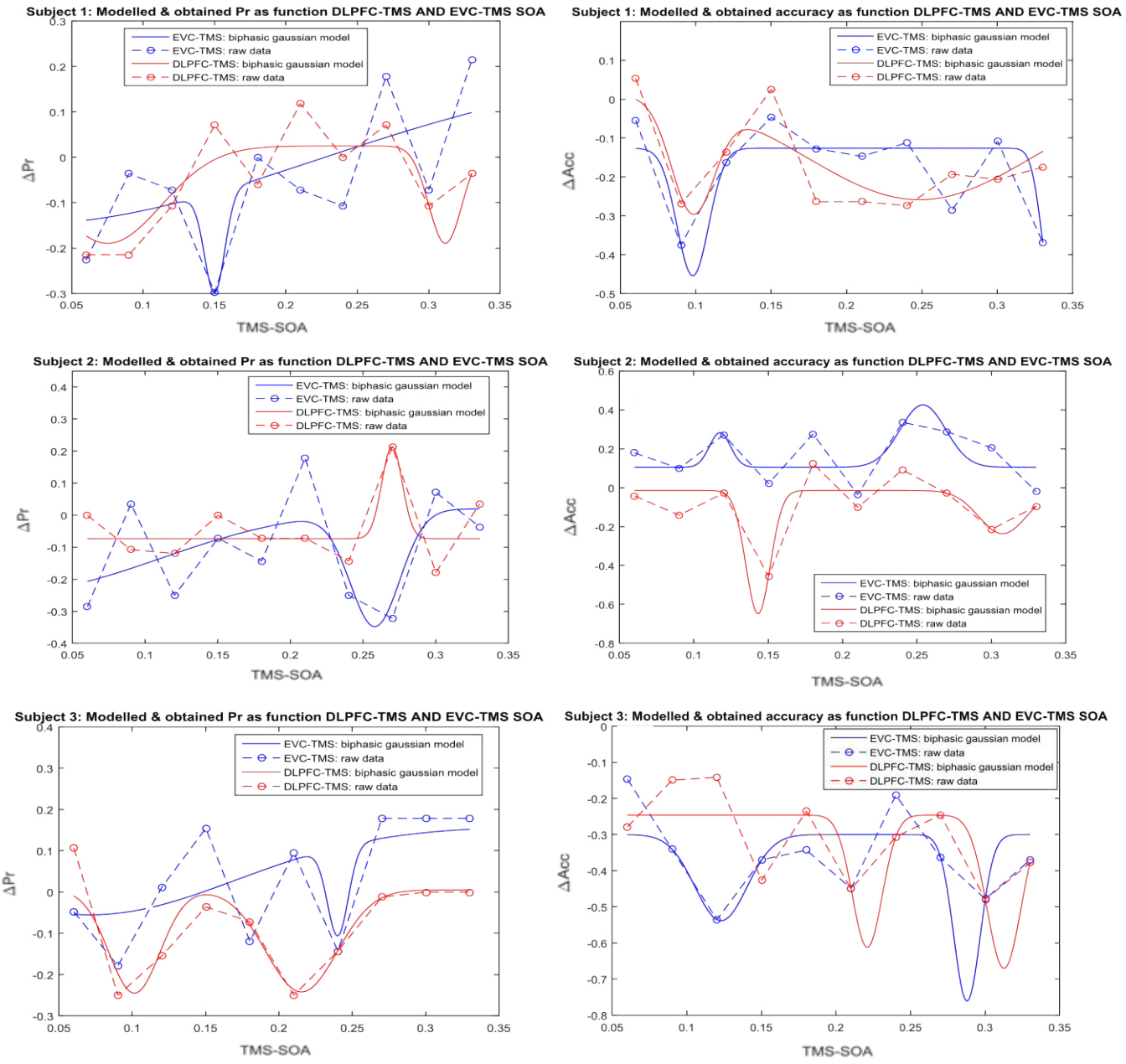

Figure 6. Biphasic Gaussian models and raw data for ΔPr as a function of EVC and left DLPFC TMS for participant 1 (top left), 2 (middle left) and 3 (bottom left). Figure 5D, 5E and 5F reveal the biphasic Gaussian models and raw data for ΔAcc as a function of EVC and left DLPFC TMS for participant 1, 2and 3, respectively.

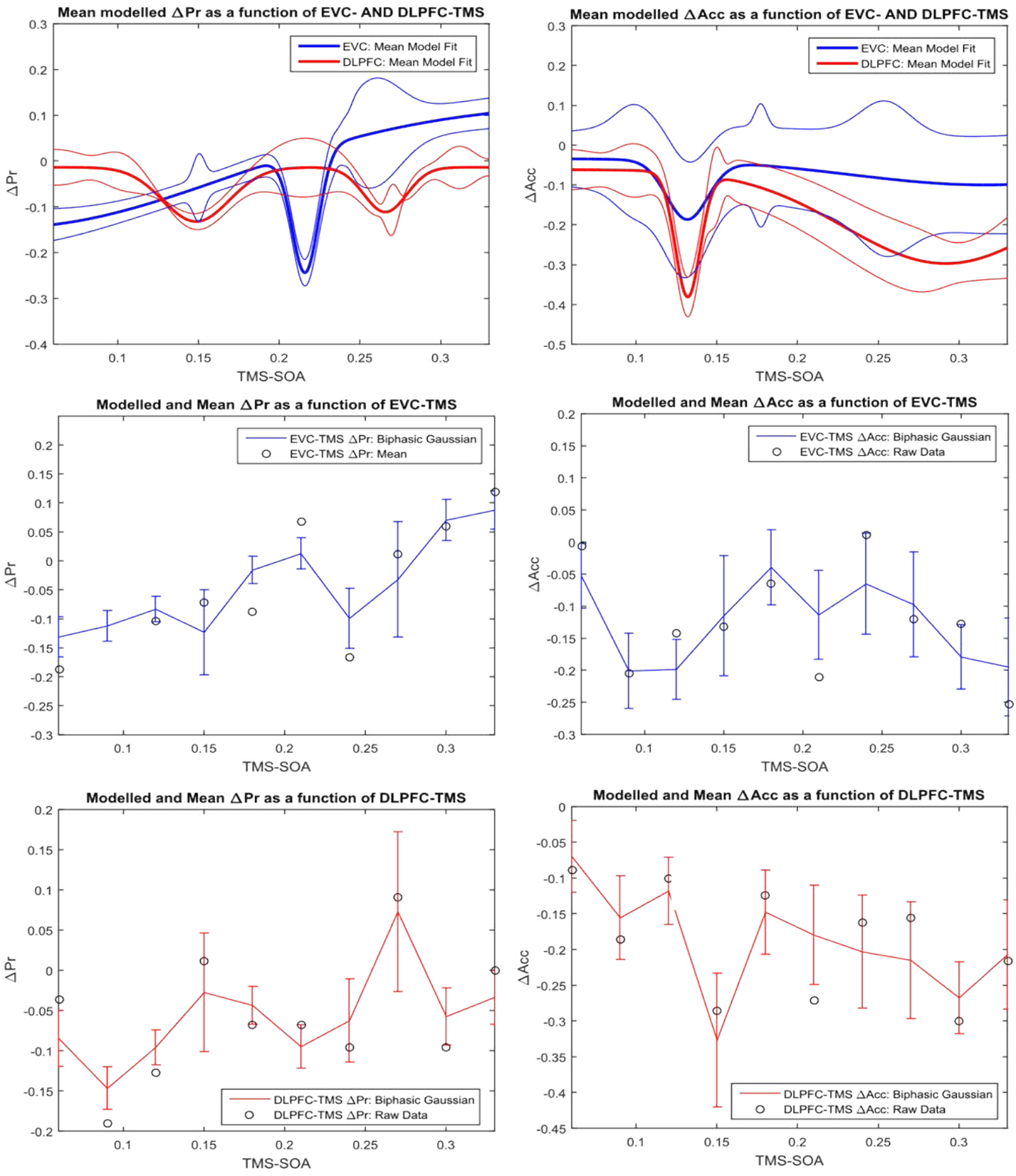

Figure 7. Top right: ΔPr as a function of EVC-TMS and left DLPFC-TMS: Thick lines represent the mean; thin lines represent the -/+ standard error. Top left: ΔAcc as a function of EVC-TMS and left DLPFC-TMS: Thick lines represent the mean; thin lines represent -/+ 1 standard error. Middle left: ΔPr as a function of EVC TMS: Raw mean and modelled mean. Error bars represent the modelled -/+ 1 standard error. Middle right: ΔAcc as a function of EVC-TMS: Raw mean and modelled mean. Error bars present the modelled -/+ 1 standard error. Bottom left: ΔPr as a function of left DLPFC-TMS: Raw mean and modelled mean. Error bars represent the -/+ 1 standard error. Bottom right: ΔAcc as a function of left DLPFC-TMS: Raw mean and modelled mean. Error bars represent the -/+ 1 standard error.

3.3.1 Simulated data and justification of Bayesian analyses: Aims

The proposed experiment aims to identify if EVC*x* significantly differs from DLPFC*x*. This section aims to investigate the likely outcomes of the experiment and to validate the GAn and SGAn as methods of addressing the aims of the proposed experiment. First of all, pilot data was collected which was then used as the basis for generating simulated data sets. The simulated data sets were then used to determine the most appropriate Bayesian statistical tests to apply to compare EVC*x* and DLPFC*x* in the GAn-2 and the SGAn-2, which aimed to reveal whether the temporal position of EVCx_1 differs from the temporal position of DLPFCx_1 and/or DLPFCx_2. The conception of a prior-distribution before data collection began was important as its parameters are subjective (Dienes, 2011). In order to decide the best way to test the pre-registered hypotheses before data collection begins, the pilot data was used to create simulated data sets that could investigate two outcomes of comparing EVCx_1 to DLPFCx_1 and DLPFCx_2. One outcome that could be expected was that the temporal position of a EVC-TMS induced effect was the same as the temporal position of the left DLPFC-TMS induced effect. Another outcome that could be expected was that the temporal position of a EVC-TMS induced effect was different from the temporal position of a left DLPFC-TMS induced effect. Both of these outcomes were simulated using the pilot data to determine the choice of Bayesian prior-distribution that is capable of producing evidence for either of these outcomes before data collection for the real experiment commenced. In order to validate these analyses, outcomes that could be expected were produced by generating separate simulated ΔPr and ΔAcc data sets based on simulated first phase coefficients produced as a function of EVC and left DLPFC TMS. All of these simulated data sets did not contain real data; these data sets were artificially produced ΔPr and ΔAcc values across all SOAs. These simulated data sets were used to answer the following questions: If EVC *and* left DLPFC TMS-induced effects on ΔPr and ΔAcc occur, which prior, a JZS (Rouder et al., 2009) or a uniform (Dienes, 2011), is most sensitive to the simulated presence and absence of a difference between EVC*x* and DLPFC*x*? As outlined previously, these simulations also assess whether it is feasible to expect an effect of EVC-TMS *and* an effect of DLPFC-TMS, as

quantified by their respectively amplitude coefficients. Moreover, effects of EVC-TMS and DLPFC-TMS are not the only hypothesis being tested here; whether the temporal onset of the DLPFC-TMS effect is after the temporal onset of the EVC-TMS effect is also under investigation. The use of simulations also enables the feasibility of both of these hypotheses to be tested *a priori*. The following sub criterions were applied to test the sensitivity of each prior:

1. When a simulated difference was absent: If both priors support the null hypothesis, which one produced a *BF* that is less than 1/3 after testing fewer participants?
2. When a simulated difference was present: If both priors support the experimental hypothesis, which produced a *BF* that was more than 3 after testing fewer participants?
3. How should the outcomes of the GAn and the SGAn on ΔPr *or* ΔAcc influence a stopping rule in the event of one of them producing support the null or experimental hypotheses?

3.3.2: Simulated data and justification of Bayesian analyses: Methods

The critical hypothesis tests that took place involved comparing one phase of the biphasic Gaussian model applied to EVC to one phase of the biphasic Gaussian model applied to DLPFC. Although the model that was applied to ΔPr and ΔAcc was biphasic, the tests which were of interest here were only concerned with the comparison of a single phase to another single phase. A biphasic Gaussian model was recruited due to interest in recurrent processing. For example, if TMS produced more than one effect across SOAs for EVC, reflecting feedforward andrecurrent processes in EVC at separate SOAs, there may be an early effect affecting feedforward processes and a later effect affecting recurrent processes. The recruitment of a biphasic Gaussian model enables these potentially discrete effects to be isolated and compared to when a DLPFC-TMS induced effect takes place. In order to identify the best approach for comparing the single constituent phases of a biphasic Gaussian across sites, simulated data based on single Gaussian models was created. A single Gaussian model was used so the comparison of one phase to another could be carried out based on simulated data

As outlined in chapter 2, the fitting of Gaussian models (in this experiment, the model is biphasic) to pilot data can be used to understand the duration (*b*), temporal position (*x*) and magnitude (*a*) of TMS-induced effects on performance. Calculating the mean and variance of each of these coefficients can be used to create distributions which identify the sort of TMS-induced effects that could be expected in a real experiment. These distributions were used to create simulated data sets for ΔPr and ΔAcc as a function of EVC-TMS and left DLPFC-TMS. Simulated data sets were generated using the mean and standard deviation of the first phase a_1 and b_1 coefficients generated from fitting a biphasic Gaussian model to ΔPr and ΔAcc as a function of EVC & left DLPFC TMS in the pilot experiment. x_1 coefficients as a function of EVC-TMS and left DLPFC-TMS were set arbitrarily to simulate the conditions when these TMS-induced effects on these sites occurred at the same time or different times. The mean of the x_1 distributions was set arbitrarily as the development of a statistical analysis that was sensitive to the presence and absence of a difference in x_1 between EVC and DLPFC was critical to the pre-registered investigation. Four simulated data sets were created. One pair simulated when EVC*x* and DLPFC*x* had the same temporal position and another pair simulated when EVC*x* and DLPFC*x* had different temporal positions. In each of these sets, EVC*x* was set at 100ms consistent which would be expected based on previous EVC-TMS research (Kammer, 2007; de Graaf et al., 2014). DLPFC*x* was set at two different values in each pair. One of the values was 100ms (the same as EVC*x*), which was done to produce conditions where EVC*x* was equal to DLPFC*x*. The other value was 220ms, which was 100ms + 120ms to simulate a 120ms mean difference between EVC*x* and DLPFC*x*. The standard deviations of the first phase EVC and DLPFC x_1 coefficients were also used in the generation of simulated data.

These means and standard deviations were used to separate generate peak amplitude, bandwidth and temporal position coefficients as a function of TMS-SOA for each site. Each of these coefficients was drawn from a normal distribution with the mean of each coefficient and the corresponding standard deviation described in chapter 2. These values were then introduced into an equation for a single Gaussian to generate ΔPr or ΔAcc scores at the TMS-SOAs that will be sampled

in the experiment, which was repeated 32 times to create data for 32 simulated participants. The equation for a single Gaussian can be found below:

$$y = y_0 + a_1 e^{\left[-\left(\frac{x - x_1}{b_1}\right)^2\right]}$$

A single Gaussian was used instead of a double Gaussian because each Bayesian *t*-test, which aimed to test whether EVC**x** significantly differs from DLPFC*x*, was only be applied to *one* phase within the biphasic Gaussian applied *to each site*. A single Gaussian model was then applied to the simulated data set to generate peak amplitude, bandwidth and temporal position coefficients for ΔPr and ΔAcc, which were then included in the GAn and the SGAn. Simulated participant coefficients as a function EVC- and DLPFC-TMS were incrementally included within the GAn and SGAn, starting with 8 participants and increasing in units of 8 to 32. After each of these increments, the GAn and SGAn were completed separately for each measure. Of critical interest here was the outcome of the simulated GAn-2 and SGAn-2, which applied a JZS prior (Rouder et al., 2009) or a uniform prior (Dienes, 2011) to test whether EVC*x* was different to DLPFC*x*.

3.3.3: Simulated data and justification of Bayesian analyses: Results

ΔPr: Difference between EVCx and DLPFCx = 0ms

Figure 8 (top left) and Figure 8 (bottom left) reveal the mean simulated ΔPr data for the ΔPr GAn and SGAn, respectively, when the difference between EVC*x* and DLPFC*x* was set at 0ms. Figure 8 (top right) reveals that the *BF* factor produced by a uniform prior was greater than that of the JZS prior, yet both provide weak support for the null after testing 32 simulated participants, which suggests that both priors are not necessarily sensitive to a the absence of a difference between EVC*x* and DLPFC*x* in the GAn. In contrast, Figure 8 (bottom left) reveals that the *BF* produced by a uniform prior in the SGAn is sensitive to the absence of a difference between EVC*x* and DLPFC*x* after testing a subgroup of 14 simulated participants who qualified for inclusion. This sensitivity to the absence of a difference was revealed by a *BF* that is less than 1/3.The *BF* produced by JZS prior, on the other hand, only produced weak support for the null after including all 14 of these simulated participants.

The outcome of these simulations is that applying a uniform prior in the SGAn appears to be the most sensitive method of assessing evidence for the absence of a difference between EVC*x* and DLPFC*x*.

ΔPr: Difference between EVCx and DLPFCx = 120ms

Figure 9 (top left) and Figure 9 (bottom left) reveal the mean simulated data that was included in the GAn-2 and the SGAn-2, respectively, when the difference between EVC*x* and DLPFC*x* for ΔPr was 120ms. Figure 9 (top right) reveals that the *BF* produced a uniform prior is more sensitive to a 120ms difference in ΔPr than a JZS prior in the GAn-2, which is evidenced by a uniform prior producing a *BF* that is more than 3 after testing all sets of simulated participants. Figure 9 (middle) reveals this difference after 8, 16 and 24 simulated participants were tested with greater resolution. Figure 9 (bottom right) also reveals that the *BF* produced by the uniform prior crosses the threshold for supporting the experimental hypothesis (*BF* > 3) at a greater frequency and with a greater magnitude than the JZS prior when the SGAn-2 is carried out on 19 simulated participants who qualified for the SGAn-2. To conclude, the outcome of the simulated GAn-2 and SGAn-2 both suggested that the uniform prior was more sensitive than the JZS prior at assessing evidence for a 120ms difference between EVC*x* and DLPFC*x* when ΔPr was used as a measure of performance.

ΔAcc: Difference between EVCx and DLPFCx = 0ms

Figure 10 (top left) and Figure 9 (top right) display the mean simulated data that was included in the ΔAcc GAn-2 and SGAn-2, respectively, when the simulated difference between EVC*x* and DLPFC*x* was 0ms. Figure 10 (top right) reveals that a uniform prior in the GAn-2 produced support for the null hypothesis (*BF* < 3) after testing 1/3 of the simulated participants that were required for the JZS prior to produce support for the null hypothesis. This demonstrates that a uniform prior was the most sensitive method of assessing the evidence for the absence of a difference EVC*x* and DLPFC*x* in the ΔAcc GAn-2. Figure 10 (bottom right) reveals that a uniform prior was also more sensitive to a 0ms than a JZS prior in the SGAn-2 as evidenced by the uniform prior

providing substantial support the null after testing 7 of the 9 simulated participants who qualified for the SGAn-2 whereas the JZS only provides moderate support for the null in one of these instances. These ΔAcc simulations suggest that GAn-2 on ΔAcc, unlike the GAn-2 on ΔPr, was the most sensitive method of assessing evidence of the absence of a difference in the GAn-2 and SGAn-2. Moreover, a uniform prior was more sensitive to the absence of a difference.

ΔAcc: Difference between EVCx and DLPFCx = 120ms

Figure 11 (top left) and Figure 11 (bottom left) display the mean simulated data for the ΔAcc GAn and SGAn, respectively, when the difference between EVC*x* and DLPFC*x* was 120ms. Figure 11 (top right) reveals that a uniform prior supports the *null* hypothesis when a simulated *difference* of 120ms exists between EVC*x* and DLPFC*x* in the GAn. The JZS prior, on the other hand, provided weak support for the *null* hypothesis in spite of a simulated difference of 120ms existing between EVC*x* and DLPFC*x* in the GAn. The lack of sensitivity demonstrated by both priors suggests that the *BF* produced by a difference between EVC*x* and DLPFC*x* using ΔAcc as a measure was not an appropriate basis for terminating data collection. Figure 11 (bottom right) reveals a similar trend in the SGAn-2, which shows both priors providing weak support the null hypothesis in spite of a simulate difference. The outcome of these simulations suggests that ΔAcc is not necessarily sensitive to simulated differences between EVC*x* and DLPFC*x*.

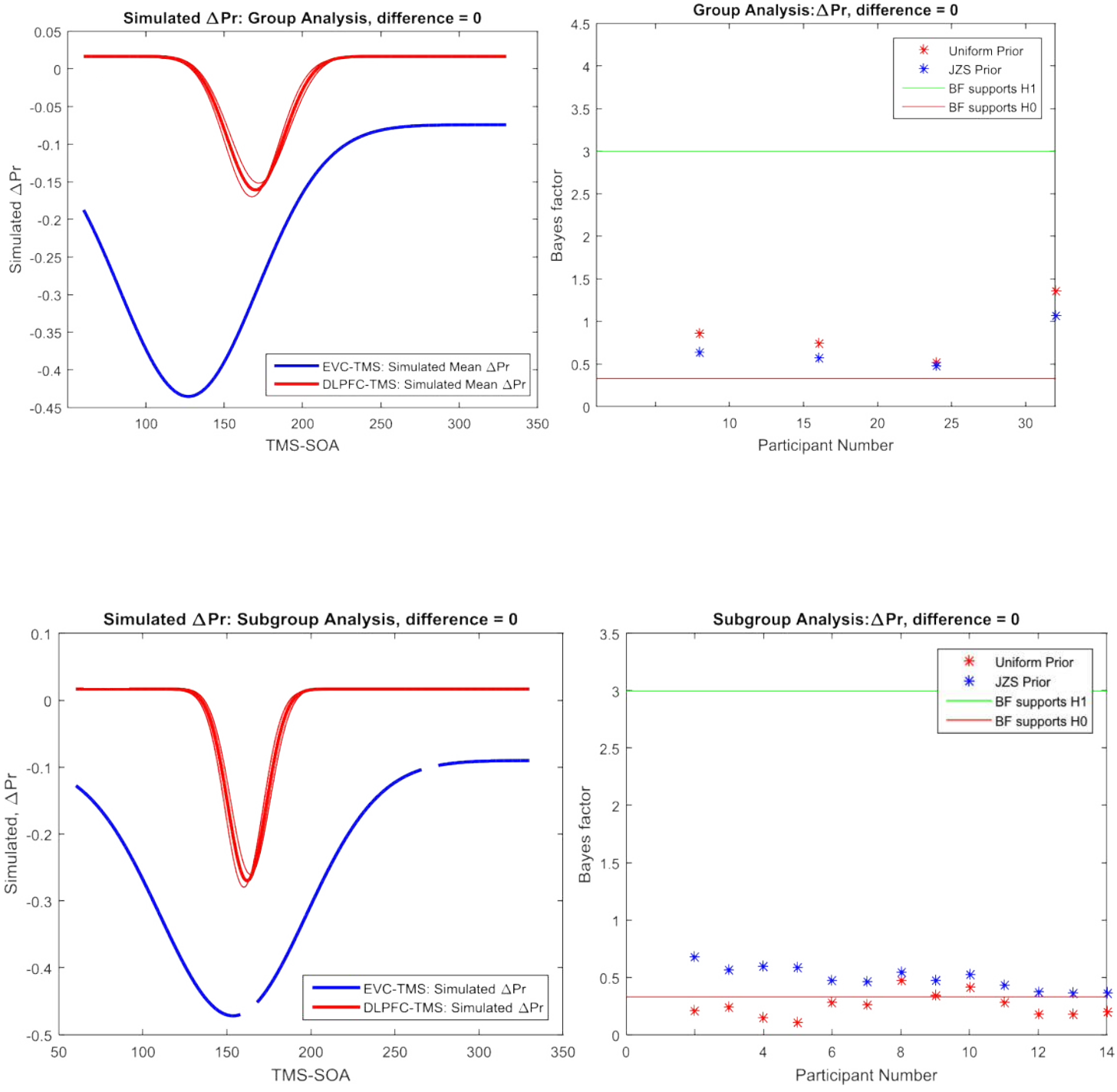

Figure 8. Top left: simulated ΔPr for the GAn-2 when the difference between EVCx and DLPFCx was 0ms. Thick lines represent the model mean; thin lines represent the -/+ 1 standard error. Top right: *BF* as a function of participant number for the GAn-2 when the difference between EVC*x* and DLPFC*x* equals 0ms. Bottom left: simulated ΔPr for the SGAn-2 when the difference between EVC*x* and DLPFC*x* equals 0ms. Thick lines represent the model mean; thin lines represent the -/+ 1 standard error. Bottom right: *BF* as a function of participant number for the SGAn-2 when the difference between EVC*x* and DLPFC*x* equals 0ms.

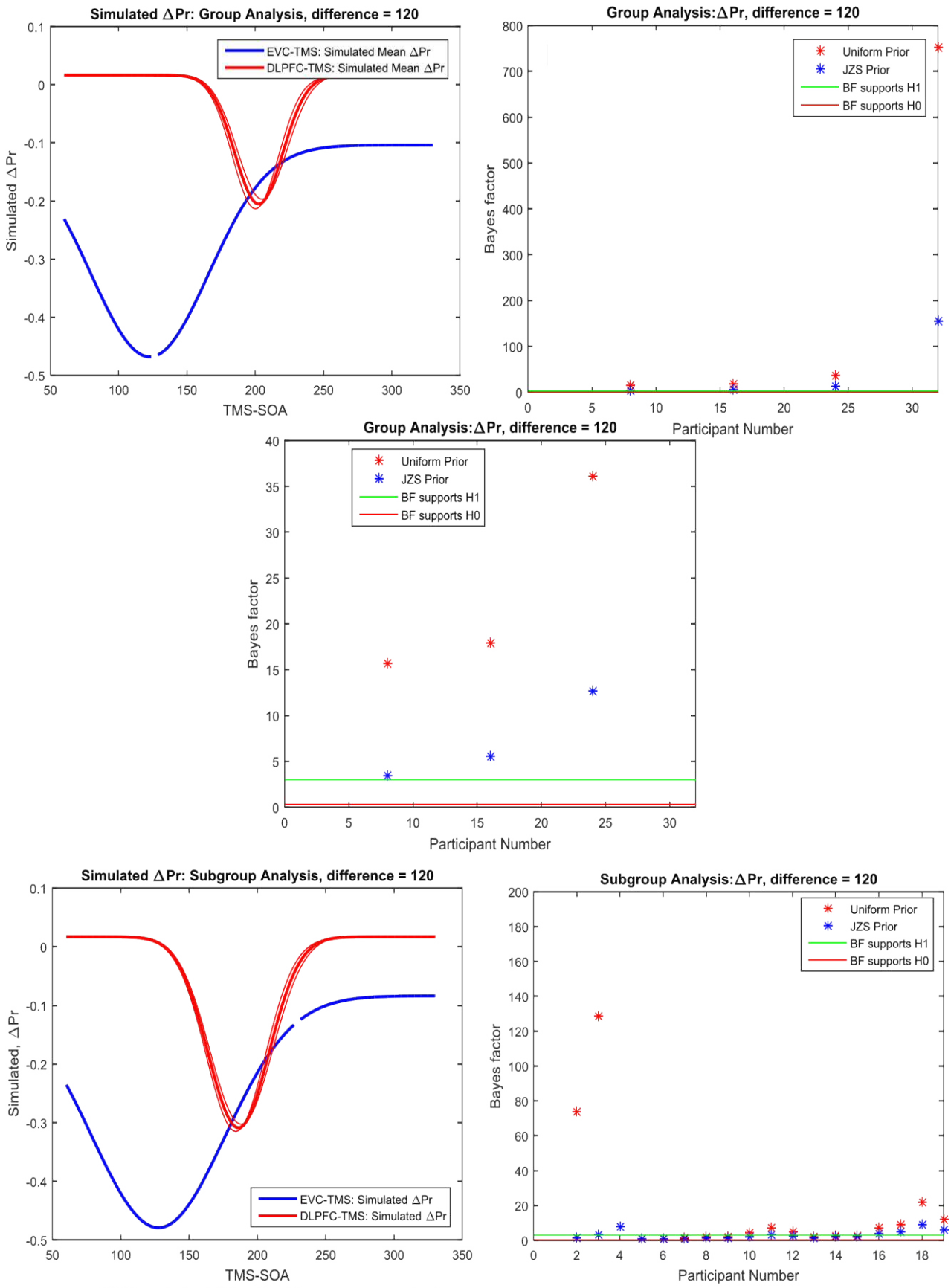

Figure 9. Top left: Simulated ΔPr for the group analysis (GAn) when the difference between EVC*x* and DLPFC*x* was 120ms. Thick lines represent the mean whereas the thin lines represent the -/+ 1 standard error. Top Right: Bayes factor (*BF*) as a function of 8, 16, 24 and 32 participants in the GAn when the simulated difference was 120ms. Middle: *BF* as a function of 16, 24 and 32 participants in the Gan when the simulated difference was 120ms. Bottom left: Simulated ΔPr for the subgroup analysis (SGAn) when the simulated difference between EVCx and DLPFCx was 120ms. Thick lines represent the mean whereas the thin lines represent the -/+ 1 standard error. *BF* as a function of participant number for the SGAn.

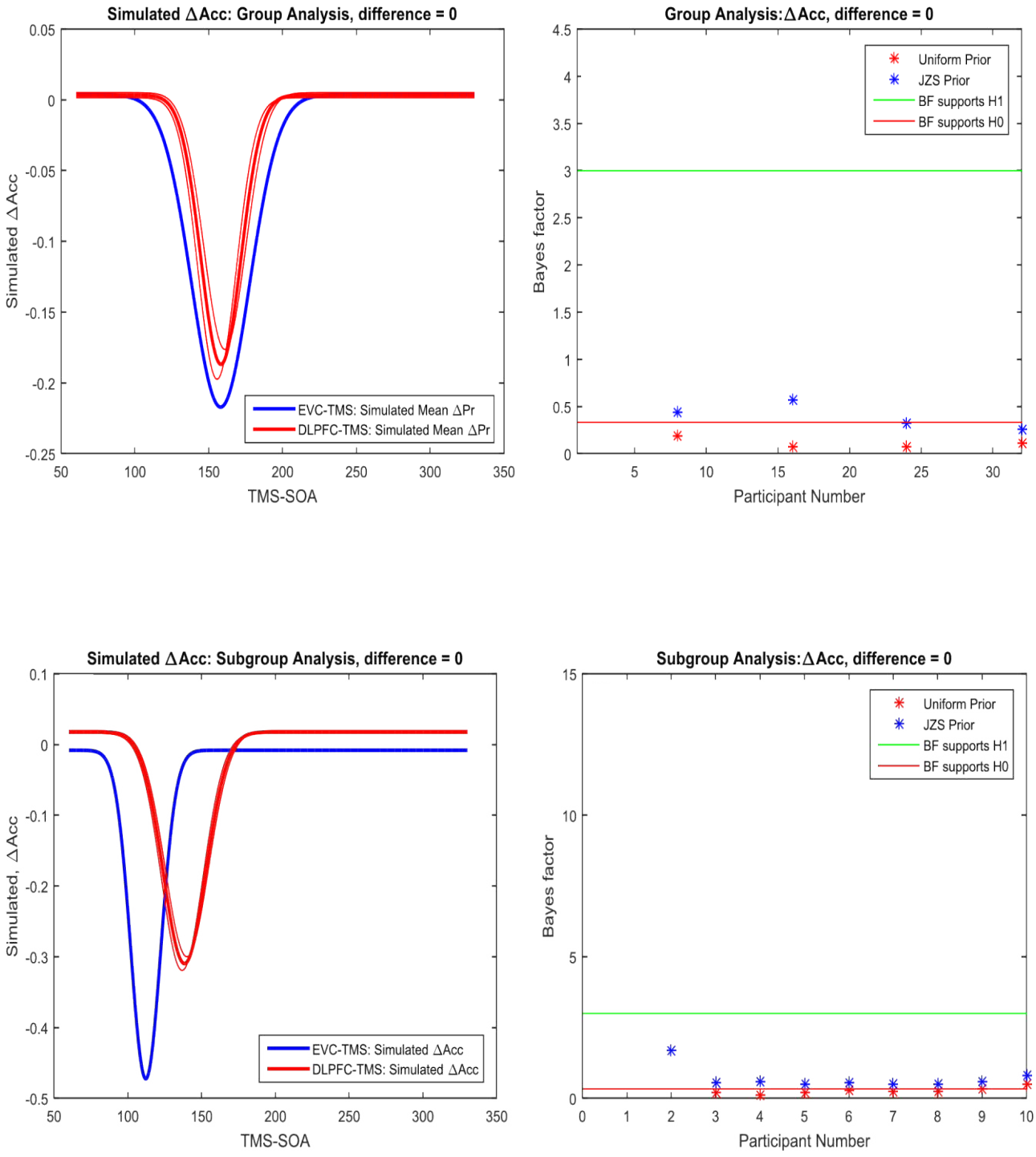

Figure 10. Top left: Simulated ΔAcc for the group analysis (GAn) when the difference between EVCx and DLPFCx was 0ms. Thick lines represent the model mean; thin lines represent the -/+ 1 standard error. Top right: Bayes factor (BF) as a function of participant number for the GAn-2 when the modelled difference between EVC*x* and DLPFC*x* was 0ms. Bottom left: Simulated ΔAcc for the SGAn when the modelled difference between EVC*x* and DLPFC*x* was 0ms. Bottom right: *BF* as a function of participant number for the SGAn when the modelled difference between EVC*x* and DLPFC*x* was 0ms.

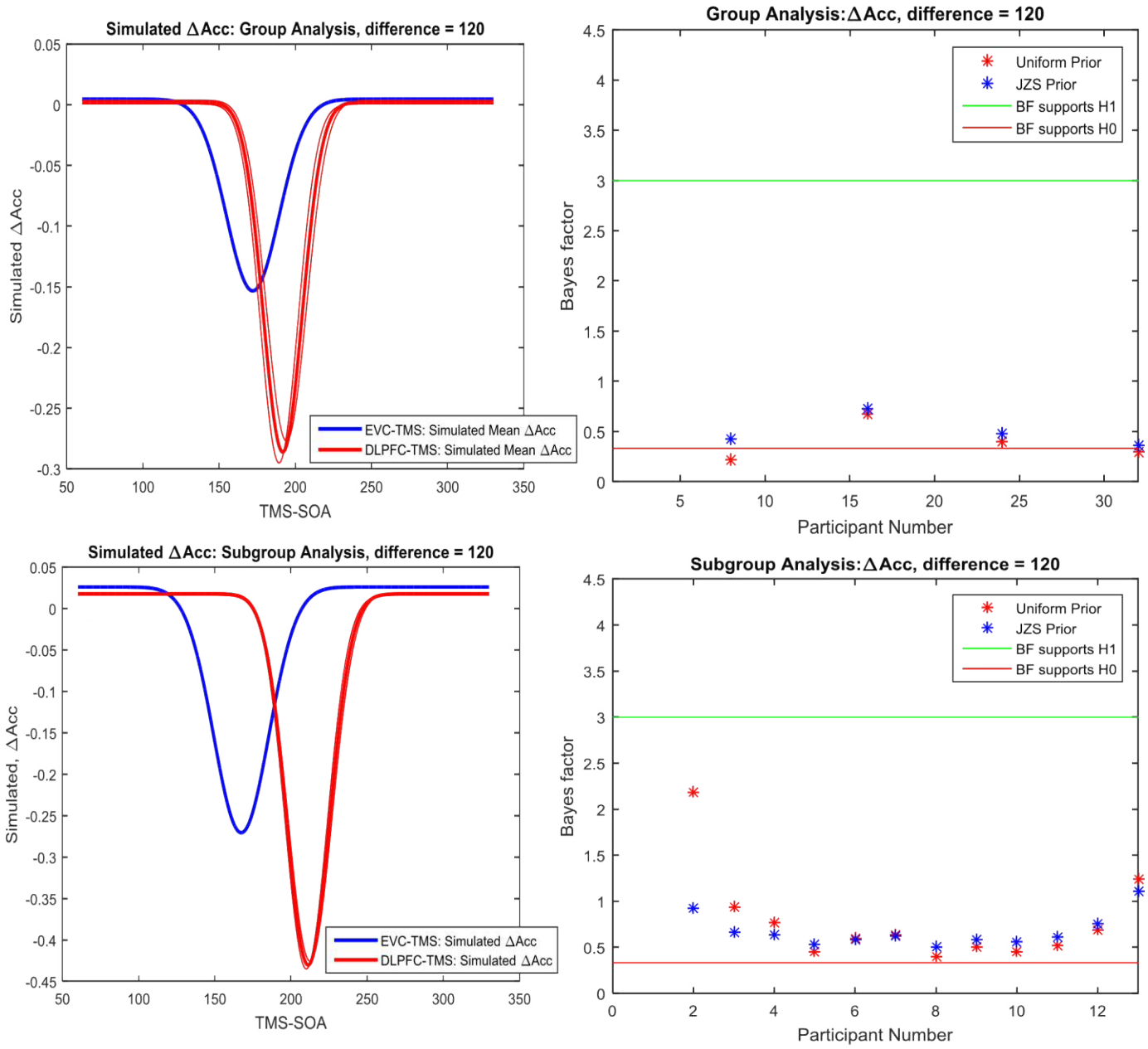

Figure 11. Top left: Simulated ΔAcc for the group analysis (GAn) when the difference between EVCx and DLPFCx was 120ms. Thick lines represent the model mean; thin lines represent the -/+ 1 standard error. Top right: Bayes factor (*BF*) as a function of participant number for the GAn-2 when the modelled difference between EVC*x* and DLPFC*x* was 0ms. Bottom left: Simulated ΔAcc for the SGAn when the modelled difference between EVC*x* and DLPFC*x* was 120ms. Bottom right: *BF* as a function of participant number for the SGAn when the modelled difference between EVC*x* and DLPFC*x* was 0ms.

3.3.4: Simulated data and justification of Bayesian analyses: Conclusions

This section aimed to identify the most sensitive method of assessing the evidence for the presence or absence of a difference between the EVC*x* and DLPFC*x* . This involved comparing two different approaches to analysing ΔPr and ΔAcc as a function of EVC-TMS and DLPFC-TMS SOA. The first approach was to compare the two different types of analysis: the GAn, which includes all participants, and the SGAn, which includes a smaller set of participants who are more likely to exhibit a difference in performance under conditions of active TMS and sham TMS. These two methods had the same aim: to identify if a difference in the temporal position of an EVC-TMS effect differs from the temporal position of a DLPFC-TMS effect. However, the simulations also aimed to identify whether a uniform or a JZS prior is the most sensitive method of assessing the evidence for the presence or absence of a simulated difference between EVC*x* and DLPFC*x*. In the absence of a simulated difference when ΔPr was used as a measure in the GAn, both priors provided *weak* support for the null hypothesis. In contrast, when applied in the ΔPr SGAn on 14 simulated participants, the uniform prior was sensitive to the simulated absence of a difference and produced substantial support for the null hypothesis whereas the JZS prior did not. These simulated outcomes suggest that both priors are capable of producing weak support for the null in the GAn but only the uniform prior is capable of demonstrating substantial evidence for the null in the SGAn given the absence of a simulated difference. Critically, it also suggests that the SGAn on ΔPr must also influence the decision to terminate data collection. When a 120ms difference between EVC*x* and DLPFC*x* was present when ΔPr was used as a measure, both priors produced a *BF* that reflected substantial support for a difference in the GAn and SGAn, suggesting that both were sensitive to a difference. However, the uniform prior produced a *BF* that supported a difference (*BF* > 3) after testing fewer participants than the JZS prior, making it a more sensitive prior for the proposed hypotheses. This greater sensitivity suggests that a uniform prior is more appropriate for the GAn

and the SGAn on ΔPr than the JZS prior. It also suggests that the GAn, in addition to the SGAn, can be used to influence the decision to terminate data collection.

When a simulated difference between EVC*x* and DLPFC*x* was absent and ΔAcc was used as a measure, both priors successfully produced a *BF* that substantially supported the null hypothesis in the GAn-2. A uniform prior was more sensitive as it produced a *BF* that is less than 3 after the inclusion of fewer participants than the JZS. The uniform prior also exhibited greater sensitivity in the SGAn-2, where a *BF* that substantially supported the absence of a difference was produced whereas the JZS prior only produced a *BF* reflecting weak support. When a simulated *difference* of 120ms was present between EVC*x* and DLPFC*x* in the GAn-2 when ΔAcc was used as measure, both priors provided weak support for the *null hypothesis* in the majority of instances. In the simulated GAn-2 a uniform prior produced substantial support for the *null* in spite of simulated difference between EVC*x* and DLPFC*x* in some instances whereas the JZS only produced weak support for the null. As a result of these simulations, ΔAcc will not influence the decision to terminate data collection. The GAn and the SGAn on ΔAcc will only serve to complement the GAn and SGAn on ΔPr. The GAn-2 and SGAn-2 on ΔAcc will apply a JZS prior, not a uniform prior.

To conclude, the outcome of the GAn-2 *or* the SGAn-2 on ΔPr will influence the decision to terminate data collection. Data collection will terminate when a one-sample *t*-test with a uniform prior in the ΔPr GAn-2 or the ΔPr SGAn-2 produces a *BF* that is more than 3 or less than 1/3. The GAn and SGAn on ΔAcc will still be carried out but their purpose will be to complement the GAn and SGAn on ΔPr. The GAn and the SGAn on ΔAcc will use a JZS prior instead of a uniform prior. The analyses using ΔAcc as measure will not influence the decision to terminate data collection.

3.4: Psychometric pilot data

3.4.1: Overview

Firstly, this section will present psychometric pilot data which will compare Pr and Acc as a function of target luminance. These two measures are being compared because they quantify

behavioural performance differently. Pr has previously been used to establish performance as a function of EVC TMS (Allen et al., 2014) whereas Acc has not. Pr measures the proportion of participant responses that the target is present on target *absent* trials and subtracts it from the proportion of participant responses that the target is present on target *present* trials, which provides a non-parametric measure of perceptual sensitivity (Corwin, 1994). In contrast, Acc measures performance as the circular difference between the presented angle and the reported angle of the target in radians. Unlike Pr, which can only measure how accurate a participant is at seeing a target after analysing *all trials*, Acc can provide a similar measure on a *trial-by-trial basis.*

As Acc has not previously been used to measure performance as a function of TMS, simulations were completed to identify the Acc values that can be expected when participants are guessing. Although similar measures have been recruited in the past (e.g. Chalk, Seitz & Series, 2010), it was decided to identify how a guess without the capacity to locate the target would manifest itself. When a guess without the capacity to locate the target takes place, any angle ranging from 1 degree to 360 degrees should be equally likely reported regardless of the angle of the target itself. Selecting an angle from 1 to 360 degrees at random along with a random location of the target, and then calculating the circular difference between these two points should reveal the circular difference that should be reported when participants are guessing without the capacity to locate the stimuli. This value will then be plotted alongside Acc as a function of target luminance to indicate the target luminance(s) where participants guessed. Acc has the advantage of being able to indicate the sort of performance that would be expected if participants are guessing on every trial. In contrast, Pr is incapable of doing this . When a participant is guessing in a detection judgment and a 'yes' or a 'no' response is being used to measure performance, a 'yes' response is just as likely to occur as a 'no' response. In order to provide further information on what Acc contributes in addition to Pr as a measure of performance. Acc was plotted as a function of target brightness on miss trials, which refers to when the target was present but the participant reported it as absent. These values

were then compared to the value that would be expected if participants were guessing without capacity to locate the target, which was obtained via simulated guessed responses. This was done to reveal whether participant's responses in the location judgment were characterized by a guess when target luminance was low followed by a deviation from a guess as target luminance increases.

Another point of interest here was how the point of inflection (POI), which is the point on the *x* axis where the Pr and Acc psychophysical function begins to *change direction* as a function of target luminance brightness. An example of where the POI can be found is illustrated in figure 12. Comparing the POI of Pr to the POI of Acc will identify whether they provided different information to one another or whether they complement one another. The POI of Pr as a function of target luminance was l be compared to the POI of Acc as a function of target luminance using a Bayesian one-sample *t*-test. If the *BF* of this comparison is less than 1/3, the lack of difference would provide evidence for POI of Pr and the POI of Acc to be the same. If the *BF* produces evidence for no difference, it would suggest that Pr and Acc provide complementary measures of a similar process. However, if the BF produced evidence for a difference by being more than 3, it would support that Pr and Acc provide different measures of performance to one another.

Finally, the number of trials that need to be sampled at each TMS-SOA was identified. The trial number was identified by plotting the standard error around the point where normalized Pr and Acc = 0.5 as a function of trial number. The asymptote of both of these functions, which represented the trial number where standard error begins to stabilize, determined the number of trials where TMS will be delivered at each SOA. A trial number was selected where the point where normalized ΔPr *and* ΔAcc = 0.5 stabilized in order to minimize the variance within ΔPr and ΔAcc at each TMS SOA for each TMS site.

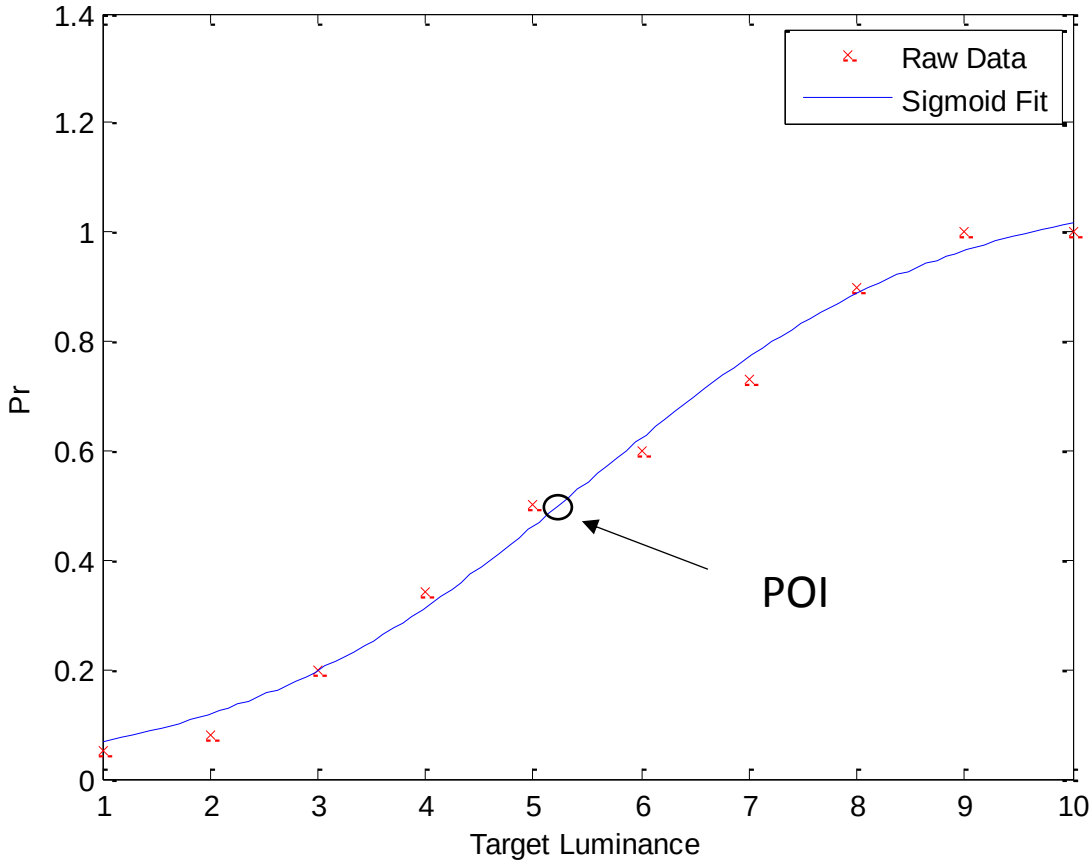

Figure 12. An example of where the point of inflection (POI) lies when a sigmoid model is fitted to Pr as a function of target luminance.

3.4.1: Participants

8 participants (the author) aged between 23 and 30 from the Cardiff University School of Psychology. One was male.

3.4.2.1: Design: Behavioural experiment

Elements of experimental design were identical to the detection threshold described above. To summarize, participants were presented with targets at 10 different luminance levels. The only difference between the protocol used here and the one described previously related to the number of trials participants completed. 5 participants completed 70 trials at each brightness level, meaning that the target was present on 49 trials (70% of trials). 5 participants were selected at this stage because 5 participants were included in the first set of behavioural pilot experiments which aimed to

validate the use of Pr and Acc in the pre-registered TMS experiment. An additional 3 participants completed 40 trials at each brightness level and the target was present on 28 trials (70% of trials).The initial 5 participants completed 70 trials because the aim was to identify how many trials would be necessary for the standard error around the point where normalized Pr/Acc to stabilize . The largest number of trials that would be feasible to complete were therefore completed. These additional 3 participants completed the TMS pilot experiment, which was completed after the behavioural pilot. These 3 participants completed a smaller number of trials because they completed the pilot TMS experiment, not the pilot behavioural experiment. The TMS experiment contained 28 trials at each luminance because this was 70% of the 40 trials, which was the number of trials that was necessary for the standard error around the point where normalized Acc = 0.5 began to asymptote. Their psychophysical functions were obtained using the target calibration method outlined in this chapter. Pr and Acc were used to measure performance as specified in section 2.1 but they were then normalized so they could be compared on the same scale.

3.4.2.2: Design: Simulated experiment

The simulated experiment was conducted using Matlab with the aim of identifying the Acc values would be obtained when participants guess without capacity to locate the stimuli, which involved generating guess responses for 5 simulated participants. On each simulated trial, the location of the target and the simulated guess response were determined by randomly choosing a number between 1 and 180. Values between 1 and 180 were chosen because those figures are the minimum and maximum differences between two points on a circle, respectively. The circular difference between the target location and the simulated response was then calculated on a trial-by-trial basis for all simulated participants. This process was repeated over 1000 iterations to smooth out variability, which produced 1000 different values for each participant. The average across the 1000 iterations was then calculated to produce 70 numbers for each simulated participant. The mean of these 70 trials was then calculated to generate single numbers for each simulated

participant. The average of these 70 trials across all simulated participants was then used as the basis for where guessed responses would lie in radians.

3.4.3: Statistical analyses: Behavioural experiment

For all 8 participants, Pr and Acc were normalized so the POI for each of the measures could be compared on the same scale. Acc and Pr were normalized by transforming both scores so the points between their maximum and minimum Pr and Acc score were distributed between 0 and 1, respectively. A sigmoid model was then separately fitted to each of the measures for each participant, which were then plotted to reveal a psychophysical function for Acc and Pr as a function of target brightness. The POI for each measure for each of the 8 participants was then calculated. The mean POI for Pr and the mean POI for Acc across all 8 participants was then subjected to a two sample t-test with a JZS prior (Rouder et al., 2009).

Data from the 5 participants who completed 70 trials at each brightness level was used to identify the number of trials required for the standard error around the point where normalized Pr and Acc = 0.5 to stabilize. In order to do so, Acc values and the target presence and target absence judgments used for measuring Pr were randomly sampled across 70 trials. Standard error around the point where Pr and Acc = 0.5 was then calculated incrementally from using 2 up to using 70 randomly sampled trials in increments of 1. This process of random sampling was repeated for 1000 iterations to smooth out the variability within the standard error as a function of each trial number. The mean was then calculated across each of the 1000 iterations from sampling 2 trials up to sampling 70 trials in order to produce 68 standard error scores. These 68 standard error scores were then plotted as a function of trial number to reveal the trial number required for Pr and Acc to asymptote.

3.4.4: Results: Behavioural experiment

The aim of the behavioural experiment was to compare Pr and Acc as measures of performance. The mean psychophysical functions in Figure 12 and individual participant functions in

Figure 13 reveal that for all 8 participants, the point where normalized Acc = 0.5 is shifted to the left of the point where normalized Pr = 0.5, which suggests that the Acc may be able to reveal more about what participants are capable of responding to as a function of TMS-SOA. The difference between Pr and Acc as measures of performance was assessed using a one-sample *t*-test with a JZS prior, which revealed weak support for a difference between Pr and Acc (t (7) = 2.2854, p = 0.1264, *BF* = 1.1126).This outcome suggests that a difference between the two measures may be obtained if more participants are included within the analysis. The absence of a difference in the POI between these normalized measures suggests that effects of TMS on ΔAcc can be used to qualify the effects of TMS on ΔAcc and vice versa.

3.4.5: Results: Simulated experiment

The aim of the simulated experiment was to identify the circular difference between the target dot and the response dot that would be expected if participants were guessing without the capacity to locate the target. The circular difference that would be expected would then be compared to participant's Acc as a function of target luminance. Acc was not normalized here. Simulating guesses for 5 participants across 49 trials revealed that the average score in radians when guesses take place is 1.556. Figure 14 (right) plots Acc guesses from the simulated experiment as a red line and averaged Acc scores as a function of target intensity as a blue line, which reveals that participants were guessing at when target brightness was low

The circular difference between the target and the response dot on trials where the target was present but participants reported it as absent was also considered. This was considered in conjunction with the value produced by the guessing simulations to reveal whether participants were guessing when they missed the target when target luminance was low. This was also considered to reveal whether participant's responses deviated from a guess as target luminance increased. Figure 14 (left) reveals that the Acc measure successfully produces a graded improvement in normalized Acc as target brightness increases on trials where participants *missed* the target. A miss was when the participant reports the target as absent when it was physically present. This

graded improvement on miss trials suggests that the Acc measure can reveal *how* inaccurate participants are at detecting a target, which is a sensitive measure of performance. However, examination of Figure 14 (right) reveals that a high proportion of misses occurred at low intensities but this proportion falls to near zero at the highest intensities. As a result, the standard error for Acc scores at high intensities on miss trials may be imprecise and affect the overall pattern shown in the data.

Inspection of the shape of the curves within Figure 15 reveals that the variance around the point where normalized Acc and Pr = 0.5 asymptotes after sampling 20 trials for both measures. Unlike the simulations mentioned in the previous paradigm, Acc was normalized to fall between 0 and 1 for this set of simulations so it fell within the same range as Pr, which was also normalized. This curve justifies our use of 40 trials at each SOA for active and sham TMS, which guarantees that variance will be minimized at each TMS SOA. The use of 40 trials mean that 28 target present and 12 target absent trials were used to measure normalized Pr (Corwin, 1994) and 28 target present trials were used to measure normalized Acc at each TMS SOA. Interestingly, Figure 15 also reveals a trend showing that the normalized Acc measure asymptotes after sampling fewer trials than the normalized Pr measure and produces less variability around the point where performance equals 0.5 across all trial numbers.

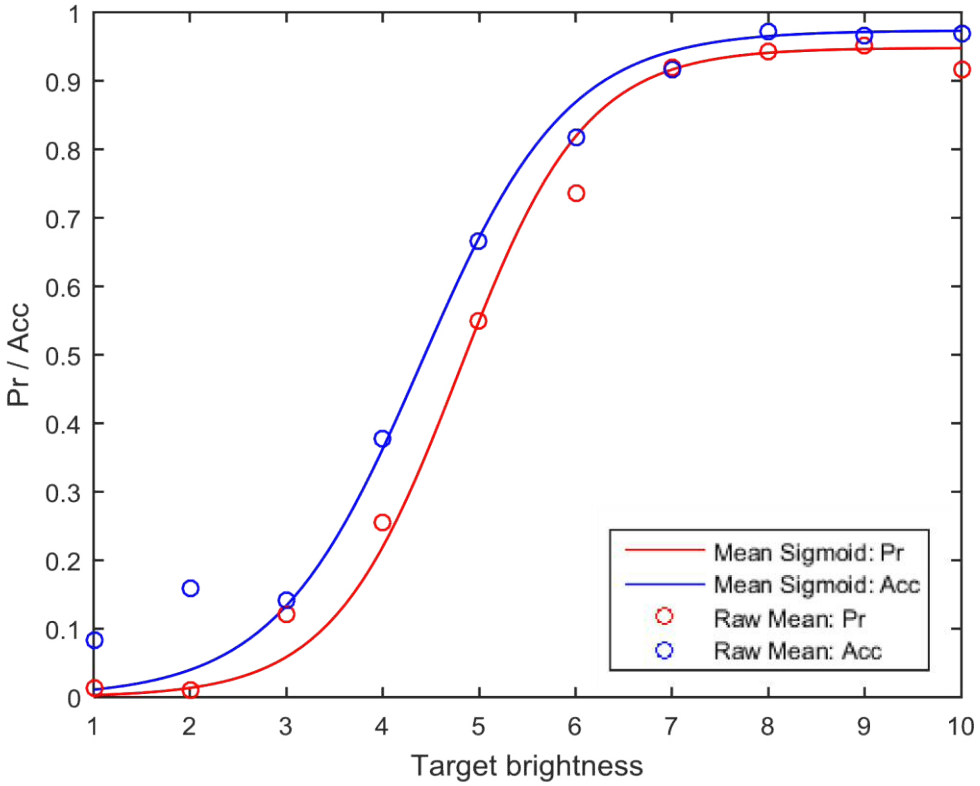

Figure 12. Mean normalized Pr, mean normalized Acc and corresponding mean sigmoid models

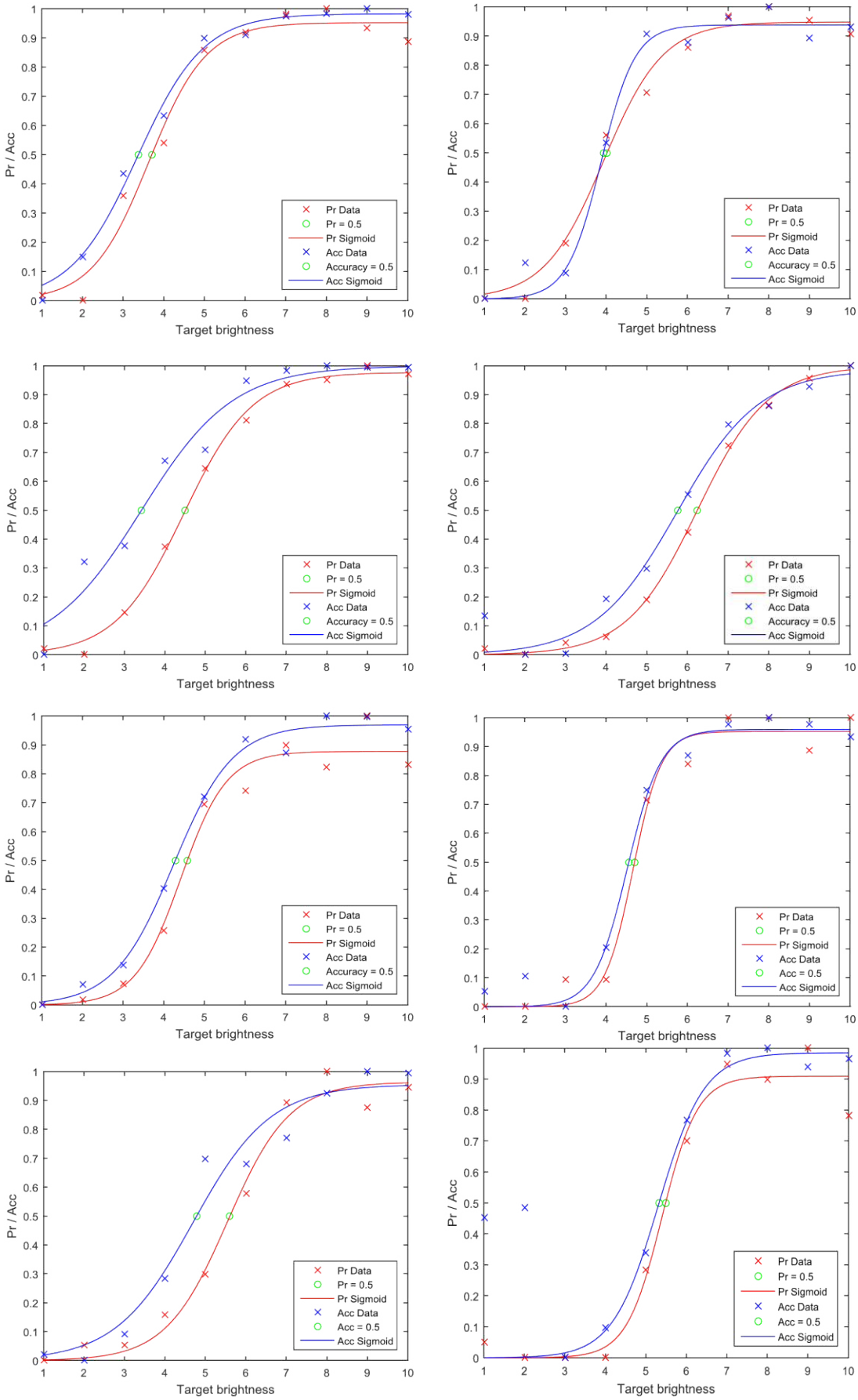

Figure 13. Individual normalized Pr and accuracy (Acc) scores for all individual participants.

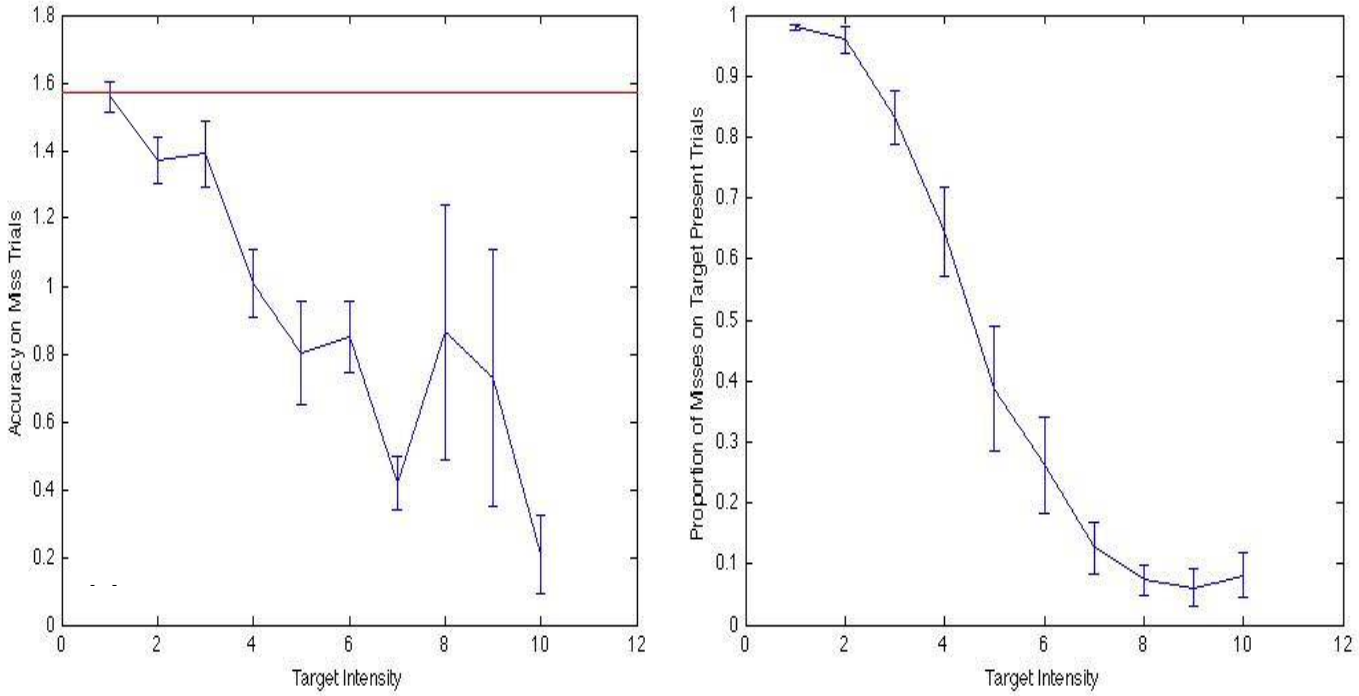

Figure 14. Right: Acc when misses took place on target present trials when the target was not seen. The red line indicates performance when guessing. Error bars display the -/+ 1 standard error. Left: Proportion of miss trials on target present trials as a function of target brightness. Error bars display the -/+ 1 standard error.

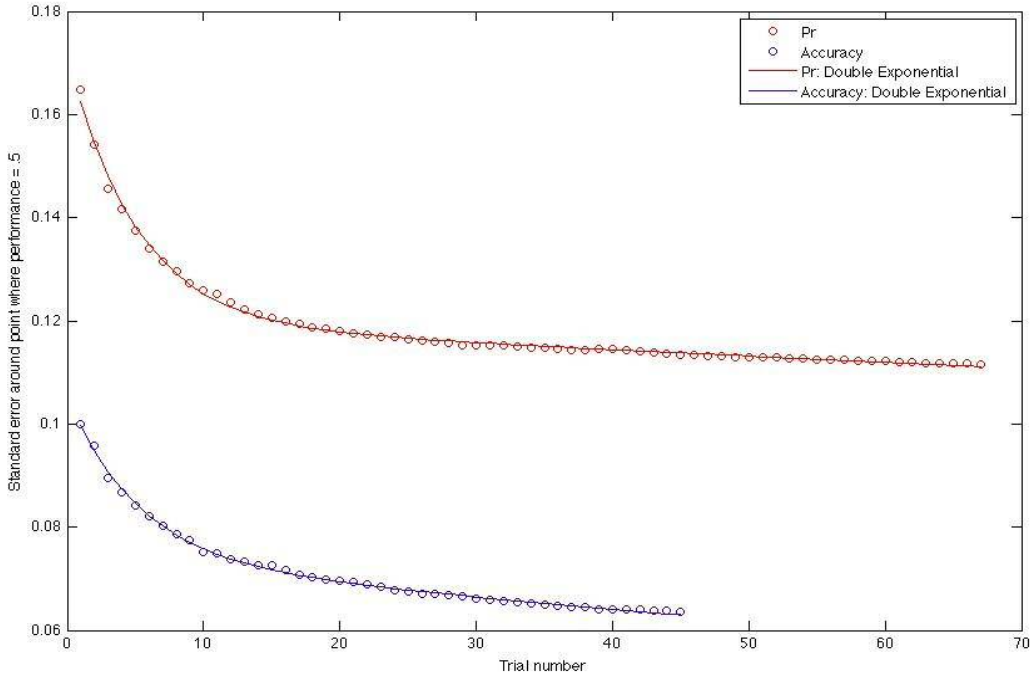

Figure 15. Standard error around the point where Pr and Acc = 0.5 as a function of trial number

4. Statement of the commencement of data collection prior to the submission of this preregistraition document

Data collection for this study commenced on January 14th 2016 due to PhD funding limitation and this document was registered on the Open Science Framework on March 11th 2017. Although data collection commenced prior to registration on the Open Science Framework, the data was not analysed and the GAn or SGAn was not applied. The data was only utilized to monitor Pr on sham TMS blocks in order to calibrate target luminance throughout the experiment.

Task Instructions

Thank you for taking part in this experiment. This experiment is interested the neural processes that underlie visual perception in humans.

In this experiment you will sometimes be presented with a dot. After this, you will need to make two judgments. First of all, you will need to indicate where you thought the dot appeared using the mouse. Click the mouse when you believe the cursor is where the target appeared. If you did not see a dot, please provide your best guess. Afterwards, you will then need to indicate whether you saw a dot with a left or right click. The experimenter will inform you which click indicates 'yes' or 'no'.

Overview: results produced by pre-registered and exploratory analyses

The first analyses that will be presented here will be the pre-registered biphasic Gaussian based analyses described above. The biphasic Gaussian analyses were split into two parts. The first part aimed to identify if effects of active TMS arose relative to sham TMS as a function of EVC-TMS or DLPFC-TMS. The second part of the analysis was contingent on at least one effect of TMS being quantified for both TMS sites. However, a number of exploratory analyses were also applied with a monophasic Gaussian or biphasic Gaussian with different constraints on the a_1 and a_2 coefficients. A biphasic Gaussian can quantify the magnitude, duration and temporal position of the two largest differences between active TMS and sham TMS. In contrast, a monophasic Gaussian can only quantify the magnitude, duration and temporal position of the one largest difference between active

TMS and sham TMS. In the set of exploratory analyses, the a_1 and a_2 coefficients were constrained in a way that prevented them from being positive, which enabled them to only detect negative differences produced by subtracting sham TMS from active TMS at each for each site.

The outcomes of the pre-registered analyses and the exploratory analyses are presented together. The pre-registered analyses are presented here in order to reveal how the data collected here related to the a priori hypothesis about the onset of a left DLPFC TMS effect coming after the onset of an earlier EVC – TMS effect. The outcome of three exploratory analyses are presented separately from this pre-registered analysis to enable the distinction between hypothesis that were conveived *a priori,* before data colletion, and additional analyses that were applied to the data after data collection had been completed. The outcomes of all of these analyses are presented in order to provide the reader with the outcome of every Bayesian analysis, which enables a judgment to be made on the onset of a EVC-TMS effect relative to a left DLPFC-TMS effect based on all the evidence that was generated from the analyses completed here.

The pre-registered analyses did not reveal an effect of active TMS relative to sham TMS for either site when ΔPr was used as a measure. Examination of the *y0* coefficients for EVC-TMS revealed that the intercept, which quantifies the baseline level of performance under conditions of TMS, appeared to quantify an effect of active TMS relative to sham TMS, whereas the a_2 coefficient ironically captured the return to baseline. The pre-registered analyses on the ΔAcc a_1 and a_2 coefficients also revealed no evidence of an EVC-TMS or left DLPFC-TMS –induced effect on ΔAcc across all SOAs. The outcome of the pre-registered analyses were surprising, especially the absence of the effect of EVC-TMS at an SOA of ~100ms (Kammer, 2007; de Graaf et al., 2014). The absence of such effect suggests a problem with the TMS parameters, visual stimulus calibration or the statistical analysis itself. However, similar TMS parameters have successfully reproduced such an effect (Chambers et al., 2013) with similar conditions of visual stimulus calibration (Allen et al., 2014). Thus, there could be a problem with the pre-registered statistical analyses. This unexpected result led to

exploratory analyses being carried out which applied different constraints to the a_1 and a_2 coefficients, which enabled them to only be negative.

To conclude, it appears that the choice of constraints which were applied to the monophasic and biphasic Gaussian models affected the ability of the *BF* to reflect evidence for EVC and DLPFC-TMS induced effects on ΔPr and ΔAcc. Only one of the *BF*s produced by the Gaussian models with positive or negative *a* coefficients successfully produced evidence for a TMS-induced effect, which was for EVC-TMS on ΔAcc. In contrast, all of the Gaussian models with negative *a* coefficients successfully quantified effects of active TMS relative to sham TMS when ΔPr and ΔAcc were used as measures. Remarkably, a consistent result was revealed in all of these analyses, regardless of whether a monophasic or biphasic Gaussian was used. The consistent result was that EVCx_1 and DLPFCx_1 occurred at the same time, which is inconsistent with the pre-registered hypothesis that DLPFCx_1 would occur after EVCx_1.#

Results

Results: Eye tracking data, Pr calibration and TMS parameters

37 participants took part in this experiment in total. Two of these only completed a PT: one decided to withdraw due to time commitments and another could not report the presence of phosphenes. Three participants were excluded because they exhibited blinks on over 40% of trials. In the participants who were included in this experiment, blinks occured on 13.4% of trials. One participant was included within the analyses despite their eye tracking data (blinks on 55% of trials) meeting our exclusion criteria due to the urgency of PhD registration deadline. Three other participants exhibited blinks on 22.3%, 21.31%, 31.87% and 39.19% of the total number of trials, which caused an entire set of active or sham TMS data to be lost at one SOA, which prevented the curve fitting procedure from being applied. The main issue that arose here is that eye tracking failed due to technical failure for complete sets of DLPFC-TMS blocks in particular. These participants were also included within the statistical analysis due to the urgency of the PhD registration deadline.

The mean level of stimulator output for TMS at 120% of PT was 75%. Mean Pr was 0.4462 as a function of sham EVC-TMS and 0.4455 (SD: 0.0290) as a function of sham DLPFC-TMS (SD: 0.0285), which is within -.1/+0.1 of a Pr of 0.5, as pre-registered.

Results: Pre-registered analyses

Pre-registered ΔPr biphasic Gaussian (-/+ a) group analyses

Four one-sample Bayesian *t*-tests were applied in the pre-registered analyses on ΔPr, which assessed whether EVCa_1 and EVCa_2 along with DLPFCa_1 and DLPFCa_2 supported TMS-induced effects on behaviour. If the Bayesian *t*-tests on EVCa_1 and DLPFCa_1 or DLPFCa_2 produced a *BF* that is more than 3, additional analyses comparing EVCx_1 and DLPFCx_1 or DLPFCx_2 were carried out.

Has an EVC-TMS induced effect occurred for ΔPr?

Consistent with the pre-registered analyses, a Bayesian one-sample *t*-test was applied after 8, 16, 24 and 32 participants were included within the analysis on ΔPr as a function of EVC-TMS. A pre-registered Bayesian one-sample t-test was completed after incrementally adding more participants, which would enable data collection to terminate if the *BF* produced evidence for the absence of an EVC-TMS effect on ΔPr. Table 2 illustrates the *BF* as a function of participant number for phase 1 and phase 2 of the biphasic Gaussian which were fitted to ΔPr as a function of EVC-TMS. After the inclusion of all 32 participants in the analysis, the *BF* for the first phase of the Gaussian produced strong support for the null hypothesis (t (31) = 0.7063, p = 0.4853, *BF* = 0.2378) whereas the *BF* for the second phase of the Gaussian produced weak support for the null hypothesis (t (31) = 1.4854, p = 0.1475, *BF* = 0.5101). The *BF* as a function of 8, 16, 24 and 32 participants can be found in table 2, which revealed that strong evidence for a_1 not differing from zero emerges after 16 participants were included in the analysis. A *BF* that is less than 1/3 when analysing EVC a_1 is surprising considering that EVC x*1* is 158.4ms, which is close to the robust and reproducible SOA where EVC-TMS reduces performance at approximately 100ms (de Graaf et al., 2014) After 32 participants were included within the analysis, the second phase of the biphasic Gaussian the *BF* was

0.5101, reflecting weak evidence for the absence of an EVC-TMS effect at 272.9ms, which suggests that support for the absence of a TMS-induced effect on performance after the effect at SOAs later than 100ms could be attained if more participants were included in the statistical analysis (de Graaf et al., 2014; Dienes, 2011). However, the results of the GAn-1 must be interpreted with caution given the absence of support for the robust and reproducible effect of EVC-TMS at 100ms in these analyses. All relevant models and raw data for this analysis can be found in figure 18.

	BF: a_1	***BF: a2***	***a_1***	***a_2***	***x_1***	***x_2***	***b_1***	***b_2***	***y0***
8	0.6854	0.7166	0.1568	0.1752	195.3ms	300.6ms	41.3ms	42.3ms	-0.1083
16	0.2767	4.1116	0.0405	0.2009	158.4ms	282ms	33.4ms	27.8ms	-0.0755
24	0.2171	1.4336	-0.0121	0.1410	150.5ms	278ms	30.6ms	39.4ms	-0.0905
32	0.2378	0.5101	0.0469	0.0953	138.4ms	272.9ms	27.3ms	39.7ms	-0.0740

Table 2. Bayes factors (BF) and mean coefficients produced by the application of a biphasic Gaussian model to ΔPr as a function of EVC-TMS when 8, 16, 24 and 32 participants were incrementally included in the analysis.

What warrants further attention here is the intercept of the model, *y0*, which quantifies the baseline of performance under conditions of TMS. When 8, 16, 24 and 32 participants are included in the analysis, qualitative reflection of the mean intercepts in table 2 reveals that none of them are approximately zero. The fact that none of intercepts are approximately zero (mean: -0.0750, SD: 0.1712) suggest that further statistical analysis could reveal that active TMS reduces the baseline level of performance relative to sham TMS. An exploratory analysis which applied a Bayesian one-sample *t*-test with a JZS prior (Rouder et al., 2009) revealed that the *BF* reflected strong support for a mean difference between the mean intercept and a mean of zero when 24 participants were included in the analysis as revealed in table 1 (t (23) = -2.6113, p = 0.0156, *BF* = 3.3401). Moreover, support was produced for a mean difference when 16 (t (15) = -2.2076, p = 0.0433, *BF* = 1.6823) and 24 participants (t (31) = -2.4443, p = 0.0204, *BF* = 2.4222 were included within the analysis as revealed in table 1. The outcomes of this exploratory analysis suggest that the amplitude coefficients, a_1 and a_2, were not sensitive to a decrement in performance produced by EVC TMS yet the intercept was successful in capturing an effect of active EVC-TMS relative to sham EVC-TMS.

However, this indicates that a difference in baseline exists between active TMS and sham TMS does exist within the data. The issue is that the biphasic Gaussian model cannot pinpoint a specific SOA where such a difference exists. For example, the biphasic Gaussian model was clearly sensitive to two decrements in performance as revealed by the left hand part of figure 16. However, the application of the same model to another participant's data reveals no evidence of such effects as revealed in the right hand part of figure 16. In fact, the right hand side of figure 16 reveals the opposite, that two improvements in performance can be detected. It is possible that these two effects can cancel one another out, which prevents EVC and DLPFC-TMS induced effects from being discovered.

Has a DLPFC-TMS induced effect occurred for ΔPr?

Consistent with the pre-registered analyses, a Bayesian one-sample *t*-test was applied after 8, 16, 24 and 32 participants were included within the analysis on ΔPr as a function of DLPFC-TMS. A pre-registered Bayesian one-sample t-test was completed after incrementally adding more participants, which would enable data collection to terminate if the *BF* produced evidence for the absence of an EVC-TMS effect on ΔPr. Figure 17 illustrates the *BF* as a function of participant number for a_1 and a_2 of the biphasic Gaussian model applied to ΔPr as a function of DLPFC-TMS. After including all 32 participants in the analysis, the *BF* produces weak support for the null hypothesis for DLPFCa_1 t (31) = -1.1806, p = 0.2467, *BF* = 0.3565) and strong support for the null hypothesis for

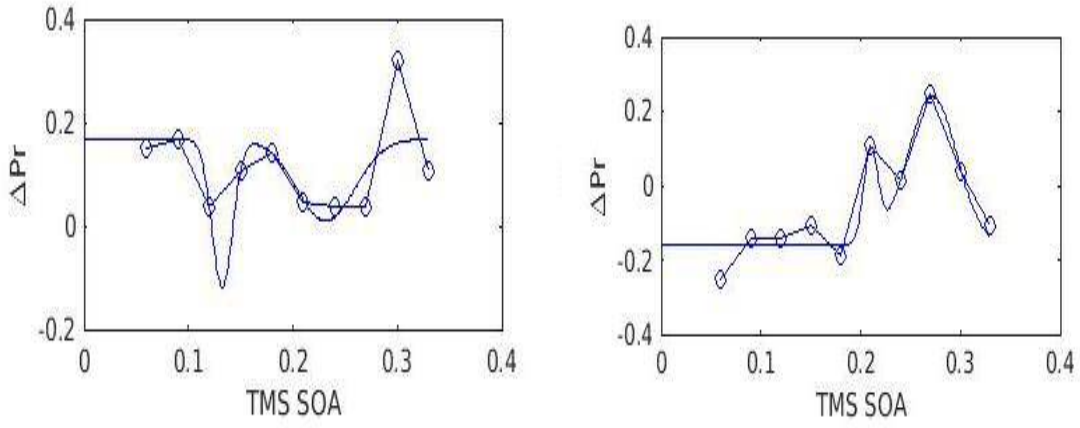

Figure 16. Left. Two decrements in TMS as quantified by the pre-registered biphasic Gaussian model. Right. Two improvements in TMS as quantified by the pre-registered biphasic Gaussian model

DLPFCa_2 (t (31) = -0.0808, p = 0.9362, BF = 0.1894). The BF as a function of 8, 16, 24 and 32 participants can be found in table 3. An exploratory Bayesian one-sample t-test also revealed that the mean intercept did not differ from a mean of zero (t (31) = -0.5936, p = 0.5571, BF = 0.2223), which suggests that there is no evidence for an effect of DLPFC-TMS on the baseline level of performance. All relevant models and raw data for this analysis can be found in figure 18.

	BF: a_1	***BF: a_2***	***a_1***	***a_2***	***x_1***	***x_2***	***b_1***	***b_2***	***y0***
8	0.3383	1.4471	-0.0141	0.2080	159.9ms	297.6ms	20.5ms	48.5ms	-0.038
16	0.2744	0.8506	0.0348	0.1443	155.6ms	274.4ms	30.2ms	35.7ms	-0.0262
24	0.2340	0.3836	-0.0323	0.0949	138.1ms	261.2ms	27ms	32.5ms	-0.0223
32	0.3565	0.1894	-0.0917	-0.0069	145.1ms	264.5ms	26.2ms	32.4ms	-0.0181

Table 3. Bayes factors (BF) and mean coefficients produced by the application of a biphasic Gaussian model to ΔPr as a function of DLPFC-TMS when 8, 16, 24 and 32 participants were incrementally included in the analysis.

Pre-registered ΔPr biphasic Gaussian (-/+ $a_{1,2}$) subgroup analyses: Does DLPFCx_1 or DLPFCx_2 occur later than EVCx_1?

A total of 4 participants qualified for inclusion within the subgroup analysis in which a Bayesian one-sample t-test with a uniform prior revealed that DLPFCx_1 does not occur after EVCx_1 (t (2) = 2.3544, p = 0.1428, BF = 0.0205). Application of a JZS prior to the same mean difference revealed weak evidence for the null hypothesis (BF = 1.3287). Only one participant qualified for the subgroup analysis which compares EVCx_1 to DLPFCx_2, which prevents exploratory Bayesian paired-sample t-tests from being carried out as there is no variance in a sample of one.

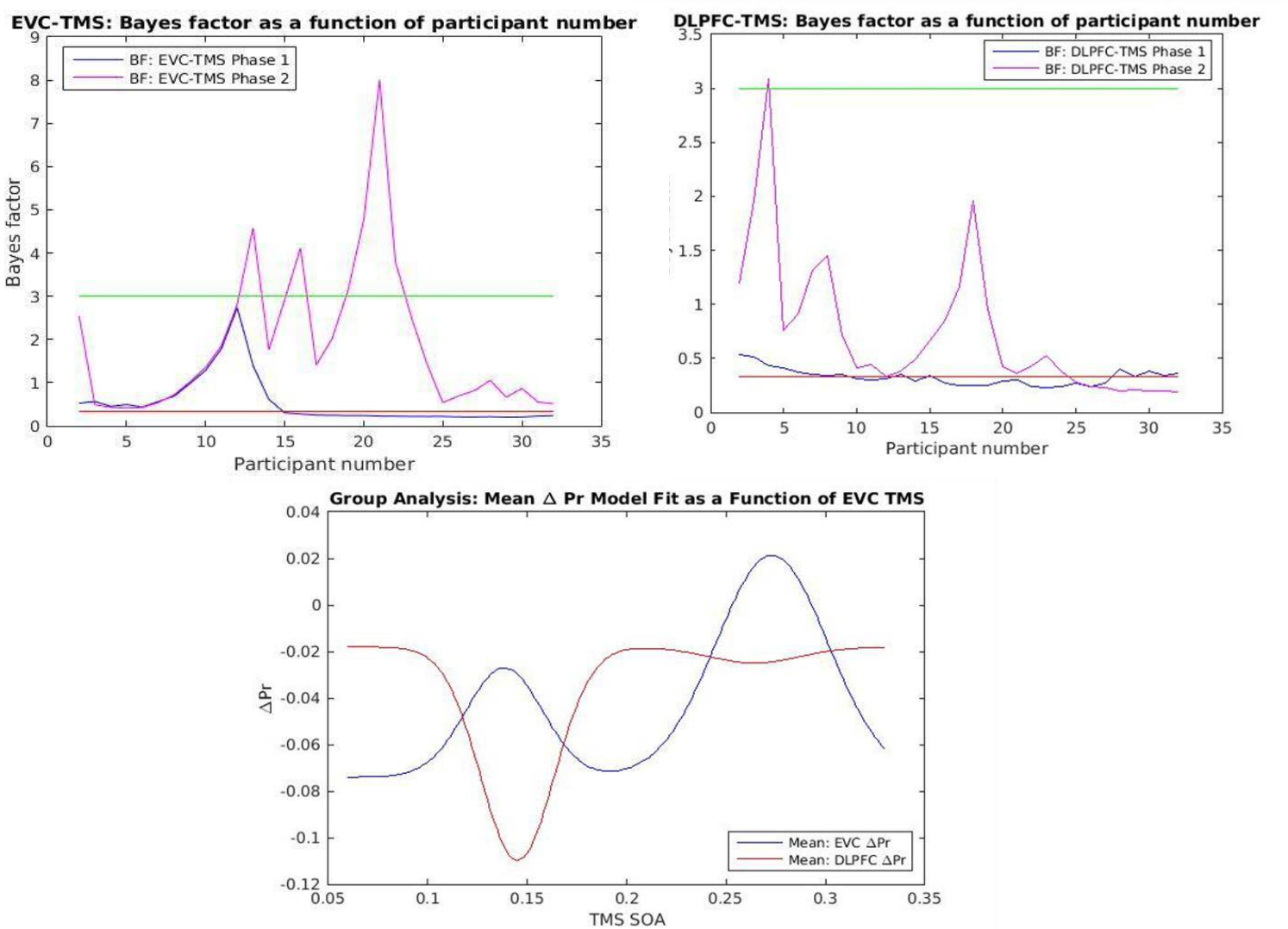

Figure 17. Top left: Bayes factor (*BF*) as a function of participant number for phase 1 and phase 2 amplitude coefficient produced by EVC-TMS. Top right: *BF* as a function of participant number for the phase 1 and phase 2 amplitude coefficients produced by DLPFC-TMS. Bottom: EVC and DLPFC biphasic models produced by the mean of EVC and DLPFC biphasic Gaussian model coefficients, respectively.

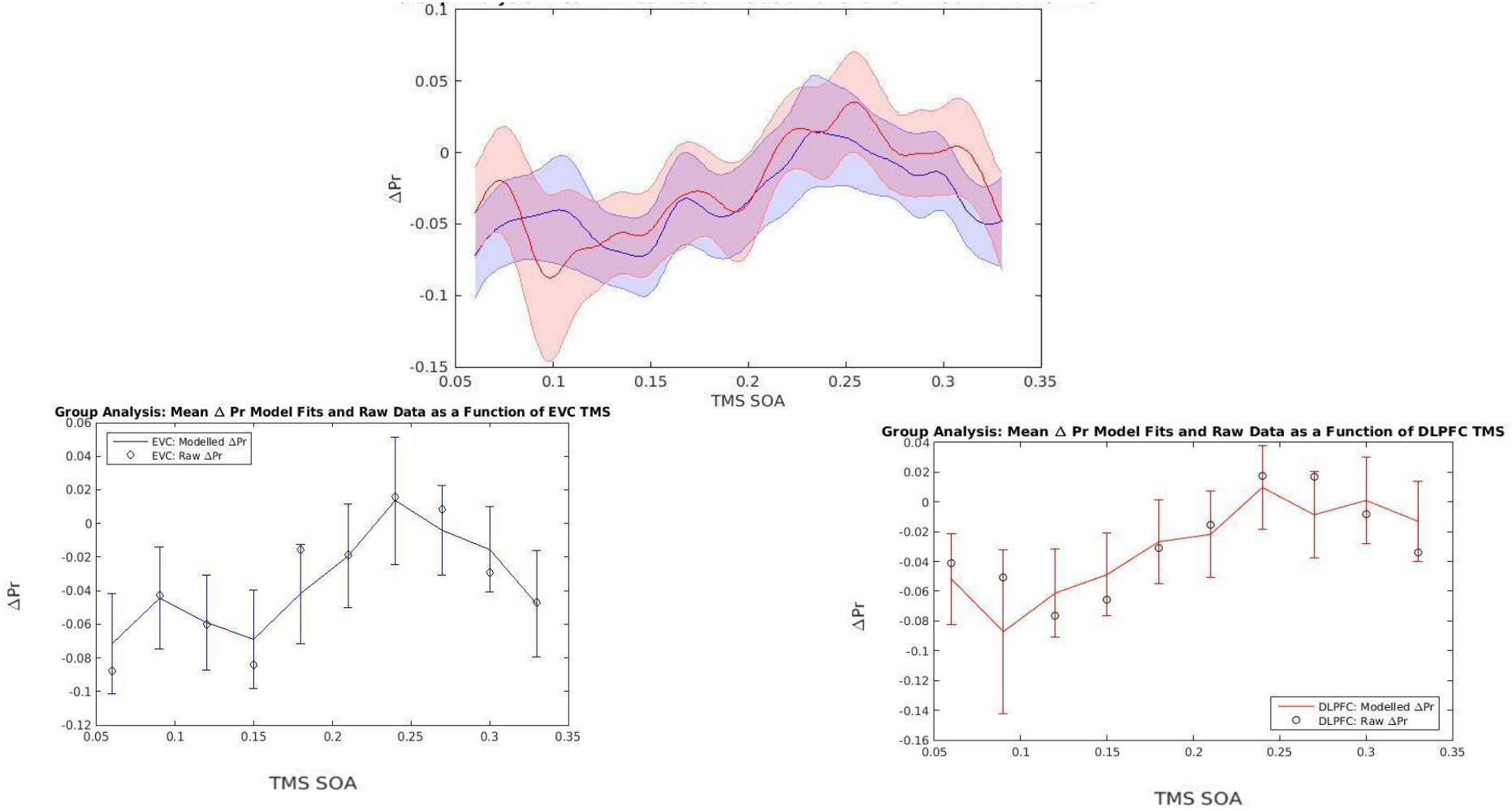

Figure 18. Top: Mean EVC (blue) and DLPFC (red) biphasic Gaussian fits for ΔPr as a function of TMS. Bottom left: Modelled ΔPr and raw ΔPr as a function of EVC-TMS. Bottom right: Modelled ΔPr and raw ΔPr as a function of DLPFC-TMS

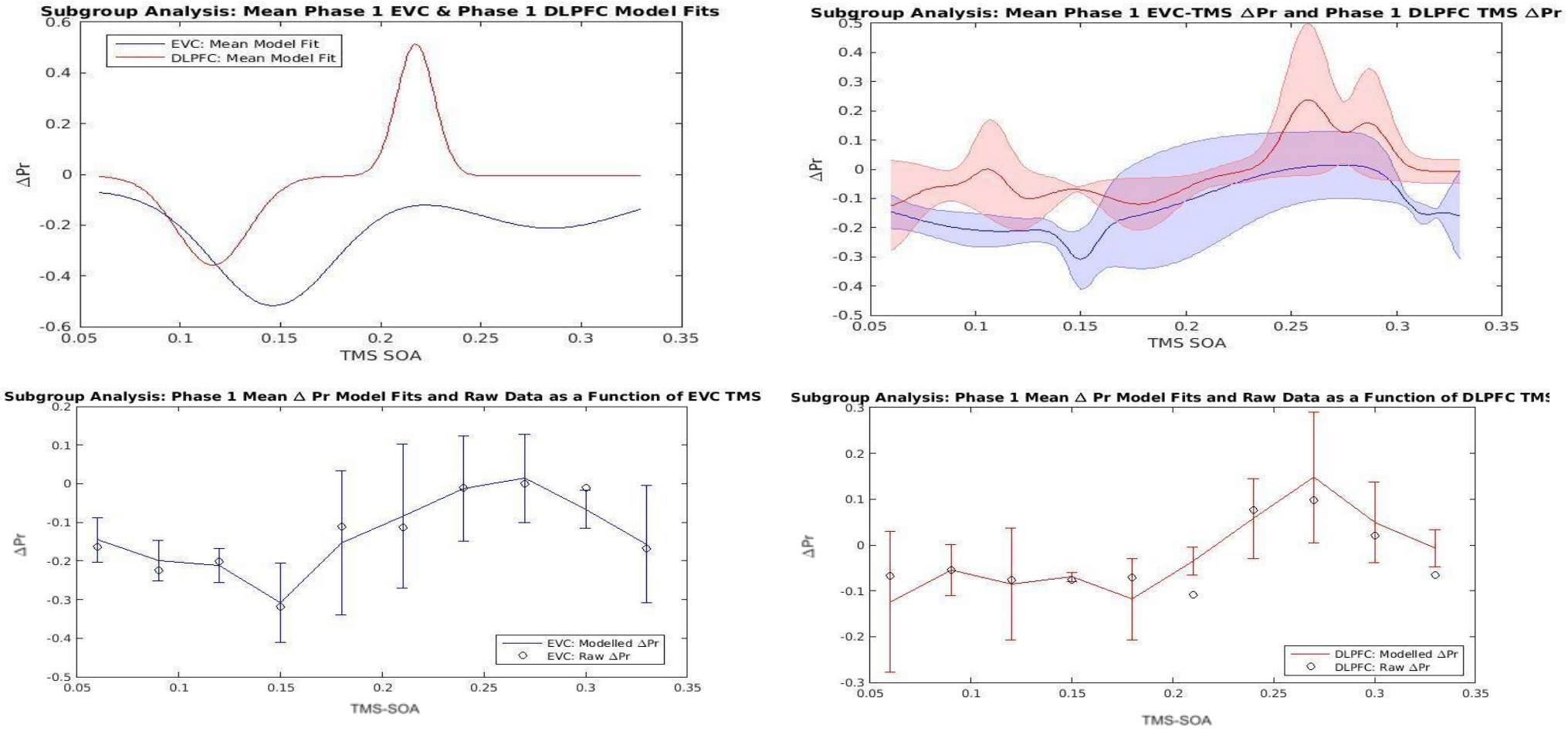

Figure 19. Top left: EVC and DLPFC models produced by EVC and DLPFC coefficients from those who qualified for the subgroup analysis not solved across values of x. Top right:EVC and DLPFC models produced by EVC and DLPFC coefficients from those who qualified for the subgroup analysis solved across values of x. Bottom left: Mean modelled and raw ΔPr as a function of EVC-TMS. Bottom right: Mean modelled and raw ΔPr as a function of DLPFC-TMS

Pre-registered ΔAcc biphasic Gaussian (-/+ $a_{1,2}$) group analyses:

There were four one-sample Bayesian *t*-tests in these pre-registered analyses, which assessed whether EVCa_1 and EVCa_2 along with DLPFCa_1 and DLPFCa_2 supported TMS-induced effects on behaviour. If the Bayesian *t*-tests on EVCa_1 and DLPFCa_1 or DLPFCa_2 produced a *BF* that is more than 3, additional analyses comparing EVCx_1 and DLPFCx_1 or DLPFCx_2 were carried out.

Pre-registered ΔAcc biphasic Gaussian (-/+ $a_{1,2}$) group analyses: Have EVC and DLPFC-TMS induced effects occurred on ΔAcc?

A Bayesian one-sample *t*-test with a JZS prior (Rouder et al., 2009) on EVCa_1 produced a *BF* that provided strong support for the null hypothesis as a function of 32 participants *t* (31) = -0.3728, *p* = 0.7119, *BF* = 0.2014) but revealed weak evidence for the null hypothesis as a function of 32 participants for EVCa_2 (*t* (31) = 1.3858, *p* = 0.1757, *BF* = 0.4501). The *BF* as a function of participant number and corresponding mean coefficients can be found in table 4. The *BF* as a function of participant number can be found in figure 20 . All models and raw data for this analysis can be found in figure 21. Examination of figure 20 (top) reveals a model that does not look biphasic with two distinct peaks; it looks multi-lobed. This is not due to an error in the curve fitting procedure. Instead, it is due to differences in how the plot in figure 18 (top) was generated. Figure 18 (top) was generated by solving each participant's biphasic Gaussian across values of x – in this instance – over values ranging from 1 – 330 milliseconds. Calculating the mean of these models solved across values of produces a curve that has variance on the *y*, enabling it to reflect individual differences in the onset, magnitude and duration of TMS-induced effects on performance. As this method captures indivudal differences in the onset, magnitude and duration of TMS effects, the curve is likely to look multi-lobed as it reflects variance in structure of TMS-induced effects across the SOAs where TMS was administered in this experiment.

	BF: a1	***BF: a2***	***a1***	***a2***	***x1***	***x2***	***b1***	***b2***	***y0***
8	0.3367	0.3882	0.0165	0.1850	114.2ms	266.9ms	35.9ms	37.9ms	-0.0432
16	0.2987	0.2555	0.1081	-0.0039	124.3ms	263.5ms	30.8ms	31ms	-0.0039
24	0.2173	0.2147	-0.0235	-0.0011	131.1ms	262ms	34.8ms	27.7ms	0.0386
32	0.2014	0.4501	-0.0457	0.1811	127.2ms	253.9ms	47.3ms	31.3ms	0.0113

Table 4. Bayes factor (*BF*) and mean ΔAcc biphasic Gaussian coefficients as a function of 8, 16, 24 and 32 participants for EVC-TMS.

A Bayesian one-sample *t*-test with a JZS prior on DLPFCa_1 revealed strong evidence for the null hypothesis as a function of 32 participants (a_1: *t* (*31*) = 0.2398, *p* = 0.8120, *BF* = 0.1940; a_1: *t* (31) = -0.2812, *p* = 0.7804, *BF* = 0.1959). The *BF* as a function of 8, 16, 24 and 32 participants and corresponding mean coefficients can be found in figure 20 . The *BF* as a function of participant number and corresponding mean coefficients can be found in table 5. Table 5 presents the *BF* produced by the Bayesian one-sample *t*-tests after 8, 16, 24 and 32 participants. The *BF* is displayed after each of these increments because analyses were applied after 8, 16, 24 and 32 people because this enabled full counterbalancing of active and sham DLPFC and EVC pairs to take place before additional data analysis was completed. None of the *BF*s produced by Bayesian one-sample *t*-tests produced evidence for a EVC-TMS or DLPFC-TMS induced effect on ΔAcc, which means that this analysis is not permitted to compare EVCx_1 to DLPFCx_1 or DLPFCx_2.

	BF: a1	***BF: a2***	***a1***	***a2***	***x1***	***x2***	***b1***	***b2***	***y0***
8	0.3921	1.6064	-0.1986	-0.5065	125.9ms	249.3ms	19.6ms	41.6ms	0.1284
16	0.3026	0.3566	0.1211	-0.1614	146ms	261.9ms	26.5ms	44.1ms	0.0034
24	0.3012	0.2170	0.123	-0.0226	141ms	260.7ms	28.4ms	37.9ms	-0.0183
32	0.1940	0.1959	0.0318	-0.0352	134ms	266.7ms	26ms	33.6ms	0.0747

Table 5. *BF* and mean ΔAcc biphasic Gaussian coefficients as a function of 8, 16, 24 and 32 participants for DLPFC-TMS.

Pre -registered ΔAcc biphasic Gaussian (-/+ $a_{1,2}$) subgroup analyses: Does DLPFCx_1 or DLPFCx_2 occur later in time than EVCx_1

In the first pre-registered ΔAcc subgroup analysis, which compared EVCx_1 to DLPFCx_1 in a sample of 7 participants whose EVCa_1 and DLPFCa_1 coefficients, respectively, qualified for inclusion. A Bayesian paired-sample *t*-test with a uniform prior (Dienes, 2011) revealed weak evidence for the null hypothesis, which suggests that the DLPFCx_1 does not occur later than EVCx_1 (t (6) = -0.5335, p = 0.6129, BF = 0.3541). Application of a JZS prior to the same mean difference revealed weak evidence for the null hypothesis (BF = 0.3973). In the second pre-registered ΔAcc subgroup analysis, which compared, which compared EVCx_1 to DLPFCx_2 in a different sample of 7 participants who EVCa_1 and DLPFCa_2 coefficients, respectively, enabled qualification for inclusion. A Bayesian paired-sample *t*-test with a uniform prior (Dienes, 2011) revealed decisive evidence for DLPFCx_2 occuring at a later point in time to EVCx_1 (t (6) = -7.7797, p = 2.3749e-04, BF = 2759315074657).All models and raw data can be found in figures 22 and 23.

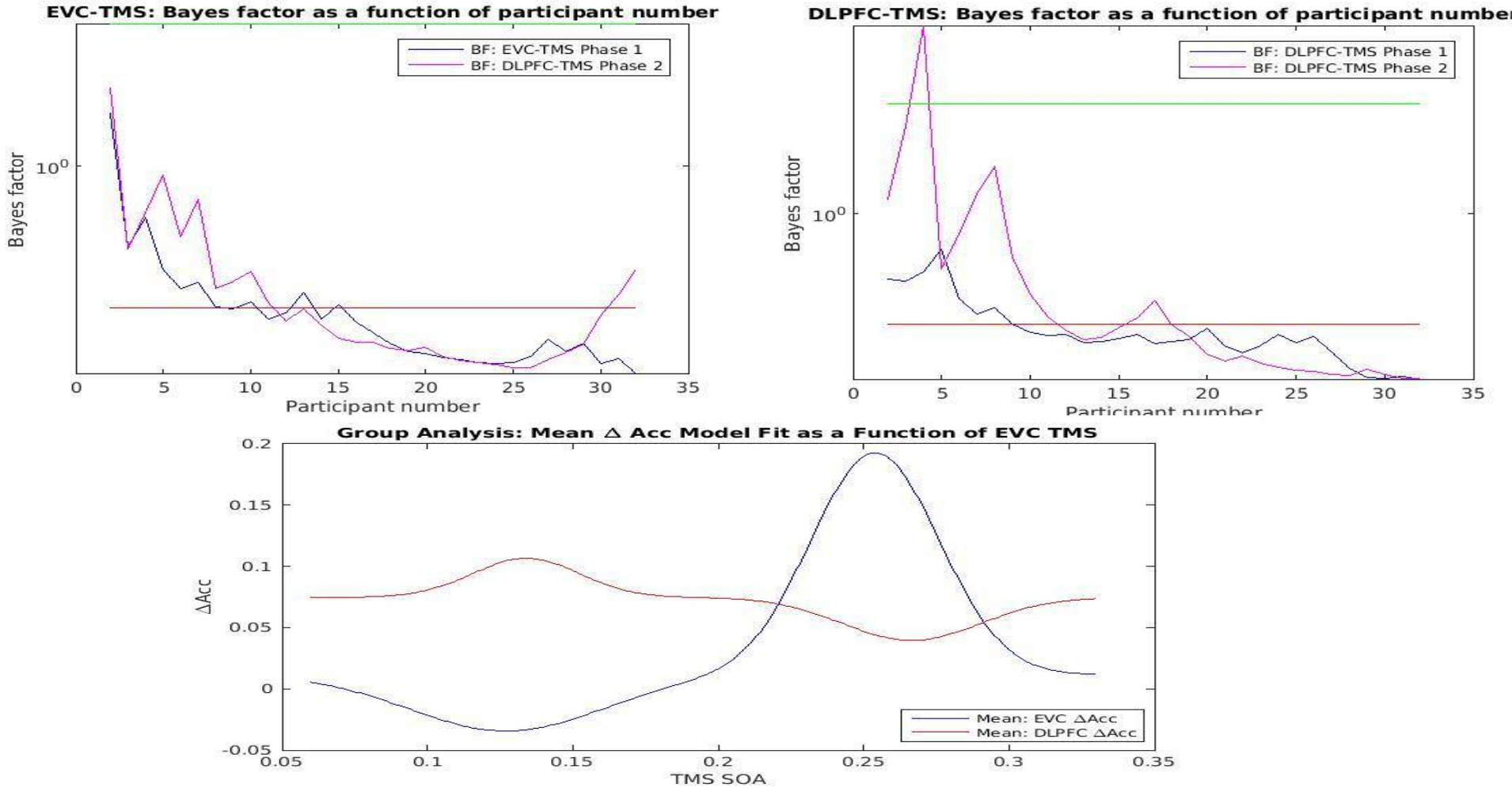

Figure 20. Top left: BF as a function of participant number for EVC-TMS. Top right: BF as a function of participant number for DLPFC-TMS.

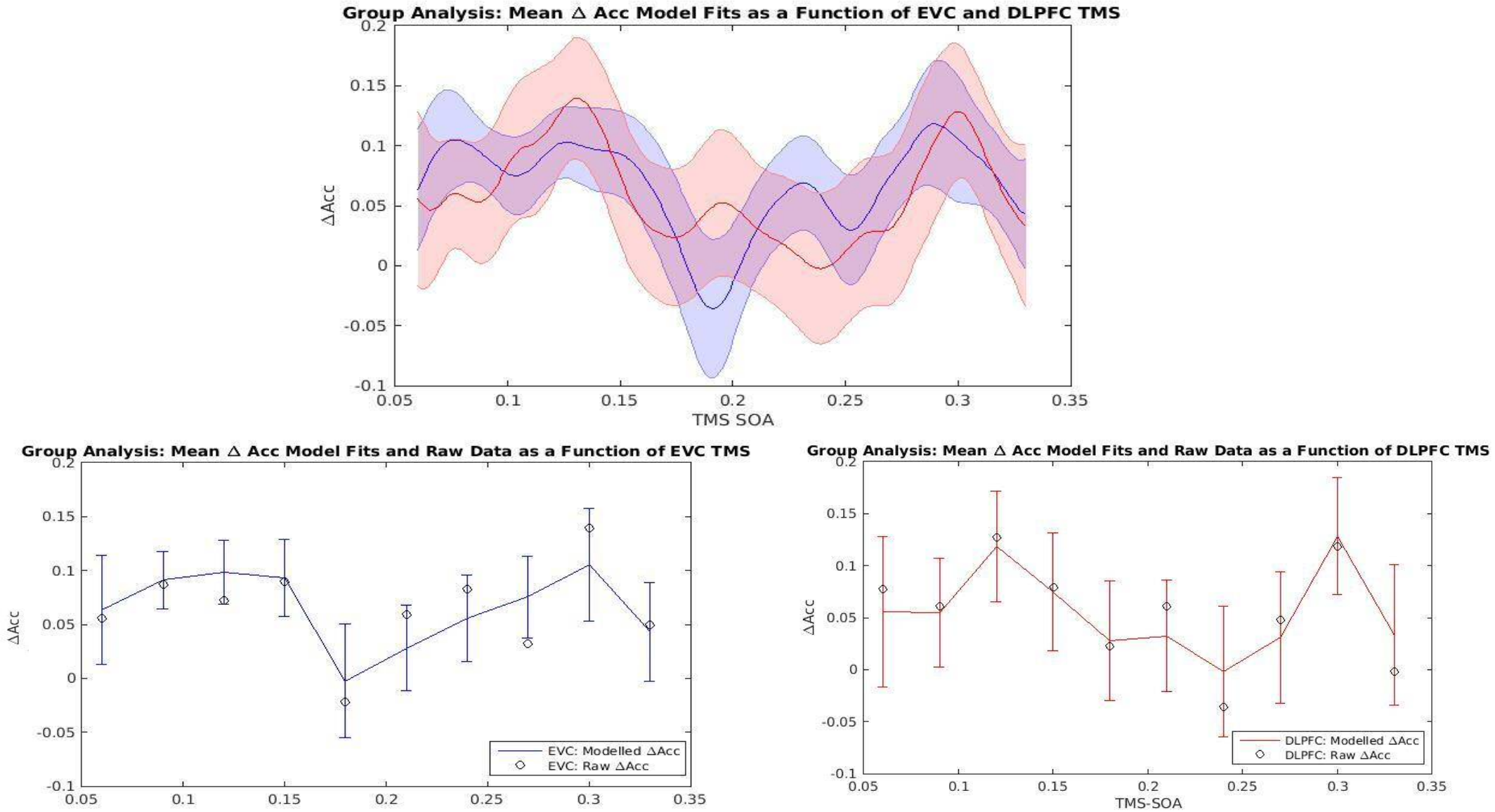

Figure 21. Top: Mean biphasic Gaussian ΔAcc fits as a function of EVC-TMS and DLPFC-TMS. Bottom left: Biphasic Gaussian model fits for ΔAcc as a function of EVC-TMS solved across the SOAs used in the experiment and corresponding raw data. Bottom right: Biphasic Gaussian model fits for ΔAcc as a function of DLPFC-TMS solved across the SOAs used in the experiment and corresponding raw data.

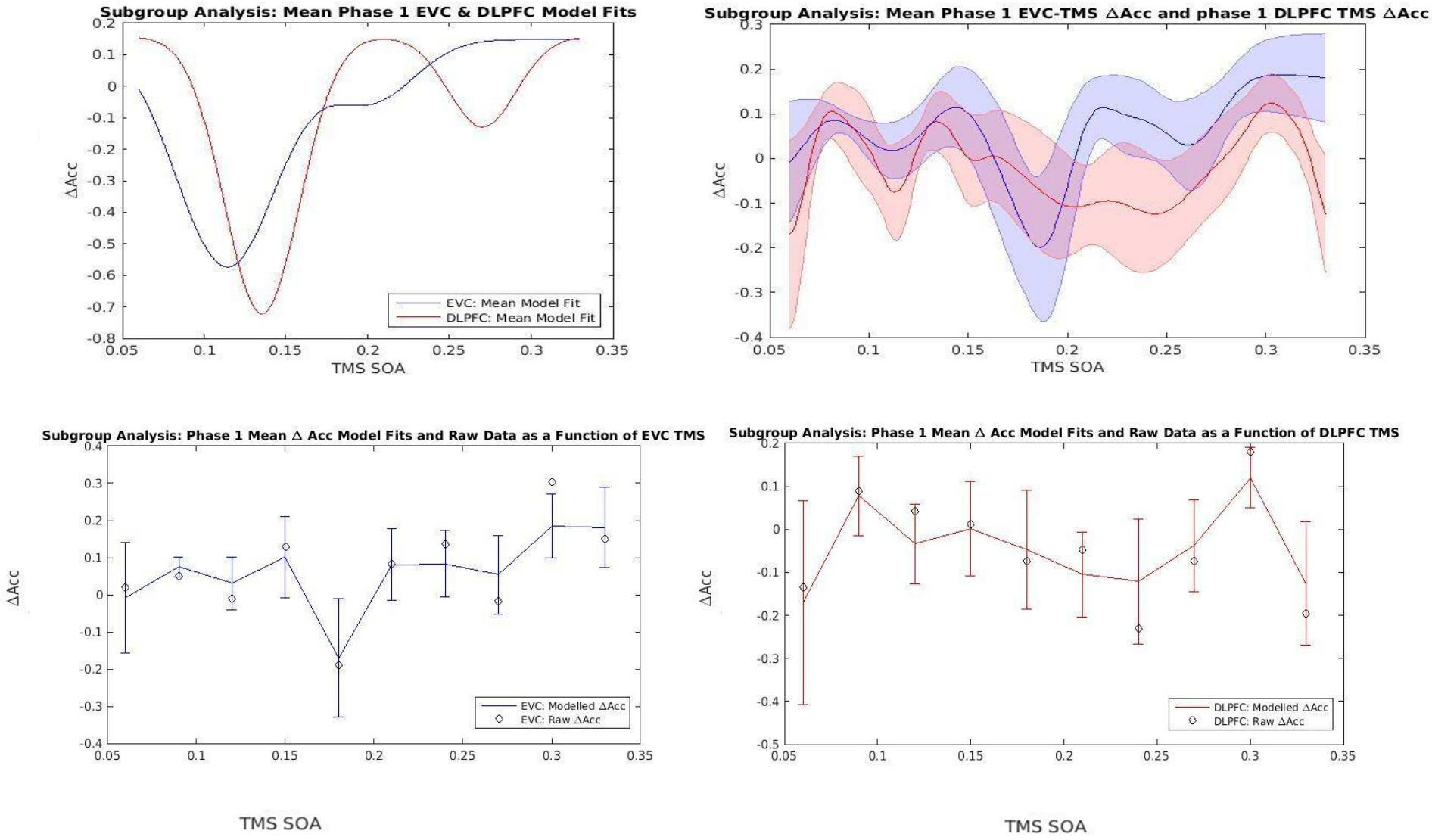

Figure 22. Top left: Mean Biphasic Gaussian models produced by the mean coefficients across all participants included in the subgroup analysis that compared EVCx_1 to DLPFCx_1. Top right: Mean biphasic Gaussian models produced by Gaussian models solved across all possible values of *x*. Bottom left: Biphasic Gaussian model fits for ΔAcc as a function of EVC-TMS solved across the SOAs used in the experiment and corresponding raw data across all participants included in the subgroup analysis that compared EVCx_1 to DLPFCx_1 Bottom right: Biphasic Gaussian model fits for ΔAcc as a function of DLPFC-TMS solved across the SOAs used in the experiment and corresponding raw data across all participants included in the subgroup analysis that compared EVCx_1 to DLPFCx_1

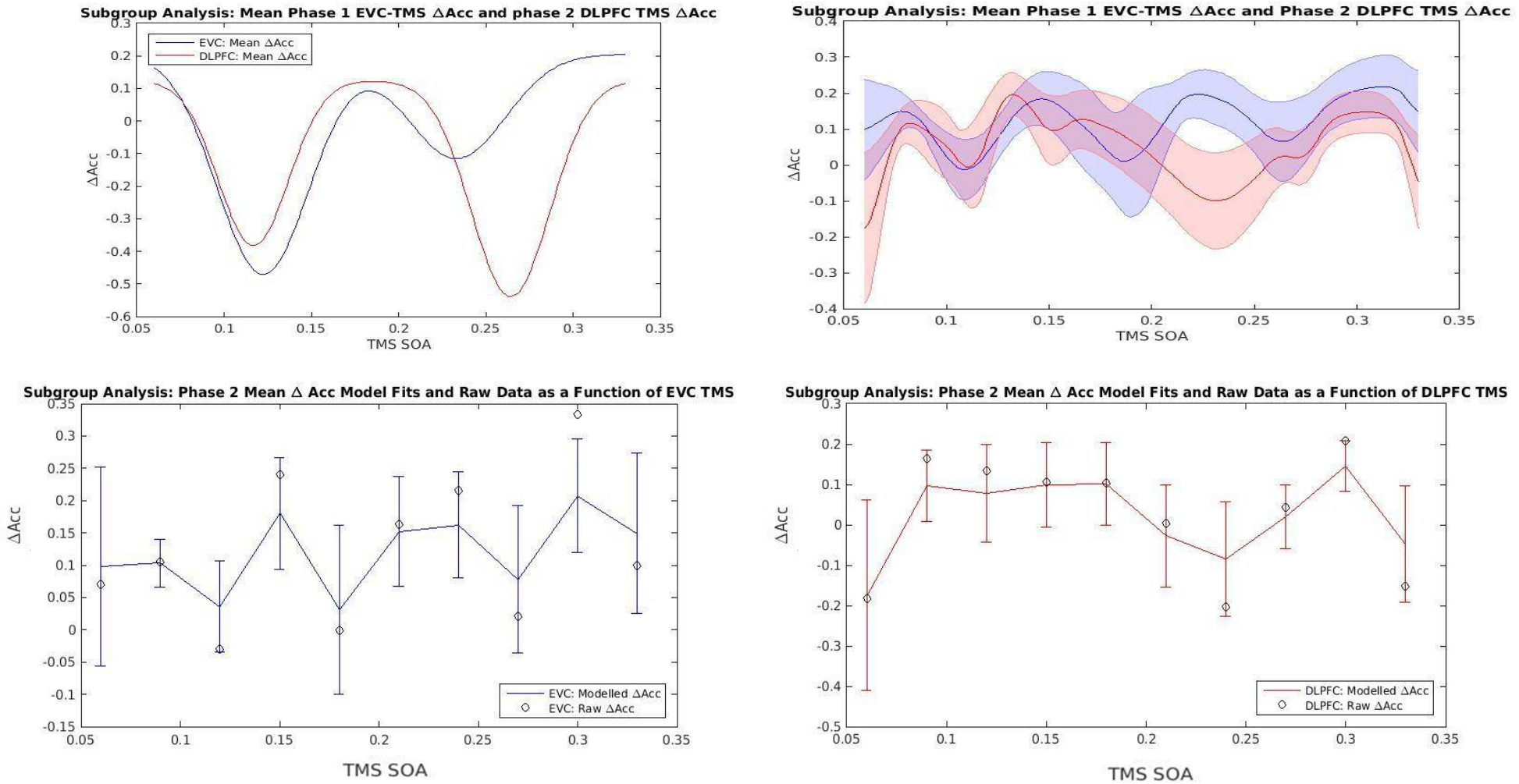

Figure 23. Top left: Mean Biphasic Gaussian models produced by the mean coefficients across all participants included in the subgroup analysis that compared EVCx_1 to DLPFCx_1. Top right: Mean biphasic Gaussian models produced by Gaussian models solved across all possible values of *x*. Bottom left: Biphasic Gaussian model fits for ΔAcc as a function of EVC-TMS solved across the SOAs used in the experiment and corresponding raw data across all participants included in the subgroup analysis that compared EVCx_1 to DLPFCx_2. Bottom right: Biphasic Gaussian model fits for ΔAcc as a function of DLPFC-TMS solved across the SOAs used in the experiment and corresponding raw data across all participants included in the subgroup analysis that compared EVCx_1 to DLPFCx_2

Pre-registered analyses: Interim discussion

As a Bayesian one-sample *t*-test with a JZS prior (Rouder et al., 2009) failed to produce evidence for the mean difference between a_1 or a_2 and zero for ΔPr or ΔAcc as a function of EVC-TMS or DLPFC-TMS. For this reason, the pre-registered analyses concerning Bayesian comparisons of EVCx_1 *to* DLPFCx_1 or DLPFCx_2 were not carried out. The comparison of EVCx_1 to DLPFCx_1 and DLPFCx_2 were not carried out because it was pre-registered that such an analysis was contingent on either of these effects being present. Given that the expected effect of EVC-TMS on performance at approximately 100ms was absent despite the fact that almost all published EVC-TMS studies have produced it (de Graaf et al., 2014), additional exploratory analyses were conducted. Additional exploratory analyses were critical considering that the biphasic Gaussian model as a function of EVC-TMS with the pre-registered constraints produced an intercept but not amplitude or temporal position coefficients that quantified a different between active TMS and sham TMS.

The pre-registered analyses assumed that peak amplitude, a_1, and temporal position, x_1, would quantify an EVC-TMS induced effect on performance at 100ms, and that peak amplitude, a_2, and its temporal position, x_2, could quantify an additional EVC-TMS effect that occurs after 100ms, if such an effect exists. However, this assumption appears to have been incorrect in the pre-registered analyses on ΔPr. The pre-registered analyses on ΔPr revealed that x_1 quantified a minor shift from the intercept at 138.4ms and x_2 quantified a larger shift from baseline at 272.9ms. The critical issue with this is that *y0* is *negative* (-0.0740 when n = 32) and significantly differs from zero when ΔPr is used as a measure. The implication of this is that a decrement in performance at earlier SOAs can be quantified as a deflection from baseline, as measured by y0, or a time-specific difference between active TMS and sham TMS, as quantified by *x* and *a*, respectively. Whether a_1 or *y0* quantifies time specific dips is determined the coefficients that produce the highest adjusted r^2. A major assumption behind the application of a Gaussian model to performance as a function of TMS SOA is that *y0* quantifies the baseline level of performance regardless of SOA, and that $a_{1,2}$ quantify positive or negative deflections from this baseline at a particular point in time. Inspection of the bottom left of

figure 16, which reveals raw and modelled ΔPr at each SOA reveals a clear decrement in performance at 100ms, followed by a brief set of SOAs at 250ms where performance returns to zero, followed by the beginning of a decrement at 300ms. The $a_{1,2}$ coefficients were constrained in a way that did not always facilitate the detection of a TMS-induced decrement in performance, which can cause *y0* to quantify such effects. Instead. *y0* appears to have quantified the maximal decrement in performance and $a_{1,2}$ have captured the maximal increments where, in this case, performance returns to baseline. $a_{1,2}$ quantify improvements relative to the intercept but in terms of absolute value, $a_{1,2}$ and corresponding $x_{1,2}$ quantify where active and sham performance *do not* differ. In contrast, the intercept of the model captured the magnitude of the difference between active performance and sham performance, which is different from zero according to a Bayesian one-sample *t*-test. However, the intercept quantifies such an effect on the *x* axis without any source of variance on *y* axis, preventing statistical analysis from revealing the temporal structure of recurrent processing within EVC.

In order to explain the unexpected results presented here, a series of exploratory analyses were carried out. These analyses involved applying a biphasic and a monophasic Gaussian to ΔPr and ΔAcc as a function of EVC-TMS and DLPFC-TMS SOA. Both of these Gaussian models were applied with two different types of constraint which was only applied to the *a* coefficients. The first type of constraint only enabled *a* to be negative, which aimed to prevent y0 from capturing decrements in performance. The second type of *a* coefficient constraint which was applied to exploratory analyses was identical to the constraints that were pre-registered.

Overview: Exploratory analyses

A series of exploratory analyses were applied in response to the issues arising from the pre-registered analyses. Reapplying the GAn and the SGAn as pre-registered to the ΔPr biphasic Gaussian model with different a_1 and a_2 constraints led to a different outcome: the *BF*s supported EVCx_1 and DLPFCx_1 occurring at the same time but supported that DLPFCx_2 occurred later in time than EVCx_1. The same exploratory analysis which constrained the ΔAcc biphasic Gaussian a_1 and a_2 coefficients

also revealed that EVCx_1 and DLPFCx_1 occurred at the same time but DLPFCx_2 occurred later on than EVCx_1. When exploratory analyses were carried out with a monophasic Gaussian which could have positive or negative a_1 coefficients similar outcomes were revealed when ΔPr and ΔAcc were used as measures. The analysis proceeded similarly to the pre-registered analyses. First, an effect of active TMS relative to sham TMS was sought using the EVC and DLPFC a_1 coefficients. Subsequently, a comparison of EVCx_1 to DLPFCx_1 took place, if the a_1 coefficients successfully quantified an effect of active TMS relative to sham TMS. When a_1 could be positive or negative, a monophasic Gaussian failed to produce evidence for an effect of EVC-TMS at ~100ms. However, when a_1 could be positive or negative and a monophasic Gaussian was applied to ΔAcc, evidence for an effect of EVC-TMS at ~100ms was produced but no evidence for a DLPFC-TMS effect was found. However, when the a_1 and a_2 coefficients could only be negative, evidence of EVC- and DLPFC-TMS induced effects was obtained, and evidence for EVCx_1 and DLPFCx_1 occurring at the same time was obtained.

Exploratory ΔPr and ΔAcc analyses: biphasic Gaussian model with negative peak amplitude coefficient constraints ($-a_{1,2}$)

The principle reason that the pre-registered analyses failed to was that $a_{1,2}$ were positive as opposed to negative, which in the case of ΔPr quantified deflections from a negative baseline (*y0*), with *y0* suggesting that a difference between active and sham EVC TMS exists. The co-occurrence of these events could have prevented the decrement in performance produced by EVC-TMS at an SOA of 100ms from being detected. The outcome of the pre-registered analyses was surprising considering that an EVC-TMS effect at an SOA of ~100ms is one of the most robust and reproducible effects in TMS research (de Graaf et al., 2014). In order to conclude whether or not such an effect is present and whether these issues also precluded the detection of a DLPFC-TMS effect, additional analyses were completed. These additional analyses applied an additional biphasic Gaussian model to ΔPr and ΔAcc as a function of EVC-TMS and DLPFC-TMS. The only constraints that differed from the pre-registered analyses are displayed below:

1. $a_{1,2} < 0$, which prevented the peak amplitude coefficients from being positive.

2. $a_{1,2}$ > the absolute difference between the maximum and minimum ΔPr/ΔAcc score obtained across all TMS SOAs multiplied by -1, which enabled the amplitude coefficients to be negative without exceeding the largest difference between data points across SOAs.

The only difference between the pre-registered model constraints the exploratory model constraints here were applied to $a_{1,2}$. In the pre-registered analyses, $a_{1,2}$ were less than the positive or negative difference between the maximum and minimum ΔPr score obtained across all TMS SOAs, respectively. In this exploratory analysis, the constraint enabling $a_{1,2}$ to be positive was removed but the constraint enabling the same coefficients to be negative was retained. Such a change was implemented in order to prevent *y0* from quantifying the difference between active and sham TMS and force $a_{1,2}$ and their corresponding $x_{1,2}$ to quantify the SOA where the largest negative difference between active and sham TMS exists, if such a difference exists.

Exploratory ΔPr biphasic Gaussian (-$a_{1,2}$) group analyses : Have EVC-TMS and DLPFC-TMS induced effects occurred?

Figure 24 reveals the *BF* supports for a mean difference between $a_{1,2}$ and zero for ΔPr as a function of EVC-TMS once 32 participants for a_1 (*t* (31) = -14.8358, *p* = 1.2531e-15, *BF* = 4823705238325) and a_2 (*t* (31) = -11.84, *p* = 4.9048e-13, *BF* = 15908887780). The implication of these analyses is that ΔPr as a function of EVC-TMS qualifies for inclusion within the temporal position test. Figure 24 reveals that the *BF* also supports a mean difference between $a_{1,2}$ and zero for ΔPr as a function as a function of DLPFC-TMS once all 32 participants have been included in the analysis for a_1 (*t* (31) = -8.7445, *p* = 7.1261e-10, *BF* = 15675129) and a_2 (*t* (31) = -11.4278, *p* = 1.2063e-12, *BF* = 6739265478). This outcome means that ΔPr as a function of DLPFC-TMS also qualifies for inclusion within the GAn-2. Model fits and corresponding raw data for this exploratory GAn can be found in figure 25.

These exploratory analyses aimed to identify whether $a_{1,2}$ successfully quantified EVC and DLPFC-TMS induced effects if the amplitude coefficients were constrained to prevent them from

being positive but enabled them to be negative. The outcome of these exploratory analyses revealedthat the *BF* supported that a mean difference between active and sham EVC TMS existed at 109.6ms, consistent with previous EVC-TMS research (Kammer, 2007; de Graaf et al., 2014) and later on at 276.5ms. Moreover, the *BF* also supported that a mean difference between active and sham DLPFC TMS existed at 109.9ms and later on at 273.4ms. To summarize, the outcome of this exploratory analysis suggested s that effects of EVC and DLPFC TMS have occurred at a particular SOA.

Exploratory biphasic Gaussian (-$a_{1,2}$) ΔPr group analyses: Does DLPFCx_1 or DLPFCx_2 later in time than EVCx_1?

As a result of the exploratory analysis on EVC a_1 and DLPFC $a_{1,2}$, an additional analysis will be carried out which aims to identify if DLPFC x_1 or DLPFC x_2 occur later in time to EVCx_1. The first temporal position test compared EVCx_1 to DLPFCx_1 using a Bayesian paired-sample *t*-test, which revealed that DLPFCx_1 does not occur later in time to EVCx_1 (*t* (31) = -0.0262, *p* = 0.9793, *BF* = 0.0617). Application of a JZS prior to the same mean difference revealed strong evidence that EVCx_1 has the same onset as DLPFCx_1 (BF = 0.1889). However, a uniform prior did reveal that DLPFCx_2 occurs later in time to EVCx_1 (*t* (31) = -12.9345, *p* = 4.9525e-14, *BF* = 2.9436e+35).

Exploratory biphasic Gaussian (-a1,2) subgroup ΔPr analyses: Does DLPFCx_1 or DLPFCx_2 later in time than EVCx_1?

The subgroup analysis applied an identical selection procedure to the exploratory subgroup analyses that were specified in the amended pre-registration document. A total of 18 participants qualified for the first subgroup analysis, which revealed that EVCx_1 and DLPFCx_1 occur at the same time (*t* (18) = -0.9310, *p* = 0.3649, *BF* = 0.21). Application of a JZS prior to the same mean difference revealed weak evidence that EVCx1 and DLPFCx1 have the same temporal onset (*BF* = 0.3555). 19 participants also qualified for the second subgroup analysis, which revealed that DLPFCx_2 occurred later in time to EVCx_1 *t* (18) = -11.5144, *p* = 9.7846e-10, *BF* = 1.0652e+28). Model fits and corresponding raw data for this exploratory SGAn can be found in figure 26 and 27 For

completeness, an additional exploratory analysis was conducted which applied a biphasic Gaussian model to ΔAcc with identical constraints to the exploratory analysis applied to ΔPr which only enabled a_1,^{2} to be negative.

Exploratory ΔAcc biphasic Gaussian (-a1,2) group analyses: Have EVC-TMS and DLPFC-TMS induced effects occurred on ΔAcc

A Bayesian one-sample *t*-test with a JZS prior (Rouder et al., 2009) on EVC$a_{1,2}$ revealed a two effects of EVC-TMS on ΔAcc: one at 132.2ms (a_1: *t* (31) = -13.6313, *p* = 1.0e- 12 * 0.0123, *BF* = 539000388210) and another effect later on at 282.4ms (a_2: *t* (31) = -13.9809, *p* = 1.0e – 12 * 0.0063, *BF* = 1032511837742). Similarly, a Bayesian one-sample *t*-test with a JZS prior (Rouder et al., 2009) on DLPFC $a_{1,2}$ also revealed decisive evidence for two effects of DLPFC-TMS on ΔAcc: one at 123.9ms (a_1: *t* (31) = -12.1705, *p* = 1.0e – 12*0.2419, *BF* = 31249028072) and another later on at 284.8ms (*t* (31) = -16.0061, *p* = 1.0e- 12*0.002, *BF* = 35855754841824). This suggests that two distinct effects of EVC-TMS and DLPFC-TMS arose between 60 and 330ms after the onset of the visual target. As a result of EVCa_1 along with DLPFCa_1 and DLPFCa_2 producing *BF*s that reflected TMS induced effects on performance, the GAn-2 was completed.

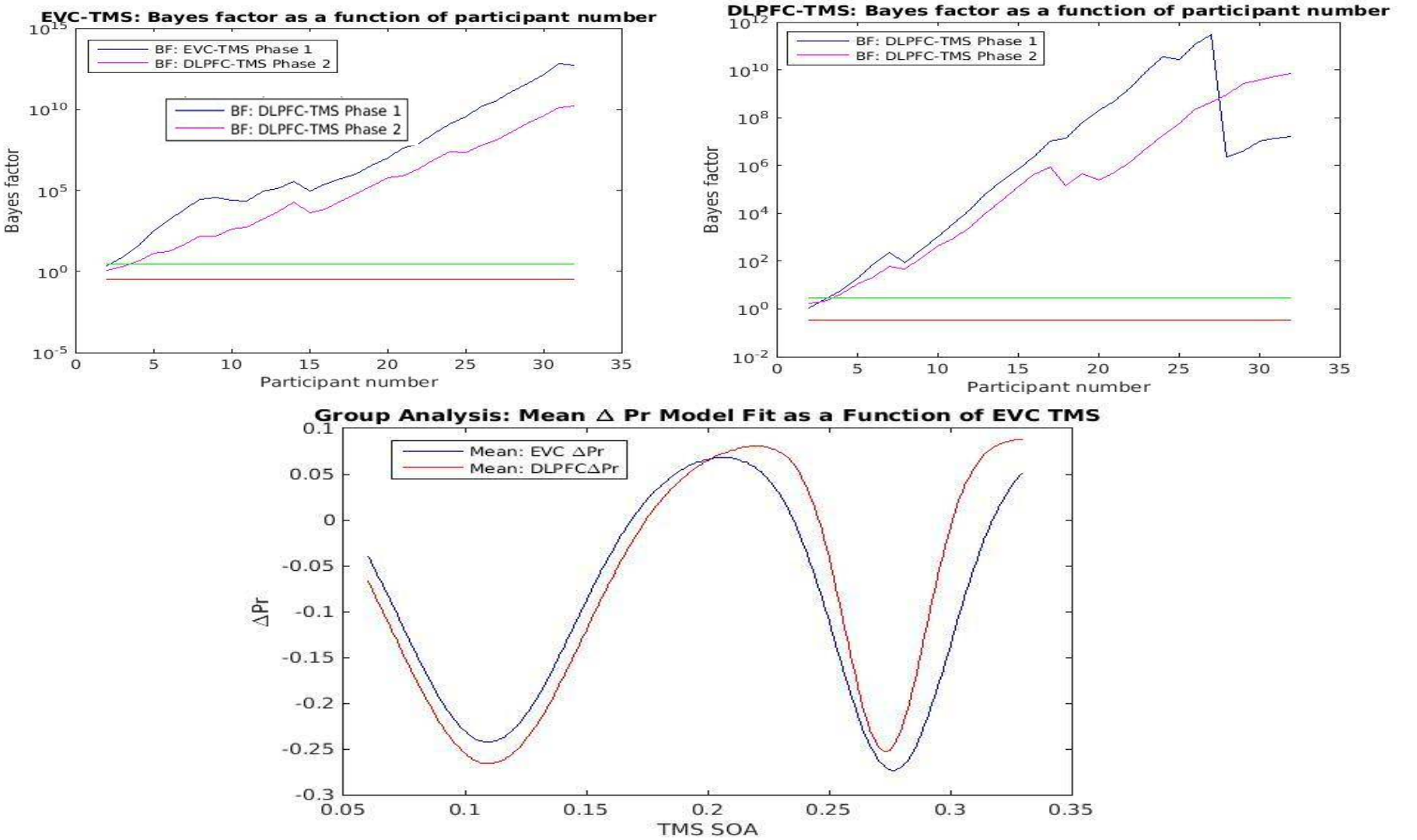

Figure 24. Top left: Bayes factor (*BF*) as a function of participant number for EVC-TMS. Top right: *BF* as a function of participant number for DLPFC-TMS. Bottom: Gaussian models produced by calculating the mean of each biphasic Gaussian ΔPr coefficient as a function of EVC-TMS and DLPFC-TMS.

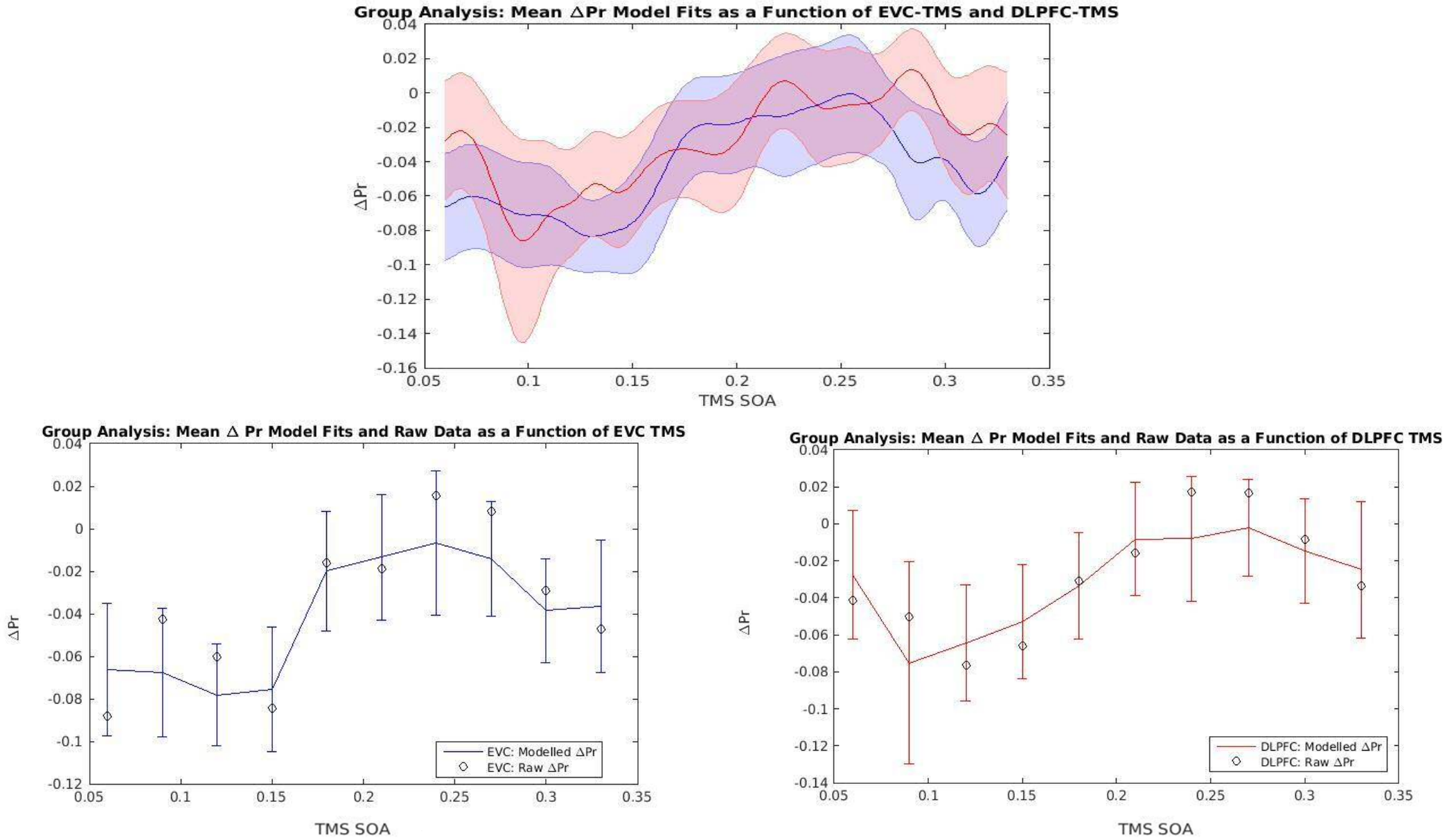

Figure 25. Top: Mean biphasic Gaussian ΔPr fits as a function of EVC-TMS and DLPFC-TMS. Bottom left: Biphasic Gaussian model fits for ΔPr as a function of EVC-TMS solved across the SOAs used in the experiment and corresponding raw data. Bottom right: Biphasic Gaussian model fits for ΔPr as a function of DLPFC-TMS solved across the SOAs used in the experiment and corresponding raw data.

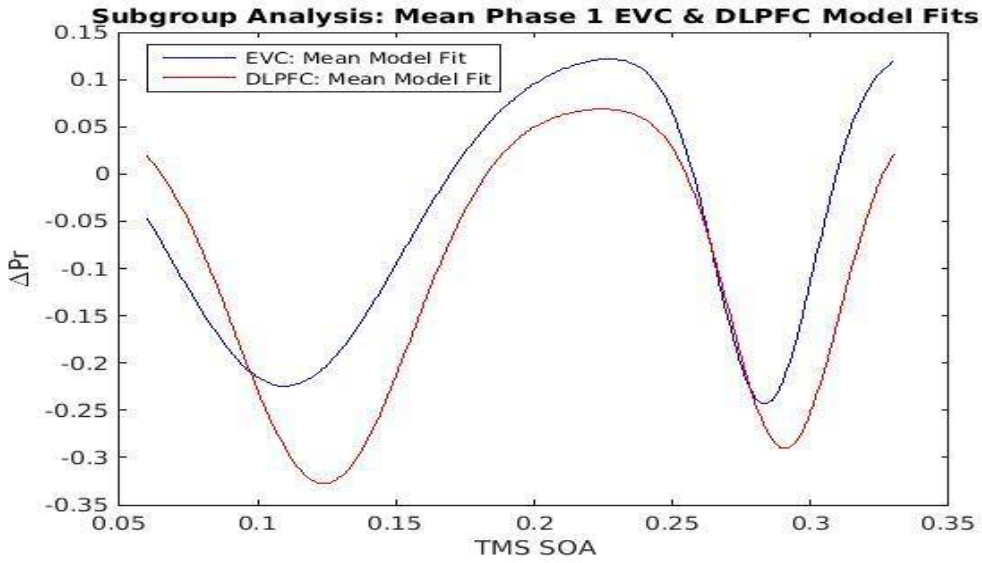

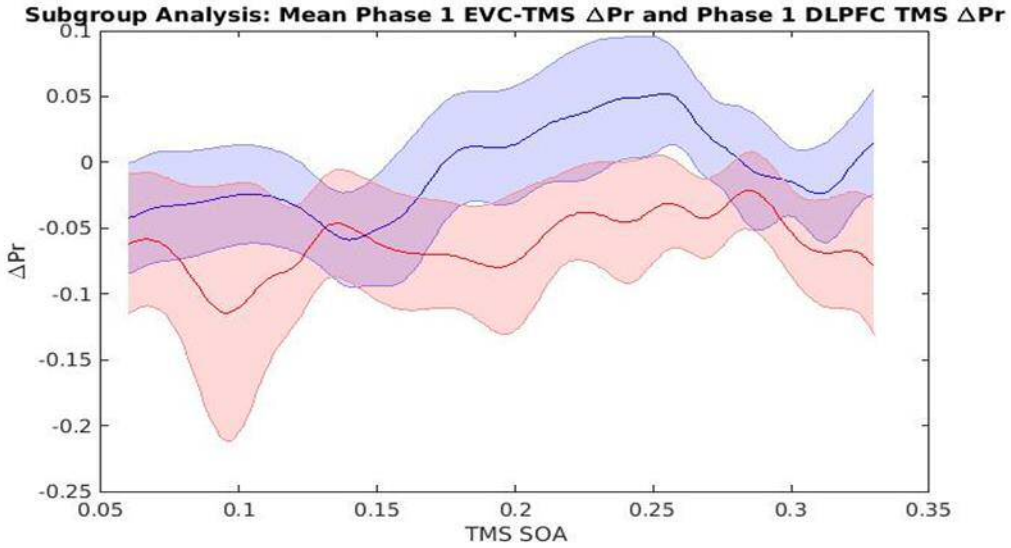

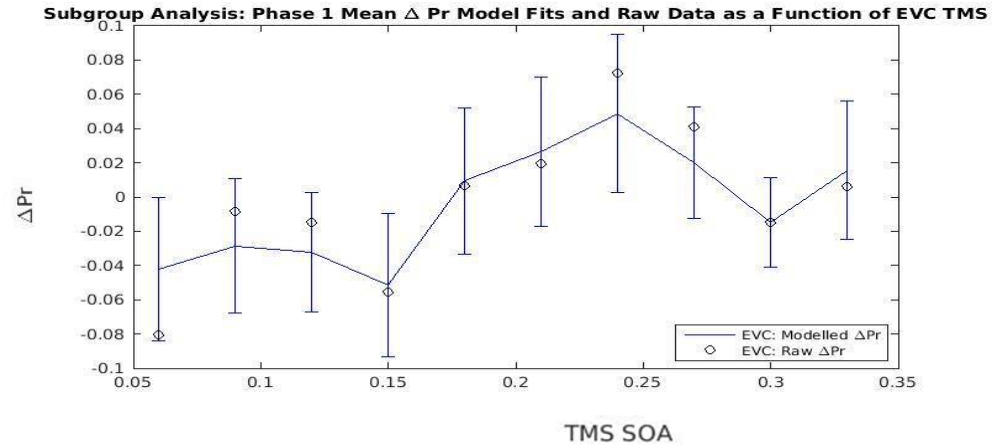

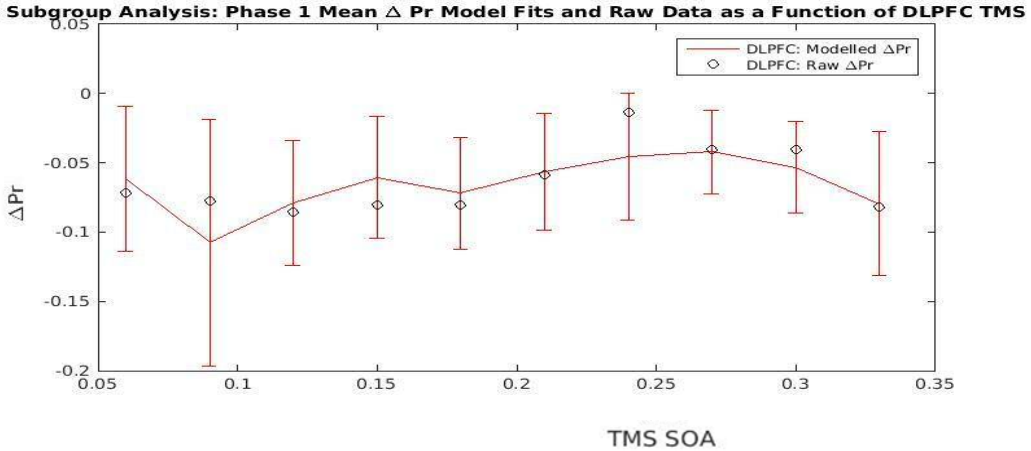

Figure 26. Top left: Mean Biphasic Gaussian models produced by the mean coefficients across all participants included in the subgroup analysis that compared EVCx_1 to DLPFCx_1. Top right: Mean biphasic Gaussian models produced by Gaussian models solved across all possible values of *x*. Bottom left: Biphasic Gaussian model fits for ΔPr as a function of EVC-TMS solved across the SOAs used in the experiment and corresponding raw data across all participants included in the subgroup analysis that compared EVCx_1 to DLPFCx_1. Bottom right: Biphasic Gaussian model fits for ΔPr as a function of DLPFC-TMS solved across the SOAs used in the experiment and corresponding raw data across all participants included in the subgroup analysis that compared EVCx_1 to DLPFCx_1

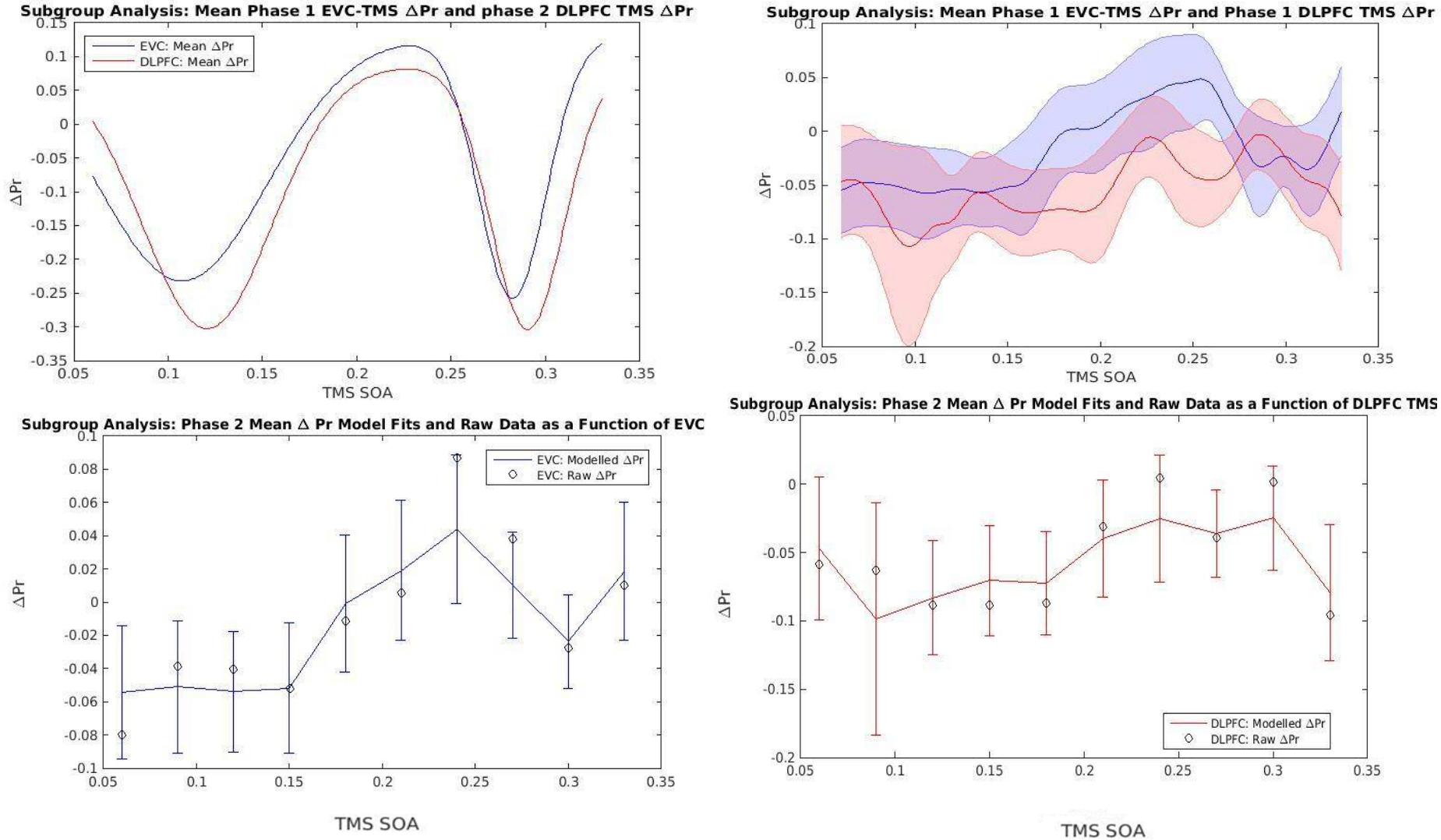

Figure 27. Top left: Mean Biphasic Gaussian models produced by the mean coefficients across all participants included in the subgroup analysis that compared EVCx_1 to DLPFCx_2. Top right: Mean biphasic Gaussian models produced by Gaussian models solved across all possible values of *x*. Bottom left: Biphasic Gaussian model fits for ΔPr as a function of EVC-TMS solved across the SOAs used in the experiment and corresponding raw data across all participants included in the subgroup analysis that compared EVCx_1 to DLPFCx_2. Bottom right: Biphasic Gaussian model fits for ΔPr as a function of DLPFC-TMS solved across the SOAs used in the experiment and corresponding raw data across all participants included in the subgroup analysis that compared EVCx_1 to DLPFCx_2

Exploratory biphasic Gaussian (-$a_{1,2}$) ΔAcc group analyses: Does DLPFCx_1 or DLPFCx_2 induced effects occur later than EVCx_1 induced effect?

A Bayesian paired-sample *t*-test with a uniform prior (Dienes, 2011) revealed that DLPFCx_1 and EVCx_1 occur at the same point in time (*t* (31) = 0.6131, *p* = 0.5443, *BF* = 0.0479). Application of a JZS prior to the same mean difference revealed strong evidence for EVCx_1 and DLPFCx_1 having the same temporal onset (*BF* = 0.2247). However, a uniform prior did reveal that DLPFCx_2 occurs at a later point in time to EVCx_1 (*t* (31) = -10.9130, *p* = 3.8208e-12, *BF* = 1.1058e+25). The *BF*s as a function of participant number produced by these Bayesian one-sample *t*-tests as a function of participant number can be found in figure 28 .

Exploratory biphasic Gaussian (- $a_{1,2}$) ΔAcc subgroup analyses: Does DLPFCx_1 or DLPFCx_2 occur later in time than EVC-TMSx_1 induced effect?

When comparing EVCx_1 to DLPFCx_1 in a sample of 30 participants who EVCa_1 and DLPFCa_1 coefficients, respectively, enabled qualification for inclusion. A Bayesian paired-sample *t*-test with a uniform prior (Dienes, 2011) revealed weak evidence for the null hypothesis, which suggests that the DLPFCx_1 does not occur later than EVCx_1 (*t* (29) = 0.4070, *p* = 0.6870, *BF* = 0.0576). When comparing EVCx_1 to DLPFCx_2 in sample of 30 participants who qualified for inclusion, the Bayesian paired-sample *t*-test revealed decisive evidence that DLPFCx_2 occurs at a later point in time to EVCx_1 (t (30) = -11.41448, *p* = 0.8301, *BF* = 1.4281e+26). All model fits and corresponding raw data concerning this analysis can be found in figure 30.

Interim discussion: Exploratory group and subgroup analyses using a biphasic Gaussian model to ΔPr and ΔAcc with negative amplitude coefficients

The pre-registered analyses had the potential to segregate two discrete TMS induced effects which could occur from SOAs ranging from 60ms to 330ms. The pre-registered analyses then compared EVCx_1 to DLPFCx_1 and DLPFCx_2. For both ΔPr and ΔAcc, EVCx_1 and DLPFCx_1 had the same temporal position whereas and DLPFCx_2 did occupy at later temporal position to EVCx_1. However, by segregating the data in into two separate Gaussian phases with a constraint that forces x_2 to occur at

a later point in time than x_1. Analyses that compare EVCx_1 to DLPFCx_2 are more likely to produce *BF*s that reflect the constraints within the curve fitting procedure rather than a genuine difference in the timing of two events that enable a visual target to be reported. In light of this criticism, additional analyses were carried out with a monophasic Gaussian, which only has one *a*, *x* and *b* along with an intercept coefficient. However, as highlighted previously two discrete effects of TMS may not reflect feedforward and recurrent processes, which could be captured by a biphasic Gaussian being applied to ΔPr and ΔAcc as a function of EVC-TMS. However, it is also possible that feedforward and recurrent processes could be reflected in a single TMS effect (de Graaf et al., 2012; de Graaf et al., 2014), which could be captured by a monophasic Gaussian. To address these methodological and theoretical concerns, additional exploratory analyses using a monophasic Gaussian with positive and/or negative a coefficients were also carried out. The interesting conclusion that has been highlighted by this analysis which can be explored further analysis is that temporal order of EVC-TMS and DLPFC-TMS effects. The hypothesis that was pre-registered, that a DLPFC-TMS effect will occur after an EVC-TMS effect was not confirmed. Instead, it appears that critical events for visual perception occur at the same time within EVC and DLPFC.

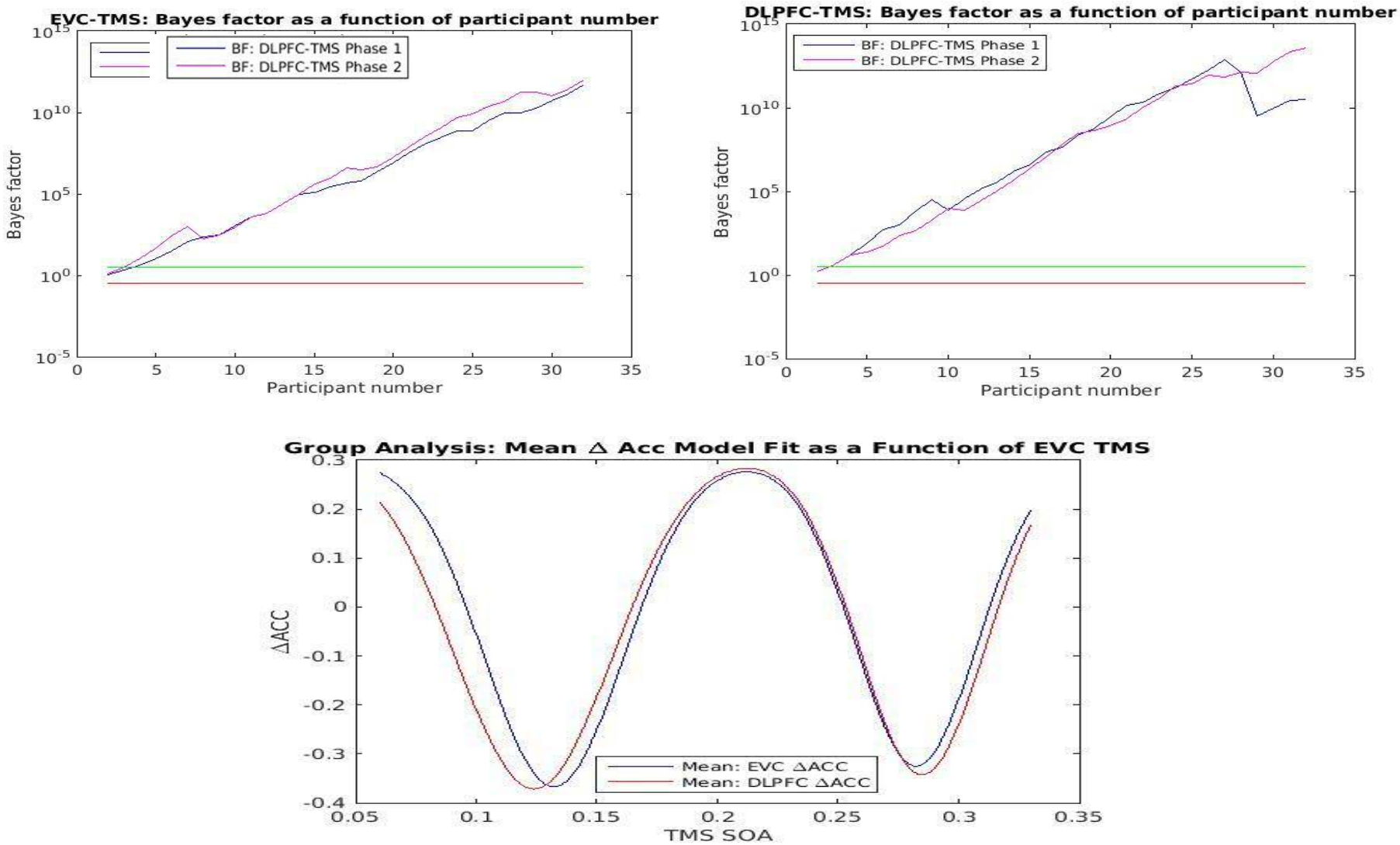

Figure 28. Top left: Bayes factor (*BF*) as a function of participant number for EVC-TMS. Top right: *BF* as a function of participant number for DLPFC-TMS. Bottom: Gaussian models produced by calculating the mean of each biphasic Gaussian ΔAcc coefficient as a function of EVC-TMS and DLPFC-TMS.

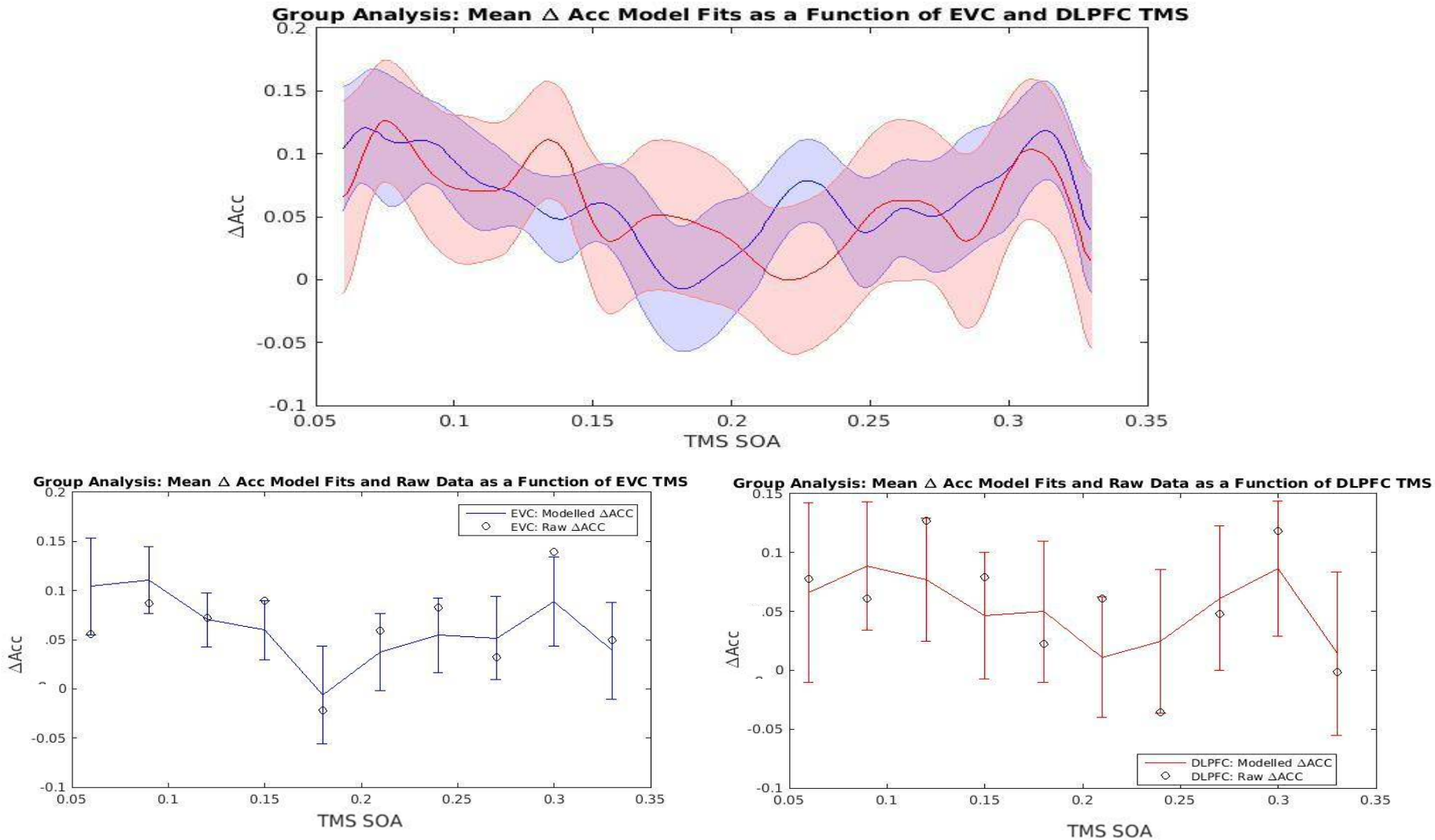

Figure 29. Top: Mean biphasic Gaussian ΔAcc fits as a function of EVC-TMS and DLPFC-TMS. Bottom left: Biphasic Gaussian model fits for ΔAcc as a function of EVC-TMS solved across the SOAs used in the experiment and corresponding raw data. Bottom right: Biphasic Gaussian model fits for ΔAcc as a function of DLPFC-TMS solved across the SOAs used in the experiment and corresponding raw data.

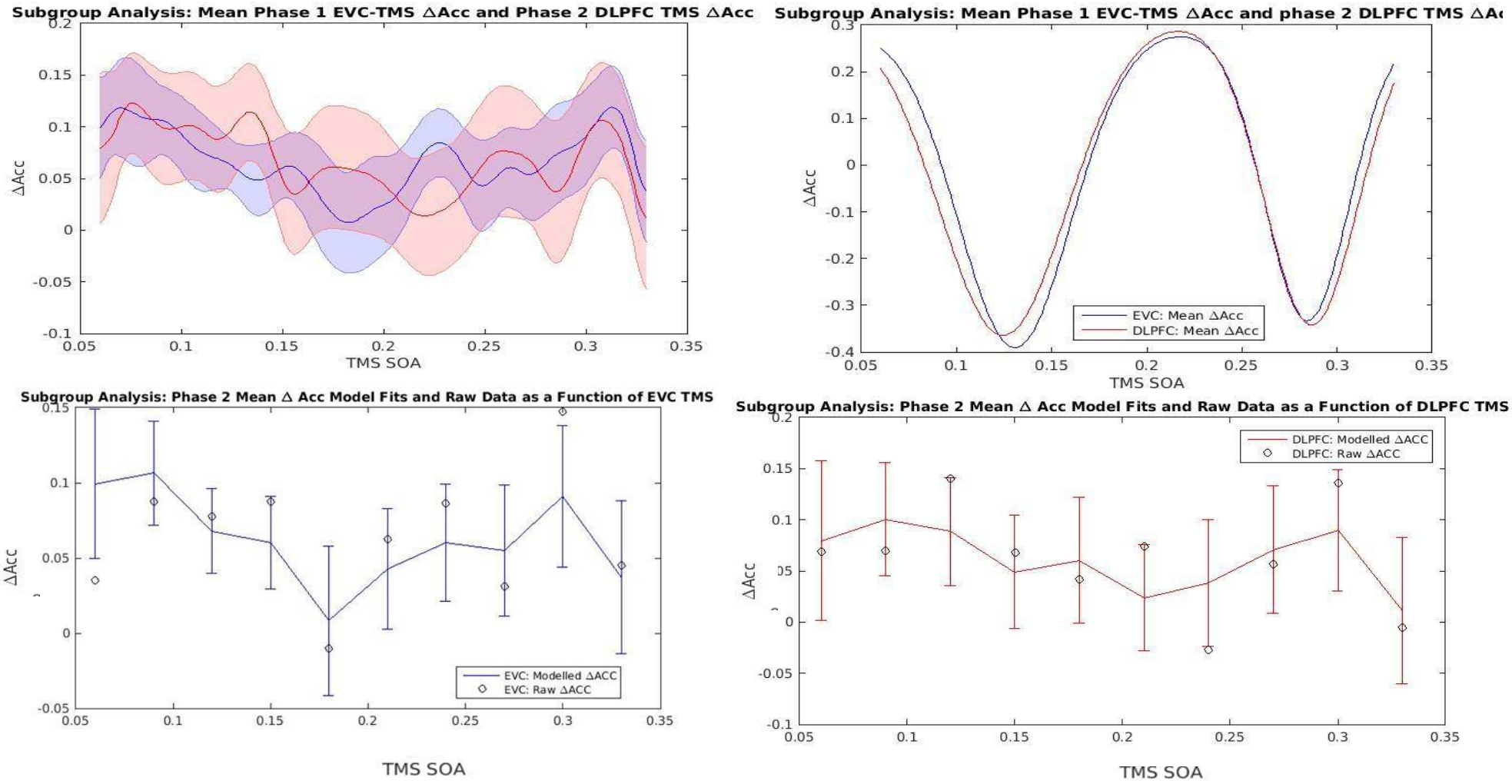

Figure 30. Top left: Mean Biphasic Gaussian models produced by the mean coefficients across all participants included in the subgroup analysis that compared EVCx_1 to DLPFCx_1. Top right: Mean biphasic Gaussian models produced by Gaussian models solved across all possible values of *x*. Bottom left: Biphasic Gaussian model fits for ΔAcc as a function of EVC-TMS solved across the SOAs used in the experiment and corresponding raw data across all participants included in the subgroup analysis that compared EVCx_1 to DLPFCx_1. Bottom right: Biphasic Gaussian model fits for ΔAcc as a function of DLPFC-TMS solved across the SOAs used in the experiment and corresponding raw data across all participants included in the subgroup analysis that compared EVCx_1 to DLPFCx_1

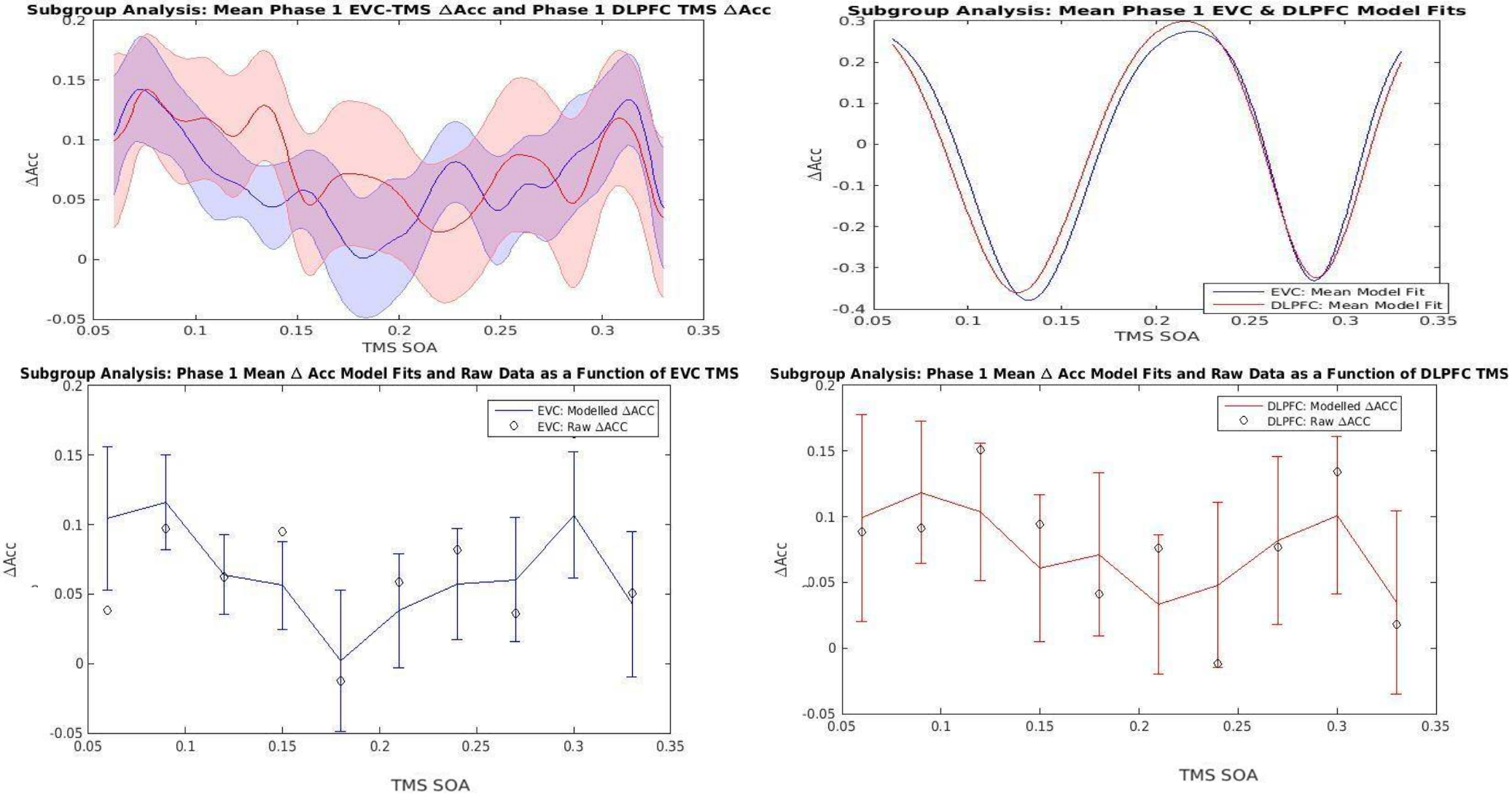

Figure 31. Top left: Mean Biphasic Gaussian models produced by the mean coefficients across all participants included in the subgroup analysis that compared EVCx_1 to DLPFCx_2. Top right: Mean biphasic Gaussian models produced by Gaussian models solved across all possible values of *x*. Bottom left: Biphasic Gaussian model fits for ΔAcc as a function of EVC-TMS solved across the SOAs used in the experiment and corresponding raw data across all participants included in the subgroup analysis that compared EVCx_1 to DLPFCx_2. Bottom right: Biphasic Gaussian model fits for ΔAcc as a function of DLPFC-TMS solved across the SOAs used in the experiment and corresponding raw data across all participants included in the subgroup analysis that compared EVCx_1 to DLPFCx_2

Exploratory ΔPr analyses: monophasic Gaussian model with positive or negative peak amplitude coefficient constraints

A monophasic Gaussian model can only quantify the largest difference between active TMS and sham TMS, unlike a biphasic Gaussian which can quantify the two largest differences between active TMS and sham TMS. A monophasic Gaussian was applied because feedforward *and* recurrent processes could be reflected in a single TMS-induced effect at ~100ms (de Graaf et al., 2014) rather than two discrete effects which could be captured by a biphasic Gaussian. In order to establish whether this was the case, a monophasic Gaussian was fitted to ΔPr as a function of EVC- and DLPFC-TMS with identical constraints to the pre-registered biphasic Gaussian model. The critical difference between the two was that the monophasic Gaussian consists only has one a_1, x_1 and b_1 along with *y0*. A monophasic Gaussian is specified below:

$$y = y_0 + a_1 e^{\left[-\left(\frac{x - x_1}{b_1}\right)^2\right]}$$

The monophasic Gaussian was applied with the following constraints:

1) a_1 < the largest absolute difference between data points across SOAs multiplied by 1.

2) a_1 > the largest absolute difference between data points across SOAs multiplied by -1.

3) x_1 > 10ms, which prevented the temporal position of the Gaussian from falling below 10ms

4) x_1 < 380ms, which prevented the temporal position of the Gaussian from increasing beyond 380ms.

5) b_1 > 10ms, which prevented the bandwidth of the Gaussian from falling below 10ms.

6) b_1 < 380ms, which prevented the bandwidth of the Gaussian from increasing beyond 380ms.

7) y0 > lowest ΔPr score & *y0* < highest ΔPr score, which prevented the intercept of the model falling below the lowest ΔPr score or exceeding the highest ΔPr score, respectively.

Exploratory ΔPr monophasic Gaussian (-/+ a_1) group analyses: Are there EVC-TMS and DLPFC-induced effects?

The *BF* produced by a one-sample *t*-test with a JZS prior (Rouder et al., 2009) on a_1 for ΔPr as a function of EVC-TMS revealed strong evidence for the null hypothesis once all 32 participants were included within the analysis (*t* (31) = -0.6613, *p* = 0.5133, *BF* = 0.2312). The *BF* as a function of participant number can be found in figure 32. The *BF* suggests that a monophasic Gaussian with constraints enabling a_1 to be positive or negative was unable to quantify the effect of EVC-TMS at an SOA of 100ms. The *BF* produced by a one-sample *t*-test with a JZS prior (Rouder et al., 2009) on a_1 for ΔPr as a function of DLPFC-TMS revealed strong evidence for the null hypothesis once all 32 participants were included within the analysis (*t* (31) = -0.6842, *p* = 0.4989, *BF* = 0.2345). The *BF* suggests that a monophasic Gaussian with constraints enabling a_1 to be positive or negative was unable to quantify an effect of DLPFC-TMS on ΔPr across all SOAs. All raw data and model fits can be found in figure 33.

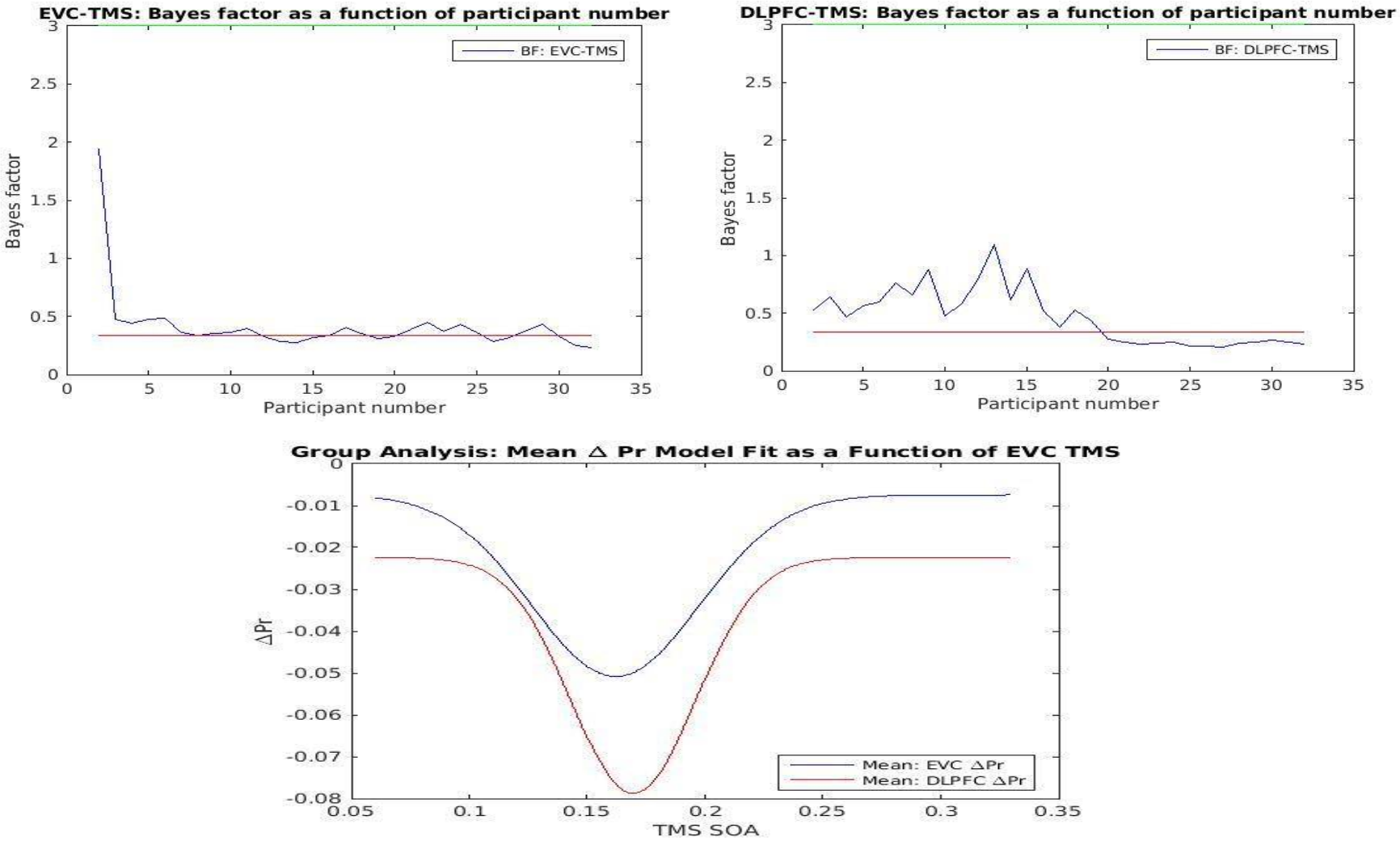

Figure 32. Top left: BF as a function of participant number for EVC-TMS. Top right: BF as a function of participant number for DLPFC-TMS. Bottom: Gaussian models produced by calculating the mean of each monophasic Gaussian ΔPr coefficient as a function of EVC-TMS and DLPFC-TMS.

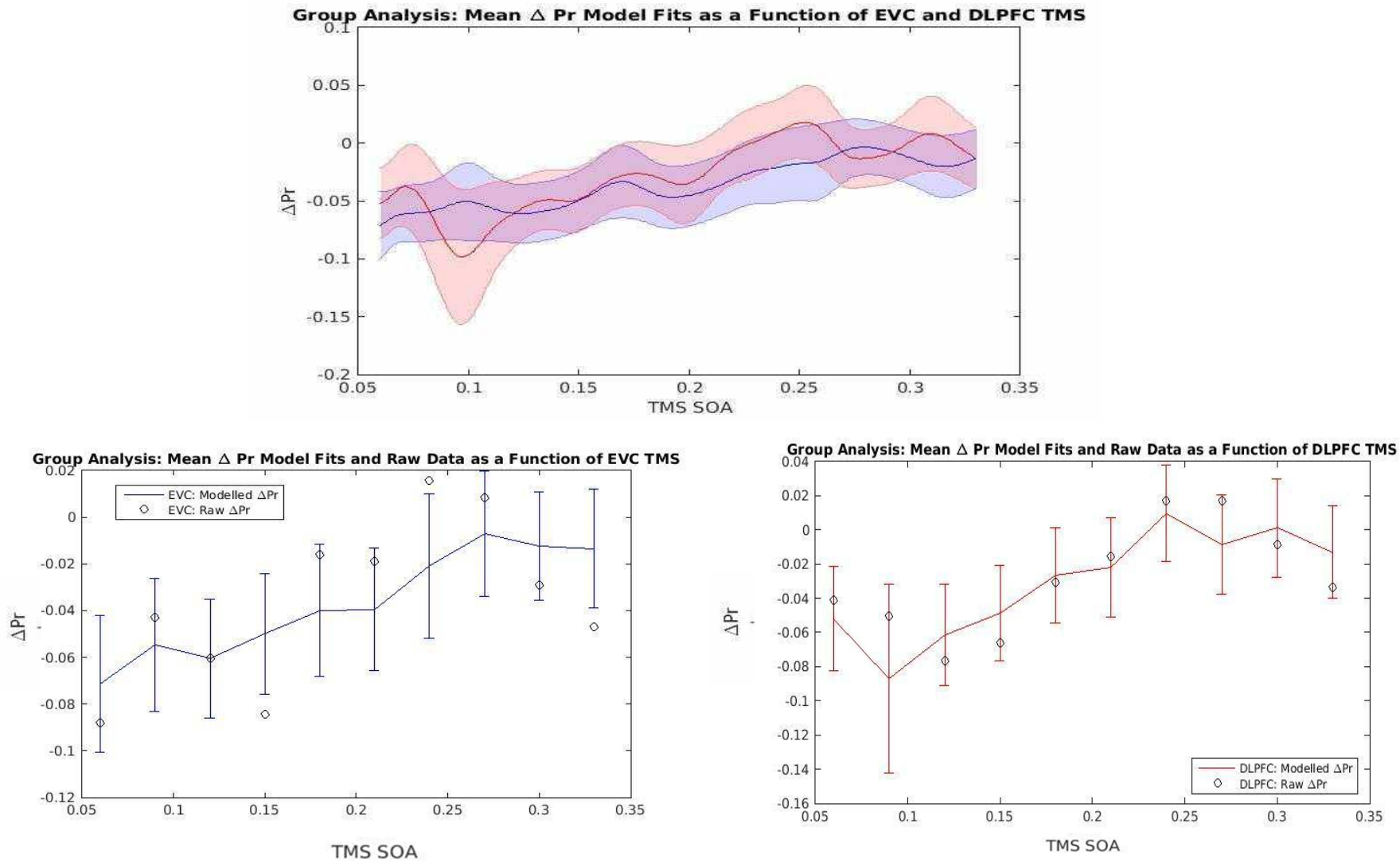

Figure 33. Top: Mean monophasic Gaussian models solved across all possible values of *x* in the group analysis. Bottom left: Mean model fits produced by solving the monophasic Gaussian models across values of *x* and corresponding raw data as a function of EVC-TMS. Bottom right: Mean model fits produced by solving the monophasic Gaussian models across values of *x* and corresponding raw data as a function of DLPFC-TMS.

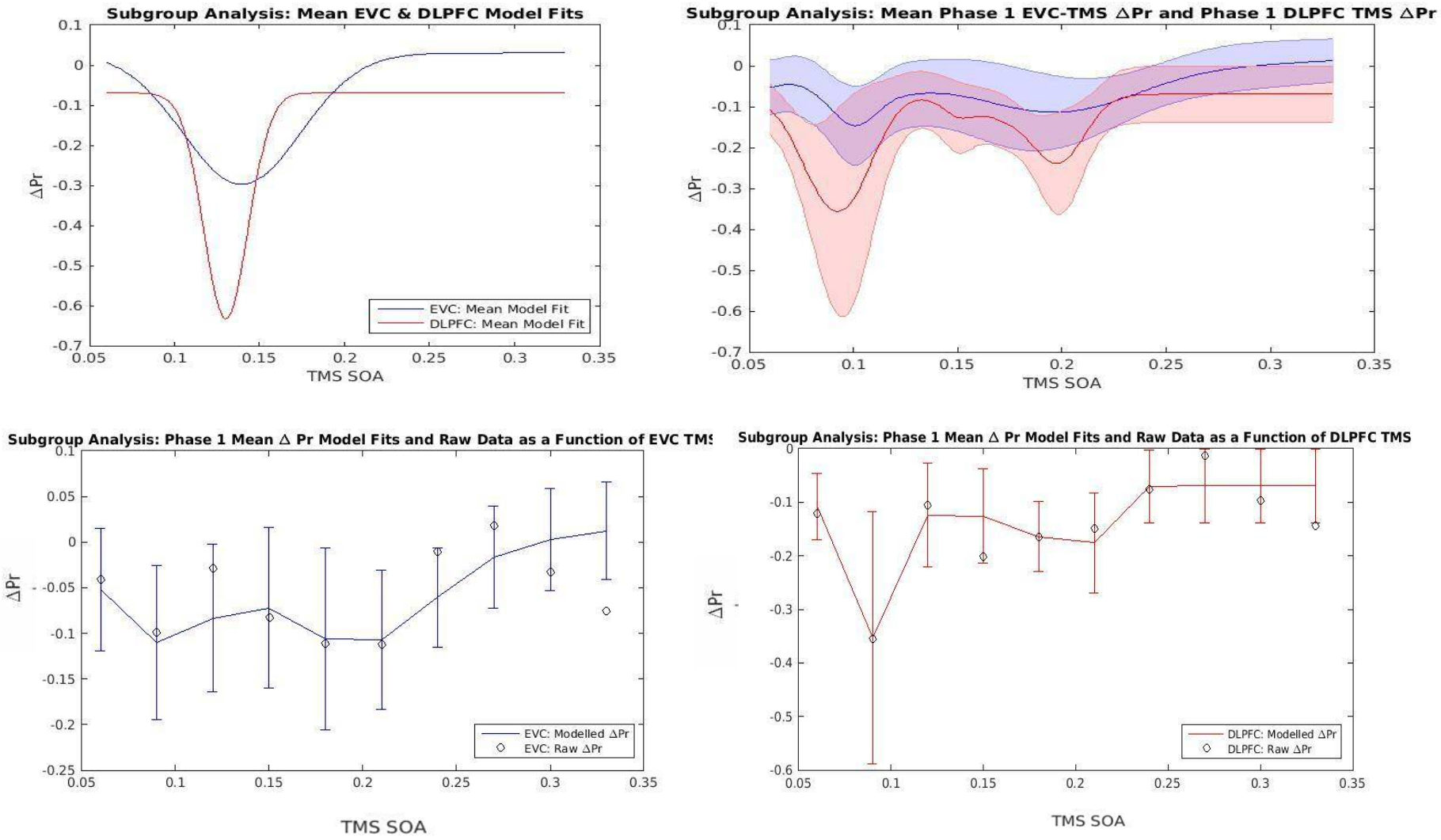

Figure 34. Top left: Mean monophasic Gaussian models produced by the mean coefficients across all participants included in the subgroup analysis that compared EVCx_1 to DLPFCx_1. Top right: Mean monophasic Gaussian models produced by Gaussian models solved across all possible values of *x* in the subgroup analysis. Bottom left: monophasic Gaussian model fits for ΔPr as a function of EVC-TMS solved across the SOAs used in the experiment and corresponding raw data across all participants included in the subgroup analysis that compared EVCx_1 to DLPFCx_1. Bottom right: Biphasic Gaussian model fits for ΔPr as a function of DLPFC-TMS solved across the SOAs used in the experiment and corresponding raw data across all participants included in the subgroup analysis that compared EVCx_1 to DLPFCx_1

Exploratory ΔPr monophasic Gaussian (-/+a) group analyses: Interim Discussion

The completion of a Bayesian paired-sample *t*-test with a pre-registered uniform prior (Dienes, 2011) depended on the *BF*s producing evidence for a TMS-induced effects on ΔPr as a function of EVC-TMS *and* DLPFC-TMS. No such evidence was obtained when a monophasic Gaussian has an a_1 for each site that can be positive or negative. As a result, a Bayesian comparison of DLPFC x_1 and EVC x_1 will not take place.

Exploratory ΔPr monophasic Gaussian subgroup analyses (-/+a): Does DLPFCx_1 or DLPFCx_2 occur later in time than EVCx_1?

The subgroup analysis applied an identical selection procedure to the exploratory subgroup analyses that were specified in the amended pre-registration document. A total of 6 participants qualified for the subgroup analysis, which revealed that EVCx_1 and DLPFC$x1$ occur at the same time (t (5) = 1.5613, p = 0.1792, BF = 0.0426) using a Bayesian one-sample *t*-test with a uniform prior (Dienes, 2011). All model fits and raw data relevant to this analysis can be found in figure 34.

Exploratory ΔAcc single Gaussian group analyses (a-/+): Have EVC-TMS and DLPFC-induced effects occurred?

A one-sample *t*-test with a JZS prior (Rouder et al., 2017) on a_1 revealed an effect of EVC-TMS (t (31) = -2.6993, p = 0.0111, BF = 4.0189) but not DLPFC-TMS (t (31) = 1.0956, p = 0.2817, BF = 0.3269) on ΔAcc. The EVCx_1 that corresponded to EVCa_1 was 128ms, which suggests that the application of a monophasic single Gaussian to ΔAcc has successfully quantified the ~100ms effect of TMS on performance (de Graaf et al., 2012). Critically, this took place without constraining the a_1 coefficient to be negative. In contrast, the *BF* did not produce any evidence for an effect of DLPFC-TMS across all SOAs. The BF as a function of participant number for both sites can be found in figure 35. As a result of the *BF* support an effect of EVC-TMS but not DLPFC-TMS on ΔAcc, a Bayesian comparison of EVCx_1 to DLPFCx_1 will not take place. All models and raw data relevant to this analysis can be found in figure 36.

Exploratory ΔAcc monophasic Gaussian subgroup analyses (α-/+): Does the temporal position of EVCx$_1$ differ from the temporal position of DLPFCx$_1$

A Bayesian paired-sample *t*-test with a uniform prior (Dienes, 2011) in a subgroup of 10 participants who qualified for inclusion revealed that DLPFCx$_1$ did not occur at a later point in time to EVCx$_1$ (*t* (9) = -0.5073, *p* = 0.6241, *BF* = 0.2576). Application of a JZS prior to the same mean difference revealed weak evidence for the null hypothesis (*BF* = 0.3446). All models and raw data relevant to this analysis can be found in figure 37.

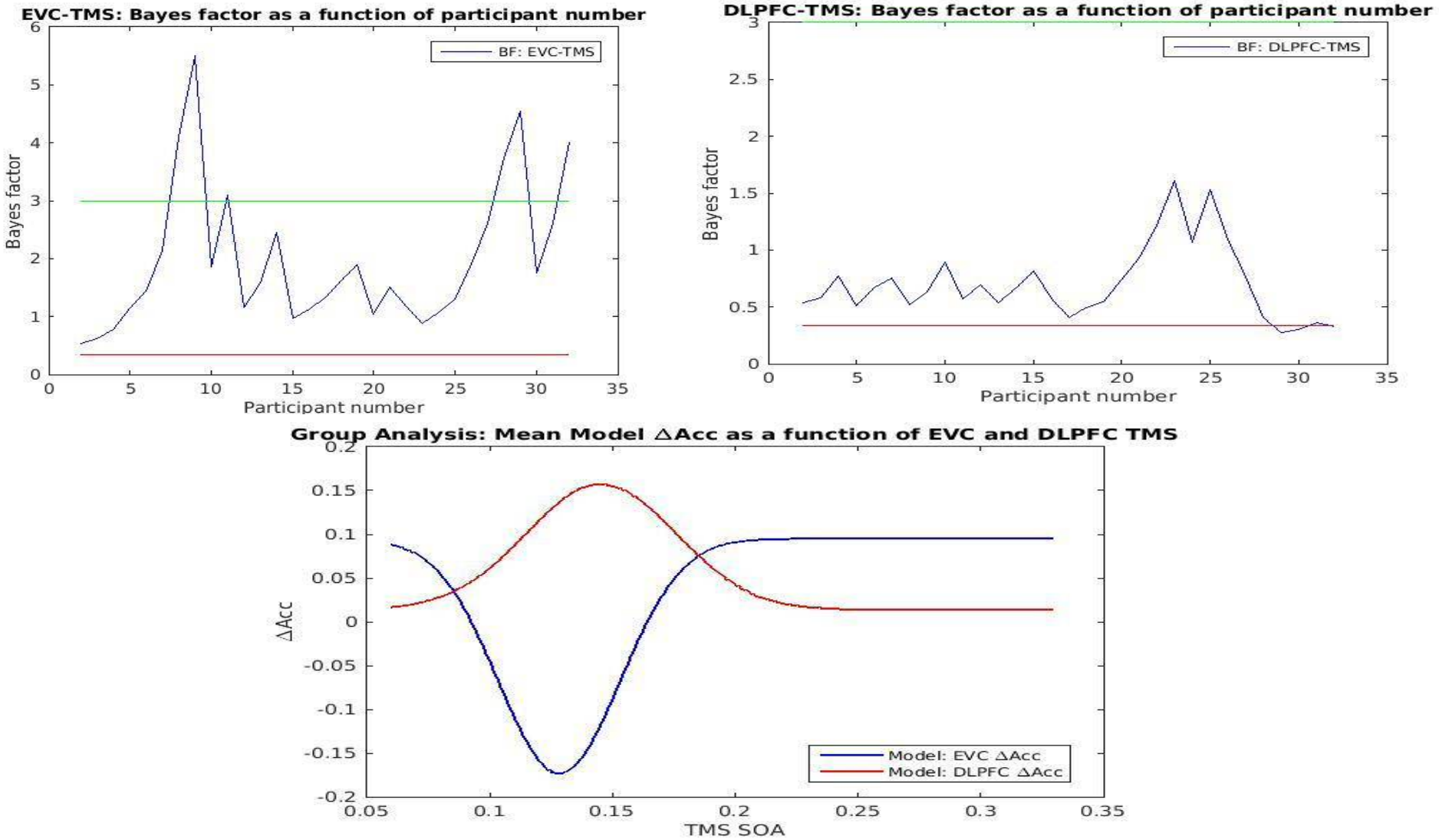

Figure 35. Top left: Bayes factor (*BF*) as a function of participant number for EVC-TMS. Top right: BF as a function of participant number for DLPFC-TMS. Bottom: Gaussian models produced by calculating the mean of each monophasic Gaussian ΔAcc coefficient as a function of EVC-TMS and DLPFC-TMS.

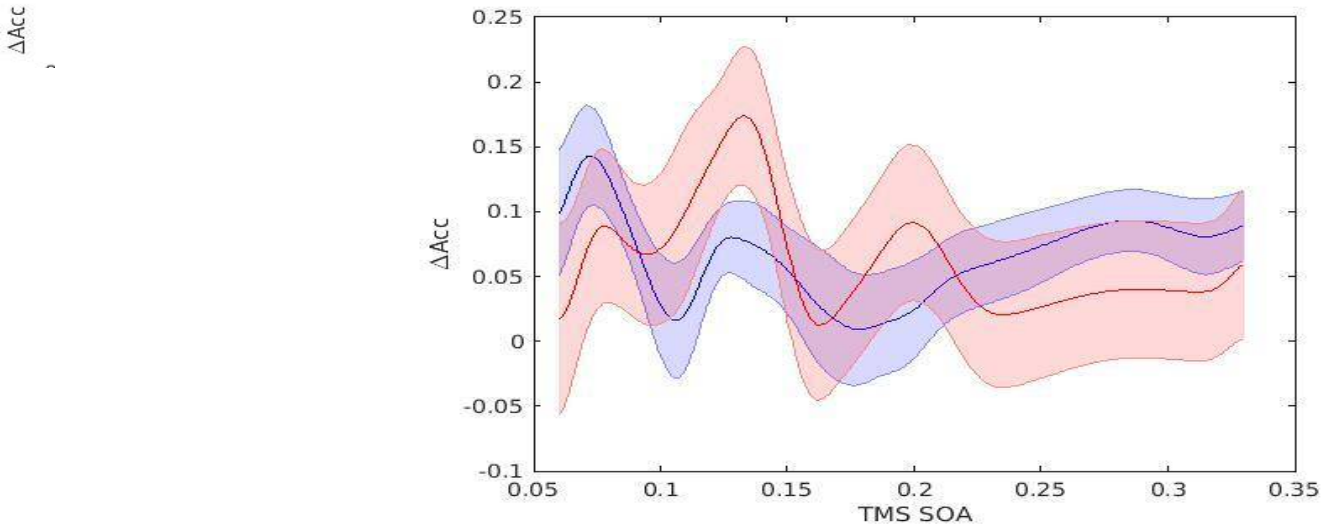

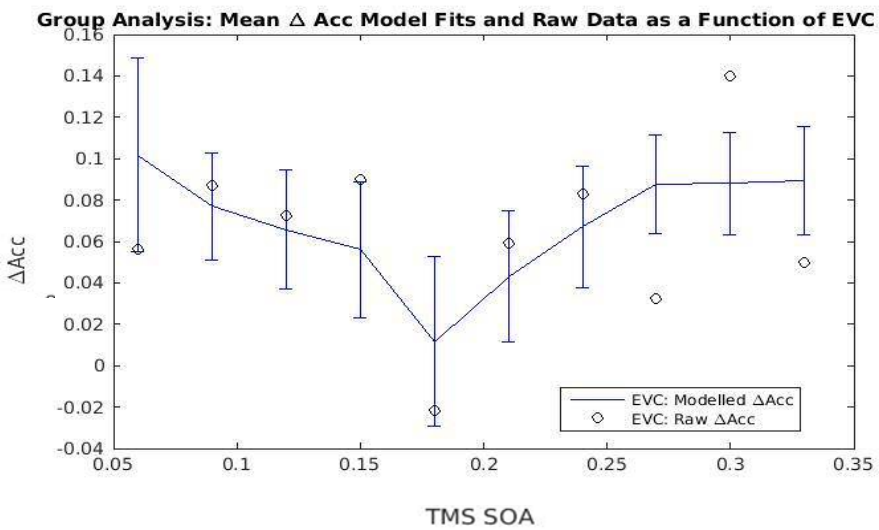

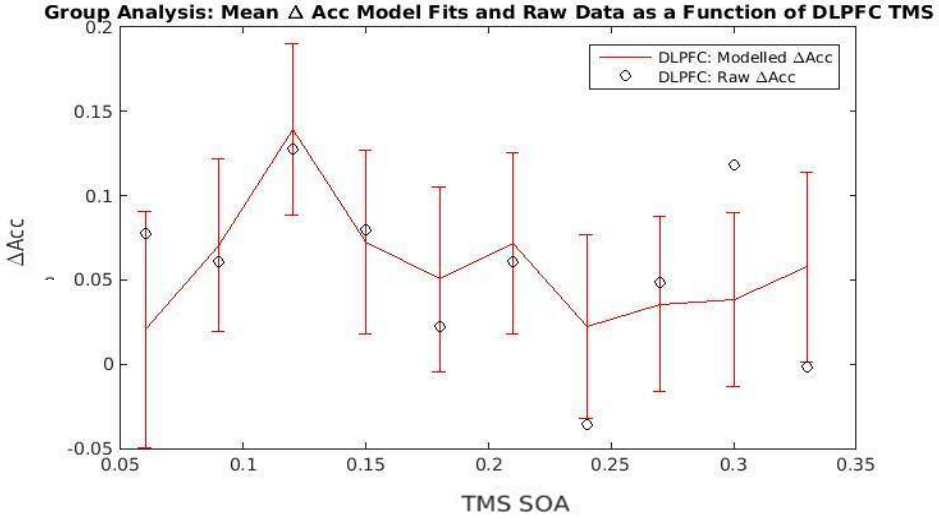

Figure 36. Top: Mean monophasic Gaussian ΔAcc fits as a function of EVC-TMS and DLPFC-TMS. Bottom left: monophasic Gaussian model fits for ΔAcc as a function of EVC-TMS solved across the SOAs used in the experiment and corresponding raw data. Bottom right: monophasic Gaussian model fits for ΔAcc as a function of DLPFC-TMS solved across the SOAs used in the experiment and corresponding raw data.

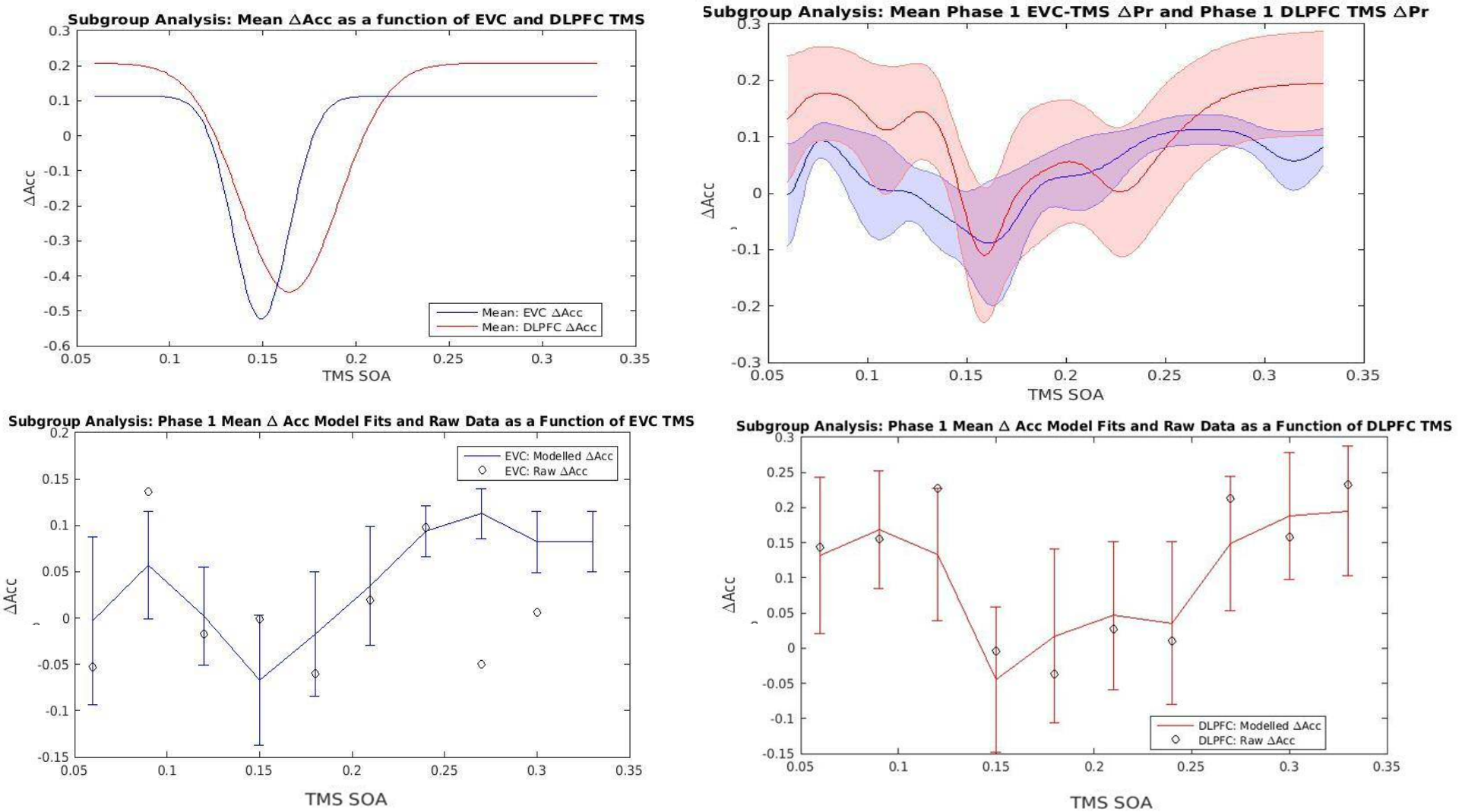

Figure 37. Top left: Mean monophasic Gaussian models produced by the mean coefficients across all participants included in the subgroup analysis that compared EVCx_1 to DLPFCx_1. Top right: Mean monophasic Gaussian models produced by Gaussian models solved across all possible values of *x*. Bottom left: monophasic Gaussian model fits for ΔAcc as a function of EVC-TMS solved across the SOAs used in the experiment and corresponding raw data across all participants included in the subgroup analysis that compared EVCx_1 to DLPFCx_1. Bottom right: Biphasic Gaussian model fits for ΔAcc as a function of DLPFC-TMS solved across the SOAs used in the experiment and corresponding raw data across all participants included in the subgroup analysis that compared EVCx_1 to DLPFCx_1

Exploratory ΔPr analyses: monophasic Gaussian model with negative peak amplitude coefficient constraints ($-a_1$)

Like the biphasic Gaussian with identical constraints for each phase, the *BF* obtained from the monophasic Gaussian failed to produce evidence for TMS-induced effects on ΔPr as a function of EVC-TMS and DLPFC-TMS. However, altering the constraints of the biphasic Gaussian preventing $a_{1,2}$ from being positive and forcing $a_{1,2}$ to be negative successfully produced a *BF* supporting an effect of a TMS-induced effect on ΔPr for both sites. For this reason and for completeness, an additional exploratory monophasic Gaussian analysis will be carried out on ΔPr, which prevents a_1 from being positive. This exploratory monophasic Gaussian analysis will have the following constraints:

1) $a_1 < 0$, which prevented a_1 from increasing beyond zero.
2) $a_1 >$ the largest absolute difference between data points across SOAs multiplied by -1.
3) $x_1 >$ 10ms, which prevented the temporal position of the Gaussian from falling below 10ms.
4) $x_1 <$ 380ms, which prevented the temporal position of the Gaussian from increasing beyond 380ms.
5) $b_1 >$ 10ms, which prevented the bandwidth of the Gaussian from falling below 10ms.
6) $b_1 <$ 380ms, which prevented the bandwidth of the Gaussian from increasing beyond 380ms.
7) *y0* > lowest ΔPr score & *y0* < highest ΔPr score, whichprevented the intercept of the model falling below the lowest ΔPr score or exceeding the highest ΔPr score, respectively.

The only difference between the monophasic Gaussian model applied here and the model applied in the previous monophasic Gaussian analysis is constraint 1. In this analysis, constraint 1 was altered to prevent a_1 from being positive. All other aspects of the group analysis will be identical: a one-sample *t*-test with a JZS prior (Rouder et al., 2009) will be applied to a_1 for both sites and a Bayesian paired-sample *t*-test with a uniform prior (Dienes, 2011) with the pre-registered prior upper and

lower limits. The subgroup analysis will also be carried out with one difference – the *p* value will one-tailed, not two-tailed, as the direction of a_1 can only be negative.

Exploratory ΔPr monophasic Gaussian group analyses (-a_1): Has EVC-TMS and a DLPFC-TMS induced effects occured?

The *BF* produced by a one-sample *t*-test with a JZS prior (Rouder et al., 2009) on EVCa_1 as a function of EVC-TMS produced evidence for evidence for a TMS-induced effect (*t* (31) = -11.2412, *p* = 1.8252e-12, *BF* = 4540095204) and on DLPFCa_1 as a function of DLPFC TMS (*t* (31) = -8.4935, *p* = 1.3579e-09, *BF* = 8522495). The EVC effect had an x_1 of 158.2ms which suggests that a single Gaussian model with negative amplitude constraints successfully produced evidence for a TMS effect at ~100ms on ΔPr (de Graaf et al., 2014). Similarly, the effect of DLPFC-TMS occurred at 153.3ms, which is at a similar mean temporal position to the EVC-TMS effect. With the *BF* supporting an effect of TMS on ΔPr for both sites, an additional Bayesian comparison will be carried out to infer whether DLPFCx_1 occurs after *EVC*x_1. All figures relevant for this group analysis can be found in figure 38.

Exploratory ΔPr monophasic Gaussian (-a_1) group analyses: Does DLPFCx_1 occur after EVCx_1?

A Bayesian paired-sample *t*-test with a uniform prior (Dienes, 2011) revealed evidence of no difference between EVCx_1 and DLPFCx_1 at the group (*t* (31) = 0.1972, *p* = 0.8450, *BF* = 0.1157). Application of a JZS prior to the same mean difference revealed strong evidence for the null hypothesis (*BF* = 0.1923), suggesting that EVCx_1 and DLPFCx_1 have the same temporal onset. All figures relevant to this group analysis can be found in figure 39 .

Exploratory ΔPr monophasic Gaussian (-a_1) subgroup analyses: Does DLPFCx_1 occur after EVCx_1?

At the subgroup level in a smaller sample of 16 participants, a Bayesian paired-sample *t*-test with a uniform prior revealed strong evidence for DLPFCx_1 does not occur later on in time than EVCx_1 (*t* (15) = 0.1382, *p* = 0.8919, *BF* = 0.2225). Application of a JZS prior to the same mean difference revealed strong evidence that EVCx_1 and DLPFCx_1 have the same temporal onset (*BF* = 0.2576). The outcomes of the group and subgroup analysis are in agreement: EVCx_1 and DLPFCx$_1$ occur in a

parallel rather than serial fashion. All figures relevant to this group analysis can be found in figure 40

.

Exploratory ΔAcc single Gaussian (-a_1) group analyses Have EVC-TMS and a DLPFC-TMS induced effects occurred?

A Bayesian one-sample *t*-test with a JZS prior (Rouder et al., 2009) produced support for an effect of EVC-TMS (*t* (31) = -14.007, *p* = 1.0e-12*0.005, *BF* = 1286779569748) at 182.7ms an effect of DLPFC-TMS (*t* (31) = -12.1631, *p* = 1.0e- 12 * 0.2457, *BF* = 30787354518) at 187.8ms. All figures relevant to this group analysis can be found in figure 41 .

Exploratory ΔAcc monophasic Gaussian (-a_1) group analyses: Does DLPFCx_1 occur after EVCx_1?

A Bayesian paired sample *t*-test with a uniform prior (Dienes, 2011) revealed that EVCx_1 does not occur at a different time to DLPFCx_1 (*t* (31) = -0.2316, *p* = 0.8183, *BF* = 0.1457). Application of a JZS prior to the same mean difference revealed strong evidence that EVCx_1 and DLPFC*x1* have the same temporal onset (*BF* = 0.1936). All figures relevant to this group analysis can be found in figure 42 .

Exploratory ΔAcc monophasic Gaussian (-a_1) subgroup analyses: Does DLPFCx_1 occur after EVCx_1?

An additional Bayesian paired-sample t-test with a uniform prior (Dienes, 2011) revealed that DLPFCx1 does not occur after EVCx1 in a subgroup of 26 participants (t (26) = -0.2134, p = 0.8327, *BF* = 0.1662). Application of a JZS prior to the same mean difference revealed strong evidence that EVCx_1 and DLPFCx_1 have the same temporal onset (*BF* = 0.2081). All figures relevant to this group analysis can be found in figure 43 .

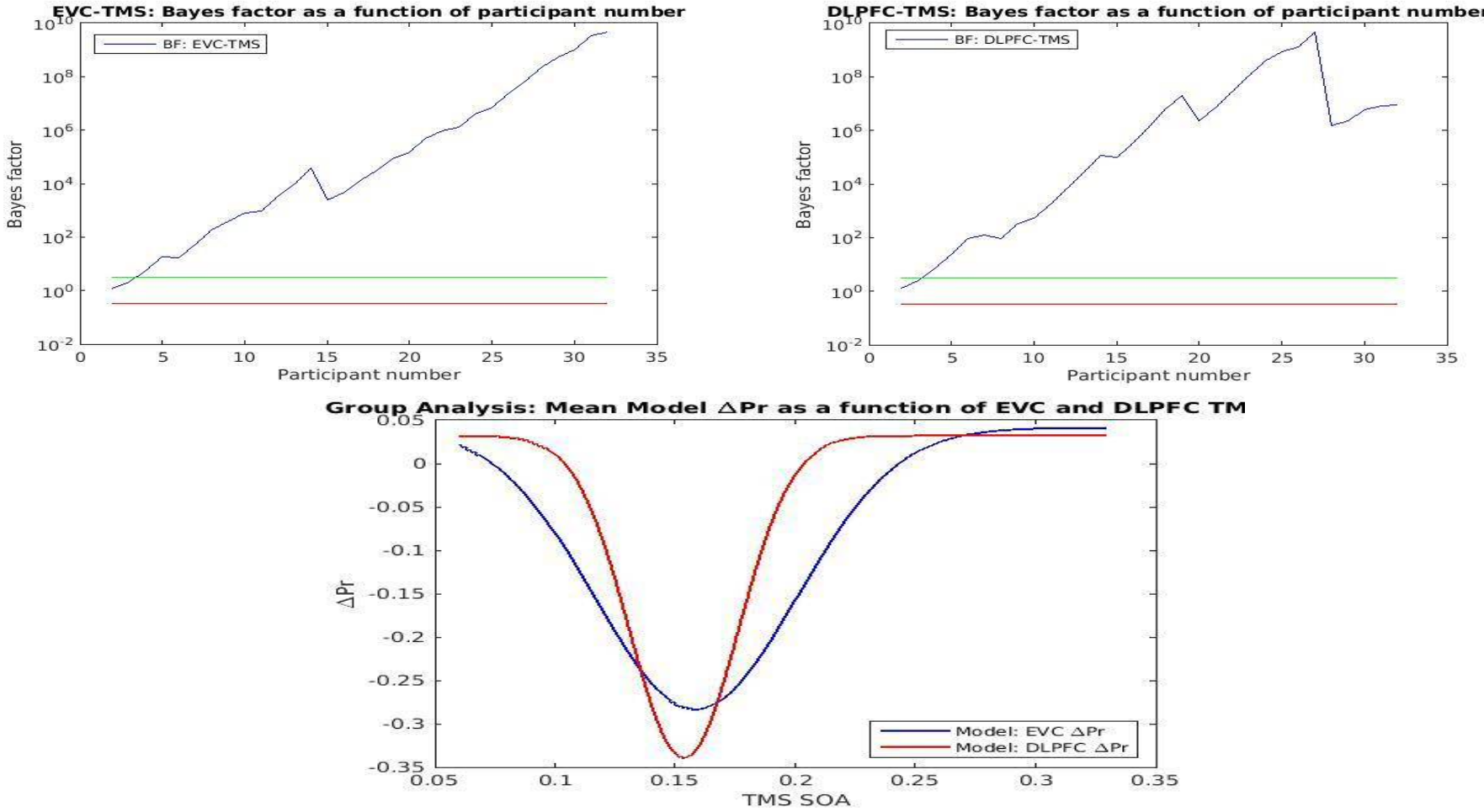

Figure 38. Top left: Bayes factor (*BF*) as a function of participant number for EVC-TMS. Top right: *BF* as a function of participant number for DLPFC-TMS. Bottom: Gaussian models produced by calculating the mean of each monophasic Gaussian ΔPr coefficient as a function of EVC-TMS and DLPFC-TMS.

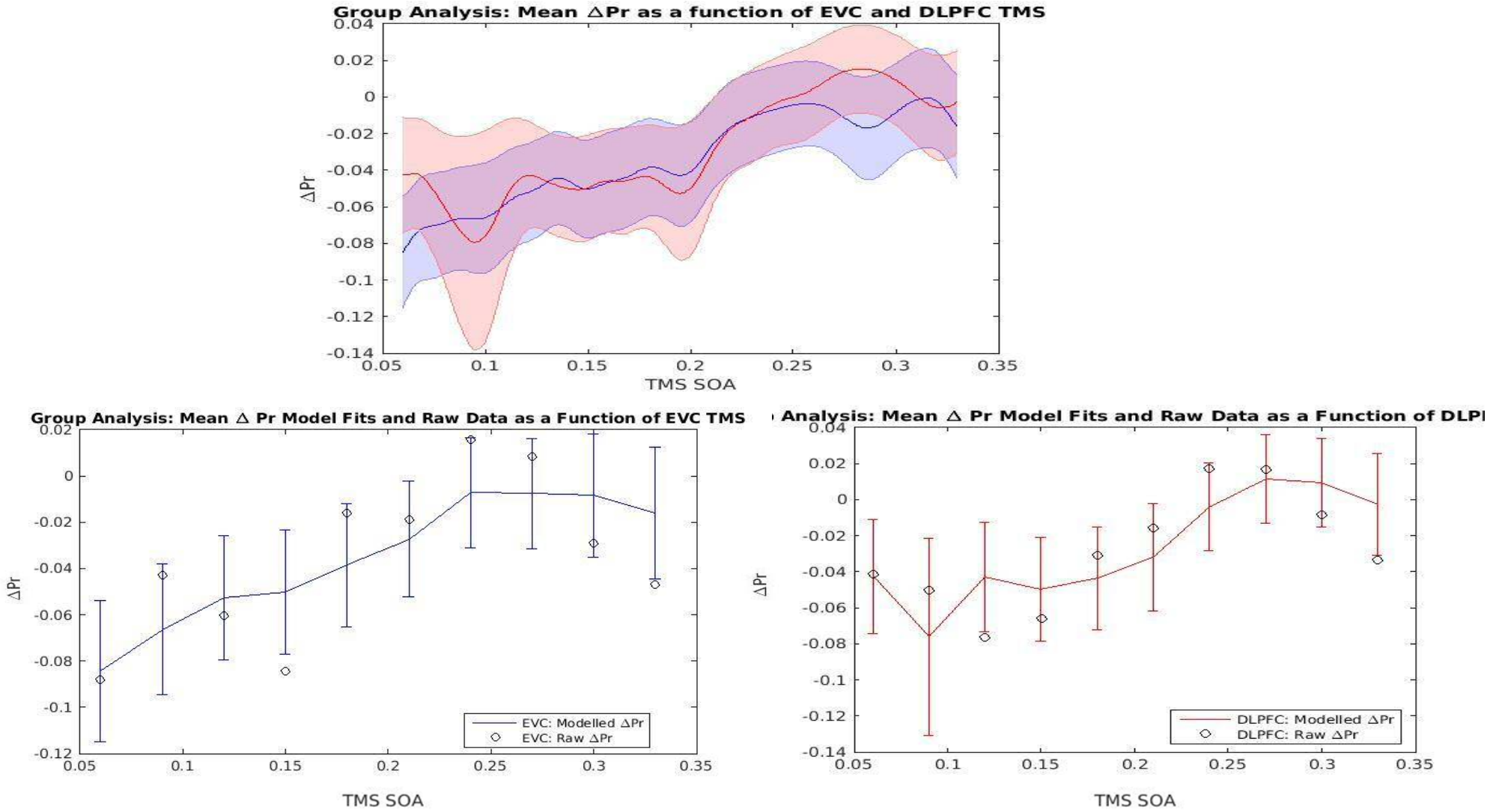

Figure 39. Top: Mean monphasic Gaussian ΔPr fits as a function of EVC-TMS and DLPFC-TMS. Bottom left: monophasic Gaussian model fits for ΔPr as a function of EVC-TMS solved across the SOAs used in the experiment and corresponding raw data. Bottom right: monophasic Gaussian model fits for ΔPr as a function of DLPFC-TMS solved across the SOAs used in the experiment and corresponding raw data.

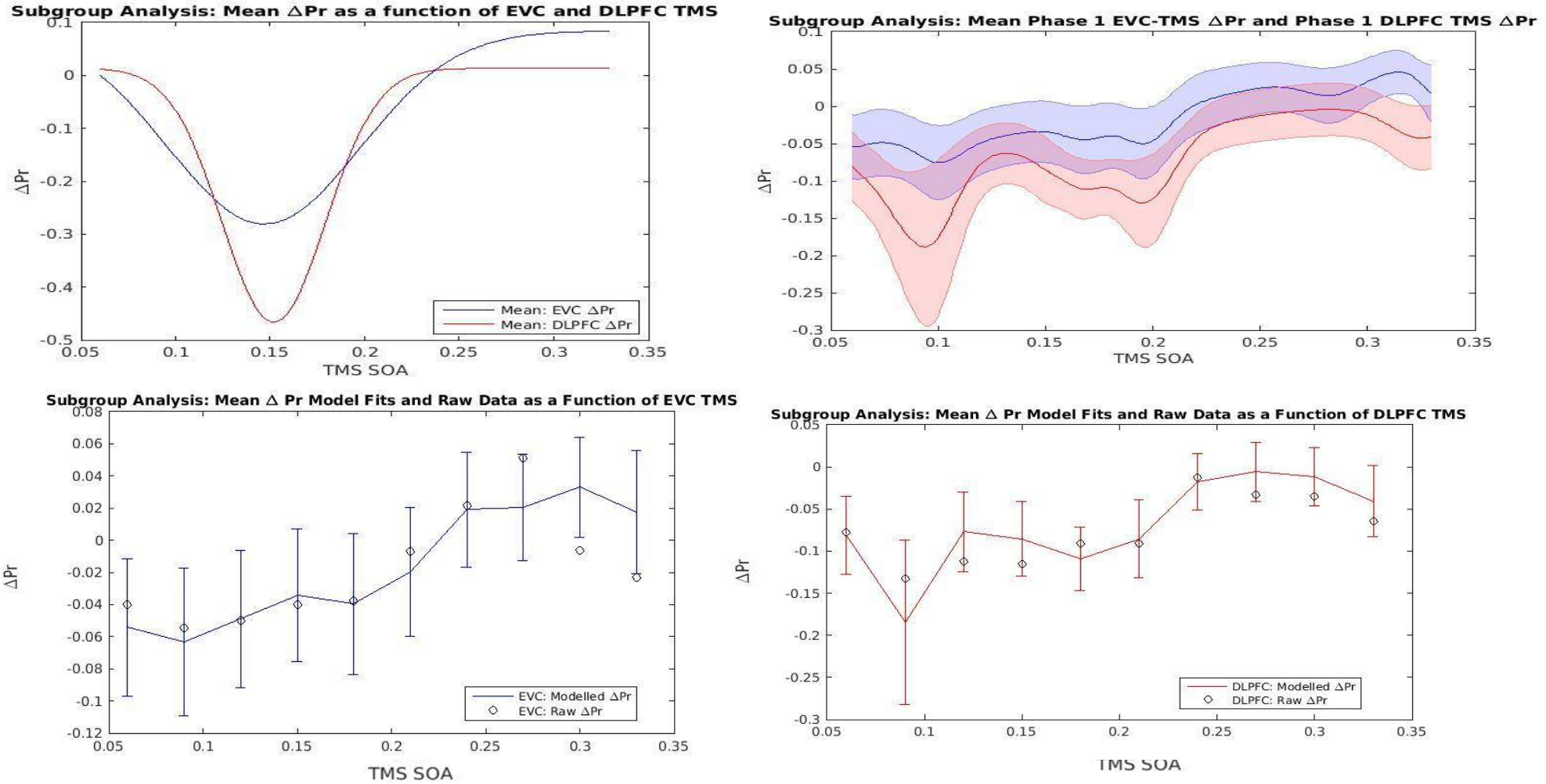

Figure 40 . Top left: Mean monophasic Gaussian models produced by the mean coefficients across all participants included in the subgroup analysis that compared EVCx_1 to DLPFCx_1. Top right: Mean monophasic Gaussian models produced by Gaussian models solved across all possible values of *x*. Bottom left: monophasic Gaussian model fits for ΔPr as a function of EVC-TMS solved across the SOAs used in the experiment and corresponding raw data across all participants included in the subgroup analysis that compared EVCx_1 to DLPFCx_1. Bottom right: Biphasic Gaussian model fits for ΔPr as a function of DLPFC-TMS solved across the SOAs used in the experiment and corresponding raw data across all participants included in the subgroup analysis that compared EVCx_1 to DLPFCx_1

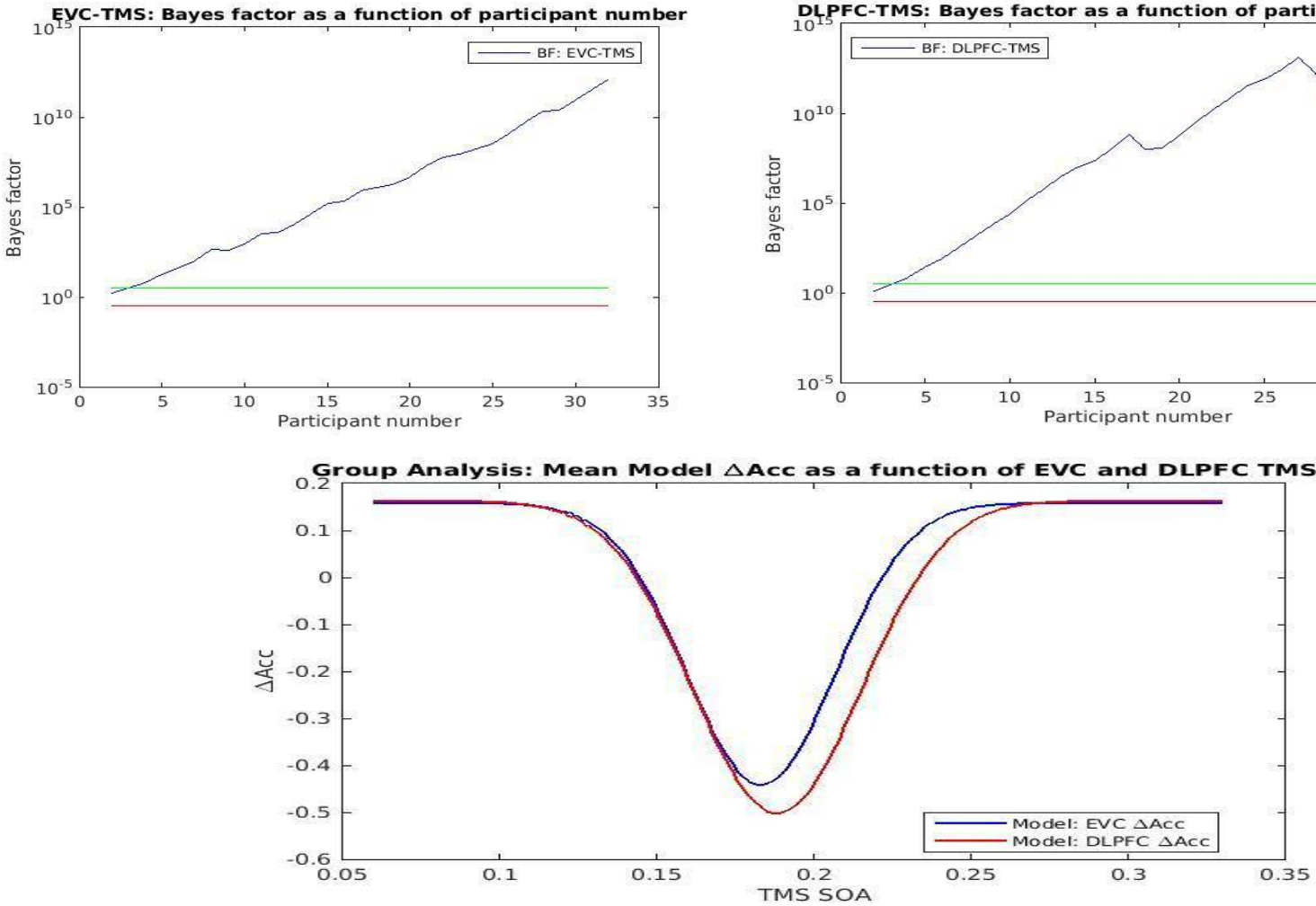

Figure 41 . Top left: BF as a function of participant number for EVC-TMS. Top right: BF as a function of participant number for DLPFC-TMS. Bottom: Gaussian models produced by calculating the mean of each monophasic Gaussian ΔAcc coefficient as a function of EVC-TMS and DLPFC-TMS.

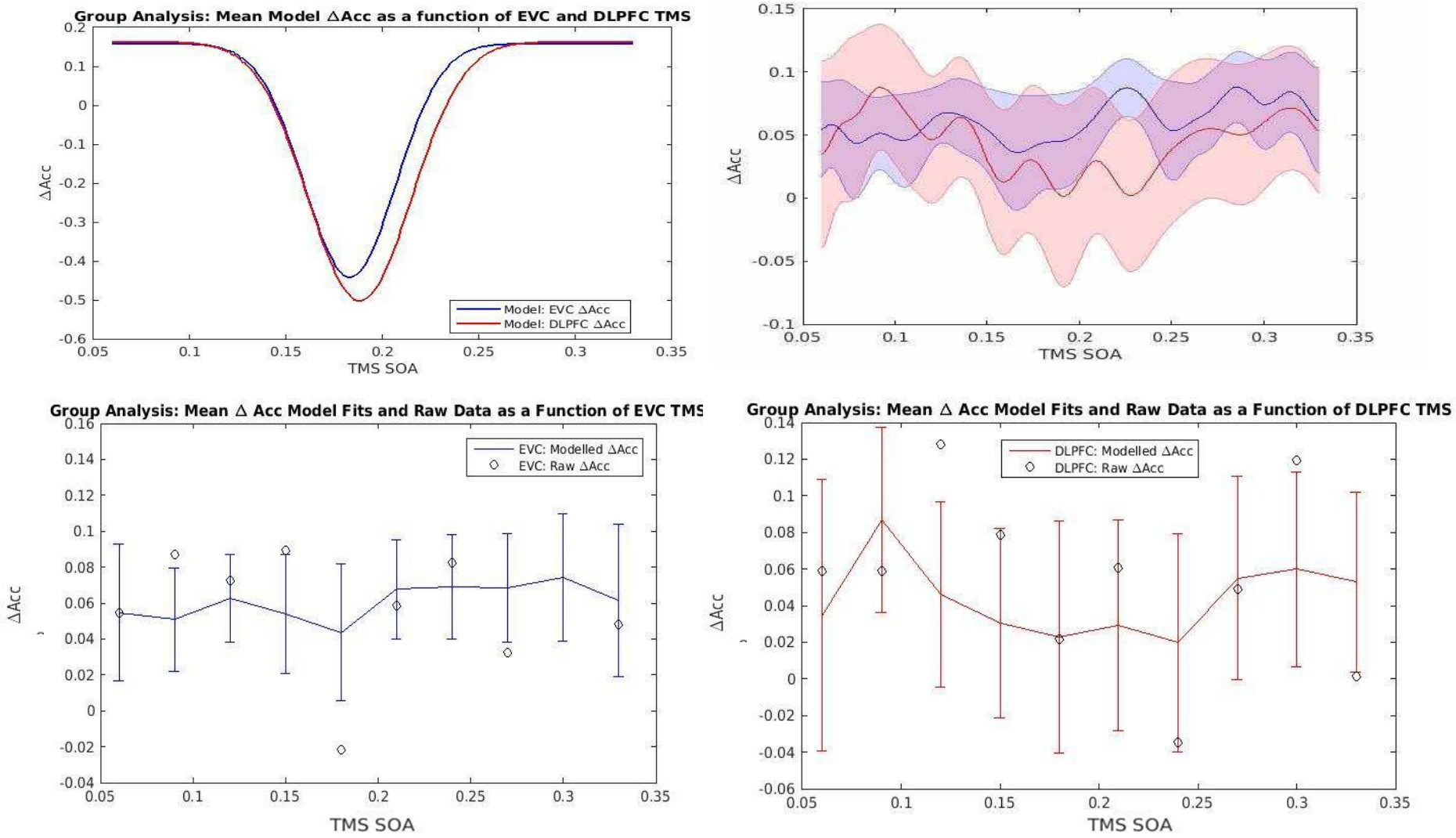

Figure 42 . Top: Mean monophasic Gaussian ΔAcc fits as a function of EVC-TMS and DLPFC-TMS. Bottom left: monophasic Gaussian model fits for ΔAcc as a function of EVC-TMS solved across the SOAs used in the experiment and corresponding raw data. Bottom right: monophasic Gaussian model fits for ΔAcc as a function of DLPFC-TMS solved across the SOAs used in the experiment and corresponding raw data.

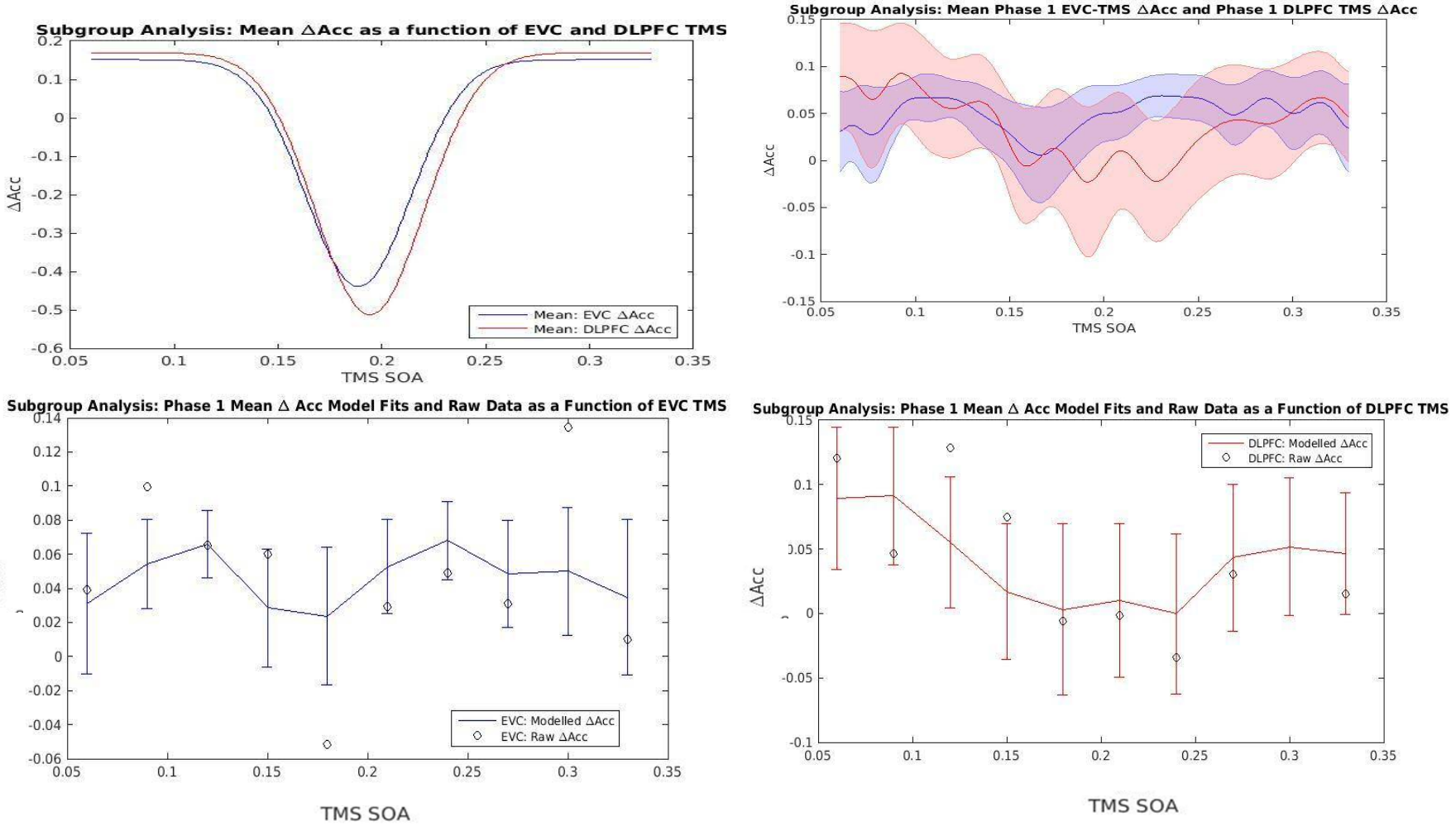

Figure 43 . Top left: Mean monophasic Gaussian models produced by the mean coefficients across all participants included in the subgroup analysis that compared EVCx_1 to DLPFCx_1. Top right: Mean monophasic Gaussian models produced by Gaussian models solved across all possible values of *x*. Bottom left: Biphasic Gaussian model fits for ΔAcc as a function of EVC-TMS solved across the SOAs used in the experiment and corresponding raw data across all participants included in the subgroup analysis that compared EVCx_1 to DLPFCx_1. Bottom right: Biphasic Gaussian model fits for ΔAcc as a function of DLPFC-TMS solved across the SOAs used in the experiment and corresponding raw data across all participants included in the subgroup analysis that compared EVCx_1 to DLPFCx_1

Exploratory linear analyses: Pr

The pre-registered analyses presented here which enabled the a_1 and a_2 coefficients produced by EVC-TMS to be positive or negative. The absence of such an effect may simply be due to this sort of analysis being uncommon in the literature. However, Chambers et al. (2013) successfully produced the effect of EVC-TMS at an SOA of ~100ms using a biphasic Gaussian model when a foveal target was presented. In spite of this, biphasic Gaussian models are not the norm in the TMS literature. In order to confirm the unexpected results produced by the pre-registered analyses no were not due to using a biphasic Gaussian model, a more conventional way of analysing TMS data was also employed. A two-way repeated measures ANOVA was applied to ΔPr as a function of EVC-TMS. EVC-TMS was selected due to the robust and reproducible SOA where TMS affects performance at ~100ms (de Graaf et al., 2014). If the ANOVA reveals presence of a TMS-induced effect, then it would suggest that choosing a biphasic Gaussian with a_1 and a_2 coefficients that can be positive *or* negative may not be appropriate way to analyse this data. Moreover, it would justify the use of different constraints that prevent a_1 and a_2 from being positive and forcing them to be negative. A two-way repeated measures ANOVA revealed that there was no significant main effect of TMS type (F (1, 31) = 2.852, p = 0.101) or SOA (F (9,279) = 1.406, p = 0.185) on Pr. However, there was a significant interaction between TMS type and SOA on ΔPr (F (9,279) = 2.008, p = 0.038), which suggests that the difference between active EVC TMS and sham EVC TMS depends on the SOA at which TMS was administered. In order to identify the SOAs where active and sham performance differed as a function of EVC-TMS, 10 paired-sample t-tests were conducted with a Bonferroni correction. Paired sample t-tests revealed significant differences between active and sham TMS at 60ms (t (31) = -2.6340, p = 0.0130), 90ms (t (31) = -1.2716, p = 0.2130), 120ms (t (31) = 2.1325, p = 0.0410), 150ms (t (31) = 2.4864, p = 0.0185) but not at 180ms (t (31) = 0.5279, p = 0.6013), 210ms (t (31) = 0.5930, p = 0.5575), 240ms (t (31) = -0.4079, p = 0.6862), 270ms (t (31) = -0.3118, p = 0.7573), 300ms (t (31) = 1.0527, p = 0.3006) or 330ms (t (31) = 1.4462, p =0.1582). Consistent with similar

analyses in the literature, statistically significant differences between active and sham EVC-TMS emerged between 60ms up to 150ms, consistent with the established TMS-induced decrement in performance at ~100ms (de Graaf et al., 2014). This suggests that the EVC-TMS effect at an SOA of ~100ms was present within this data set when the analysis is carried out conventionally, which justifies the alteration of a_1 and a_2 constraints.

Chapter 3: Discussion

This experiment aimed to identify whether a DLPFC-TMS induced effect occurred after an EVC-induced effect at ~100ms. If subsequent effects of EVC-TMS were revealed at SOAs later than ~100ms, DLPFC-TMS could be a source of feedback to EVC. The pre-registered analyses failed to detect effects of EVC-TMS or DLPFC-TMS on ΔPr and ΔAcc. Such an outcome is surprising, especially when considering the EVC-TMS effect at ~100ms is among the most robust and reproducible effects in TMS research (de Graaf et al., 2014). However, this may be due to the pre-registered analyses methods chosen, as an exploratory analysis on ΔPr revealed that the intercept (*y0*) of a biphasic Gaussian model, and not the amplitude coefficients ($a_{1,2}$), reflected the time specific decrement of ΔPr at an SOA of ~100ms. Such an outcome is likely to arise from the *a* coefficient being able to detect positive *and* negative differences when subtracting sham performance from active performance at each SOA. When the *y0* is negative and captures a fall in performance due to TMS, the *a* coefficient is then forced to be positive in order to accommodate performance at the SOAs where performance returns to baseline. As a result of this, additional exploratory analyses were carried out with a biphasic Gaussian model. When the amplitude coefficients were constrained in a way that forced them to be negative and prevented them from being positive, exploratory analyses on ΔPr and ΔAcc successfully quantified two effects of EVC-TMS *and* DLPFC-TMS on performance. The earlier effects of EVC-TMS and DLPFC-TMS, as quantified by EVCx_1 and DLPFCx_1, respectively, occurred at the same time as one another, which was contrary to our hypothesis.

One issue with how the biphasic Gaussian model was constrained was that it forced x_1 to occur earlier in time than x_2, which would force DLPFCx_2 to occur later in time than EVCx_1 because the constraints we used meant that an x_2 coefficient always had a higher value than an x_1 coefficient regardless of site. The decisive evidence for a mean difference produced by all DLPFCx_2 and EVCx_1 comparisons are therefore likely to reflect artefactual constraints in the curve fitting procedure rather than a genuine neural phenomenon. This issue precludes our analysis from revealing whether critical events in DLPFC occur earlier, and may be related to, *later* critical events if EVC. By later critical events in EVC, I refer to events in EVC after the ~100ms effect. However, regardless of whether the Gaussian model was monophasic or biphasic, the onset of EVCx_1 invariably around 100ms and the onset of DLPFCx_1 took place at the same time when the amplitude coefficients were constrained in a way that forced them to be negative.

Studies applying TMS to the frontal lobe and considering its effects on visual representation are sparse. One applied repetitive TMS to the left DLPFC in a paradigm where participants had to quickly and accurately indicate whether a high or low quality image contained a face or a car (Philiastides et al., 2011). Active rTMS was found to reduce accuracy and increase reaction times relative to sham rTMS. A drift diffusion model was fitted to the active and sham data. A drift diffusion model assumes that a decision between two choices is made by the accumulation of evidence in support of one choice compared to another. The rate at which evidence is accumulated for one decision over another is called the drift rate. This process of evidence accumulation evolves over time until support for one choice reaches a threshold, the decision is made and a response is executed. Active TMS was proposed to reduce the drift rate relative to sham TMS, which suggests that the rate at which evidenced accumulated for one choice over another was reduced (Philiastides et al., 2011). Critically, this finding was also decrement in performance, in this case, successfully categorizing a car or a face, can be produced by DLPFC-TMS. Thus, it may not be due to the constraints in our curve fitting procedure that a DLPFC-TMS induced effect was produced at ~100ms.

It is difficult to compare the paradigm used here to that used in Philiastides et al. (2011). In experiment 1, a small visual target was presented at 1.5^{o} eccentricity for 10ms with single pulse TMS administered at 120% of each participants phosphene threshold to left DLPFC. Philiastides et al. (2011), on the other hand, administered TMS at a frequency of 1Hz to left DLPFC for 12 minutes and then participants worked out whether a low or high quality image was a face or a car. Each image occurred for up to 1250ms.. If the results of this study are *not* due to the constraints of the curve fitting procedure, the resolution of the drift rate in left DLPFC relative to visual inputs is ~100ms. However, a comprehensive study which combined fMRI with theta-bust TMS revealed evidence that DLPFC is engaged more in *how* the perceptual decision (Rahnev et al., 2016) should be made based on a pre-defined criteriaA comprehensive study found that the application of theta-burst TMS to DLPFC (based on each participant's fMRI activation within the site) reduced the difference in reaction time when instructions to make fast responses or accurate were emphasized (Rahnev et al., 2016). According to these findings, DLPFC engages in a process that determines how long the process of evidence accumulation should take place as opposed to the drift rate, which is the process by which evidence is accumulated. Once again, it is difficult to compare this study to the findings presented here as Rahnev et al. (2016) measured and modelled reaction time. However, the findings here point to left DLPFC being engaged in the rate of evidence accumulation, otherwise it cannot be explained why active DLPFC TMS reduced performance relative to sham DLPFC TMS in the paradigm employed in experiment 1, where only one set of instructions had to be followed.

What is remarkable about the findings here is the fact that EVC-TMS and DLPFC-TMS induced effects appear to be carried out in parallel. Evidence from functional neuroimaging and theoretical formulation suggest that accompany visual inputs are accompanied by a cascade of feedforward and recurrent processes (Lamme & Roelfsema, 2000; Friston, 2005; Ahissar & Hochstein, 2004). Evidence for a recurrent processes taking place could be when when the time course of a neuron within one site is altered at a later point in time, which could orginate from feedback connections from elsewhere in the brain or horizontal connections within the same brain

region (Lamme & Roelfsema, 2000). The proposed study set out to identify whether it is possible to reveal recurrent interactions between DLPFC and EVC with time locked TMS, where such recurrent interactions may be critical for decisions of target presence or target location. The results suggest that left DLPFC and EVC are engaged in such processes at approximately the same time, which makes it difficult to establish whether a recurrent interaction is happening between these two sites. The left DLPFC site that was stimulated along with EVC may have been engaged in recurrent processing with sites elsewhere in the brain. Many theories emphasize that recurrent interactions take place when feedback from higher-level sites in the cortex, such as DLPFC, are sent back in response to inputs from lower-level sites in the cortex, such as EVC (Friston, 2005; Ahissar & Hochstein, 2004). The implication of this study is that an interaction between DLPFC and EVC is not a simple as one site triggering or modulating the response of another; these two sites appear to be engaged at the same time when the presence or absence and the location of a visual target needs to be determined. For feedback from left DLPFC to modulate the responses sites throughout the brain that are critical for visual awareness, it would be expected for left DLPFC to become critical for visual processing very early on.

The questions that the participants were asked to answer - did you see the target and where was the target – provide a glimpse of what processes could be affected by such feedback. Lau & Passingham (2006) revealed a dissociation between proportion correct and a participant's ability to know they were responding correctly. Such an effect was only observed when a metacontrast mask, which was presented at a long SOA of 33ms, and which did not affect proportion correct but did affect a participant's ability to report the presence of the target. In that experiment, participant's ability to know the target was present was associated with a greater response within left mid-DLPFC (Lau & Passingham, 2006). Based on these findings, it would be expected that left DLPFC TMS would disrupt judgments of target presence or absence (ΔPr) whilst leaving the ability to locate the target unhindered (ΔAcc). However, this was not the case in the current experiment: both capacities were affected by DLPFC-TMS at early SOAs.

Other studies such as Rahnev, Koizumi, McCurdy, D'Esposito & Lau (2015) provide evidence that suggests that confidence judgments take place within the frontal lobe. If confidence was being reduced by early DLPFC-TMS, it would be expected that participants would be more likely to say 'no' in response to target presence. Moreover, it would also be feasible that reduced confidence would cause participant's to be less likely to successfully report the location of the target. Rahnev et al. (2015) revealed that processes related to confidence may be taking place the anterior prefrontal cortex. Participants completed reported the dominant colour of a letter presented within an array or letters and subsequently reported their confidence. Confidence, but not accuracy or RT, on the one task was found to found to affect confidence on other task. This effect suggests that assessment of the dominant signal in the letter prevalence judgment affect the assessment of which colour was most prevalent. The lack of relationship between accuracy and RT and confidence suggests that being more accurate or quick at responding at one of the judgments made participants more confident with the other judgment. Analysis of functional MRI data revealed that a greater influence of confidence in one task on the other was associated with greater grey matter volume within the right prefrontal cortex (Rahnev et al., 2015). Although the right, not the left, prefrontal cortex was associated with such an effect it suggests that the frontal lobes could be involved in confidence judgments, which is compatible with the interepretation presented here.

It is difficult to conclude that the temporal order of events that were disrupted in this study are due to recurrent processing. Instead, the process is more complicated than frontal responses being driven by posterior responses. However, this study did reveal that events which are critical for locating a visual target and successfully reporting its presence occur early on within DLPFC that coincide with a critical event within EVC at ~100ms. It is conceivable that there are candidate regions within the ventral stream or elsewhere in the dorsal stream, such as parietal cortex, that engage in a recurrent interaction with DLPFC and/or EVC. Moreover, it is also likely that there are candidate sites whose responses are determined by the critical events at ~100ms in both EVC and DLPFC. A likely candidate for such an interaction is parietal cortex. EVC-TMS affects conscious detection of the

colour or shape of targets at SOAs of 30 – 120ms whereas the intraparietal sulcus (IPS) TMS impaired conscious detection at 90ms (Koivisto et al., 2014). The idea that feedback from IPS to EVC – including V1 – is a recurrent interaction is reflected by the larger number of SOAs (30 – 120ms) where EVC-TMS reduced performance compared to the smaller number of SOAs (90ms) where IPS-TMS reduced performance. The response of EVC at SOAs prior to 90ms (IPS-TMS effect) may be determined by feedforward inputs, horizontal processes within V1 or feedback from V1, V2 or V3, all of which may be disrupted by the administration of TMS to EVC (Thielscher et al., 2010). However, the effects of EVC-TMS at 120ms *after* the IPS-TMS effect at 90ms may affect feedback from IPS is integrated within EVC. Parietal cortex is also a candidate site for influence from DLPFC. Vernet et al. (2015) applied pulses to IPS 70ms before the onset of a stimulus that can be perceived in the same way to a previous presentation or in a different way to a previous presentation. When pulses were applied at 70ms, participants reported a change in the stimulus more often (Vernet et al., 2015). In contrast, when the 70ms IPS pulse was followed by a right DLPFC pulse 10ms later, the effect of IPS on the likelihood of perceiving the stimulus a different way disappeared (Vernet et al., 2015). In light of this evidence, there is potential to use single pulse TMS to compare the critical time course of EVC, IPS, and DLPFC to reveal the temporal structure of recurrent processing within the human brain.

In conclusion, this experiment revealed that EVC-TMS and DLPFC-TMS effects on a visual target presence and location task could occur in parallel. Such a finding may be due to constraints in the curve fitting procedure which only revealed evidence for a DLPFC-TMS induced effect when amplitude coefficients were forced to be negative. Although this is not the first experiment to reveal a DLPFC-TMS induced effect on behavioural performance in the visual domain, the current findings do not rule out DLPFC and/or EVC participating in recurrent interactions with sites elsewhere in the dorsal stream, such as the intraparietal sulcus.

Chapter 4. Does the violation of a top-down prediction trigger more recurrent processing within early visual cortex

Chapter 4: Overview

Chapter 4 aimed to develop a behavioural paradigm that could be used to demonstrate an influence of a prior-probability on behavioural performance, which varied as a function of an experimental manipulation. The development of such a paradigm was initially to integrate it with single pulse TMS and Bayesian modelling of behavioural performance. However, issues with the Bayesian predictive coding approach itself, along with methodological issues with measuring the influence of a prior-probability (in a Bayesian sense) on performance led to a revision in the aims of this set of experiments.

Introduction

The idea of feedforward and feedback based - or recurrent - interactions is becoming an influential and accepted notion of how the human brain operates (Lamme & Roelfsema, 2000). Predictive coding models offer a theoretical framework that can characterize the functional significance of feedforward and recurrent processes with implications for functional stages of visual cognition (e.g. Rao & Ballard, 1999; Friston, 2005; Spratling, 2008; Clark, 2013). Predictive coding models argue that feedback from a higher level cortical site and the site below reflect a top-down prediction of what is going on, whereas feedforward processes from a lower-level site to the higher level cortical site indicate that the prediction is wrong (Rao & Ballard, 1999). Bayesian predictive coding goes one step further and proposes that the constituents and the process of Bayes theorem characterizes how and why feedforward and recurrent processes take place in the human brain (Friston, 2005).

One issue with predictive coding models is that they are difficult to falsify, and when the premises of a Bayesian approach are supported in data, simpler models that make the same predictions are often ignored (Bowers & Davis, 2012). These issues have led to researchers questioning the validity of the Bayesian approach (Bowers & Davis, 2012). Here, we aimed to run an experiment to test and falsify the Bayesian approach by examining the temporal structure of events under the predictive coding, and how such events would be affected by TMS. If Bayes theorem characterized the process by which prediction errors are integrated with prior-probabilities to create a posterior within the human brain, such processes should evolve in a predictable chronological order.

Bayesian predictive coding proposes that feedback from a higher order site to a lower order site is a prior-probability – the most likely cause of sensory inputs (Friston, 2005). In contrast, a feedforward input from a lower order site to a higher order site is a prediction error, which reflects the prior-probability failing to represent the most likely cause of sensory inputs, and the prediction

error is conveyed forwards to trigger a revision of the prior-probability (Friston, 2005). The revision of the prior-probability takes place by integrating the prediction error and the prior-probability using Bayes theorem in order to produce the posterior. The posterior represents a revised top-down prediction which aims to resolve the prediction error (Friston, 2005). The process by which Bayes theorem is implemented within a predictive coding framework offers a number of predictions that can be investigated using TMS.

The critical premise of Bayesian predictive coding is that feedforward inputs to the rest of the brain from EVC are not triggered by retinal stimulation *per se*; they are triggered by a mismatch between the most likely cause of sensory inputs and the current source of sensory inputs, which causes a prediction error to be fed forward (Rao & Ballard, 1999; Friston, 2005). The implication of this is that the first event that needs to take place is the establishment of a prior-probability within EVC. According to Bayesian predictive coding, no feedforward inputs can take place from V1 without a prior-probability being present prior to additional sensory inputs, otherwise no prediction error can be fed forwards (Friston, 2005). The critical implication of this premise is that feedback from elsewhere must take place *first* before any feedforward events. Once the most likely cause of sensory inputs has been established, feedforward inputs to the rest of the brain can be produced in response (Friston, 2005). The presence of these prediction errors then produces a revised prior-probability – the posterior – in order to recapture the most likely cause of sensory inputs (Friston, 2005). The posterior is then fed back to V1 in order to represent the causes of sensory inputs (Friston, 2005).

It becomes apparent that a set of discrete temporal events can be predicted from Bayesian predictive coding and each of these events relates to part of the process of integrating two sources of information according to Bayes theorem (Friston, 2005). First of all, the prior-probability attempts to represent the most likely cause of sensory inputs. Afterwards, prediction errors can be conveyed forwards in response to the prior-probability being an unsuccessful representation of sensory inputs.

After a prediction error, the revision of the prior-probability is produced by integrating it with the prediction error produces the posterior. The process of feedback (prior-probability being sent back), feedforward (prediction error in response to prior-probability) and feedback (the revised posterior in response to prediction error) lays out a series of temporal events that must be present in order for Bayesian predictive coding to be a feasible model of brain function. The application of single pulse TMS provides an opportunity to isolate each of these constituents at different time points and in turn, there is the potential to provide evidence for or against this approach.

In order to isolate the prior-probability, prediction error and posterior at discrete time points, it now becomes important to consider how Bayes theorem is implemented. When a prior-probability is integrated with a prediction error using Bayes theorem, the relative influence of the prior-probability and the prediction error is determined by the precision of the one relative to the other (Feldman & Friston, 2010). When TMS adds noise to the prediction error it is *imprecise,* which means that the influence of the prior-probability will be greater when the two are integrated to produce the posterior (Feldman & Friston, 2010). In contrast, when the precision of the prediction error is greater than the precision of the prior-probability, the influence of the sensory input will be greater than the influence of the prior-probability when they are integrated to form the posterior (Feldman & Friston, 2010). Here, the initial aim was to utilize the influence of TMS to add noise to neural processes (Walsh & Cowey, 2000) to identify whether the addition of TMS-induced noise can reduce the precision of the prediction error and/or the prior-probability. When TMS-induced noise reduces the precision of the prior-probability, performance could be improved by increasing the precision of the prediction error relative to the prior-probability. In contrast, performance should be impaired *and* influenced by a prior-probability when TMS-induced noise reduces the precision of the prediction error relative to the prior-probability.

The experiments presented here initially aimed to develop a paradigm that could be used to probe for the representation of a prior-probability, a prediction error and a posterior within EVC.

Predictive coding proposes that a prior-expectation – a prior-probability according to the Bayesian approach - must be in place within V1 before a prediction error can take place (Rao & Ballard, 1999). Once a prior-probability has been established, a prediction error can subsequently be triggered or not triggered in the event of violation or confirmation of the prior-probability, respectively (Friston, 2005). In the event of prior-probability violation, a posterior, which is a revised prior-probability, is produced by integrating the prediction error with the prior-probability (Friston, 2005). Thus, for Bayesian predictive coding framework to be correct, the first temporal event must affect the prior-probability, otherwise no prediction errors could be generated. The second temporal event must be the prediction error, which occurs when the prior-probability is incorrect. Finally, the final temporal event must be the posterior, which reflects the integration of the prior-probability with the prediction error to complete perceptual inference.

No study, that I am aware of, has applied single pulse TMS to EVC with the aim of revealing whether Bayesian predictive coding is taking place within EVC. However, it is possible to survey the literature and identify whether TMS produces effects at early SOAs that are consistent with TMS affecting the precision of a prior-probability rather than the precision of a prediction error. Under certain conditions, it can be envisaged that a prior-probability can hinder performance when participants make perceptual judgments; when a prior-probability is absent – or less influential -, performance could improve. For example, participant's thresholds for perceiving head directed motion are greater when participants are pursuing a moving dot with their gaze compared to their threshold when they are fixating elsewhere whilst the dot moves across their visual field (Freeman et al., 2010). Thresholds are greater for head directed motion when pursuing a dot compared to fixated a dot because sensory signals are derived from two different sources of information under these conditions. When fixated, perceptual judgments are based on movement derived from the retina. In contrast, there is less retinal motion when judgments were made during pursuit and motion judgments are also based on the velocity of gaze whilst pursuing the dot (Freeman et al., 2010).

Freeman et al. (2010) applied a Bayesian model to their data and revealed that retinal motion and gaze velocity differ in terms of their precision; retinal image motion is more precise than gaze velocity. The difference in precision between these two sources of information causes differences in how the posterior is integrated with a prior-probability. Retinal image motion had greater precision in the Bayesian model compared to eye velocity, which lead to a posterior that was influenced more by sensory signals than the prior-probability. Under these conditions, the prior-probability was a zero motion prior-probability based on the assumption that most objects in the visual environment are not moving. As a result of this, the lack of precision within eye velocity signals caused the posterior to be influenced by the prior-probability more than the sensory data itself, which in turn, increased a participant's threshold. An increase a participant's threshold means that participants were less sensitive to motion during pursuit and more susceptible to a prior-probability that impairs performance. It must be noted here that Freeman et al. integrated a prior-probability with a sensory signal itself rather than integrating a prior-probability with a prediction error. However, this still reveals evidence about how a prior-probability can *bias* perceptual judgments in a particular direction. Moreover, the relative influence of the prior-probability is determined by the precision of what it is integrated with – in this case a sensory signal – which in turn, determines the position of the posterior.

Similar results are also revealed when participants made judgments without moving their eyes, such as when participant simply report the direction a field of dots are moving in (Kok et al., 2013). When a cue indicated upcoming rightward motion, participant's rated the motion as moving rightward to a greater extent compared to reporting motion moving upwards (Kok et al., 2013). Moreover, a rightward cue-induced bias could be accompanied by a change in representation within visual cortex itself as visual cortex voxels (V1, V2, V3, V4 V3A & MT+) that were more responsive to rightward motion within exhibited greater BOLD during motion presentation compared to voxels that more responsive to upward motion (Kok et al., 2013). Thus it becomes apparent, that simple motion judgments, eye movements and representation within visual cortex can be biased by prior-

representation. Here, we aimed to probe a process more directly within visual cortex by altering the precision of these two sources of information using TMS by developing a paradigm where these two sources of information can be manipulated.

All experiments outlined in this chapter aimed to induce a prior-probability within the experiment itself, which EVC-TMS could then interfere with when visual inputs are presented. Experiment 2 used a detection paradigm where participants had to indicate whether a triangle was present or absent. The luminance of the target was low and presented within visual noise in order to increase task difficulty. The target was presented in two different blocked contexts: a high probability context (HPC) and a low probability context (LPC). In the high probability context, the target had a high probability of appearing and in the low probability context the target had a low probability of appearing. The likelihood of target occurrence in each was made explicit to the participant. An 'H' also served as fixation in the high-probability context and an 'L' served as a fixation in the low-probability context to avoid any ambiguity of the context. These contextual manipulations were introduced to set a precise prior-probability of target occurrence in each context under conditions where sensory inputs are imprecise.

Recall that target luminance was deliberately set at a low level. This combination of a precise prior-probability combined with an imprecise sensory signal was expected to bias the participant's pattern of errors in a particular direction. If incoming sensory signals are unclear, then the precision of the prediction error should be low.. When the precision of the prediction error is low, the relative influence of the prior-probability should be greater than the influence of the prediction error. This should lead to differences in the pattern of errors in each context. In the high-probability context where the target is highly likely to appear, it will be expected that participants will make a false alarm when the target is absent. When the likelihood of target occurrence was high and the target was *absent*, participants were expected to make false alarms. In contrast, when the likelihood of

target occurrence was low and the target was *present*, participants were expected to miss the target.

The establishment of a precise prior-probability in each context enables the predictions of the predictive coding framework to be tested, which would differ in each context. In the HPC, it was expected that participants would make more false alarms when the target is present. This is because the target is difficult to detect; and the presence of a strong prior-probability indicating target is likely to be there. This pattern in performance is likely to reflect a prior-probability induced change in a participant's criterion (Br) (Corwin, 1994). When participants are informed of the high prior-probability of target occurrence and such a target is difficult to see, they are likely to make more judgments of target presence than judgments of target absence. As a result, the number of hits *and* false alarms they make is likely to increase, which would reflect participant's adopting a more liberal criterion. In contrast, in the LPC a different pattern of results was expected, despite the fact that target identity is the same. In the LPC it was expected that the precise prior-probability led to a different pattern of errors but this time on target present trials. As the luminance of the target was low but the LPC biases participants towards judgments of target absence, participants were expected to make more misses relative to the HPC. This was also expected to produce a change in participant's criterion, but in the opposite direction to what was revealed in the HPC. In the LPC the low probability was expected to cause participants to make more judgments of target absence than judgments of target presence. Consequently, the number of correct rejections *and* misses was expected to increase, which should be reflected in a participant's criterion becoming more conservative. It was predicted that criterion would significantly differ between contexts, which was assumed to reflect the difference in the prior-probability between the HPC and the LPC. The confirmation of each of these predictions would establish that the combination of a precise prior-probability with an imprecise prediction error can lead to two opposite types of perceptual judgment despite the fact that stimulus calibration is identical across both contexts.

An effect on perceptual sensitivity (Pr) was not expected. In order for Pr to improve, the number of target present judgments on target present trials should increase and the number of target absent judgments on target absent trials must increase. However, target present judgments on target absent trials and target absent judgments on target present trials must be minimal. Such an outcome is incompatible with the predictions of Bayesian predictive coding here. As outlined above, the number of target present judgments must increase on target present trials *and* target absent trials must take place in the HPC. Also, the number target absent judgments must increase on target absent *and* target present judgments in the LPC. Thus, a change in Pr between the HPC and the LPC is not compatible with predictions of Bayesian predictive coding. Thus, a difference in Br but not Pr was expected between the HPC and the LPC.

If a difference in criterion between the HPC and the LPC is successfully established, then the effects of TMS outlined above can be taken into consideration for this contextual paradigm. The posterior is formed by integrating the prior-probability with the prediction error. The relative influence of each of these sources of information is determined by their precision. When the precision of the prior-probability is greater than the precision of the prediction error, the prior-probability has a greater bearing on the formation of the posterior. In contrast, when the precision of the prediction error was greater than the precision of the prior-probability, the prediction error would have a greater bearing on the formation of the posterior. It was expected that TMS would reduce the precision of the prior-probability or the prediction error depending on SOA at which TMS is administered. The critical premise of predictive coding is that feedforward outputs from V1 are not sensory inputs per se, but the difference between what has the highest prior-probability and what is currently being presented – a prediction error. Therefore, the earliest effect of TMS that can be observed with the detection paradigm is an effect of TMS on the prior-probability as a feedforward output from V1 is contingent on a prior-probability being established beforehand.

If the prior-probability is being integrated with a prediction error consistent with Bayes theorem, an improvement in performance should be revealed on target present trials in the HPC and target absent trials in the LPC. These effects were expected at the *earliest SOAs* where TMS successfully produces an effect on performance regardless of the context the participant is in. In the HPC, participants should be biased towards making judgments of target presence when the target is absent due to a higher prior-probability of target occurrence in this context and the target itself being difficult to detect. The target being difficult to detect would promote the influence of the prior. On the other hand, in the LPC the effect of TMS on performance was expected on target present trials. In the LPC, the integration of the prior-probability with the prediction error biases perceptual judgments towards errors of target absence on target present trials. In the LPC, participants should be biased towards making judgments of target absence when the target is present due to the prior-probability of target occurrence being low and the target being difficult to detect. However, on target present trials the administration of TMS would reduce the precision of the prior-probability relative to the prediction error, which would reduce the influence of the prior-probability relative to the prediction error when forming the posterior. This should manifest itself as a judgment of target *presence* on a target absent trial, which would improve performance on target present trials. To conclude, regarding effects of TMS on the prior-probability, the effect of TMS is expected to reduce the influence of the prior-probability in opposite ways in each context despite target identity being the same in each case.

Under Bayesian predictive coding, the prediction error is carried forward which is conditional on a prior-probability being established in V1. Consequently, an effect of TMS on the precision of the prediction error was expected after the effects on the precision of the prior-probability. The effect of TMS on the precision of the prediction error was expected to occur *after* the effect of TMS on the precision of the prior-probability. These later effects on the precision of the prediction error will be distinct from what will be expected of the early effects on the precision of the prior-probability. When TMS affects the precision of the prediction error, then its precision

relative to the prior-probability would l be reduced even further due to luminance being calibrated so low. Under these circumstances, the prior-probability will have greater precision than the prediction error, and a bias in perceptual judgment consistent towards the prior-probability would be expected. Thus, if the only effect of TMS that is observed is an improvement in performance on target present trials in the LPC and target absent trials in the HPC, the outcome of the experiment will not be consistent with Bayesian predictive coding. Two effects of TMS are therefore expected – an early improvement and a later impairment in performance - depending on the context the participant is in and whether they are experiencing a target present or a target absence trial.

Experiment 2: Methods

Participants

Participants were 18 undergraduates and postgraduates who were recruited from the Cardiff University School of Psychology. Participants were paid 5 pounds for their participation.

Design

Participants were presented with a difficult to detect target in two different contexts. In one context the target was relatively likely, present on 80% of trials. In the other context, the target was relatively unlikely, present on 20% of trials. These contexts are referred to as the HPC and the LPC, respectively. A 'H' served as fixation during the HPC whereas an 'L' served as fixation in the LPC. In both contexts participants had to indicate if a triangular target had been present or absent. If the target was present, participants indicated its presence by pressing 'c' on a keyboard. If the target was absent, participants indicated its absence by pressing 'm' on a keyboard. Two different contexts were used to set the prior-probability that the target had of occurring on each trial within a block. An illustration of the paradigm employed in experiment 2 can be found in figure 1. The order in which each context was completed was counterbalanced which meant that participants completed the experiment in this order: HPC, LPC, HPC, LPC or this order: LPC, HPC, LPC, HPC. The participant completed 50 trials when each context took place, which meant that 200 trials were completed in

total. In the HPC, the target was present on 40 trials and the target was absent on the remaining 10 trials. In contrast, the target was present on 10 trials and it was absent on the remaining 40 trials in the LPC. Before each context began, the participant was explicitly told with on screen instructions that the HPC or LPC was about to begin. In the HPC, the participant was told: ''HIGH PROBABILITY CONTEXT. The target has a high likelihood of appearing. It will occur on 80% of trials''. In the LPC the participant was told: ''LOW PROBABILITY CONTEXT. The target has a low likelihood of appearing. It will occur on 20% of trials''. Performance was measured using Pr, a non-parametric measure of perceptual sensitivity (Corwin, 1994). Pr was calculated by subtracting each participant's false alarm rate (FAR) from their hit rate (HR). A hit occurred when participants indicated target presence when the target was present whereas a miss took place when participants indicated target absence when the target was absent. Their HR was the number of target present responses on target present trials divided by the total number of target present trials. The FAR was the number of target present responses on target absent trials divided by the total number of target absent trials. Br, a non-parametric measure of criterion, was also calculated, which is as follows: FAR / (1 – Pr).As outlined previously, a non-parametic version of criterion, Br, was selected here due to issues that can arise from very high (> 0.95) and very low (< 0.05) hit and false alarm rates (Bor et al., 2017) once a *z* function is fitted to hit rate and false alarm rates. Hit rates and false alarm rates can approach positive or negative infinity when they are more than 0.95 or less than 0.05, respectively (see Bor et al. 2017, for an example).

The precision of the sensory data was manipulated by altering the luminance of an upright triangle, which was presented within visual noise. The luminance of triangle was manipulated using an up-down staircase procedure (Levitt, 1970) to identify an intensity that was accompanied by a Pr score that was within -0.1/+0.1 of 0.293). A Pr score that was very low was chosen in order to reduce the precision of the sensory data by making the task difficult. Under these conditions where Pr was low, it was predicted that participants would be rendered sensitive to the contextual manipulations indicating the likelihood of target appearance. Participants completed six interleaved adaptive

staircases and a total of six reversals needed to be obtained within each staircase in order to complete the calibration. Six of the staircases were completed in the HPC and the remaining six

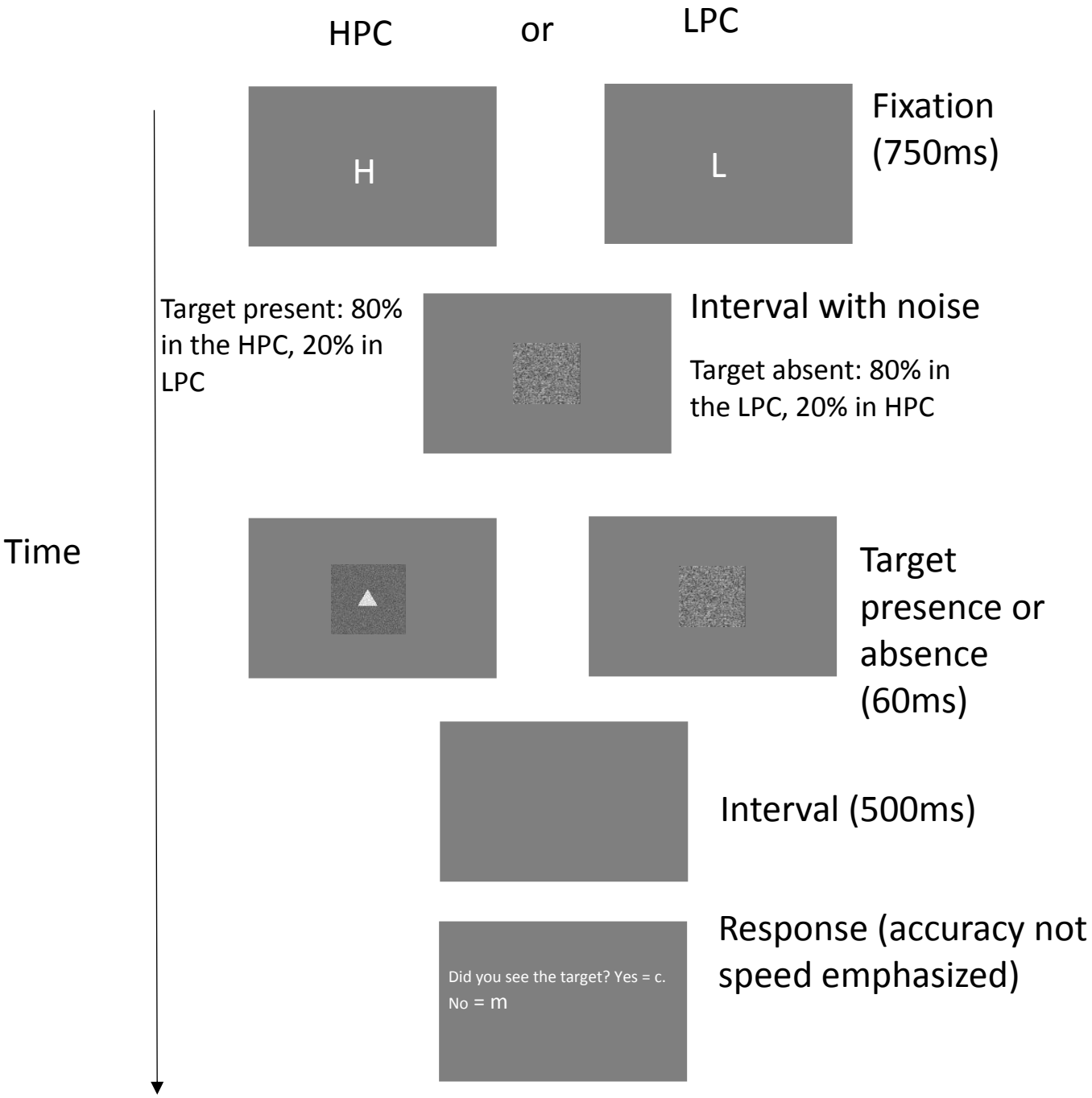

Figure 1. Illustration of the experimental paradigm employed in experiment 2. First of all, a 'H' or an 'L' was used as fixation depending on whether participants were in the high probability context (HPC) or low probability context (LPC), repectively. Following fixation, visual noise was presented for 60ms prior to a frame where the target could be present or absent. The target was present on 70% of trials in the HPC and the target was present on 30% of trials in the LPC. A response was then made after a 500ms interval. Images not drawn to scale.

staircases were completed in the LPC. This meant that a total of 36 reversals needed to be obtained. There were two types of reversal that could take place, which determined the luminance of the triangle on the next trial within a staircase. A positive reversal, which refers to when participants make two consecutive incorrect responses, needed to take place in order to the luminance of the triangle to be increased (Levitt, 1970). A negative reversal, which refers to when participants made a correct response that was preceded by an incorrect response, or a correct response by itself, needed to take place in order for luminance to be decreased (Levitt, 1970).

Once 36 reversals had been obtained, participants completed 30 trials with the luminance of the triangle set at the mean luminance on the last 3 reversals of each staircase. An implication of this was that luminance was set based on the last 3 reversals in the HPC *and* LPC rather than calibrating luminance of the HPC and LPC separately. If Pr was within -0.1/+0.1 of 0.293, participants went on to complete the rest of the experiment. In contrast, if Pr was not within -0.1/+0.1 of 0.293, participants completed the stimulus luminance calibration procedure again. The procedure was be repeated until a Pr within -0.1/+0.1 of 0.293 was obtained.

Equipment

This experiment was completed on a 13'' MacBook Pro with a refresh rate of 60Hz (Apple Inc.).

Procedure

First of all, participants completed the calibration procedure until it succeeded in calibrating Pr to the pre-specified range. Once this level had been attained, participants then completed 200 trials which was segregated into four 50 trial context sets. Participants could take a break between contexts, if they wished.

Experiment 2: Results

Pr in the LPC and HPC can be found in figure 1. A Bayesian paired-sample *t*-test with a JZS prior (Rouder et al., 2009) revealed that Pr did not differ between contexts (*t* (17) = -0.2992, *p* = 0.7684, *BF* = 0.2530). However a Bayesian paired-sample *t*-test with a JZS prior (Rouder et al., 2009) did reveal weak evidence for a difference in Br between contexts (*t* (17) = 2.2770, *p* = 0.0360, *BF* = 1.8672). Br in the HPC and LPC can be found in figure 2. It must be noted that although Br between the LPC and HPC was statistically significant with orthodox statistics, the *BF* only revealed weak support for a difference in Br.

Of critical interest to our hypotheses was how FARs differed between the LPC and the HPC. It was expected that the HRs would be higher in the HPC relative to the LPC, which is due to the prior-probability of target occurrence being greater in the HPC than the LPC. Under conditions of imprecise sensory data (Pr ~= 0.293) in the HPC, reliance on the prior-probability would lead to a higher FAR; when participants are unsure if the target is there or not, they should rely on the prior-probability. In contrast, the opposite should be the case in the LPC, when the sensory data is imprecise and the prior-probability is low, participants should have a lower false alarm rate (FAR). A Bayesian paired-sample *t*-test with a JZS prior confirmed that were more false alarms in the HPC than the LPC (*t* (17) = 2.3892, *p* = 0.0287, *BF* = 2.2336) although the *BF* quantified weak evidence for such a difference. Despite the fact that participants made more false alarms in the HPC compared to the LPC, the FAR was 0.2111 (SD -/+ 0.2076) compared to 0.1056 (SD -/+ 0.0938) in the LPC, meaning false alarms only occurred on just less than a quarter of stimulus absent trials in the HPC. This is a striking finding as the FAR was expected to be greatest in HPC. Even more striking is the finding that only, 61% of participants had a greater false alarm rate in the HPC than the LPC, which is quite low and close to the number of participants who would show the effect due to chance (50%).

The second critical interest to our hypotheses was how the HRs differed between the LPC and the HPC. In the HPC, imprecise sensory data would lead to participants indicating target

presence more than target absence. In contrast, imprecise sensory data would lead participants making the opposite pattern of response in the LPC; participants would indicate target absence more than target presence. A Bayesian one-sample *t*-test with a JZS prior revealed that participants had a greater hit rate in the HPC than the LPC (t (17) = 2.1416, p = 0.0466, *BF* = 1.5242) although the *BF* only quantified weak evidence for such a difference.

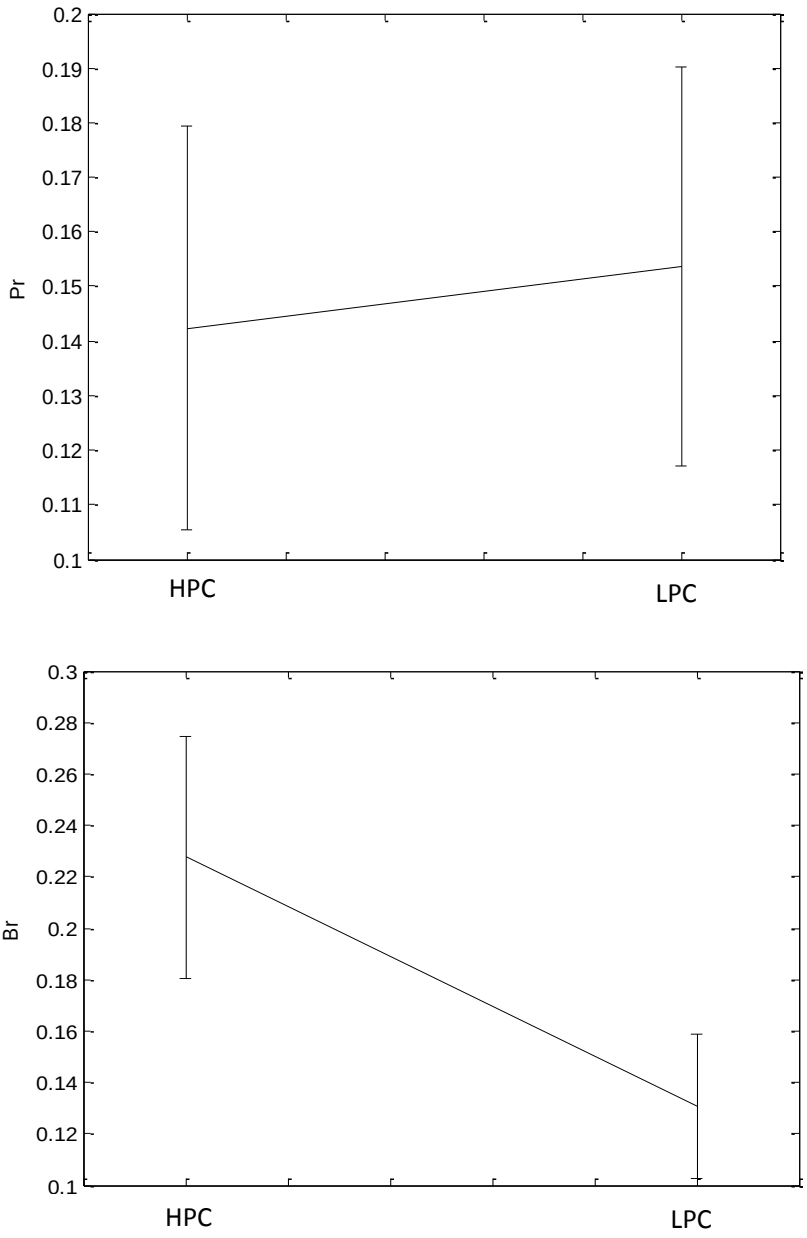

Figure 2. Top: Pr (perceptual sensitivity) in the HPC and LPC. Bottom. Br (criterion) in the HPC and LPC. Errors bars represent the -/+ 1 standard error.

Interim discussion: Experiment 2

Experiment 1 aimed to manipulate two different prior-probabilities of target occurrence in a HPC and an LPC. Different effects were predicted in each context when the participant was presented with imprecise sensory data (luminance where Pr ~= 0.293). Participants were expected to make more false alarms in the HPC than the LPC and more misses in the LPC than the HPC. Both of these hypotheses were confirmed, albeit weakly, which suggests that the influence of the prior-probability increases when sensory data is imprecise. Such an effect could have been present due to a change in a participant's criterion.

A differential effect of the prior-probability in each context when the sensory data is imprecise means that this paradigm can be considered for application with single pulse TMS. By adding noise to processes within EVC with TMS, it would be expected that an effect of reducing the precision of the prior-probability would be obtained before any effect on the prediction error. What is critical about the paradigm here and the pattern of behavioural responses is that the prior-probability made participants make errors when visual information was inconsistent with the prior-probability on a given trial. Performance was worse in the HPC because participants have a greater false alarm rate, due to the prior-probability indicating target presence despite the target being absence trials. In contrast, performance was worse in the LPC because participants had a lower hit rate, due to the prior-probability indicating target absence despite the target being present.

How would TMS affect the precision of the prior-probability and the prediction error using this paradigm?

Experiment 2 was conducted in order to develop a paradigm that can be integrated with EVC-TMS. Recall that a top-down prediction needs to be established in EVC before any feedforward inputs can take place (Rao & Ballard, 1999). Recurrent processes take place in response to prediction errors whereby the top-down prediction – or prior-probability in a Bayesian sense – is revised to represent sensory inputs (Rao & Ballard, 1999; Friston, 2005). The prior-probability needs to

established first, which means that TMS-induced effects on the prior-probability should occur before the well-documented TMS effect produced at ~100ms (Kammer, 2007; de Graaf et al., 2014). Such a prediction is feasible as improvements in performance when applying EVC-TMS have been revealed, whichcan occur before or at ~100ms (Abrahamyan, Clifford, Arabzadeh & Harris, 2011; Allen et al., 2014). The visual evoked latency of V1, V2 and V3 visual evoked latencies occur as early as 34ms, 84ms and 55ms, respectively (Schmolesky, Wang, Hanes, Thompson, Leutgeb, Schall & Leventhal, 1998). This TMS-effect at ~100ms does not quantify the latency of EVC activity to retinal stimulation; it quantifies the time taken for EVC to become critical to make a visual judgment. This delay relative to the latency of early EVC responses may mean that recurrent processes are necessary for reporting or discriminating visual stimuli. Bayesian predictive coding would argue that the latency of V1 responses reflects a prior-probability attempting to represent sensory inputs (Rao & Ballard, 1999; Friston, 2005; Clark, 2013). Later responses at ~100ms would then reflect the process whereby a prediction error is fed forward, which triggers a recurrent processing in order to integrate the prediction error with the prior-probability to produce the posterior (Rao & Ballard, 1999; Friston, 2005).

Single pulse TMS would be in used in conjunction with this paradigm to interfere with the prediction error or the prior-probability, which are integrated according to Bayes theorem in order to produce the posterior (Friston, 2005). By adding noise to neural processes within EVC (Walsh & Cowey, 2000), it is possible that the addition of noise would reduce the precision of the prior-probability or the prediction error, depending on the SOA when TMS is applied. Reducing the precision of the prior-probability or the prediction error would affect each of their relative contributions to the formation of the posterior (Feldman & Friston, 2010). Now the effects of TMS will be considered if EVC-TMS was to reduce the precision of the prior-probability and the prediction error. As a prior-probability needs to be established before prediction errors can be fed forward, an effect of EVC-TMS on the precision of the prior-probability will be expected at earlier SOAs prior to 100ms. In contrast, effects on the prediction error will be expected at SOAs at ~100ms or afterwards.

How this sequence of EVC-TMS effects on behaviour would emerge will now be considered using the paradigm presented in experiment 2.

First of all, an effect on the prior-probability will be predicted. The effects of reducing the precision of the prior-probability must occur at earlier SOAs than the effects of reducing the precision of the prediction error (Feldman & Friston, 2010; Friston, 2005). Reducing the precision of the prior-probability distribution using single pulse TMS would promote the influence of the prediction error when the two are integrated to form the posterior. This is because EVC-TMS would add noise to neural processes within EVC, which would in turn promote the relative precision of the prediction error relative to the prior-probability (Walsh & Cowey, 2000; Feldman & Friston, 2010). The effect of altering precision of the prior-probability on the formation of the posterior should lead to an *improvement* in performance on trials where an unexpected event takes place. An unexpected event refers to when the target is absent in the HPC and when the target is present in the LPC. An improvement would take place in the HPC on a target absent trial because the prior-probability is misleading on these trials; the target is *absent* but the prior-probability is indicating the target is likely to be present. As a result of TMS reducing the precision of the prior-probability, the participant would be less likely to make a false alarm on a target absent trial. An improvement would take place in the LPC on a target present trial because the misleading prior-probability indicates that the target would be absent on target present trials. As a result of TMS reducing the precision of the prior-probability, the participant would be less likely to make a miss response on a target present trial because the precision of the misleading prior-probability indicating target absence would be reduced. The effects of EVC-TMS on the precision of the prior-probability would be reflected in a participant's criterion (Corwin, 1994). The effect of EVC-TMS on criterion will also differ in the HPC and the LPC. In the HPC, a participant's criteria would become more conservative. In contrast, their criterion would become more liberal in the LPC. Their criterion would become more conservative in the HPC because the participant would make less target present responses on target absent trials. As a result, the participant's false alarm rate would be reduced. In contrast, their criterion would

become more liberal in the LPC because participants would make more target present responses on target present trials. As a result, the participant's hit rate would be increased.

Experiment 2: Methodological limitations

Despite the results of experiment 2 being consistent the predictions of predictive coding, there may be a number of methodological issues that prevent this paradigm being integrated with TMS. One issue was specific to the HPC. In the HPC, where participants were expected to make more false alarms due to the prior-probability of target presence, the false alarm rate (FAR) was low. Even in the HPC where the FAR was expected to be highest, the FAR was 0.2111 (SD -/+ 0.2076) compared to 0.1056 (SD -/+ 0.0938) in the LPC, meaning false alarms only occurred on just less than a quarter of stimulus absent trials in the HPC. There was also a lot more variability in the FAR in the HPC – some participants appeared to make no false alarms at all. False alarms are important in the current paradigm because they determine whether the precise prior-probability creates a representation of the target when the precision of the prediction error is low, despite the fact that the target itself is not present. In order to probe this phenomena using TMS, the phenomena needs to be present in a large number of participants, otherwise it may not be possible to detect the effect in first place (de Graaf & Sack, 2011). Overall, 61% of participants had a greater false alarm rate in the HPC than the LPC, which is quite low and close to the number of participants who would show the effect due to chance (50%). When considering the number of misses, which reduces a participant's hit rate, 72% of participants had a lower hit rate in the LPC compared to the HPC. In order for the predicted effects of TMS to be present and achievable, a high percentage of participants would need to display both effects. Without such effects being present in their control data, which is what this experiment was emulating, it would not be possible to use EVC-TMS to interfere with the precision of prior-probability distribution to cause improvements in performance. If an effect of the prior-probability is not present behaviourally, how would it be possible to utilize TMS to interfere with such a distribution?

An additional issue is the emergence of a TMS-induced effects to begin with. Not all participants exhibit effects of EVC-TMS (Camprodon et al., 2011 - see experiment 1 for a null result), which can be due to choosing incorrect TMS parameters, poor coil placement (de Graaf & Sack, 2011), inaccessible neuroanatomy, or inappropriate choice of visual stimulus calibration. It could be unreasonable to expect participants to make a large number of false alarms in the HPC -why would participants report a target as present when a target is not there? The combination of these issues mean that it may be a tall order to expect these hypotheses to be confirmed. This means that it may not be feasible to rely on this paradigm to reduce the precision of the prior-probability distribution using EVC-TMS if a prior-probability might is not influencing every participant's responses.

Another issue with the paradigm here is the blocked structure of each context. It is likely that blocked structure and the explicit nature of the instructions set up a prior-probability that is too strong and potentially difficult or impossible to interfere with using TMS. Here the HPC and the LPC were presented separately and likely contributed to the criterion shift that led to the difference in false alarms and misses between each context. The context the participant was in was made very clear – at the beginning of each context block, where the probability of target occurrence was told to them explicitly. The context they were in was also made clear at the beginning of each trial where an 'H' or an 'L' indicating that participants were in the HPC or LPC condition, respectively. These manipulations were introduced to maximize the likelihood that participants were aware of the context they were experiencing. It was essential that participants were aware of being in the HPC or LPC in order for the effect of prior-probability to affect performance in each of these contexts. Similar paradigms published after experiment 2 had been completed have made participants aware of how likely a target is to appear in blocks where the likelihood of target occurrence is low or high (Sherman, Seth, Barrett & Kanai, 2015). Interestingly, the paradigm introduced by Sherman et al. (2015) was combined with EEG to reveal that pre-stimulus activity within the occipital lobe predicts whether a participant will make a yes or a no response (Sherman, Kanai, Seth & VanRullen, 2016). In particular, pre-stimulus alpha phase predicted whether a prior-expectation of stimulus presence or

absence would be reflected in participant's responses. This means that a common substrate exists for prior-probabilities for target presence *and* target absence. Such a substrate is a likely candidate for mediating the effect of the prior-probability in the HPC and the LPC in the paradigm presented here.

However, when considering the design of this paradigm, it is important to determine whether the effect of the prior-probability is due to integration of a prediction error with the prior-probability which fed back into EVC or whether the effect is due to a bias in participant's responses regardless of whether they see or do not see the target. Given that the target is very difficult to see, it is possible that participants did not know whether the target was present or not, which led to a bias in their responding based on how obvious the experimental manipulation was in this experiment. An implication of this is that the paradigm was not feasible for probing whether Bayesian integration of a prediction error with a prior-probability occurs within EVC using TMS. In response to this criticism, it would be useful to employ a paradigm which retains the probabilistic element to the task, such as using a cue that indicates what is most likely to occur on a given trial. To probe the existence of the prior-probability, it would also be useful to have a target that is present on every trial, which eliminates the problem of relying on consistently high false alarm rates as the principle dependent variable, which may be an unreasonable requirement of the task. Instead, it may be useful to rely on the cue to indicate how likely a particular characteristic of the target is, such as its identity or location, rather than how likely a target is to appear or not appear at all.

In conclusion, the hypotheses of this experiment were confirmed; there was evidence of a prior-probability influencing responses. However, the prior-probability did not affect all the participants consistently, which complicates the use of EVC-TMS to probe the nature of such a prior-probability in perceptual processes. The influence of prior-probability is most likely to have arisen because of how the experiment was structured. The probability of target occurrence was made so obvious in each experiment and the target was very difficult to see. It is likely that participants did

not see anything and went with what was most likely. As an alternative, a paradigm will be employed where the stimulus is always present, thus eliminating the problem of relying on false alarms as one of the measures of a prior-probability. Rather making participants make judgments of target presence of absence, a task will be employed which relies on an arrow cue to determine how likely a target is to appear in one visual hemifield or another. Judgments of target location to probe the existence of a prior-probability and the temporal dynamics of prediction error integration with a prior-probability using TMS.

Experiment 3: Introduction

Experiment 2 utilized a block structure where the prior-probability was made very explicit to participants. It is possible that this was *too* explicit and in spite of this, some participants revealed no evidence of a prior-probability on performance. In experiment 2, the prior-probability was not set in a block-like structure. Instead, a prior-probability was used to indicate the most likely location of target occurrence on each trial. The likelihood of the target occurring in one these locations varied on a trial-to-trial basis and the precision of the prior-probability itself was varied on a trial-to-trial basis. By designing the experiment this way, it was possible to retain a probabilistic element to the experiment without using a blocked contextual design which leads to a bias in participant's responses.

Posner cueing has proven useful in the study of Bayesian predictive coding (Feldman & Friston, 2010). In a Posner cueing paradigm, participants are required to fixate at a central location on a screen and respond as soon as a target appears, which is usually in peripheral location to the site of fixation (Posner, 1980). Prior to target occurrence, a cue appears which can be central (usually an arrow) or peripheral (in the same location as upcoming target) which indicates the likelihood that a target will appear in a certain location. The cue can be valid or invalid; when the cue is valid, the target appears in the cued location whereas when the cue is invalid, the target appears in a different location to the cued location. In some variants of this paradigm, The cue is a valid predictor of

upcoming target location, for instance predicting the upcoming target position on ~80% of trials (Feldman & Friston, 2010). The consequence of presenting a cue before target occurrence is on reaction time (RT). When the cue is valid, RTs tend to be faster than when the cue is invalid (Feldman & Friston, 2010). Here we attempted to utilize the probabilistic element to the Posner (Posner, 1980) cueing paradigm to develop a task that could be integrated with TMS to probe the existence of Bayesian integration of a prior-probability with a prediction error to create a posterior.

Experiment 3 employed a Posner cueing-like paradigm to induce a trial-by-trial prior-probability of where a visual target could appear. An arrow cue could be a valid or invalid indicator of target location. On a valid trial, the arrow indicated the hemifield where the target would appear whereas on an invalid trial, the arrow indicated the opposite hemifield to where the target would appear. Two arrows appeared in a diamond-like shape (<>). One of these arrows was a valid cue of upcoming target location (70% of trials) which was always presented at maximum luminance. The remaining arrow served as a non-cue arrow and the luminance of this non-cue arrow was altered on a trial-by-trial basis. There is also evidence that altering the certainty of a target appearing in a particular location by increasing or decreasing the ambiguity of a cue that can indicate the upcoming location of a target affects the overall influence of a cue on performance (Huang, Liang, Xue, Wang, Hu & Chen, 2017). For example, reaction time increases when cues occupy all the locatins where a target could appear. In contrast, reaction time decreases when a valid cue only occupies a single location, where the target subsequently appears. In a similar manipulation, more akin to the classic Posner cueing paradigm, the luminance of the non-arrow cue was altered in order to modulate the precision of the prior-probability. When the non-arrow cue and the arrow cue had equal luminance, the prior-probability was imprecise as it does not provide a certain upcoming location for the target. The luminance of the non-cue arrow ranged from both having equal luminance to the cue arrow, creating an imprecise prior-probability, to one of arrows having identical luminance to the screen background (thus rendering it invisible), creating a precise prior-probability. When both arrows had equal luminance, it was expected that the prior-probability would be imprecise because these arrow

cues conveyed no information surrounding the location of the upcoming target. As as result, the prior-probability is imprecise because it is uncertain as to where the upcoming target will appear. In contrast, when the non-arrow cue had an identical luminance to the background and the difference in luminance between the arrow and non-arrow cue was largest, it was assumed that the precision of the prior-probability would be at its highest.

In experiment 3, a 2 (cue validity) x 5 (non-cue arrow luminance) repeated measures ANOVA was applied to RT, PC and the number of errors in the cued hemifield. The cue arrow was expected to improve performance on valid trials compared to invalid trials. However, such a benefitdepended on the difference in luminance between the cue arrow and the non-cue arrow. Such differences would reflect the greater precision of the prior-probability as the difference in luminance between the cue arrow and the non-cue arrow increases. When the difference in luminance between the cue arrow and the non-cue arrow is large, the prior-probability will be precise, which would lead to a greater effect of the cue on RT and PC. In contrast, when the difference in luminance between the cue arrow and the non-cue arrow is large, the upcoming target location will be uncertain and the prior-probability will be imprecise, which would reduce the effect of the cue on RT and PC. As the difference in luminance between the cue arrow and the non-cue arrow increases, a greater PC for valid trials compared to invalid trials should emerge. This luminance difference dependent increase in PC will manifest itself as an interaction between cue validity and non-cue arrow luminance. A similar effect was expected for RT. However, RT was expected to be greater on invalid trials compared to valid trials. Such an effect would reflect quicker detection of a target has appeared in the cued hemifield compared to when the target has not occurred in the cued hemfield (Posner, 1980). However, such a benefit would depend on the difference in luminance between the cue arrow and the non-cue arrow. As the difference in luminance between the cue arrow and the non-cue arrow increased, a greater RT for invalid trials compared to invalid trials would emerge. As the difference between the cue arrow and the non-cue arrow increases, RT will be shorter for valid trials compared to invalid trials. This luminance dependent decrease in RT for valid trials compared to

invalid trials would manifest itself as an interaction between cue validity and non-cue arrow luminance. In terms of the errors that participants make, a slightly different pattern of results was expected. The influence of cue on the errors would vary as a function of the difference in luminance between the cue arrow and the non-cue arrow. When the difference was large, the prior-probability of target occurrence in the cued hemifield would l be clearer than when the difference in luminance is not large. As a result of this, a main effect of non-cue arrow luminance was expected; as the luminance difference between the non-cue arrow and the cue arrow increases, participants would make more judgments in the cued hemifield.

Here, the participant has the option to report one of four quadrants to indicate where the target has appeared. Under Bayesian predictive coding, the arrow cue indicates where the target is most likely to appear, which would manifest itself as a higher prior-probability of target occurrence within the hemifield where the arrow cue is pointing towards. When the target appears on a valid trial, the integration of the prediction error with the prior-probability would lead to a judgment that the target has appeared in either of the quadrants corresponding to where the arrow cue was pointing. For example, if the arrow cue was pointing right, the integration with prediction error with the prior-probability would indicate that the target could appear in either one of the locations in the upper right or lower right quadrants on the screen. Such integration would lead to a benefit in terms of PC on valid trials: the prior-probability indicates that the target will appear in the half of the screen that corresponds to where the target actually appears. Such a process could also lead to a bias in participant's errors on valid trials. When a participant makes an incorrect response on a valid trial, they are reporting the target to be present in the hemifield cued by the arrow cue, but not the quadrant in the cued hemifield where the target appeared. For example, this would arise when the left hemifield was cued and the target appeared in the bottom left quadrant but the participant reports the target present in *top* left quadrant. On valid trials this pattern of responses mean that an effect of the prior-probability on performance can be measured in terms of PC being greater as the

cue is expected to bias responses towards the cued hemifield. However, it can also be expected that the errors participants make will also be biased towards the cued hemifield on valid trials.

It was intended that experiment 3 would be integrated with single pulse EVC-TMS to test the predictions of Bayesian predictive coding (Rao & Ballard, 1999; Friston, 2005). As outlined previously, TMS is expected to reduce the precision of the prior-probability before TMS can reduce the precision of the prediction, which is due to prediction errors being conditional on a prior-probability being established beforehand (Feldman & Friston, 2010). The effect of the prior-probability on performance was measured in terms of a greater PC for valid trials compared to invalid trials. The effect of the prior-probability was also measured as faster RT on valid trials compared to invalid trials. Both of these effects relied on the arrow cue being an uninformative indicator of upcoming target location. Reducing the precision of the prior-probability by adding noise to neural processes within EVC at earlier SOAs was expected to reduce the influence of this misleading source of information (Walsh & Cowey, 2000; Feldman & Friston, 2010). This would reduce RT and increase proportion correct on invalid trials, which would reduce the magnitude of the difference in PC between valid trials and invalid trials.

To conclude, experiment 3 aimed to develop a different paradigm from experiment 2 to test the predictions of predictive coding across different TMS SOAs. Similarly, to experiment 1, effects of TMS reducing the precision of the prior-probability were expected before effects of TMS reducing the precision of prediction error. On valid trials, an effect of reducing the precision of the prior-probability would reduce the benefit garnered by a valid cue when indicating where the target appeared. On valid trials, it is difficult to tease apart the promotion of the relative influence of the prediction error compared to the prior-probability as the target and the cue both appear in the same hemifield. Are incorrect responses in the cued hemifield due to the cue pointing (prior-probability) there or due to the target appeared there (prediction error)? As a result of this, invalid trials will be more informative to the hypotheses present here. On an invalid trial, incorrect responses in the cued

hemifield would reflect an influence of the prior-probability and correct responses in the uncued hemifiled would reflect an influence of the prior-probability. If this predictions were confirmed, this paradigm would have been considered for integration with single pulse TMS.

Experiment 3: Methods

Participants

12 participants who were undergraduates and postgraduates from the Cardiff University School of Psychology, who were paid £6 or reimbursed with course credit for their participation.

Design

A minor variation of a Posner cueing (Posner, 1980) paradigm was employed here. Participants had to indicate where a target appeared. The target was a square. The target could appear in the centre of one of four quadrants. Each quadrant was marked by the top left (Q1), top right (Q2), bottom left (Q3) or bottom right (Q4) of the screen. Participants had to indicate which quadrant the target appeared in by pressing a button on a keyboard (Q1: 'z', Q2: 'n', Q3: 'x', Q4: 'm'). Prior to target occurrence, an arrow cue appeared, which was either a valid or invalid indicator of where the target would appear in the left or right of the screen. The arrow cue was valid when the arrow cue pointed left and target appeared on the left hand side of the screen, which was in either Q1 or Q3. The arrow could also be valid when the arrow cue pointed right and the target appeared on the right hand side of the screen, which was in either Q2 or Q4. The arrow cue was a valid indicator of target location on 75% of trials. On an invalid trial, the target appeared on the opposite side of the screen to where the cue indicated. When the arrow cue was pointing right, the target appeared on the left hand side of the screen, which was in either Q1 or Q3. On an invalid cue when the arrow cue was pointing left, the target appeared on the right hand side of the screen, which was in either Q2 or Q4. Performance was measured using proportion correct. The number of times the participant indicated the target was in a cued quadrant where the target did *not* occur was also calculated, along with RT. The calculation of RT as a measure of performance meant that participants

were instructed to emphasize speed *and* accuracy in their responses. The proportion of errors (PE) that were made in the cued hemifield were also calculated as an additional measure of the precision of the prior-probability on performance. PE was calculated by dividing the number of errors in the cued hemifield (left arrow cue: Q1 + Q3 responses & right arrow cue: Q2 + Q4 responses) by the total number of errors the participant made.

The principle differences between the paradigm used here and the conventional Posner (1980) cueing paradigm were the duration of time that separated the onset of the arrow cue and the onset of target (1000ms) and the nature of the arrow cues. In this experiment, two arrows cues were presented at once, which formed a diamond shape (<>). One of these arrows served as the cue specified above, which indicated the hemifield where the target would occur on 75% of trials. The luminance of the second non-cue arrow, which did *not* indicate the hemifield where the target would appear was used to manipulate the precision of the prior-probability. Five differences in luminance between the cue arrow and the non-cue arrow were used, which are illustrated in figure 3. One had identical luminance to the arrow cue pointing in the opposite direction. In another set of trials, the non-cue arrow was absent. Two more non-cue arrows were used that had intermediate differences in luminance in-between background luminance and a luminance that was identical to the opposing arrow cue. When the difference in luminance between the cue and the non-cue arrow was at its largest, the prior-probability was at its most precise as only one arrow as visible which was valid on 75% of trials. When the cue arrow and the non-cue arrow had equal luminance, the prior-probability was most imprecise as no information was present to indicate the hemifield the target was most likely to appear in. At intermediate differences in luminance between the arrow cue and the non-cue arrow, the precision of the prior-probability was expected to incrementally increase as the luminance of the non-arrow cue decreased.

Each type of non-cue arrow luminance occurred 120 times and there were four different non-cue arrows. These were presented randomly across six blocks which meant there were 600

trials in total. For each non-cue arrow luminance there were 84 valid trials and 36 invalid trials. The order in which each non-cue arrow luminance occurred was randomized. On valid and invalid trials, the target appeared in the upper and lower quadrants an equal number of times, enabling counterbalancing to take place. Counterbalancing meant that the target appeared in the upper quadrant and the lower quadrant on 42 trials when the cue was valid for each non-cue arrow luminance. When the arrow cue was invalid, the target appeared in the upper quadrant and the lower quadrant on 18 trials for each non-cue arrow luminance. The luminance of the target was fixed throughout the part of the experiment. Illustration of the experimental design can be found in figure 3.

Participants completed a luminance manipulation procedure prior to the part of the experiment where the luminance of target was altered. Participants were presented with 15 different target luminances. Each luminance occurred on 28 trials and the order in which each luminance was presented was randomized. There were 420 trials in total during the luminance calibration procedure. The arrow cues were valid on 75% of trials and the left and right pointing arrows were presented by themselves; there were no non-cue arrows presented during the calibration procedure. There were 21 valid trials and 7 invalid trials for each target luminance. Once all 420 trials had been completed, PC was calculated for each luminance level and a sigmoid or linear function was fitted (depending on which model had the highest adjusted r^2) (Allen et al., 2014). The model with the best fit was then solved to identify the value of luminance that corresponded to a PC (y) of 0.7. Target luminance was set of this luminance value for the rest of the experiment.

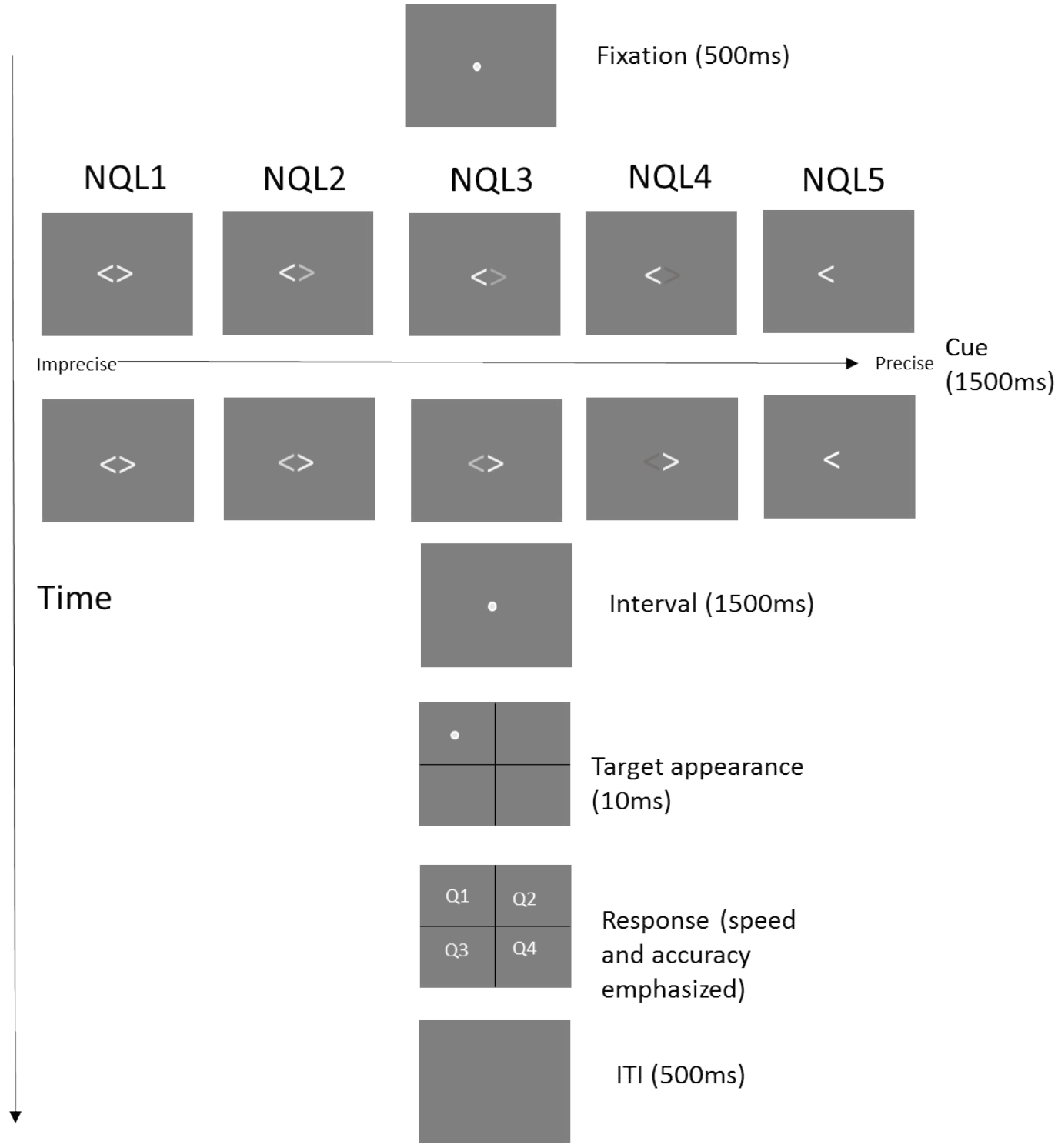

Figure 3. Illustration of the paradigm employed in experiment 3. First of all, fixation took place, which was followed by the presentation of a right or left pointing arrow cue, which was a valid predictor of the hemifield the target could appear in on 70% of trials. Two different types of valid trial could place. When the arrow cue pointing left and the target appeared in quadrant 1 (Q1) or quadrant 3 (Q3) or when the arrow cue pointed right and the target appeared in quadrant 2 (Q2) or quadrant 4 (Q4) Five differences in luminance between the valid or invalid cue arrow and the non-cue arrow were presented. There was either no difference in luminance between the cue arrow and the non-cue arrow (NQL1) and ascending differences between the cue arrow and the non-cue arrow, which are referred to as NQL2, NQL3, NQL3, N1L4 and NQL5. After the appearance of the cue, a 1500ms interval took place prior to the appearance of the target, which took place for 10ms. Immediately after cue appearance, the participant could report the cue's location in one of four quadrants in Q1, Q2, Q3 and Q4. Speed and accuracy was emphasized in their responses. Once the response had taken place, an ITI of 500ms took place.

Equipment

Visual stimuli were produced by Matlab running the Psychophysics Toolbox 3 on a gamma-corrected 21" Mitsubishi CRT monitor (refresh rate: 100 Hz). Visual stimuli were also presented on this monitor in experiment 3.

Procedure

Firstly, participants completed the luminance manipulation procedure. Subsequently, participants completed the second part of the experiment where the luminance of one of the cues was altered. Participants were instructed to emphasize speed and accuracy in their responses.

Experiment 3: Results

Proportion correct (PC)

Mean PC as function of cue validity and non-cue arrow luminance can be found in figure 4. Critical to the hypothesis, a 2 x 5 ANOVA revealed a significant interaction between cue validity and cue luminance (F (4, 44) = 3.667, p = 0.012), which meant that a difference between PC as a function of cue luminance existed but depended on cue validity. A main effect of cue validity (F (1, 11) = 19.903, p = 0.001) was also revealed, which meant that PC was higher when the arrow cue was valid regardless of the luminance of the non cue arrow. However, a main effect of cue brightness was also revealed (F (4, 44) = 3.551, p = 0.014), which suggested that PC was also significantly differed as a function of cue luminance.

In order to identify the differences in cue luminance where PC differed as a function of cue validity, a Bayesian paired-sample t-test with a JZS prior (Rouder et al., 2009) compared PC on valid trials to PC on invalid trials at each cue luminance. This test is important as it reveals the how the effect of arrow cue validity varies as a function of non-cue arrow luminance. It was expected that no difference between valid and invalid trials when non cue arrow luminance is equal to cue arrow luminance (NQL1) but it was expected that a PC will be greater for valid trials than invalid trials when the difference in luminance between the cue arrow and the non-cue arrow increases between NQL2

up to NQL5. The use of Bayesian *t*-tests is particularly important here as the production of evidence for the null hypothesis is just as important as evidence against the null hypothesis (Dienes, 2011). As expected, PC did not differ as a function of validity at NQL1 (t (11) = 0.4253, p = 0.6788, BF = 0.3108). Decisive evidence for a difference in PC as a function of validity at NQL2 (t (11) = 3.4528, p = 0.0054, BF = 9.7907), NQL3 (t (11) = 3.9287, p = 0.0024, BF = 19.4772) and NQL5 (t (11) = 4.5834, p < 0.001, BF = 49.1371). Surprisingly *inconclusive* evidence for a mean difference was found at NQL4 (t (11) = 2.1988, p = 0.0502, BF = 1.6525). When the prior-probability was imprecise (arrow cue and the non-cue arrow with equal luminance), no benefit of cueing was presence within PC. However, the *BF* revealed incrementally greater support for a mean difference in PC between valid trials and invalid as the difference in luminance between the arrow cue and the non-arrow cue increased. As the prior-probability became more precise, the difference in PC between valid and invalid arrow cues also became greater. The only exception to this statement is the *BF* revealed by NQL4.

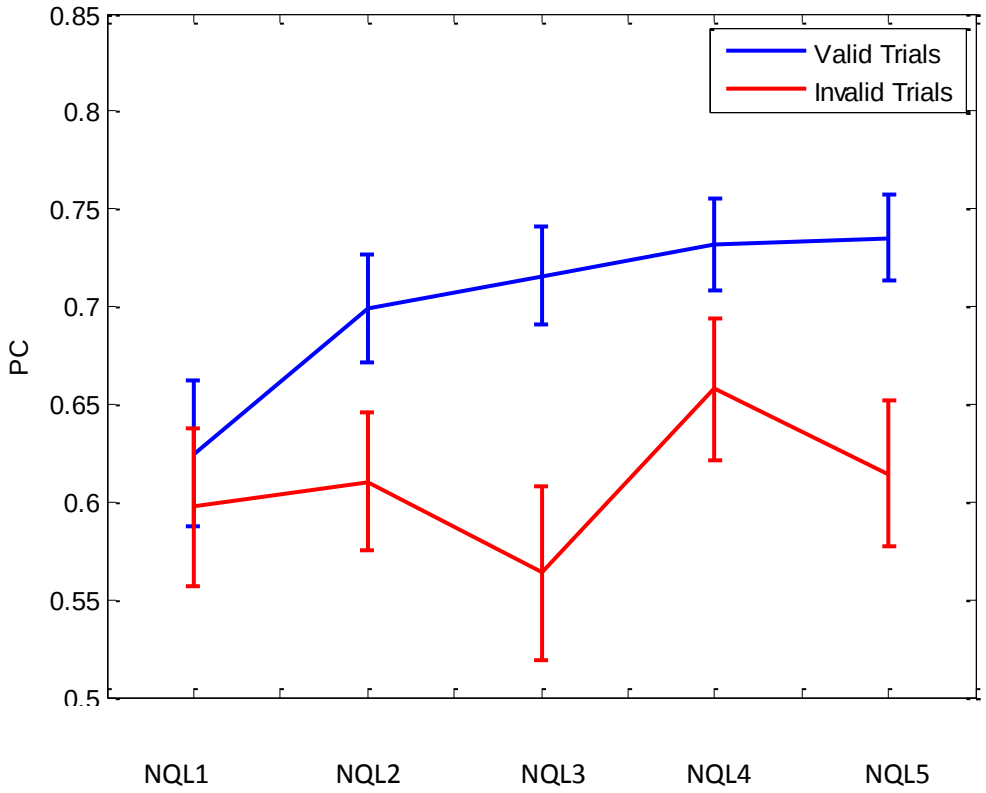

Figure 4. Proportion correct (PC) as a function of non-cue arrow luminance 1 (NQL1), 2 (NQL2), 3 (NQL3), 4 (NQL4) and 5 (NQL5) for valid and invalid trials.

Reaction time (RT)

Mean RT as function of cue validity and non-cue arrow luminance can be found in figure 5. A 2 X 5 ANOVA revealed a main effect of cue validity (F (1, 11) = 12.179, $p < 0.005$), which meant PC was higher when the arrow cue was valid compared to when it was invalid, as expected. However, a main effect of cue brightness (F (1, 44) = 1.482, p = 0.224) was not found nor an interaction (F (1, 44) = 1.984, p = 0.114).

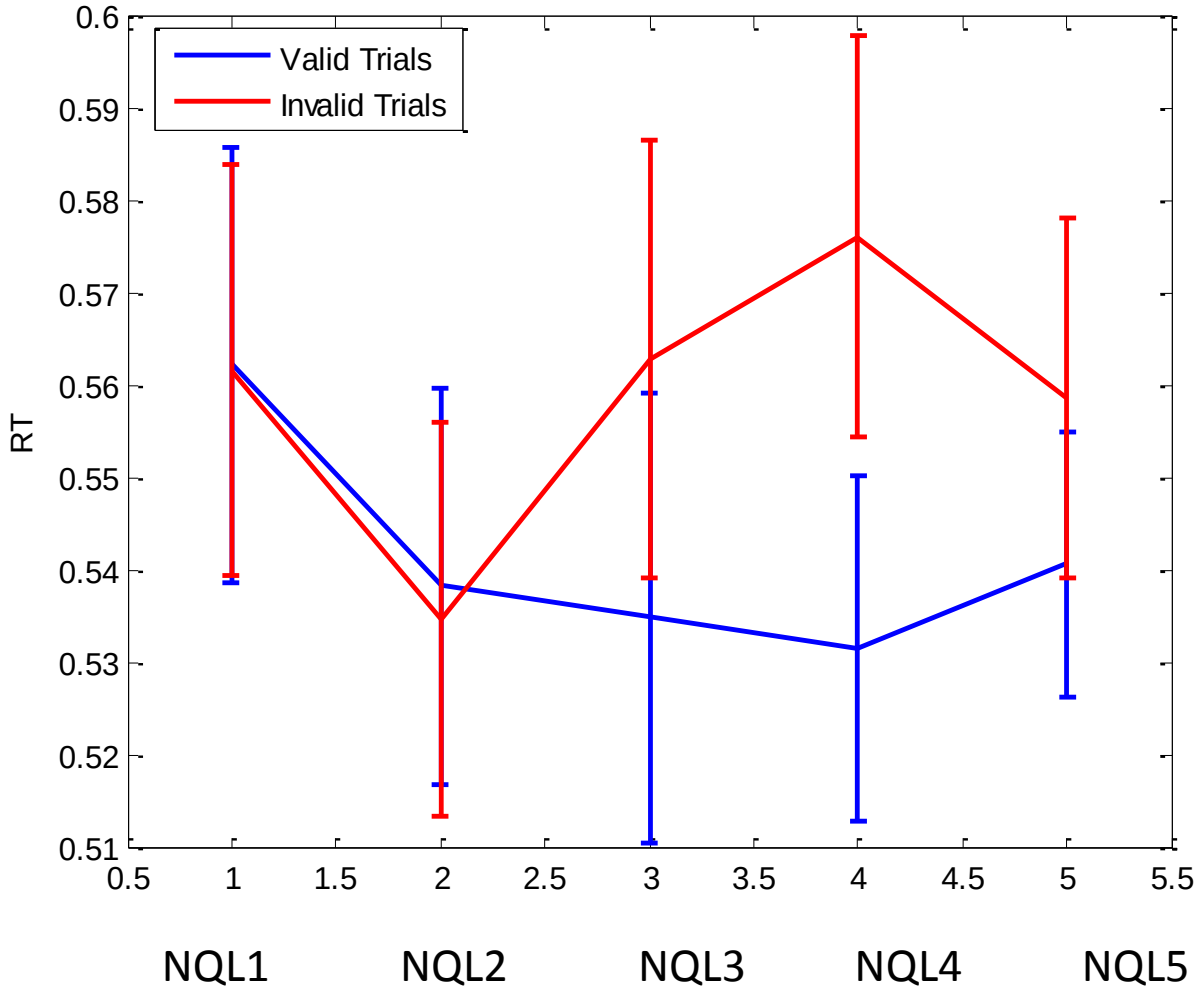

Figure 5. Reaction time (RT) as a function of non-cue arrow luminance 1 (NQL1), 2 (NQL2), 3 (NQL3), 4 (NQL4) and 5 (NQL5) for valid and invalid trials.

Errors in the direction of the prior

Mean errors in the cued hemifield as function of cue validity and non-cue arrow luminance can be found in figure 6. A 2 x 5 ANOVA did not reveal that a main effect of cue validity (F (1, 11) = 1.226, p = 0.292) reached statistical significance. However, a main effect of non cue arrow luminance

did reach statistical significance (F (4, 44) = 4.606, p = 0.003), which meant that participants made more errors in the cued hemifield when the difference in luminance between the cue arrow and the non-cue arrow as the difference in luminance increased. An interaction between validity and cue brightness did not reach statistical significance (F (4, 44) = 1.529, p = 0.210).

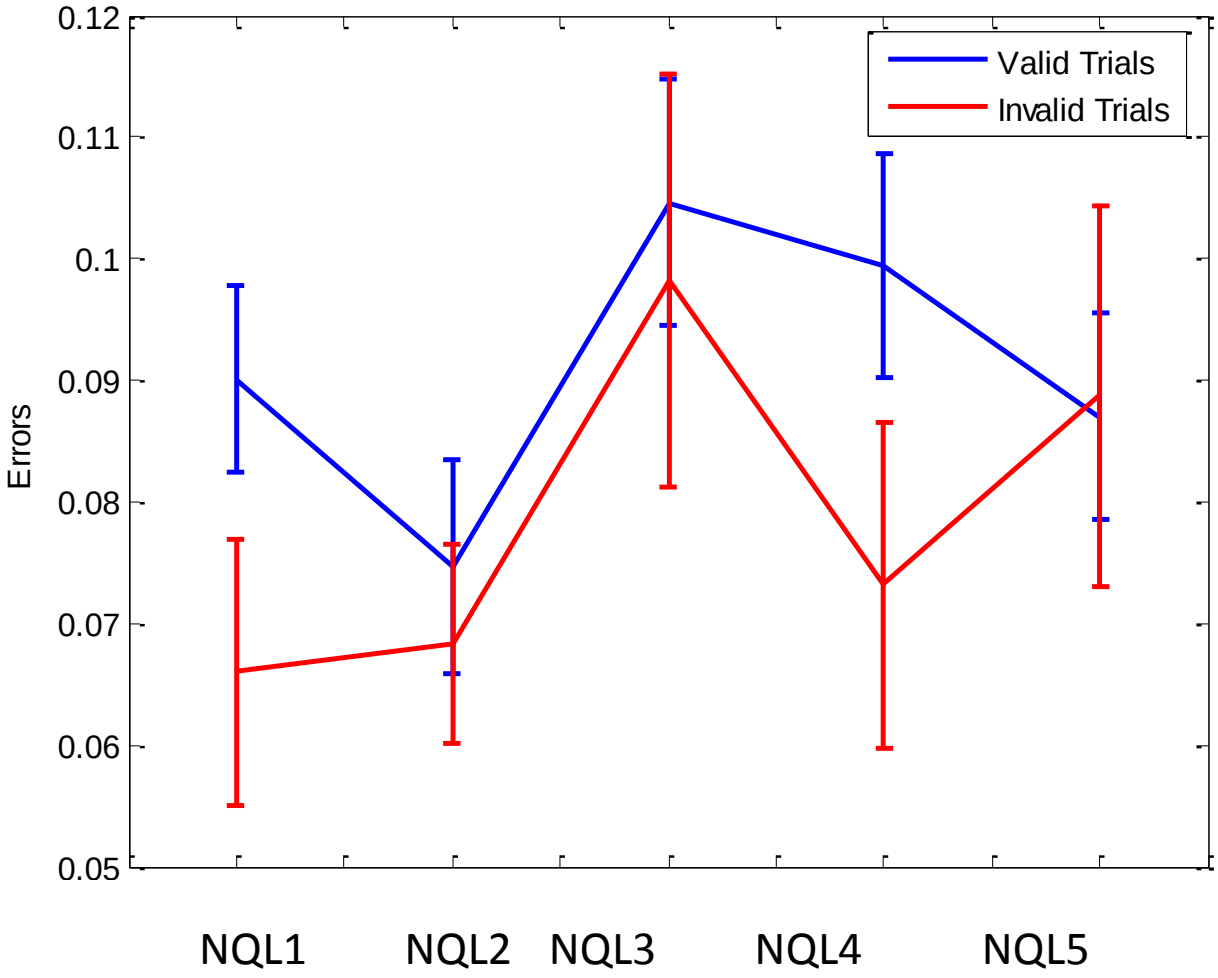

Figure 6. Errors in the direction of the prior (Errors, PE) as a function of the five differences in luminance between the cue arrow and the non-cue arrow. 5 ascending differences were used, which are marked by NQL1, NQL2, NQL3, NQL4 and NQL5.

Experiment 3 Discussion

Experiment 3 aimed to manipulate the precision of the prior-probability distribution by altering the difference in luminance between the cue arrow and the non-cue arrow. When both arrows had equal luminance, the precision of the prior-probability was low, as the neither cue carries information about the hemifield the target could appear in. However, when only one arrow cue was visible, the precision of the prior-probability was high, as the cue validly indicated the

hemifield the target could appear in.t It was assumed that the precision of the prior-probability would incrementally increase at intermediate luminances between these two extremes. Here, we investigated the effect of altering the precision of the prior-probability on PC, RT and the pattern of participant's errors. As expected, an interaction between cue validity and cue luminance was found, the direction of these differences meant that a greater PC was obtained on valid trials when the difference between the cue arrow and non-cue arrow was high, but not when there was no difference in luminance. Surprisingly, no such statistically significant effect was observed for RT. An effect of the precision of the prior-probability was also found on the errors that participants made, which was expressed as a main effect of cue brightness on the bias to report that the target appeared in the cued hemifield.

Although the majority of the hypotheses for this experiment were confirmed, further investigation of how the effects of the cue could arise led to the conclusion that this paradigm was not an appropriate candidate for integration with TMS. This conclusion was based on intimate relationship between the process of visual attention and the process of stimulus representation (Summerfield & Egner, 2009). The use of an arrow cue enhances stimulus representation in the cued hemifield (Posner, Synder & Davidson, 1980), which increases the relevance of the cued hemifield during the a task (Desimone & Duncan, 1995). Such a process can be distinguished from the process by which descending top-down predictions and ascending predictions errors work synergistically to represent sensory inputs consistent with Bayes theorem (Rao & Ballard, 1999; Friston, 2005; Feldman & Friston, 2010). The findings of the experiment in relation to predictive coding (Rao & Ballard, 1999; Friston, 2005; Feldman & Friston, 2010) and theories of visual attention (Desimone & Duncan, 1995) will now be discussed.

It was assumed that altering the difference in luminance between the cue arrow, which could a valid or invalid probabilistic indicator of where a target would appear, and a non-cue arrow would alter the precision of the prior-probability. When cue arrow and the non-cue arrow luminance

were equal, it was expected that the precision of the prior-probability would be low. This assumption was made because both arrows had equal luminance and the participant had no way of utilizing one of them to anticipate the upcoming hemifield the target would appear in. In contrast, when the difference in luminance between the cue arrow and the non-cue arrow was highest (when the cue was absent), it was expected the precision of the prior-probability would be greatest. This assumption was made because the cue could be utilized as a valid predictor of upcoming target location. The difference in precision between the prior-probability and the prediction error determines the relative each one has when the two are integrated to form the posterior (Feldman & Friston, 2010). An effect of the cue was found to alter PC and the number of errors participants made in the cued hemifield, which suggests that the precision of the prior-probability successfully altered participant's perceptual judgments. Moreover, an effect of the precision of the prior-probability was found to alter perceptual judgments but not RT, which suggests that its effect may have been on what participant's perceived as opposed to an artefact of speeded responses to validly cued, but not invalidly cued locations (Posner, 1980).

Experiment 3 found an effect of the precision of the prior-probability. Although a probabilistic element to this experiment cannot be ruled out, it is important to be distinguish between effects of prior-probability on target identity and target location. Bayesian predictive coding proposes that a prior-probability must be in place for feedforward outputs to the rest of brain from V1 (Friston, 2005). In theparadigm used in experiment 3, the presentation of a cue that can produce a precise but not an imprecise prior-probability, leads to feedback to EVC which signals the hemifield where the target is most likely to occur. It was assumed that presentation of the target would trigger a prediction error, which would be integrated with the prior-probability to form a posterior. When a cue precedes the target, it was assumed that the posterior would reflect the prior-probability. For example, when an arrow pointing right appeared, target appearance would more likely to create a representation of target shape *and* target location in the right hemifield.

However, it must be considered that in our paradigm that the effects of prior-probability in visual cortex can be expressed in two different ways. The one probability is the likelihood of target *location*, which increases cortical excitability and enhances spatial resolution of forthcoming sensory inputs in an expected location (Yeshurun & Carasco, 2013; Bestmann, Ruff, Blakemore, Driver & Thilo, 2007). This processes can be distinguished from processes that relate to expecting a stimulus of a particular identity taking place, which can also alter responses within EVC (Kok et al., 2013). However, the process of expecting a target in a particular location and the process of expecting a target of a particular identity, are often confounded (Summerfield & Egner, 2009). In experiment 3, the target was always the same – a square – and this target could be expected to appear in a cued location. Consequently, the process of expecting a target of a particular identity and the process of expecting a target to appear in a particular location could be confounded as explained by Summerfield & Egner (2009). The effects of expecting a target to appear in a particular location relate to attention, which can be flexibly allocated depending on the goal of a particular task (Desimone & Duncan, 1995).

There is strong evidence that arrow cues affect how attention is deployed, which has consequences for how stimuli are subsequently processed. It must be noted that these effects are related to processes related to stimulus identity, but the effect of attention is to improve representation of a particular stimulus depending on where a stimulus is presented within the visual field. For example, presented a cue that indicates the upcoming location of a target produces a significant increase in V2 and V4 in the retinotopic location where the target would subsequently appear in all participants during a 10 second expectation period (Kastner, Pinsk, De Weerd & Ungerleider, 1999). This included a greater increase in BOLD from baseline prior to visual stimulation in V1, V2 and V4 (Kastner et al., 1999), which is consistent with primate electrophysiological recordings revealing a significant increase in the spikes per second in V1, V2 and V4 when attention is directed to a location within their receptive field (Luck, Chelazzi, Hillyard & Desimone, 1997). Thus, it is clear that a probabilistic cue can alter pre-stimulus activity within EVC, which prepare EVC for

forthcoming visual stimulation. Such effects increase the cortical excitability of retinotopic visual cortex as unpredictably substituting a real visual stimulus that would be presented in a cued location for an EVC-TMS pulse leads to a lower TMS stimulation intensity inducing a phosphene (Bestmann et al., 2007). It becomes apparent that a process that increases cortical excitability in a cued location is at work in the paradigm used here, which would account for PC was higher for valid trials than invalid trials when the difference in luminance between the cue arrow and non-cue arrow was largest.

However, there is still the result that participants made more errors in the hemifield indicated by the cue arrow when the difference in luminance between the cue arrow and the non-cue arrow was at its highest, which could relate to what the participants saw. Processes related to what participants see are of relevance here because they relate to how top-down predictions induced by the cue affect the representation of sensory input (Rao & Ballad, 1999; Friston, 2005). Unlike PC which varied as a function of cue validity and non-cue arrow luminance, a main effect of non-cue arrow luminance was found on the proportion of errors that participants made in the cuedhemifield . What is interesting about this is that the precision of the prior-probability affected whether or not participant's errors were biased, which suggests that a prior-probability is important in perceptual judgments. However, the main issue with this paradigm remains to be that processes that contribute to enhancing representation in one part of the visual field cannot be distinguished from the processes that contribute towards creating the visual representation that can enhanced in the first place. To put it simply, if this task was integrated with TMS, it could not dissociate the processes that are responsible for representing the target from the processes that *improve* the representation of the target. The latter process relates to visual attention (Desimone & Duncan, 1995), which is not of interest to the investigations here.

Based on the evidence presented so far, it remains unclear whether the retinotopic effects of target identity expectation can be revealed in EVC and whether effects of target identity

expectation can be distinguished from retinotopic effects of target location expectation (c.f. Summerfield & Egner, 2009). There is evidence that the prior-probability of upcoming motion direction induced by a tone can bias representation in visual cortex (Kok et al., 2013). In particular, voxels in V1, V2, V3, V4, V4A and MT+ with estimated motion tuning curves for rightward motion exhibiting a greater BOLD response when rightward motion was predicted compared to when upward motion was predicted (Kok et al., 2013). In this case, it is clear that a cue and the prior-probability it induces can alter stimulus representation throughout EVC. It has also become apparent that a template of the stimulus that is most likely to occur on a current trial can also be evoked by a tone (Kok, Failing & de Lange, 2014). The BOLD response is greater in V1 and V2 when participants make grating orientation judgments when the stimuli appear one after the other and the *second* stimulus is unexpectedly absent (Kok et al., 2014). It becomes clear that the prior-probability of stimulus occurrence has implications for how visual representation takes place within EVC. What must now be considered is whether the current arrow cueing paradigm is appropriate to probe such a mechanism using TMS. The current paradigm has been successful in demonstrating that the precision of the prior-probability can influence PC and the direction of the errors participants made, as expected. However, there is an element to this paradigm that lends itself to interpretations that do not require Bayes theorem to explain the results (c.f. Bowers & Davis, 2012). Consider if an EVC-TMS effect was obtained on PC or the nature of participant's errors when applied after the onset of the arrow cue but before the onset of the target. The Bayesian interpretation would be that reducing the precision of the prior-probability distribution improves performance by promoting the relative influence of the prediction error produced by the target in forming the posterior (Feldman & Friston, 2010). However, EVC-TMS could also affect the process of allocating attention to where the target is most likely to appear, which maximizes the likelihood of success in this paradigm (Desimone & Duncan, 1995). It is not possible to tease apart these two confounding explanations with this paradigm.

The critical point is that the paradigm itself appears to be inappropriate for integration with single pulse TMS because there are processes related to selective attention that make it difficult to rule out non-Bayesian explanations (c.f. Bowers & Davis, 2012). All that is necessary for stimulus representation according to Bayesian predictive coding are the prior-probability and the prediction error, which are integrated in order to produce a posterior (Friston, 2005; Feldman & Friston, 2010). It appears to be difficult to devise a paradigm where it is feasible to alter the precision of the prediction error and the prior-probability *and* interfere with these constructs using TMS, which can or cannot falsify the Bayesian approach compared to another approach (c.f. Feldman & Friston, 2010). It is still possible to generate support for the central tenet of predictive coding within EVC, although such an approach would not show that Bayes theorem was responsible for such a process, such as the model of predictive coding proposed by Rao & Ballard (1999). The central tenet of predictive coding with visual cortex is that perception is achieved by the exchange of top-down predictions from higher-cortical levels to lower-cortical levels (Rao & Ballard, 1999). If the top-down prediction is an unsuccessful representation of the visual field, then a prediction error is fed forwards from *lower* levels to higher levels (Rao & Ballard, 1999). Such a process is repeated until the top-down prediction successfully represents what is being presented and suppresses prediction error arising from the level below (Rao & Ballard, 1999). The temporal dynamics of such events also provide an opportunity to test predictive coding models. First and foremost, a top-down prediction must be established in EVC- without this initial stage, there cannot be any feedforward outputs from EVC (Rao & Ballard, 1999; Friston, 2005).

Regardless of whether Bayes theorem is used to achieve such a top-down prediction, the central tenant of predictive coding is in the exchange between feedforward processes in response to unpredictable inputs and the recruitment of feedback to successfully re-predict sensory inputs (Rao & Ballard, 1999). The top-down prediction must be established in EVC first, which triggers the feedforward prediction error in response, if a discrepancy exists between top-down predictions and sensory inputs. This discrepancy triggers the revision of a top-down prediction in response to the

prediction error (Rao & Ballard, 1999). When considering the basic premises of predictive coding it becomes apparent that more processes need to be completed when a top-down prediction is unsuccessful at suppressing prediction error compared to when it is successful (Rao & Ballard, 1999). This is because a successful top-down prediction does not trigger a prediction error. A successful top-down prediction only requires establishment in EVC, which *suppresses* activity in the level below (Rao & Ballard, 1999). In contrast, an unsuccessful top-down prediction also requires establishment in EVC first. The top-down prediction then triggers a prediction error that is fed forward and in turn, requires additional feedback until the prediction error has been resolved. In short, events where successful top-down predictions occur are shorter than events where top-down predictions are unsuccessful. Single-pulse EVC-TMS could be used to probe the duration of such events. When a recurrent process that is critical for performance takes place for a longer period of time, TMS should affect performance over a larger number of SOAs compared to when a critical event takes place for a shorter period of time (de Graaf et al., 2012).

In conclusion, experiment 3 manipulated the precision of the prior-probability in a modified version of the Posner (1980) cueing paradigm. An effect of the precision of prior-probability, as induced by the difference in luminance between a cue arrow and a non-cue arrow, had an effect on PC and participants bias . An interaction between cue validity and cue luminance was found on PC. PC was the same when the arrow cues had the same luminance, when the prior-probability was imprecise. However, as cue luminance increased, PC became higher on valid trials relative to invalid trials, which suggests that the precision of the prior-probability distribution influenced on performance. Participants also made more errors in the cued direction as the difference in cue luminance increased. In particular, participants did not report the target to occur in the 'cued' hemifield when both arrow cues had the same luminance. Despite the fact that an effect of prior-probability precision was found, the effects of EVC-TMS in these circumstances are still open to non-Bayesian interpretations and do not test the heart of the predictive coding models. As a result, a different premise of predictive coding will be investigated, which will be the duration of processing

within EVC under conditions where a top-down prediction is successful or unsuccessful at predicting current sensory inputs.

Experiment 4.1: Introduction

Experiment 2 and 3 highlighted the difficulties in developing a paradigm that creates a prior-probability that can influence performance and be modulated by TMS. It also becomes apparent that an appropriate paradigm needs to isolate the feedback-based processes that create a probabilistic representation of the visual field (Rao & Ballard, 1999; Friston, 2005) from the feedback-based processes that enhance representation in one part of the visual field relative to another based on task goals (Yesherun & Carrasco, 2013; Desimone & Duncan, 1999). Here a paradigm was developed that presented frequently occurring or infrequently occurring stimuli in order to indirectly manipulate the top-down prediction of stimulus occurrence. To avoid issues arising from the difficulty arising from feedback-based processes contributing to enhancing representation in selected parts of the visual field, the frequent and infrequent stimuli l only appeared in one location. Foveal stimuli that only appeared in one location can be contrasted from the peripheral stimuli that can appear in four different locations that were used in experiment 3, which should preclude the involvement of processes that enhance processing in one hemifield relative to another (Posner, 1980; see also Summerfield & Egner, 2009).

In experiment 3, participants completed a same-different judgment on foveally presented gabor patches. One pair of Gabor patcheswere identical in terms of phase, size and contrast which had the same orientation occurred on 50% of trials when the same pair of Gabor patches appeared. This type of same trial was coined a familiar same trial. Another pair of Gabor patches, which were identical in terms of phase, size and luminance but had different orientations occurred on 50% of trials when a different pair of Gabor patches appeared. This type of different trial was coined a familiar different trial. On remaining same trials, one orientation was selected at random from the remaining orientations that remained once the familiar same and familiar different orientations

were excluded. On remaining different trials, two different orientations were selected at random from the orientations that were not familiar same or different stimuli.

The manipulation of stimulus frequency (or familiarity) was used to probe whether this was a feasible paradigm to integrate with single pulses of EVC-TMS, which could reveal whether infrequent events produce more recurrent processes within EVC than frequent events, consistent with predictive coding (Rao & Ballard, 1999; Friston, 2005)Familiarity was manipulated by making the proportion of trials where two oriented pairs of Gabor patches greater than the likelihood of all other pairs of Gabor patches. By making these pairs of trials occur more often, it was expected that the participant would become more familiar with them relaive to other pairs, which could manifest itself in behavioural performance. The initial aim of these experiments was to identify whether PC or Pr (Corwin, 1994) was greater for familiar stimuli than unfamiliar stimuli. The benefit of familiarity on PC or Pr was initially assumed to be due to an increased frequency of presentation improving the representation of familiar stimuli, which produces an effect that can be measured using behaviour. An additional aim of these experiments was to identify how many trials were necessary for PC or Pr to become greater for familiar stimuli compared to unfamiliar stimuli. In order for each pair of stimuli that occurred on a greater proportion of trials to 'become' familiar stimuli, these pairs more occur more often as the experiment proceeds. Thus, it would be expected that an increasein PC for familiar stimuli relative to unfamiliar stimuli would emerge as trial number increases. These experiments had the aim of identifying the exact number of trials where such an effect emeges, as this would enable a minimum trial number to be identified that is necessary to produce a familiar effect. If such an effect is then to be modulated by TMS, this minimum number of trials must be presented in order for a familiar effect that can subsequently be probed with TMS to be present in this experiment.

Experiment 4.1: Methods

Participants

Fourteen participants were recruited from the Cardiff University School of Psychology took part in this experiment. They were reimbursed for their participation with course credit.

Design

Participants were presented with two Gabor patches, which were presented at 1.5^{o} eccentricity to the left and to the right of a fixation dot. Each Gabor had a width and height of 1^{o}. Both Gabor patches were presented for 10ms. The two patches had an orientation that was the same or an orientation that was different. Participants had to indicate whether the orientations were the same or different using a left or right click of a mouse, which was counterbalanced. Illustration of this paradigm can be found in figure 7. Gabor patches which were the same appeared on 50% of trials and Gabor patches that were different appeared on 50% of trials.On each trial, participants were presented with a pair of Gabor patches which had the same orientation, which occurred more often. These two patches were labelled as the familiar same Gabor patches, which occurred on 50% of same trials (25% of the total number of trials). There were also a pair of Gabor patches which had different orientations and this pair of orientations that were different occurred more often on different trials. These two patches were labelled as the familiar *different* patches, which occurred on 50% of different trials (25% of the total number of trials). The familiar different Gabors consisted of two orientations; the one orientation always appeared to the left of fixation and the remaining orientation always appeared to the right fixation. Thus, participants were presented with the same familiar Gabors on 25% of same trials and same unfamiliar Gabors on 25% of different trials (50% of overall trials). On remaining same trials, which were labelled as unfamiliar same trials, orientations was selected from the remaining 177 angles between 1 and 180 degrees at random. Similarly, on remaining different trials two different orientations were selected from the remaining 177 angles between 1 and 180 degrees at random and these two Gabor orientations were presented

to participants. Performance was measured using proportion correct (PC) and Pr of the same-different judgment, which were calculated separately for familiar Gabors and unfamiliar Gabors. For the calculation of Pr (Corwin, 1994), a hit was defined as a 'same' response on a same trial and a 'miss' was defined as a 'different' response on same trial. A false alarm was defined as a 'same' response on different trials and a correct rejection was defined as a different response on a different trial.

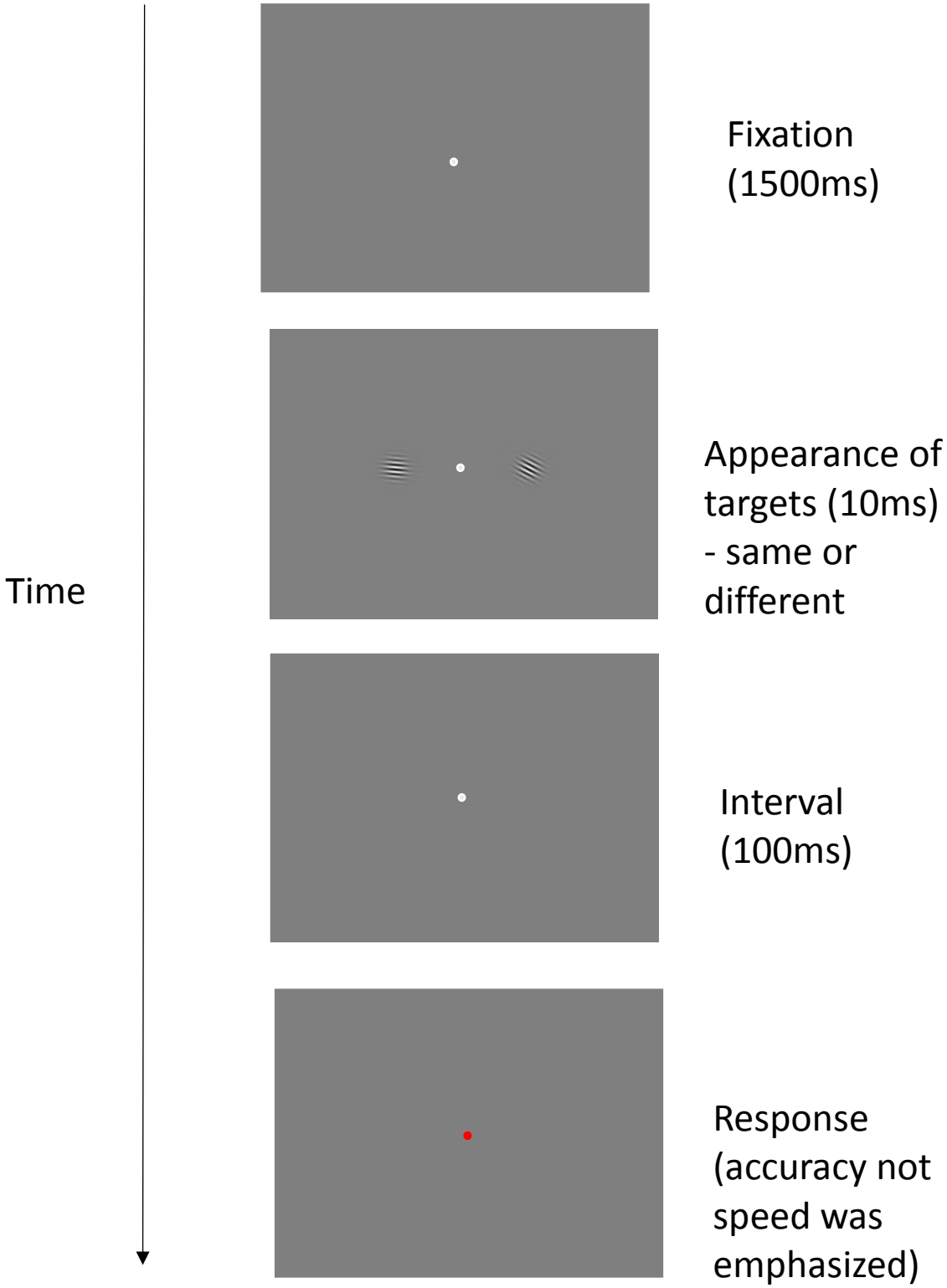

Figure 7. Illustration of the paradigm employed in experiment 4. First of all, fixation took place for 1500ms, which was followed by two Gabors. These Gabors were either of the same orientation of or different orientations. Familiar Gabors that were same which occurred on 50% of same trials, whereas on the remaining 50% of same trials two different Gabors were selected at random. Familiar different Gabors were also presented on 50% of different trials, on the remaining 50% of different trials two Gabors with different orientations were selected at random. It was impossible for Gabor orientations on familiar trials to occur on unfamiliar trials. After an interval, participants indicated whether the Gabors had the same orientation or different orientations using a left or a right click. The use of a left or a right click to indicate whether the Gabors were the same or different was counterbalanced.

Manipulation of Gabor Contrast

Contrast of the familiar and unfamiliar Gabor patches were altered using an up-down staircase procedure, which was designed to identify the luminance where PC in the same-different judgment equals 0.707 (Levitt, 1970). The format of the staircase procedure was identical to the format of the experiment itself with one major difference: all orientations of Gabor patch were equally likely to take place on same and different trials. Whether or not a same or different trial would take place was randomly determined prior to each trial. Two changes in the participant's response sequences could take place which affected target contrast on the upcoming trial. The contrast of the Gabors was increased after the participant made an incorrect response by itself, or a correct response followed by an incorrect response, which fall into the category of a negative reversal (Levitt, 1970). In contrast, the contrast of the Gabors was decreased after the participant made a correct response by itself, or made a correct response that was preceded by an incorrect response, which falls into the category of a positive reversal (Levitt, 1970). The procedure was completed until six reversals had been attained in three separate staircases. The occurrence of each staircase on each trial was determined at random, which meant that the occurrence of all thee staircases was interleaved throughout the contrast manipulation procedure. This procedure continued until six reversals had been obtained in each staircase, which meant that a total of 18 reversals occurred in total

Once 18 reversals had been obtained throughout all six staircases, the mean was calculated across contrast e values that were presented for the last three reversals of each staircase (Levitt, 1970), which was then presented to participants to verify whether a PC within -0.1/+0.1 of 0.707 had been attained. Participants completed 40 trials at this contrast and PC was calculated. If PC was within -0.1/+0.1 of 0.707, contrast manipulation ceased and participants moved on to the next part of the experiment. However, if PC was not within -0.1/+0.1 of 0.707, participants completed the staircase procedure until a PC within these boundaries was attained. Once such a PC was identified,

the corresponding contrast identified by the staircase procedure was presented to participants throughout the entire experiment.

Procedure

Firstly, participants completed the calibration procedure until a PC within -0.1/+0.1 of 0.707 was attained. Subsequently, participants completed the exposure phase, which consisted of 1000 trials.

Experiment 4.1: Results

Figure 8 reveals PC as a function of trial number for familiar and unfamiliar trials. Contrary to the prediction that familiarity conferred an advantage over unfamiliar stimuli in terms of PC, mean unfamiliar PC was greater than mean familiar PC. Figure 8 reveals mean PC as a function of trial number on same or different familiar or unfamiliar Gabor patches, which reveals that overall, participants performed best on same familiar trials and unfamiliar same trials whereas performance was worst on unfamiliar different trials. Within figure 8, familiar and unfamiliar PC do not begin at the same point because PC was calculated incrementally at each trial number. This pattern of PC with PC being higher on same trials than different trials regardless of whether the Gabors were familiar or unfamiliar may reflect a pattern of response bias. Participants may be biased to respond with same judgments. In order to accommodate response bias, Pr (Corwin, 1994) was also calculated. Mean Pr as a function of trial number can be found in figure 8. Pr is a measure of PC which accounts for response bias, and evidence of such a bias is revealed in mean Pr scores that are lower overall than PC scores. A general bias to say that the Gabor patches were the same led to the pattern of results in figure 7. However, as figure 8 reveals, accommodating for response bias to say that stimuli are the same still reveals a Pr score that is a higher for unfamiliar stimuli than familiar stimuli. However, familiar and unfamiliar PC (t (13) = -1.2204, p = 0.2440) and Pr (t (13) = -1.1489, p = 0.2713) were not significantly different from one another.

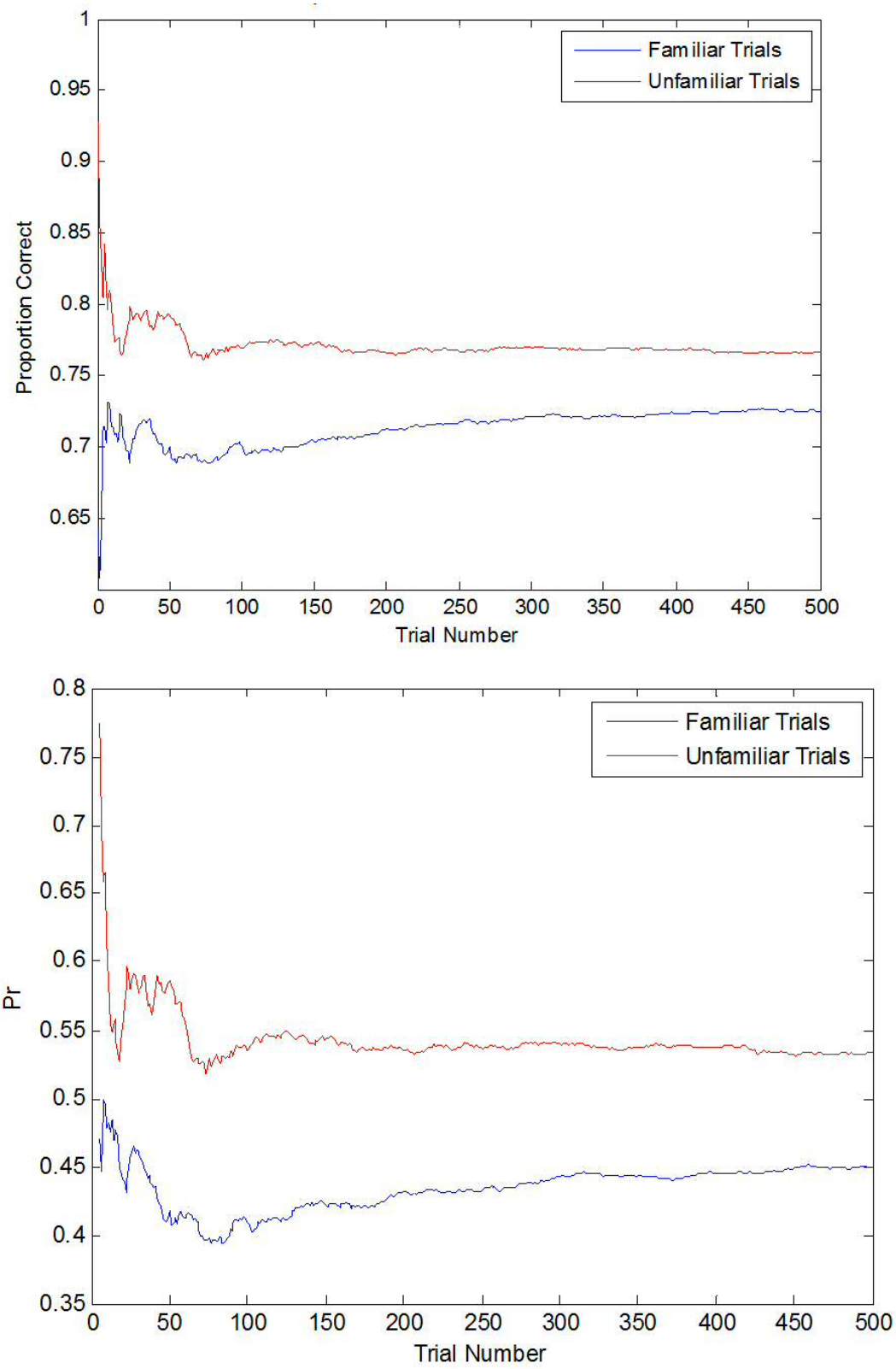

Figure 8. Top: Proportion correct (PC) as a function of familiar and unfamiliar trials. Bottom: Perceptual sensitivity (Pr) (Corwin, 1994) as a function of familiar and unfamiliar trials.

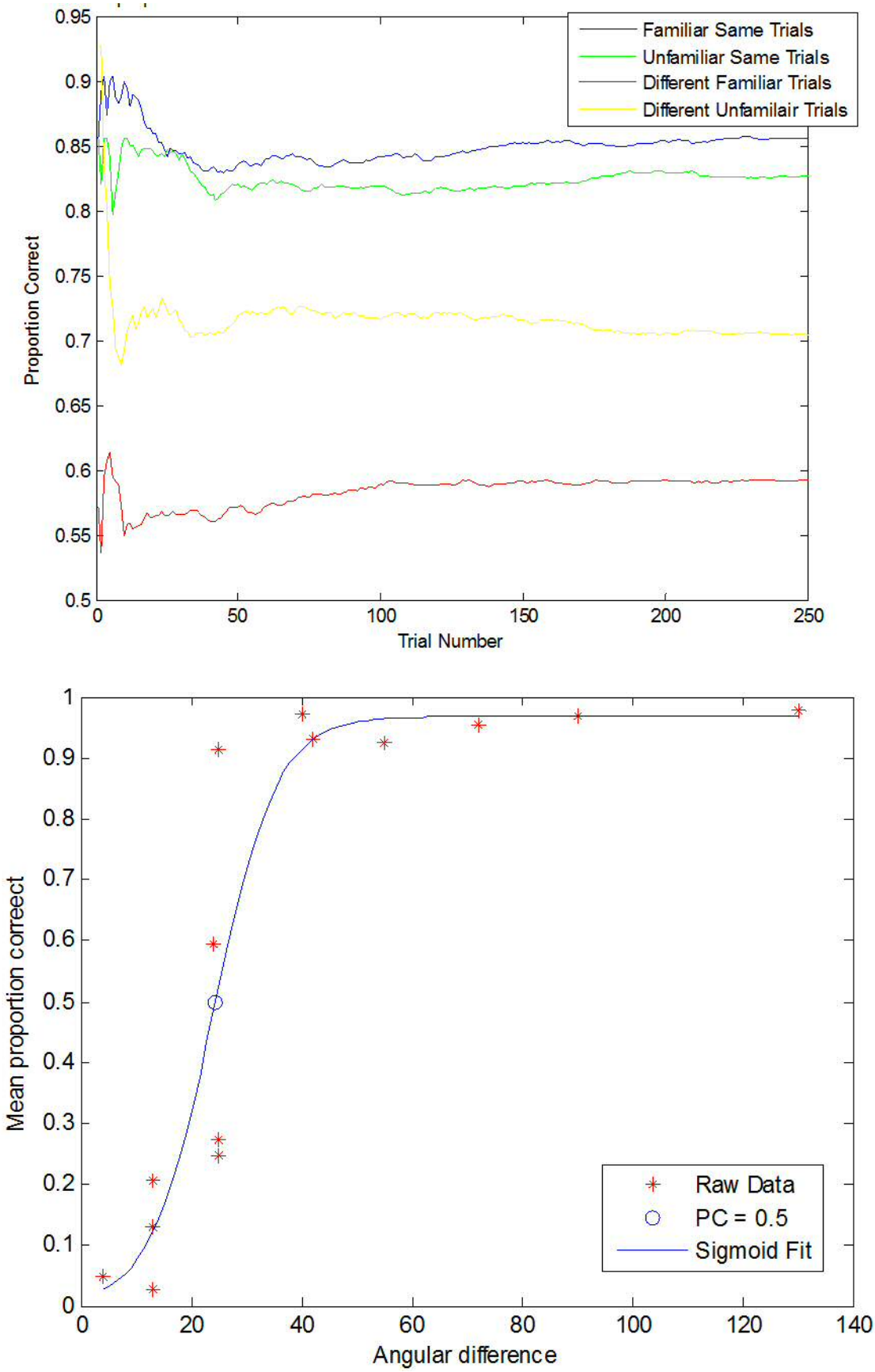

Figure 9. Top: Proportion correct (PC) as a function of familiar and unfamiliar same and fifferent trials trials. Bottom: Proportion correct as a function of the angular difference between the two orientations selected on familiar different trials.

One problem with stimuli here that can be revealed with the current paradigm is the angular difference between the two orientations that were selected to serve as the familiar *different* stimuli. The familiar different stimuli were selected by choosing two orientations that differed from one another at random. Choosing the two stimuli that served as the familiar different stimuli at random meant that all angular differences between 1^{o} and 180^{o} were equally likely to occur. An implication of this is that the task would be very difficult on familiar different trials when the angular difference is small compared to when the angular difference is large. It is feasible to predict that PC would be low on familiar different trials when the angular difference is small compared to when it is large. Examination of figure 9 reveals that this is the case. The false alarm rates for the 4 participants who achieved a PC that is less than 0.5 on familiar different trials were 0.916, 0.74, 0.98 and 0.9320, which suggests that the difference in orientation on familiar different trials was not successfully discriminated.

Interim discussion: Experiment 4.1:

Experiment 4.1 aimed to identify whether an effect of prior expectation (generated through increased frequency) could be found in the form of a higher PC for familiar Gabor patches relative to unfamiliar Gabor patches. No such evidence was revealed. There are a number of potential reasons for this outcome. The first reason could be that participants were not exposed to the 'familiar' stimuli enough for an effect of familiarity to emerge. Two different familiar (same or different) stimuli occurred on 25% (250 trials in total) of trials each throughout the experiment. This may not have been enough. Another reason may be the difficulty of the task, which is determined by the duration the Gabor patches appear for, the luminance of the Gabor patches and the angular difference in orientation between the two Gabor patches on different trials.

It is difficult to disentangle the relative contribution of the stimulus duration and stimulus luminance due to the use of a calibration procedure to determine stimulus luminance for each participant. It would be expected that participants would have a higher PC when stimulus duration is

longer compared to when stimulus duration is shorter. An up-down staircase procedure (Levitt, 1970) would control for such effects – a higher luminance would accompany a PC of 0.707 when stimulus duration is short whereas a lower luminance would accompany a PC of 0.707 when stimulus duration is longer. One potential solution would be to abandon the calibration procedure entirely and present stimuli for a fixed duration and a fixed luminance. However, such a solution would be not be well integrated with TMS, which these experiments are designed to support; the use of visual stimulus calibration is often essential for TMS to produce an effect on performance (see Camprodon et al., 2010 – Experiment 1 for a null result).. The implication of this is that it may not be possible to produce a familiarity effect that can be produced with a stimulus luminance that is also compatible with TMS.

Examination of false alarm rates reveal that some participants made a large number of 'same' responses on unfamiliar different trials, which suggests that the angular difference was too small for participants to identify that the two familiar Gabor patches were different, regardless of the number of times the familiar different stimuli were presented. In contrast, all angular differences between 1^{o} and 180^{o} could occur on unfamiliar different trials, which meant that the unfamiliar different task could be easier than the familiar different task. This could explain why familiar PC was *lower* than unfamiliar PC, which was contrary to the predictions of this experiment.

In conclusion, experiment 4.1 did not y reveal an advantage of presenting familiar stimuli compared to unfamiliar stimuli in a same different judgment. The absence of this advantage appears to be due to how the difference in orientation was selected on familiar different trials. The difference in orientation was selected at random, which meant that orientation differences that were too small to discriminate emerged. This issue was reflected in some participants having high false alarm rates, which indicate that the familiar different stimuli were perceived as being the same. This issue was to be addressed in the next experiment.

Experiment 4.2: Introduction

The motivation behind experiment 4.2 was identical to the motivation behind experiment 4.1, which was to identify if an effect of familiarity can be found and to identify whether this paradigm is suitable for TMS. This additional experiment took place to identify whether PC or Pr is higher for familiar trials than familiar trials, which would be an indicator that a familiarity effect is present. The angular difference on different familiar and unfamiliar different trials was fixed throughout experiment 4.2 to prevent insufficient angular differences causing participants to make false alarms on familiar different trials. The hypothesis being tested in experiment 4.2 is the same as the hypothesis in 4.1. It will be expected that Pr or PC for familiar stimuli will be greater than Pr or PC for unfamiliar stimuli.

Experiment 4.2: Methods

Participants

15 additional participants who had not taken part in experiment 4.1 were recruited from the Cardiff University School of Psychology, who were reimbursed for their participation with course credit.

Design & Procedure

The format of experiment 4.2 was the same as experiment 4.1 with two differences, which was that the number of familiar same and familiar different trials was increased. Angular differences could be 10^{o}, 20^{o}, 30^{o} or 40^{o} throughout the contrast manipulation procedure and was presented on different trials until 18 reversals had been obtained from 3 separate staircases, as outlined previously. The way in which same trials were presented throughout the contrast manipulation procedure was identical to how same trials were conducted in experiment 3.1. If a PC within -0.1/+0.1 of 0.707 was obtained from 40 trials with luminance set at the mean luminance of the last three reversals within each staircase, the experiment proceeded with the angular difference that was presented throughout the calibration. However, if a PC within -0.1/+0.1 of 0.707 was not

obtained from the calibration procedure, the angular difference was increased if PC was below 0.707 and decreased if performance was above 0.707. The contrast manipulation procedure was repeated and the angular difference was altered until a PC within -0.1/+0.1 of 0.707 was obtained. Once the luminance value that accompanied such a PC was obtained, this luminance was presented for the entire experiment. Increasing the amount of familiar trials meant there were 600 (out of 1000) familiar trials in total; 300 of these were familiar same trials and 300 of these were familiar different trials. The way experiment 4.3 proceeded was identical to experiment 4.1.

Experiment 4.2: Results

Unlike experiment 4.2, examination of figure 10 reveals that experiment 4.2 produced an overall mean PC and mean Pr that was greater for familiar Gabor patches than unfamiliar Gabor patches, which suggests that fixing the angular difference on all different trials was successful in equating familiar and unfamiliar different trials in terms of difficulty. However, there was no effect of either making unfamiliar difficult trials easier nor increasing the number of times familiar same or familiar different Gabors appeared. Neither PC (t (14) = -1.4698, p = 0.2616, BF = 1.5614) nor Pr (t (14) = -0.0218, p = 0.9829) were greater for familiar stimuli than unfamiliar stimuli.

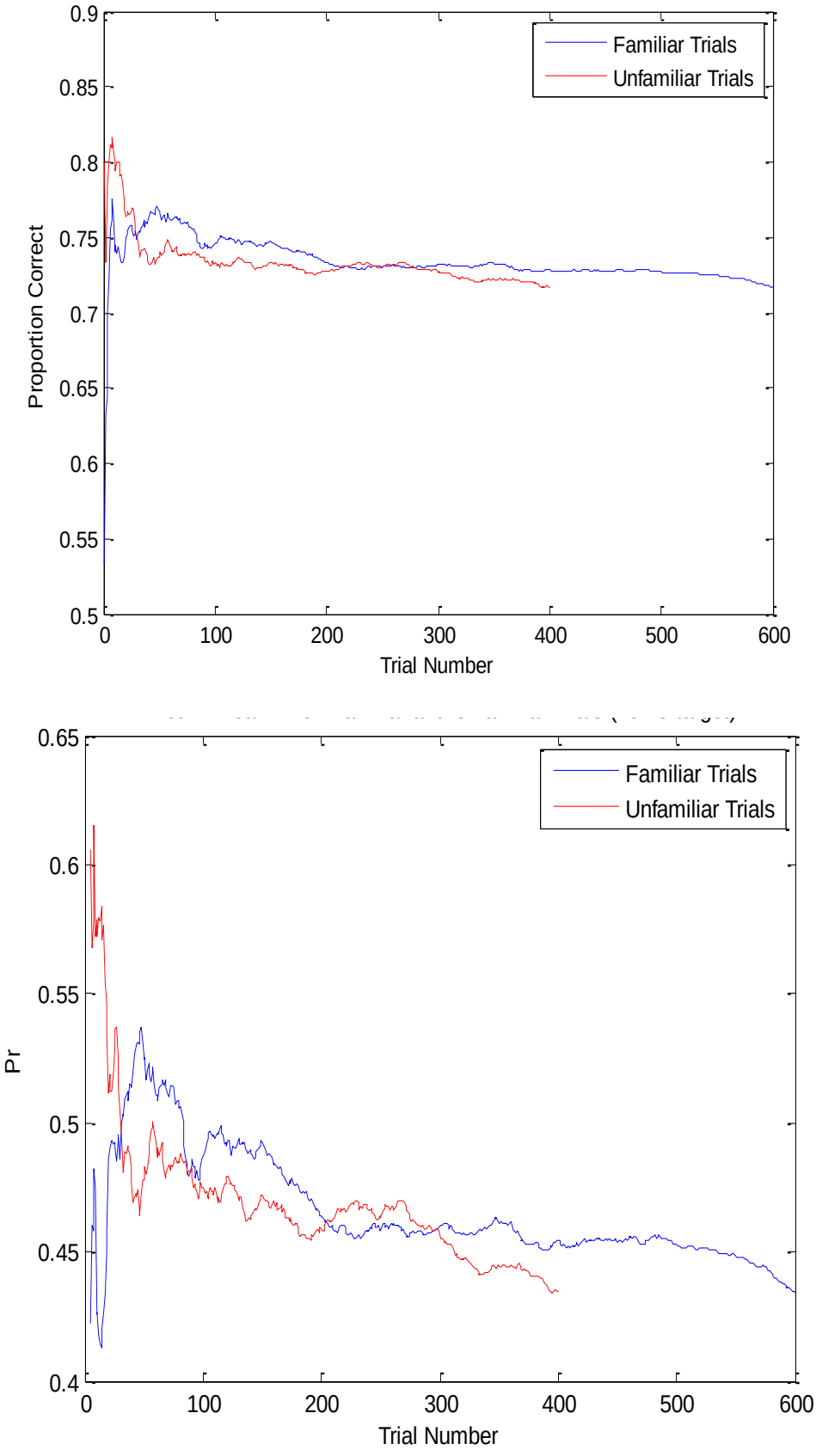

Figure 10. Top: Propotion correct as a function of trial number for familiar and unfamiliar trials. Bottom: Perceptual sensivity (Pr) (Corwin, 1994) as a function of trial number familiar and unfamiliar trials.

Experiment 4.2: Interim discussion

Experiment 4.2 aimed to identify if equating familiar and unfamiliar trials in terms of difficulty along with increasing the number of familiar trials relative to the number of familiar trials, caused PC or Pr to be greater for familiar trials than unfamiliar trials. Although fixing the angular difference appeared to be successful in terms of equating familiar and unfamiliar different trials in terms of difficulty, there was only weak evidence for PC or Pr for familiar trials being greater than PC or Pr for unfamiliar trials.

As outlined previously, an additional explanation for the lack of a familiarity effect (PC: familiar > unfamiliar) is the duration of time the stimuli are being presented for. Presenting the stimuli for 10ms may not have been long enough for participants to be able to distinguish whether two patches are the same or different but too short for an effect of familiarity toemerge . Therefore, an additional experiment was carried out which increased the duration of stimulus presentation.

Experiment 4.3: Introduction:

Experiment 4.3 aimed to identify whether increasing the duration the pair of Gabor patches appeared for increased PC or Pr for familiar trials relative to PC or Pr for unfamiliar trials.

Experiment 4.3: Methods

Participants

15 participants who had not taken part in experiment 4.1 or experiment 4.2 were recruited from the Cardiff University School of Psychology, who were reimbursed for their participation with course credit.

Design & Procedure

The only difference between experiment 4.3 and experiment 4.2 was the duration that stimuli were presented for, which was increased to 80ms for experiment 4.3. Such a duration was chosen as a previous experiment revealed that this was sufficient for a PC of 71.3% to be obtained in

same-different paradigm when pairs of stimuli were presented in the fovea (Chambers et al., 2013), which closely corresponds to the PC of 70.7% (0.707) which had be chosen for these experiments.

Experiment 4.3: Results

Here, only Pr was analysed as no differences in the outcome of the analyses above existed between PC and Pr. Inspection of figure 11 reveals that the direction of the results is the opposite of what was obtained in experiment 4.2: Pr is greater for unfamiliar trials than familiar trials.The *BF* revealed weak support for a mean difference in Pr between familiar trials and unfamiliar trials (t (14) = =1.3936, p = 0.1852, *BF* = 1.699161).

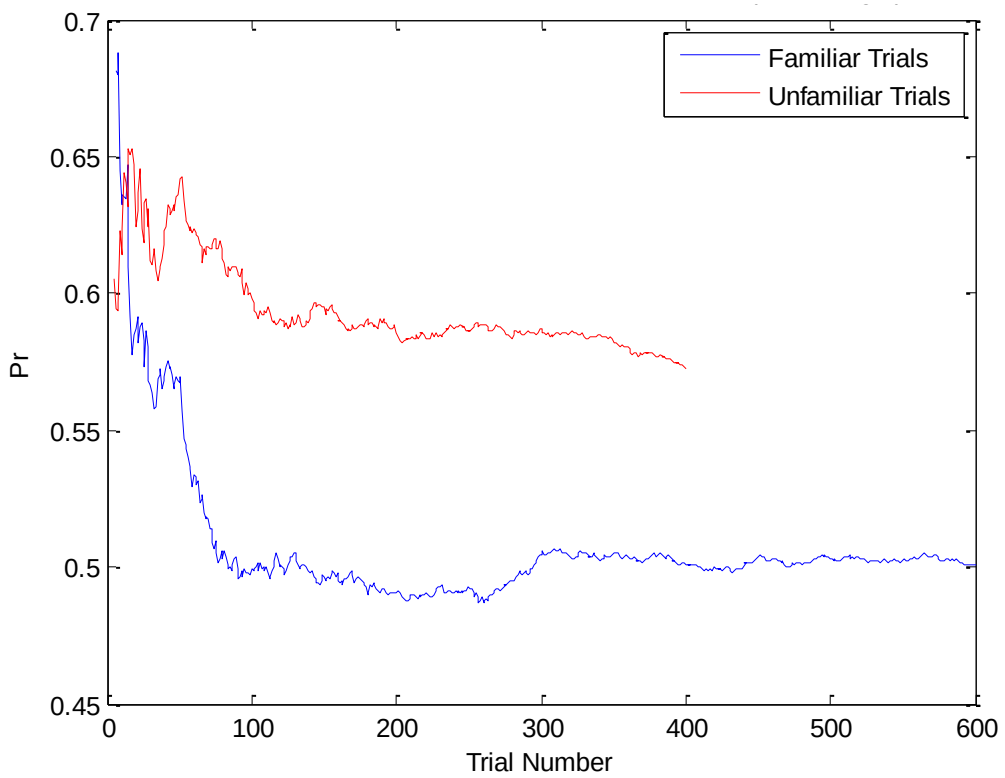

Figure 11. Perceptual sensitivity (Pr) (Corwin, 1994) as a function of trial number for familiar and unfamiliar trials.

Discussion: Experiment 4

Experiment 4 aimed to reveal an effect of a top-down prediction on performance which would have been expressed as a greater in PC or Pr on trials when a same-different judgment was made on a familiar pair of Gabor patches compared to when an identical judgment was made on an unfamiliar pair of Gabor patches. Such a difference was not revealed. Instead, a series of considerations were uncovered that must be taken into account when using a calibration procedure and a difference in orientation to probe such an effect.

The first issue was how the difference in orientation was selected for familiar different trials. The difference in orientation was selected at random, which caused some participants made a large number of false alarms in experiment 4.1. A large number of false alarms indicated that two patches were perceived as having the same orientation when they were physically different. This outcome is likely to be due to the difference in the orientation being too small for them to be seen as different. To control for this, the difference in orientation was kept constant for familiar and unfamiliar trials. However, a difference in PC or Pr between unfamiliar and familiar stimuli did not occur even with this control in place, nor when participants were given more time to see the patches. It is likely that the thresholding procedure and/or the choice of stimuli are likely causes of this phenomena

The absence of a difference in PC between familiar – or expected stimuli – and unfamiliar, unexpected,stimuli has been revealed before in behavioural data in support of an fMRI experiment (Kok et al., 2014). In this experiment, a difference in RT but not PC was found for expected gratings compared to unexpected gratings (Kok et al., 2014). There were methodological differences between this experiment and Kok et al. (2014). The principal difference was that a tilt judgment had to take place in Kok et al. and the grating stimuli were presented sequentially rather than simultaneously. Another difference was that Kok et al. presented a low-frequency or a high-frequency tone that preceded to expected grating with 100% validity, which was likely to induce a stronger prior-probability – or top-down prediction – than experiment 4. In the present study, the

top-down prediction was assumed to emerge as a function of exposure to one set of Gabor patches compared to every other possible set of Gabor patches. However, in spite of the prior-probability being stronger in Kok et al., no effect on PC was presented despite the fact that PC was calibrated to 75% in Kok et al. and ~70% (~0.707) in these experiments.

The difference between the effect of familiarity in Kok et al. (2014) and experiment 4 was that Kok et al. found an effect of familiarity on RT but not on PC. The lack of evidence of an effect in these experiments must be because RT was not used as a measure. In experiment 4, RT was not chosen as a measure of performance as it aimed to look at how visual representation takes place rather than the time it takes to make judgments. When RT is used as a measure, responses must be speeded (c.f. Posner, 1980). When responses accurate and speeded responses are emphasized as opposed to emphasizing accuracy alone, it is possible that the processes that surround visual representation could be confounded with processes that produce the fastest motor response (Swensson, 1972). The aim of these experiments was to show that more recurrent processes are taking place within EVC when a top-down prediction is revised in response to a prediction error compared to when a top-down prediction is not accompanied by prediction error (Rao & Ballard, 1999; Friston, 2005). If such processes are related to visual representation in EVC, much stronger evidence for predictive coding would be garnered if EVC-TMS produced an effect on performance when participants were responding as accurately as possible

It is likely that the decision to manipulate PC to ~0.707 (Levitt, 1970) is the primary reason for the absence of effects of familiarity in these experiments, even though the difference in orientation was fixed for familiar and unfamiliar stimuli with presentation time for up to 60ms (c.f. Chambers et al., 2013). When the difference in orientation is fixed, any benefit in making a different judgment on familiar or unfamiliar trials is countered by a decrease in Gabor contrast to ensure PC remains within 0.707. A similar principle can be applied to any benefit produced by increasing Gabor presentation time to 60ms. When presentation time is increased, participants have more time to

examine whether one Gabor patch differs from the other. Any benefit of increased examination time would also be countered by the contrast manipulation procedure. When presentation time was 10ms, Gabor luminance would need to be greater in order for PC to reach 0.707 otherwise the Gabors would not be bright enough for discrimination to be successful. In contrast, when presentation time was 60ms, Gabor contrast would be lower than when presentation time was 10ms, as participants do not need the Gabors to be as bright for discrimination to be successful. In short, it could be that luminance was too low for a familiarity effect to arise within these experiments.

It is essential to Gabor calibration to take place otherwise the effect of EVC-TMS at ~100ms (de Graaf et al., 2014) may be prevented due to ceiling effects. Without thresholding, stimulus contrast could be too high and TMS would be unable to suppress this visual representation. However, it is possible to change the stimuli and procedure in a way that could facilitate a familiarity effect being present. The choice of a same-different judgment may be partially responsible. In order for Pr (Corwin, 1994) to be calculated, two different types of mutually exclusive responses need to take place; a same response or a different response. In order for Pr as a function of familiarity to be present, there must be two types of same or different stimuli; familiar same stimuli and familiar different stimuli. Even in experiments 4.2 and 4.3, where familiar same and familiar different stimuli occurred on 60% of trials in total, the familiar pair or the different pair only occurred on 30% of trials each. This method of manipulating familiarity may have weakened the magnitude of a familiarity effect compared to when an identical stimulus would have been present on 60% of trials.

Another issue is the choice of stimuli: Gabor patches. Every Gabor patch had the same size and contrast; they only differed in terms of their orientation if they were presented on a different trial. The familiar Gabor patches may not have been distinct enough from other Gabor patches for participants to become familiar with them. Gabor patches were selected due to their close

relationship with the classical receptive field within V1 (Hubel & Wiesel, 1962). It is desirable to have stimuli that have a close relationship with the area of interest, which may constrain the effects of TMS to processes and areas of interest (c.f. de Graaf et al., 2012). However, changing the stimuli to simple shapes that can be more distinct from one another may be one method of overcoming the issues arising from Gabor patches looking similar to one another. However, the same issue could arise when using different shapes. The task would become easier as shapes become more distinct from another and the calibration procedure would prevent any benefit garnered from increased shape distinction. It was expected that shape luminance would be higher to achieve a PC of 0.707 when shape distinctiveness was low and that shape luminance would be lower to achieve a PC of 0.707 when shape distinctiveness was high. This idea was developed further in experiment 5.

It is also possible to alter the contrast manipulation procedure to counter these issues. In all of these experiments, target luminance or contrast was decreased to make the task harder and increased to make the task easier (Levitt, 1970). A negative reversal took place was broadly defined as when an incorrect response followed a correct response as specified in Levitt (1970). When a negative reversal took place, luminance was reduced in order to bring target luminance closer to the luminance of the background, which made the task harder. A positive reversal was defined as when correct response followed an incorrect response (Levitt, 1970). When a positive reversal took place, the luminance of the target was increased, which made it more distinct from the background and reduced task difficulty. When calibrating the stimuli in this way, the desired level of performance is achieved by reducing the difference in luminance between the stimuli to be detected or discriminated and the background. This means that the shapes can be presented at a low luminance, which may have prevented them from being distinct and recognizable. All experiments in experiment 4 presented stimuli at a low luminance, which meant there were difficult to recognize and could explain why an effect of familiarity is absent. Alterations in the process of stimulus calibration were introduced in experiment 5.

In conclusion, experiment 4 attempted to present participants with familiar Gabor patches and unfamiliar Gabor patches and explore whether PC was greater for familiar patches than for unfamiliar patches in a same-different judgment. A benefit of Gabor patches being familiar did not emerge for PC or Pr. It was concluded that this was due to the recruitment of a same-different paradigm, the use of Gabor patches as stimuli and the way in which contrast e was altered following a correct or incorrect response, was responsible for the absence of a familiarity effect. The familiar Gabor patches on the other hand could have been difficult recognize due their size and position being identical, combined with their contrast being altered to achieve a corresponding PC of 0.707. The following section will address these issues by identifyingwhether unfamiliar stimuli are processed for longer, which could reflect the revision of a top-down prediction relative to familiar stimuli (Rao & Ballard, 1999; Friston, 2005).

Experiment 5: Introduction

Experiments 2 and 3 revealed the difficulty in devising a paradigm that reveals evidence of Bayesian predictive coding (Friston, 2005; Feldman & Friston, 2010) that is appropriate for integration with single pulse TMS. The prior-probability created in experiment 2 produced a criterion shift, which may not be affected by. In contrast, experiment 3 struggled to dissociate the effects of enhancing visual representation in task relevant parts of the visual field (Desimone & Duncan, 1995) from effects of feedback that create a probabilistic representation of the visual environment (Friston, 2005). Experiment 4 attempted to address these issues by presenting foveal stimuli that were frequent or infrequent and had participants complete a same-different judgment. However, the identity of the stimuli (Gabor patches) and the way in which stimuli contrast was manipulated experiment 4 may have prevented participants from become familiar with the frequently presented stimuli. Moreover, in experiment 4, an increase in stimuli presentation time also failed to produce a familiarity effect. Experiment 5 attempted to change the calibration procedure along with the identity of the stimuli to see if such changes could produce an effect of familiarity that can be

modulated by EVC-TMS. The modulation of familiarity that would be expected by applying EVC-TMS would be determined by whether a stimulus violates a top-down prediction or not (Rao & Ballard, 1999). As outlined previously, more EVC-TMS would be expected to interfere with recurrent processing across a greater number of SOAs when a top-down prediction is violated compared to when a top-down prediction is not (Rao & Ballard, 1999). An increase in recurrent processing would be expected because the revision a top-down prediction requires more processing compared to when a top-down prediction does not need to be revised (Rao & Ballard, 1999).

Experiment 4 may have failed to produce an effect because the differential contributions of a top-down prediction or a prediction error to visual representation may not produce an observable change in PC or Pr. The difference in the exchange between top-down predictions and prediction errors highlights a potential reason for why experiment 4 failed to produce a PC or Pr that was greater for familiar stimuli compared to unfamiliar stimuli. The relative contribution of top-down predictions and prediction errors changes depending the precision of prediction error and the precision of the top-down prediction (Feldman & Friston, 2010). When top-down predictions are confirmed, a visual representation is accommodated by top-down predictions (Rao & Ballard, 1999; Friston, 2005). In contrast, when a discrepancy exists between a top-down prediction and sensory input, a prediction error is incorporated into a revised top-down prediction to successfully represent sensory inputs (Rao & Ballard, 1999; Friston, 2005). In experiment 4, top-down predictions may have been more responsible representation of the familiar stimuli than prediction errors due to stimulus frequency enabled them to be incorporated within top-down predictions. In contrast, in experiment 4, prediction errors may have been more responsible for representation of the unfamiliar stimuli than top-down predictions due to their infrequency preventing them from being incorporated within top-down predictions. The relative contribution of top-down predictions and prediction errors differed between stimuli but PC or Pr did not differ. It is therefore the process that underlies predictive coding that is important here, not the behavioural consequences of different types of integration of a top-down prediction and a prediction error (Rao & Ballard, 1999; Friston, 2005).

Experiment 5 presented participants with 9 different shapes. One of these shapes served as a familiar stimulus and occurred on a higher proportion of trials. The remaining 8 shapes were selected as unfamiliar stimuli which occurred on a lower proportion of trials. Participants were required to indicate whether the lower half or the upper half of the shape was brighter. Performance was measured using PC. The way that the stimuli were calibrated was altered to accommodate the problem in lowering luminance to produce a PC of ~0.707 (Levitt, 1970) to such an extent that the stimuli may not be recognizable. The use of different shapes would become feasible if the relationship between the difficulty of the task and the luminance of the background was altered. For example, the calibration of the targets could be changed if participants completed a discrimination task where they identify which half of a shape is brighter. The luminance of one half of the shape would be set the maximum possible luminance and the other half will be have a lower luminance. By presenting the stimuli this way *reducing* the luminance of stimulus would make the task easier and *increasing* the luminance would make the task harder. This method of altering the difficulty of the task, and in turn PC, is the opposite to the method used to alter the difficulty of the task in experiments 2, 3 and 4. Critically, increasing the luminance of the dimmer half of the shape reduces the overall difference in luminance between the two halves of the shape, which meant that the shape as a whole is easier to recognize. By calibrating stimulus luminance in this way, it was possible to manipulate PC relative to luminance without compromising a participant's ability to recognize the shapes.

Experiment 5 administered EVC-TMS at SOAs ranging from 30ms to 220ms separated by 30ms increments after the onset of the stimulus. In order to quantify the TMS-induced change in PC in the luminance judgment for familiar stimuli and unfamiliar stimuli, two different types of TMS were be administered: active TMS and vertex TMS. Active TMS and vertex TMS were calculated at each SOA. The TMS-induced change in PC, ΔPC, was calculated by subtracting PC for vertex TMS at one SOA by the corresponding active TMS score at the same SOA. The outcome of this subtraction was expected to be negative for familiar and unfamiliar stimuli, reflecting that active TMS has

impaired performance relative to vertex TMS at the robust and reproducible EVC-TMS SOA of ~100ms (de Graaf et al., 2014). Such an effect was quantified by fitting a single Gaussian model to ΔPC as a function of EVC-TMS for familiar stimuli and unfamiliar stimuli, which has previously been used to quantify the time course of TMS-induced effects on performance (Stevens et al., 2009; Rusconi et al., 2013; Chambers et al., 2013). A single Gaussian model produces an peak amplitude (a_1) coefficient, which refers to the magnitude and direction of a TMS-induced effect on ΔPC. a_1 will be used to identify whether active TMS has been impaired relative to sham TMS. Additional coefficients that are produced by a single Gaussian model are the temporal position coefficient (x_1), bandwidth coefficient (b_1) and the intercept ($x0$). The temporal position, x_1, coefficient refers to the point in time – or SOA – where a_1 takes place. The bandwidth coefficient, b_1, refers to the duration of TMS-induced effect a_1 at x_1, which quantifies duration of time that active TMS successfully suppressed performance relative to vertex TMS.

The a_1 and b_1 coefficients were of critical interest here. The first question was to identify whether a_1 has quantified an effect of active TMS relative to vertex TMS, which will be done with a Bayesian one-sample *t*-test (Rouder et al., 2009). If this analysis revealed that a_1 for familiar stimuli and a_1 for familiar stimuli are different from zero, an additional analysis would be carried out investigating whether unfamiliar stimuli are processed for longer than familiar stimuli. What was of interest in the additional analysis is the duration of time – or the number of SOAs – that TMS suppressed performance for. The b_1 coefficient for familiar targets and the b_1 coefficient for unfamiliar targets quantified the amount of recurrent processing that was being devoted to these different types of stimuli. If top-down prediction triggers a prediction error, which is followed by a revised top-down prediction that attempts to suppress prediction error (Rao & Ballard, 1999; Friston, 2005), unfamiliar stimuli should be suppressed by TMS for a relatively long period of time. In contrast, familiar stimuli only require the top-down prediction as they are more likely to occur on a given trial (Rao & Ballard, 1999; Friston, 2005). Familiar stimuli would produce less or no prediction error, and would not require as much or any revision of the top-down prediction (Rao & Ballard,

1999; Friston, 2005). As less processes need to be completed for familiar stimuli to be represented, it was expected that familiar stimuli will be affected by TMS for a smaller number of SOAs than unfamiliar stimuli. In order to identify whether b_1 for unfamiliar targets is greater than b_1 for familiar targets, mean b_1 for familiar targets will be subtracted from mean b_1 for unfamiliar targets. If the outcome of this subtraction is positive, it will mean that the duration of TMS effect for familiar stimuli is greater than the duration of TMS effect for familiar stimuli, supporting the hypothesis that more recurrent processing accompanies unfamiliar stimuli compared to familiar stimuli. In contrast, a negative value produced by the same subtraction would provide evidence against this hypothesis. A Bayesian one-sample *t*-test will be used to produce evidence for or against this hypothesis (Dienes, 2011).

The statistical analyses within experiment 5 were pre-registered on the Open Science Framework. Pilot data is presented here which was subjected to simulation procedure outlined in chapter 2, which aimed to identify the best prior distribution for Bayesian analysis and whether the hypotheses outlined here were feasible. Once the most sensitive prior was identified, it was then selected to identify whether the bandwidth for familiar stimuli was greater than the bandwidth for unfamiliar stimuli. This prior was then used to analyse the data in experiment 5.

Experiment 5: Methods

Introduction to methods

Firstly, the procedure and design and the experiment will be outlined. Subsequently, the calibration of the visual stimuli and TMS parameters are described. Statistical analyses are outlined and pilot data will be presented. After the presentation of pilot data, a series of analyses will be presented which assess the feasibility of the experiment. The feasibility analyses suggested that it is possible to use b_1 coefficients to test the hypothesis that more recurrent processes take place for unfamiliar stimuli compared to familiar stimuli. Consequently, the prior identified using the feasibility analyses is then applied in a set of pre-registered statistical analyses. These feasibility

analyses suggested that a half-normal prior (Dienes, 2011), not a JZS prior (Rouder et al., 2009) was most suited to the statistical analyses that were going to be recruited here.

Design

Experiment 5 aimed to identify whether the bandwidth (b_1) of a TMS-induced effect on performance across TMS-SOAs differs for familiar stimuli compared for unfamiliar stimuli. Participants completed a discrimination paradigm where they discriminated if the upper or lower half of a target is brighter than the opposite half. The target appeared for 10ms. Active and vertex TMS – the latter serving as a control condition – was administered at one of 7 SOAs ranging from 30ms to 210ms in increments of 30ms (30, 60, 90, 120, 150, 180 & 210ms) on each trial. Active TMS and vertex TMS was administered in a blocked format, which meant that active TMS and vertex TMS were not administered together within a block. Accuracy, not speed, was emphasized to the participant when they made their responses. Illustration of the paradigm can be found in figure 12.

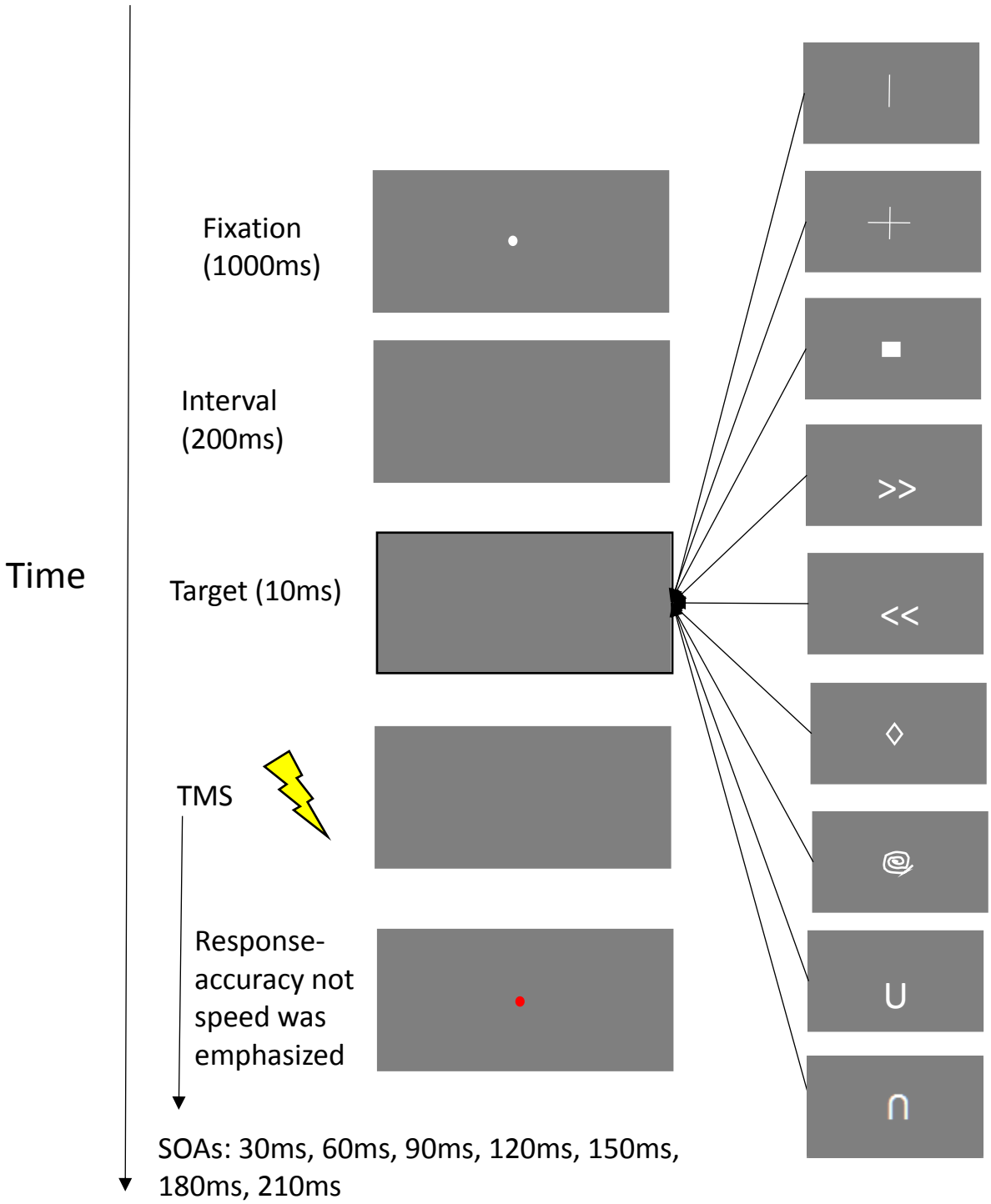

Figure 12. Illustration of the paradigm employed in experiment 5. First of all fixation took place followed by a brief interval prior to occurrence of the target. The familiar target was one of the 9 shape illustrateded on the right hand side, which occurred on 2/3 of trials. The remaining 8 shapes occurred an equal number of times on the remaining 1/3 of trials. Following target occurrence, transcranial magnetic stimulation (TMS) was administered to early visual cortex (EVC) at one of 7 stimulus onset asynchronies (SOAs) which ranged from 30ms to 210ms in increments of 30ms. After TMS administration, the response screen appeared whereby participants had to indicate whether the upper half or the lower half of the shape was brighter with a left click or a right click, which was counter balanced. Images are not drawn to scale.

The main familiarity manipulation involved conditions where stimuli are frequently presented and comparing these to the conditions where infrequent stimuli were presented. The frequent target was presented on 2/3 of trials whereas the infrequent target was presented on the remaining third. A total of 9 targets were presented; one served as the familiar target. The familiar target was maintained for each participant throughout the experiment. The remaining 8 served as the unfamiliar stimuli, which were presented in a randomized order throughout a block. An attempt was made to ensure that each of the 9 targets served as the familiar target for an equal number of participants to ensure that counterbalancing took place. However, the stopping rule specified in the next section prevented this from taking place. The task involved the participant indicating if the upper or lower half of the shape was brighter using a left or right mouse click. The responsemapping between left and right mouse key upper or lower half is brighter was counterbalanced. Half of the participants used a left click to say the upper half is bright and the other half used a right click to indicate that the lower half is brighter and vice versa.

Participants completed the experiment in ten 168-trial blocks. Five of these blocks were active TMS and five of these blocks were vertex TMS, which meant that there were a total of 1680 trials. Within a block, there were 24 trials of TMS administered at each SOA; there were 16 familiar target trials (2/3 of trials) and 8 (1/3 of trials) unfamiliar target trials at each SOA. This method ensured that each of the 8 unfamiliar targets occurred an equal number of times throughout each block whilst maximizing the number of trials containing the familiar target. In total, there were 840 active TMS trials and 840 vertex TMS trials; there were 120 trials at each SOA as a function of active TMS and vertex TMS. The familiar target appeared 80 times. The unfamiliar target was present on 40 trials in total. Participants underwent TMS in active and vertex pairs. This format was adopted so performance could be monitored after vertex blocks to ensure that proportion correct did not deviate from -0.1/+0.15 of 0.707 (Levitt, 1970). This procedure was completed separately for the familiar and unfamiliar targets. There were two possible orders that participants could experience active and vertex TMS: active TMS followed by vertex TMS or vertex TMS followed by active TMS,

which was counterbalanced. 50% of participants received active TMS followed by vertex TMS in a pairs and 50% of participants received vertex TMS followed by active TMS in a pairs.

Performance was measured using proportion correct (PC), which was calculated separately at each TMS SOA for familiar and unfamiliar targets as a function of active TMS and vertex TMS. ΔPC was calculated by subtracting PC as a function of vertex TMS from PC as a function of active TMS at each SOA. ΔPC was calculated separately for PC as a function of EVC-TMS for familiar and unfamiliar targets.

Calibration: Target luminance

Luminance of the dimmer upper or lower half of the shape was determined using 3 interleaved staircases in order to produce a PC within – 0.1 /+ 0.15 of 0.707 (Levitt, 1970). It is worth noting here that the brighter half of the stimulus was set at the maximum screen luminance value of 255. Thus, increasing the luminance reduces the difference between the current luminance and 255, making discrimination harder. In contrast, reducing the luminance of the stimuli increases the difference between current luminance and 255, making discrimination easier. The luminance of the dimmer half was reduced after a negative reversal, which increased the difference in luminance between the upper and lower half of the shape after participants made an incorrect response (Levitt, 1970). A negative reversal had taken place when participants made an incorrect response following a correct response (Levitt, 1970). The luminance of the dimmer upper or the lower half was increased after a positive reversal where participants make two consecutive correct responses (Levitt, 1970), which makes the difference in luminance smaller.

The thresholding procedure for familiar and unfamiliar stimuli was completed separately and each of them continued until 6 separate reversals have been attained within each staircase (Levitt, 1970), which meant that 18 reversals took place in total for familiar and unfamiliar stimuli. The brighter half of the shape was always set at maximum luminance. The luminance of the dimmer half that was supposed to produce a proportion correct of 0.707 was the mean luminance of the

three final reversals across each of the staircases (Levitt, 1970). The half that was brighter (upper or lower) was determined at random on each trial. For the thresholding of the familiar targets, only the familiar target appeared. For the thresholding of the unfamiliar stimuli, the 8 remaining targets were presented. It was attempted to have each unfamiliar target occur an equal number of times during the unfamiliar target calibration. However, it was not be possible to have each unfamiliar appear equally with certainty as the onset of a reversal could not predicted. Throughout the thresholding of the unfamiliar stimuli, the 8 unfamiliar targets were presented in sequences of 8 to ensure that each of the unfamiliar stimuli occurred *as close to* an equal number of times until a reversal took place. The order of each sequence was determined at random.

After six reversals were obtained for each of the three staircases, the participant automatically completed 40 trials. Luminance was set at the mean luminance of the three final reversals for each of the staircases. If proportion correct was within -0.1/+0.15 of 0.707, target calibration of the current stimulus type (familiar or unfamiliar) was complete. The target luminance that was attained by the luminance manipulation procedure was always be used for the first active sham pair within a session. Target luminance manipulation continued to be monitored after vertex blocks to control for effects of fatigue and/or learning. If proportion correct for familiar or unfamiliar targets was within -0.1/+ 0.15 of 0.707, familiar or unfamiliar target luminance was not changed on the next active vertex pair. However, if proportion correct was outside of -0.1 or + 0.15 of 0.707 for either familiar or unfamiliar targets, the luminance was decreased or increased, respectively. The exact magnitude of the increase or decrease was not specified during pre-registration so luminance could be changed flexibly throughout the experiment.

Calibration: Phosphene threshold

Where possible, participants who were recruited had already completed a phosphene threshold (PT). These participants completed the study specified here: https://osf.io/7t3z5/ or here: https://osf.io/d7uik/. However, if participants had not completed a phosphene threshold procedure

in our laboratory, the following procedure, similar to Allen et al. (2014), will be completed. The only difference between the procedure here and Allen et al. (2014) is that the proportion of phosphenes reported will be worked out as a function of TMS intensities ranging from 80%, 90%, 100%, 105%, 110% and 115% of an initial PT gathered using a single up-down staircase.

Procedure

If the participant had not completed a PT in our laboratory before (https://osf.io/d7uik/; https://osf.io/d7uik/), the PT outlined above was completed first. Prior to TMS blocks, the participant completed the familiar and unfamiliar staircases separately. Each of the staircases was repeated until the participant achieved the desired PC. If the participant did not achieve the desired PC after completing the staircase 3 times, the participant completed 40 trials with target luminance throughout the block set manually by the experimenter until the desired PC was achieved. Once target luminance for familiar and unfamiliar stimuli had successfully been calibrated, the scalp location that accompanied a reasonably clear phosphene that covers part of the centre of participant's visual field when TMS is administered was sought. Once such a scalp location had been found, TMS blocks began. Within each session, TMS blocks were completed in pairs to ensure that each active block was paired with a vertex block. This meant that a minimum of one active and one sham block was completed within a session. Participants usually completed one 4 block session and one 6 block session. However, the number of blocks a participant completed was ultimately determined by their availability and the experimenter's availability.

Equipment

TMS was administered by a Magstim single 90mm round coil connected to a Magstim Rapid^2 biphasic stimulator (Magstim). Visual stimuli were delivered on an ASUS VG248QE 24" NVIDIA 2D V2 monitor (refresh rate: 100Hz). The TMS coil was placed above one site (EVC or vertex) throughout a block. Before the first active or vertex block of the session, the scalp location that accompanied a reasonably clear phosphene covering part of the participant's visual field was identified. Once this

scalp location had been identified, the location was marked on the participant's MRI scan using Brainsight 2 (Rogue Research Inc.). Prior to each EVC-TMS block, a pulse of TMS was delivered to this site to confirm a reasonably clear phosphene covering part of the participant's visual field was still present. If a phosphene was present, the block commenced. If a phosphene was not present, a phosphene covering part of the centre of their visual field was re-identified. The TMS coil location was marked on the participant's MRI scan before each EVC-TMS block commenced.

Pre-registered statistical analyses

The basis for all the statistical analyses pre-registered here was ΔPC (active – vertex) as a function of SOA for familiar and unfamiliar targets, which was calculated separately for each participant. First of all, proportion correct as a function of each SOA was calculated separately for active TMS and vertex TMS for familiar targets and unfamiliar targets. ΔPC as a function of SOA for familiar and unfamiliar targets was calculated separately by subtracting vertex performance at each SOA from active PC at the corresponding SOA. This generated the TMS-induced change in performance, ΔPC, as a function of time for familiar and unfamiliar targets. These two different sets of ΔPC scores were the basis for statistical analysis involving the fitting of monophasic Gaussian models to quantify TMS-induced effects.

Each participant generated two separate monophasic Gaussian models; one for ΔPC as a function of familiar targets and one for ΔPC as a function of SOA for unfamiliar targets. These models will be generated using the curve fitting toolbox provided with MATLAB 2015a (Mathworks Inc.). The Gaussian models are comprised of four coefficients: an amplitude coefficient, a_1, which refers to the magnitude of a potential TMS-induced deflection effect on ΔPC, b_1, a bandwidth coefficient, which refers to the *duration* of potential TMS-induced effect on ΔPC; x_1 a temporal position coefficient, which refers to the timing of a_1 with duration b_1; and an intercept *y0,* which refers to the baseline level of performance. The formula for the single Gaussian model can be found here:

$$y = y_0 + a_1 e^{\left[-\left(\frac{x - x_1}{b_1}\right)^2\right]}$$

The single Gaussian model was applied with the following constraints:

1) $a_1 < 0$, which meant that the amplitude coefficient couldnot t be greater than zero. This ensured that the model detected a decrement in performance as a result of EVC-TMS.
2) a_1 < the absolute difference between the largest ΔPC score and the smallest ΔPC score multiplied by -1. This was also to ensure that the model detected a decrement in performance as a result of EVC-TMS.
3) $x_1 > 5$ms & $x_1 <$ 235ms. These x_1 constraints were introduced to prevent x_1 from falling outside the range of TMS-SOAs where TMS was administered in this experiment.
4) $b_1 > 5$ms & $b_1 <$ 235ms. These b_1 constraints were introduced to prevent b_1 from being greater than the range of TMS-SOAs where TMS was administered in this experiment. A minimum b_1 wasselected to prevent b_1 from being less than zero, which is impossible given the theory behind applying single Gaussian models to these data sets.
5) *y0* < the highest ΔPC score & *y0* > the lowest ΔPC score. These constraints were chosen to prevent the intercept of the model from being greater than or less than the ΔPC scores obtained across SOAs.

a_1 was the first coefficient of interest when carrying out the analysis pipeline that was pre-registered. The a_1 produced by fitting the model to ΔPC as a function of EVC-TMS for familiar and unfamiliar targets was used to establish EVC-TMS had successfully produced an effect on performance. A Bayesian one-sample *t*-test with a JZS prior (scaling factor: 0.3) was applied to a_1 for familiar targets and a_1 for unfamiliar targets separately. An additional statistical analysis was carried out because the Bayes factor (*BF*) produced by one-sample *t*-test supported that an effect of EVC-TMS was present for familiar and unfamiliar stimuli. This additional statistical analysis involved a Bayesian paired sample *t*-test with a half-normal prior (Dienes, 2011) on the mean difference produced by subtracting the familiar b_1 from the unfamiliar b_1. If the difference is positive, this will

meant that b_1 for unfamiliar stimuli was greater than b_1 for familiar stimuli, supporting the hypothesis that more recurrent processing occurs for familiar stimuli. In contrast, if the difference was negative or centred around zero, b_1 for unfamiliar targets would be lesser than or approximately equal to the b_1 for familiar targets, going against the hypothesis that more recurrent processing occurs for unfamiliar stimuli. The mean of the half-normal prior was zero and the standard deviation was 27.2ms (Dienes, 2011). This prior was selected because it was most sensitive to 10ms, 20ms and 30ms simulated differences in b_1 when simulated data was generated using the methods outlined below.

Pilot data: Results

Mean model fits and mean raw ΔPC acquired from pilot data can be found in figure 13. Mean model fits as raw ΔPC acquired from 3 participants from the pilot can be found in figure 14.

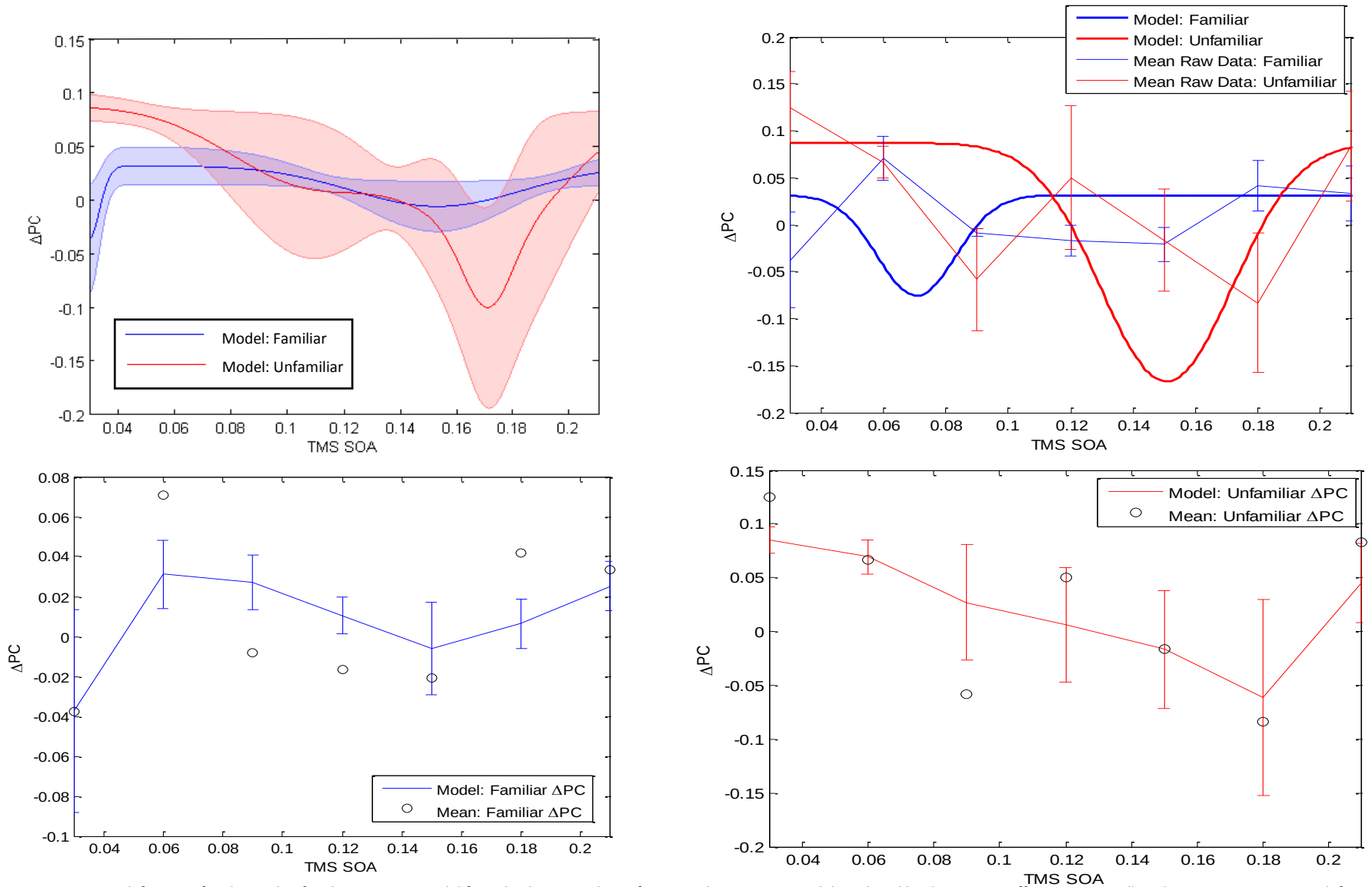

Figure 13. Top left: Mean familiar and unfamiliar Gaussian model fits solved across values of x. Top right: Gaussian model produced by the mean coefficients across all 3 pilot participants. Bottom left: Mean and standard error of Gaussian model fits to ΔPC and corresponding mean ΔPC as a function of TMS under conditions of familiarity. Bottom right: Mean and standard error of Gaussian model fits to ΔPC and corresponding mean ΔPC as a function of TMS under conditions of unfamiliarity.

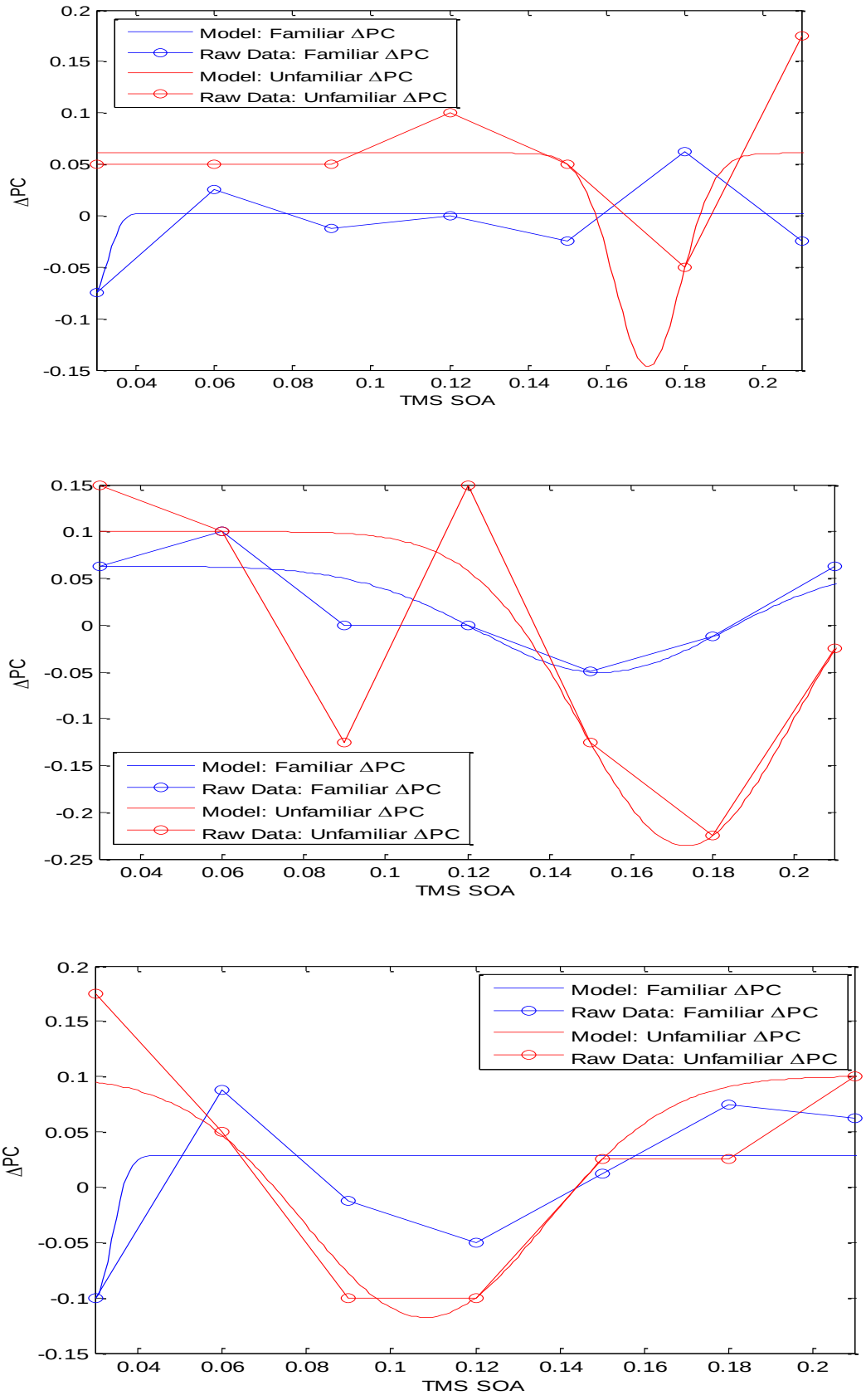

Figure 14. Pilot data revealing proportion correct (PC) for familiar and unfamiliar targets as function of EVC-TMS SOA.

Pilot analyses: Bayesian prior sensitivity and hypothesis feasibility analyses

It was uncertain whether a mean difference between two b_1 coefficients produced by EVC-TMS was a feasible hypothesis to test with a realistic number of participants. This uncertainty relates to the power argument proposed by de Graaf & Sack (2011), which refers to the difficulty in concluding whether a null result is genuine or whether a significant result could be attained if a larger number of participants was included within the analysis. Simulations were carried out to assess whether simulated differences in b_1 coefficients were accompanied by a *BF* which suppored that a mean difference is present. These simulations suggested that it was feasible to rely on the difference between b_1 coefficients to provide evidence for or against the hypothesis that more recurrent processing occurs for unfamiliar stimuli compared to familiar stimuli.

Three simulated experiments are presented here, which assessed the feasibility of the pre-registered statistical analyses presented here. One was based on simulations where 'perfect data' is introduced into the analysis pipeline presented. The second set of simulations was based on the mean of the single Gaussian coefficients obtained from a pilot data set. A third set of simulations was based on the mean of single Gaussian coefficients obtained from experiment 1 that generated 32 sets of single Gaussian coefficients produced by EVC-TMS. The analysis pipeline was identical to pre-registered analysis pipeline presented here with one major difference. The major difference was that a JZS prior with a scaling factor of 0.3 or 0.7 (Rouder et al., 2009) or a half-normal prior (Dienes, 2011) (mean: 0ms, standard deviation, 27.2ms) was applied to the mean difference between simulated familiar and unfamiliar b_1 coefficients. Three different priors were applied to the mean difference between simulated b_1 coefficients to identify which one was most sensitive at producing support for 10ms, 20ms and 30ms simulated differences in b_1. The most sensitive prior was the half-normal prior (Dienes, 2011).

The first stage of creating simulated data involved fitting a monophasic Gaussian model to a real pilot data set which contains the difference between active TMS and sham TMS across the SOAs

that will be used in the proposed study. The constraints applied to this Gaussian model were identical to the constraints that were specified for the pre-registered monophasic Gaussian models. The mean and standard deviation of each set of coefficients was then calculated across participants, which quantifies how a_1, x_1, b_1 and *y0* were distributed within the data set. These distributions which were characterized by the mean and standard deviation of each coefficient were then used as the basis for creating a simulated data set. First of all, a_1, x_1, b_1 and *y0* coefficients were randomly drawn from their respective distributions. These coefficients were then inserted into the equation for a monophasic Gaussian and solved across values of *x* that correspond to the TMS-SOAs that were used in experiment 5. Once this process had been completed, one set of simulated ΔPC data points will have been created across the SOAs that were used in experiment 5. A monophasic Gaussian model was then fitted to simulated ΔPC as a function of TMS-SOAs.

The process outlined above was used to generate three differences in b_1 between the familiar and unfamiliar simulated data sets, simulating potential outcomes of the experiment. One was when the difference in b_1 (b_1Diff) is 10ms, another was where the b_1Diff is 20ms another was where the b_1Diff is 30ms. Each one of these differences was selected in order simulate a 10ms, 20ms and 30ms b_1Diff for familiar and unfamiliar targets. These three simulated b_1Diffs were generated using three different means and standard deviations of the a_1, x_1, b_1 and *y0* distributions. These three different distributions were then used to generate values which are inserted into the equation for a single Gaussian to generate ΔPC as a function of TMS-SOA. The first set of means and standard deviations which were used to create simulated ΔPC were those with a very small amount of variance in ΔPC as a function of TMS-SOA. In the second set of simulations, the means and standard deviations of the distributions which were used to generate simulated ΔPC as a function of TMS-SOA were based on the monophasic Gaussian coefficients obtained from the pilot data presented here. In the third set of simulations, the means and standard deviations of the distributions which were used to generate simulated ΔPC as a function of TMS-SOA were based on the outcome of a monophasic Gaussian curve fitting procedure from experiment 1 (https://osf.io/d7uik/) investigating

EVC and dorsolateral prefrontal cortex (DLPFC). Data from experiment 1 was included here because TMS as applied to EVC with identical stimulation parameters with a large sample of 32 participants, which may reduce the influence of variance on the stopping rule for experiment 5. Variance may have effect because the the pilot data from experiment 5 contained a small sample of 3 pilot participants.The means and standard deviations for each distribution for each simulated analysis can be found in table 1.

		a_1		x_1		b_1		*y0*	
		Mean	***St. Dev***	***Mean***	***St. Dev***	***Mean***	***St. Dev***	***Mean***	***St. Dev***
Perfect	***Fam.***	-0.1	0.015	100ms	15ms	30ms	15ms	0	0.015
	Unfam.	-0.1	0.015	100ms	15ms	40ms, 50ms or 60ms	15ms	0	0.015
Pilot	***Fam.***	-0.1072	0.0256	70.7ms	71.1ms	17.7ms	21.6ms	0.0315	0.0303
	Unfam.	-0.2540	0.0711	150.7ms	36.8ms	27.7ms, 37.7ms or 47.7ms	15.6ms	0.0871	0.0227
EVC-DLPFC	***Fam.***	-0.3248	0.1635	158.2ms	104.9ms	59.2ms	74.4ms	0.0418	0.1373
	Unfam.	-0.3248	0.1635	158.2ms	104.9ms	69.2ms, 79.2ms or 89.2ms	74.4ms	0.0418	0.1373

Table 1. Mean and standard deviations (St. Dev) of the a_1, x_1, b_1 and *y0* distributions which were the basis for generating simulated ΔPC as a function of familiar (Fam) or unfamiliar targets (Unfam) as a function of TMS-SOAs ranging from 30ms to 220ms separated in increments of 30ms . Simulations were based on 'perfect data ' with very little variance, the coefficients generated from the pilot experiment or ΔPr. ΔPr was calculated from an experiment investigating early visual cortex (EVC).

Bayesian prior sensitivity and hypothesis feasibility analysis: Perfect data

An analysis on simulated data drawn from a_1, x_1, b_1 and *y0* distributions with very little variance (a_1 & *y0*: 0.015; x1 & b1: 15ms) enabled identification of whether it was feasible to detect a difference between two b_1 coefficients under ideal conditions. Moreover, simulated a range of differences (10ms, 20ms & 30ms) can reveal a specific b_1 difference in milliseconds where the *BF* successfully crosses the threshold for support for a difference between the simulated familiar and unfamiliar bandwidths. Alternatively, this analysis on 'perfect' data could also reveal a specific difference in milliseconds in bandwidth where it is unfeasible to produce a *BF* that crosses the threshold for support for a difference. The absence of such a *BF* would be critical as a difference would be present in the simulated data but the analysis using single Gaussian models would be unable to measure such a difference. The absence of a *BF* that supports a difference in 'perfect' data would suggest that bandwidth coefficients are not an appropriate measure of the duration of temporal events in EVC that are being disrupted as a function of TMS SOA.

Figure 15 reveals the *BF* as a function of participant number in simulations of 'perfect' data, where the bandwidth for unfamiliar targets is 10ms (figure 15, top), 20ms (figure 15, middle) and 30ms (figure 15, middle) greater than the bandwidth for familiar targets. What is striking about figure 15 is that a half-normal prior (Dienes, 2011) was always more sensitive than the JZS prior (Rouder et al., 2009) regardless of whether the scaling factor of the JZS is 0.3 or the default of 0.707 across all simulated differences. In fact, the choice of prior distribution (half-normal or JZS) appears to be the critical determinant of how sensitive the *BF* was to a simulated difference in bandwidth. This is illustrated by the fact the half-normal prior is shifted to the left of both JZS priors in figures 15, which illustrates that the *BF* produced by a half-normal prior is more sensitive to a simulated difference in bandwidth after including a smaller sample of participants than the *BF* produced by either JZS prior. Critically, however, the outcome of these analyses make it clear that the difference between a familiar and unfamiliar bandwidth, when the unfamiliar bandwidth is increased by 10ms, 20ms and 30ms, was reflected in a *BF* that exceeds 6 which reflects strong support for a difference

between two means (JZS (0.707): *BF* > 6, n = 6; JZS (0.4): *BF* > 6, n = 7; Half Normal: *BF* > 6, n = 4). In conclusion, the outcomes of the simulated analyses of 'perfect' data suggests that a greater bandwidth for unfamiliar targets than the bandwidth for familiar targets is a feasible hypothesis to test using monophasic Gaussian models that measure performance as a function of EVC-TMS SOA.

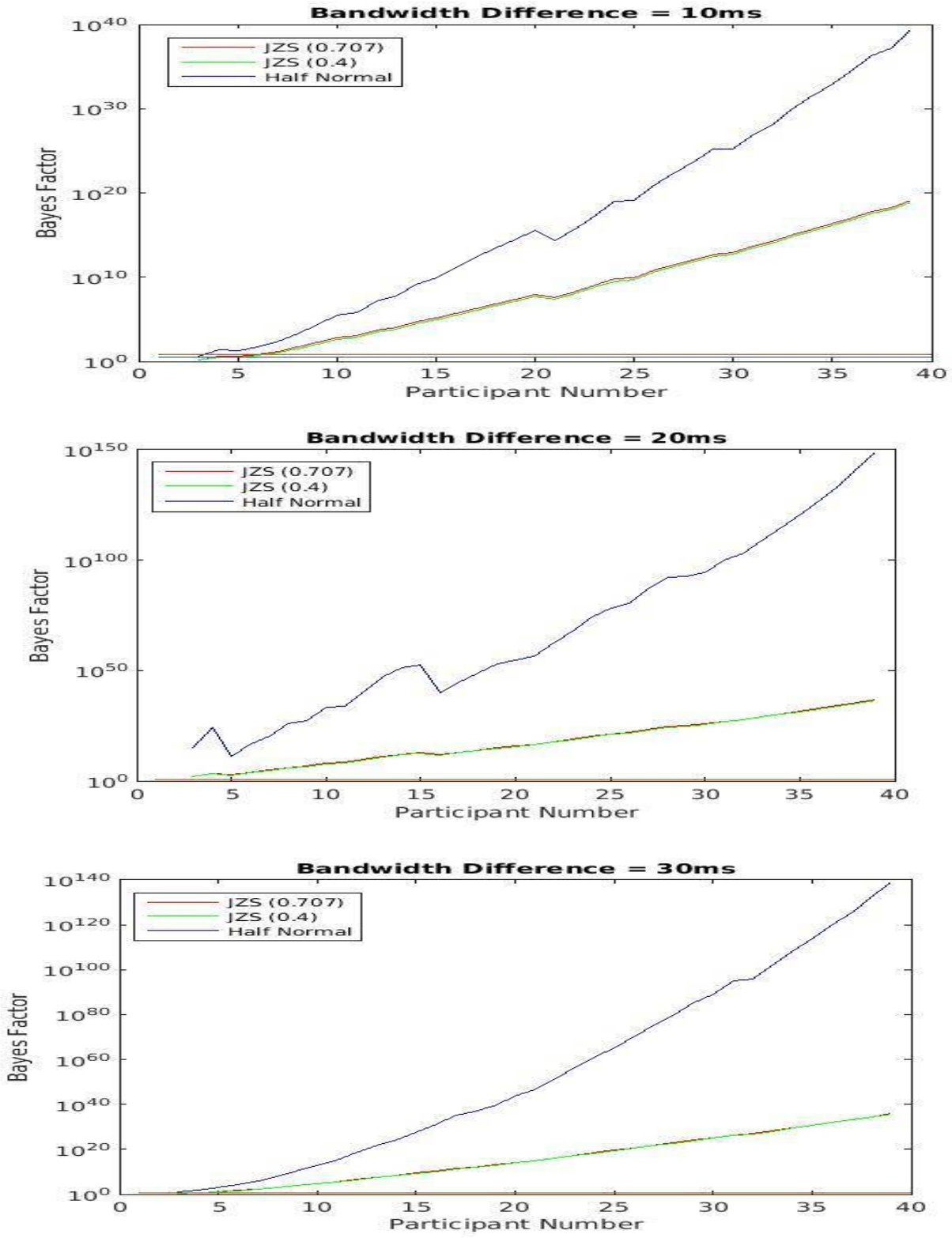

Figure 15. Bayes factor as a function of participant number for mean differences of 10ms, 20ms and 30ms in bandwidth coefficient (b_1) based on 'perfect data'.

Bayesian prior sensitivity and hypothesis feasibility analysis: Pilot data

The outcomes of the simulated analyses of 'perfect' data suggests that the use of a bandwidth coefficient is a feasible measure of temporal events within EVC. Moreover, it also suggested that a *BF* can produce support for one mean coefficient being 10ms, 20ms or 30ms greater than another bandwidth coefficient. However, the presence of such low variance is that it increased the likelihood of two means being different from one another. In a real TMS experiment, it is unlikely that the variance will be low. As a result, it is important to run additional simulations with a realistic amount of variance for each of the coefficients.

Figure 16 reveals the *BF* as a function of participant number in simulations based on the mean and variance of the a_1, x_1, b_1 and *y0* coefficients from a pilot experiment with an identical protocol to the experiment pre-registered here. Like the simulations of the 'perfect' experiment, the mean bandwidth for unfamiliar targets was increased by 10ms, 20ms and 30ms relative to the mean bandwidth for familiar targets. The variance, however, was determined by the variance of the bandwidth coefficients obtained from the pilot experiment. The mean of the a_1, x_1 and *y0* distributions which were the basis for simulated ΔPC as a function of familiar and unfamiliar targets were also determined by bandwidth coefficients obtained in the pilot experiment. Thus, these simulations could identify whether it was still feasible to obtain a *BF* that supports a difference between two mean bandwidths with a realistic data set. Unlike all the other simulations presented here, the mean difference of 10ms is revealed as a function of 120 simulated participants. The simulations go up to 120 here to identify whether all three priors are capable of eventually producing a *BF* that is more than 3 for a mean difference of 10ms. Unlike the simulations based on 'perfect' data, figure 15 (top) suggests that it would be unfeasible to detect a difference in bandwidth of 10ms with a half-normal prior (Dienes, 2011) but it would be feasible with both JZS priors (Rouder et al., 2009). A JZS Prior with a scaling factor of 0.707 produces a *BF* that is more than 3 after 107 participants are included in the analysis. A JZS prior with a scaling factor of 0.4, on the other hand, produces a *BF* that is more than 3 after 103 participants are included in the analysis.

In contrast, figure 16 (middle & bottom) reveals that it is feasible for a half-normal prior and both JZS priors to produce a *BF* that is sensitive to a 20ms (figure 16, middle) and a 30ms (figure 16, bottom) difference between familiar and unfamiliar bandwidths. However, whether or not the *BF* produces support for the presence or absence of a difference of 20ms and 30ms depends on the number of participants that are included in the statistical analysis. Initially, both prior distributions produced *BF*s that supportedr the null hypothesis until eventually beginning to rise and exceed the threshold for strong support for a difference between two bandwidths ($BF > 6$). In conclusion, the outcome of these simulated analyses suggested that the choice of prior determines whether it is feasible to detect a difference in bandwidth that is less than or equal to 10ms. However, it is feasible to produce support for a difference between two mean bandwidths of 20ms or 30ms regardless of the prior that is chosen.

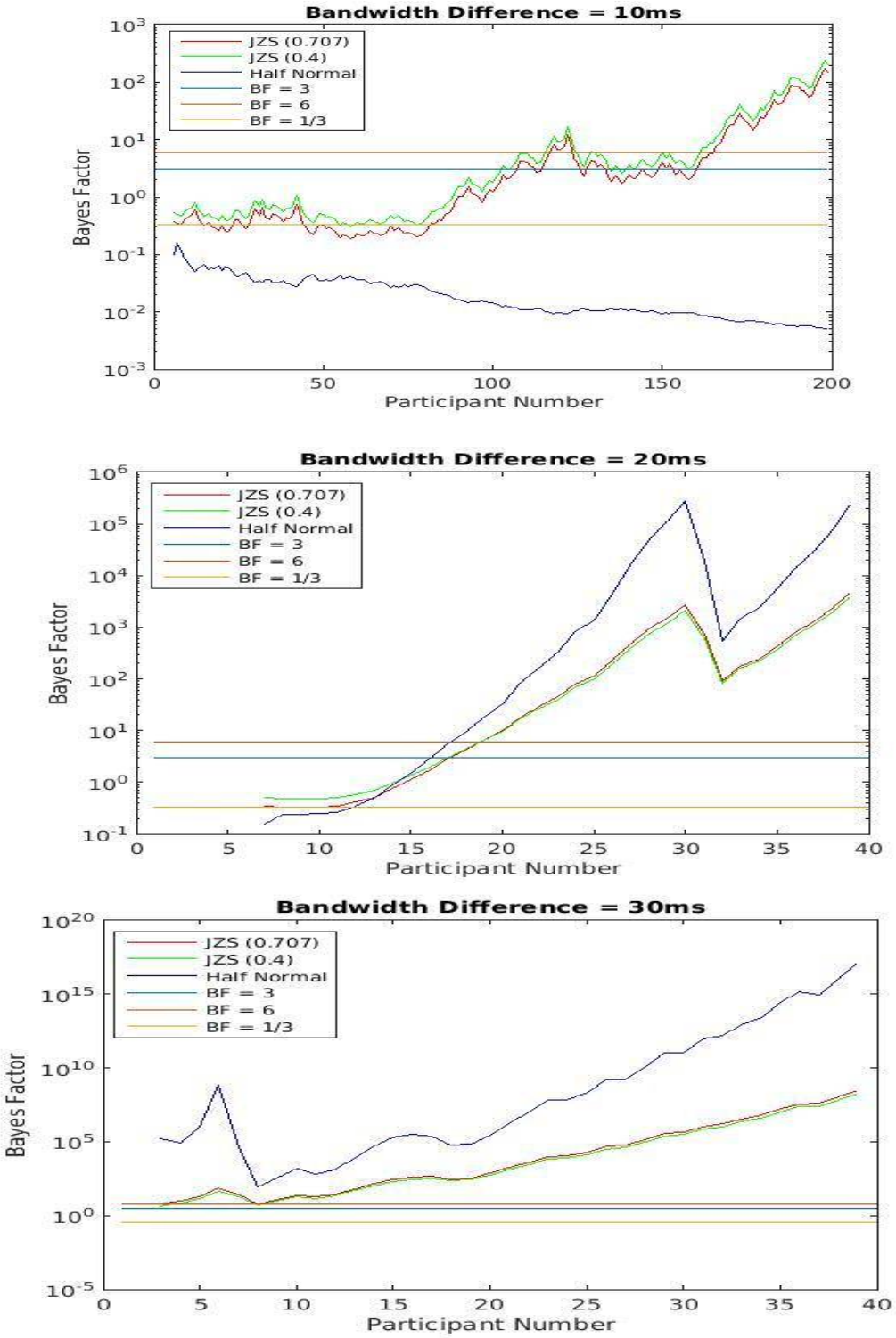

Figure 16. Bayes factor as a function of participant number for mean differences of 10ms, 20ms and 30ms in bandwidth coefficients (b_1) based on pilot data.

Bayesian prior sensitivity and hypothesis feasibility analysis: EVC-DLPFC experiment

The simulations based on pilot data relied on coefficients derived from monophasic Gaussian fits to ΔPC for familiar and unfamiliar targets as a function of TMS SOA obtained from 3 participants. Thus, the mean a_1, x_1, b_1 and *y0* were obtained from a small sample of 3 participants, which may mean that the simulations did not accurately represent the duration of processing within EVC. Inaccuracies may be present due to a large amount of variance in a small pilot data set. In order to confirm the validity of the simulated analyses based on pilot data, an additional set of simulations were completed in which the simulated coefficients for a single Gaussian were derived from the mean coefficients from 32 single Gaussian fits to ΔPr, a non-parametric measure of perceptual sensitivity (Corwin, 1994), as a function of EVC-TMS SOA from experiment 1 (https://osf.io/7t3z5/). The distributions that determined the coefficients that went into the simulated analyses presented here were based on the mean and variance of a_1, x_1 and *y0* coefficients from a larger sample of 32 participants. A larger sample was used as it is more likely to be an accurate measure of the duration of processing within EVC. The task and measure that generated these coefficients was different to the task outlined here. This experiment was a simple detection task where participants had to report the presence of absence of a small dot presented in the participant's fovea. Pr, which is a different measure of performance was also used. Pr, subtracts a participant's false alarm rate from their hit rate, to provide a bias free measure of performance (Corwin, 1994). However, the TMS parameters that were used in this experiment were identical to TMS parameters registered here (120% of phosphene threshold).

Figure 17 reveals the *BF* as a function of participant number for simulated differences in b_1 of 10ms (figure 17, top), 20ms (figure 17, middle) and 30ms (figure 17, bottom). Examination of figure 16 (top) reveals considerable variation of the *BF* produced by half-normal prior (Dienes, 2011) when the simulated difference between mean bandwidths was 10ms. Initially, the *BF* garners very strong

support for the absence of a mean difference in bandwidth when n = 4 before becoming inconclusive and finally returning to very strong support for a mean difference in bandwidth when n = 29 . In contrast, JZS priors (Rouder et al., 2009) that expect effect sizes of 0.4 and 0.707 remain inconclusive until 31 participants are included in the analysis, where they exhibit substantial support for a mean difference. However, the *BF* produced by both JZS priors never exceeded the threshold for very strong support for a mean difference in bandwidth. The implication of this analysis suggest that it is feasible for a half-normal prior to detect a mean difference in bandwidth of 10ms providing that a sufficient number of participants (~20) are included within the statistical analysis.

Examination of figure 17 (middle and bottom) reveal that it is feasible to obtain a *BF* that reflects very strong support for a mean difference in bandwidth with all 3 prior distributions after including at least 5 participants in the analysis. Once again, the *BF*s produced by a half-normal prior distribution are shifted to the left of the *BF*s produced by a JZS prior, which suggests that a half-normal produces stronger evidence for a mean difference in bandwidth after including a smaller number of participants in the statistical analysis.

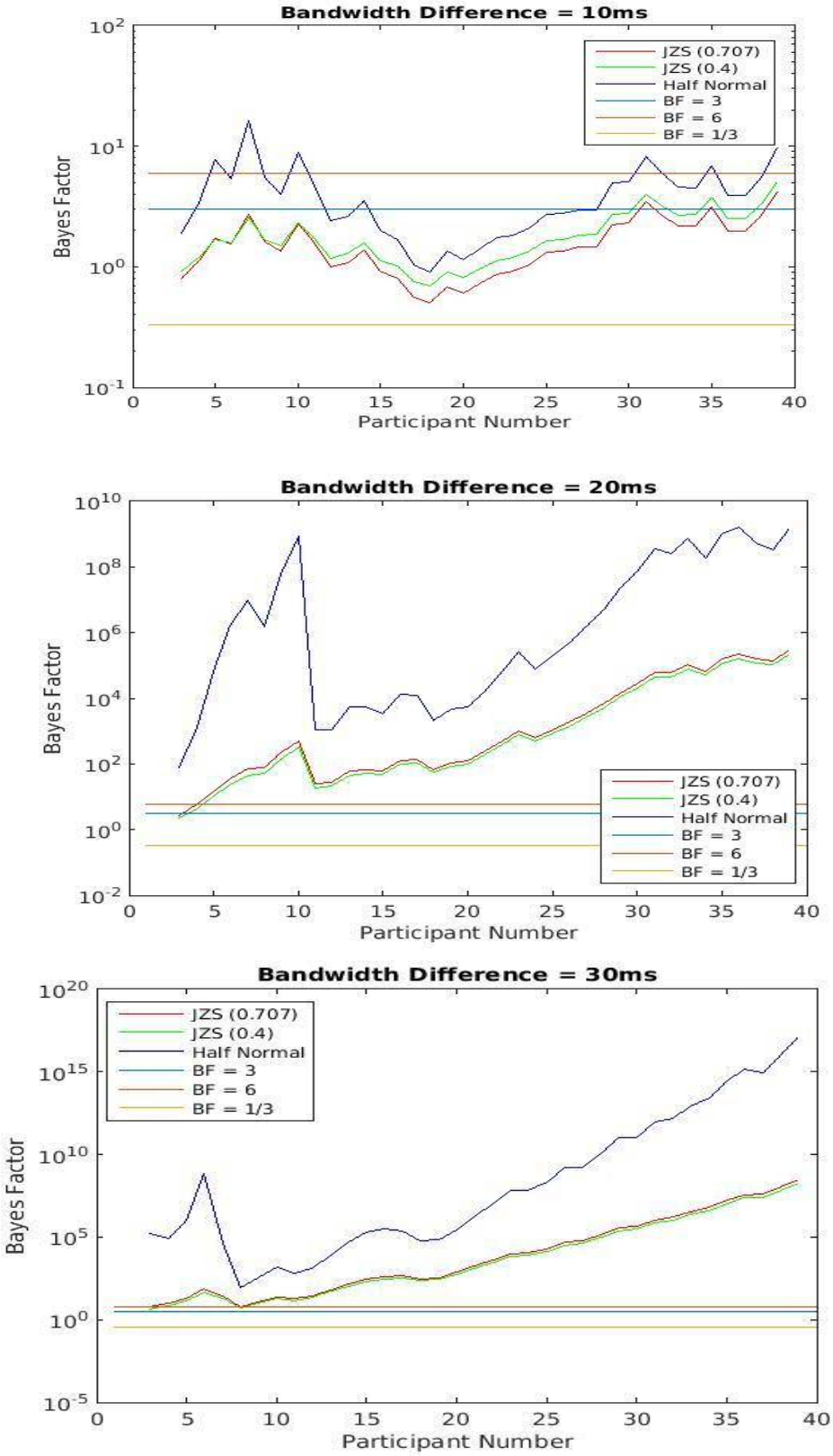

Figure 17. Bayes factor as a function of participant number for mean differences of 10ms, 20ms and 30ms in bandwidth coefficients (b_1) based on negative amplitude monophasic Gaussian model fits to ΔPr as a function early visual cortex TMS and dorsolateral prefrontal cortex TMS from experiment 1.

Experimental analyses and stopping rule

The first stage of the pre-registered analyses identified whether TMS has successfully reduced ΔPC for familiar and unfamiliar targets, which would indicate that PC for active TMS has been reduced relative to PC for sham TMS. In order to identify whether such effects have taken place, a Bayesian one-sample *t*-test with a JZS prior with a scaling factor of 0.3 (Rouder et al., 2009) was applied to each set of a_1 coefficients for ΔPC as a function of TMS-SOA for familiar and unfamiliar targets. If the *BFs* produced by *both* one-sample Bayesian *t*-tests were more than 3, an additional analysis on the b_1 coefficients will be completed. The additional analysis then tested the hypothesis that more recurrent processing takes place for unfamiliar stimuli compared to unfamiliar stimuli. This involved the application of a Bayesian one-sample *t*-test with a half-normal prior (Dienes, 2011) with a mean of 0ms and a standard deviation of 27.2ms. This experiment terminated on August 11th 2017.

Statement that data collection has already commenced for this experiment

Due to a student registration deadline approaching, data collection commenced prior to this experiment being pre-registered on the Open Science Framework on August 16th 2017. This data was not analysed in any way other than in the tracking of sham performance in line with the above procedure prior to August 11th 2017.

Results: Pre-registered analyses

The first stage of the pre-registered analyses was to identify whether EVC-TMS has produced an effect on ΔPC for familiar and unfamiliar targets. The initial stage involved the application of a Bayesian one-sample *t*-test with a JZS prior (Rouder et al., 2009) with a scaling factor of 0.3 to the mean familiar and unfamiliar a_1 coefficients. The purpose of this initial stage was to identify if TMS effects were present in both conditions, which would enable an additional analyses to take place to identify whether the b_1 coefficients for unfamiliar targets were greater for the b_1 coefficients for familiar using a Bayesian one-sample *t*-test with a half-normal prior (Dienes, 2011).

Mean and modelled ΔPC for familiar and unfamiliar targets can be found in figure 18 whereas the mean monophasic Gaussian models solved and not solved across values of x can be found in figure 19. A one-sample *t*-test with a JZS prior (scaling factor: 0.3) (Rouder et al., 2009) on the a_1 coefficients for familiar and unfamiliar targets produced a *BF* that was more than 3 once 5 participants were included in the analysis. Once 6 were included, a *BF* that was more than 3 was not revealed. However, once 7 up to 16 participants were included a *BF* that is more than 3 was consistently revealed. The *BF* as a function of participant number for the Bayesian one-sample *t*-test on the familiar and unfamiliar a_1 coefficients can be found in figure 18. This consistent *BF* that supports that the a_1 coefficients for familiar and unfamiliar targets are different from zero, meaning that active TMS has produced an effect relative to vertex TMS. In short, the pre-registered criteria for moving on the second stage of the analysis, which sought to identify whether b_1 for unfamiliar targets was greater than b_1 for familiar targets was met.

The second stage of the pre-registered analysis involved a Bayesian one-sample *t*-test with a half-normal prior (Dienes, 2011) to the mean difference of a subtraction of the b_1 for familiar targets from b_1 for unfamiliar targets. If the outcome of this subtraction were positive, it would mean the b_1 for familiar targets is greater than b_1 for unfamiliar targets, supporting the idea that more recurrent processing occurs unfamiliar targets than familiar targets. If the outcome of this subtraction was negative, it would mean that b_1 for familiar targets is greater than b_1 for unfamiliar targets, supporting the hypothesis that more recurrent processing occurs for unfamiliar targets compared familiar targets. In contrast, if the outcome of this subtraction is positive, it would mean that b_1 for unfamiliar targets is greater than familiar targets, providing evidence for the hypothesis than more recurrent processing occurs for unfamiliar targets than for familiar targets. The *BF* produces by a one sample *t*-test with a half-normal prior (Dienes, 2011) as a function of participant number can be found in figure 18. All 16 participants were included in the analysis which sought to identify whether unfamiliar b_1 was greater than familiar b_1. Weak evidence for a positive difference was found after subtracting the familiar b_1 from the unfamiliar b_1 (t (15) = -1.6301, p = 0.1239, *BF* = 2.5333),

providing that weak evidence for the hypothesis that more recurrent processing accompanies unfamiliar stimuli compared to familiar stimuli.

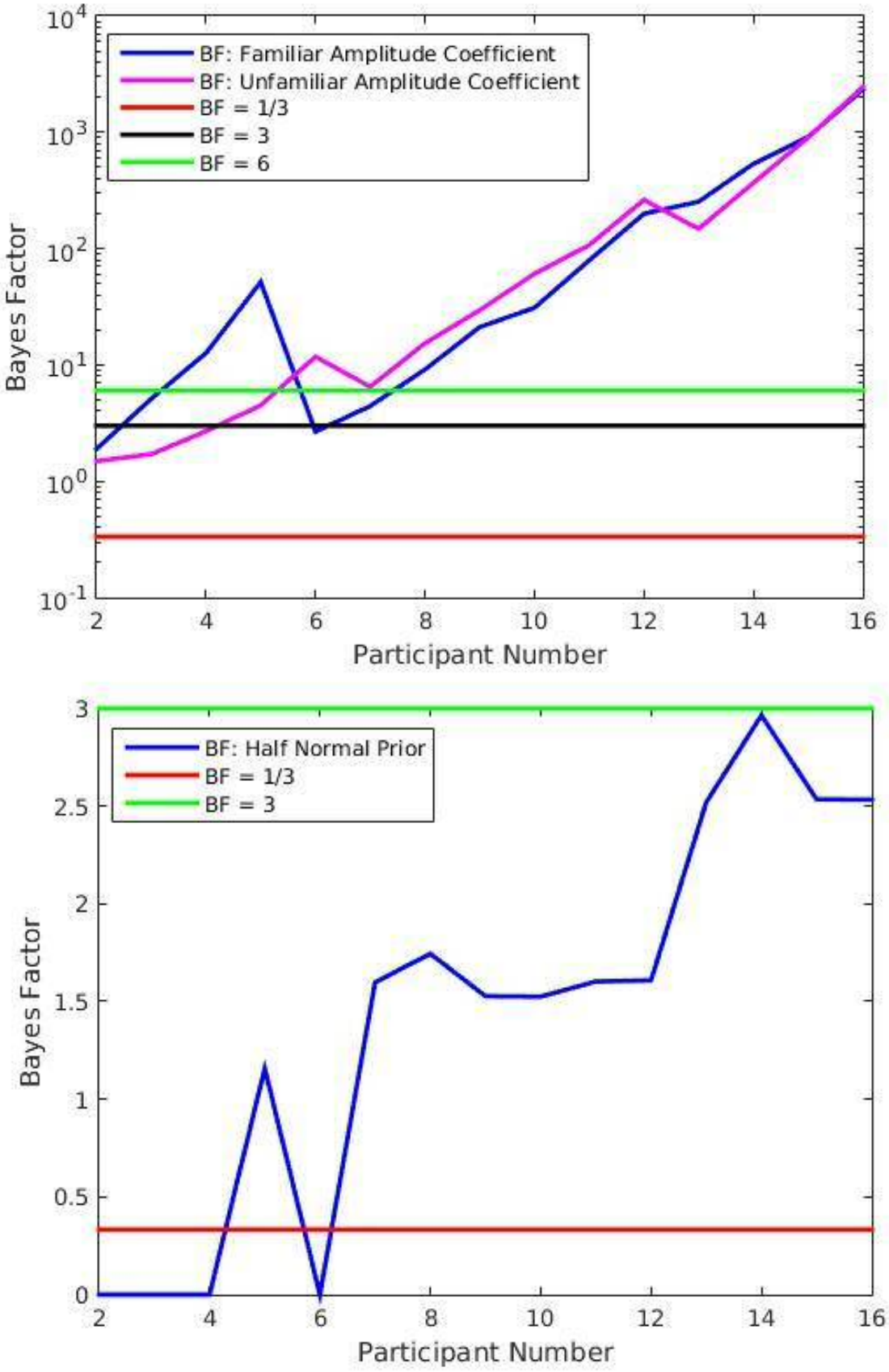

Figure 17. Top: Raw data and monophasic Gaussian model fits to ΔPC as a function of EVC-TMS SOA for familiar targets. Error bars represent the -/+ 1 standard error. Middle: Raw data and monophasic Gaussian model fits to ΔPC as a function of EVC-TMS SOA for unfamiliar targets. Error bars represent the -/+ 1 standard error. Bottom: Raw ΔPC for familiar and unfamiliar targets as a function of EVC-TMS SOA. . Error bars represent the -/+ 1 standard error.

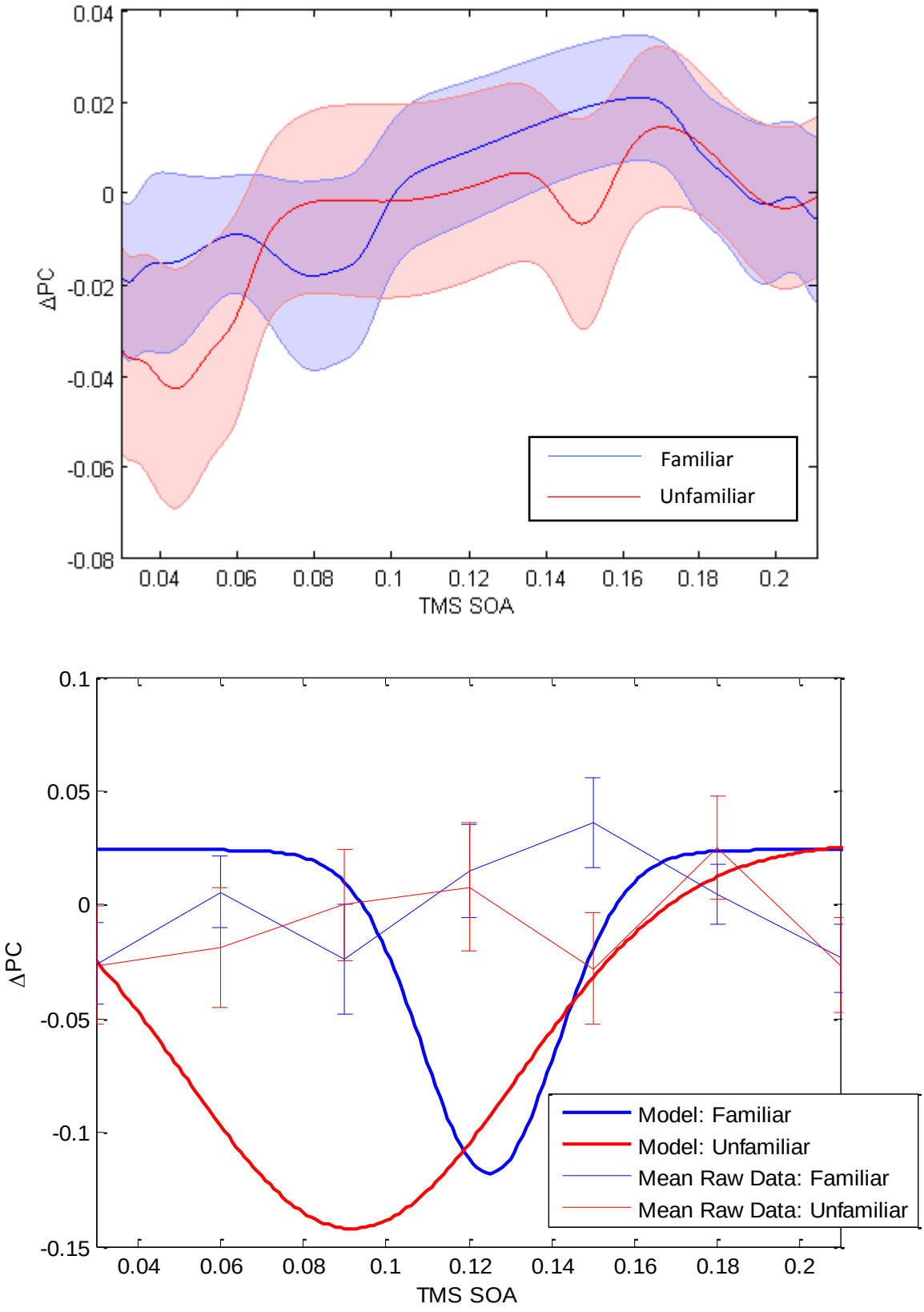

Figure 18. Top: Modelled ΔPC as a function of EVC-TMS solved across values of *x* for familiar and unfamiliar targets Line represent the model mean. Shaded regions represent the -/+ 1 standard error. Bottom: Modelled ΔPC as a function of EVC-TMS not solved across values of *x* for familiar and unfamiliar targets. Error bars represent the -/+ 1 standard error of the raw data.

Experiment 5: Discussion

Experiment 5 sought to identify if unfamiliar targets were subjected to more recurrent processing within EVC than familiar targets. This experiment presented participants with a familiar shape at a greater frequency than an unfamiliar shape and applied a single Gaussian model to ΔPC as a function of EVC-TMS for familiar and unfamiliar shapes. The a_1 coefficient was used to quantify whether EVC-TMS successfully produced an effect on ΔPC. The b_1 coefficient was used to quantify the duration of recurrent processing that was devoted to familiar targets and unfamiliar targets, as induced by the duration that active EVC-TMS successfully supressed performance compared to vertex EVC-TMS. The *BF* quantified weak evidence for b_1 for unfamiliar targets being greater than b_1 for familiar targets, which suggests that strong support for a difference in the duration of recurrent processing for unfamiliar targets compared to familiar targets could be obtained if more participants were included within the analysis. This suggests that the central tenet of predictive coding, that sensory inputs that are unexpected trigger more processes within EVC than sensory inputs that are expected (Rao & Ballard, 1999; Friston, 2005) may be an appropriate framework for brain function. Unfortunately, temporal constraints on data collection prevented more participants from being included in the current study.

Experiment 5 used b_1 coefficients to measure the duration of TMS-induced effects between two different conditions: conditions when a familiar target was presented and conditions when an unfamiliar target was presented. Unlike a previous investigation of recurrent processing (de Graaf et al., 2012), the results here were based on a measure that is more sensitive to duration of TMS-induced effects on behaviour. This previous investigation compared the duration of processing within EVC as measured by the number of SOAs that EVC-TMS suppresses performance for (de Graaf et al., 2012). Based on this assumption, more recurrent processing for face stimuli compared to simple Gabor patches was revealed, suggesting that it is possible to rely on EVC-TMS to interfere with recurrent processes of different durations. This is interesting because it was influential in the

notion that the EVC-TMS induced effect at ~100ms could reflect feedforward and recurrent processing (de Graaf et al., 2014). However, in de Graaf et al. (2012) the duration of recurrent processing was measured indirectly. Mean performance was calculated *within* an SOA, which meant a source of variance was available to apply statistics to the magnitude of a TMS induced effect at one SOA. However, a source of variance was not available *across* SOAs, which is the critical variable of interest here as SOA at which TMS is administered measures the duration of TMS-induced effect over time. Here, we bypassed this issue using the b_1 coefficients generated by a monophasic Gaussian model. The advantage of using b_1 coefficients is that they directly measure the number SOAs that TMS-induced effect extends over, meaning that they can quantify the duration of recurrent processing within EVC

The outcome of these results demonstrate that predictive coding could be a feasible model of the feedforward and recurrent processes that go into creating a visual representation within EVC (Rao & Ballard, 1999; Friston, 2005). Weak support for a mean difference between the b_1 coefficients for unfamiliar targets being greater than the b_1 coefficient for familiar targets was obtained. This suggests that the mismatch between a top-down prediction and what is currently presented is a candidate mechanism that could determine what is fed forward and fed back within EVC (Rao & Ballard, 1999; Friston, 2005). Here, it was assumed that presenting a familiar target at a greater frequency would enable it to be incorporated into a top-down prediction of what will occur on a current trial. When the familiar target occurs, less prediction error would be produced because it is consistent with top-down predictions (Friston, 2005). In contrast, it was assumed that an unfamiliar target would not incorporated within into top-down predictions (as much as the familiar target) because it occurred at a lower frequency. As a result of being incorporated within top-down predictions to a lesser extent, it was assumed that unfamiliar targets will trigger a prediction error to a greater extent than familiar stimuli. The difference in the amount of prediction error that accompanies familiar and unfamiliar stimuli was the basis for probing the duration of recurrent processing that accompanied familiar unfamiliar stimuli.

It was assumed that more recurrent processing would occur for unfamiliar stimuli than familiar stimuli. On each trial, a top-down prediction would ultimately be conveyed to V1 in order capture the statistical regularity the environment (Rao & Ballard, 1999; Friston, 2005). Familiar stimuli would incorporated within such predictions as they occur at a greater frequency than unfamiliar stimuli. When an unfamiliar stimulus occurs, the top-down prediction would need to be revised as prediction error would be produced as a result of an unlikely target being presented. More recurrent processing was expected to accompany the unfamiliar stimuli because more prediction error was assumed to accompany, which would in turn, trigger a revision of the top-down prediction (Rao & Ballard, 1999; Friston, 2005). The revision of a top-down prediction would require the prediction error to be conveyed forwards to higher order sites and would subsequently require a new top-down prediction to be fed back to lower levels in response (Rao & Ballard, 1999; Friston, 2005). The b_1 coefficient was used to measure the duration of time taken to revise a top-down prediction. The revision of top-down prediction of an infrequent, unfamiliar stimulus was predicted to produce a larger b_1 coefficient than that which accompanied the revision of a frequent, familiar stimulus. Such a prediction was confirmed, which suggests that the mismatch between a top-down prediction and a a sensory input could determines the magnitude of feedforward processing *and* what is fed back as a within EVC (Rao & Ballard, 1999; Friston, 2005).

There are some models that make similar predictions to predictive coding that are often ignored within the literature (Bowers & Davis, 2012). For example, Rescorla & Wagner (1972) proposed that stimuli that are not expected trigger larger responses than stimuli that are not expected, such responses become the basis for learning about an unexpected event. Moreover, Pearce & Hall (1980) proposed an alternative explanation for such an event: unexpected events are subjected to more processing than expected events because they attract attention. Both of these explanations could be compatible with the results here. However, this experiments highlight something more fundamental about the processes within EVC. For example, if the b_1 coefficient was greater for *familiar* stimuli than unfamiliar stimuli. All three theories would have offered incorrect

predictions for the outcome of the experiment (Rao & Ballard, 1999; Rescorla & Wagner, 1972; Pearce & Hall, 1980). Moreover, if b_1 coefficients were the same for familiar targets and unfamiliar targets, it could also be suggested that all three theories do not offer a competent explanation for what occurs within EVC or that TMS can be used to probe such mechanisms within EVC. The outcome of this study suggests that something remarkable is going on within EVC, and such a process could be related to the mismatch between a top-down prediction and what is current presented, which has previously being highlighted with functional MRI (Kok et al., 2013).

An alternative explanation to the results here may exist due to visual adaptation, which refers to a reduction in the neural response to a repeated stimulus (Gibson & Radner, 1937). Here, repeated stimuli was a critical manipulation that was assumed to incorporate one target into a top-down prediction but not others, as predicted by predictive coding (Rao & Ballard, 1999; Friston, 2005). Consequently, the conditions that led to a formulation of a top-down prediction could also lead to visual adaptation. Unlike other experiments, which jittered the position of a Gabor patch that to avoid visual adaptation with the fulfilment of a top-down prediction (Sherman et al., 2015; Sherman et al., 2016), experiment 5 presented the familiar target in the same foveal position on a trial-by-trial basis. However, there are is evidence from neuroimaging that a reduction in the response of a neural population to repeated stimuli relates to the absence of a discrepancy between a top-down prediction and a sensory input (Summerfield et al., 2008). Summerfield et al. (2008) demonstrated that a greater reduction in BOLD within the FFA occurred within a block where repetitions of the same face pairs occurred on a trial compared to when different face pairs occurred on a trial. Such a finding was revealed when *unique* faces were repeated on the same trial, which rules out the findings being due to presented of the same face (Summerfield et al., 2008). However, unlike Summerfield et al. (2008) experiment 5 presented the *same* stimuli in the same location. Alternative interpretations therefore must be sought rule out visual adaptation as explanation of the results here.

Evidence has recently emerged that the state of a neural population, such as whether the neural population has undergone visual adaptation, can alter the effect of TMS (Silvanto, Muggleton & Walsh, 2008). For example, the application of a TMS pulse to EVC after adaptation to colour has taken place has been reported to alter the characteristics of a phosphene depending on whether adaptation to red or green took place (Silvanto, Muggeton, Cowey & Walsh, 2007). Following adaptation, a phosphene was more likely to be reported as the adapted colour, but not the non-adapted colour, which led to the conclusion that TMS affects adapted neural populations to a greater extent than non-adapted populations. Whether adaptation to the familiar targets took place in this experiment is uncertain and it is also unclear how such adaptation would affect the coefficients of the monophasic Gaussian model. In particular, is uncertain whether the duration of visual suppression at ~100ms (de Graaf et al., 2014) is greater for adapted stimuli compared to non-adapted stimuli. If the duration of visual suppression is greater for adapted stimuli, then it would have an impact on the b_1 coefficient which was of critical interest to the results presented here.

In order to determine whether visual adaptation has an impact on the b_1 coefficients, an additional experiment would need to be completed. Visual adaptation can be demonstrated by presenting the participant with a grating tilting to the left for a minimum of 5 seconds causes a vertical grating to be reported as rotated to the right (Gibson & Radner, 1937). An adaption paradigm like that employed by Gibson & Radner (1937) could be integrated with single pulse EVC-TMS to demonstrate whether adaptation prolongs the duration of TMS-suppression at an SOA ~100ms. Such an experiment could have participants undergo foveal adaptation and subsequently present the Gabor patch that underwent adaptation again, which would then be followed by TMS at the SOAs used in this experiment. Participants could report whether the Gabor patch presented later on is tilted to one direction or another. A monophasic Gaussian model would then be applied to proportion correct as a function of TMS-SOA for adapted and non-adapted targets. If adaption prolongs the period of visual suppression, then the b_1 coefficient should be greater for adapted targets than non-adapted targets.n additional methodological issue in experiment 5 is the fact that

some of the stimuli are more similar to one another than others. For example, the pairs of arrows pointing left (< <) are similar to the arrows pointing right (> >), which may have had an impact on the magnitude of the difference between the familiar and unfamiliar bandwidth coefficients. It is possible that some participants may have mistaken these stimui for being the same, which would reduce the overall magnitude of the familiarity effect expected here. However, a BF which provided weak support *for* not against a familiarity effect was found despite such potential similiarities between stimuli. It could also be suggested that additional analyses are carried out which exclude stimuli that are similar to one another. A potential issue with such analyses is that the exclusion of trials where 'similar' stimuli occur could increase the overall amount of variance in trials where familiar and unfamiliar stimui take place. A consequence of increasing variance is the risk of noise promoting spurious outcomes that could be avoided if a greater number of trials are included within each analysis. The implication of this is that future research could test an identical hypothesis by choosing stimuli that differ from one another to a greater extent whilst simultaeneously including a sufficient number of trials to avoid increased variance producing spurious results.

Finally, a discrepancy appears to exist between the two different methods of averaging the monophasic Gaussian models. The first method involves averaging each set of monophasic Gaussian coefficients and subsequently inserting these averaged coefficients into the equation for a monophasic Gaussian. This methods appears to generate a model that does not correspond to the raw data points. However, an alternative method to averaging monophasic Gaussian models which is also displayed here. The alternative method involves solving each participant's monophasic Gaussian model across all values of x, which is over milliseconds in this instance. The alternative method then averages all participants models which have been solved across values of x, which produces a model that corresponds to the raw data to a greater extent.

To conclude, experiment 5 relied on b_1 coefficients to measure the duration of recurrent processing in EVC. It was expected that unfamiliar targets that occurred infrequently would trigger

more recurrent processing than familiar targets that occurred frequently (Rao & Ballard, 1999; Friston, 2005). The use of a b_1 coefficient to measure such a difference revealed that this prediction could be confirmed if more participants were included within the statistical analysis. This outcome suggests that the feedback of top-down prediction to EVC – and potentially V1 itself – could be responsible for the extent to which a feedforward input is triggered, which is in turn, accompanied by a revised top-down prediction that is fed back in response (Rao & Ballard, 1999; Friston, 2005). A potential confound exists, which relates to the phenomena of visual adaptation (Gibson & Radner, 1937). Repeating the familiar target could affect the duration of visual suppression at ~100ms (de Graaf et al., 2014). An additional experiment that could address this issue was outlined.

Chapter 4: Discussion

This chapter reports a series of experiments that set out to test the premises of the predictive coding approach to brain function (Rao & Ballard, 1999; Friston, 2005; Feldman & Friston, 2010). The critical premise of predictive coding that these experiments set out to investigate was whether top-down predictions are established in EVC that subsequently determine feedforward inputs to the rest of the brain in the form of prediction errors (Rao & Ballard, 1999; Friston, 2005). In the event of a prediction error, additional feedback is sent to V1 in order to suppress prediction error using a revised top-down prediction (Friston, 2005; Rao & Ballard, 1999). Experiments 2 and 3 set out to test a specific type of predictive coding: Bayesian predictive coding, which proposes that a top-down prediction is a prior-probability that represents the most likely causes of sensory input, given past experience (Friston, 2005). Under Bayesian predictive coding, prediction errors are produced when the prior-probability fails to represent the most likely causes of sensory inputs (Friston, 2005). When such events take place, the prediction error is integrated with the prior-probability according to Bayes theorem to produce a revised top-down prediction – the posterior, which is ultimately fed back to V1 (Friston, 2005). Evidence of such a process taking place was sought

in experiments 1 and 2, with the aim of creating a paradigm that manipulated such processes which could then be subjected to single pulse EVC-TMS.

One way of providing evidence for or against a process of Bayesian integration is to identify how differences in the precision of the prior-probability and the precision of the prediction error, affect the relative influence each one has on the formation of the posterior (Feldman & Friston, 2010). The posterior represents a revision in the most likely cause of sensory inputs, given the prediction error (Friston, 2005). Experiment 2 manipulated the precision of the prior-probability by explicitly informing participants of a high or low likelihood of target occurrence in a high probability context and a low probability context, respectively. The precision of the prediction error was made imprecise by calibrated Pr to 0.293, which is low. This meant that the relative precision of the prior-probability was greater than the prediction error, which should lead to a greater relative influence of the prior-probability when participants are presented with sensory inputs that are inconsistent with the prior-probability (Feldman & Friston, 2010). In the high probability context, an unlikely event – the target *not* appearing –should be influenced more by the prior-probability, leading to participants making more false alarms. In contrast, in the high probability context an unlikely event – the target *appearing* – should be influenced more the prior-probability, leading to participants making more misses. Both of these predictions were confirmed. The confirmation of an effect of a prior-probability on performance meant that the prediction of single pulse EVC-TMS in conjunction with such a paradigm could be considered.

It was assumed that TMS would reduce the precision of the prior-probability, which would improve performance on stimulus absent trials in the high probability context and improve performance on stimulus present trials in the low probability context (c.f. Feldman & Friston, 2010). However, the change in the pattern of participant's response in these two different contexts would rely on TMS reducing the precision of prior-probability in a way that was sufficient to produce a change in a participant's criterion (Corwin, 1994). A change a participant's criterion would reduce

the number of 'yes' responses in the high probability and context and increase the number of 'yes' responses in the low probability context. The way in which the criterion shift was produced in experiment 1 was by making the context too explicit to participants: contexts occurred in blocks and fixation served as a reminder of the current context on every trial. It is likely that prior-probability was too strong in this context, which meant that relying on TMS to reduce the precision of the prior-probability, which would in turn alter the participant's likelihood of making a target present response in the high probability context and a target absent response in the low probability context. There was also a concern regarding the number of false alarms that participants made in the high probability context. The false alarm rate was low in this context, not present in all participants judgments and was highly variable, suggesting that one of the behavioural phenomena that would be necessary for the existence of a prior-probability was absent during experiment 2. It may be unreasonable to expect participants to make false alarms – why would they report a target being present when there is nothing there, regardless of the task explanation? Experiment 3 aimed to address these concerns by changed the precision of the prior-probability on a trial-by-trial basis, and had participants make judgments of where a target appeared as opposed to judgments of whether a target appeared at all.

Experiment 3 relied on a modified version of Posner cueing paradigm (Posner, 1980), whereby the difference in luminance between a cue arrow, which could a valid or invalid indicator of target location on each tria and a non-cue arrow was manipulated on a trial-to-trial basis.. Manipulating the difference in luminance between the cue arrow and the non-cue arrow was expected to also manipulate the precision of the prior-probability (Feldman & Friston, 2010). When the difference between the cue arrow and the non-cue arrow and the cue arrow was large, the prior-probability was assumed to be precise. In contrast, when the difference in luminance between the cue arrow and the non-cue arrow was small (or they were equal) it was assumed that the prior-probability would be imprecise. Intermediate differences in the precision of the prior-probability were assumed to exist when intermediate differences in luminance existed between the cue arrow

and the non-cue arrow. It was predicted that PC and RT would vary as a function of the difference in luminance between the cue arrow and the non-cue arrow.

When the difference in luminance between the cue arrow and the non-cue arrow was large, it was expected that PC would be higher for valid trials than invalid trials. In contrast, when there was no difference in luminance between the cue arrow and the non-cue arrow, it was expected that no difference in PC would exist between valid trials and invalid trials. These predictions were confirmed. It was also predicted that a higher PC for valid trials than invalid trials would emerge at one of intermediate difference in luminance between the cue arrow and the non-cue arrow. This prediction was also confirmed. This confirms that the precision of the prior-probability that was set by the arrow cue can produce observable effects on behaviour. A similar pattern was expected for RT but an interaction between cue validity and cue luminance was not revealed. The invocation of a precise prior-probability at the beginning of each trial was also expected to affect participant's judgments on invalid trials when incorrectly judged the location of the target. When the precision of the prior-probability is high and target presence triggers a prediction error, the integration of the two to produce the posterior should display reveal evidence of the prior-probability (Feldman & Friston, 2010). This should lead to more errors in the hemifield cued by the cue arrow as the difference in luminance between the cue arrow and the non-cue arrow increases. This prediction was also confirmed. Taken together, this suggests that the integration of a precise prior-probability with a prediction error increases the likelihood that a target will be reported in the most likely location– the cued hemifield (Feldman & Friston, 2010; Friston, 2005).

Although an effect of the prior-probability was found here, a concern was raised about this paradigm as non-Bayesian explanations can account for the results without any mention of Bayes theorem. For instance, a prominent theory of attention, biased competition, would state that attention would be allocated to the cued hemifield due to participants being informed of the higher likelihood of target occurrence there (Desimone & Duncan, 1995), which can explain why PC was

higher for valid trials than invalid trials when the difference in luminance between the cue arrow and the non-cue arrow was largest. It may also be feasible that participants reported the target to be present in the cued hemifield on invalid trials because responses were speeded. If accuracy, not speed, was emphasized in the instructions participants such an effect may disappear. The issue of speeded responses is a major problem here. These experiments aimed to probe how establishment of a prior-probability that is integrated with a prediction error creates a visual representation (Friston, 2005). It may be that a visual representation is being created with the target appearing in the uncued hemifield but are not reporting it as present there because of the cue invalid cue preceding it.

In short, experiments 2 and 3 raise issues with paradigms that aim to use an experimentally induced prior-probability to probe the existence of Bayesian predictive coding (Friston, 2005; Feldman & Friston, 2010). Experiment 2 ran into problems with creating a criterion (Corwin, 1994) shift that reflected a precise prior-probability (Feldman & Friston, 2010) that could be too strong to be affected using EVC-TMS. Experiment 3 attempted to address this issue by altering the precision of the prior-probability on a trial-by-trial basis using an arrow cue that could differ in luminance from a non-cue arrow. Despite overcoming the issue of creating a precise prior-probability that was too strong, experiment 3 ran into theoretical issues concerning the effect of the prior-probability on visual representation. In experiment 3, was difficult to dissociate the process of creating a visual representation using the mismatch between the prior-probability and the current cause of sensory inputs – the prediction error – from the process that enhances representation in a location where a cue is expected to appear (Rao & Ballard, 1999; Friston, 2005; Desimone & Duncan, 1995; Summerfield & Egner, 2009). Experiment 4 and 5, however, did not run into these issues.

Experiments 3 and 4 aimed to elucidate a process similar to experiment 2: the process by which top-down predictions shape a visual representation within EVC (Rao & Ballard, 1999; Friston, 2005). However, experiment 4 aimed to investigate a fundamental prediction of predictive coding:

that feedforward input from EVC is conditional on the establishment of a top-down prediction beforehand (Rao & Ballard, 1999). This means that a top-down prediction must be established within V1 *before* V1 can provide outputs for the rest of the brain. (Rao & Ballard, 1999). The extent to which recurrent processes occur within EVC would be determined by whether sensory inputs are incorporated within such a top-down prediction. If sensory inputs are not incorporated within a top-down prediction, feedforward prediction error will be greater compared to when sensory inputs - captured by top-down predictions (Rao & Ballard, 1999). Experiment 4 aimed to test this fundamental assumption of predictive coding models rather than testing whether Bayes theorem can explain how prediction errors are integrated with a prior-probability to produce a revised top-down prediction – the posterior (Rao & Ballard, 1999; Friston, 2005). Moreover, experiment 4 and 5 attempted to demonstrate that this process created a visual representation as opposed to enhancing a visual representation via the recruitment of visual attention (Rao & Ballard, 1999; Desimone & Duncan, 1995).

Experiments 4 and 5 employed a similar experimental manipulation: some stimuli were more likely than others to occur any other trial. Experiment 4 presented participants with Gabor patches which could be the same or different on a given trial. There were Gabor patches that were the same that could occur more often and Gabor patches that were different from one another that could occur more often. Participants had to identify whether the stimuli were the same or different. Initially, it was expected that PC would be greater for the familiar Gabors relative to the unfamiliar Gabors. Such an outcome was not revealed despite addressing potential methodological issues. One issue was selecting the different in orientation between the two same Gabor patches on familiar same trials at random. For some participants, the difference in orientation on familiar same trials was too small to be discriminated and participants made a high number of false alarms. Note that a false alarm in this paradigm is considered to be when participants report stimuli that are different to be the same, unlike in experiment 1 when participants made a judgment of target presence when the target was absent. However, even when the difference in orientation wasfixed on familiar same

and familiar different trials, a higher PC for familiar Gabors relative to unfamiliar Gabors was not revealed. The absence of such a result persisted, even when the duration of Gabor presentation was increased from 10ms to 60ms, consistent with previous experiments that have integrated same-different judgments with EVC-TMS (Chambers et al., 2013). The reason for the lack of such an effect could have been due to how the stimuli were calibrated or the differential contribution of top-down predictions and prediction errors for familiar and unfamiliar targets.

Experiment 5 altered the method by which contrast was set (Levitt, 1970) in order to make the familiar stimuli recognizable whilst retaining task difficulty. Experiment 4 calibrated the stimuli by reducing the difference in contrast between the Gabors and the background, which meant that the stimuli were quite faint and difficult to make out. Experiment 5 employed a different paradigm whereby participants had to indicate whether the upper half or the lower half of a shape is brighter. The stimuli in experiment 5 were made recognizable by presenting one half of the shape at maximum luminance whilst changing the difference in luminance of the other to calibrate the stimuli. This way the stimuli are always presented a high luminance, increasing the ease at which one target can be differentiated from another whilst enabling the difficulty of the task to be manipulated simultaneously. However, it may not be the choice of target manipulation that led to the absence of a higher PC for familiar trials compared to unfamiliar trials. It may be that top-down predictions are more responsible for representing familiar stimuli than unfamiliar stimuli and that the revision of a top-down prediction due to a prediction is responsible for representation of unfamiliar stimuli (Rao & Ballard, 1999; Friston, 2005). The differential contribution of these processes may not produce a difference in PC; they could be two different ways of processing that achieve the same level of performance. As a result of this, experiment 5 did not contain any behavioural experiments and instead solely relied on EVC-TMS to probe the existence of an interaction between top-down predictions and prediction error.

As outlined previously, experiment 5 sought to identify whether more recurrent processing takes place for infrequently occurring, unfamiliar stimuli compared to frequently occurring familiar stimuli. The existence of these processes in response to these different types of stimuli would reveal that the violation of a top-down prediction - which is established in V1 prior to and conditional for – a feedforward prediction error to the rest of the brain (Rao & Ballard, 1999). A recurrent process takes place in response to prediction error, which involves conveying a revised top-down prediction back to V1 (Rao & Ballard, 1999). The extent to which recurrent processing took place was measured by fitting a monophasic Gaussian model to ΔPC as a function of EVC-TMS for familiar and unfamiliar targetsand calculating difference between the familiar b_1 coefficient and the unfamiliar b_1 coefficient. If the difference between these two coefficients was positive, it would suggest that the effect of EVC-TMS for unfamiliar targets extends over more SOAS than the effect of EVC-TMS for familiar targets. Such a difference would indicate that more recurrent processing accompany familiar targets compared to unfamiliar targets. Weak evidence for such a difference was revealed, which suggests that strong evidence for such a difference could be revealed if more participants were included within the analysis. It was not feasible to include more participants in the analysis due to time constraints on when this experiment needed to be completed.

Taken together, it appears that the presence of a top-down prediction within EVC could determine the extent to which feedforward outputs are sent to the rest of brain, which is consistent the key premise of predictive coding (Rao & Ballard, 1999). However, it remains unclear whether Bayesian inference is the process by which a top-down prediction is revised and sent back to V1 to create a new visual representation (Friston, 2005). In order to probe such a mechanism, a paradigm must be developed which avoids strong criterion (Corwin, 1994) shifts like in experiment 2 and avoids implicating the allocation of attention in order to meet task goals like in in experiment 3 (Desimone & Duncan, 1995). One candidate paradigm is to use random dot kinematograms (RDK) or moving dots in which responses can be made with eye movements or with simple yes or no responses. Freeman et al. (2010) revealed that the precision of sensory inputs determines the

relative influence of a zero motion prior-probability, based on the assumption that the majority of objects in the visual environment are stationary. Moreover, there have been demonstrations of the potential of recurrent interactions taking place between EVC and V5 (Silvanto et al., 2005a; Pascual-Leone & Walsh, 2001) and EVC and IPS (Koivisto, Mäntylä & Silvanto, 2010), which contribute to the representation of moving stimuli. Suppression of discriminating the direction of motion using V5 TMS takes place before EVC-TMS suppresses the same task with the same responses (Silvanto et al., 2005a), which suggests that top-down predictions concerning the direction of motion may be conveyed from V5 to EVC. Moreover, the presence of a moving phosphene after administering EVC-TMS is conditional on a V5 TMS pulse being presented beforehand (Pascual-Leone & Walsh, 2001), providing causal evidence for feedback, which could be in the form of a top-down prediction being sent to EVC. A natural question that arises from the results of these experiments is why motion was not used to probe the existence of Bayesian integration and the relative contribution of the precision of a prior-probability and a prediction error within EVC.

In order to the critical premises of predictive coding to be tested, a paradigm needs to be employed that enables events that occur over a short time period to be distinguished from one another. It appears to be easier to distinguish these short events using static stimuli compared to when using motion stimuli. For example, Silvanto et al. (2005a) presented RDKs for 48ms or 64ms, which required two pulses of V5 TMS or EVC TMS to successfully suppress the discrimination of motion direction. In order for motion to be perceived, the position of stimulus on screen must change on a frame-to-frame basis. This means that multiple frames need to be presented to the participants in order for the stimuli to be perceived as moving. Such a process means that stimuli must be present on screen for more than one frame. Presenting stimuli in such a way evokes a recurrent process whereby V5 relays information back to V1 (Silvanto et al., 2005a; Pascual-Leone & Walsh, 2001). However, when stimuli are presented for more than one frame, more pulses of TMS are required to suppress performance (Silvanto et al., 2005a), which means that some of the temporal resolution of TMS is lost. In contrast, presenting stimuli for one frame enables finer

resolution of events taking place within EVC, as demonstrated by Camprodon et al. (2010) who presented stimuli for one frame (14ms) and revealed two discrete windows whereby EVC TMS is critical for the categorization of an image to be a bird or a mammal at 100ms and 220ms, respectively.

Thus, the use of motion prevents TMS from being used to probe the existence of temporal events within EVC that occur on a narrow time scale. It is likely that the process of revising a top-down prediction within EVC occurs on a very narrow time scale (Rao & Ballard, 1999; Friston, 2005). Thus, it is critical that the stimuli employed in the experiment are presented for a very short period of time so the feedback-feedforward-feedback loop evoked by target occurrence occurs for a short time, enabling single pulses of TMS to isolate the discrete temporal events that enable a top-down prediction to be revised in response to a prediction error. It is important that future work avoids recruit Posner-cueing (Posner, 1980) like paradigms that are likely to recruit attention (Desimone & Duncan, 1995) and blocked paradigms with explicit instructions to probe the existence of Bayes theorem in the revision of a top-down prediction.

In conclusion, chapter 4 set out to investigate whether the predictions of Bayesian predictive coding (Friston, 2005) offer a feasible account of brain function, which could have been tested using TMS. Two paradigms were explored but were dismissed as unfeasible. Experiment 2 invoked a prior-probability that caused a strong criterion (Corwin, 1994) shift that TMS is likely to unable to change. Experiment 3 employed a paradigm that made it difficult to rule out the role of attention (Desimone & Duncan, 1995) in improving or worsening performance. In response to these issues, experiments 4 and 5 set out to investigate a more fundamental assumption of predictive coding models (Rao & Ballard, 1999), that establishing a top-down prediction in EVC needs to take place before any feedforward inputs take place in the form of prediction errors. Such prediction errors trigger the revision of a top-down prediction (Rao & Ballard, 1999). The existence of such a mechanism was explored using paradigms that enabled one set of stimuli (or stimulus) to occur more than another

set of stimuli (or stimulus). Experiment 4 offered a paradigm that was unfeasible, which was likely to be due to presenting stimuli at a low contrast that made them difficult to recognize as familiar. Experiment 5 addressed this concern by presenting familiar, frequently occur stimuli that were distinct from unfamiliar, infrequently occurring unfamiliar stimuli. All stimuli were presented at high luminance, enabling an easier process of recognition. The integration of such a paradigm with single pulse EVC-TMS revealed that more recurrent processing could take place for unfamiliar stimuli compared to familiar stimuli, which could be consistent with predictive coding (Rao & Ballard, 1999; Friston, 2005). Time limitations on data collection preventing conclusive evidence for such a difference from being obtained.

General discussion

General discussion: Summary

In this final chapter, the experimental findings will initially be considered in relation to the main hypotheses. The theoretical implications of these findings for recurrent processing will then be discussed (Lamme & Roeflsema, 2000), focusing on the relationship between DLPFC and EVC, how recurrent processes can take place within EVC, and how frontal and occipital sites could implement predictive coding in the human brain (Rao & Ballard, 1999; Friston, 2005). Methodological issues will then be addressed and reconciled where possible. Finally, suggestions for future research will be considered.

Experimental findings

These experiments set out to investigate how recurrent processing takes place within the human brain. The existence of a recurrent process were assumed to occur later on during visual processing, which reflects a change in the tuning of a neuron over the course of its response (Lamme & Roelfsema, 2000). In addition to this proposition, the idea of global recurrent processing whereby information exchange between frontal and occipital sites takes place during visual processing was

also under investigation (Lamme, 2006). Experiment 1 investigated the temporal dynamics of TMS-induced effects on two separate brain regions – EVC and DLPFC. Each of the TMS-induced effects occurred at approximately the same time, suggesting that processing that is critical for visual awareness and reporting target location occurred in parallel within DLPFC and EVC. Experiment 5 investigated how recurrent processing takes place within EVC itself. This experiment revealed weak support for a longer duration of processing accompanying unexpected events relative to an expected events.

Despite considerable interest in DLPFC in visual processing (e.g. Heekeren, Marrett & Ungerleider, 2008; Rahnev et al., 2016), experiment 1 was the first experiment to investigate when DLPFC becomes critical for basic visual processing using single pulse TMS. It also contained novel pre-registered statistical analyses. A main hypothesis of Experiment 1 was that a DLPFC-TMS induced effect would arise after the robust and reproducible EVC-TMS induced effect at ~100ms (Kammer, 2007; de Graaf et al., 2014). However, the fact that these two events appeared to be occurring at the same time suggests that recurrent processes are taking place outside the sites investigated here. Rather than the process being characterized by an event in EVC being triggered by DLPFC or vice versa, it appears that events are taking place within these areas simultaneously or in parallel. Such an effect may reflect a genuine neural phenomena or a limitation of TMS when used to distinguish discrete events happening between two different sites. The finding that such events occur in parallel was revealed using two different measures, which provide a hint at the process which DLPFC in particular is implicated in. The application of TMS to both sites affected judgments of target presence or absence and when participants reported the location of the target. The function being carried out within DLPFC must accommodate these two processes. Previous research has implicated DLPFC in the process of knowing whether a visual stimulus has been presented whilst the ability to report stimulus characteristics is unaffected (Lau & Passingham, 2006; Rounis et al., 2010). Here, it has been revealed left DLPFC is implicated in the ability to report a target as seen *and* characteristics of the target, such as its characteristics. However, the difference between the paradigms employed

in experiment 1 and Lau & Passingham (2006) must be examined. In Lau & Passingham (2006), it was possible for participants to successfully report the characteristics of a target without being aware of their success. However, in experiment 1 an effect of left DLPFC-TMS on the capacity to report the target as seen and the ability to locate the target may *both* require awareness. Instead, experiment 1 revealed that it might not be feasible to demonstrate the existence of recurrent processes between two sites by showing that a discrete DLPFC-TMS effect occurs after a discrete EVC- TMS effect. All that was revealed was the temporal order of TMS-induced effects was not consistent with the idea that serial recurrent processing was taking place between the sites that were stimulated. It is still possible that these sites are engaging in recurrent processing with sites that were not stimulated throughout the experiment. One potential candidate for such an interaction is the IPS, where there is potential for an interaction with EVC (Koivisto et al., 2014) and DLPFC (Vernet et al., 2015).

Chapter 4 investigated how recurrent processing takes place within EVC. Three experiments were completed which were subsequently considered for integration with EVC-TMS. Initially, Bayesian predictive coding was considered to generate predictions based on how recurrent processing would take place within EVC. The focus here was on the precision of the prior-probability and the precision of the prediction error (Feldman & Friston, 2010). The precision of the prior-probability relative to the precision of the prediction error determines the influence these sources of information have on the formation of the posterior (Feldman & Friston, 2010). The posterior represents a revised top-down prediction that represents the most likely cause of sensory inputs, given the prediction error. Experiments 2 and 3 aimed to establish a prior-probability that could be misleading indicator of what would occur on a small number of trials, which would cause participants to make predictable mistakes. Reducing the precision of the prior-probability was expected to reduce the relative influence of misleading prior-information and promote the relative influence of the prediction error (Feldman & Friston, 2010). In experiment 2 explicitly informing participants of high (HPC) or low likelihood (LPC) of target occurrencecaused false alarms when a target was absent and misses when the target was present, respectively. In experiment 2, the

application of EVC-TMS pulses could reduce the precision of the prior-probability when a target was unexpected present or unexpectedly absent, which would in turn, promote the relative influence of prediction error. This effect would lead a posterior that is influenced by the informative prediction error rather than the misleading prior-probability and improve performance. However, the manipulation produced a shift in criterion (Corwin, 1994) that was potentially too strong to be modulated by EVC-TMS. Experiment 3 flexibly altered the precision of the prior-probability on a trial-by-trial basis to avoid large criterion shifts but the use of a modified version of the Posner (1980) cueing paradigm implicated effects of EVC-TMS due to goal-directed attention (Desimone & Duncan, 1995). This confounding explanation led to the paradigm employed in experiment 3 to be dismissed as unfeasible.

An alternative hypothesis was generated based on a different premise of predictive coding (Rao & Ballard, 1999; Friston, 2005). The premise of predictive coding that was under investigation was whether a discrepancy between the top-down prediction and sensory input causes a prediction error to be fed forward which triggers a revision of the top-down prediction that is attempting to represent the visual environment. A discrepancy between the top-down prediction and the sensory input requires more processing to achieve visual representation compared to when no discrepancy exists. Initially, Gabor patches were chosen as stimuli (experiment 4) but then simple shapes were chosen instead, which were used in experiment 5. Experiment 5 manipulated the familiarity (or predictability) of a target decreases the amount of time that a stimulus is processed for relative to unfamiliar (or unpredictable) target. Weak evidence for this prediction was revealed, which suggests that the discrepancy between what is predicted and what is observed could be feasible mechanism that determines the magnitude of processing within EVC. When an unfamiliar target appears, it was hypothesized that a greater feedforward volley from EVC would take place. The magnitude of feedforward and recurrent processing that would take place was formulated using the predictive coding framework (Rao & Ballard, 1999; Friston, 2005). Under predictive coding, feedforward inputs to the rest of the brain are conditional upon a top-down prediction being established in EVC. Top-

down predictions represent was is most likely to occur given the statistical regularities of the visual environment. If top-down predictions successfully represent visual inputs, the magnitude of feedforward inputs w ould bereduced. This prediction error is conveyed to higher levels of the cortex, which in turn feed back a revised top-down prediction to V1. This experiment manipulated the statistical regularity of target appearance by making one target more likely to occur than others and revealed that unlikely, or unfamiliar targets were found to be affected by EVC-TMS for more SOAs than familiar targets. The finding, albeit based on weak evidence, suggests that statistical regularity could be one of the determinants of recurrent processes within EVC.

Gaussian modelling and hypothesis testing

Experiments 1 and 5 relied on the use of Gaussian models to identify whether TMS-induced effects took place and characterise the temporal dynamics of such effects. The constraints that were used appeared to be a critical determinant of whether a difference between active TMS and control TMS was discovered. A Gaussian model generated coefficients which describe the nature of a TMS-induced effect on performance. The TMS-induced difference between active TMS and control TMS was quantified used an amplitude coefficient. A biphasic Gaussian model produces two amplitude coefficients, a_1 and a_2, which means that two differences between active TMS and sham TMS can be produced as a function of TMS-SOA. A biphasic Gaussian model was used in the pre-registered analyses in experiment 1. A monophasic Gaussian model was also used, which produces one amplitude coefficient, a_1, which means that only one difference between active TMS and sham TMS can be quantified. All the pre-registered statistical analyses presented here depended on the a_1 or a_2 coefficients being significantly different from zero using a Bayesian one-sample *t*-test. Without such a difference being presented, the analyses could not proceed any further. In experiment 1, a_1 coefficients needed to different from zero as a function EVC-TMS and DLPFC-TMS in order to identify whether an DLPFC-TMS –induced effect occurred later in time than an EVC-TMS –induced effect. In contrast, experiment 5 relied on a_1 coefficients quantifying a difference between active TMS and

vertex TMS for familiar and unfamiliar targets. This condition had to be fulfilled in order for the duration of each of these effects - as measured by the bandwidth (b_1) coefficients – to be compared. Gaussian models were only successful at detecting a decrement in performance when the a_1 and/or a_2 coefficients were prevented from being greater than zero.

Experiment 1 used a biphasic and a monophasic Gaussian model with altered constraints to identify whether a difference between sham TMS and active TMS exists and whether it occurred at a specific time. The only alteration in constraints was applied to the amplitude (a_1 or a_2) coefficients. Some constraints enabled the a_1 or a_2 coefficients to be positive or negative whereas other constraints enabled the a_1 or a_2 coefficients to only be negative. Negative constraints were applied to specifically search for effects where active TMS impaired performance relative to sham TMS. Experiment 5 on the other hand used a monophasic Gaussian model with a constraint which prevented the a_1 coefficient from being greater than zero. Such a constraint was implemented in order to maximize the likelihood of the a_1 coefficient capturing the point where the largest decrement in performance between active TMS and vertex TMS was largest. In experiment 5, it was expected that such a constraint would quantify the robust and reproducible impairment produced by EVC-TMS at ~100ms (Kammer, 2007; de Graaf et al., 2014). Although previous experiments have used such models to capture the point where a TMS-induced effect is largest (e.g. Stevens et al., 2008; Rusconi et al., 2013; Chambers et al., 2013), these experiments went one step further and used the coefficients to test hypotheses about the nature of processing within difference cortical areas. Two different coefficients were used to test hypotheses about recurrent processing. In experiment 1, the temporal position coefficient, x_1, was used to identify if DLPFC-TMS-induced effect arise after the EVC-TMS at ~100ms. In experiment 4, the bandwidth coefficient, b_1, was used to identify whether EVC-TMS affected performance over a larger number of SOAs when a familiar target was presented compared to when a familiar target was presented. In experiment 1, a Gaussian model was successfully at demonstrating that a DLPFC-TMS induced effect occurs at the same point time to an EVC-TMS, suggesting that such a model is useful at demonstrating whether

discrete temporal events take place at two distal sites. In experiment 5 on the other hand, produced weak support for a difference in the duration of processing under different conditions of visual stimulation, which suggests that Gaussian models could also be useful at probing the magnitude of processing under different conditions.

Moreover, the use of monophasic Gaussian models also enabled an analysis pipeline to be developed in advance of data collection which enabled the choice of a Bayesian prior-probability (Dienes, 2011) to represent the likely outcomes of the experiment, given what was hypothesized. Monophasic Gaussian models also facilitated the choice of such prior-probabilities by enabling the creation of simulated data which could be used to assess the sensitivity of different types of prior-probability distributions to potential differences between conditions in advance of data collection. The most sensitive prior could then be included within a pre-registration protocol which is uploaded to the Open Science Framework. The use of pre-registration complements the use of Bayesian statistics because the parameters of the prior-probability, such as the mean difference that is most likely and the standard deviation around such a difference is subjective (Dienes, 2011). Pre-registering these parameters before statistical analyses are completed prevented the subjective parameters from being altered once data was collected, ensuring that an *a priori* hypothesis was tested once data collection had been completed.

Theoretical implications

Theoretical implications: Summary

The experimental findings presented here have implications for how recurrent processes take place between EVC and DLPFC and the nature of recurrent processes within EVC. Lamme (2006) distinguished between two different types of recurrent processing: local recurrent processing and global recurrent processing. Local recurrent processing refers to the initial phases of recurrent processing that occur after the feedforward sweep whereby sites within visual cortex exchange information with one another (Lamme, 2006). In contrast, global recurrent processing refers to

when a bidirectional exchange takes place between frontal regions, parietal regions and visual cortex following the feedforward sweep (Lamme, 2006). The finding that EVC and DLPFC become critical at approximately the same time during visual representation, and what this means for the idea of global recurrent processing throughout the brain isdiscussed (Lamme & Roelfsema, 2000; Lamme, 2006b). The early role of DLPFC at ~100ms was an unpredicted result, so this result is discussed in relation to other studies of the frontal lobe in visual processing. In particular, speculation is revealed about *how* visual information could reach the frontal lobe, potentially via the magnoceullar pathway and visual information from low spatial frequencies (Bar, 2003). Recurrent processing within EVC is also discussed. Here, sources of feedback to EVC are discussed and along with implications of early frontal involvement during recurrent processing in neural implementation of how predictive coding in the human brain (Friston, 2005).

Theoretical implications for recurrent processing: DLPFC and its relationship with EVC

TMS has successfully demonstrated that the application of an EVC-TMS pulse ~100ms after the onset of visual target can suppress awareness of target presence (de Graaf et al., 2014). It has recently been proposed that EVC-TMS effect at ~100ms reflects feedforward and recurrent processing (de Graaf et al., 2014). Experiment 5 indicated that the magnitude of recurrent processing can increase on the wider context in which a visual stimulus takes place. Moreover, de Graaf et al. (2012) revealed that the type of stimulus that is presented – a face or a house – affects the number of SOAs that an EVC-TMS induced effect lasts for, despite the fact that both effects arise at a similar time. This also suggests that recurrent processes are being affected by TMS in addition feedforward processes. Such findings are of relevance to TMS in studies of recurrent processing, as some researchers propose that recurrent processing is a critical determinant of whether a visual target is reported as seen (Lamme, 2006). The effect of EVC-TMS at ~100ms is likely to be due to the stimulation of V1, V2d and V3 (Thielscher et al., 2010). However, the latencies of V1, V2 and V3 responses are 34ms, 84ms and 55ms, respectively, which marks the beginning of the feedforward

sweep (Schmolesky et al., 1998; Lamme & Roelfsema, 2000). The suppression of awareness at ~100ms is considerably later than these latencies, which suggests that EVC-TMS is interfering with recurrent processes in addition to feedforward processes.

In particular, Lamme (2006b) distinguishes between two different types of recurrent processing: localized recurrent processing and global recurrent processing. Localized recurrent processing refers to when recurrent processing takes place within visual cortex itself, enabling the exchange of information between sites within visual cortex (Lamme, 2006). In contrast, global recurrent processing is characterized by the exchange of information between frontal sites, parietal sites and visual cortex (Lamme, 2006). Experiment 1 applied single pulses of TMS to EVC and DLPFC in order to identify when the largest difference between active TMS and sham TMS arises as a function time. Evidence against the hypothesis that the DLPFC-TMS effect would occur after the EVC-TMS at ~100ms was found. Instead, these events appeared to occur in parallel. Moreover, the DLPFC effect was revealed in a judgment where participants had to reveal whether not they saw the target, which suggests that events within DLPFC are taking place that are critical for awareness of visual stimuli (Lau & Passingham, 2006). However, the application of TMS to DLPFC also impaired a judgment of target location, suggesting that processes related detection and discrimination are taking place within DLPFC. What is interesting here are the implications of experiment 1 for the chronological order of local and global recurrent processing in DLPFC and EVC. Global recurrent processes whereby the feedforward sweep triggers a response within fronto-parietal regions occurs at the same time as local recurrent processes within EVC (Lamme, 2006). Thus, a mechanism appears to be in place that enables recurrent processes in DLPFC to be completed at the same time. It is important to distinguish between the feedforward sweep and local recurrent processing here.

It is likely that DLPFC and EVC are engaging in a recurrent interaction with sites elsewhere within the brain. Experiment 1 did not provide evidence against the idea of recurrent processing. Instead, it revealed that the temporal position of an EVC-TMS effect and the corresponding position

of a DLPFC-TMS effect are not consistent with a serial, discreate account of recurrent processes in EVC feed forward processing is completed prior to recurrent processes within DLPFC. Such an effect may be partially due to the resolution of TMS to probe such processes.

Theoretical implications for the role of DLPFC during recurrent processing

Experiment 1 revealed an effect of DLPFC-TMS at ~100ms, which had the same temporal position as the well documented EVC-TMS at ~100ms (de Graaf et al., 2014). DLPFC-TMS successfully produced a negative difference between active TMS and sham TMS when sham performance was subtracted from active performance. Such an effect was present within two different measures of performance. One of the effects was on participant's capacity to report a visual target as present and another effect was on a participant's ability to report the location of a visual target. Both of these effects had a temporal position that did not differ from the temporal position of the EVC-TMS at ~100ms. DLPFC appears to co-ordinate inputs from and has outputs to multiple sensory modalities, including the visual system (Klemen & Chambers, 2012). However, there is also potential for feedback based recurrent processing whereby DLPFC could modulate the initial response of stimuli of other posterior sites within the processing hierarchy during global recurrent processing (Lamme, 2006b). The process by which DLPFC could become engaged in visual processing early on will now be considered.

Although a large number of studies have applied rTMS to DLPFC and observed the effects on visual-based tasks (Rounis et al., 2010; Philiastides et al., 2011;Chiang et al., 2014; Rahnev et al., 2016), none have used single pulses of TMS to isolate when DLPFC is critical for post-stimulus visual representation. The early involvement of DLPFC highlighted here suggests that DLPFC is activated quickly by incoming sensory information. The question remains here is how, considering that such events take place at such a pace that they can be considered to occur in parallel to recurrent processes within EVC that also contribute to visual representation. Higher-order sites, such as the frontal lobes appear to be involved in an early process that could be taking place at ~100ms after the

onset of a visual stimulus (Bar, Kassam, Ghuman, Boshyan, Schmid, Dale, Hämäläinen, Marinkovic, Schacter, Rosen & Halgren, 2006). DLPFC, along with other sites within the frontal lobe, could be implicated in a process that utilizes a coarse representation to guide subsequent processing throughout the brain (Bar, 2003). A coarse representation has been proposed to be created via the magnocellular (M) pathway, which conveys low resolution, achromatic information at a high speed (Maunsell, Nealey & dePriest, 1990; Shapley, 1990; Merigan & Maunsell, 1993; Bullier & Nowak, 1995; Chen, Lakatos, Shah, Mehta, Givre, Javitt & Schroeder, 2006), which has been hypothesized to create a coarse representation of a visual input early in time (Bar, 2003). Bottom-up processing may be facilitated by such a bias because other processing streams, such as the parvocellular and koniocullular pathways, are conveyed at lower speeds and then complete the bottom-up phase of the representation (Tootell, Hamilton & Switkes, 1988). The coarse representation that is created using the M pathway facilitates recognition by biasing subsequent stimulus processing elsewhere in the brain (Kveraga, Boshyan & Bar, 2007; Bar, 2003). The early DLPFC-TMS effect may have been revealed at ~100ms because it is also involved in the process of utilizing a coarse representation to facilitate subsequent visual processing.

In an fMRI experiment, participants were presented with line drawings of everyday objects which were achromatic and low contrast (M-biased) or chromatic and isoluminant (parvocellular-biased) and their task was to indicate whether or not each object was greater in size than a shoe box (Kveraga et al., 2007). A greater BOLD response within a frontal site, the orbitofrontal cortex (OFC), was observed when M-biased stimuli were presented compared to parvocellular-biased stimuli (Kveraga et al., 2007). Firstly, when participants were presented with a target to be recognized in between two masks and to indicate whether or not they recognized the target during magnetoencephalography (MEG), a difference between recognized and not recognized objects emerged in the left OFC 130ms after the stimulus was presented was revealed (Bar et al., , 2006). Critically, a significant difference between presenting images of high (parvocellular-biased) and low spatial (M-biased) frequencies peaked 115ms after the onset of stimulation (Bar et al., 2006). This

peak at 115ms is similar to the onset of the DLPFC-TMS at ~100ms, which suggests that a tentative link may exist between DLPFC and OFC responses to visual stimulation.

The work of Moshe Bar and colleagues (2003, 2006, 2007) provides a potential explanation for how the frontal lobes can become critical for visual representation early on at ~100ms. The frontal lobes, the OFC in particular, is involved in process of achromatic visual information of a low spatial frequencies as a means of facilitating object recognition (Bar, 2003). Experiment 1 highlights that left DLPFC may also be involved in such a process. In experiment 1, stimuli were achromatic and of a relatively low spatial resolution. It can be stated that stimuli were of a low spatial resolution because stimuli were calibrated against a grey background at a luminance where Pr = ~0.5. It is difficult to compare the paradigm employed here to the paradigms employed by Bar and colleagues (2006, 2007) as their paradigms relied on participants being able to categorize stimuli rather than detect the presence of stimuli. However, the finding that the frontal lobes are involved early in visual processing in order to facilitate processing elsewhere within the brain is of interest here.

It must be highlighted that neither Kveraga et al., (2007) nor Bar et al. (2006) revealed any evidence of DLPFC being implicated in the process of object recognition using fMRI or MEG. However, an additional fMRI study has revealed evidence of DLPFC engaging in similar processes to those described by Bar and colleagues (2006, 2007) whereby the process of visual representation relies on a changing balance between higher-order and lower-order sites (Mundy, Downing, Honey, Singh, Graham & Dwyer, 2014). Here, participants completed difficult discriminations of natural stimuli (faces and natural scenes) and unnatural stimuli (random static dot patterns) during functional MRI. It was revealed improvements in discrimination were accompanied by a fall in BOLD response within V1 and V2 and increase in the BOLD response within V3 and V4 (Mundy et al., 2014). DLPFC also exhibited changes in the BOLD response as a function of accuracy: as accuracy increased DLPFC responses also fell (Mundy et al., 2014). Based on this evidence, it appears that the early responses of higher order sites, such as OFC and DLPFC, may have implications for the extent

to which visual representation relies on V1 and V2 or V3 and V4. DLPFC may be involved in a process that determines the extent to which re-entrant processing takes place in sites situated below it in the processing hierarchy.The early ~100ms DLPFC-TMS effect on ΔPr and ΔAcc may represent an effect on a process that determines the extent to which stimulus representation relies on the feedforward or recurrent processes. It can be speculated that DLPFC is implicated in an early response to visual inputs in addition to other sites within the frontal lobe, such as OFC (Kveraga et al., 2007; Bar et al., 2006), which could have implications for later stages of visual representation. In order for such a proposition to be demonstrated, an influence of DLPFC-TMS on posterior sites could be revealed. Consistent with the idea that re-entrant processing within stimulus-selective cortex within visual regions could be take place via early involvement of DLPFC, remote effects of DLPFC-TMS have been revealed in stimulus selective-regions, such as the face selective fusiform face area (FFA) and the house selective parahippocampal place area (PPA) during TMS-fMRI (Feredoes et al., 2011). Effects of DLPFC-TMS on BOLD responses outside the site of stimulation were revealed in a paradigm where participants have to retain a target in working memory (WM) and DLPFC-TMS was applied during a retention period when distractors were present or absent. Effects of DLPFC-TMS on sites outside the site of stimulation were only observed when distractors were present and within sites that were selective for the targets being retained in WM (Feredoes et al., 2011). This meant that DLPFC-TMS produced a remote effect upon the FFA when houses were retained and distracting face stimuli were present but not absent (Feredoes et al., 2011). This also meant DLPFC-TMS produced a remote effect upon the PPA when houses were retained and distracting face stimuli were present but not absent (Feredoes et al., 2011). It must be noted that a working memory paradigm was employed here and the questions within this TMS-fMRI experiment go beyond investigating visual representations that can be reported as present or absent. However, this experiment does demonstrate that DLPFC is capable of affecting representation in stimulus selective regions. Moreover, the effect of DLPFC-TMS was dependent on the presence of a distractor that was not selectivefor the currently presented item that was being retained in memory. What this suggests

is that DLPFC could be capable of biasing responses in favour of one representation over another representation in stimulus selective cortex. Such a process would represent a feedback-based recurrent interaction wherebyDLPFC and OFC could work in unison at ~130ms to bias processing in stimulus selective cortex (Bar, 2003). Whether this can occur whilst stimuli are currently being presented, rather than when stimuli need to be retained in working memory, is an interesting question for future research. Moreover, whether an interaction between DLPFC and OFC takes place in order to implement such an process remains to be determined. It would be a coincidence that both sites become involved in visual processing ~100ms after stimulus onset if they were not working in unison.

What remains unclear is whether feedback from the frontal lobes can have a direct or indirect effect on processing within EVC. Such feedback could indirectly reach EVC via the IPS, the PPA or the FFA under particular sets of circumstances (Kovisto et al., 2014; Vernet et al., 2015; Feredoes et al., 2011). For example, DLPFC would bias PPA responses when houses are presented and would bias FFA responses when houses are presented. Such feedback would be consistent with the idea of global recurrent processing proposed by Victor Lamme and Pieter Roelfsema (Lamme, 2006b; Lamme & Roelfsema, 2000). Experiment 5 revealed evidence that recurrent processing within EVC could change under different conditions of visual stimulation. No effort was made in experiment 1 to alter the amount of recurrent processing that occurred. Experiment 1 was motivated by to reveal distinct phases of visual representation in the frontal and occipital lobes rather than to demonstrate that different magnitudes of recurrent processing can occur within the same site to create a visual representation, which was a motivation of experiment 5. The early DLPFC effect at ~100ms could become the basis for future paired-pulse paradigms similar to Vernet et al. (2015). For example, a paradigm that attempts to alter the magnitude of recurrent processing within EVC under different conditions of visual stimulation but with paired pulses of TMS being delivered to DLPFC and IPS could be explored by future research. This idea will be explored further in a forthcoming section.

To conclude, the effect of DLPFC-TMS occurring in parallel to the effect of EVC-TMS was an unpredicted result. Instead, it was predicted that the DLPFC-TMS effect would occur after the EVC-TMS effect. However, previous research indicates that frontal influences can emerge early on during the process of visual representation. The early involvement of the frontal lobe could be caused by the fast transmission of information of low spatial frequency information to OFC in particular. However, it remains uncertain whether the early DLPFC response occurs via the magnocellular pathway in a similar way to OFC (Bar et al., 2006; Kveraga et al., 2007), which could affect representation in posterior sites such as the PPA, FFA and/or EVC (Bar, 2003). Such a bias appears to emerge at ~130ms (Bar et al., 2006), which coincides with the temporal position of the DLPFC-TMS effect at ~100ms revealed by experiment 1. Anatomical studies of the macaque brain have revealed that connections exist between OFC and DLPFC which may enable such an interaction to take place (Cavada, Company, Tejedor, Cruz-Rizzolo & Reinuso-Suarez, 2000). Moreover, there is evidence from TMS-fMRI demonstrating that DLPFC-TMS can modulate stimulus selective cortex in favour of one stimulus over another, which suggests that the frontal lobes may bias stimulus selective cortex in favour of one representation over another (Feredoes et al., 2011). Whether effects of the frontal lobes exert their influence on EVC via stimulus selective cortex or parietal cortex is unknown. All of these prospects are promising yet challenging avenues for future research on recurrent processing.

Theoretical implications: recurrent processing in early visual cortex and predictive coding

Experiment 1 set out to compare when EVC and DLPFC are critical for visual representation whereas experiment 5 set out to specifically investigate the process of visual representation within EVC itself. Previous experiments had revealed that the magnitude of recurrent processing within EVC can differ depending on what is presented to a participant (de Graaf et al., 2012). For example, the presentation of a face stimulus is suppressed by EVC-TMS for a larger number of SOAs compared to when a grating stimulus is presented despite that the fact the onset of such effects both arise at ~100ms (de Graaf et al., 2012; de Graaf et al., 2014). An increase in the number of SOAs where EVC-

TMS affects performance under one visual condition compared to another despite similar onsets of such an effect suggests that feedforward and recurrent processes are affected by the application of EVC-TMS pulses at ~100ms (de Graaf et al., 2014).

Experiment 5 revealed that recurrent processing within EVC could differ depending on the frequency at which a target of one identity appears compared to targets of other identities. Here, it was assumed that the bandwidth coefficient of a monophasic Gaussian model can successfully measure the amount of time where EVC-TMS has affected performance.. It was hypothesized that unfamiliar stimuli would be affected by EVC-TMS for a longer duration than familiar stimuli, which would reflected in the bandwidth coefficients applied to ΔPC as a function of EVC-TMS for familiar and unfamiliar targets, respectively. Such a difference would arise from the violation of a prior-expectation being greater when an unfamiliar stimulus is being presented compared to when a familiar stimulus is presented (Rao & Ballard, 1999; Friston, 2005). According to predictive coding, feedforward inputs from V1 to the rest of the brain are conditional on a top-down prediction being established in V1 (Rao & Ballard, 1999). The discrepancy between the top-down prediction and current sensory input is then the basis for feedforward inputs to the rest of the brain in the form of prediction error (Rao & Ballard, 1999). The prediction error is conveyed forwards in the processing hierarchy and a revised prior-expectation is fed back to V1 in response (Rao & Ballard, 1999). Unfamiliar stimuli were predicted to trigger more prediction error as they were less likely to occur on each trial than familiar stimuli which were more likely to occur on each trial. It was expected that more recurrent processing would occur when unfamiliar stimuli were presented because they would not match top-down predictions due to their low likelihood of occurring on each trial. More recurrent processing would take place in order to feed back a revised top-down prediction in response to the prediction error to V1 (Rao & Ballard, 1999; Lamme & Roelfsema, 2000). The Bayes factor produced quantified weak support for a difference in the duration of the EVC-TMS effect for unfamiliar stimuli compared to familiar stimuli, which suggests that such a conclusion is tentative. This outcome suggests that the extent to which recurrent processing takes place within EVC may not

be solely determined by the physical attributes of the visual stimulus as suggested by de Graaf et al. (2012), such as whether it constitutes a face or a grating, but could instead be determined by the greater context in which a visual stimulus appears. In particular, it appears that the frequency (or familiarity) of a target is critical to the amount of processing that accompanies it within EVC.

EVC and recurrent processing: Implications for visual awareness

Lamme (2006) proposed that recurrent processes rather than feedforward processes may be necessary for conscious representation. Lamme & Roelfsema (2000) proposed that recurrent processes can be distinguished from feedforward processes within a particular brain area based on the time that they are taking place. Thus, the proposition by Lamme (2006) is that a representation that can be consciously perceived occurs later on in time and can be distinguished from earlier feedforward processes that are prerequisite for the later recurrent phases for conscious representation. Initial support was garnered for this proposition. Silvanto et al. (2005) applied pulses of TMS at sub phosphene threshold levels to V5 followed by a supra-phosphene threshold pulse to V1, a moving phospene was perceived. The authors concluded that feedback to V1 must take place in order for what is represented in V5 to be consciously perceived (Silvanto et al., 2005). This is particularly interesting in light of predictive coding models, as such models can explain why TMS-effects at later SOAs arise because they feedback could be responsible. Under predictive coding, the feedback could be representation that is available for conscious report and such feedback must be conveyed to V1 (Rao & Ballard, 1999; Friston, 2005; Clark, 2013). The emergence of such feedback in response to prediction error, could be a critical determinant of what is consciously reported (Clark, 2013). However, evidence from TMS suggesting that early EVC-TMS effects affect nonconscious processes and later EVC-TMS effects affect conscious processes is not always revealed (Koivisto et al., 2010).

The absence of a difference between unconscious and conscious perception at early and late SOAs, led to the proposition that recurrent processing is not critical for awareness but for enhancing

the visual representation that reaches awareness (Koivisto, Kastrati & Revonsuo, 2013). This was supported by an experiment which had participants categorize images as animals or non-animals during EEG (Koivisto et al., 2013). The images of the animals or non-animals to be categorized were masked or not masked. Presenting a mask was found to reduce the reported clarity of the image but left the ability to categorize the stimuli as animals or non-animals in tact (Koivisto et al., 2013). EEG recordings revealed that a reduction in image clarity but a preservation of accuracy that was produced by the mask emerged between 150ms and 250ms whereas no difference emerged up 150ms after stimulus onset. On the basis of this result, it was concluded that recurrent processing is not critical for awareness *per se* but for the improvement of a coarse representation that has already reached awareness (Koivisto et al., 2013). Consistent with this, Camprodon et al. (2010) revealed that EVC-TMS affects performance at early SOAs of 100ms and late SOA of 220ms, which were inferred as effects on feedforward and recurrent processes, respectively. However, a participant's capacity to report something as present has been also affected by EVC-TMS at SOAs beyond ~100ms (Allen et al., 2014, Heinen et al., 2005; Wokke et al., 2012; Koivisto et al., 2014). Thus, the investigation of TMS effects beyond ~100ms at later SOAs does appear to be of relevance to awareness but it remains uncertain whether such effects can be exclusively attributed to conscious processes. The investigation of unconscious and conscious processes has implications for how feedforward and recurrent processes reach awareness under the predictive coding framework (Clark, 2013).

Predictive coding may offer a feasible account of how feedforward and recurrent processes operate and how they contribute to visual awareness (Clark, 2013). Bayesian predictive coding argues that a participant will perceive the feedback recurrent product which is triggered by a prediction error (Friston, 2005; Clark, 2013). Experiment 5 did not test this proposition, rather it intended to show that the extent to which recurrent processing taking place is determined by the likelihood a target has of occurring on each trial. In experiment 5, it was revealed that targets that are unlikely to appear are subjected to more recurrent processing than stimuli that are likely to

appear. This could confirm one of the critical premises of predictive coding – that top-down predictions attempt to represent current sensory inputs based on the regularities of the visual environment (Rao & Ballard, 1999) or what is most likely to occur given past experience (Friston, 2005). When current sensory inputs are not regular (Rao & Ballard, 1999) or unlikely to occur based on past experience (Friston, 2005), a prediction error is generated in response to, and conditional on, a top-down prediction failing to represent sensory inputs. The confirmation of this central tenet of predictive coding suggests that predictive coding could be of use to the study of awareness as suggested by Clark (2013). Instead of focusing on whether EVC-TMS affects unconscious processing at the early SOAs and conscious processing at later SOAs (e.g. Koivisto et al., 2014), it may prove useful to explore whether use the central tenets of Bayesian predictive coding to explore how feedforward and recurrent processes contribute to the creation of a visual representation that can be consciously reported (Clark, 2013).

Probing feedforward and recurrent processes with TMS: Do early EVC-TMS effects interfere with feedforward processing and later EVC-TMS effects interfere with recurrent processing?

A debate that has arisen from applying EVC-TMS at different SOAs is how the emergence of discrete TMS-induced effects as a function of TMS-SOA relate to feedforward and recurrent processes (de Graaf et al., 2014). The term discrete TMS-induced effects refers to differences between conditions arising at two SOAs, which are separated by SOAs where no differences exist between active TMS and control TMS (e.g. Camprodon et al., 2010). Some experiments have applied EVC-TMS at SOAs of 60ms and 90ms post-stimulus and reveal dissociable effects on unconscious and conscious processing, respectively (Hurme, Koivistio, Revonsu & Railo, 2017). This suggests that a dissociation could exist between early, feedforward conscious processes and later, recurrent processes that take place around 100ms (de Graaf et al., 2014). Other experiments only apply EVC-TMS at early SOAs of 40 – 60ms, 40 – 80ms, 90 – 130ms and very late SOAs of 280 – 320ms and reveal differential EVC-TMS induced effects at all but the 40-80ms window(Allen et al., 2014). Another experiment that applied TMS over a range of SOAs reveal EVC-TMS induced effects at

100ms and 220ms with no effects of TMS at SOAs of 120ms – 200ms (Camprodon et al., 2010). What becomes apparent here is that feedforward and recurrent processes could be occurring at ~100ms but then additional effects beyond 200ms also emerge at later SOAs (de Graaf et al., 2014; Hurme et al., 2017; Allen et al., 2014; Camprodon et al., 2010). One reason for this discrepancy is that some experiments do not apply TMS at SOAs that are late enough to produce EVC-TMS induced effects beyond 200ms. Another reason is the choice of stimuli and TMS stimulation parameters. For example, Camprodon et al. (2010) fixed stimulator output for all participants and no participants reported phosphenes whereas experiments 1 and 5 along with Allen et al. (2014) all applied TMS at 120% of each participant's phosphene threshold. However, it still becomes apparent that different kinds of recurrent processing could be taking place in each of the experiments presented here. The inconsistency between different studies that reveal or do not reveal early or late and TMS effects in the literature may arise from the choice of different TMS parameters and visual stimuli.

The choice of stimuli or the choice of response the participant needs to make appears to be what enables an effect of EVC-TMS to emerge at ~200ms. Camprodon et al. (2010) presented participants with animals or birds and asked participants to categorize them as such and revealed an EVC-TMS induce effect at 220ms. However, Allen et al. (2014) simply asked participants to report whether they saw a stimulus and report its characteristics and produced an effect of EVC-TMS at an SOA of 280 – 320ms (Allen et al., 2014). Thus, the emergence of an additional window which is likely to be due to recurrent processes (Allen et al., 2014) is not likely to be due to higher-order categorization but could instead be due to higher-order processes related to determining whether something is present or absent. In support of this, EVC-TMS applied at SOAs of 236 – 259ms (Wokke et al., 2012) and 250 – 280ms (Heinen et al., 2005) impaired performance when participants had to identify whether a frame differed orthogonally from a background of line segments. Thus, it appears to be whether or not a particular type of visual stimulus is seen as opposed to relying on higher order categorization alone. As experiment 5 suggests, it may be difficult to dissociate early TMS effects on feedforward processing from later TMS effects on recurrent processing because the two

are intimately related and may overlap in time. Experiment 5 suggested that the magnitude of recurrent processing could be intimately related to the feedforward processing that precedes it. In particular, experiment 5 suggests that prediction error that was triggered by unfamiliar stimuli is accompanied by more recurrent processing than familiar stimuli. More recurrent processing takes place when an unfamiliar target takes place because these targets may equire the revision of a top-down prediction to be represented, which trigger recurrent processes to a greater extent (Friston, 2005).

It is apparent that feedforward and recurrent processes are occurring at ~100ms but process underlying additional TMS effects beyond ~200ms remain elusive. From this discussion it appears that the existence of early feedforward and late recurrent processes within EVC using TMS can be revealed in two different ways. One way is to demonstrate that EVC-TMS produces an effect an early SOAs and later SOAs with no effects of TMS in between the late and early effects. An example of this is Camprodon et al. (2010), who revealed two SOAs where active TMS differed from control TMS: one at ~100ms and another at 220ms. Alternatively, another method is to demonstrate that EVC-TMS effects on feedforward and recurrent processes both take place around ~100ms (de Graaf et al., 2014). Feedforward processes occur prior to ~100ms and recurrent processes take place to a greater extent beyond ~100ms without being separated by SOAs where differences between active TMS and control TMS are absent. An example of this can be found in the findings of experiment 5, which revealed that EVC-TMS effects could occur over a larger number of SOAs when recurrent processes are taking place. Similar findings were revealed by de Graaf et al. (2012) who demonstrated that EVC-TMS effects occur over a larger number of SOAs when a judgment is made on faces compared to when a judgment is made on gratings despite the fact the latency of these effects both emerge at ~100ms. Experiment 5 and de Graaf et al. (2012) suggest that the interference of recurrent processes within EVC using TMS is revealed by an EVC-TMS effect occurring at ~100ms but also persists over a larger number of SOAs.

It may be the case that these two different ways of demonstrating recurrent processes are not mutually exclusive. Rather than EVC-TMS interfering with two discrete windows, it may simply be that the effect of EVC-TMS at ~100ms affects feedforward and recurrent processes, and later effects such as those revealed at and beyond ~200ms reflect the tail end of this process such as the findings of experiments applying TMS beyond 200ms (e.g. Camprodon et al., 2010; Allen et al., 2014; Wokke et al., 2012; Heinen et al., 2005). It should also be noted that it is uncertain whether the recurrent processing in EVC at ~100ms is due to horizontal connections, feedback connections or a mixture of the two (Lamme & Roelfsema, 2000). Thielscher et al. (2010) revealed that the induced electric field is greatest in V2d when EVC-TMS is applied at ~100ms but V3 and V1 are also affected. The implication of this is that EVC-TMS could be affecting feedback from V3 to V2 or V2d to V1 or horizontal connections within V1, V2 and V3 themselves. It is likely to be a mixture of three but the limitations of relying on Faraday's law of electromagnetic induction within EVC prevent the distinction between these different types of recurrent processing within EVC.

To conclude, examination of the literature suggests that are two discrete windows whereby visual representation in EVC is affected by recurrent interactions. However, experiment 5 and the findings of de Graaf et al. (2012) suggest that feedforward and recurrent processes are present at ~100ms. Early segments of this effect could be attributed to feedforward processes and later segments of this effect could be attributed to recurrent processes. Such an effect could arise from horizontal connections and/or feedback connections.

Bayesian predictive coding: Potential implications for recurrent processing

A series of experiments were carried out which had the initial aim of producing a behavioural paradigm that could generate the conditions that would be required to probe whether Bayesian inference/predictive coding characterize human brain activity (Rao & Ballard, 1999; Friston, 2005). The development of a paradigm that produced behavioural conditions that could successfully be affected by TMS *and* test predictions generated by the Bayesian predictive coding framework,

that are distinct from alternative accounts, proved challenging. To recap, Bayesian predictive coding proposes that the top-down prediction is a prior-probability, which represents the sensory input that is most likely to take place given past experience (Friston, 2005). In the most relevant implantation top-down prediction is fed back to V1 via feedback connections (Friston, 2005; Felleman & Van Essen, 1991). Like the predictive coding approach proposed by Rao & Ballard (1999), the prior-probability needs to be established in V1 before feedforward inputs to the rest of the brain can take place in the form of a prediction error (Friston, 2005). When the revision of the prior-probability takes place, it is integrated with the prediction error according to Bayes theorem to produce the posterior (Friston, 2005). The posterior represents a revised top-down prediction given the prediction error which aims to successfully represent future sensory inputs (Friston, 2005). The relative influence of the prior-probability and the sensory information, when there is a discrepancy between the two, results in prediction error. The integration process results in a posterior which is determined by their precision of the prediction error relative to the prior, which then constitutes a new prior (Feldman & Friston, 2010). The term precision in the context of Bayesian processes refers to uncertainty of the causes of the prediction error or uncertainty of the most likely causes of sensory inputs, given past experience (Feldman & Friston, 2010). When the precision of the prior-probability is greater than the precision of the prediction error, the posterior will represent what has been most likely in the past to a greater extent than the prediction error (Feldman & Friston, 2010). In contrast, when the precision of the prediction error is greater than the precision of the prior-probability, the posterior will reflect the prediction error to a greater extent than what has been most likely given past experience (Feldman & Friston, 2010).

Experiments 2 and 3 aimed to produce a paradigm where a participant's responses could be influenced by what has been most likely to occur in the past and the discrepancy between past experience and current sensory inputs. Single pulse TMS was then intended to isolate the relative contribution of the prior-probability and the prediction error when they are integrated to form the posterior (Friston, 2005; Feldman & Friston, 2010). In experiment 2 this involved explicitly informing

participants of the likelihood of target occurrence throughout a block. Two different types of block could take place – a high probability context (HPC) and a low probability context (LPC) where the target had a high and low probability of occurring, respectively. In each of these contexts, visibility of the target that was identical in each context was low, which was intended to reduce the precision of the prediction error. In the HPC, prediction error would be triggered on trials where the target was absent. In the LPC, prediction error would be triggered on trials where the target was present. The experiment was designed so the precision of the prediction error would be low in each of these contexts. The experiment was also designed to make the prior-probability explicit in each context. The combination of an experimentally induced difference in precision whereby the precision of the prior-probability is greater than the precision of the prediction error, which would leading to a posterior, or percept, that is influenced more by top-down predictions.

However, experiment 2 represents a cautionary note on how prior-probability can be made explicit to participants, especially when the aim of an experiment is to reduce the precision of the prior-probability using TMS. The effect of the explicit prior-probability was likely to have been too strong, producing a criterion that is unlikely to be manipulated by TMS. Experiment 3 attempted to address this issue by flexibly changing where a target could appear on a trial-to-trial basis using a modified version of Posner (1980) cueing paradigm (Feldman & Friston, 2010). As predicted, participants were better at detecting targets that appeared in the visual hemifield indicated by an arrow cue compared to when a target appeared in the opposite hemifiled to an arrow cue. Moreover, participants made more errors in the direction of the arrow cue when they unsuccessfully reported target location. The effect of the cue on proportion correct and errors suggesting that an influence of a prior-probability could be adjusted on a trial-to-trial basis. However, the use of a modified version of th Posner-cueing paradigm (Posner, 1980) implicated goal-directed attention in performance (Desimone & Duncan, 1995). The use of goal-directed attention to bias representation explains the advantage of presenting an arrow cue which can validly indicate upcoming target location. The paradigm employed in experiment 3 cannot distinguish

between effects of EVC-TMS on a prior-probability that indicates the sensory input that is most likely to take place, given past experience and the effects of EVC-TMS on preparing visual cortex for a target in an expected location (Desimone & Duncan, 1995; Friston, 2005). Such a paradigm does not test the core of predictive coding models which state that there are relative contributions of top-down prediction and prediction error to visual representation (Rao & Ballard, 1999; Friston, 2005, but see Feldman & Friston, 2010).

Paradigms developed by other laboratories have also developed paradigms that test central tenets of predictive coding (Sherman, Seth, Barrett & Kanai, 2015). Sherman et al. (2015) had participants complete a visual search task in conjunction with a near-threshold Gabor detection task. Similarly to experiment 2, the likelihood of the Gabor target appearing differed in each block of trials. Participants were instructed to search for a letter within a visual search array and detect the Gabor which had a different likelihood of occurring in a block or to ignore the Gabor and just perform the visual search task (Sherman et al., 2015). An effect of expectation and report was revealed, which suggested that participants were more likely to make judgments of target presence when the likelihood of target occurrence was high but not when it was low. Such decisions were also made with greater confidence. These effects did not interact with an attention manipulation, which had participants to divert or not their attention to a visual search array whilst completed a Gabor detection task. The probabilistic information provided in this experiment related to the likelihood of the Gabor appearing within a block, which meant that attention and expectation were manipulated orthogonally, which prevents attention and expectation from being confounded (Summerfield & Egner, 2009). Such a manipulation prevents goal-directed top-down attention from being viewed as an alternative mechanism for effects of probabilistic cues on target detection, like in the case of experiment 2 (Desimone & Duncan, 1999).

Such a task has also been successful in revealing how prior-expectations affect how incoming information is represented within EVC. The use of this task in conjunction with EEG

revealed evidence that top-down predictions of stimulus presence and stimulus absence are conveyed by oscillations in the alpha band (Sherman et al., 2016). Calculating the average time-frequency point on the occipital electrode that responded more to hits than misses revealed that pre-stimulus (-119ms) alpha at 10Hz predicted whether a yes or a no response would be made under each expectation condition (25% or 75%) (Sherman et al., 2016). Thus, it appears that expectations set prior to target occurrence, which are probabilistic in their nature, can determine the response that will be made afterwards. Recall that the behavioural paradigm used here and mentioned (Sherman et al., 2015) revealed that there was no interaction between attention and expectation; instead, expectation conveyed an independent benefit to Gabor detection. The independent contribution of expectation to performance suggests that pre-stimulus alpha at 10Hz and its effect on judgments of stimulus presence is not due to attention.

Experiment 5 demonstrates that the ongoing context in which targets appear could also give rise to a prior-expectation that could determine how sensory information is processed within EVC. Sherman et al. (2016) reveal the pre-stimulus processes that could determine how forthcoming visual information is processed whereas experiment 5 demonstrates the post-stimulus consequences of such expectations. The fact that pre-stimulus alpha predicted 'yes' and 'no' responses in Sherman et al. (2016), suggests that a common substrate could exist for the establishment of prior-expectations in early visual cortex, which determine how forthcoming sensory information is processed. Pre-stimulus occipital activity in the alpha band 10Hz may be the means by which a top-down prediction as established in experiment 5, whereby unexpected, unfamiliar stimuli were subjected to more recurrent processing than expected, familiar stimuli. Taken together, these experiments provide tentative confirmation of some the central tenets of predictive coding.

Top-down predictions are stated to arise from higher-order sites within the brain, which are fed back to lower-order sites within the brain (Rao & Ballard, 1999; Friston, 2005). However, an

outstanding question is where do top-down predictions arise from? Frontal regions, such as OFC appear to be a promising candidate based on the finding that low spatial frequencies of an image triggered a left OFC response ~130ms after stimulus onset (Bar et al., 2006) which could be achieved via the M pathway (Kveraga et al., 2007). The early involvement of DLPFC at ~100ms suggests that DLPFC may also be involved in the process of creating an early coarse representation that has implications for subsequent processing. Such effects draw a parallel between predictive coding (Rao & Ballard, 1999; Friston, 2005) and the 'initial guess' generated by low spatial frequencies and the M pathway (Bar, 2003; Kveraga et al., 2007; Bar et al., 2006). Whether DLPFC generates top-down predictions that represent prior-probability distributions is unknown. Moreover, how such influences are conveyed via feedback connections is uncertain. There is evidence from functional MRI suggesting that DLPFC (Fletcher, Anderson, Honey, Carpenter, Donovan, Papadakis & Bullmore, 1999) and OFC (Nobre, Coull, Frith & Mesulam, 1999) exhibit a greater BOLD signal in response to the violation of a prior-expectation. Such findings are of limited use when examining the central tenets of predictive coding because the BOLD signal is ambiguous, in that, the increased BOLD signal could represent a prediction error or the creation of a new top-down prediction or the integration of the top-down prediction and the prediction error to create a posterior (Rao & Ballard, 1999; Friston, 2005). Of critical importance here are the temporal order of events and direction of information flow from higher-order sites, such as DLPFC and OFC, to sites below in order to represent visual information. Such effects could be exerted via DLPFCs influence on stimulus selective cortex (Feredoes et al., 2011) or on the IPS (Vernet et al., 2015).

Although experiment 5 revealed weak support for more recurrent processing taking place when a discrepancy exists between top-down predictions and sensory inputs compared to when no dissonancy exists, the origin of top-down predictions remains uncertain. An answer to the origin of such a question is important, as the idea of 'initial guesses' could arise from the frontal cortices (Bar, 2003) and early visual cortex itself within V1, V2d or V3 (Rao & Ballard, 1999). Such a question is important to the relevance of predictive coding as a theory of cortical responses or an explanation of

extra-classical receptive field properties within EVC (Friston, 2005; Rao & Ballard, 1999). Such a question relates to where top-down predictions originate from and whether such top-down predictions determine the contents of feedforward processes and relative contribution of recurrent processes during visual representation (Lamme & Roelfsema, 2000). For example, visual representation via the revision of top-down predictions could take place within visual cortex itself, without assistance from DLPFC.

To conclude, the experiments here provide tentative support for the key tenet of predictive coding (Rao & Ballard, 1999). Predictive coding proposes that top-down predictions that arise from feedback must established in V1 before any feedforward inputs can be sent to the rest of the cortex (Rao & Ballard, 1999; Friston, 2005). Feedforward inputs are prediction errors, which represent a discrepancy between the top-down prediction and current sensory inputs. After a series of preliminary experiments, experiment 5 revealed weak evidence for this proposition. Top-down predictions represent the regularity of the environment (Rao & Ballard, 1999), which may be understood as a probability distribution based on what is most likely to occur given past experience (Friston, 2005). When a prediction error takes place, additional feedback is necessary to convey a revised top-down prediction back to V1 to suppress prediction error (Friston, 2005). Experiment 5 manipulated the frequency at which one target occurred relative to other targets, and identified whether more processing takes place in EVC when an infrequent event takes place. Weak evidence for this proposition was revealed, suggesting that more recurrent processing takes place when unlikely stimuli take place. The increase in recurrent processing could be due a revised top-down prediction being fed back to V1 in response to prediction error. A parallel could be drawn between the early DLPFC effect revealed in experiment 1 and the coarse representation formed within OFC, potentially via low spatial frequency elements of an image and the M pathway (Bar, 2003). Whether early responses with these frontal sites have the potential to modulate EVC is unknown. The influence of DLPFC could be exerted on parietal cortex or stimulus selective cortex, such as the PPA and the FFA.

Methodological limitations

Methodological limitations: summary

A number of methodological concerns were identified that may have an impact on the interpretation of the results. First of all, issues with Gaussian model fitting and overfitting are discussed, together with mitigating counterarguments. Furthermore, examination of two key studies from the literature reveals different ways that evidence of recurrent processing can be revealed when TMS is applied to two different sites. These different explanations are outlined and formulated into an additional method of determining whether recurrent processing is taking place. Finally, measures of stimulus visibility and confidence in visual judgments are discussed as such measures are prevalent in the literature but were not included in the experiments presented here. Such measures are discussed and their implications for studies of predictive coding and recurrent processing are outlined.

Overfitting using monophasic and biphasic Gaussian models

In experiment 1 and experiment 5, the earliest SOA where a pulse of TMS was delivered to EVC was 60ms. However, the model fits sometimes produced adjusted r^2 values that were negative, which may be the product of fitting a Gaussian model with too many coefficients relative to the number of data points (Hawkins, 2004). Such values were negative or low due to overfitting whereby a large number of coefficients are fitted to an insufficient number of data points. Examples can be found in the appendix.The adjusted r^2 value is reduced in order to penalize models that fit a large number of coefficients to a small number of data points.

In order to provide a more comprehensive investigation of recurrent processing and produce Gaussian models with better adjusted r^2 values, it would be beneficial to increase the number of SOAs where TMS is administered. Increasing the number of SOAs where TMS is administered would increase the number of data points to which the Gaussian model are fitted and as a consequence reduce the reduction adjusted r_2 for fitting a Gaussian model to a small number of data points. It

appears that administering TMS at a number of SOAs prior to visual stimulus onset could be useful in this respect (see Sherman et al., 2016). This adjustment would be particularly useful when investigating pre-stimulus influences on recurrent processes within EVC. Pre-stimulus impairments produced by the application of EVC-TMS have also been found to prevent awareness of visual stimuli when TMS is applied at SOAs of 60ms and 80ms prior to stimulus onset are of relevance here (Jacobs et al., 2012). Pre-stimulus effects may affect the top-down prediction that needs to be established prior to a sensory input, which is conditional for a feedforward prediction error to take place (Rao & Ballard, 1999; Friston, 2005). Experiment 5 revealed that prior-expectations, which have been demonstrated to be present prior to stimulus onset (Sherman et al., 2016), could also determine the extent to which recurrent processes are devoted to incoming sensory information. By applying EVC-TMS to SOAs prior to stimulus onset, the experiments presented here may provide a better window to investigate the extent to which prior-expectation shapes subsequent processing within EVC at ~100ms. This would also enable TMS to be administered at more SOAs than in the TMS experiments presented here, which could prevent overfitting from taking place when fitting Gaussian models to performance as a function of TMS-SOA.

The presence of some negative r^2 values in experiment 1 does not invalidate the results. In experiment 1 pilot data was used to calculate the standard error around the point where Pr = 0.5 and was calculated as a function of trial number and the point where the standard error began to asymptote was identified. This is illustrated in figure 1. This process can be found in figure 1. Such a trial number is important because it indicates the number of trials where standard error begins to stabilize given the variability of responses. The trial number where variance stabilizes could then be selected, which ensures that reasonably stable data points could be obtained at each TMS SOA. As a result of this precaution, the negative r^2 values do not indicate that anything is wrong with the data set; instead, it indicates that TMS was not administered at a sufficient number of SOAs to compensate for the penalty that is applied to an adjusted r^2 value when a monophasic or biphasic Gaussian is applied to data. Overfitting was more prevalent when a biphasic Gaussian was applied

compared to when a monophasic Gaussian was applied, which is because a biphasic Gaussian model has more coefficients. Examples of this can be found in the appendix. Practical issues can also be used to counter the potential issue posed by negative r^2 values produced by the model fits. In some cases, it is not feasible to include a large number of SOAs because it is not feasible to complete an experiment where active TMS and control TMS due to the time taken for a participant to complete the experiment. To illustrate this further, TMS is usually completed in control blocks and active blocks, with a break in between each block. TMS experiments are usually completed in sessions. In the case of the TMS experiments presented here, the smallest number of sessions was two 2 hour sessions. The largest number of sessions was four 2 hour sessions. To conclude, negative r^2 values do not indicate problematic data. Instead, it can be argued that they reflect a necessity to administer TMS at a feasible number of SOAs.

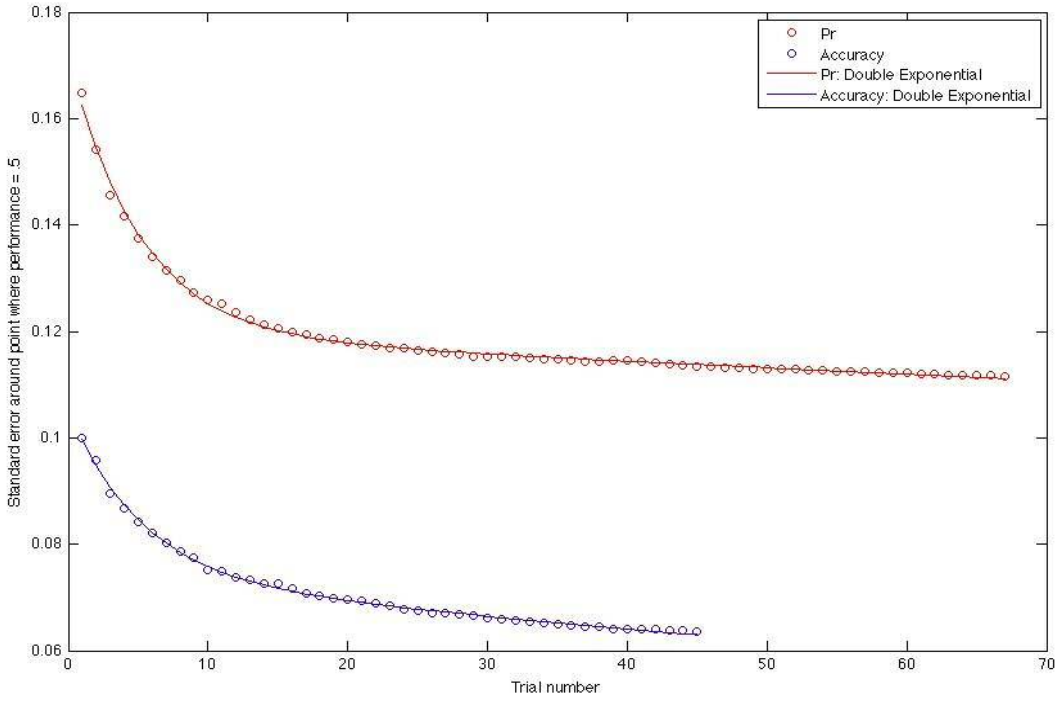

Figure 1. An illustration of where the standard error around the point where normalized measures of performance equal 0.5 begins to asymptote as a function of trial number.

The use of Gaussian models and how their coefficients relate to recurrent processes

In experiment 1, evidence for recurrent processes taking or not taking place relied on the use of temporal position coefficients. If the mean difference between temporal position coefficients for DLPFC- and EVC-TMS induced effects was different, it could be concluded that a recurrent interaction was taking place. Experiment 5, on the other hand, relied on a mean difference between bandwidth coefficients to determine whether recurrent processing was taking place within EVC. Two influential experiments regarding how recurrent interactions taking place will be discussed and a potential revision to the use of Gaussian models in TMS research will be proposed. This discussion will revolve around how it is potentially misleading to rely on the temporal position of one TMS effect relative to another TMS effect to demonstrate whether recurrent processing is taking place or not. This is because some experiments have revealed evidence of recurrent processes taking place when EVC-TMS and IPS-TMS effects emerge at the same temporal position but the duration of these effects differ. The duration of one TMS effect relative to another TMS effect may be of use when using Gaussian models to investigate recurrent processes.

A number of different approaches have been developed which enable the existence of a recurrent interaction between two different cortical sites to be revealed by the application of single pulse TMS. One approach was presented which relies on the temporal order of when TMS-induced effects emerge for one site relative to TMS-induced effects arising for another site (Silvanto et al., 2005a). The sites that were stimulated in Silvanto et al. (2005a) were V5 and EVC. Evidence of a recurrent interaction taking place was inferred by revealing two discrete SOAs where EVC-TMS affected motion direction discrimination at 40-60ms and at 80 – 100ms. However, there was an SOA lying in between these two SOAs - 60 - 80ms - where EVC-TMS produced no effect on performance. It was at the SOAs of 60 – 80ms that an effect of V5 –TMS emerged. Silvanto et al. (2005a) concluded a temporal dissociation between feedforward processing and recurrent processing exists at 40 – 60ms and 80 – 100ms, respectively, within EVC. They also concluded that evidence of recurrent processing could be found that a V5 effect emerged where no EVC effect was present (60 – 80ms),

which was followed by an additional period (80 – 100ms) where EVC was critical. Using this logic evidence of feedforward and recurrent processes can be concluded based on mutually exclusive TMS effects that arise one after the other at a series of SOAs. However, this is not the only method of concluding whether a recurrent interaction is taking place. In a similar experiment, Koivisto et al. (2014) applied single pulses of TMS to IPS and EVC in task where participants had to discriminate different shapes. In this experiment, evidence of a recurrent interaction between IPS and EVC was concluded in a different way. The application of EVC-TMS impaired shape discrimination at SOAs of 60ms, 90ms and 120ms. IPS-TMS did not impair performance at an SOA where EVC-TMS had no effect; instead, IPS-TMS impaired performance at 90ms, which co-occurred with and was in-between a sequence of EVC-TMS induced effects. This raises the question as to whether there are different ways to conclude that a recurrent interaction is taking place.

Koivisto et al. (2014) revealed evidence of a recurrent interaction using the overlap of EVC-TMS and IPS-TMS induced effects whereas Silvanto et al. (2005b) revealed evidence of a recurrent interaction by revealing a mutually exclusive sequence of EVC-TMS and V5-TMS induced effects. If the logic of Silvanto et al. (2005b) was applied to Koivisto et al. (2014), no evidence of recurrent processing would be revealed because effects of IPS-TMS and EVC-TMS did not arise in a sequence of mutually exclusively SOAs. Instead, in Koivisto et al. (2014) IPS-TMS produced an effect that overlapped with a sequence of EVC-TMS effects. This suggests that an additional method of revealing recurrent processing is to demonstrate that two sites become critical for processing at a similar time, but then to also demonstrate that the duration of processing within one site is greater than processing within another. This has implications for how Gaussian models are used to conclude that recurrent interactions are taking place between two different cortical sites. Experiment 5 revealed weak evidence that the bandwidth of a monophasic Gaussian model can be used to distinguish between different types of recurrent processing. Experiment 1, on the other hand, revealed that the temporal position coefficients can be used to distinguish whether critical events within EVC and DLPFC are happening at the same time or different times. If the temporal position

coefficients were being used to determine whether EVC and V5 were engaging in recurrent processing, the analysis would be successful in revealing such evidence based on the findings of Silvanto et al. (2005b). However, if the temporal position coefficients were being used to determine whether a recurrent interaction was taking place using the results of Koivisto et al. (2014), no evidence of a recurrent interaction would not be revealed because the centre of the EVC-TMS and IPS-TMS induced effects would both be at 90ms. This means that temporal position coefficients alone cannot solely be used to determine whether recurrent processing is taking place, which was the logic behind the pre-registered hypotheses tested in experiment 1. Instead, the duration of one TMS effect relative to another may also be of interest when investigating recurrent processing.

In order for Gaussian models to successfully produce evidence for recurrent interactions like those reported between EVC and IPS by Koivisto et al. (2014), Gaussian models need to be used to demonstrate that two processes are taking place at the same time but differ in their overall duration. It appears that the temporal position coefficients and the bandwidth coefficients need to be used to determine whether a recurrent interaction is taking place. In the case of Koivisto et al. (2014), the temporal position coefficients would need to be used in conjunction with Bayesian statistics to show that IPS and EVC are engaged in critical processing at the same time. Evidence for feedback from IPS subsequently modulating processes within EVC would then need to be obtained using bandwidth coefficients. A mean difference in bandwidth coefficients would then demonstrate that processing within EVC, which occurs for a greater duration than IPS, could be subjected to recurrent feedback from IPS. There is evidence to suggest that the amount of recurrent processing that takes place in EVC is susceptible to change. For example, de Graaf et al. (2012) revealed that EVC becomes critical for longer periods of time depending on the stimuli that are presented and experiment 5 revealed weak evidence for changes in recurrent processing depending on the likelihood of a particular target appearing. Moreover, experiment 1 revealed that the use of Gaussian models in conjunction with Bayesian statistics can be used to demonstrate temporal positon coefficients produced by two different TMS sites have the same onset.

To conclude, the experiments presented here introduced two ways of using the coefficients from Gaussian models to demonstrate the existence of recurrent processes between and within different cortical sites. However, examination of two different studies of recurrent processing reveal that the premises behind the statistical analyses presented here may not be sufficient to demonstrate that recurrent processes are taking place. The use of temporal position coefficients may lead to evidence for recurrent processing in some circumstances and against recurrent processing in others, despite the fact that conventional methods of analysing data produce evidence for recurrent processing. In order to accommodate these potential issues, an additional, revised method is proposed. The revised method relies on using temporal position coefficients to show that two different sites become critical for processing at the same time, and the bandwidth coefficients to illustrate the potential for feedback from one site to affect processes within the other.

Future directions

Future directions: summary

Key findings that require further investigation are why DLPFC becomes involved in visual processing very early on following the onset of visual stimulation, and the determinants of recurrent processing within EVC itself. Here, future experiments are proposed that aim to investigate the interaction between coarse representations in frontal sites and whether they affect processing elsewhere within the brain. In particular, it is also important to identify whether early DLPFC responses can be triggered by the magnocellular pathway. An interaction may also be taking place between IPS and DLPFC, which is also of interest to how recurrent processing takes place within the human brain.

DLPFC, OFC and recurrent processing: Suggestions for future research

There has been renewed interest in investigating the involvement of frontal sites in perceptual decision making processes despite interest usually arising from cognitive control studies relating to attention and motor control (Rahnev et al., 2016; Heekeren et al., 2008). Here, it was

revealed that an effect of DLPFC-TMS emerges at ~100ms, which is early on during visual processing. The orbitofrontal cortex (OFC) has also been implicated in visual processing early at ~130ms (Bar et al., 2006). What remains uncertain is whether early events within OFC are related to the early events within DLPFC reported in experiment 1. The work of Moshe Bar and colleagues suggests that the early response within OFC takes place in order to recruit low spatial frequencies and achromatic visual information to modulate subsequent, slower visual processes (Bar, 2003; Bar etal. 2006; Kveraga et al. 2007). It remains uncertain whether DLPFC is also implicated in these processes, which is an interesting question for future research.

Previous research has revealed that DLPFC can modulate the responses of stimulus selective cortex, such as the face selective FFA and the house selective PPA (Feredoes et al., 2011). Early DLPFC responses reported at ~100ms and early OFC responses at ~130ms (Bar et al., 2006) may be related, whereby OFC and DLPFC could work in unison to recruit visual information from the M pathway to modulate subsequent, slower visual processes (Bar, 2003). The first question that naturally arises from this is whether the early response of DLPFC, like OFC, is triggered by visual information conveyed by the M pathway. The second question is contingent on the DLPFC response being triggered by the M pathway. This second question is whether the early response of DLPFC (that could be) triggered by the M pathway can subsequently modulate visual processing in distal sites throughout the brain.

One way to address both of these questions is to use stimuli that bypass or do not bypass the M pathway in conjunction with DLPFC-TMS, which could reveal whether the early DLPFC is specific visual information conveyed back via the M pathway. This demonstration could implicate the early DLPFC response with the early OFC response which has been reported to be specific to information conveyed by the M pathway (Bar et al., 2006; Kveraga et al., 2007). This would implicate DLPFC in the process of utilizing a coarse visual representation to modulate subsequent, slower visual processing throughout the brain (Bar, 2003). Stimuli have been developed which bypass the

magnocellular pathway, called S-cone stimuli (Sumner, 2006; Sumner, Nachev, Vora, Husain & Kennard, 2004; Sumner, Adamjee & Mollon, 2002). S-cone stimuli stimulate short wave cones but not long and medium wave cones, which have previously been successful at revealing processes that the magnocellular pathway has been implicated or not implicated in (Sumner, 2006; Sumner et al., 2004; Sumner et al., 2002). These S-cone stimuli that bypass the M pathway could be used in conjunction with luminance stimuli that do not bypass the M pathway. Participants could make exactly the same judgments as experiment 1: judgments about target presence or absence along with judgments of stimulus location. This task would be completed in conjunction with single pulses of DLPFC-TMS at the SOAs used in experiment 1 (60ms to 330ms in increments of 30ms). If the effect of early DLPFC-TMS is specific to medium to long wavelengths that are conveyed by the M pathway, but not short wavelengths that are not conveyed by the M pathway, then the early DLPFC-TMS affect should depend on the stimuli that are presented. If the early DLPFC-TMS effect is specific visual information conveyed by the magnocellular pathway, then the early DLPFC-TMS effect would be present for luminance stimuli but not S-cone stimuli.

An additional experiment that could be carried out could incorporate S-cone and luminance stimuli with TMS-fMRI. Such an experiment could reveal whether early DLPFC responses that could be triggered by the magnocellular pathway modulate the response of distal sites within the brain. In such a paradigm, participants would be presented with luminance or S-cone stimuli whilst pulses of DLPFC-TMS are administered during functional MRI. If DLPFC utilizes visual information conveyed by the M pathway in order to modulate processing elsewhere as suggested by Bar (2003), then a remote effect of DLPFC-TMS on BOLD response should be specific to stimuli that are conveyed by the M pathway. The administration of DLPFC-TMS should add noise (Walsh & Cowey, 2000) to processes involved in utilizing magnocellular information. The addition of noise could preclude the process by which DLPFC modulates subsequent, slower processing. If DLPFC modulates visual processing by utilizing information conveyed by the M pathway, then remote effects of TMS elsewhere in the brain would be revealed when luminance stimuli are presented but not when S-

cone stimuli are presented. This dissociation would emerge because luminance stimuli do not bypass the M pathway, which would implicate DLPFC and in turn, enable DLPFC-TMS to modulate the BOLD response elsewhere within the brain. However, if early DLPFC response is specific to information conveyed by the magnocellular pathway, then administration of DLPFC-TMS during fMRI whilst S— cone stimuli – that bypass the M pathway – would not affect BOLD response. In contrast, if the early DLPFC response is not determined by the wavelength of visual information and is instead responsible for a general modulation of posterior sites, no difference in the modulation of the BOLD response would be revealed when comparing S-cone stimuli to luminance stimuli.

To conclude, the early DLPFC response at ~100ms revealed by experiment 1 is an interesting result because other sites have been implicated in visual processing at a similar time, albeit with different measures of neural events (Bar et al., 2006). The OFC appears to be involved in utilizing information conveyed by the M pathway in order to modulate subsequent, slower visual processing (Bar, 2003, Bar et al., 2006; Kveraga et al., 2007). In order to demonstrate whether DLPFC is partaking in similar processes, an experiment has been proposed which presents stimuli that bypass or do not bypass the M pathway. If the early DLPFC response is specific to the M pathway, then effect of DLPFC-TMS should be specific to luminance stimuli but not S-cone stimuli. Moreover, if DLPFC modulates subsequent, slower processes in the brain like OFC, by utilizing information conveyed by the M pathway, remote effects of DLPFC-TMS on the BOLD response should be specific to also be these luminance stimuli but not S-cone stimuli.

DLPFC, IPS and recurrent processing: Suggestions for future research

IPS appears to be important in processes that relate to judgments of stimulus presence (Koivisto et al., 2014). Experiment 1 revealed that DLPFC is also important for judgments of stimulus presence. The exact relationship between these sites is unclear yet has potentially important implications for global recurrent processing, whereby frontal and parietal regions engage in bidirectional information exchange with each other and EVC (Lamme, 2006). Tentative evidence for

an interaction between DLPFC and IPS was revealed by Vernet et al. (2015) who revealed that a DLPFC-TMS pulse cancels out the effect of an IPS-TMS pulse when participants report whether a change in a bistable stimulus has taken place. However, Vernet et al., (2015) did not apply single pulses of TMS to IPS or DLPFC post-stimulus. Instead, pulses of TMS were applied in between two consecutive presentations of a bistable stimulus. This methodological difference comparison of the findings of Vernet et al. (2015) to experiment 1 and the findings of Koivisto et al. (2014) difficult. In order to reconcile these experiments, which may be revealing evidence of recurrent processing, a comprehensive study that compares the onset of an IPS-TMS effect to DLPFC-TMS effect should be carried out.

Such an experiment would apply single pulses of TMS to DLPFC or IPS after the onset of a visual target and investigate how these effects relate to one another using single Gaussian models. Comparison of experiment 1 of the DLPFC-TMS effect revealed at ~100ms along with the finding that IPS-TMS effects can emerge at 90ms (Koivisto et al., 2014), suggests that these events are going on at the same time. However, Koivisto et al. (2014) revealed evidence of a recurrent interaction going on between two sites by demonstrating an *overlap* of two TMS-induced effects rather than showing that one TMS effect arose before or after another. A single pulse TMS experiment comparing the nature of IPS and DLPFC-TMS induced effects appears to be necessary in order to conclusively demonstrate that IPS and DLPFC are or are not engaging in a recurrent interaction. As outlined in the methodological limitations section, an additional method of revealing recurrent processing is to demonstrate that two sites become critical for processing at the same time, but then to also demonstrate that the duration of processing within one site is greater than processing within another. This logic could be applied to an experiment investigating recurrent processes between IPS and DLPFC.

The application of single Gaussian models would be useful in such an experiment. It would be expected that the temporal position coefficients for IPS-TMS and DLPFC-TMS effects would arise

at approximately the same time. The bandwidth coefficients could be used to determine whether the duration of one of these effects differ. Recall that Koivisto et al. (2014) demonstrated that an overlap between EVC and IPS-TMS effects at 90ms with EVC-TMS producing an effect over a larger number of SOAs at 60ms, 90ms and 120ms. It is possible that feedback from IPS is modulating processes that take place within EVC between 90ms and 120ms. Similar logic could be used to generate predictions about recurrent interactions between DLPFC and IPS. Experiment 5 demonstrated that bandwidth coefficients could be used to quantify the duration of a TMS-induced effect. The bandwidth coefficients could be used to determine whether more processing occurs within DLPFC than IPS despite the fact that TMS-induced effects for both sites emerge at the same time. If feedback from DLPFC is modulating responses within IPS, then the bandwidth of the IPS effect would be greater than the bandwidth of the DLPFC effect, but both TMS-induced effects would arise at the same time. In contrast, if DLPFC recurrent processes within are being modulating by recurrent processes within IPS, the bandwidth of the DLPFC-TMS effect would be greater than the bandwidth of the IPS-TMS effect. Such an experiment would confirm whether an interaction between IPS and DLPFC is taking place as suggested by Vernet et al. (2015).

To conclude, IPS may be implicated in visual processing along with DLPFC but methodological differences between the findings of experiment 1 and other studies which investigated DLPFC and IPS using TMS make comparison difficult. To address this difficulty, an experiment has been proposed which applied pulses of TMS to DLPFC and IPS during the same task in order to compare their critical time course.

Mental imagery within EVC reflect the influence of DLPFC or elsewhere within the frontal lobe?

DLPFC has been implicated in visual working memory (Ester, Sprague & Serences, 2015) but there is growing evidence that EVC is also involved in the generation of images that are sustained within working memory (Albers, Kok, Toni, Dijkerman & de Lange, 2013; Kok et al., 2014; Cattaneo, Bona & Silvanto, 2012). Here, we reveal that the application of TMS to DLPFC at ~100ms affects

more basic processes, such as those related to stimulus presence. This evidence, combined with the idea that the frontal lobes may bias processing in stimulus selective cortex due to their early responses (Bar et al., 2006), suggests that imagery within EVC and coarse representations evoked by stimulus onset (Bar, 2003) may be related to one another. Early coarse representation may be responsible for the process of bias within stimulus selective cortex (Bar, 2003), which could evoke templates that correspond to such a coarse representation within EVC (Cattaneo et al; 2012). The use of a coarse representation may correspond to a top-down prediction which needs to be conveyed to V1 before feedforward inputs can take place to the rest of the cortex (Rao & Ballard, 1999; Friston, 2005).

Evidence for this proposition is as follows. The work of Moshe Bar and colleagues revealed that the M pathway and low spatial frequencies of an image evoke early responses within OFC at ~130ms (Bar et al., 2006; Kveraga et al., 2007). Moreover, experiment 1 revealed that the application of TMS to DLPFC revealed an effect at ~100ms. DLPFC is implicated in the maintenance of images within visual working memory (Ester et al., 2015). Interestingly, there is evidence from TMS and fMRI studies suggesting that vision and imagery may share a substrate within EVC (Cattaneo et al., 2012; Kok et al., 2014). Causal evidence for imagery taking place within EVC was revealed by an experiment which requested participants to imagine clock hands representing different times after a period of visual adaptation (Cattaneo et al., 2012). The application of EVC-TMS facilitated mental imagery when an overlap existed between the adapted region of space and the location where a spatial judgment had to be made. A link also exists between top-down predictions and mental images (Kok et al., 2014). The association of a tone with a grating of a particular orientation leads to a greater BOLD response in voxels responsive to the associated orientation when the grating is absent (Kok et al,. 2014). This suggests that a link exists between top-down predictions in EVC and the process of mental imagery. Taken together, this suggests that low spatial frequency information and the M pathway could evoke an early coarse representation (Bar,

2003; Kveraga et al., 2007; Bar et al., 2006), which may evoke a template of the stimulus itself within EVC (Kok et al., 2014; Cattaneo et al., 2012).

Evidence of DLPFC being able to evoke such representations comes from a TMS-fMRI experiment, which stimulated DLPFC whilst faces or houses had to be maintained in working memory (Feredoes et al., 2011). Effects of DLPFC-TMS on BOLD responses in the FFA emerged when faces had to be retained and effects of DLPFC-TMS on BOLD responses in in the PPA emerged when houses had to be retained during distraction. What remains uncertain is whether *top-down predictions* of such visual representations are sent back to EVC in order to perceive an object as opposed to retaining such an object within working memory. Investigating whether such feedback takes place may provide a potential explanation for the early effect of DLPFC-TMS on performance, which may or may not be related to translating a coarse representation into a template that represents top-down predictions (Bar, 2003; Rao & Ballard, 1999; Friston, 2005). Such top-down predictions may be conditional on feedforward inputs to the rest of the cortex in the form of prediction errors (Rao & Ballard, 1999; Friston, 2005).

One method of examining whether the frontal lobes (OFC and/or DLPFC) are responsible for such representations within EVC is to adopt a similar paradigm to Kok et al. (2014). Kok et al. (2014) identified the voxels within EVC that were responsive to a grating which was associated with a tone that appeared beforehand. The association of the tone with such a grating was assumed to create a top-down prediction of the grating when the tone was presented. The same approach could be adopted in a TMS-fMRI experiment that applied TMS to DLPFC in circumstances where a top-down prediction of target identity, which evokes a 'template' of the expected stimulus within EVC (Kok et al., 2014). An effect of DLPFC could be established not by seeking a remote effect of DLPFC-TMS within EVC per se, but seeking a remote effect of DLPFC in EVC voxels that represent an expected visual stimulus. The demonstration of such a mechanism would elaborate on why weak evidence for a difference in recurrent processing when unexpected, unfamiliar stimuli were presented compared

to expected, familiar stimuli in experiment 5. For example, if the top-down prediction represents a *template* that matches an expected sensory input, prediction error would be suppressed within EVC (Rao & Ballard, 1999). However, if the top-down prediction represents a template that does not match an unexpected input, prediction error would be increased within EVC (Rao & Ballard, 1999).

To conclude, in addition to being implicated in studies of awareness, DLPFC has also been implicated in working memory processes (Ester et al., 2015; Feredoes et al., 2011). The maintenance of an image within working memory implicates EVC (Catteneo et al., 2012), which might be related to top-down predictions within EVC (Kok et al., 2014). Additional studies on how DLPFC affects remote regions, such as EVC, must be carried out to assess whether templates are evoked by coarse representation within frontal sites, such as OFC and DLPFC, are conveyed back to EVC as a top-down prediction with the aim of successfully represented visual information (Bar, 2003; Friston, 2005). Carrying out such research would elaborate on why DLPFC is involved early in visual processing and offer a potential explanation for more recurrent processing taking place when sensory inputs are unexpected compared to when they are expected.

General discussion: Summary

This research aimed to identify how feedforward and recurrent processes in the frontal and occipital lobes contribute to visual representation (Lamme & Roelfsema, 2000). Investigation of when the frontal lobes contribute to visual representation compared to the occipital lobes revealed evidence of parallel processing, with the frontal lobes appearing to be critical at the same time as EVC at ~100ms. Early involvement of DLPFC may be related to additional frontal processes within OFC occurring at ~130ms (Bar et al., 2006), which could be speculated to provide a coarse representation of visual inputs based on low frequency information and the magnocellular pathway (Kveraga et al., 2007; Bar, 2003). Predictive coding offers a framework to explain when and why feedforward and recurrent processes take place (Rao & Ballard, 1999; Friston, 2005). Weak evidence was revealed for more recurrent processing taking place when an unfamiliar, unexpected stimuli

take place relative to familiar, expected stimuli when TMS was applied to EVC. This suggests that the discrepancy between a top-down prediction and a current sensory input may determine the extent to which recurrent processing takes place (Rao & Ballard, 1999; Friston, 2005). Critically, this finding shows that the regularity of the environment affects how stimuli are processed (Rao & Ballard, 1999). Under predictive coding, a top-down prediction that reflects the statistical regularity of the environment must be established before feedforward inputs can take place (Rao & Ballard, 1999; Friston, 2005). If a top-down prediction is unsuccessful, additional feedback is necessary to revise a top-down prediction to represent incoming sensory information (Rao & Ballard, 1999; Friston, 2005). Evidence presented here suggests that predictive coding may explain processes that occur within EVC. An additional promising approach is to identify whether a template based on a coarse OFC representation is conveyed back to EVC from DLPFC, which in turn, determines the amount of recurrent processing that takes place within EVC. Another promising avenue for future research is to identify whether the early DLPFC response is triggered by the M pathway. In order to investigate if this is the case, single pulse DLPFC-TMS could be combined with stimuli that bypass or do not bypass the M pathway, which could reveal whether the early effect is specific to visual information conveyed by the M pathway. Moreover, such a paradigm could be combined with fMRI to identify whether effects of DLPFC-TMS on the BOLD response elsewhere in the brain are contingent on DLPFC being presented with information from the M pathway. Finally, studies that compare the temporal structure of DLPFC and IPS-TMS effects should also be carried out to identify whether IPS can mediate a recurrent interaction between EVC and DLPFC.

Appendices

Appendices: Experiment 1: ΔPr model fits produced by monophasic and biphasic Gaussian models with positive and negative or negative amplitude ceofficients and raw data from experiment 1 (-/+) refers to positive and negative amplitude coefficients (-) refers to negative amplitude coefficients.

Participant 1	a_1 (-/+)	a_2 (-/+)	x_1	x_2	b_1	b_2	*y0*	*Adjusted* r^2
EVC	0.24137	-0.34259	0.20248	0.22222	0.094068	0.023181	-0.2353	0.5188
DLPFC	-0.22619	0.19025	0.28065	0.28556	0.023275	0.085844	0.17838	0.16856
	a_1 (-)	a_2 (-)	x_1	x_2	b_1	b_2	*y0*	*Adjusted* r^2
EVC	-0.34259	-0.16169	0.22358	0.3232	0.01461	0.010792	-0.14127	-0.23049
DLPFC	-0.17993	-0.22619	0.11571	0.28192	0.086632	0.016739	0.32237	-0.18395
	a_1 (-/+)	x_1	b_1	*y0*	*Adjusted* r^2			
EVC	0.34259	0.17136	0.013555	-0.17143	0.44641			
DLPFC	-0.22619	0.13557	0.01789	0.24893	0.27217			
	a_1 (-)	x_1	b_1	*y0*	*Adjusted* r^2			
EVC	-0.16475	0.33698	0.010639	-0.14286	-0.33178			
DLPFC	-0.22619	0.13557	0.017887	0.24891	0.27206			

a_1 & a_2 (-/+) a_1 (-/+) a_1 & a_2 (-) a_1 (-)

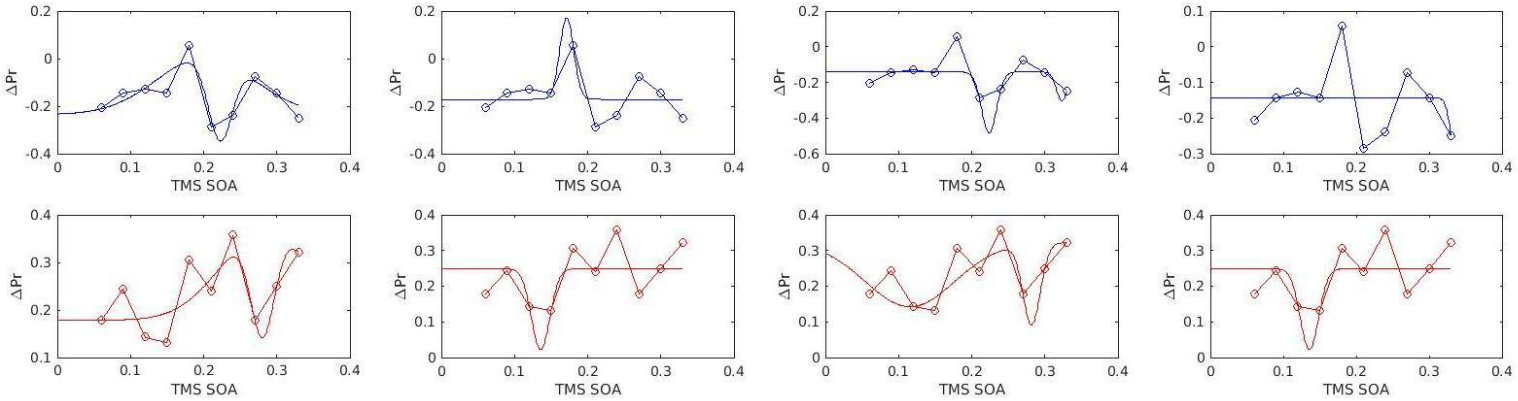

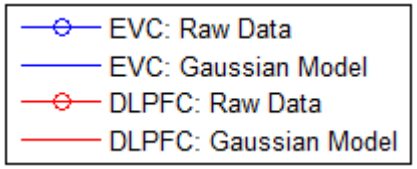

Participant 2	a_1 (-/+)	a_2 (-/+)	x_1	x_2	b_1	b_2	y0	Adjusted r^2
EVC	-0.28521	-0.38994	0.082422	0.28402	0.024657	0.021446	0.13665	0.5491
DLPFC	0.37018	0.43207	0.17368	0.38	0.058873	0.095852	-0.20238	0.48934
	a_1 (-)	a_2 (-)	x_1	x_2	b_1	b_2	y0	Adjusted r^2
EVC	-0.28521	-0.38993	0.082422	0.28402	0.024657	0.021446	0.13665	0.5491
DLPFC	-0.45833	-0.32558	0.069199	0.26372	0.052599	0.069044	0.2422	0.19534
	a_1 (-/+)	x_1	b_1	y0	Adjusted r^2			
EVC	0.25835	0.16887	0.061145	-0.02769	0.18908			
DLPFC	0.31674	0.18239	0.026373	-0.05821	0.22472			
	a_1 (-)	x_1	b_1	y0	Adjusted r^2			
EVC	-0.38994	0.28415	0.018063	0.093415	0.10121			
DLPFC	-0.45833	0.073887	0.017004	0.032868	0.18493			

a_1 & a_2 (-/+) ***a_1 (-/+)*** ***a_1 & a_2 (-)*** ***a_1 (-)***

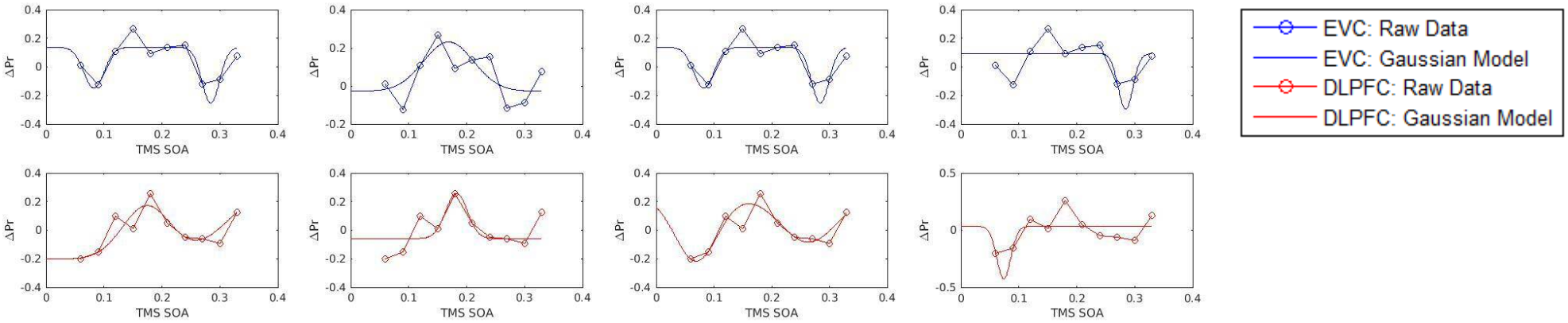

Participant 3	a_1 (-/+)	a_2 (-/+)	x_1	x_2	b_1	b_2	y0	Adjusted r^2
EVC	0.55925	0.44541	0.23128	0.37988	0.015602	0.097115	-0.15446	0.80404
DLPFC	-0.51996	0.60979	0.1666	0.30874	0.01309	0.01466	-0.01486	0.79601
	a_1 (-)	a_2 (-)	x_1	x_2	b_1	b_2	y0	Adjusted r^2
EVC	-0.39972	-0.55952	0.10195	0.2833	0.12505	0.012434	0.19617	0.26015
DLPFC	-0.31343	-0.60979	0.14745	0.25614	0.083314	0.013931	0.1911	-0.11911
	a_1 (-/+)	x_1	b_1	y0	Adjusted r^2			
EVC	-0.48811	0.061365	0.26323	0.30952	0.42497			
DLPFC	0.60979	0.30867	0.015696	-0.03669	0.69516			
	a_1 (-)	x_1	b_1	y0	Adjusted r^2			
EVC	-0.48811	0.061366	0.26323	0.30952	0.42497			
DLPFC	-0.25262	0.18304	0.081322	0.095138	0.46143			

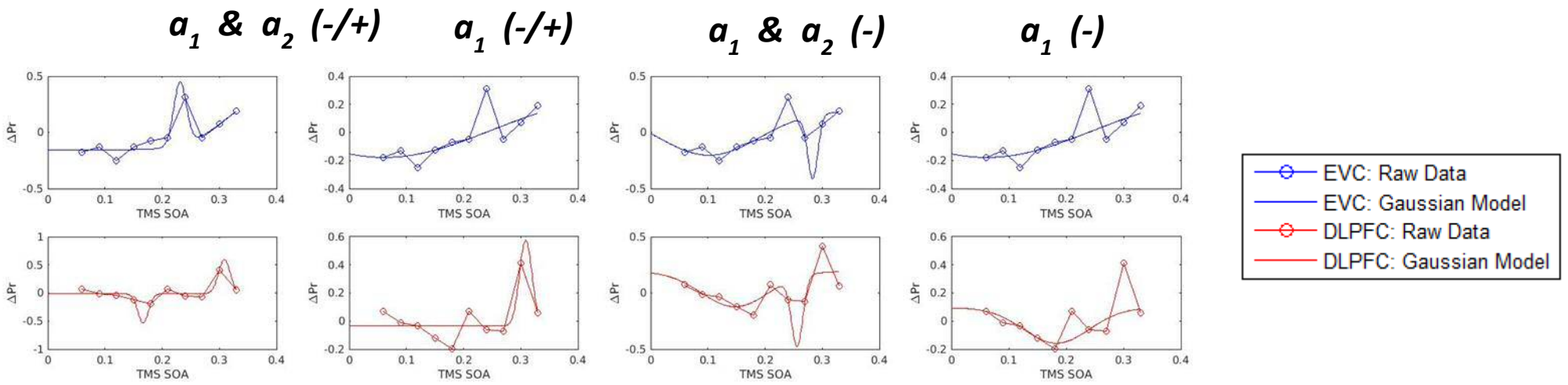

Participant 4	a_1 (-/+)	a_2 (-/+)	x_1	x_2	b_1	b_2	y0	Adjusted r^2
EVC	-0.22163	0.27035	0.20679	0.26995	0.10968	0.010195	-0.0966	-0.10711
DLPFC	0.29111	0.22251	0.1299	0.23816	0.023826	0.049036	-0.02863	0.32869
	a_1 (-)	a_2 (-)	x_1	x_2	b_1	b_2	y0	Adjusted r^2
EVC	-0.37698	-0.37698	0.16297	0.22599	0.017426	0.016353	-0.14051	-0.07532
DLPFC	-0.29111	-0.2911	0.077191	0.30977	0.023636	0.013977	0.14295	0.21775
	a_1 (-/+)	x_1	b_1	y0	Adjusted r^2			
EVC	-0.31987	0.17872	0.14439	0.019841	-0.13121			
DLPFC	-0.29111	0.076919	0.020945	0.12302	0.23591			
	a_1 (-)	x_1	b_1	y0	Adjusted r^2			
EVC	-0.32109	0.17803	0.14315	0.019841	-0.13257			
DLPFC	-0.29111	0.076919	0.020945	0.12302	0.23591			

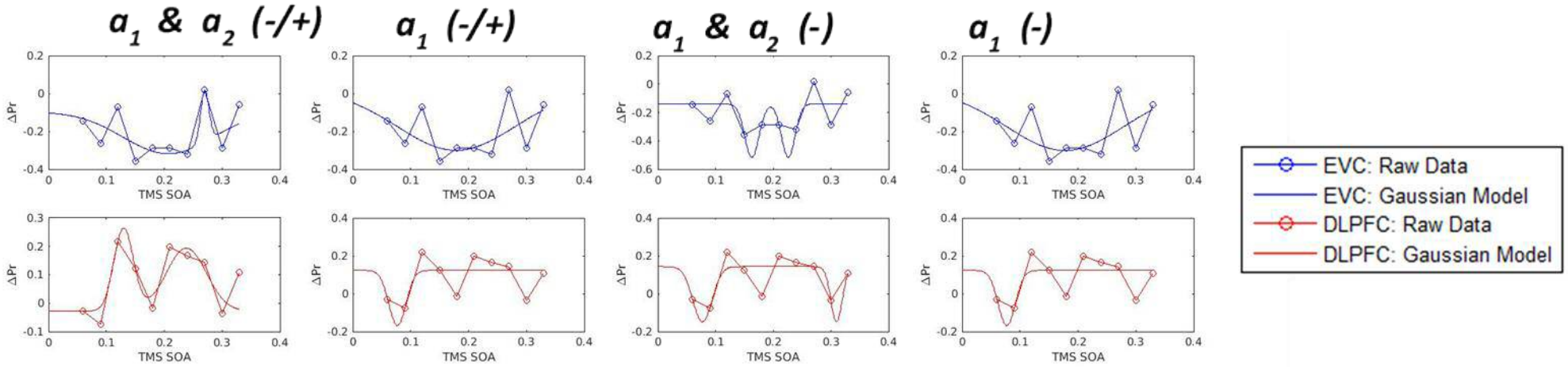

Participant 5	a_1 (-/+)	a_2 (-/+)	x_1	x_2	b_1	b_2	y0	Adjusted r^2
EVC	0.30692	0.28331	0.20998	0.30318	0.013251	0.048093	-0.18967	0.77594
DLPFC	0.39051	-0.34212	0.077922	0.3245	0.012755	0.017273	0.036675	-0.31297
	a_1 (-)	a_2 (-)	x_1	x_2	b_1	b_2	y0	Adjusted r^2
EVC	-0.33658	-0.34358	0.071234	0.24877	0.16037	0.011837	0.11264	0.29928
DLPFC	-0.27699	-0.36743	0.11985	0.32672	0.010541	0.022991	0.088328	0.28919
	a_1 (-/+)	x_1	b_1	y0	Adjusted r^2			
EVC	-0.36937	0.01	0.20341	0.098555	0.34348			
DLPFC	0.46841	0.077348	0.013594	-0.001	-0.01935			
	a_1 (-)	x_1	b_1	y0	Adjusted r^2			
EVC	-0.36937	0.01	0.20342	0.098557	0.34348			
DLPFC	-0.40494	0.32272	0.017771	0.069915	0.14898			

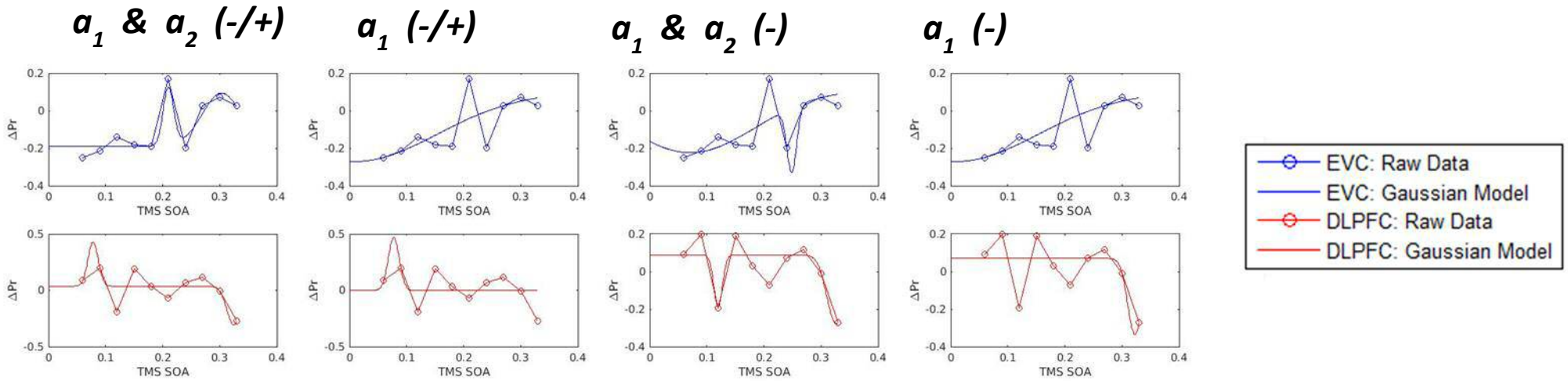

Participant 6	a_1 (-/+)	a_2 (-/+)	x_1	x_2	b_1	b_2	y0	Adjusted r^2
EVC	-0.09804	0.22705	0.24735	0.29994	0.047185	0.010676	0.11931	0.47407
DLPFC	-0.19596	0.17946	0.14915	0.20877	0.01189	0.090421	-0.2378	0.11023
	a_1 (-)	a_2 (-)	x_1	x_2	b_1	b_2	y0	Adjusted r^2
EVC	-0.28571	-0.1583	0.13233	0.23145	0.014001	0.039151	0.16733	-0.11974
DLPFC	-0.28571	-0.20671	0.14038	0.3313	0.016243	0.01	-0.1177	0.20764
	a_1 (-/+)	x_1	b_1	y0	Adjusted r^2			
EVC	-0.11477	0.24	0.0912	0.15048	0.25685			
DLPFC	0.13804	0.23999	0.054843	-0.20946	0.084484			
	a_1 (-)	x_1	b_1	y0	Adjusted r^2			
EVC	-0.11477	0.24	0.0912	0.15048	0.25685			
DLPFC	-0.28571	0.14061	0.017505	-0.10714	-0.18656			

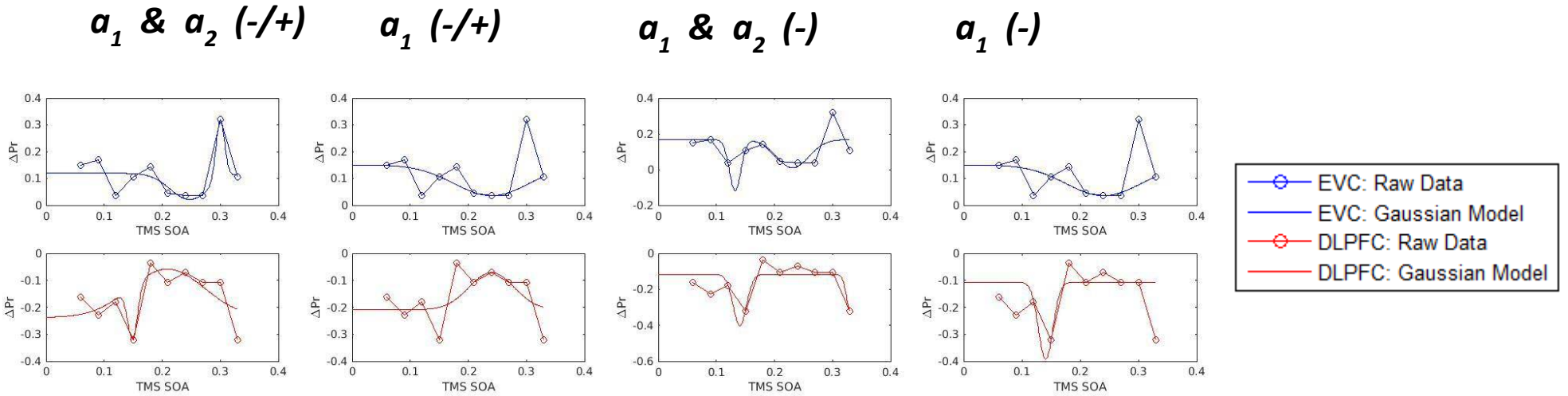

Participant 7	a_1 (-/+)	a_2 (-/+)	x_1	x_2	b_1	b_2	y0	Adjusted r^2
EVC	0.50666	0.50831	0.16394	0.3741	0.015466	0.092403	-0.28572	0.54133
DLPFC	-0.15021	0.29762	0.15081	0.31476	0.01	0.017667	-0.05282	0.51163
	a1 (-)	a2 (-)	x1	x_2	b1	b_2	y0	Adjusted r^2
EVC	-0.41316	-0.31448	0.076445	0.24802	0.11075	0.048168	0.11905	0.54622
DLPFC	-0.22288	-0.29001	0.14171	0.25634	0.08888	0.01573	0.09276	-0.14954
	a_1 (-/+)	x_1	b_1	y0	Adjusted r^2			
EVC	0.43426	0.36104	0.07696	-0.25	0.31582			
DLPFC	0.29762	0.31475	0.019098	-0.06868	0.30406			
	a_1 (-)	x_1	b_1	y0	Adjusted r^2			
EVC	-0.40536	0.050792	0.24055	0.11905	0.40168			
DLPFC	-0.1677	0.1503	0.12004	0.095238	0.14185			

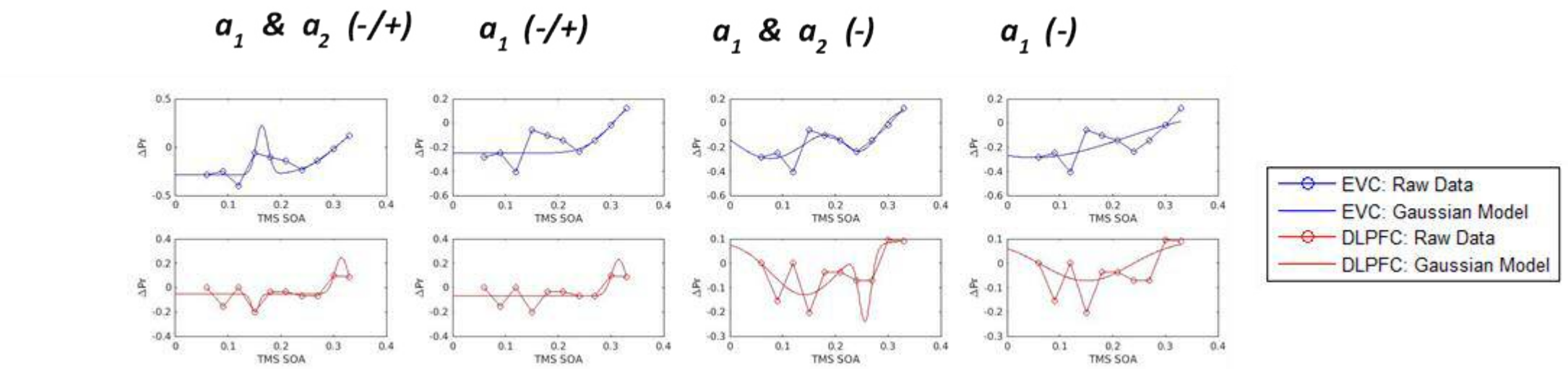

Participant 8	a_1 (-/+)	a_2 (-/+)	x_1	x_2	b_1	b_2	y0	Adjusted r^2
EVC	0.24526	0.39971	0.21022	0.27153	0.010274	0.035077	-0.16087	0.8059
DLPFC	-0.07205	0.074549	0.15078	0.32028	0.010001	0.017056	0.017569	-0.22539
	a_1 (-)	a_2 (-)	x_1	x_2	b_1	b_2	y0	Adjusted r^2
EVC	-0.43988	-0.49868	0.061243	0.31865	0.18867	0.01582	0.24868	0.21568
DLPFC	-0.0516	-0.07496	0.12552	0.14754	0.2416	0.010046	0.066397	-0.64969
	a_1 (-/+)	x_1	b_1	y0	Adjusted r^2			
EVC	0.39212	0.27125	0.032413	-0.14286	0.47768			
DLPFC	-0.08289	0.149	0.01	0.026874	0.15303			
	a_1 (-)	x_1	b_1	y0	Adjusted r^2			
EVC	-0.32735	0.01	0.1507	0.043782	0.32608			
DLPFC	-0.08273	0.14908	0.01	0.026841	0.15296			

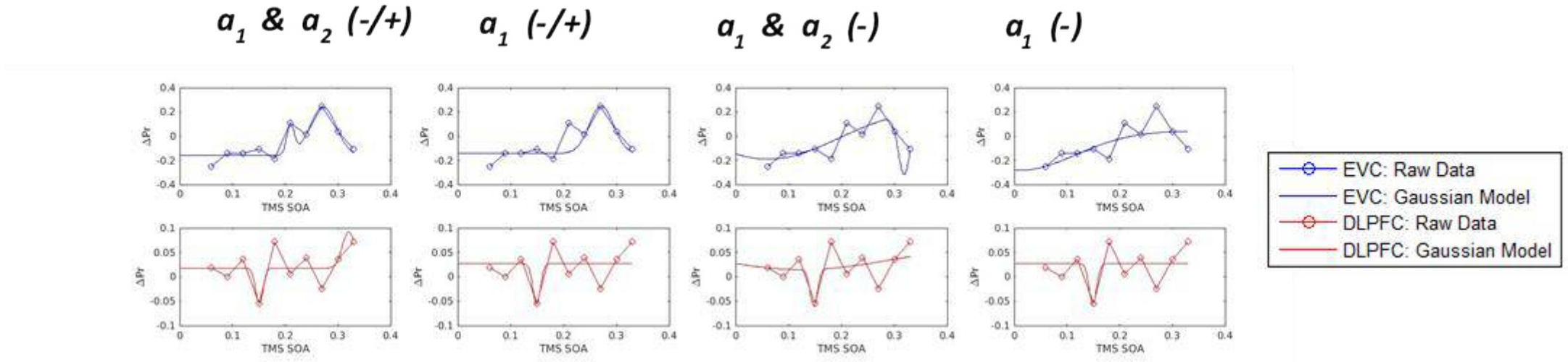

Participant 9	a_1 (-/+)	a_2 (-/+)	x_1	x_2	b_1	b_2	y0	Adjusted r^2
EVC	0.37616	0.38571	0.1698	0.23261	0.015349	0.011601	0.021399	0.48294
DLPFC	-0.30747	-0.30682	0.17252	0.31475	0.027972	0.04455	0.089337	0.85878
	a_1 (-)	a_2 (-)	x_1	x_2	b_1	b_2	y0	Adjusted r^2
EVC	-0.23184	-0.12073	0.12347	0.3251	0.017441	0.068483	0.1157	-0.72194
DLPFC	-0.30877	-0.29936	0.17236	0.31476	0.027671	0.050105	0.08933	0.85878
	a_1 (-/+)	x_1	b_1	y0	Adjusted r^2			
EVC	0.38236	0.16971	0.014359	0.034513	-0.0645			
DLPFC	0.31069	0.025306	0.23718	-0.19697	-0.00085			
	a_1 (-)	x_1	b_1	y0	Adjusted r^2			
EVC	-0.19755	0.12411	0.01	0.059744	-0.03584			
DLPFC	-0.32035	0.31488	0.024754	0.037037	0.27897			

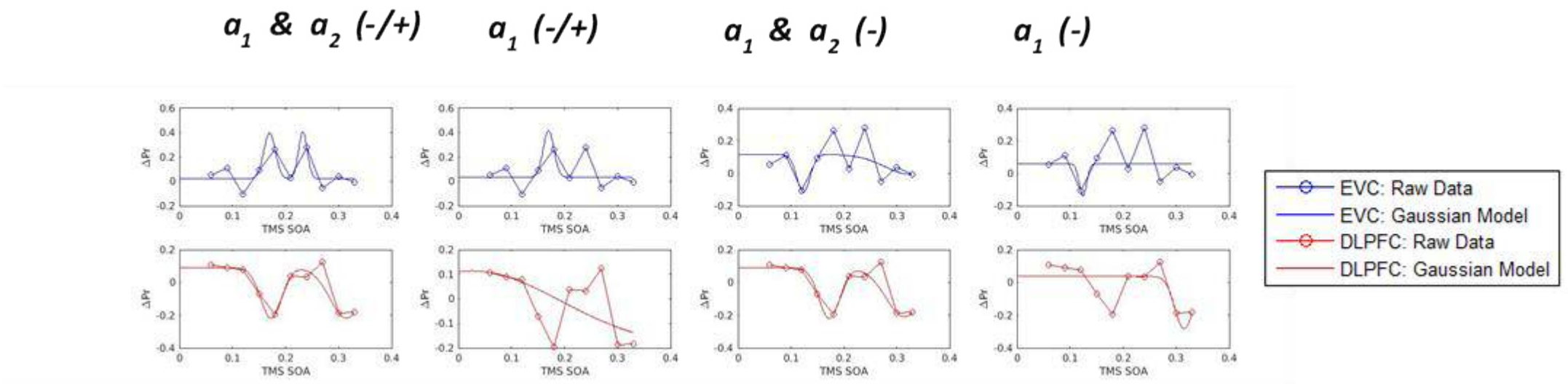

Participant 10	a_1 (-/+)	a_2 (-/+)	x_1	x_2	b_1	b_2	y0	Adjusted r^2
EVC	0.21805	0.24011	0.10372	0.27828	0.066016	0.013338	-0.10557	0.55705
DLPFC	0.23304	-0.4291	0.26627	0.26993	0.054527	0.011785	0.092989	-0.33118
	a_1 (-)	a_2 (-)	x_1	x_2	b_1	b_2	y0	Adjusted r^2
EVC	-0.17841	-0.2967	0.22337	0.31576	0.046118	0.017553	0.055216	0.1066
DLPFC	-0.24576	-0.38771	0.15938	0.27007	0.043201	0.011526	0.22255	-0.40115
	a_1 (-/+)	x_1	b_1	y0	Adjusted r^2			
EVC	0.16824	0.095363	0.075281	-0.09922	0.186			
DLPFC	-0.41176	0.26998	0.010577	0.16477	0.040144			
	a_1 (-)	x_1	b_1	y0	Adjusted r^2			
EVC	-0.19832	0.3025	0.16589	0.093988	0.045218			
DLPFC	-0.51001	0.16691	0.013046	0.15062	-0.3803			

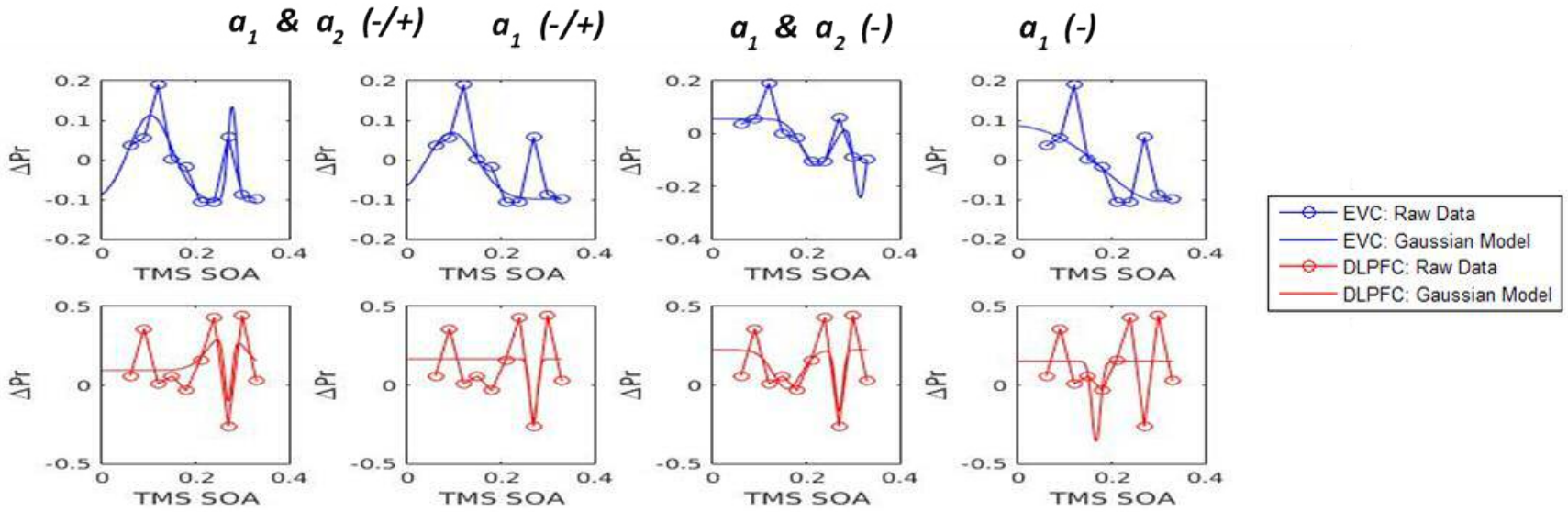

Participant 11	a_1 (-/+)	a_2 (-/+)	x_1	x_2	b_1	b_2	y0	Adjusted r^2
EVC	0.23698	0.23698	0.082138	0.16212	0.0168	0.017162	-0.10175	0.81728
DLPFC	0.26864	0.14384	0.1756	0.29944	0.028824	0.010088	-0.08591	0.60142
	a_1 (-)	a_2 (-)	x_1	x_2	b_1	b_2	y0	Adjusted r^2
EVC	-0.15567	-0.13273	0.11986	0.29558	0.010005	0.10127	0.013934	-0.06221
DLPFC	-0.23618	-0.1911	0.01	0.25133	0.073632	0.035671	0.042123	-0.33583
	a_1 (-/+)	x_1	b_1	y0	Adjusted r^2			
EVC	0.23698	0.16221	0.015441	-0.08459	0.42203			
DLPFC	0.29062	0.17598	0.030828	-0.10714	0.26509			
	a_1 (-)	x_1	b_1	y0	Adjusted r^2			
EVC	-0.12305	0.29213	0.074668	-0.00884	-0.18631			
DLPFC	-0.28191	0.25423	0.015945	-0.00116	-0.11801			

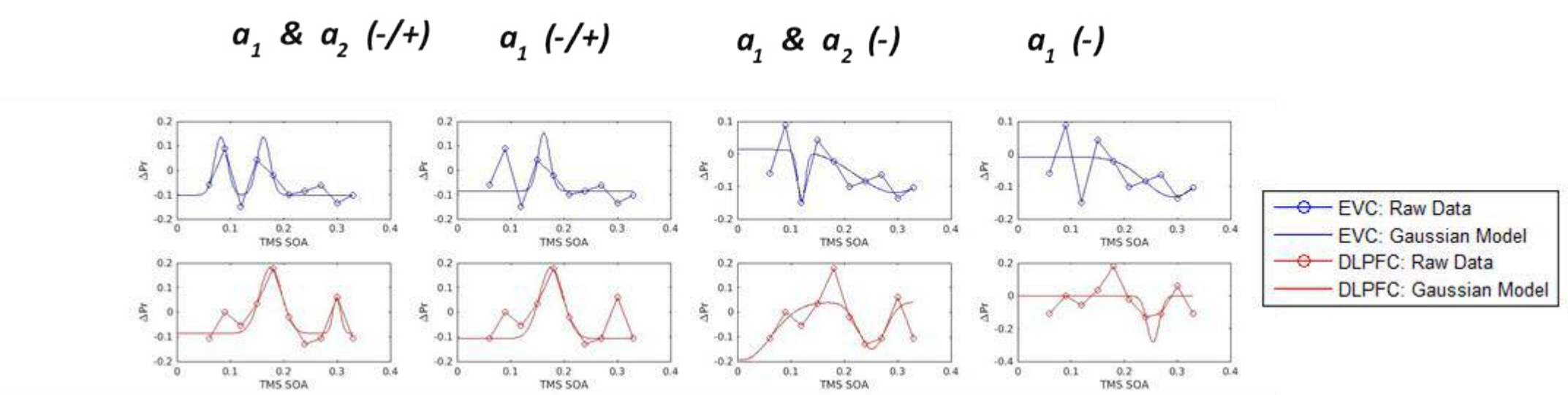

Participant 12	a_1 (-/+)	a_2 (-/+)	x_1	x_2	b_1	b_2	y0	Adjusted r^2
EVC	0.27927	0.28571	0.072352	0.22174	0.01573	0.017973	0.063543	0.38002
DLPFC	0.39286	-0.39286	0.077545	0.19469	0.016575	0.016021	-0.09241	0.68558
	a_1 (-)	a_2 (-)	x_1	x_2	b_1	b_2	y0	Adjusted r^2
EVC	-0.25936	-0.28416	0.14999	0.2987	0.06349	0.037554	0.24908	0.10557
DLPFC	-0.3298	-0.26564	0.19375	0.30406	0.042902	0.031293	0.035734	0.22624
	a_1 (-/+)	x_1	b_1	y0	Adjusted r^2			
EVC	-0.28571	0.16896	0.013747	0.11411	0.055426			
DLPFC	0.39286	0.077651	0.017987	-0.11426	0.4234			
	a_1 (-)	x_1	b_1	y0	Adjusted r^2			
EVC	-0.28571	0.16895	0.013753	0.11418	0.055536			
DLPFC	-0.39286	0.19467	0.017917	-0.06102	0.26889			

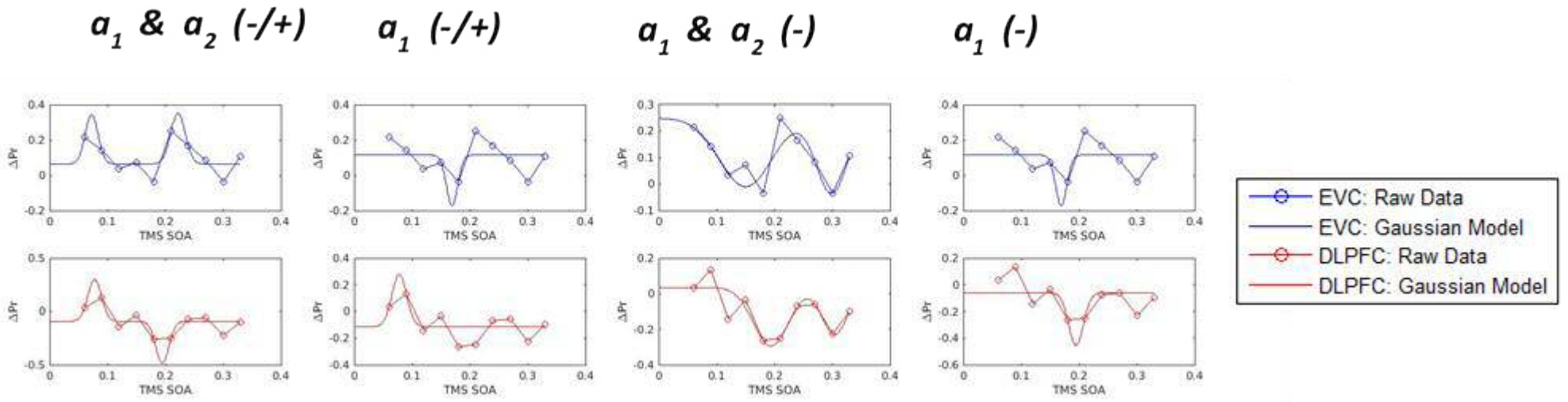

Participant 13	a_1 (-/+)	a_2 (-/+)	x_1	x_2	b_1	b_2	y0	Adjusted r^2
EVC	-0.24919	0.3176	0.26032	0.29595	0.014143	0.010988	-0.26004	-0.71368
DLPFC	0.38336	0.38336	0.1085	0.22591	0.017016	0.040807	0.017744	0.18724
	a_1 (-)	a_2 (-)	x_1	x_2	b_1	b_2	y0	Adjusted r^2
EVC	-0.17122	-0.46215	0.06389	0.25782	0.010061	0.013305	-0.21485	-0.76116
DLPFC	-0.30139	-0.30675	0.010385	0.29639	0.15743	0.028874	0.31191	-0.34448
	a_1 (-/+)	x_1	b_1	y0	Adjusted r^2			
EVC	-0.46215	0.25784	0.013115	-0.21909	-0.24032			
DLPFC	0.34233	0.22592	0.023023	0.12628	0.26811			
	a_1 (-)	x_1	b_1	y0	Adjusted r^2			
EVC	-0.23199	0.050335	0.01	-0.27116	-0.29525			
DLPFC	-0.31821	0.069708	0.013614	0.16983	-0.20098			

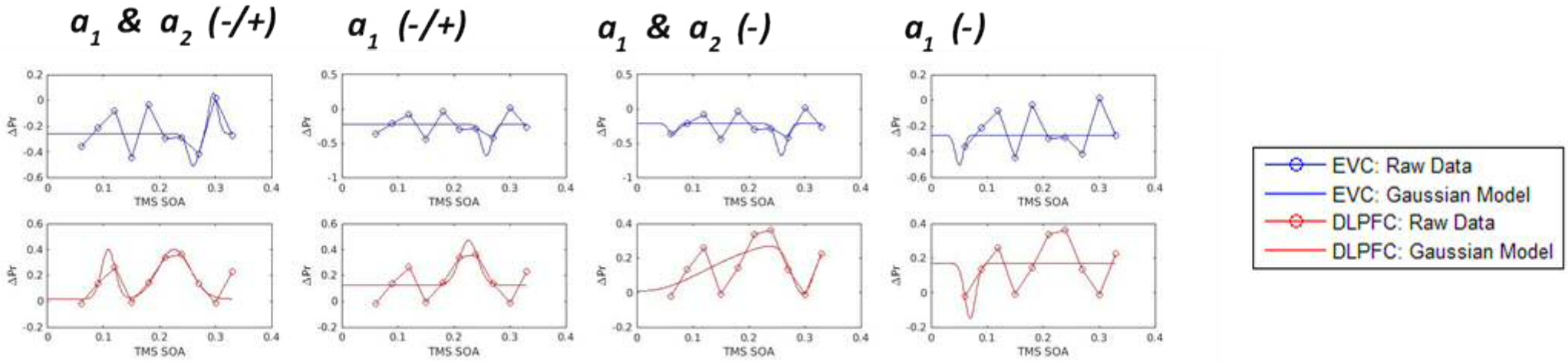

Participant 14	a_1 (-/+)	a_2 (-/+)	x_1	x_2	b_1	b_2	y0	Adjusted r^2
EVC	-0.44393	-0.33397	0.18364	0.33249	0.055684	0.010319	-0.07723	0.6632
DLPFC	-0.33555	0.4748	0.17779	0.28707	0.027297	0.01264	0.04763	0.64183
	a_1 (-)	a_2 (-)	x_1	x_2	b_1	b_2	y0	Adjusted r^2
EVC	-0.44653	-0.36834	0.18365	0.3339	0.055639	0.010003	-0.07624	0.66343
DLPFC	-0.37727	-0.28366	0.17892	0.33682	0.035054	0.01	0.10675	0.67867
	a_1 (-/+)	x_1	b_1	y0	Adjusted r^2			
EVC	-0.37263	0.18314	0.045241	-0.13748	0.40312			
DLPFC	-0.36692	0.17801	0.029729	0.079572	0.5619			
	a_1 (-)	x_1	b_1	y0	Adjusted r^2			
EVC	-0.37264	0.18314	0.045241	-0.13748	0.40312			
DLPFC	-0.36692	0.17801	0.029729	0.079572	0.5619			

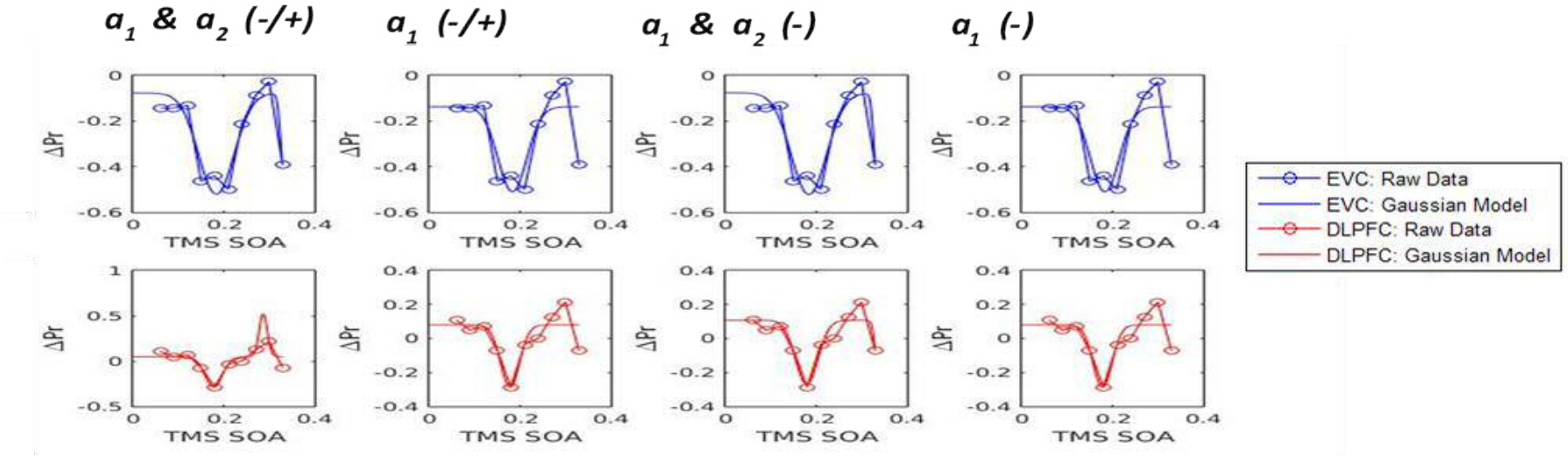

Participant 15	a_1 (-/+)	a_2 (-/+)	x_1	x_2	b_1	b_2	y0	Adjusted r^2
EVC	-0.80929	0.45101	0.053478	0.33565	0.010014	0.01	0.041432	0.35046
DLPFC	0.47466	0.47467	0.075828	0.22994	0.017479	0.026595	-0.20906	0.61872
	a_1 (-)	a_2 (-)	x_1	x_2	b_1	b_2	y0	Adjusted r^2
EVC	-0.67737	-0.85713	0.01	0.28647	0.17183	0.01615	0.35711	0.17207
DLPFC	-0.41027	-0.38804	0.14535	0.33536	0.055438	0.065573	0.15405	-0.41456
	a_1 (-/+)	x_1	b_1	y0	Adjusted r^2			
EVC	-0.85608	0.053463	0.01	0.0703	0.46834			
DLPFC	0.47467	0.22906	0.020277	-0.1339	0.46294			
	a_1 (-)	x_1	b_1	y0	Adjusted r^2			
EVC	-0.85609	0.053468	0.01	0.070637	0.46844			
DLPFC	-0.11763	0.15268	0.041752	-0.04055	-0.26634			

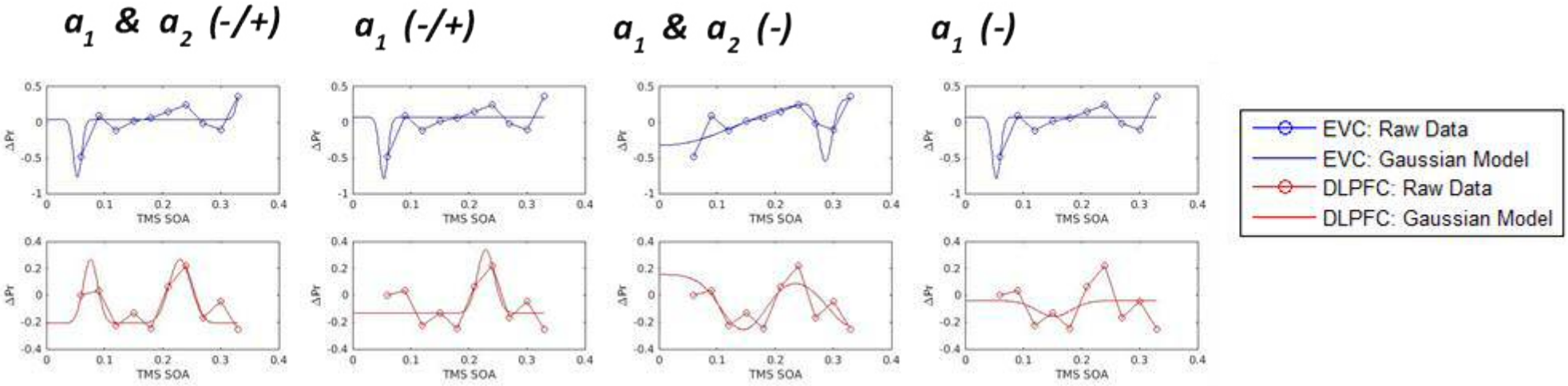

Participant 16	a_1 (-/+)	a_2 (-/+)	x_1	x_2	b_1	b_2	y0	Adjusted r^2
EVC	-0.21461	0.22947	0.053904	0.24815	0.01	0.015394	0.076565	0.056998
DLPFC	-0.44048	0.29748	0.15654	0.18798	0.12969	0.020904	0.023568	-0.05164
	a_1 (-)	a_2 (-)	x_1	x_2	b_1	b_2	y0	Adjusted r^2
EVC	-0.2551	-0.18319	0.055241	0.14272	0.01	0.024503	0.13198	0.11005
DLPFC	-0.41452	-0.24409	0.089125	0.2397	0.16575	0.021875	0.032197	-0.14017
	a_1 (-/+)	x_1	b_1	y0	Adjusted r^2			
EVC	-0.17977	0.059164	0.01	0.10708	0.10485			
DLPFC	-0.43092	0.093374	0.18193	0.035714	0.049134			
	a_1 (-)	x_1	b_1	y0	Adjusted r^2			
EVC	-0.20533	0.056255	0.01	0.10704	0.10492			
DLPFC	-0.43092	0.093375	0.18193	0.035714	0.049129			

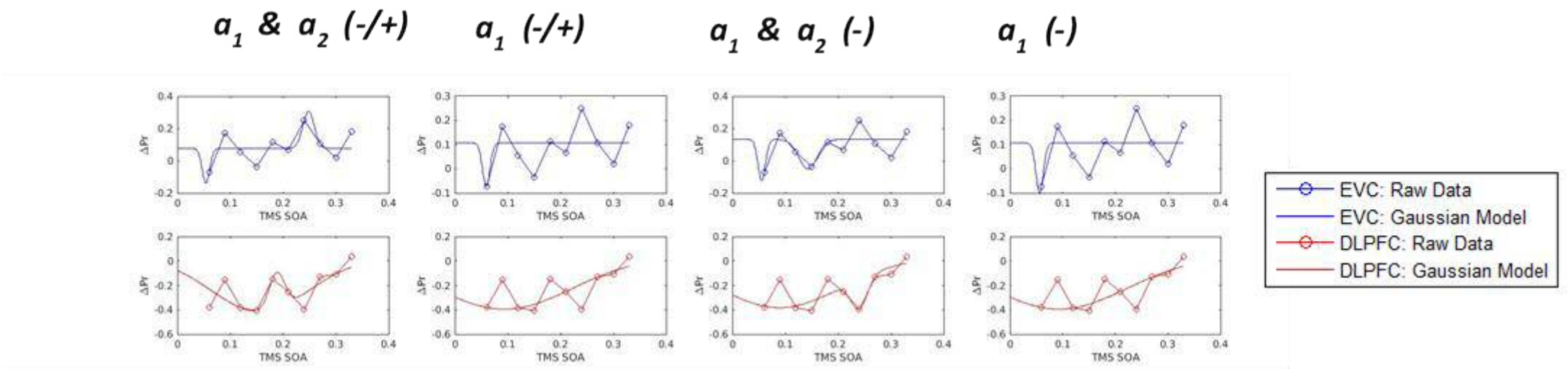

Participant 17	a_1 (-/+)	a_2 (-/+)	x_1	x_2	b_1	b_2	$y0$	Adjusted r^2
EVC	-0.56388	-0.44589	0.1057	0.31266	0.063891	0.014928	0.24286	0.92644
DLPFC	-0.35693	0.3535	0.056216	0.10733	0.020917	0.01195	-0.0863	-0.03443
	a_1 (-)	a_2 (-)	x_1	x_2	b_1	b_2	$y0$	Adjusted r^2
EVC	-0.56392	-0.43218	0.1057	0.31259	0.063885	0.015171	0.24286	0.92646
DLPFC	-0.37617	-0.18313	0.060393	0.27022	0.01746	0.010691	-0.04969	0.24876
	a_1 (-/+)	x_1	b_1	$y0$	Adjusted r^2			
EVC	-0.51263	0.10306	0.067001	0.23822	0.90258			
DLPFC	-0.36284	0.059088	0.010088	-0.07186	0.39469			
	a_1 (-)	x_1	b_1	$y0$	Adjusted r^2			
EVC	-0.51263	0.10306	0.067002	0.23822	0.90258			
DLPFC	-0.36413	0.058905	0.010037	-0.07192	0.3947			

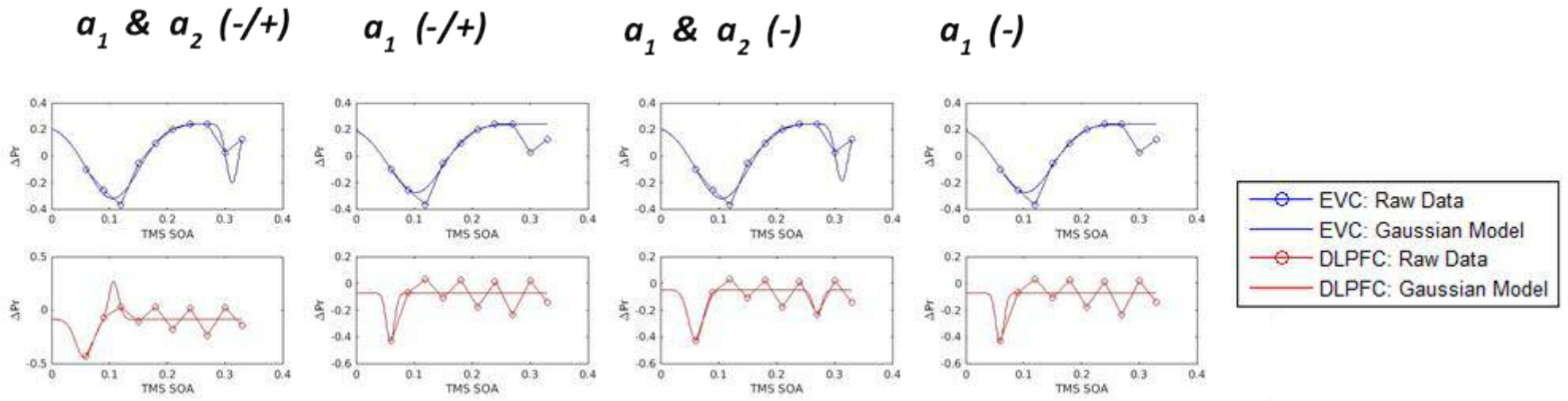

Participant 18	a_1 (-/+)	a_2 (-/+)	x_1	x_2	b_1	b_2	y0	Adjusted r^2
EVC	-0.35175	0.33489	0.15021	0.21005	0.010002	0.1343	-0.35673	0.50045
DLPFC	-0.35988	0.73371	0.11471	0.25768	0.027516	0.015401	0.017854	0.62706
	a_1 (-)	a_2 (-)	x_1	x_2	b_1	b_2	y0	Adjusted r^2
EVC	-0.21368	-0.33526	0.077289	0.14982	0.030123	0.011328	-0.08798	0.23951
DLPFC	-0.5148	-0.73371	0.11854	0.31234	0.044763	0.014962	0.20011	0.188
	a_1 (-/+)	x_1	b_1	y0	Adjusted r^2			
EVC	0.21284	0.21873	0.056804	-0.24468	-0.06374			
DLPFC	0.73371	0.25783	0.01779	-0.05456	0.52522			
	a_1 (-)	x_1	b_1	y0	Adjusted r^2			
EVC	-0.25199	0.077802	0.03202	-0.05952	-0.59404			
DLPFC	-0.38716	0.11515	0.029926	0.04818	0.1116			

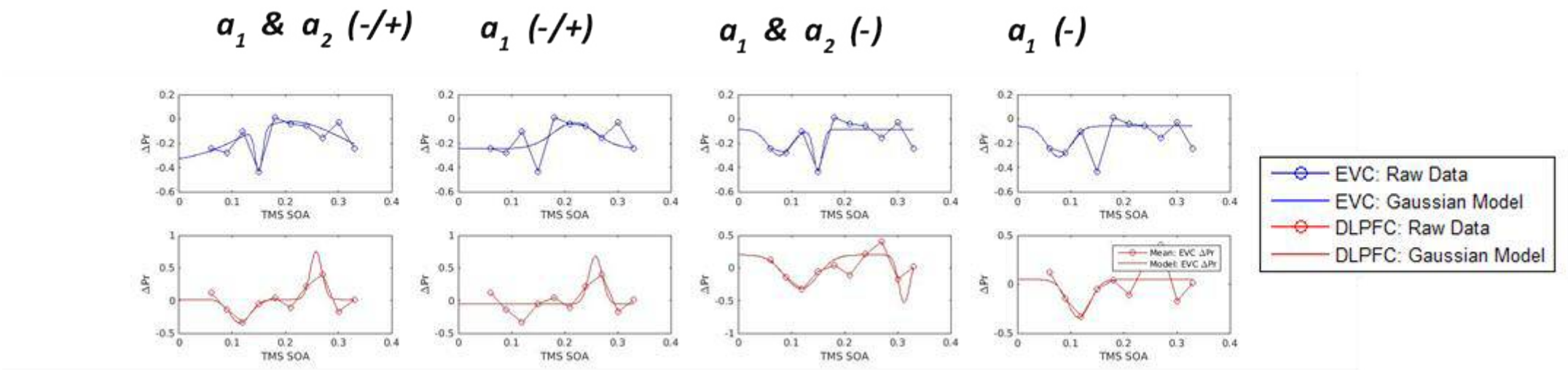

Participant 19	a_1 (-/+)	a_2 (-/+)	x_1	x_2	b_1	b_2	y0	Adjusted r^2
EVC	0.43237	0.38809	0.10717	0.26106	0.020007	0.074694	-0.33333	0.4389
DLPFC	-0.3053	-0.45659	0.12075	0.34804	0.010645	0.044315	0.11281	0.45015
	a_1 (-)	a_2 (-)	x_1	x_2	b_1	b_2	y0	Adjusted r^2
EVC	-0.30528	-0.34547	0.0659	0.15807	0.020076	0.012875	-0.05247	-0.02454
DLPFC	-0.30486	-0.4615	0.12029	0.3488	0.010001	0.044779	0.11291	0.4508
	a_1 (-/+)	x_1	b_1	y0	Adjusted r^2			
EVC	0.22751	0.27	0.030897	-0.12434	0.13161			
DLPFC	-0.24043	0.12005	0.010011	0.048118	-0.1623			
	a_1 (-)	x_1	b_1	y0	Adjusted r^2			
EVC	-0.30188	0.06664	0.017757	-0.07085	0.022321			
DLPFC	-0.46364	0.3415	0.03819	0.13839	0.58736			

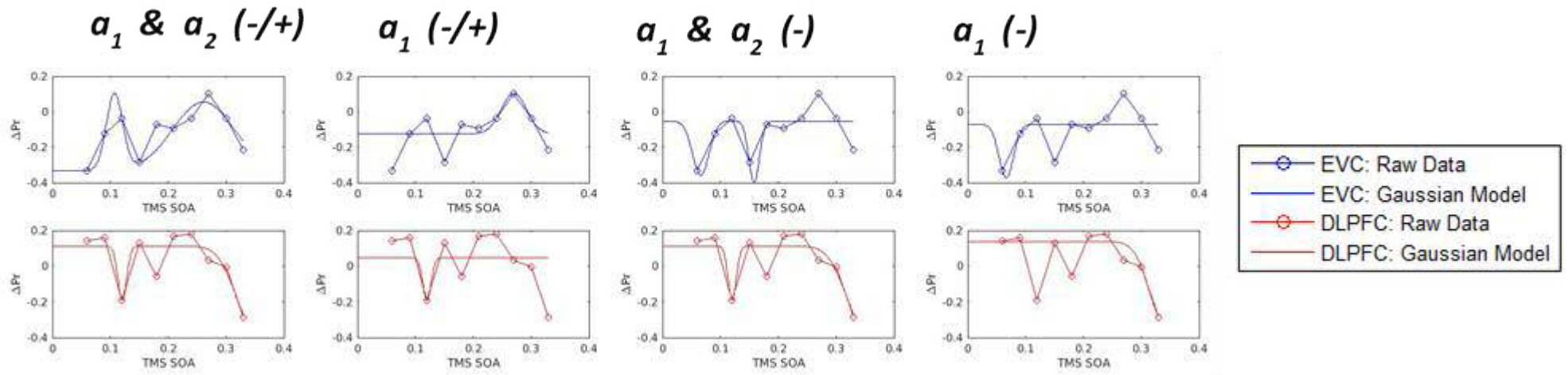

Participant 20	a_1 (-/+)	a_2 (-/+)	x_1	x_2	b_1	b_2	y0	Adjusted r^2
EVC	0.27636	0.332	0.1102	0.25817	0.036363	0.023484	-0.10938	0.34184
DLPFC	-0.63012	-0.78874	0.051599	0.19946	0.01	0.017969	0.047775	0.56435
	a_1 (-)	a_2 (-)	x_1	x_2	b_1	b_2	y0	Adjusted r^2
EVC	-0.24176	-0.32935	0.057539	0.31331	0.01	0.018518	0.044278	-0.09897
DLPFC	-0.44655	-0.78875	0.053884	0.19946	0.010191	0.017974	0.048105	0.41913
	a_1 (-/+)	x_1	b_1	y0	Adjusted r^2			
EVC	-0.19733	0.057735	0.01	0.003958	-0.02588			
DLPFC	-0.78875	0.19937	0.01666	-0.00101	0.50462			
	a_1 (-)	x_1	b_1	y0	Adjusted r^2			
EVC	-0.18928	0.058508	0.01	0.001612	-0.02703			
DLPFC	-0.78875	0.19937	0.016654	-0.00116	0.50454			

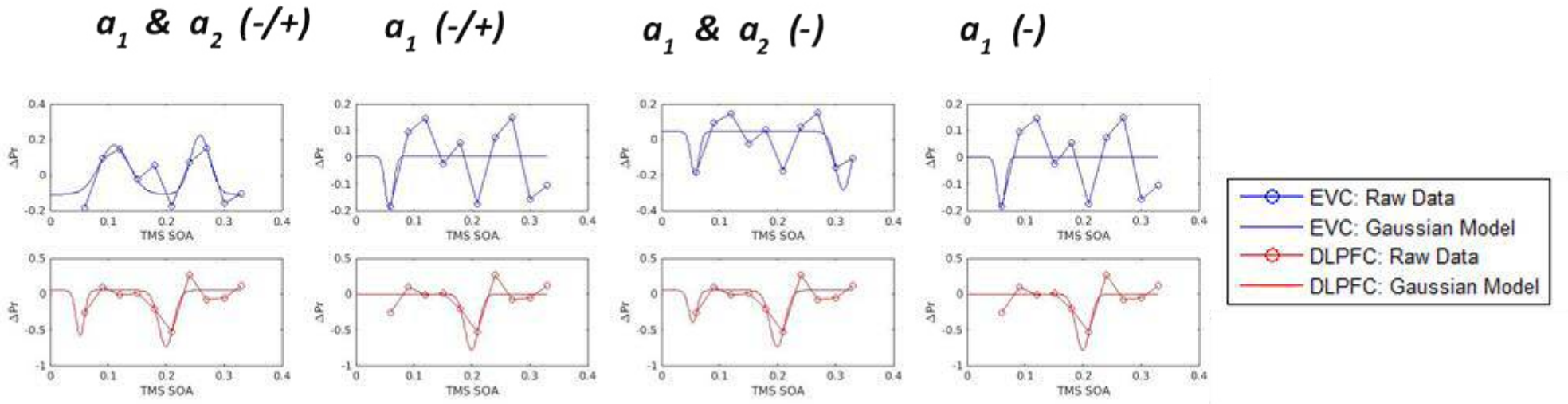

Participant 21	a_1 (-/+)	a_2 (-/+)	x_1	x_2	b_1	b_2	y0	Adjusted r^2
EVC	-0.46764	0.41623	0.10435	0.20896	0.020469	0.19367	-0.36267	0.64264
DLPFC	-0.21269	-0.19983	0.085447	0.14514	0.021216	0.01	-0.11157	-0.32031
	a_1 (-)	a_2 (-)	x_1	x_2	b_1	b_2	y0	Adjusted r^2
EVC	-0.40656	-0.15037	0.09777	0.31437	0.038426	0.022566	0.021658	0.52556
DLPFC	-0.21316	-0.22521	0.08542	0.14405	0.021229	0.01	-0.11122	-0.32029
	a_1 (-/+)	x_1	b_1	y0	Adjusted r^2			
EVC	-0.39021	0.099078	0.039025	0.006411	0.61962			
DLPFC	-0.2888	0.080656	0.014385	-0.1253	-0.14738			
	a_1 (-)	x_1	b_1	y0	Adjusted r^2			
EVC	-0.39021	0.099078	0.039025	0.006411	0.61962			
DLPFC	-0.29513	0.080527	0.014238	-0.12511	-0.14766			

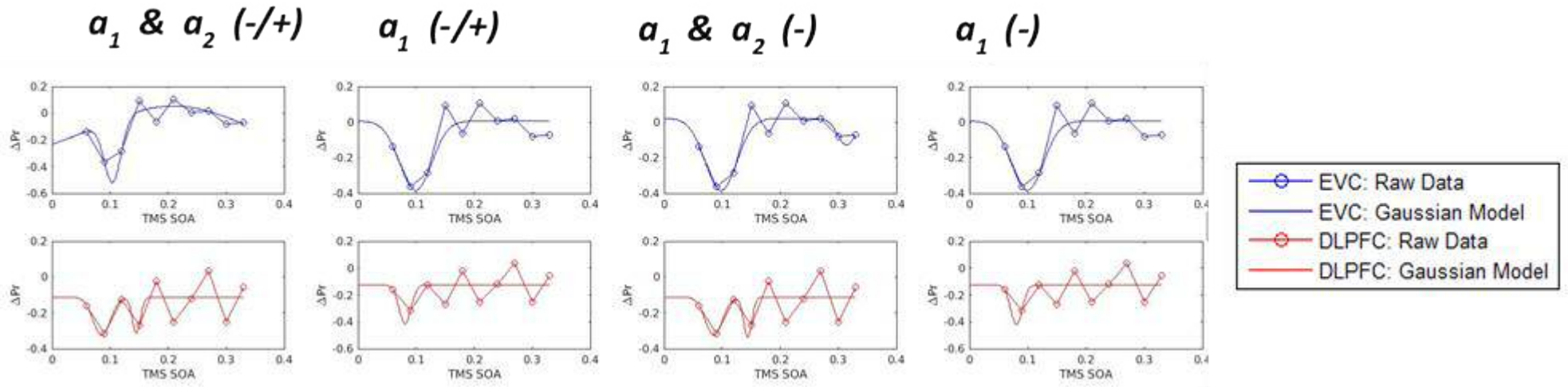

Participant 22	a_1 (-/+)	a_2 (-/+)	x_1	x_2	b_1	b_2	y0	Adjusted r^2
EVC	-0.1729	-0.30995	0.15276	0.24003	0.016316	0.010342	-0.07677	0.30427
DLPFC	0.57952	0.39516	0.16413	0.27004	0.017705	0.01	0.062279	0.18646
	a_1 (-)	a_2 (-)	x_1	x_2	b_1	b_2	y0	Adjusted r^2
EVC	-0.19191	-0.31437	0.15512	0.23948	0.014605	0.01	-0.07651	0.3059
DLPFC	-0.43723	-0.33904	0.055169	0.23693	0.010007	0.012056	0.21776	-0.74605
	a_1 (-/+)	x_1	b_1	y0	Adjusted r^2			
EVC	-0.27833	0.24011	0.011271	-0.09821	0.36519			
DLPFC	-0.3401	0.057938	0.01	0.19737	-0.02628			
	a_1 (-)	x_1	b_1	y0	Adjusted r^2			
EVC	-0.18738	0.15455	0.015515	-0.07493	-0.4584			
DLPFC	-0.35896	0.056896	0.01	0.19741	-0.02631			

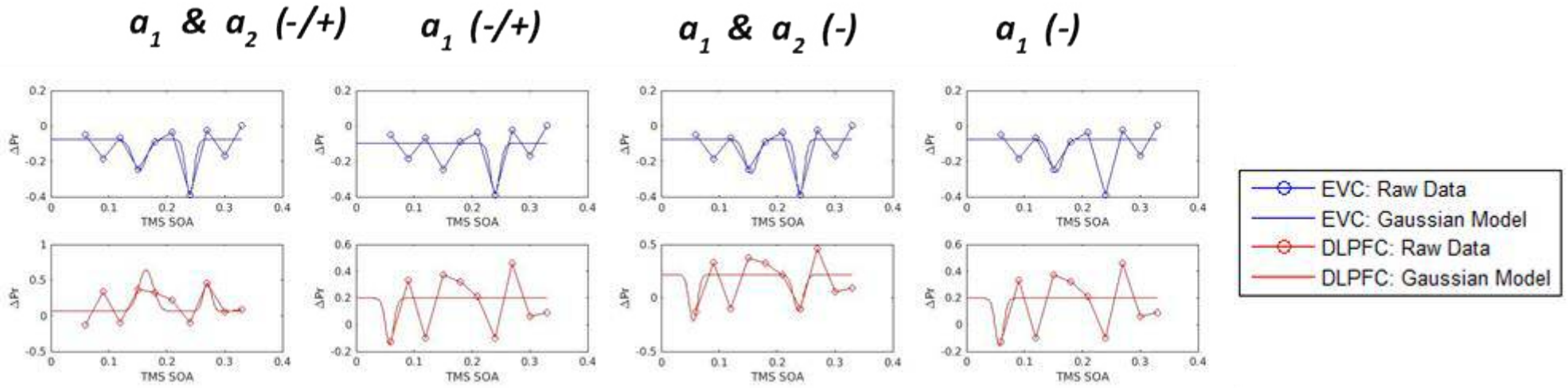

Participant 23	a_1 (-/+)	a_2 (-/+)	x_1	x_2	b_1	b_2	y0	Adjusted r^2
EVC	0.24223	-0.21145	0.24236	0.35134	0.017683	0.031685	0.15817	0.1314
DLPFC	0.21825	0.35833	0.090767	0.21761	0.010707	0.089519	-0.43333	0.77481
	a_1 (-)	a_2 (-)	x_1	x_2	b_1	b_2	y0	Adjusted r^2
EVC	-0.36557	-0.35583	0.13853	0.38	0.012756	0.065609	0.22289	-0.24811
DLPFC	-0.39319	-0.39319	0.056156	0.31833	0.10292	0.026402	-0.04069	0.69015
	a_1 (-/+)	x_1	b_1	y0	Adjusted r^2			
EVC	0.25458	0.24144	0.020439	0.14279	0.34599			
DLPFC	0.358	0.21711	0.089143	-0.43333	0.73738			
	a_1 (-)	x_1	b_1	y0	Adjusted r^2			
EVC	-0.13706	0.14609	0.01	0.17763	-0.1228			
DLPFC	-0.39319	0.053269	0.010141	-0.18026	0.14259			

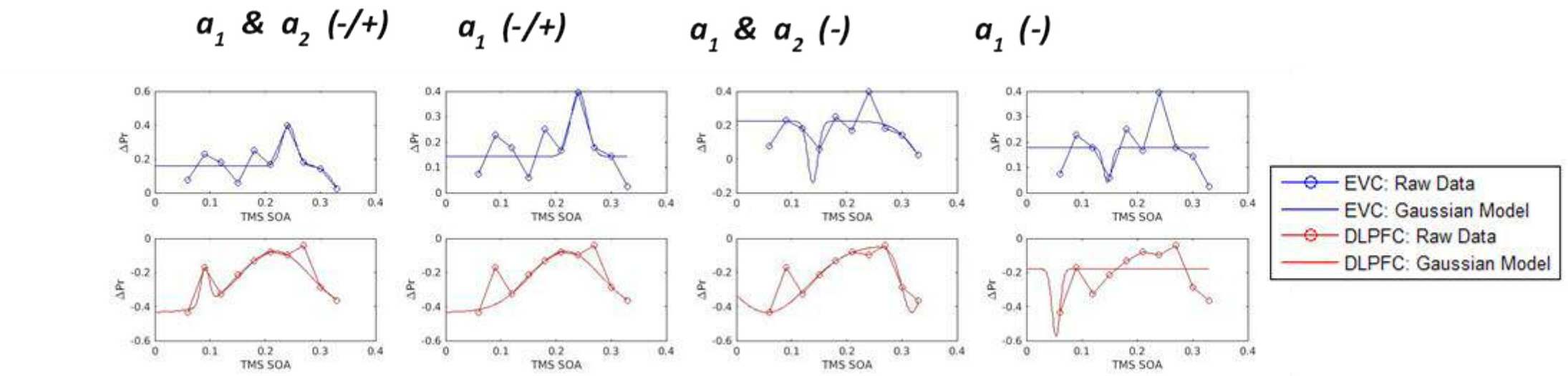

Participant 24	a_1 (-/+)	a_2 (-/+)	x_1	x_2	b_1	b_2	y0	Adjusted r^2
EVC	-0.33333	-0.33333	0.10574	0.31693	0.016617	0.017874	-0.12606	0.31937
DLPFC	-0.26422	-0.42859	0.14044	0.33231	0.04662	0.01	0.27527	0.61141
	a_1 (-)	a_2 (-)	x_1	x_2	b_1	b_2	y0	Adjusted r^2
EVC	-0.33333	-0.33333	0.10574	0.31694	0.016641	0.017902	-0.12572	0.15023
DLPFC	-0.27578	-0.43642	0.14333	0.3322	0.046766	0.010015	0.28541	0.37616
	a_1 (-/+)	x_1	b_1	y0	Adjusted r^2			
EVC	-0.33332	0.31687	0.016672	-0.14217	-0.08344			
DLPFC	0.21616	0.24907	0.05442	0.063566	-0.09447			
	a_1 (-)	x_1	b_1	y0	Adjusted r^2			
EVC	-0.33314	0.31687	0.016677	-0.14218	-0.08341			
DLPFC	-0.33299	0.1337	0.020654	0.25011	-0.42803			

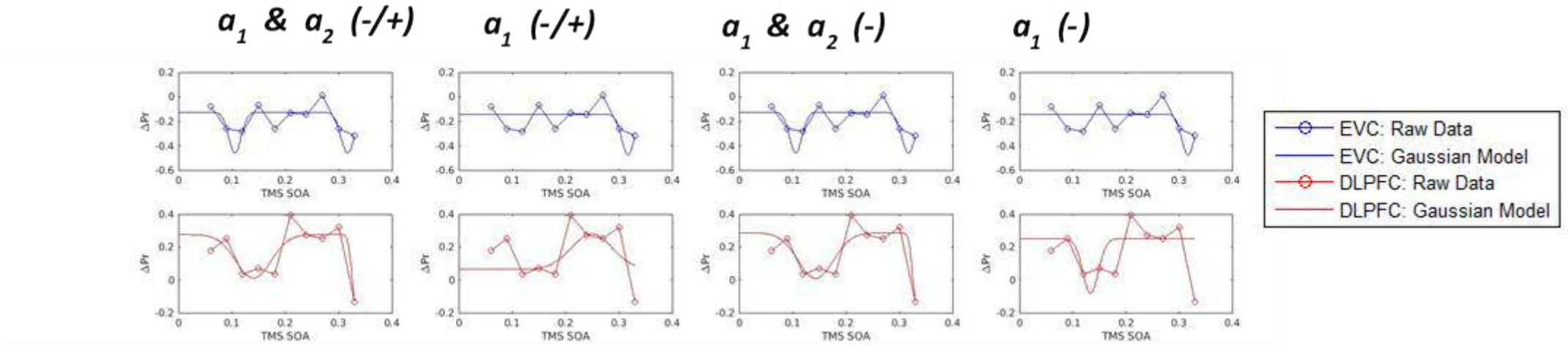

Participant 25	a_1 (-/+)	a_2 (-/+)	x_1	x_2	b_1	b_2	y0	Adjusted r^2
EVC	-0.23751	-0.74087	0.12022	0.33979	0.028911	0.02531	0.2537	0.71053
DLPFC	-0.60148	-0.60071	0.13041	0.19302	0.02956	0.020471	0.22377	0.85494
	a_1 (-)	a_2 (-)	x_1	x_2	b_1	b_2	y0	Adjusted r^2
EVC	-0.23756	-0.75554	0.12022	0.34058	0.028914	0.025726	0.25374	0.71057
DLPFC	-0.58246	-0.51544	0.13029	0.19225	0.028762	0.022737	0.20638	0.81443
	a_1 (-/+)	x_1	b_1	y0	Adjusted r^2			
EVC	0.25994	0.05598	0.01	0.15735	-0.13386			
DLPFC	-0.58498	0.14938	0.080972	0.29394	0.73033			
	a_1 (-)	x_1	b_1	y0	Adjusted r^2			
EVC	-0.61159	0.3324	0.01	0.19266	0.71497			
DLPFC	-0.58498	0.14938	0.080972	0.29394	0.73033			

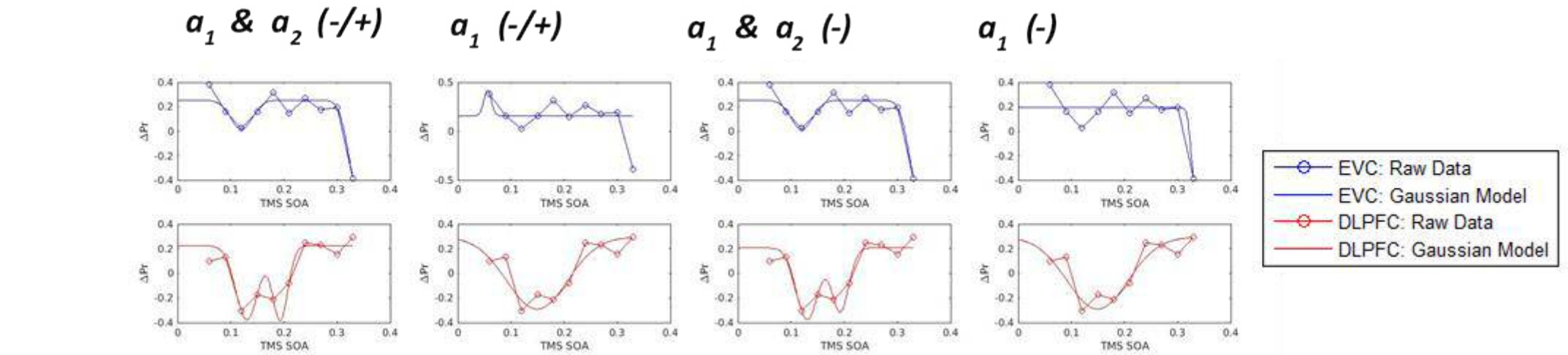

Participant 26	a_1 (-/+)	a_2 (-/+)	x_1	x_2	b_1	b_2	y0	Adjusted r^2
EVC	0.54453	0.4216	0.10934	0.23687	0.013041	0.039737	-0.01335	0.15376
DLPFC	0.32138	-0.4489	0.17874	0.21977	0.023343	0.1604	0.37787	0.3415
	a_1 (-)	a_2 (-)	x_1	x_2	b_1	b_2	y0	Adjusted r^2
EVC	-0.42573	-0.55387	0.012489	0.30901	0.18691	0.032916	0.40572	0.37018
DLPFC	-0.29267	-0.4489	0.11432	0.25628	0.06984	0.064038	0.37128	0.44086
	a_1 (-/+)	x_1	b_1	y0	Adjusted r^2			
EVC	0.40495	0.23746	0.038003	0.002586	0.19473			
DLPFC	-0.1838	0.25454	0.056801	0.11115	0.53018			
	a_1 (-)	x_1	b_1	y0	Adjusted r^2			
EVC	-0.44764	0.073615	0.015758	0.19886	-0.49512			
DLPFC	-0.1838	0.25454	0.056804	0.11115	0.53018			

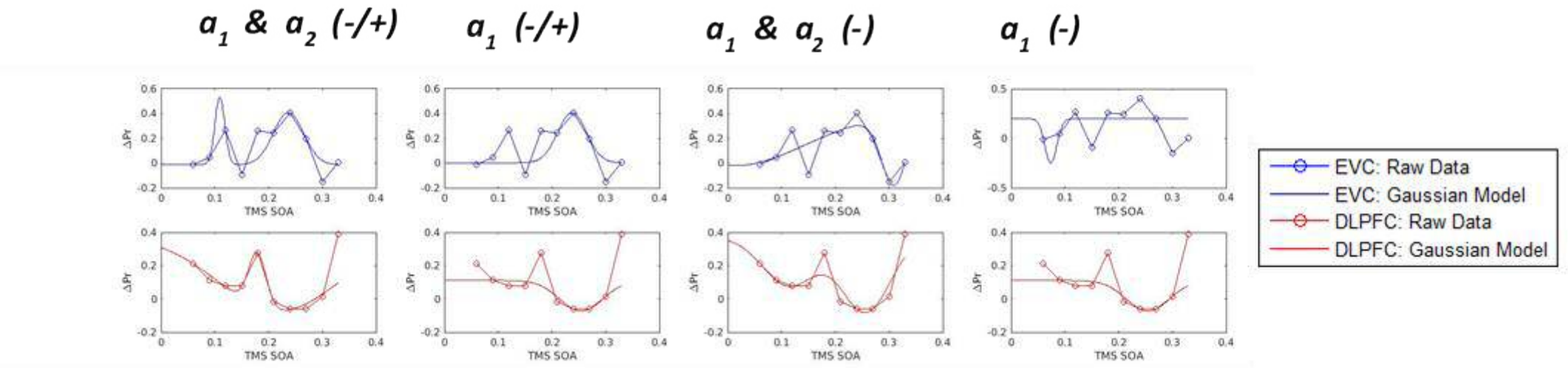

Participant 27	a_1 (-/+)	a_2 (-/+)	x_1	x_2	b_1	b_2	y0	Adjusted r^2
EVC	0.30678	0.22597	0.081028	0.33141	0.01891	0.078881	-0.08471	0.13164
DLPFC	-0.49862	-0.21833	0.097019	0.29975	0.015166	0.01	-0.02844	0.61554
	a_1 (-)	a_2 (-)	x_1	x_2	b_1	b_2	y0	Adjusted r^2
EVC	-0.23302	-0.22173	0.12713	0.19339	0.01	0.054923	0.097041	0.24
DLPFC	-0.50639	-0.22447	0.097182	0.29879	0.015093	0.01	-0.02819	0.61615
	a_1 (-/+)	x_1	b_1	y0	Adjusted r^2			
EVC	-0.28032	0.15816	0.13535	0.17857	0.030172			
DLPFC	-0.48242	0.096718	0.013437	-0.05588	0.43079			
	a_1 (-)	x_1	b_1	y0	Adjusted r^2			
EVC	-0.28032	0.15816	0.13533	0.17857	0.030239			
DLPFC	-0.4984	0.097024	0.013286	-0.05567	0.431			

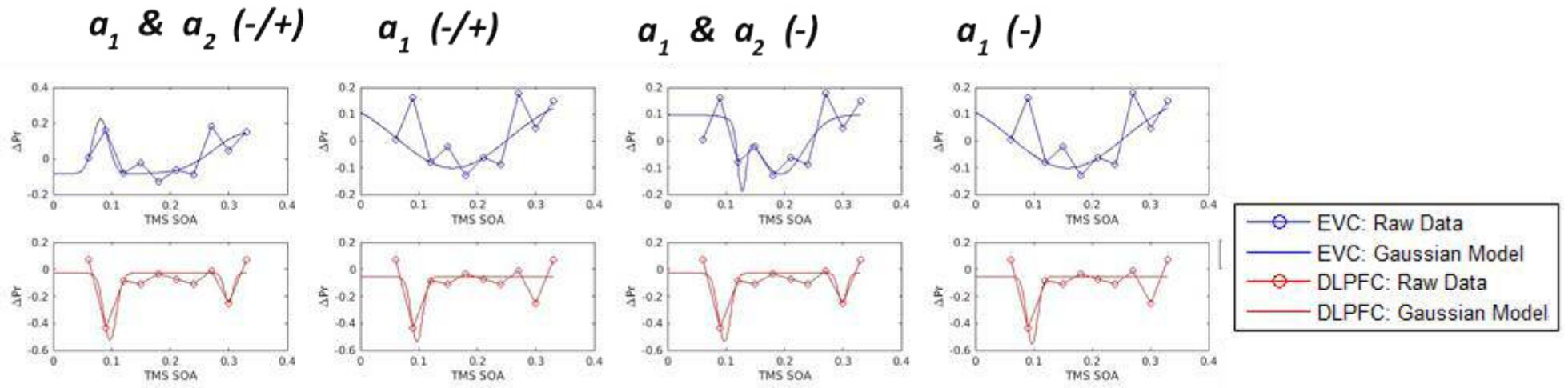

Participant 28	a_1 (-/+)	a_2 (-/+)	x_1	x_2	b_1	b_2	y0	Adjusted r^2
EVC	0.34888	0.34383	0.055375	0.23764	0.01	0.094912	-0.16865	0.1667
DLPFC	-1.4593	-1.4593	0.096195	0.34167	0.019279	0.010122	-0.16351	0.79447
	a_1 (-)	a_2 (-)	x_1	x_2	b_1	b_2	y0	Adjusted r^2
EVC	-0.27697	-0.41887	0.11658	0.31545	0.077773	0.019234	0.20726	-0.08922
DLPFC	-1.436	-0.63733	0.096616	0.33758	0.018252	0.01003	-0.18991	0.73174
	a_1 (-/+)	x_1	b_1	y0	Adjusted r^2			
EVC	-0.41887	0.10038	0.014245	0.050681	0.24271			
DLPFC	-1.4593	0.096204	0.019215	-0.16667	0.76905			
	a_1 (-)	x_1	b_1	y0	Adjusted r^2			
EVC	-0.41887	0.10038	0.014251	0.050774	0.24299			
DLPFC	-1.4593	0.096204	0.019215	-0.16667	0.76905			

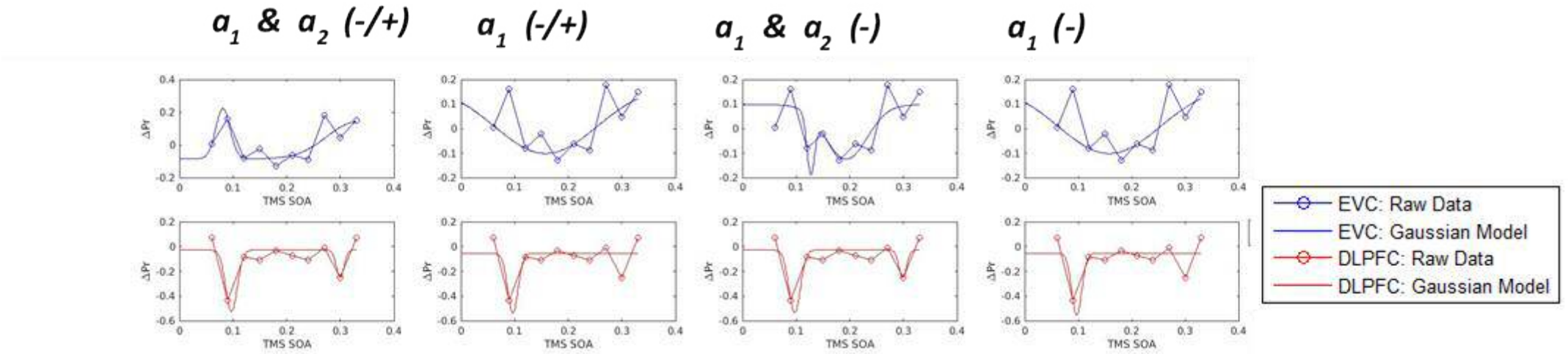

Participant 29	a_1 (-/+)	a_2 (-/+)	x_1	x_2	b_1	b_2	y0	Adjusted r^2
EVC	-0.28359	-0.4277	0.20165	0.27024	0.023161	0.011546	0.24721	0.70528
DLPFC	0.39491	-0.48121	0.22133	0.24002	0.030257	0.010434	-0.36763	0.34199
	a_1 (-)	a_2 (-)	x_1	x_2	b_1	b_2	y0	Adjusted r^2
EVC	-0.493	-0.49237	0.19801	0.26779	0.015871	0.01	0.25511	0.80702
DLPFC	-0.22494	-0.31701	0.15304	0.24209	0.019234	0.010674	-0.28836	-0.5174
	a_1 (-/+)	x_1	b_1	y0	Adjusted r^2			
EVC	-0.26828	0.21763	0.041746	0.2381	-0.34918			
DLPFC	-0.18568	0.15003	0.01	-0.32622	-0.29738			
	a_1 (-)	x_1	b_1	y0	Adjusted r^2			
EVC	-0.58084	0.19755	0.013965	0.23867	0.076923			
DLPFC	-0.18767	0.15056	0.01	-0.32483	-0.29757			

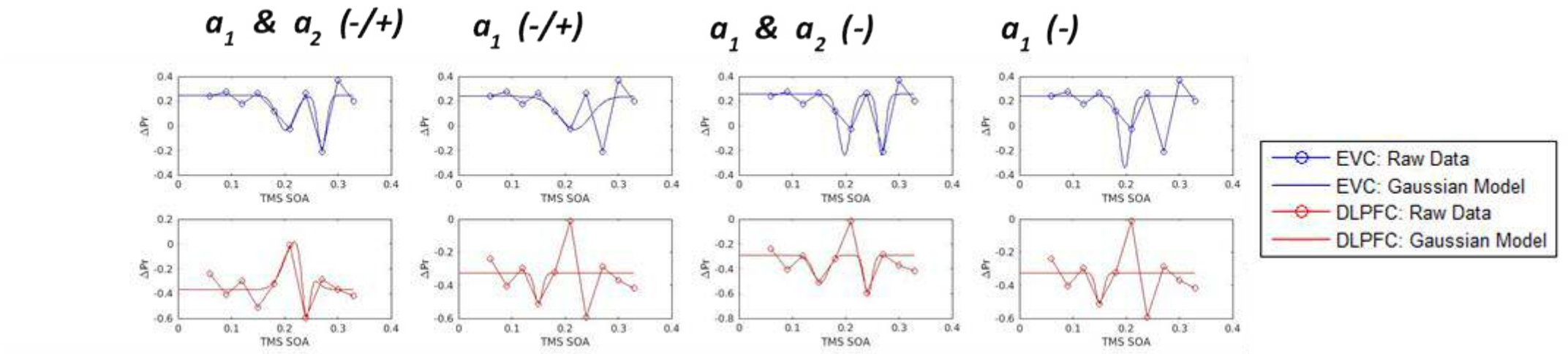

Participant 30	a_1 (-/+)	a_2 (-/+)	x_1	x_2	b_1	b_2	y0	Adjusted r^2
EVC	0.3013	0.40473	0.095979	0.19683	0.019173	0.014923	-0.11384	-0.24961
DLPFC	-0.38757	0.3244	0.22818	0.33775	0.015301	0.010043	0.095015	-0.01333
	a_1 (-)	a_2 (-)	x_1	x_2	b_1	b_2	y0	Adjusted r^2
EVC	-0.2824	-0.29181	0.14193	0.33595	0.014362	0.010076	-0.0083	-0.90254
DLPFC	-0.39286	-0.16257	0.22834	0.29995	0.018002	0.010013	0.13917	-0.13522
	a_1 (-/+)	x_1	b_1	y0	Adjusted r^2			
EVC	0.40476	0.098838	0.012975	-0.06402	0.1706			
DLPFC	-0.39286	0.22815	0.01563	0.10202	0.26717			
	a_1 (-)	x_1	b_1	y0	Adjusted r^2			
EVC	-0.21431	0.33412	0.01	-0.03346	-0.07876			
DLPFC	-0.39286	0.22815	0.015617	0.1018	0.26664			

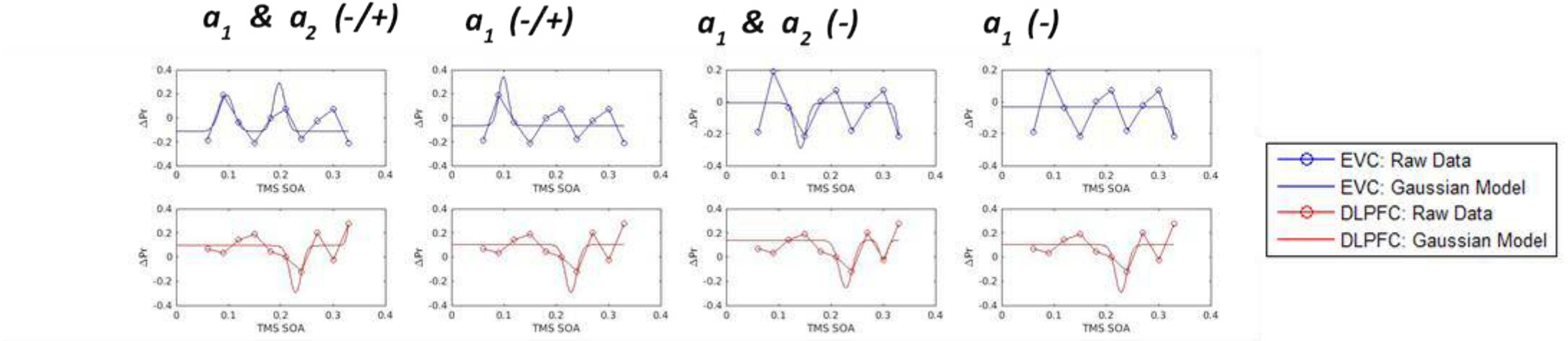

Participant 31	a_1 (-/+)	a_2 (-/+)	x_1	x_2	b_1	b_2	y0	Adjusted r^2
EVC	0.57143	-0.46802	0.10106	0.28924	0.0158	0.012437	-0.17151	0.56636
DLPFC	0.17857	0.17857	0.19443	0.30809	0.031163	0.017425	-0.21534	0.6092
	a_1 (-)	a_2 (-)	x_1	x_2	b_1	b_2	y0	Adjusted r^2
EVC	-0.38912	-0.33825	0.051274	0.29088	0.01003	0.017046	-0.13883	-0.15633
DLPFC	-0.14792	-0.17381	0.010009	0.25508	0.10672	0.023784	-0.11388	-0.17124
	a_1 (-/+)	x_1	b_1	y0	Adjusted r^2			
EVC	0.57143	0.10099	0.01672	-0.19252	0.51274			
DLPFC	0.17491	0.195	0.024243	-0.19071	0.16405			
	a_1 (-)	x_1	b_1	y0	Adjusted r^2			
EVC	-0.34231	0.29074	0.016664	-0.14153	-0.06135			
DLPFC	-0.1761	0.051606	0.01	-0.16295	-0.10128			

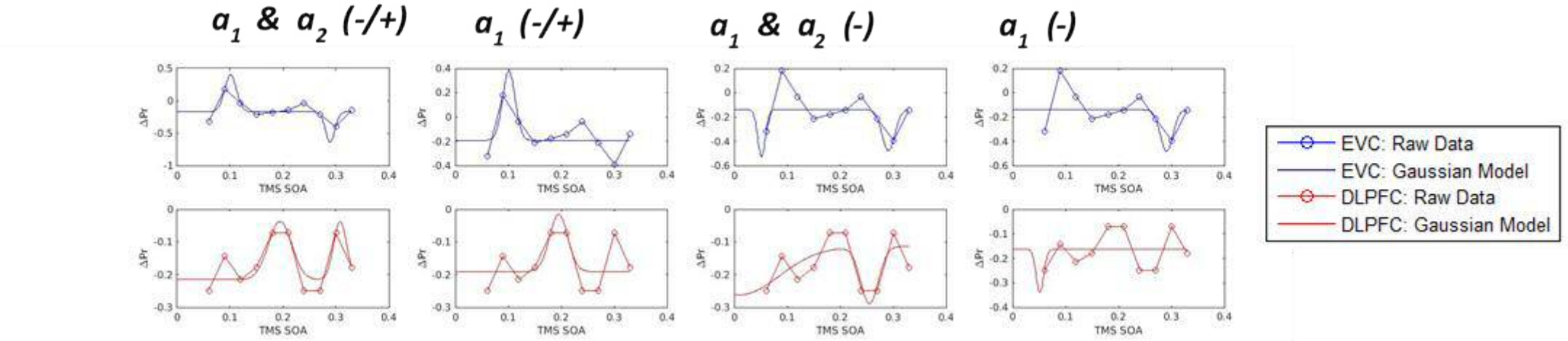

Participant 32	a_1 (-/+)	a_2 (-/+)	x_1	x_2	b_1	b_2	y0	Adjusted r^2
EVC	0.241	-0.09572	0.05288	0.16138	0.01	0.046413	-0.14436	-0.35563
DLPFC	-0.10776	0.20912	0.18245	0.25495	0.026293	0.018441	0.035397	0.55289
	a_1 (-)	a_2 (-)	x_1	x_2	b_1	b_2	y0	Adjusted r^2
EVC	-0.12158	-0.14906	0.093926	0.1894	0.010002	0.27011	-0.0156	-0.53757
DLPFC	-0.12517	-0.14786	0.096867	0.18162	0.020309	0.034557	0.076068	0.056072
	a_1 (-/+)	x_1	b_1	y0	Adjusted r^2			
EVC	0.18781	0.056228	0.01	-0.1629	0.25215			
DLPFC	0.19222	0.255	0.02396	0.012963	0.48694			
	a_1 (-)	x_1	b_1	y0	Adjusted r^2			
EVC	-0.14304	0.14998	0.010007	-0.14267	-0.02885			
DLPFC	-0.10839	0.18232	0.026405	0.036127	-0.03369			

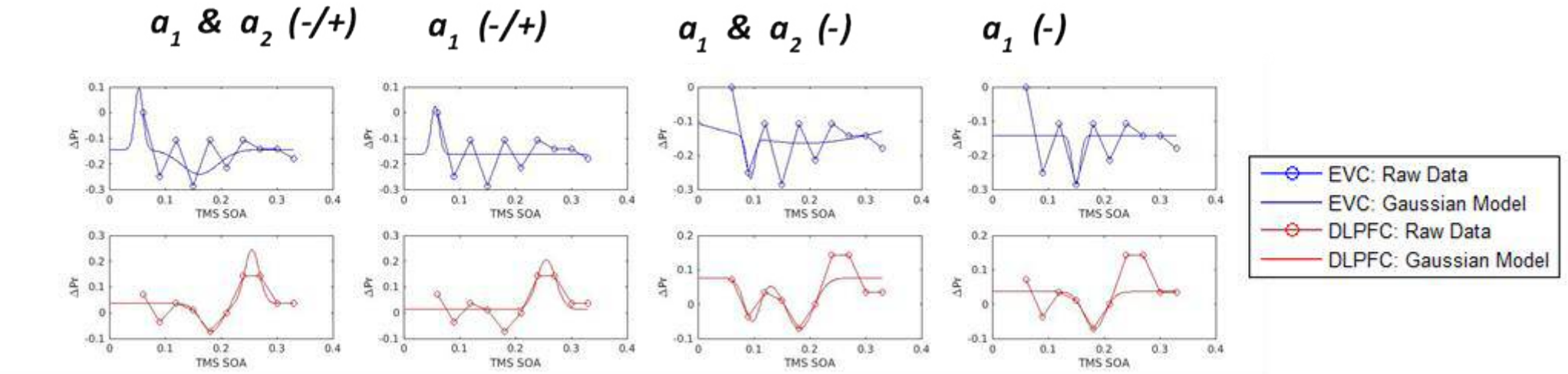

Experiment 1 : ΔAcc model fits produced by monophasic and biphasic Gaussian models with positive and negative or negative amplitude ceofficients and raw data from experiment 1 (-/+) refers to positive and negative amplitude coefficients (-) refers to negative amplitude coefficients.

Participant 1	a_1 **(-/+)**	a_2 **(-/+)**	x_1	x_2	b_1	b_2	***y0***	***Adjusted r^2***
EVC	0.57698	0.57698	0.13568	0.22455	0.024703	0.025089	-0.17835	0.16256
DLPFC	1.0264	-0.38133	0.11091	0.2706	0.013371	0.01	0.022944	0.5246
	a_1 **(-)**	a_2 **(-)**	x_1	x_2	b_1	b_2	***y0***	***Adjusted r^2***
EVC	-0.34018	-0.36831	0.27005	0.33425	0.011737	0.010097	0.076257	-0.6789
DLPFC	-0.54287	-0.58513	0.26602	0.37062	0.010003	0.044022	0.10887	-0.48655
	a_1 **(-/+)**	x_1	b_1	***y0***	***Adjusted r^2***			
EVC	0.57698	0.18007	0.14654	-0.31849	-0.36572			
DLPFC	1.0269	0.11088	0.013528	0.017161	0.52338			
	a_1 **(-)**	x_1	b_1	***y0***	***Adjusted r^2***			
EVC	-0.57667	0.079137	0.019266	0.19135	0.20363			
DLPFC	-0.31583	0.38	0.10623	0.112	-0.25721			

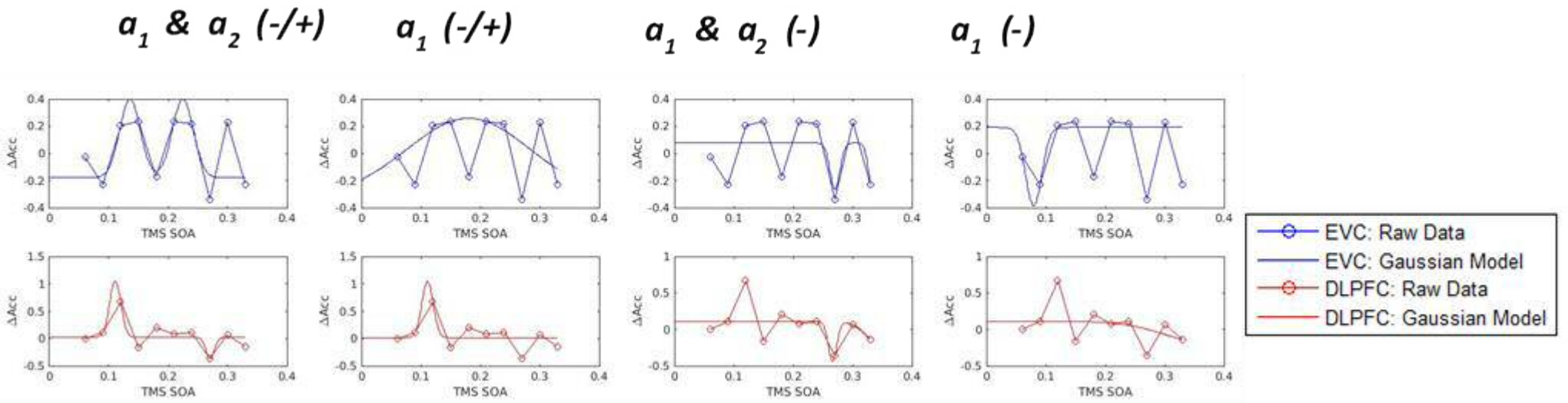

Participant 2	a_1 (-/+)	a_2 (-/+)	x_1	x_2	b_1	b_2	y0	Adjusted r^2
EVC	0.95801	0.79742	0.10167	0.38	0.024192	0.14904	-0.43472	0.61241
DLPFC	-0.899	-0.91142	0.037142	0.1643	0.030123	0.02151	0.15618	0.36728
	a_1 (-)	a_2 (-)	x_1	x_2	b_1	b_2	y0	Adjusted r^2
EVC	-0.95801	-0.74831	0.056703	0.20367	0.01002	0.10083	0.47803	0.2108
DLPFC	-0.86326	-0.91142	0.038357	0.1643	0.029579	0.021508	0.15612	0.36726
	a_1 (-/+)	x_1	b_1	y0	Adjusted r^2			
EVC	-0.95801	0.1639	0.016381	0.044975	0.073964			
DLPFC	-0.68294	0.16427	0.03032	0.11474	0.11544			
	a_1 (-)	x_1	b_1	y0	Adjusted r^2			
EVC	-0.95801	0.1639	0.016386	0.045208	0.074008			
DLPFC	-0.68285	0.16427	0.030404	0.11539	0.1141			

a_1 & a_2 (-/+) a_1 (-/+) a_1 & a_2 (-) a_1 (-)

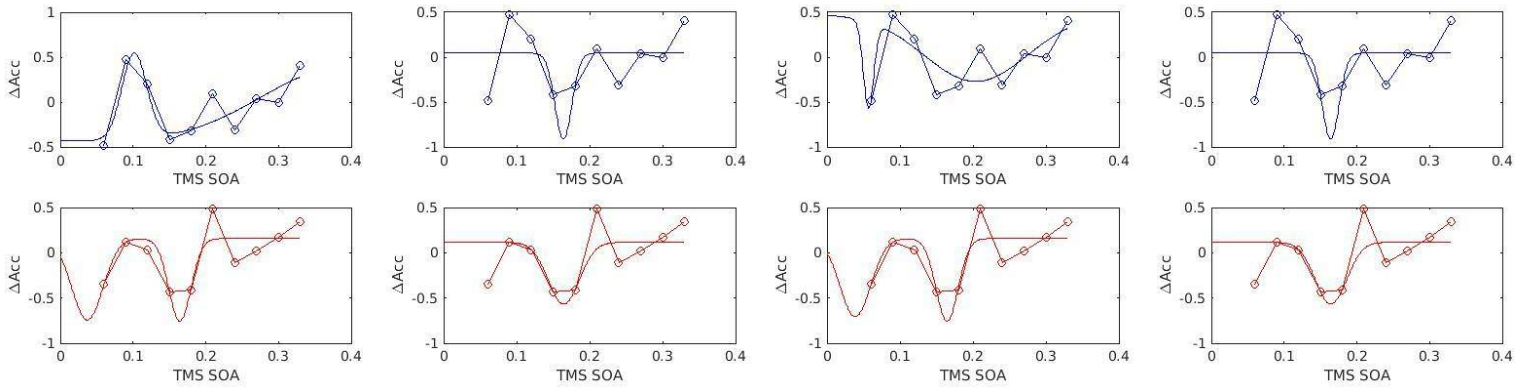

Participant 3	a_1 (-/+)	a_2 (-/+)	x_1	x_2	b_1	b_2	y0	Adjusted r^2
EVC	-0.67023	-0.64446	0.1119	0.23613	0.026736	0.040207	0.36762	0.28541
DLPFC	-1.1056	-0.58059	0.11489	0.23213	0.011553	0.034719	0.41638	0.71558
	a_1 (-)	a_2 (-)	x_1	x_2	b_1	b_2	y0	Adjusted r^2
EVC	-0.67051	-0.64489	0.1119	0.23613	0.026759	0.040225	0.36805	0.28567
DLPFC	-0.90379	-0.5996	0.11994	0.23423	0.010371	0.03384	0.42964	0.72834
	a_1 (-/+)	x_1	b_1	y0	Adjusted r^2			
EVC	-0.96653	0.10792	0.013593	0.1949	-0.15662			
DLPFC	0.90759	0.07485	0.011622	0.23978	-0.41853			
	a_1 (-)	x_1	b_1	y0	Adjusted r^2			
EVC	-0.55318	0.23585	0.035943	0.27496	-0.0681			
DLPFC	-0.61464	0.1202	0.01149	0.27864	0.2933			

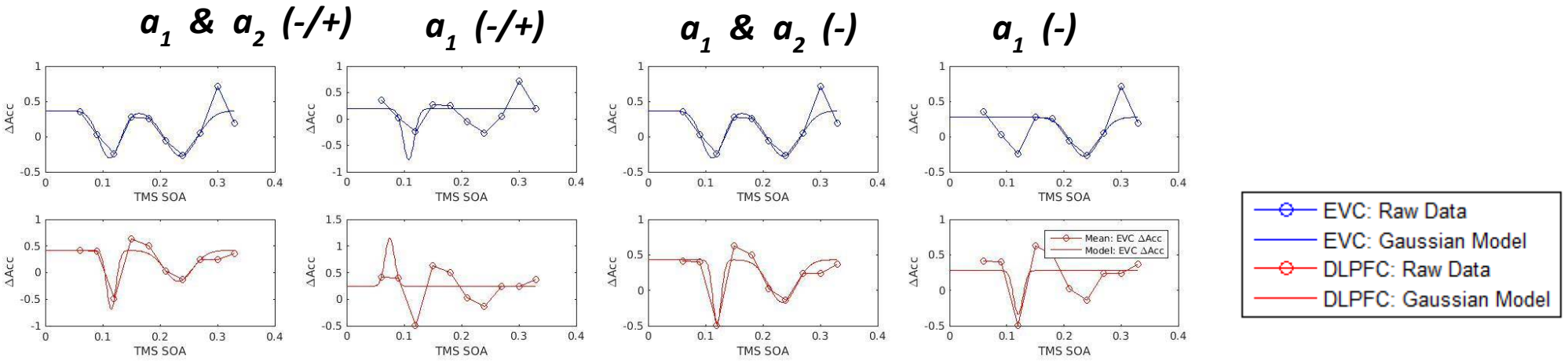

Participant 4	a_1 (-/+)	a_2 (-/+)	x_1	x_2	b_1	b_2	y0	Adjusted r^2
EVC	0.84767	1.1826	0.14476	0.30251	0.061876	0.030246	-0.48674	0.56895
DLPFC	-0.68488	-0.83669	0.089933	0.24155	0.011281	0.1014	0.077214	0.65824
	a_1 (-)	a_2 (-)	x_1	x_2	b_1	b_2	y0	Adjusted r^2
EVC	-1.192	-0.71959	0.076026	0.23901	0.015798	0.032882	0.21137	0.34844
DLPFC	-0.68358	-0.83691	0.089788	0.24164	0.011177	0.10158	0.078127	0.65836
	a_1 (-/+)	x_1	b_1	y0	Adjusted r^2			
EVC	-0.67793	0.23896	0.031343	0.16961	-0.00222			
DLPFC	0.98924	0.13184	0.015512	-0.57063	0.06598			
	a_1 (-)	x_1	b_1	y0	Adjusted r^2			
EVC	-1.192	0.076039	0.013659	0.085626	-0.20334			
DLPFC	-0.81576	0.23055	0.095151	0.079115	0.035745			

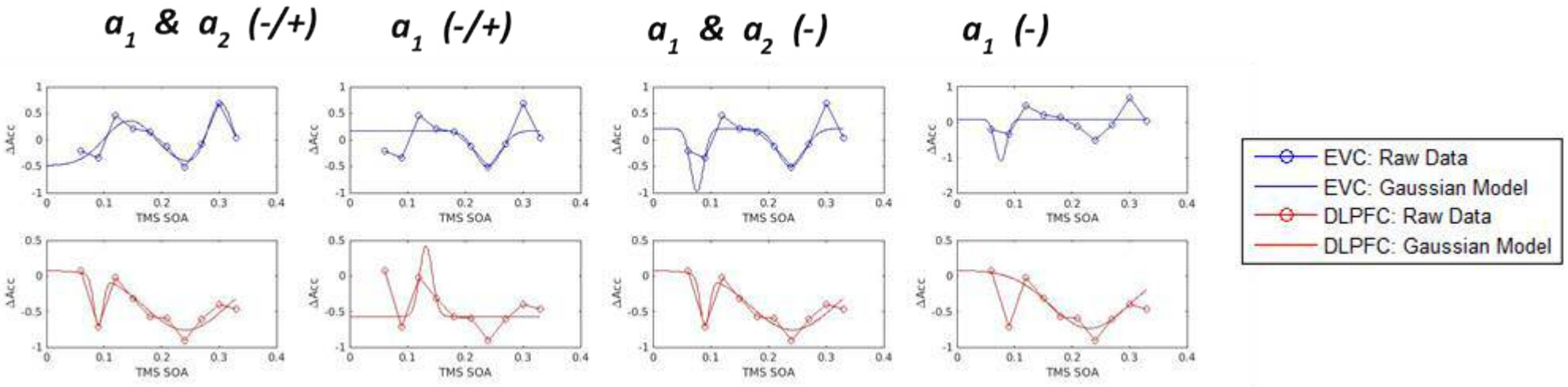

Participant 5	a_1 (-/+)	a_2 (-/+)	x_1	x_2	b_1	b_2	y0	Adjusted r^2
EVC	-0.69127	0.63247	0.18284	0.20729	0.072859	0.015237	0.19004	0.56897
DLPFC	-0.81587	0.98213	0.1996	0.22557	0.039133	0.022946	-0.07299	0.69026
	a_1 (-)	a_2 (-)	x_1	x_2	b_1	b_2	y0	Adjusted r^2
EVC	-0.7241	-0.65397	0.16544	0.25109	0.028313	0.012447	0.11856	0.63058
DLPFC	-0.70901	-0.41078	0.17859	0.2826	0.028139	0.014033	0.012968	0.13424
	a_1 (-/+)	x_1	b_1	y0	Adjusted r^2			
EVC	-0.7241	0.16579	0.027304	0.078159	0.62792			
DLPFC	-0.61564	0.17917	0.025205	-0.07536	0.4517			
	a_1 (-)	x_1	b_1	y0	Adjusted r^2			
EVC	-0.7241	0.16579	0.027304	0.078159	0.62792			
DLPFC	-0.61564	0.17917	0.025205	-0.07536	0.4517			

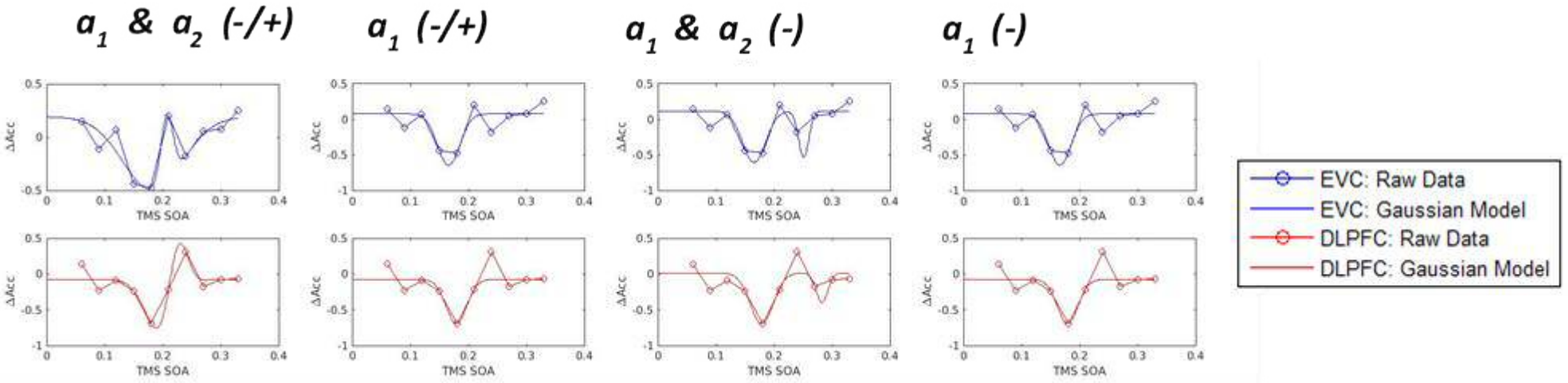

Participant 6	a_1 (-/+)	a_2 (-/+)	x_1	x_2	b_1	b_2	y0	Adjusted r^2
EVC	-0.43598	-0.55811	0.056024	0.33286	0.01002	0.010001	0.071814	-0.07102
DLPFC	1.0378	-1.0699	0.29401	0.34653	0.028627	0.044699	0.026954	0.47383
	a_1 (-)	a_2 (-)	x_1	x_2	b_1	b_2	y0	Adjusted r^2
EVC	-0.63495	-0.66627	0.052707	0.33507	0.010001	0.01	0.07179	-0.071
DLPFC	-0.69756	-1.0616	0.053715	0.32998	0.24214	0.011193	0.64434	0.096038
	a_1 (-/+)	x_1	b_1	y0	Adjusted r^2			
EVC	-0.32745	0.057147	0.01	0.000584	-0.06224			
DLPFC	0.99389	0.13773	0.012262	0.023694	-0.35522			
	a_1 (-)	x_1	b_1	y0	Adjusted r^2			
EVC	-0.49659	0.053062	0.01	0.0056	-0.05957			
DLPFC	-0.84446	0.077028	0.01247	0.089335	-0.39547			

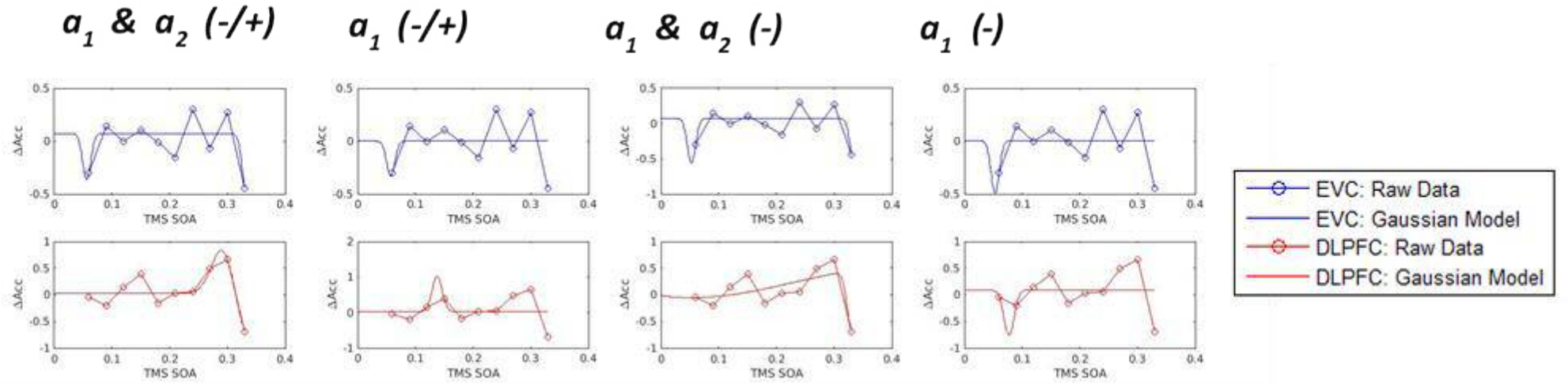

Participant 7	a_1 (-/+)	a_2 (-/+)	x_1	x_2	b_1	b_2	$y0$	Adjusted r^2
EVC	0.55116	0.79348	0.12633	0.25851	0.046877	0.017171	-0.08468	0.039991
DLPFC	0.62535	-0.82747	0.1026	0.29061	0.012854	0.016077	0.2973	0.88749
	a_1 (-)	a_2 (-)	x_1	x_2	b_1	b_2	$y0$	Adjusted r^2
EVC	-0.79348	-0.49445	0.056081	0.31181	0.01	0.20709	0.54472	-0.21365
DLPFC	-0.48359	-0.7262	0.049358	0.29315	0.01001	0.021504	0.36519	0.64333
	a_1 (-/+)	x_1	b_1	$y0$	Adjusted r^2			
EVC	-0.47039	0.056306	0.01	0.16189	0.025327			
DLPFC	0.33122	0.14661	0.084956	0.097093	-0.06606			
	a_1 (-)	x_1	b_1	$y0$	Adjusted r^2			
EVC	-0.55634	0.054556	0.01	0.16511	0.027567			
DLPFC	-0.79664	0.29118	0.017903	0.33391	0.74885			

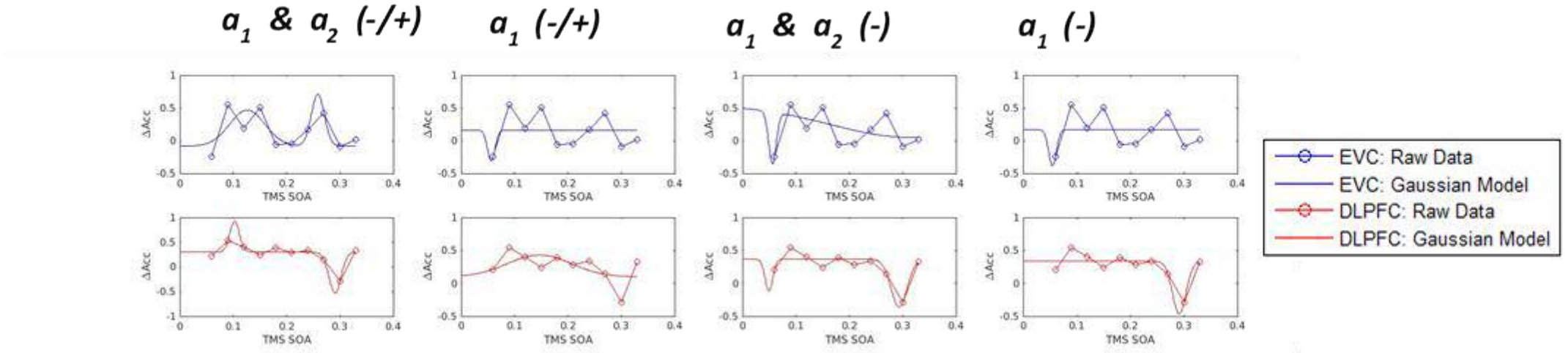

Participant 8	a_1 (-/+)	a_2 (-/+)	x_1	x_2	b_1	b_2	y0	Adjusted r^2
EVC	-1.0046	-1.3005	0.054755	0.1937	0.020109	0.016133	0.20918	0.012538
DLPFC	-0.77285	-0.42696	0.058413	0.22328	0.01	0.081654	0.10349	0.31776
	a_1 (-)	a_2 (-)	x_1	x_2	b_1	b_2	y0	Adjusted r^2
EVC	-1.2762	-1.3061	0.046716	0.19371	0.023956	0.016101	0.20952	0.25951
DLPFC	-0.76186	-0.44492	0.060078	0.22632	0.010288	0.091469	0.13382	0.094117
	a_1 (-/+)	x_1	b_1	y0	Adjusted r^2			
EVC	-0.84107	0.059359	0.01	0.10771	0.050452			
DLPFC	-0.60345	0.056639	0.010091	-0.11838	0.13199			
	a_1 (-)	x_1	b_1	y0	Adjusted r^2			
EVC	-0.87066	0.057993	0.01	0.10638	0.1866			
DLPFC	-0.58112	0.05689	0.010037	-0.13055	0.46588			

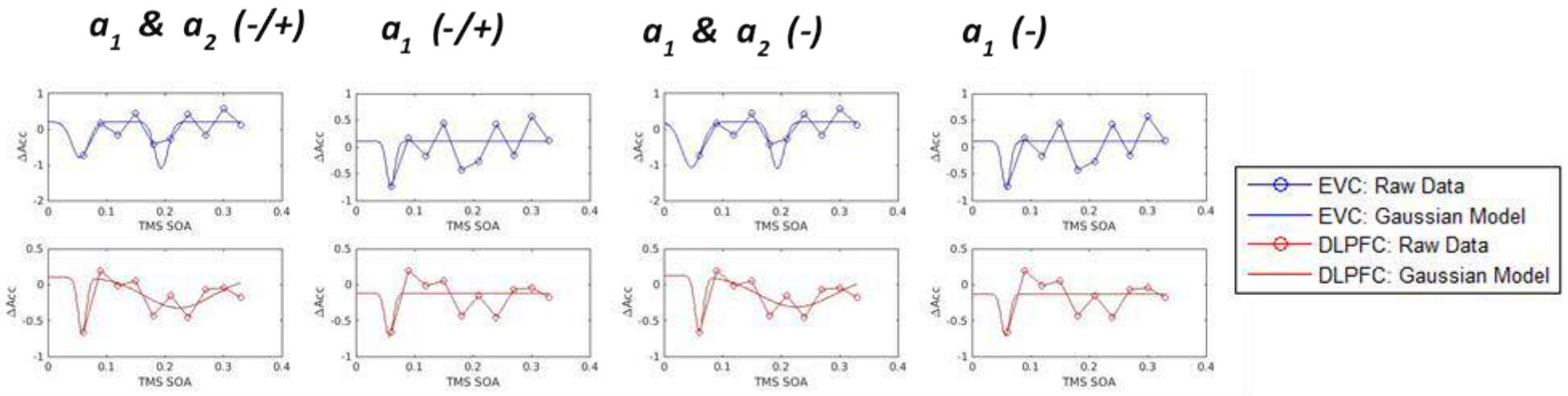

Participant 9	a_1 (-/+)	a_2 (-/+)	x_1	x_2	b_1	b_2	y0	Adjusted r^2
EVC	0.45229	0.42713	0.19494	0.29591	0.02879	0.036767	-0.11457	0.87269
DLPFC	0.71559	0.92818	0.1284	0.29173	0.053498	0.016307	-0.19099	0.30339
	a_1 (-)	a_2 (-)	x_1	x_2	b_1	b_2	y0	Adjusted r^2
EVC	-0.37976	-0.37398	0.084745	0.24899	0.072869	0.016809	0.22713	0.078758
DLPFC	-0.87947	-0.67693	0.22266	0.33516	0.014276	0.01	0.20854	-0.23002
	a_1 (-/+)	x_1	b_1	y0	Adjusted r^2			
EVC	-0.28584	0.065795	0.08002	0.14628	0.19262			
DLPFC	0.65586	0.11759	0.029273	-0.03332	0.010126			
	a_1 (-)	x_1	b_1	y0	Adjusted r^2			
EVC	-0.28584	0.065795	0.08002	0.14628	0.19262			
DLPFC	-0.5566	0.3341	0.01	0.16027	0.037454			

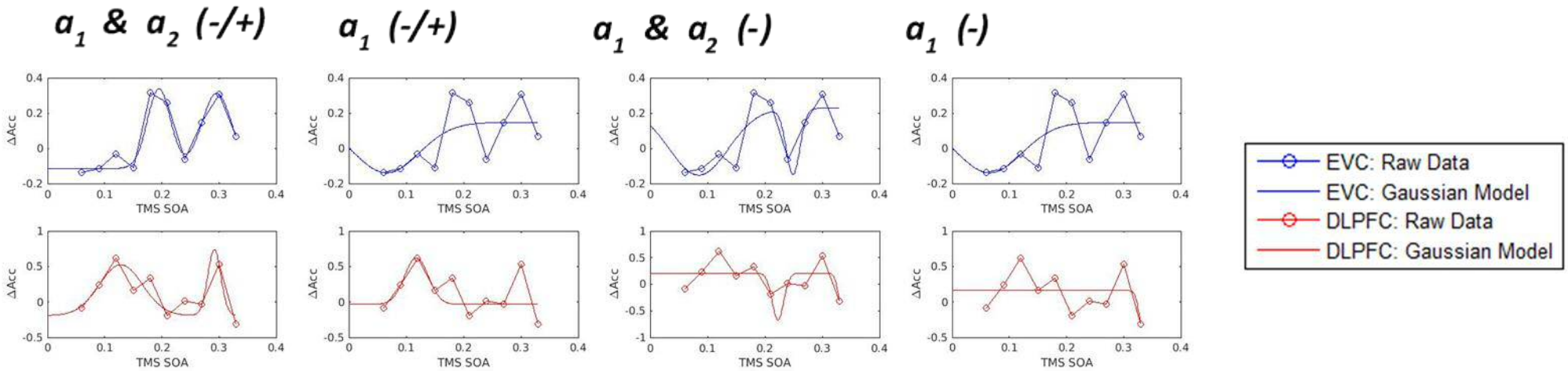

Participant 10	a_1 (-/+)	a_2 (-/+)	x_1	x_2	b_1	b_2	y0	Adjusted r^2
EVC	0.70119	0.43855	0.12049	0.21832	0.013477	0.042352	-0.177	0.5989
DLPFC	0.93733	0.70603	0.19464	0.29967	0.0209	0.010252	-0.53365	0.33136
	a_1 (-)	a_2 (-)	x_1	x_2	b_1	b_2	y0	Adjusted r^2
EVC	-0.9407	-0.57579	0.076491	0.30036	0.013957	0.036657	0.18288	0.077455
DLPFC	-0.2482	-0.67476	0.061087	0.33601	0.068541	0.01	-0.24365	-0.76816
	a_1 (-/+)	x_1	b_1	y0	Adjusted r^2			
EVC	0.55076	0.11999	0.011491	-0.05129	0.28404			
DLPFC	0.93733	0.19434	0.020637	-0.51209	-0.01119			
	a_1 (-)	x_1	b_1	y0	Adjusted r^2			
EVC	-0.45735	0.30033	0.030832	0.064595	0.054702			
DLPFC	-0.88354	0.076132	0.012561	-0.3421	-0.3645			

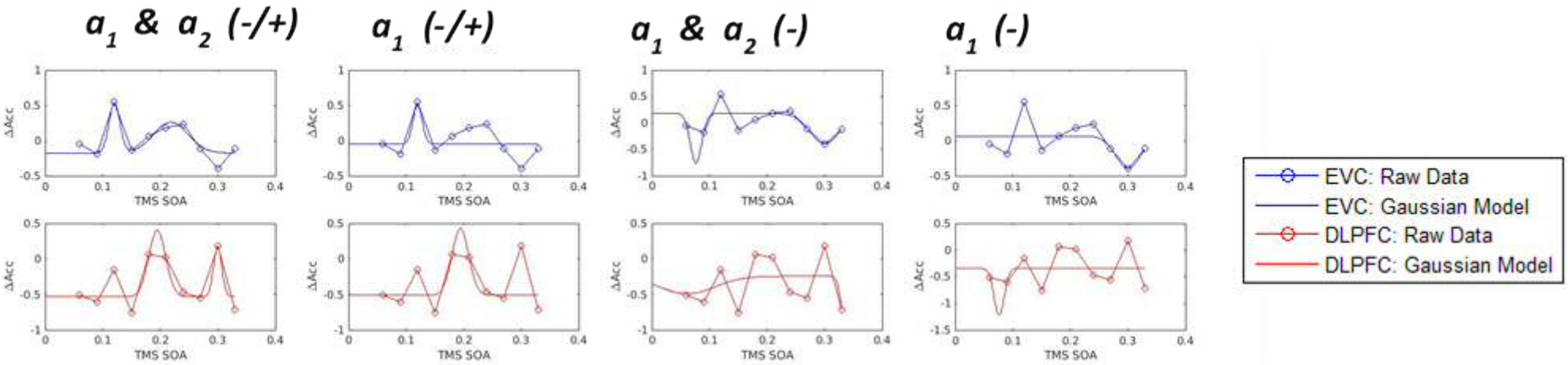

Participant 11	a_1 (-/+)	a_2 (-/+)	x_1	x_2	b_1	b_2	y0	Adjusted r^2
EVC	-0.65953	-0.73891	0.21035	0.29957	0.023824	0.011294	0.13885	0.43964
DLPFC	0.35329	0.6257	0.14886	0.33569	0.01	0.010035	-0.13854	0.17994
	a_1 (-)	a_2 (-)	x_1	x_2	b_1	b_2	y0	Adjusted r^2
EVC	-0.67031	-0.77459	0.21036	0.29997	0.024023	0.01058	0.14534	0.45234
DLPFC	-0.666	-0.28952	0.10886	0.21288	0.016207	0.041239	0.066124	-0.64929
	a_1 (-/+)	x_1	b_1	y0	Adjusted r^2			
EVC	-0.72401	0.21028	0.026043	0.19215	-0.35201			
DLPFC	-0.666	0.10898	0.012924	-0.02888	-0.15175			
	a_1 (-)	x_1	b_1	y0	Adjusted r^2			
EVC	-0.6124	0.30023	0.010948	0.033178	0.13456			
DLPFC	-0.666	0.10898	0.012926	-0.02881	0.012835			

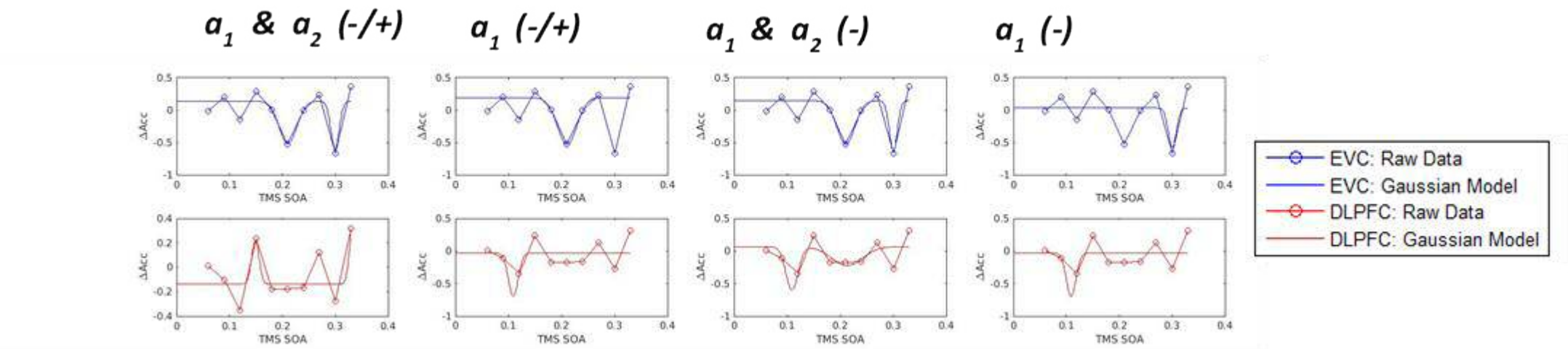

Participant 12	a_1 (-/+)	a_2 (-/+)	x_1	x_2	b_1	b_2	y0	Adjusted r^2
EVC	0.65957	-0.70522	0.14899	0.17348	0.045259	0.01963	-0.20739	0.55521
DLPFC	0.54513	0.54513	0.13287	0.31272	0.01839	0.01505	-0.32813	0.46181
	a_1 (-)	a_2 (-)	x_1	x_2	b_1	b_2	y0	Adjusted r^2
EVC	-0.43612	-0.37826	0.1808	0.26848	0.012472	0.042946	0.024604	-0.32617
DLPFC	-0.54513	-0.53893	0.19067	0.25972	0.017368	0.013653	-0.16244	0.19842
	a_1 (-/+)	x_1	b_1	y0	Adjusted r^2			
EVC	0.71493	0.13551	0.021705	-0.18074	0.59321			
DLPFC	0.54513	0.13298	0.016521	-0.28797	0.20962			
	a_1 (-)	x_1	b_1	y0	Adjusted r^2			
EVC	-0.29128	0.27045	0.028055	-0.08919	-0.21498			
DLPFC	-0.54513	0.19084	0.014776	-0.22097	0.17091			

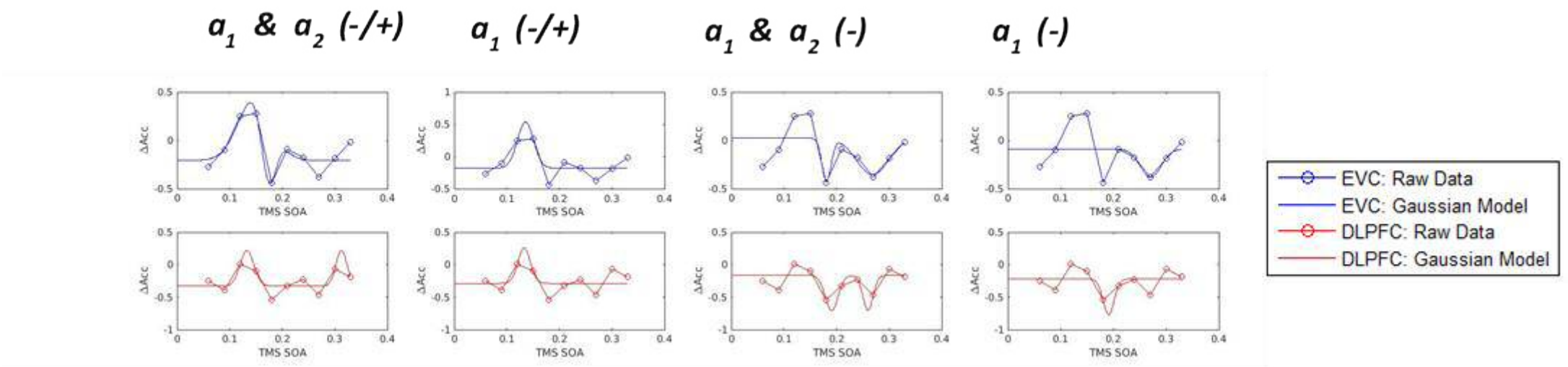

Participant 13	a_1 (-/+)	a_2 (-/+)	x_1	x_2	b_1	b_2	y0	Adjusted r^2
EVC	0.93867	0.96939	0.073789	0.29323	0.014075	0.016804	-0.02771	0.77564
DLPFC	-0.63693	0.54614	0.23962	0.26194	0.013299	0.11545	-0.07434	0.04447
	a_1 (-)	a_2 (-)	x_1	x_2	b_1	b_2	y0	Adjusted r^2
EVC	-0.89743	-0.69247	0.16837	0.33006	0.12831	0.010762	0.80115	-0.01903
DLPFC	-0.45187	-0.56607	0.055853	0.23999	0.11801	0.011656	0.40477	-0.09857
	a_1 (-/+)	x_1	b_1	y0	Adjusted r^2			
EVC	-0.48429	0.1863	0.10172	0.41911	-0.19946			
DLPFC	-0.47199	0.059986	0.010004	0.3006	-0.36651			
	a_1 (-)	x_1	b_1	y0	Adjusted r^2			
EVC	-0.48261	0.18633	0.10147	0.41746	-0.19894			
DLPFC	-0.79784	0.13004	0.017509	0.34312	0.31094			

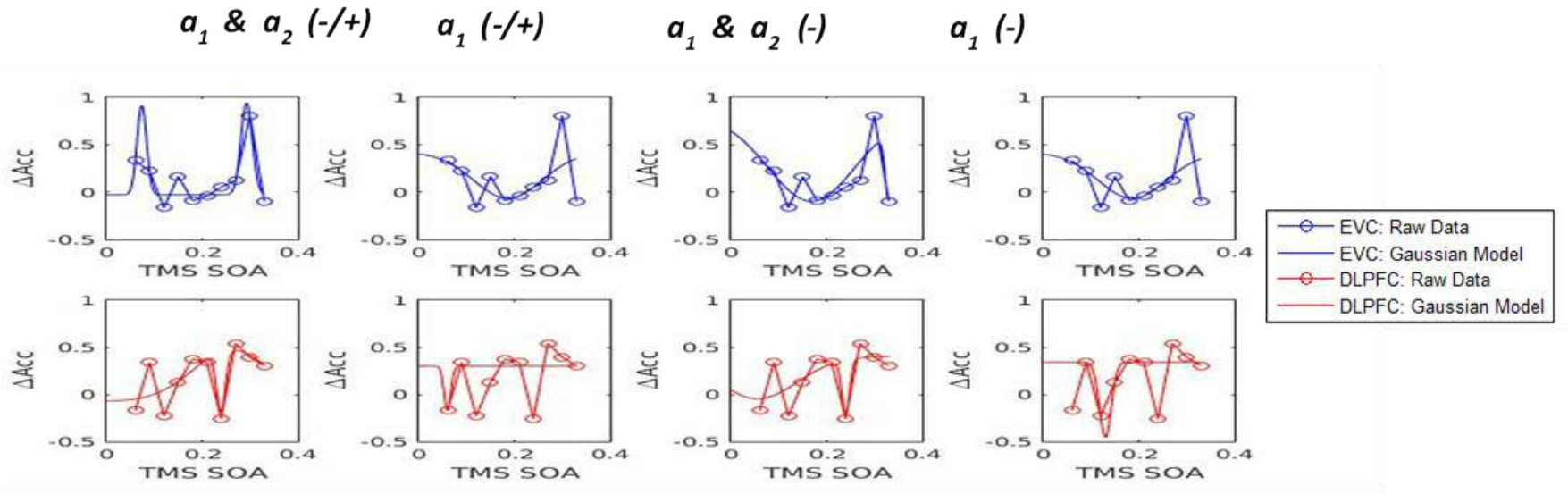

Participant 14	a_1 (-/+)	a_2 (-/+)	x_1	x_2	b_1	b_2	$y0$	Adjusted r^2
EVC	-0.70353	-0.58804	0.10695	0.3326	0.017944	0.01	0.30446	0.68259
DLPFC	0.62161	-0.50889	0.20833	0.27433	0.12428	0.010005	-0.21226	0.11047
	a_1 (-)	a_2 (-)	x_1	x_2	b_1	b_2	$y0$	Adjusted r^2
EVC	-0.70374	-0.58487	0.10695	0.33249	0.017941	0.01	0.30447	0.6826
DLPFC	-0.80825	-0.80824	0.052718	0.28107	0.010024	0.013508	0.26455	-0.06058
	a_1 (-/+)	x_1	b_1	$y0$	Adjusted r^2			
EVC	-0.70588	0.10698	0.017627	0.29447	0.44277			
DLPFC	0.65793	0.21068	0.11595	-0.21226	-0.06297			
	a_1 (-)	x_1	b_1	$y0$	Adjusted r^2			
EVC	-0.70588	0.10698	0.017627	0.29446	0.44277			
DLPFC	-0.48781	0.055579	0.01	0.18895	0.0568			

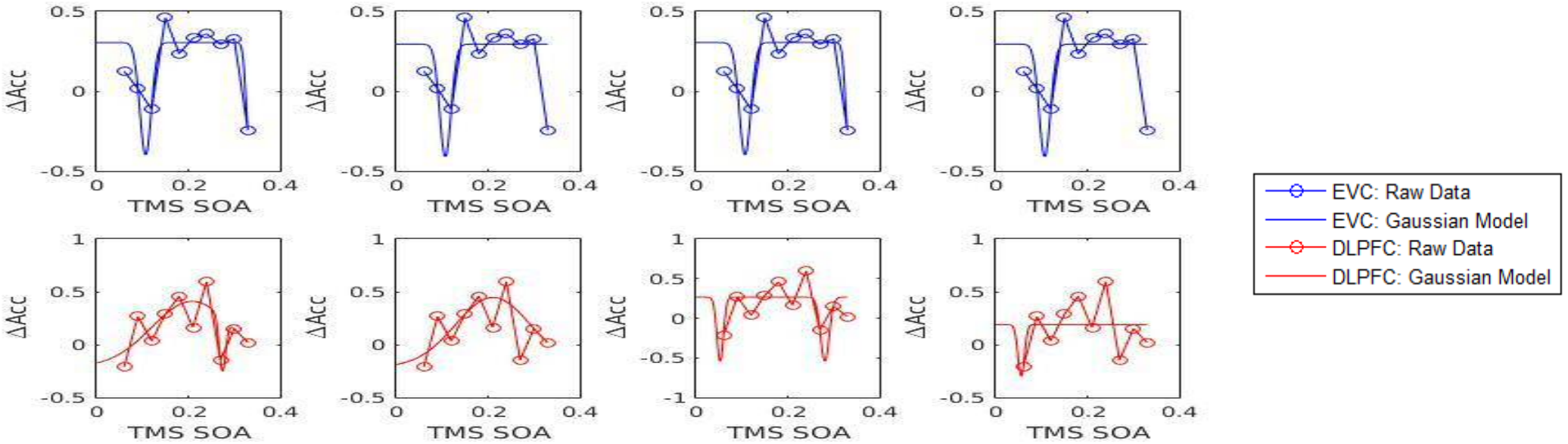

Participant 15	a_1 (-/+)	a_2 (-/+)	x_1	x_2	b_1	b_2	y0	Adjusted r^2
EVC	0.70023	-0.94151	0.062901	0.19094	0.015488	0.012147	0.03944	0.68434
DLPFC	0.50256	-0.80382	0.15016	0.20918	0.012473	0.14963	0.4064	0.10272
	a_1 (-)	a_2 (-)	x_1	x_2	b_1	b_2	y0	Adjusted r^2
EVC	-0.34792	-0.79098	0.18057	0.22275	0.010003	0.17407	0.7149	-0.07845
DLPFC	-0.98192	-0.75222	0.10442	0.22679	0.016081	0.11098	0.40812	-0.11038
	a_1 (-/+)	x_1	b_1	y0	Adjusted r^2			
EVC	0.84856	0.066051	0.016149	-0.02187	0.52385			
DLPFC	0.4895	0.15023	0.011411	-0.18881	0.014991			
	a_1 (-)	x_1	b_1	y0	Adjusted r^2			
EVC	-0.77176	0.1931	0.21917	0.71553	0.1354			
DLPFC	-0.96277	0.19224	0.012867	-0.18425	-0.25373			

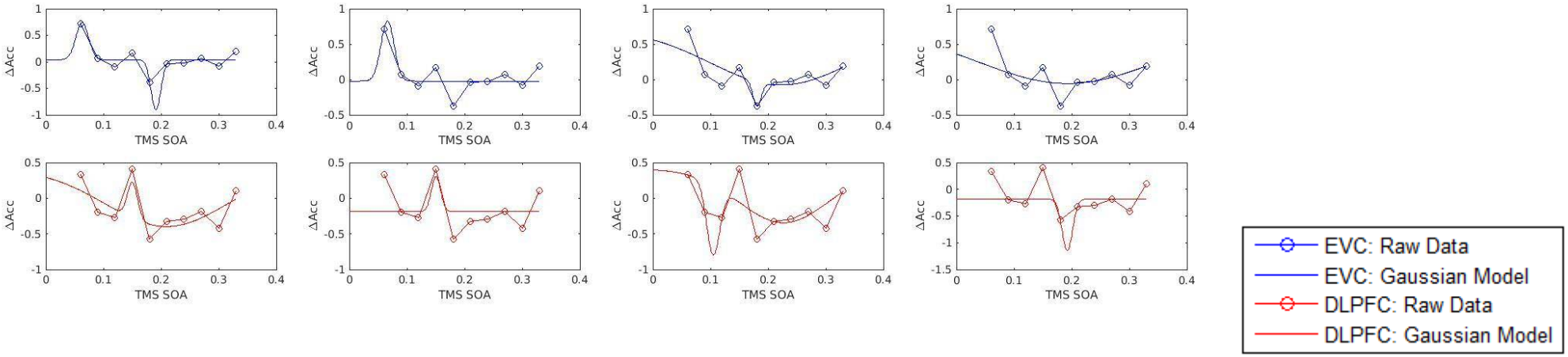

Participant 16	a_1 (-/+)	a_2 (-/+)	x_1	x_2	b_1	b_2	y0	Adjusted r^2
EVC	-0.49156	-0.40429	0.15592	0.27591	0.046952	0.043124	0.32746	0.35549
DLPFC	0.4882	-0.5685	0.12499	0.21088	0.01415	0.045751	0.097715	0.4625
	a_1 (-)	a_2 (-)	x_1	x_2	b_1	b_2	y0	Adjusted r^2
EVC	-0.49158	-0.40376	0.1559	0.27581	0.046476	0.042766	0.32542	0.36434
DLPFC	-0.7637	-0.72331	0.21234	0.31915	0.058175	0.014516	0.2913	0.48282
	a_1 (-/+)	x_1	b_1	y0	Adjusted r^2			
EVC	-0.29771	0.15817	0.036063	0.13496	0.11052			
DLPFC	-0.58922	0.21584	0.048164	0.11344	0.39342			
	a_1 (-)	x_1	b_1	y0	Adjusted r^2			
EVC	-0.29771	0.15817	0.036063	0.13496	0.11052			
DLPFC	-0.58921	0.21584	0.048164	0.11344	0.39342			

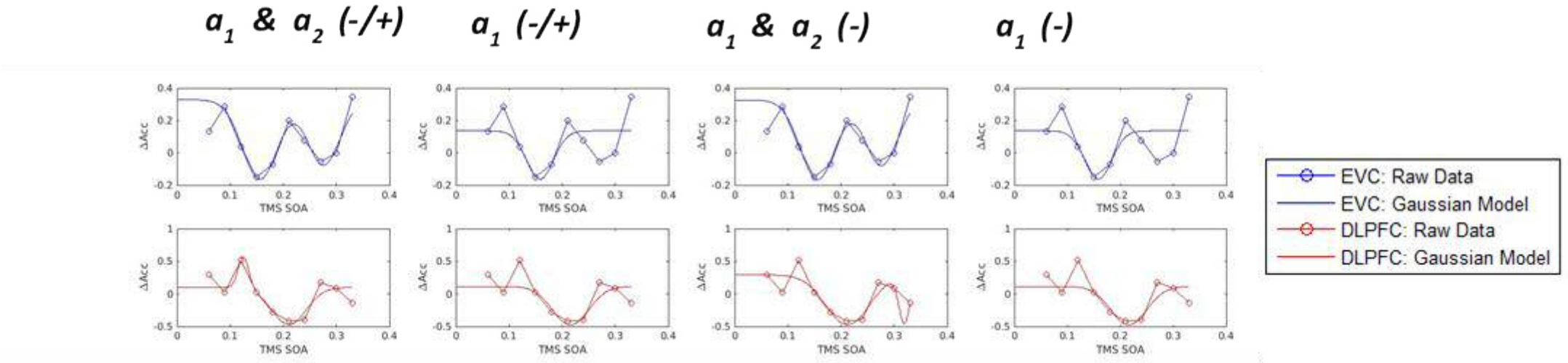

Participant 17	a_1 (-/+)	a_2 (-/+)	x_1	x_2	b_1	b_2	y0	Adjusted r^2
EVC	-0.36684	-0.7963	0.12028	0.26466	0.038345	0.018211	0.28092	0.9094
DLPFC	-0.42233	-0.72514	0.15096	0.23684	0.01	0.02935	0.04503	0.48861
	a_1 (-)	a_2 (-)	x_1	x_2	b_1	b_2	y0	Adjusted r^2
EVC	-0.36667	-0.7963	0.12101	0.26447	0.038027	0.017781	0.28055	0.88079
DLPFC	-0.42372	-0.72524	0.15104	0.23683	0.010001	0.029341	0.044965	0.48862
	a_1 (-/+)	x_1	b_1	y0	Adjusted r^2			
EVC	-0.30473	0.11768	0.033191	0.21735	0.16985			
DLPFC	-0.71562	0.23686	0.0301	0.042361	0.34999			
	a_1 (-)	x_1	b_1	y0	Adjusted r^2			
EVC	-0.57672	0.26986	0.011672	0.16971	0.5486			
DLPFC	-0.71562	0.23686	0.0301	0.042361	0.34999			

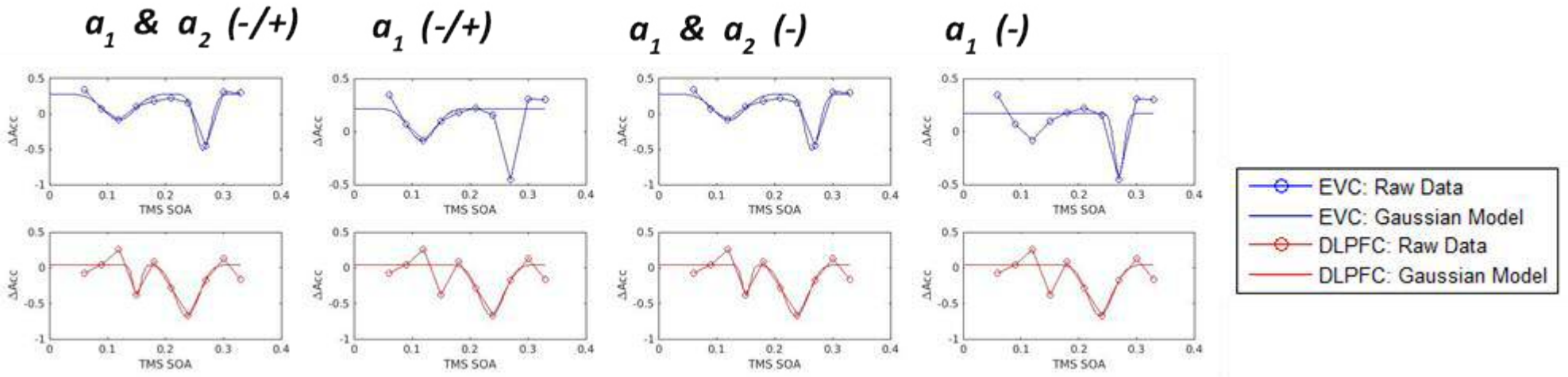

Participant 18	a_1 (-/+)	a_2 (-/+)	x_1	x_2	b_1	b_2	y0	Adjusted r^2
EVC	-0.43016	0.45082	0.1063	0.17087	0.015793	0.011817	0.19107	-0.248
DLPFC	0.2902	0.66012	0.055856	0.22354	0.01	0.027117	-0.33607	0.76429
	a_1 (-)	a_2 (-)	x_1	x_2	b_1	b_2	y0	Adjusted r^2
EVC	-0.32231	-0.24724	0.1087	0.33411	0.032478	0.010456	0.27417	-0.55377
DLPFC	-0.66012	-0.55053	0.12015	0.31572	0.068245	0.056211	0.20959	0.21797
	a_1 (-/+)	x_1	b_1	y0	Adjusted r^2			
EVC	-0.30954	0.1075	0.023905	0.22391	0.004908			
DLPFC	0.66012	0.22287	0.025996	-0.30708	0.70276			
	a_1 (-)	x_1	b_1	y0	Adjusted r^2			
EVC	-0.30954	0.1075	0.023905	0.22391	0.004908			
DLPFC	-0.1868	0.11387	0.048527	-0.22839	-0.25415			

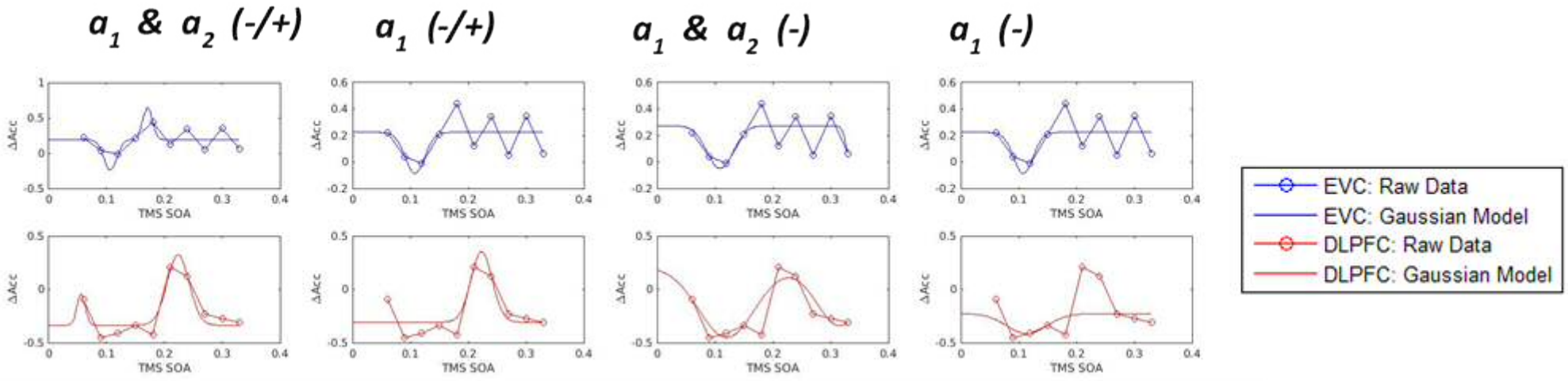

Participant 19	a_1 (-/+)	a_2 (-/+)	x_1	x_2	b_1	b_2	y0	Adjusted r^2
EVC	-1.0513	0.88904	0.24964	0.33732	0.012517	0.010153	0.13005	-0.10134
DLPFC	0.28096	0.41962	0.13081	0.21357	0.032823	0.015168	-0.23848	0.5351
	a_1 (-)	a_2 (-)	x_1	x_2	b_1	b_2	y0	Adjusted r^2
EVC	-0.876	-0.31031	0.24595	0.29023	0.01181	0.018839	0.23092	-0.4786
DLPFC	-0.46315	-0.38064	0.075768	0.38	0.013933	0.1382	-0.01897	0.16431
	a_1 (-/+)	x_1	b_1	y0	Adjusted r^2			
EVC	-0.23817	0.2247	0.076616	0.22324	-0.43869			
DLPFC	0.35898	0.14412	0.13816	-0.39732	0.18001			
	a_1 (-)	x_1	b_1	y0	Adjusted r^2			
EVC	-1.1097	0.25016	0.014014	0.20508	0.10115			
DLPFC	-0.32154	0.38	0.098083	-0.14937	-0.10656			

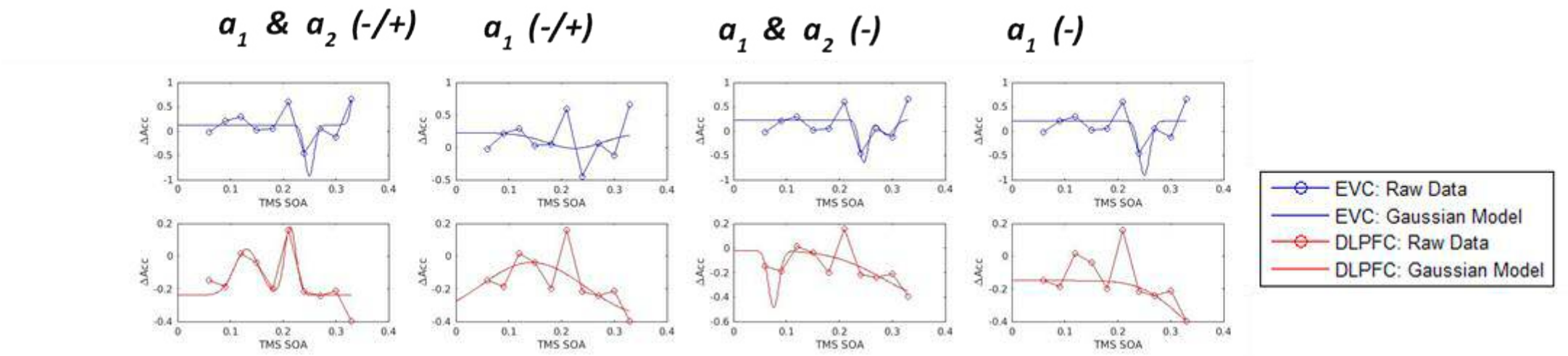

Participant 20	a_1 (-/+)	a_2 (-/+)	x_1	x_2	b_1	b_2	y0	Adjusted r^2
EVC	0.68978	0.72884	0.076824	0.27805	0.06623	0.025483	-0.29712	0.6778
DLPFC	0.65718	0.94622	0.055832	0.14323	0.01	0.037557	-0.23927	0.82858
	a_1 (-)	a_2 (-)	x_1	x_2	b_1	b_2	y0	Adjusted r^2
EVC	-0.65358	-0.80531	0.19038	0.32705	0.067431	0.025822	0.36557	0.64092
DLPFC	-0.81595	-1.0214	0.084298	0.27246	0.025851	0.10725	0.67751	0.72338
	a_1 (-/+)	x_1	b_1	y0	Adjusted r^2			
EVC	0.62541	0.076245	0.051757	-0.21719	0.11942			
DLPFC	0.88934	0.14207	0.034176	-0.16519	0.53233			
	a_1 (-)	x_1	b_1	y0	Adjusted r^2			
EVC	-0.46447	0.33056	0.01	0.0233	0.01674			
DLPFC	-0.6654	0.274	0.082729	0.32088	0.35307			

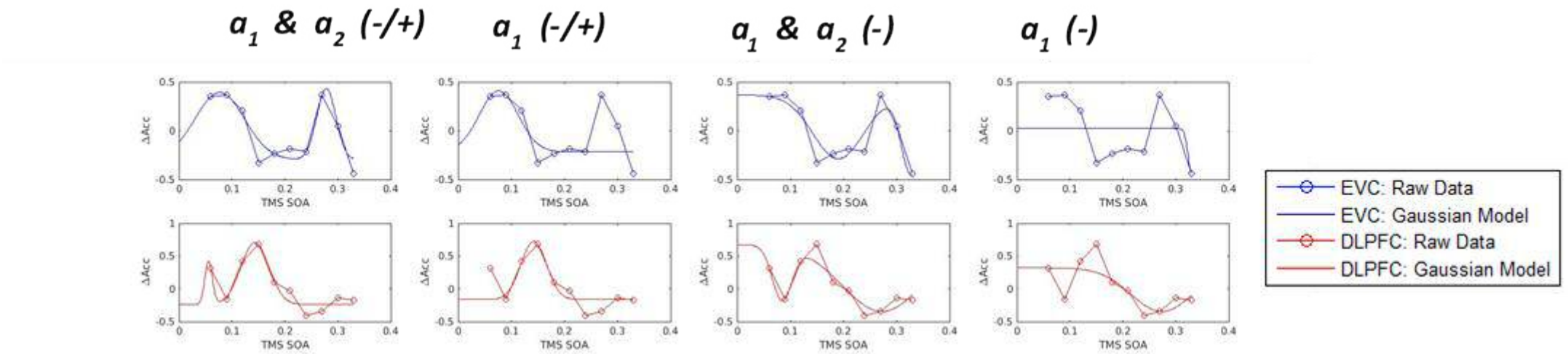

Participant 21	a_1 (-/+)	a_2 (-/+)	x_1	x_2	b_1	b_2	y0	Adjusted r^2
EVC	-0.82521	-0.73337	0.020959	0.18611	0.037155	0.024269	0.04661	0.8315
DLPFC	-0.68352	0.57384	0.26332	0.30149	0.12683	0.01412	0.19214	0.80983
	a_1 (-)	a_2 (-)	x_1	x_2	b_1	b_2	y0	Adjusted r^2
EVC	-0.82521	-0.73337	0.020959	0.18611	0.037155	0.024269	0.04661	0.8315
DLPFC	-0.61144	-0.46232	0.22465	0.33488	0.095183	0.010028	0.20873	0.27734
	a_1 (-/+)	x_1	b_1	y0	Adjusted r^2			
EVC	-0.72128	0.18665	0.02277	0.020489	0.6896			
DLPFC	0.56527	0.067487	0.082252	-0.35187	0.19263			
	a_1 (-)	x_1	b_1	y0	Adjusted r^2			
EVC	-0.72128	0.18665	0.02277	0.020489	0.6896			
DLPFC	-0.71452	0.2645	0.12424	0.20873	0.097681			

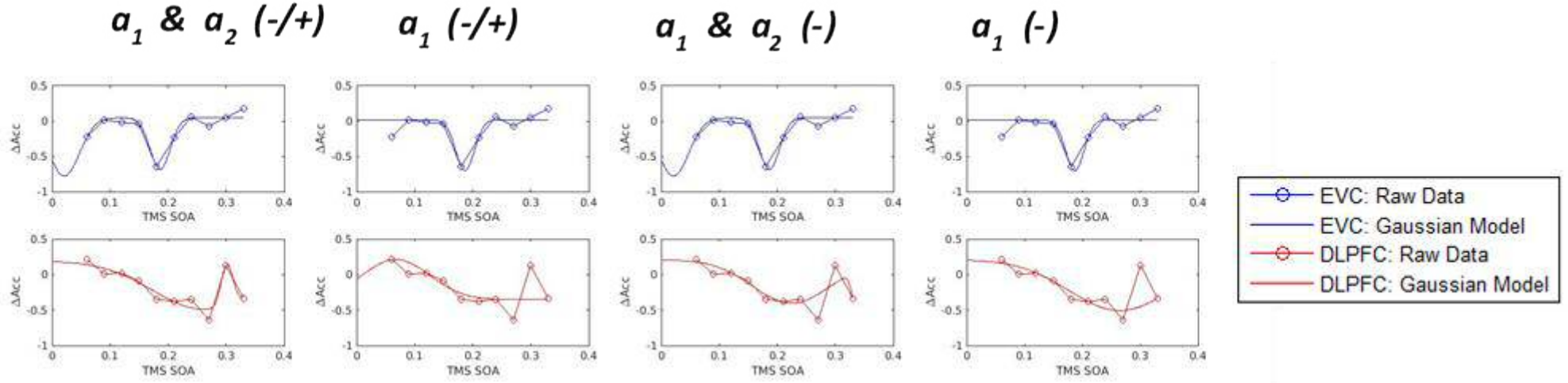

Participant 22	a_1 (-/+)	a_2 (-/+)	x_1	x_2	b_1	b_2	y0	Adjusted r^2
EVC	0.50616	-0.51326	0.18212	0.284	0.010006	0.045109	0.23894	0.59064
DLPFC	-0.32716	-0.79201	0.21039	0.3413	0.012106	0.023158	0.51664	0.45077
	a_1 (-)	a_2 (-)	x_1	x_2	b_1	b_2	y0	Adjusted r^2
EVC	-0.98886	-0.67616	0.13805	0.28347	0.01423	0.057994	0.40906	0.26547
DLPFC	-0.37115	-0.67582	0.20963	0.33561	0.011484	0.021163	0.52363	0.47793
	a_1 (-/+)	x_1	b_1	y0	Adjusted r^2			
EVC	0.30009	0.01	0.17241	0.016094	0.016898			
DLPFC	0.61194	0.16518	0.28754	-0.1065	-0.05557			
	a_1 (-)	x_1	b_1	y0	Adjusted r^2			
EVC	-0.49592	0.27757	0.060154	0.25808	0.17825			
DLPFC	-0.62406	0.33255	0.01	0.47824	0.43641			

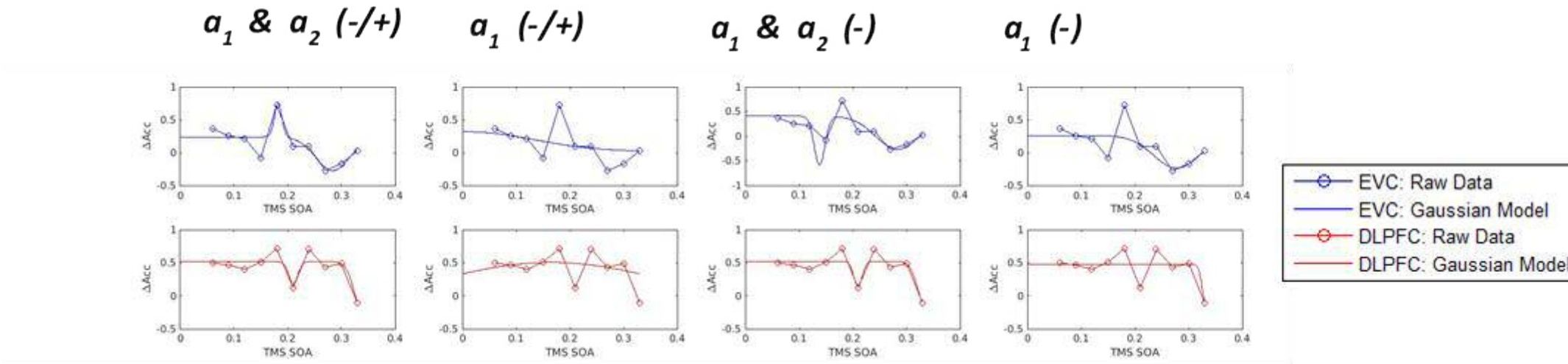

Participant 23	a_1 (-/+)	a_2 (-/+)	x_1	x_2	b_1	b_2	$y0$	Adjusted r^2
EVC	-0.45542	0.34552	0.1909	0.26693	0.14989	0.010057	0.39525	0.22195
DLPFC	0.5733	0.46291	0.043412	0.28226	0.038665	0.013243	0.10571	0.55993
	a_1 (-)	a_2 (-)	x_1	x_2	b_1	b_2	$y0$	Adjusted r^2
EVC	-0.48795	-0.48795	0.15991	0.31245	0.10397	0.015951	0.39387	-0.1354
DLPFC	-0.51075	-0.50842	0.18664	0.31706	0.11787	0.017545	0.58262	0.011299
	a_1 (-/+)	x_1	b_1	$y0$	Adjusted r^2			
EVC	0.36525	0.057767	0.01	0.04779	0.2024			
DLPFC	0.5733	0.040508	0.033854	0.17108	0.60942			
	a_1 (-)	x_1	b_1	$y0$	Adjusted r^2			
EVC	-0.29979	0.1584	0.10006	0.23059	0.043936			
DLPFC	-0.55708	0.22656	0.013376	0.21242	0.30558			

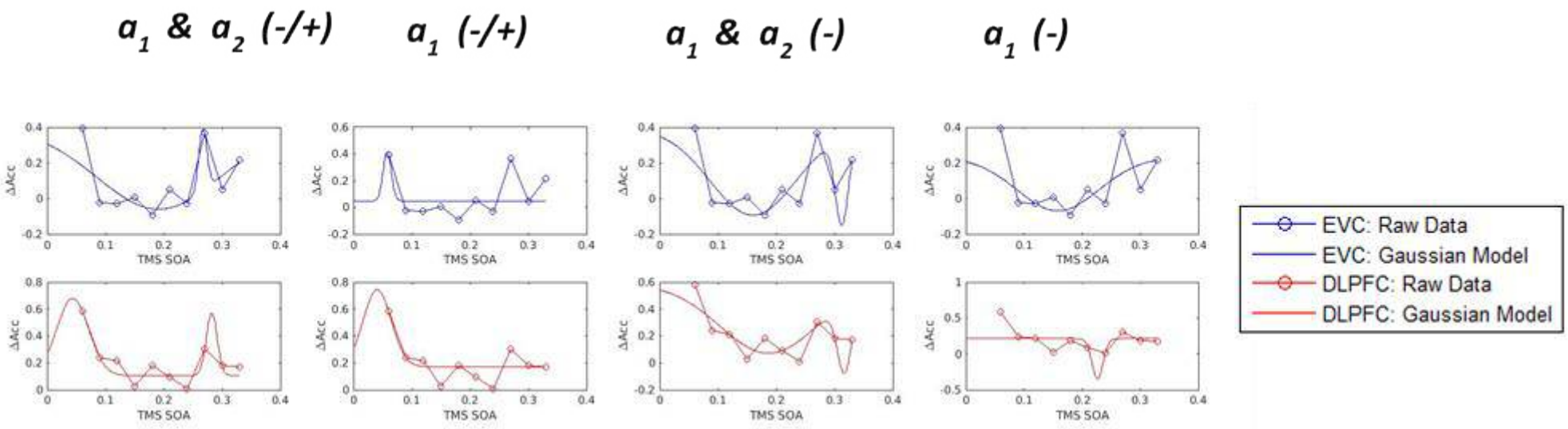

Participant 24	a_1 (-/+)	a_2 (-/+)	x_1	x_2	b_1	b_2	y0	Adjusted r^2
EVC	-0.35955	-0.33567	0.21023	0.28545	0.012674	0.023422	0.003602	-0.39607
DLPFC	0.64425	0.49299	0.13916	0.32454	0.016117	0.044468	0.33876	0.57415
	a_1 (-)	a_2 (-)	x_1	x_2	b_1	b_2	y0	Adjusted r^2
EVC	-0.50972	-0.6928	0.20901	0.28537	0.010024	0.017204	0.040814	-0.2031
DLPFC	-0.41969	-0.64275	0.080644	0.22618	0.06551	0.055962	0.83019	0.60674
	a_1 (-/+)	x_1	b_1	y0	Adjusted r^2			
EVC	-0.37211	0.059955	0.010001	0.007618	-0.31084			
DLPFC	-0.56501	0.2273	0.01744	0.51833	0.058346			
	a_1 (-)	x_1	b_1	y0	Adjusted r^2			
EVC	-0.38127	0.20993	0.011491	-0.0379	-0.04941			
DLPFC	-0.58395	0.2272	0.017041	0.51799	0.05748			

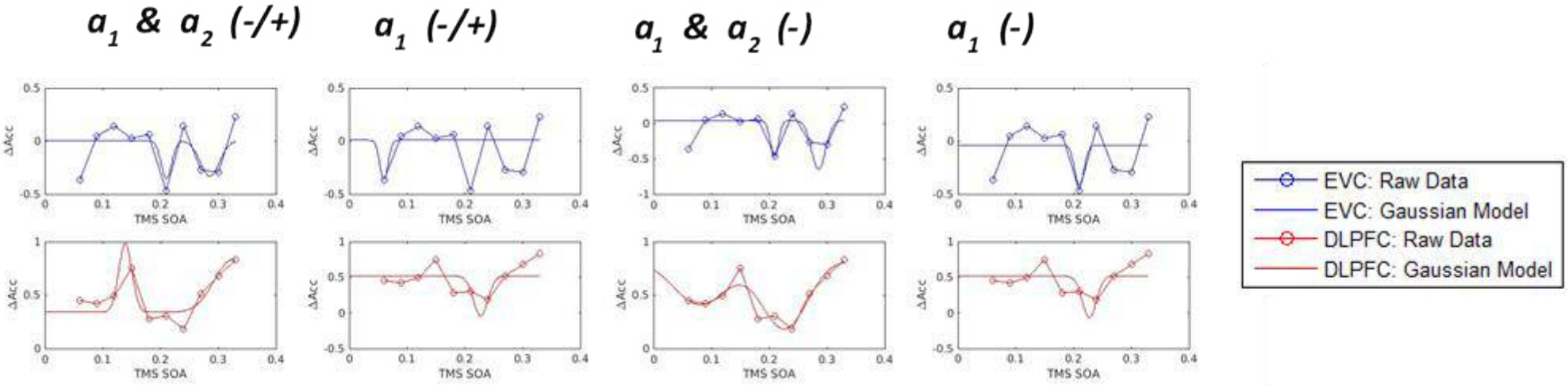

Participant 25	a_1 (-/+)	a_2 (-/+)	x_1	x_2	b_1	b_2	y0	Adjusted r^2
EVC	-0.36438	0.1977	0.077711	0.33543	0.016018	0.012184	0.19114	0.3306
DLPFC	-0.27964	0.8211	0.18036	0.33252	0.010684	0.011473	-0.02208	0.54946
	a_1 (-)	a_2 (-)	x_1	x_2	b_1	b_2	y0	Adjusted r^2
EVC	-0.26917	-0.36438	0.010015	0.29082	0.20652	0.013423	0.33769	0.35061
DLPFC	-0.91146	-1.0632	0.125	0.28808	0.18203	0.013492	0.76105	0.051529
	a_1 (-/+)	x_1	b_1	y0	Adjusted r^2			
EVC	-0.35742	0.077963	0.018465	0.22258	0.21257			
DLPFC	0.84315	0.33202	0.01	-0.04827	0.6926			
	a_1 (-)	x_1	b_1	y0	Adjusted r^2			
EVC	-0.35567	0.07798	0.018484	0.22192	0.21432			
DLPFC	-0.96065	0.13693	0.21712	0.76105	0.23676			

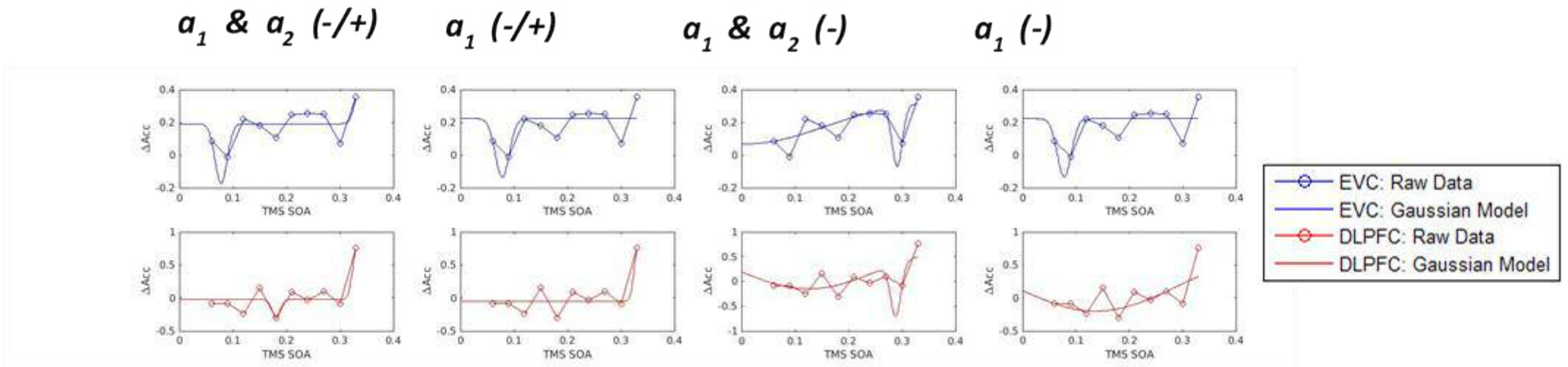

Participant 26	a_1 (-/+)	a_2 (-/+)	x_1	x_2	b_1	b_2	y0	Adjusted r^2
EVC	-0.75202	0.57116	0.13821	0.1532	0.02612	0.10187	-0.05828	0.36642
DLPFC	0.36528	0.34689	0.055141	0.2489	0.010105	0.026883	-0.03934	-0.24461
	a_1 (-)	a_2 (-)	x_1	x_2	b_1	b_2	y0	Adjusted r^2
EVC	-0.75202	-0.43559	0.13675	0.33264	0.019754	0.019016	0.30265	0.4029
DLPFC	-0.49111	-0.4911	0.16029	0.31448	0.018532	0.018699	0.1586	0.020257
	a_1 (-/+)	x_1	b_1	y0	Adjusted r^2			
EVC	-0.75202	0.13678	0.017503	0.19512	0.24751			
DLPFC	-0.49111	0.16058	0.013283	0.057904	0.031685			
	a_1 (-)	x_1	b_1	y0	Adjusted r^2			
EVC	-0.75202	0.13679	0.017589	0.19769	0.25108			
DLPFC	-0.49111	0.16058	0.013305	0.058363	-0.1288			

a_1 & a_2 (-/+) a_1 (-/+) a_1 & a_2 (-) a_1 (-)

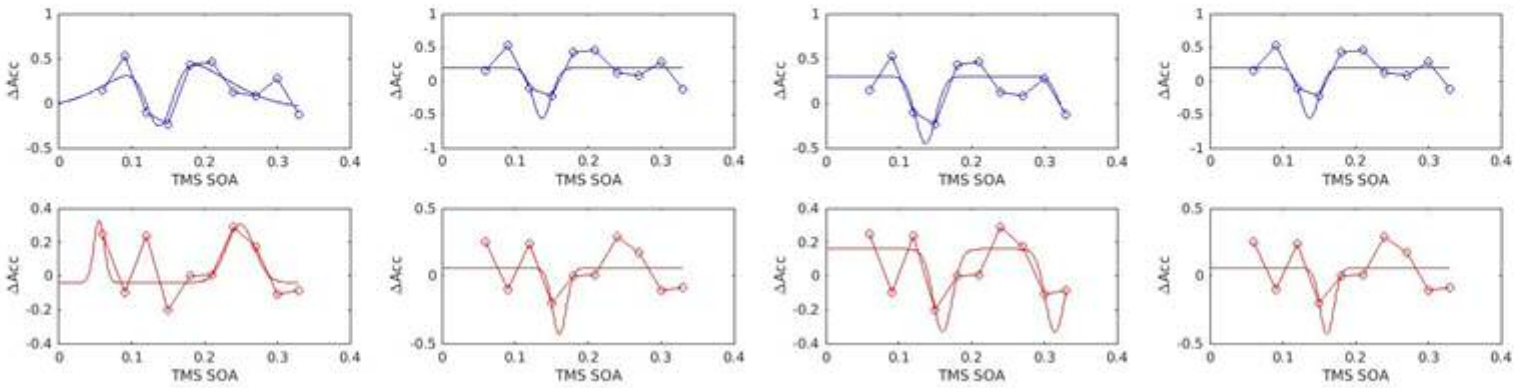

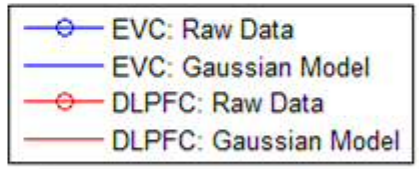

Participant 27	a_1 (-/+)	a_2 (-/+)	x_1	x_2	b_1	b_2	y0	Adjusted r^2
EVC	-1.019	1.019	0.17208	0.17976	0.02176	0.12248	-0.59395	0.47391
DLPFC	-0.59878	-0.46536	0.10024	0.33727	0.016639	0.010022	0.087631	-0.26291
	a_1 (-)	a_2 (-)	x_1	x_2	b_1	b_2	y0	Adjusted r^2
EVC	-1.019	-1.019	0.17019	0.34884	0.013892	0.032569	0.10934	0.18268
DLPFC	-0.59893	-0.2847	0.10027	0.33201	0.016503	0.010111	0.086606	-0.26289
	a_1 (-/+)	x_1	b_1	y0	Adjusted r^2			
EVC	-0.51848	0.17838	0.010824	-0.00075	-0.12729			
DLPFC	-0.59907	0.10037	0.014877	0.046338	0.2064			
	a_1 (-)	x_1	b_1	y0	Adjusted r^2			
EVC	-0.65237	0.32799	0.013756	0.018855	0.072869			
DLPFC	-0.59907	0.10037	0.01488	0.046394	0.20642			

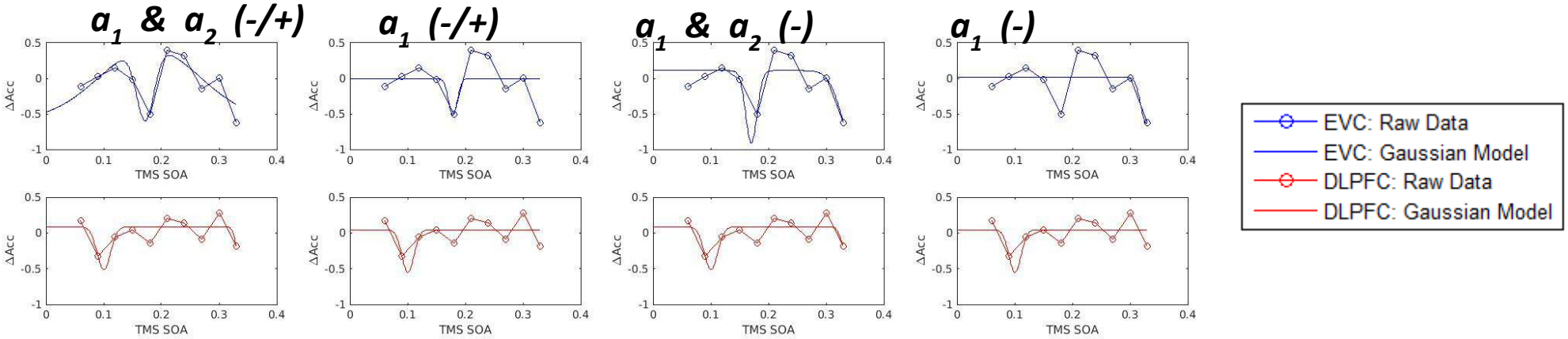

Participant 28	a_1 (-/+)	a_2 (-/+)	x_1	x_2	b_1	b_2	y0	Adjusted r^2
EVC	0.4257	0.57417	0.01	0.26076	0.20251	0.020925	-0.11602	0.59862
DLPFC	-0.99414	-0.39506	0.15055	0.21353	0.015595	0.017613	0.62247	0.63752
	a_1 (-)	a_2 (-)	x_1	x_2	b_1	b_2	y0	Adjusted r^2
EVC	-0.26027	-0.5742	0.16463	0.31499	0.061492	0.028568	0.32303	0.50456
DLPFC	-1.2916	-0.39302	0.15396	0.20794	0.011846	0.022751	0.64616	0.77178
	a_1 (-/+)	x_1	b_1	y0	Adjusted r^2			
EVC	-0.5742	0.31494	0.019195	0.19733	0.41662			
DLPFC	-1.2916	0.15534	0.013884	0.60438	0.74391			
	a_1 (-)	x_1	b_1	y0	Adjusted r^2			
EVC	-0.5742	0.31494	0.019236	0.19814	0.4176			
DLPFC	-1.2916	0.15534	0.013513	0.59545	0.7452			

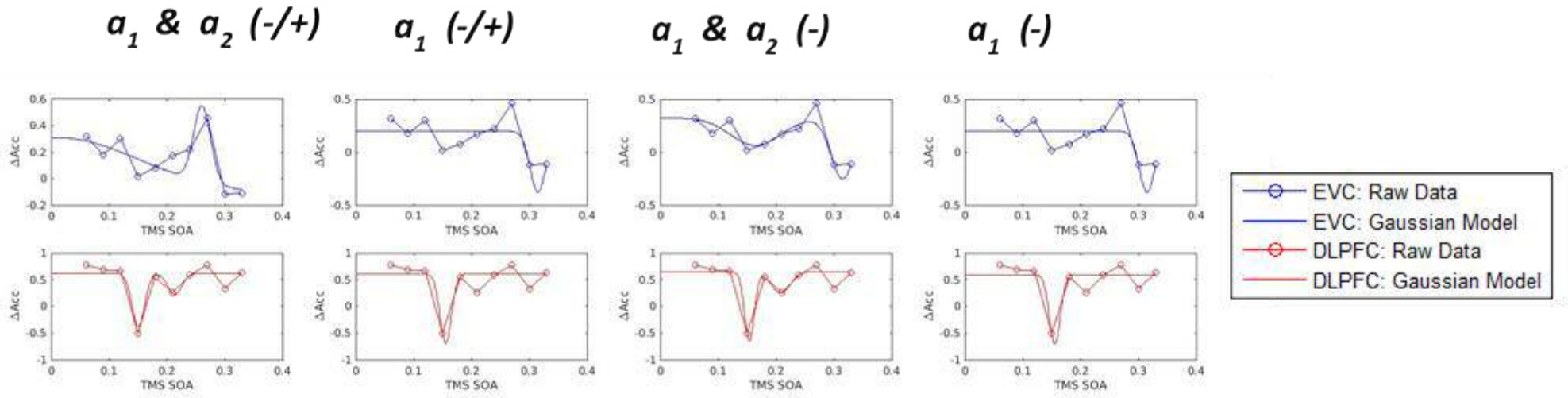

Participant 29	a_1 (-/+)	a_2 (-/+)	x_1	x_2	b_1	b_2	y0	Adjusted r^2
EVC	-0.4725	0.4725	0.13487	0.14959	0.089553	0.026901	0.53894	0.63737
DLPFC	-1.7588	-1.3669	0.060004	0.33504	0.012374	0.012202	0.33337	0.41989
	a_1 (-)	a_2 (-)	x_1	x_2	b_1	b_2	y0	Adjusted r^2
EVC	-0.39367	-0.258	0.095216	0.19936	0.050761	0.045098	0.54869	-0.04799
DLPFC	-1.9495	-1.1671	0.060017	0.33022	0.010259	0.01028	0.35487	0.44465
	a_1 (-/+)	x_1	b_1	y0	Adjusted r^2			
EVC	-0.26811	0.097598	0.040194	0.41716	0.14353			
DLPFC	-1.3123	0.059992	0.012229	0.16497	0.29861			
	a_1 (-)	x_1	b_1	y0	Adjusted r^2			
EVC	-0.26811	0.097598	0.040194	0.41716	0.14353			
DLPFC	-1.8152	0.059777	0.010573	0.22495	0.37221			

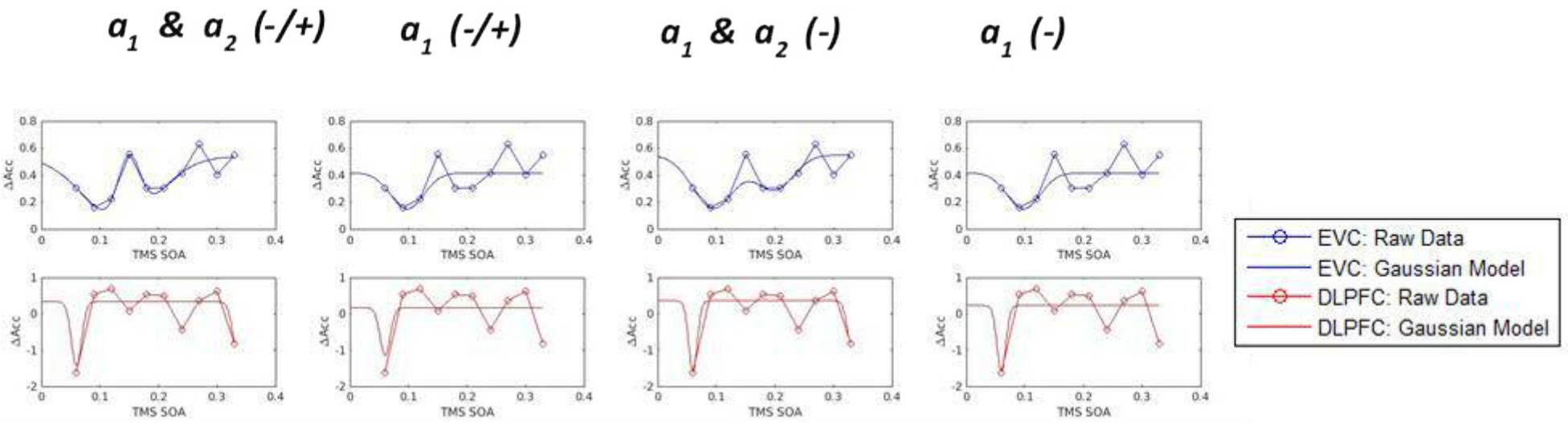

Participant 30	a_1 (-/+)	a_2 (-/+)	x_1	x_2	b_1	b_2	y0	Adjusted r^2
EVC	0.87672	1.4352	0.01	0.29015	0.24173	0.021595	-0.60063	0.77125
DLPFC	0.69521	0.43664	0.059995	0.25188	0.013395	0.052857	0.24193	0.58924
	a_1 (-)	a_2 (-)	x_1	x_2	b_1	b_2	y0	Adjusted r^2
EVC	-1.0051	-1.2535	0.1688	0.32998	0.11899	0.010368	0.83455	0.44102
DLPFC	-0.59585	-0.7663	0.14154	0.35616	0.085256	0.064057	0.82391	-0.37958
	a_1 (-/+)	x_1	b_1	y0	Adjusted r^2			
EVC	0.89769	0.072114	0.015417	-0.06717	-0.39402			
DLPFC	0.55178	0.056412	0.01	0.45202	0.30148			
	a_1 (-)	x_1	b_1	y0	Adjusted r^2			
EVC	-0.83908	0.33402	0.01	0.11348	0.17122			
DLPFC	-0.46123	0.32158	0.014544	0.5008	-0.22226			

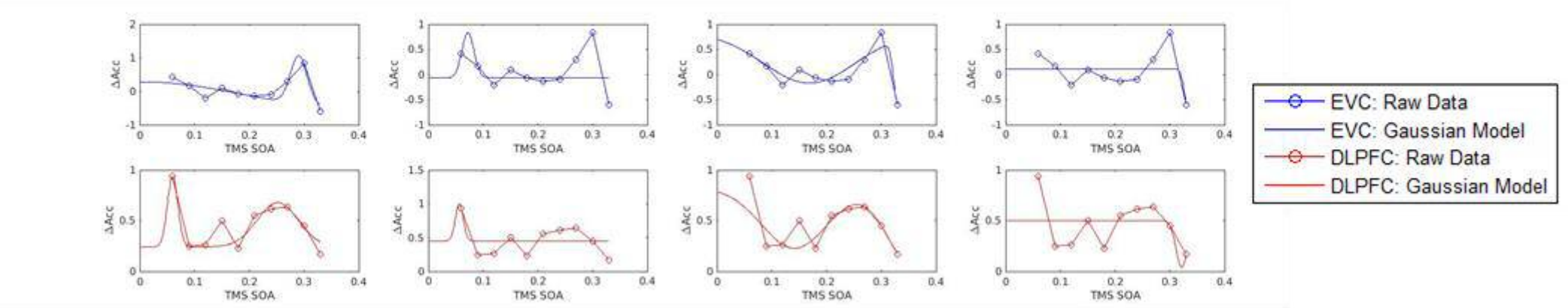

Participant 31	a_1 (-/+)	a_2 (-/+)	x_1	x_2	b_1	b_2	$y0$	Adjusted r^2
EVC	-0.40685	0.73863	0.22254	0.23903	0.063236	0.013466	0.27292	0.27662
DLPFC	0.90904	0.42186	0.20018	0.33486	0.018595	0.010019	-0.03505	0.10646
	a_1 (-)	a_2 (-)	x_1	x_2	b_1	b_2	$y0$	Adjusted r^2
EVC	-0.46104	-0.45465	0.18619	0.27242	0.031905	0.01	0.32549	-0.37998
DLPFC	-0.58143	-0.90892	0.12836	0.28885	0.017417	0.01419	0.24829	-0.95908
	a_1 (-/+)	x_1	b_1	$y0$	Adjusted r^2			
EVC	-0.78022	0.19522	0.014692	0.2243	-0.11272			
DLPFC	0.90904	0.1999	0.016209	0.050586	0.41784			
	a_1 (-)	x_1	b_1	$y0$	Adjusted r^2			
EVC	-0.78022	0.19522	0.014691	0.22427	-0.11276			
DLPFC	-0.34352	0.12137	0.01	0.12366	-0.09881			

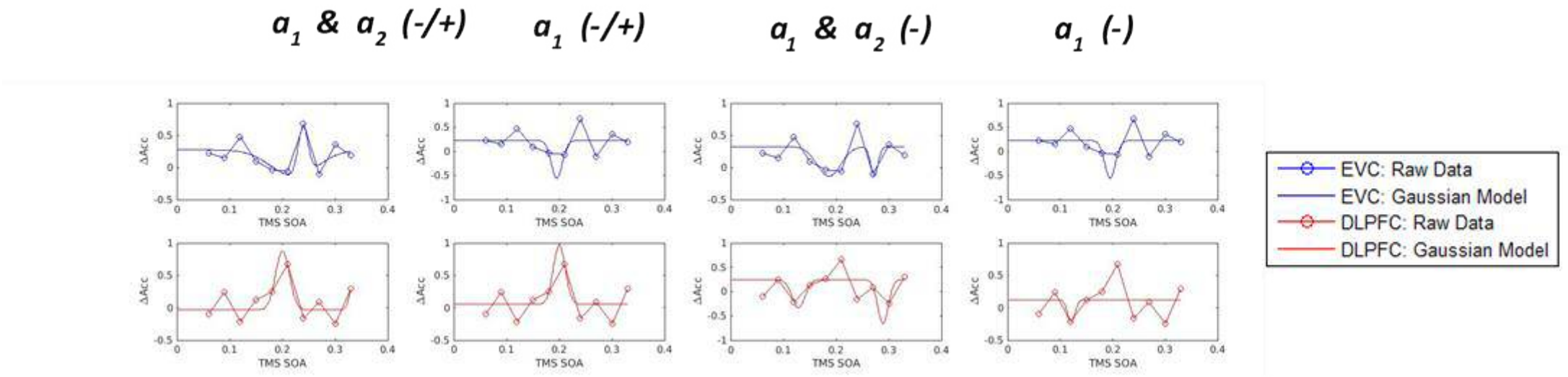

Participant 32	a_1 (-/+)	a_2 (-/+)	x_1	x_2	b_1	b_2	y0	Adjusted r^2
EVC	0.81306	0.81306	0.15967	0.22778	0.015354	0.018041	-0.1981	0.50452
DLPFC	-0.27056	-0.3811	0.097143	0.22289	0.054898	0.025828	0.76289	0.74233
	a_1 (-)	a_2 (-)	x_1	x_2	b_1	b_2	y0	Adjusted r^2
EVC	-0.79971	-0.81306	0.10418	0.28059	0.022372	0.015333	0.070926	0.07056
DLPFC	-0.27056	-0.3811	0.097143	0.22289	0.054898	0.025828	0.76289	0.74233
	a_1 (-/+)	x_1	b_1	y0	Adjusted r^2			
EVC	-0.81306	0.10436	0.017734	-0.04199	0.19792			
DLPFC	-0.3124	0.13829	0.17153	0.84536	0.089989			
	a_1 (-)	x_1	b_1	y0	Adjusted r^2			
EVC	-0.81306	0.10436	0.017743	-0.04171	0.19819			
DLPFC	-0.22262	0.096046	0.04717	0.71586	0.30258			

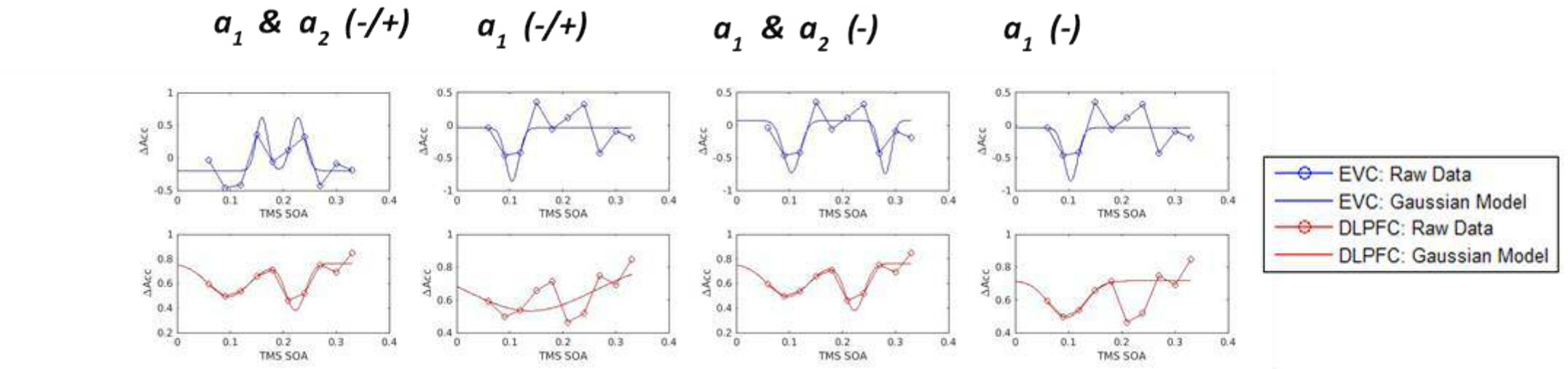

Experiment 5: : ΔPC raw data and model fits

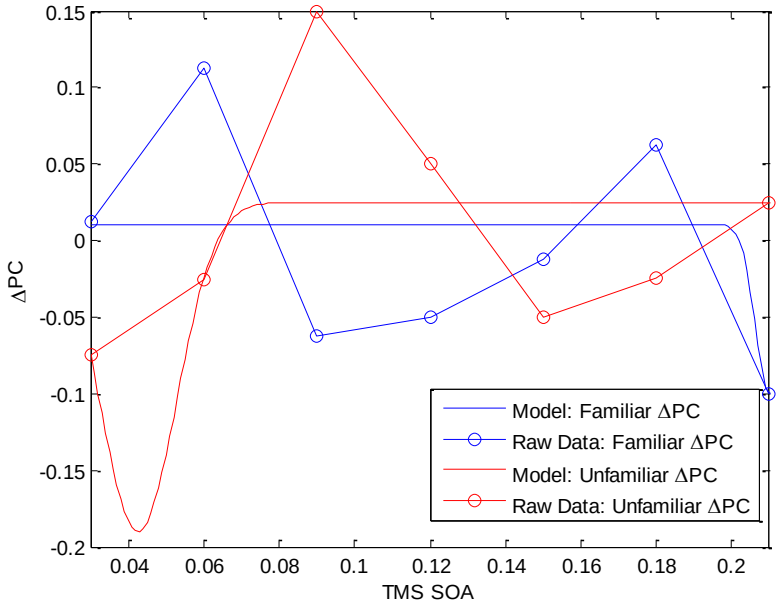

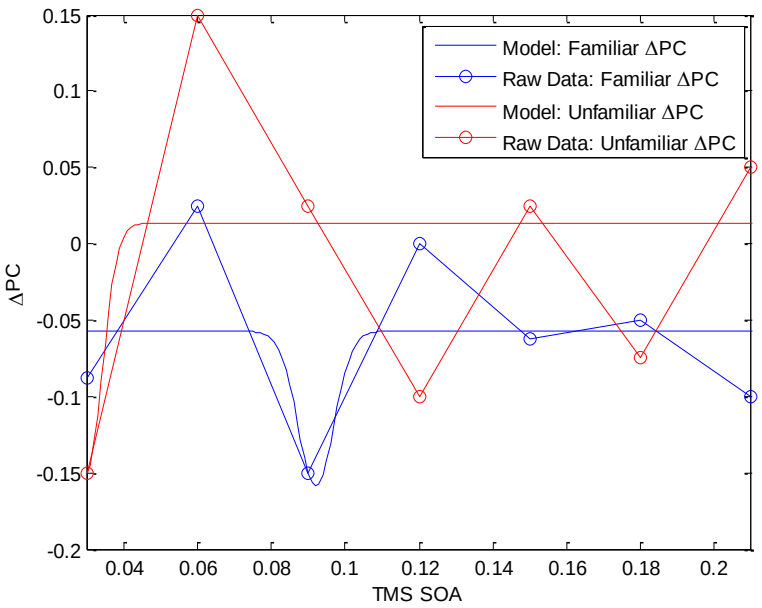

Participant 1						**Participant 2**					
Familiar	a_1	b_1	c_1	***x0***	***Adjusted r^2***	**Familiar**	a_1	b_1	c_1	***x0***	***Adjusted r^2***
	-0.11042	0.21002	0.0052439	0.010416	-0.3682		-0.10167	0.092096	0.0068861	-0.057324	0.013378
Unfamiliar	a_1	b_1	c_1	***x0***	***Adjusted r^2***	**Unfamiliar**	a_1	b_1	c_1	***x0***	***Adjusted r^2***
	-0.21501	0.042603	0.014404	0.025	-0.3682		-0.16338	0.029994	0.0059191	0.013378	0.013378

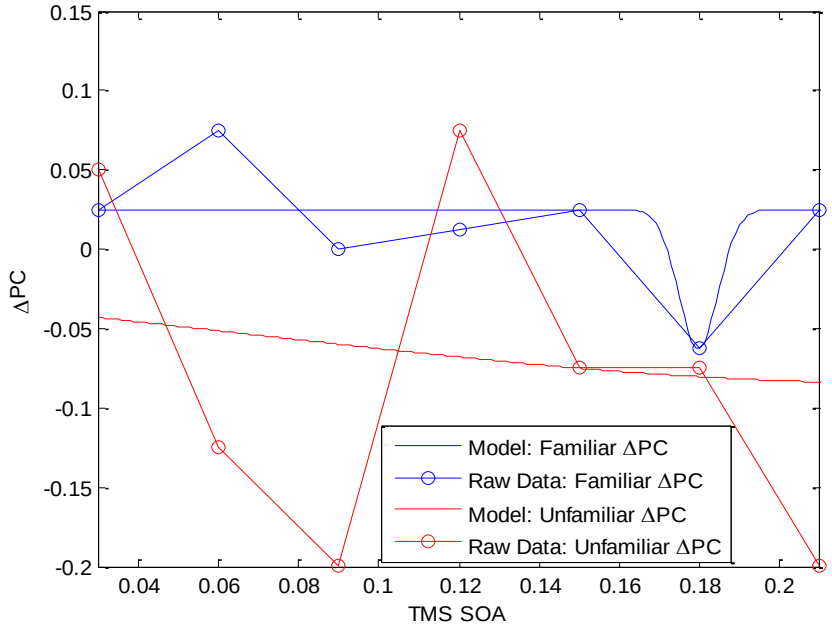

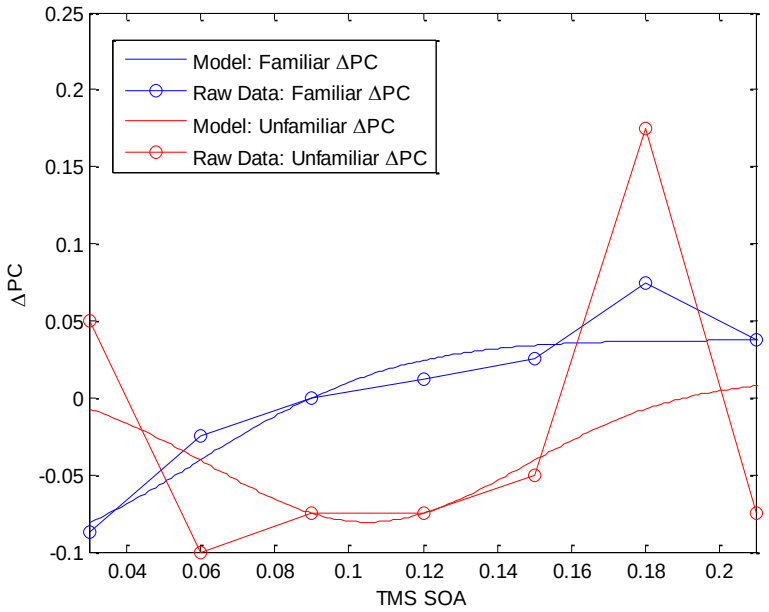

Participant 3						**Participant 4**					
Familiar	a_1	b_1	c_1	***x0***	***Adjusted r^2***	**Familiar**	a_1	b_1	c_1	***x0***	***Adjusted r^2***
	-0.087726	0.17965	0.0069318	0.025	0.3524		-0.13193	0.005	0.075674	0.037359	0.8145
Unfamiliar	a_1	b_1	c_1	***x0***	***Adjusted r^2***	**Unfamiliar**	a_1	b_1	c_1	***x0***	***Adjusted r^2***
	-0.077874	0.235	0.23489	-0.0066838	-0.4147		-0.092583	0.105	0.059733	0.011924	-0.5834

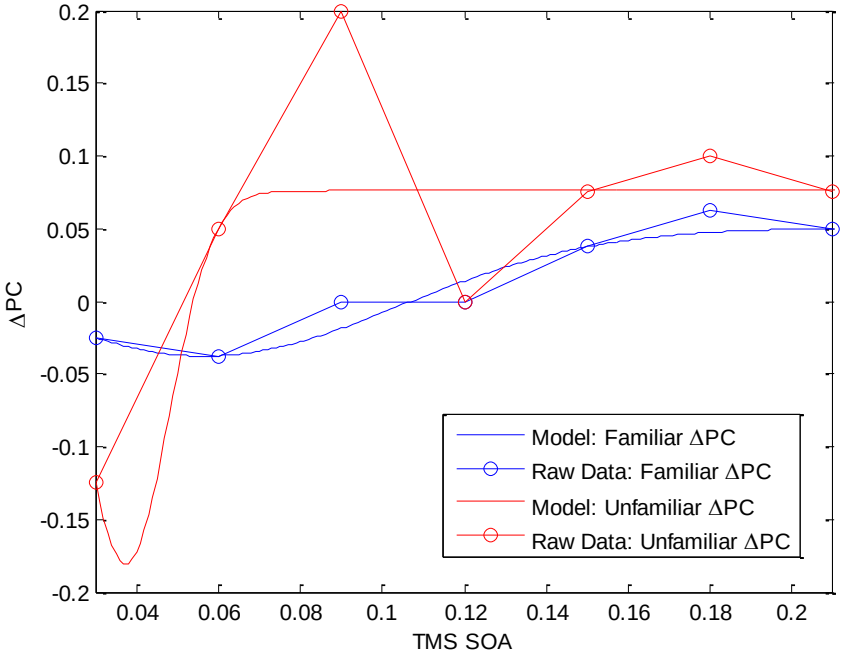

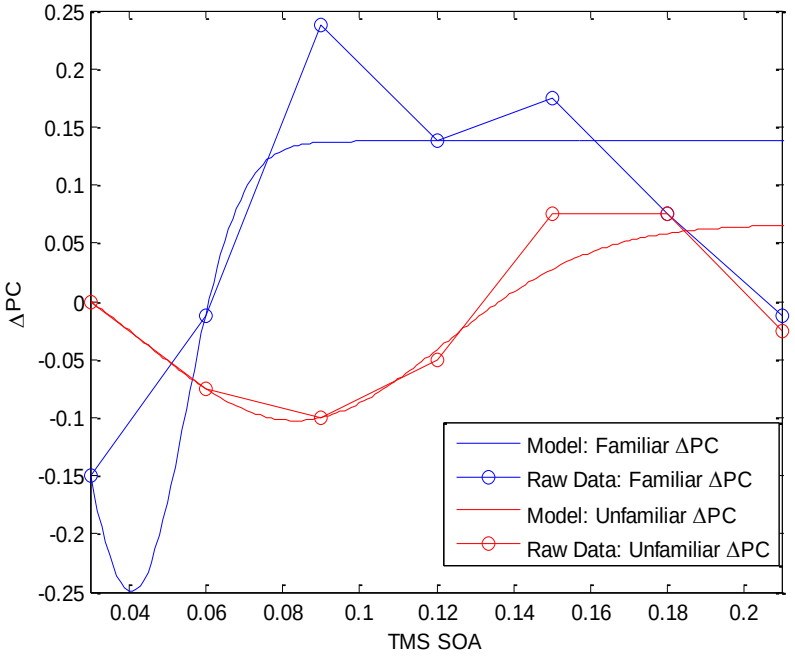

Participant 5						**Participant 6**					
Familiar	a_1	b_1	c_1	***x0***	***Adjusted r^2***	**Familiar**	a_1	b_1	c_1	***x0***	***Adjusted r^2***
	-0.088235	0.056629	0.067492	0.050515	0.8243		-0.3875	0.040779	0.01973	0.1375	0.4599
Unfamiliar	a_1	b_1	c_1	***x0***	***Adjusted r^2***	**Unfamiliar**	a_1	b_1	c_1	***x0***	***Adjusted r^2***
	-0.25668	0.037389	0.014946	0.076029	0.8243		-0.16846	0.083212	0.054926	0.065904	0.2497

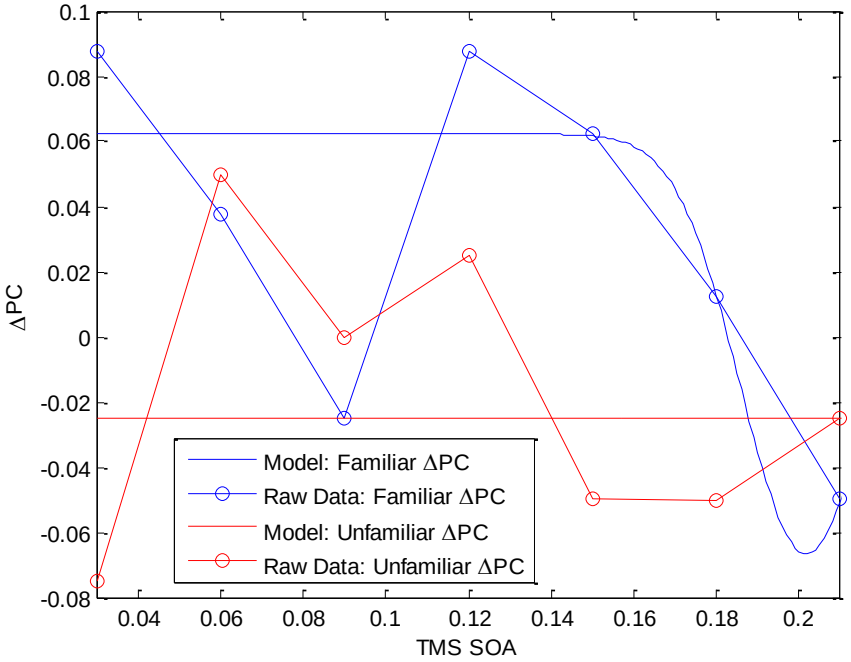

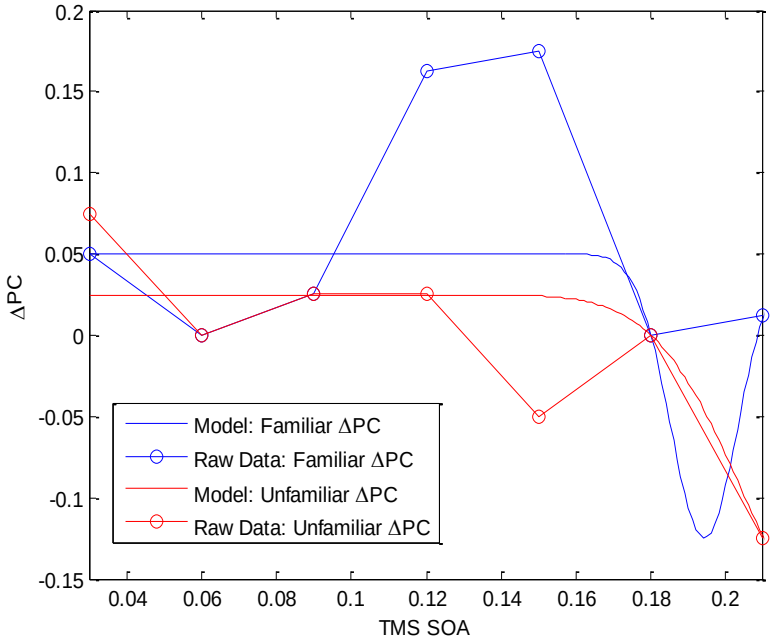

Participant 7						**Participant 8**					
Familiar	a_1	b_1	c_1	***x0***	***Adjusted r^2***	**Familiar**	a_1	b_1	c_1	***x0***	***Adjusted r^2***
	-0.12891	0.20172	0.022249	0.062223	-0.0882		-0.17482	0.19422	0.012714	0.05	-0.8202
Unfamiliar	a_1	b_1	c_1	***x0***	***Adjusted r^2***	**Unfamiliar**	a_1	b_1	c_1	***x0***	***Adjusted r^2***
	-2.2205e-014	0.06	0.12	-0.025	-0.5441		-0.2	0.22777	0.033125	0.024989	-0.8202

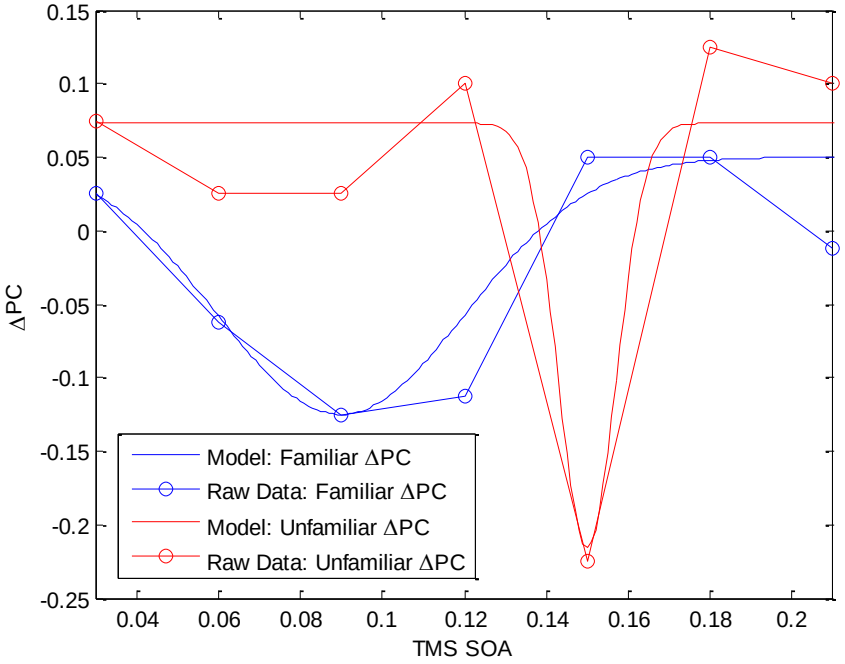

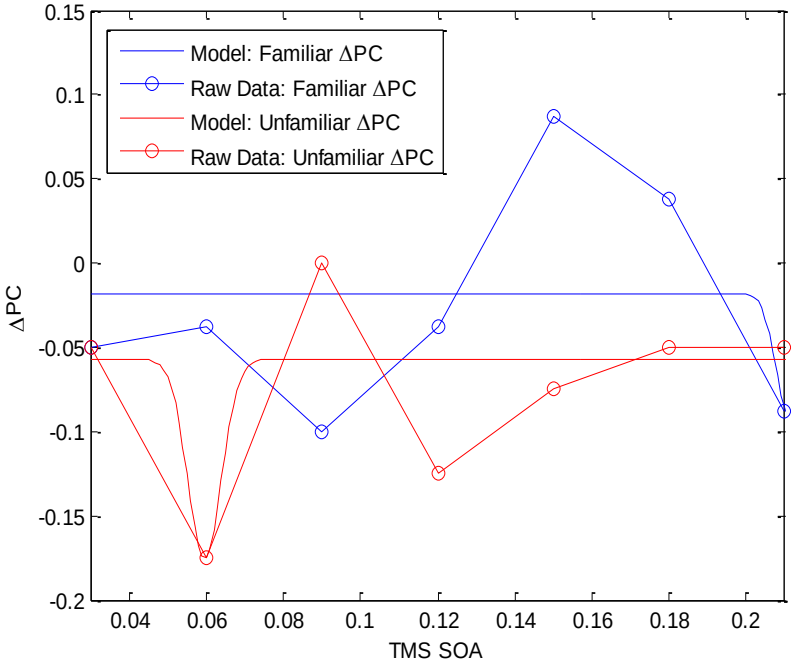

Participant 9						**Participant 10**					
Familiar	a_1	b_1	c_1	***x0***	***Adjusted r^2***	**Familiar**	a_1	b_1	c_1	***x0***	***Adjusted r^2***
	-0.175	0.089897	0.04304	0.049999	0.6545		-0.074203	0.21129	0.005	-0.018091	-0.2618
Unfamiliar	a_1	b_1	c_1	***x0***	***Adjusted r^2***	**Unfamiliar**	a_1	b_1	c_1	***x0***	***Adjusted r^2***
	-0.28846	0.14998	0.0099683	0.07308	0.7935		-0.11847	0.059601	0.0061776	-0.057026	0.1656

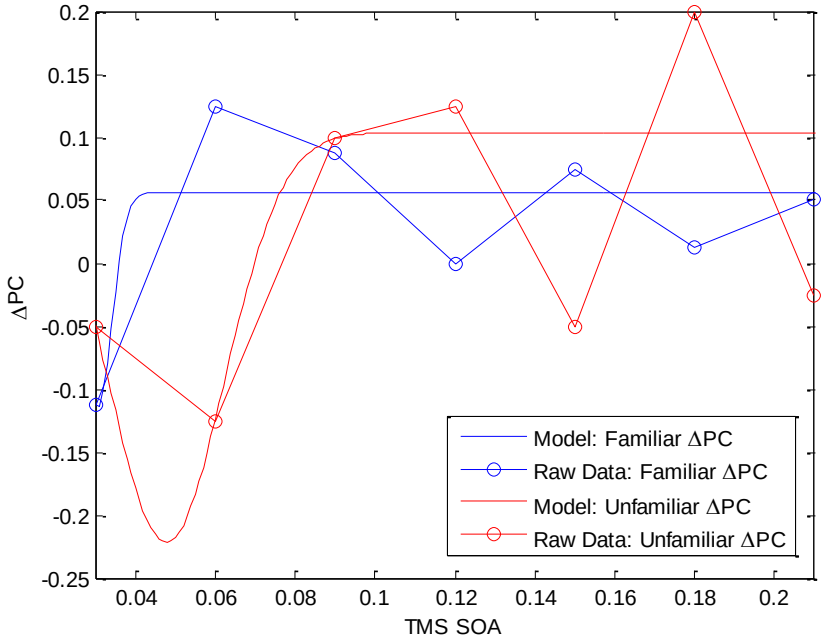

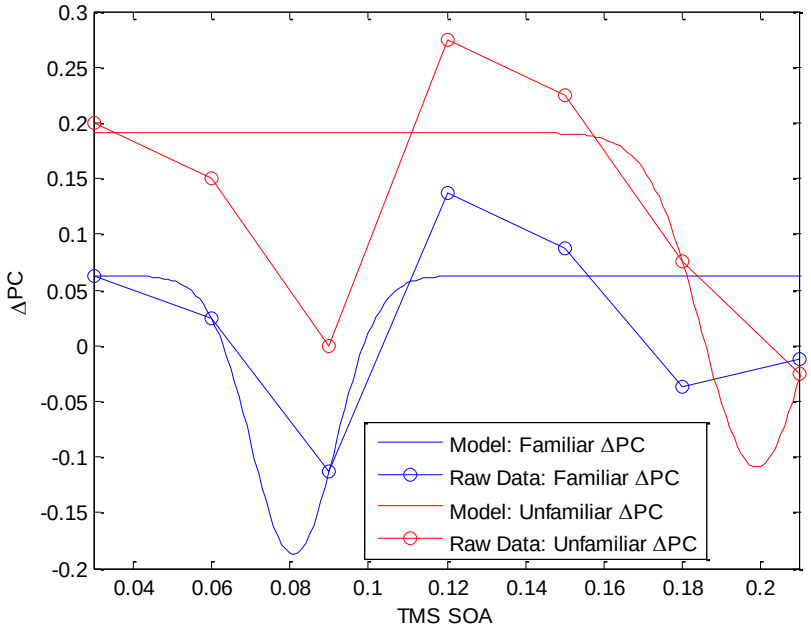

Participant 11						**Participant 12**					
Familiar	a_1	b_1	c_1	***x0***	***Adjusted r^2***	**Familiar**	a_1	b_1	c_1	***x0***	***Adjusted r^2***
	-0.17073	0.030608	0.0050046	0.055729			-0.25	0.080926	0.015193	0.062503	0.2188
Unfamiliar	a_1	b_1	c_1	***x0***	***Adjusted r^2***	**Unfamiliar**	a_1	b_1	c_1	***x0***	***Adjusted r^2***
	-0.325	0.047802	0.02056	0.10357			-0.3	0.19889	0.019351	0.19072	0.1216

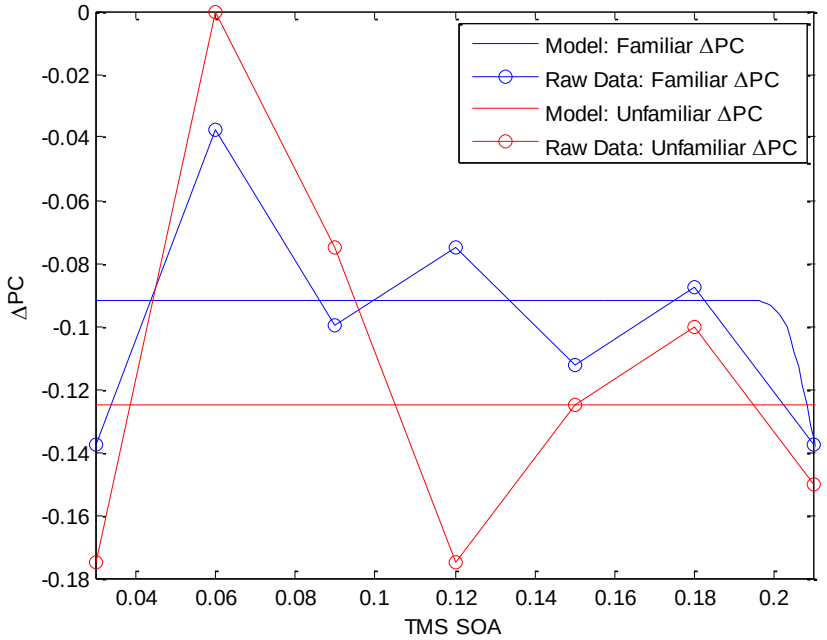

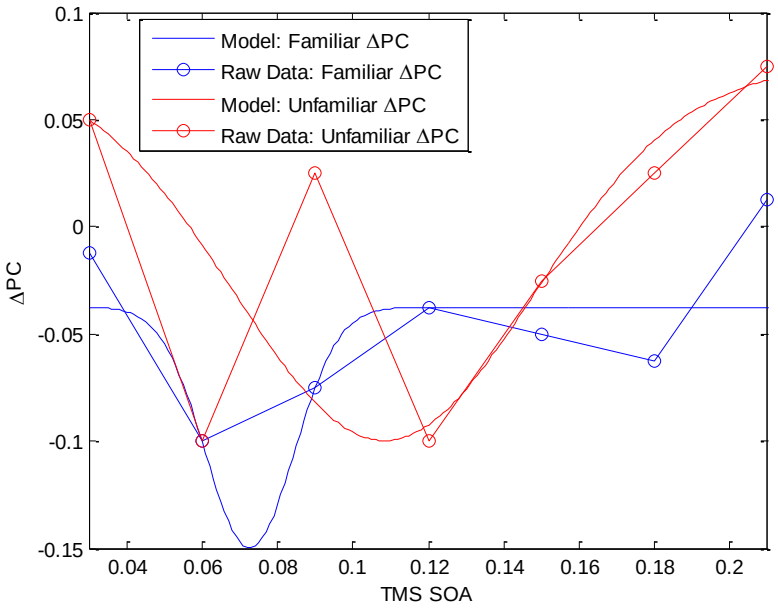

Participant 13						**Participant 14**					
Familiar	a_1	b_1	c_1	***x0***	***Adjusted r^2***	**Familiar**	a_1	b_1	c_1	***x0***	***Adjusted r^2***
	-0.060283	0.21424	0.0080923	-0.091667	-0.0632		-0.1125	0.072673	0.016537	-0.037469	0.3226
Unfamiliar	a_1	b_1	c_1	***x0***	***Adjusted r^2***	**Unfamiliar**	a_1	b_1	c_1	***x0***	***Adjusted r^2***
	-2.3296e-014	0.0050058	0.23494	-0.125	-0.5511		-0.17476	0.10843	0.056245	0.075	-0.0220

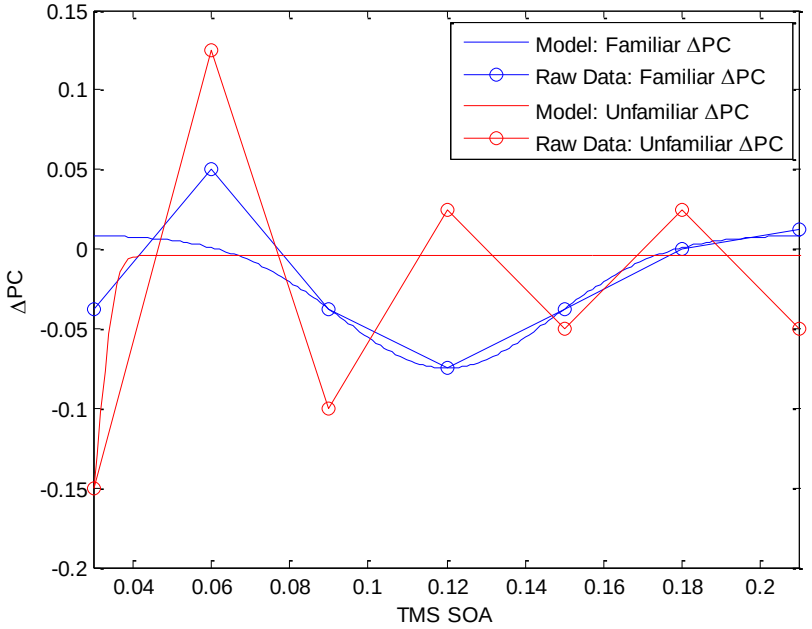

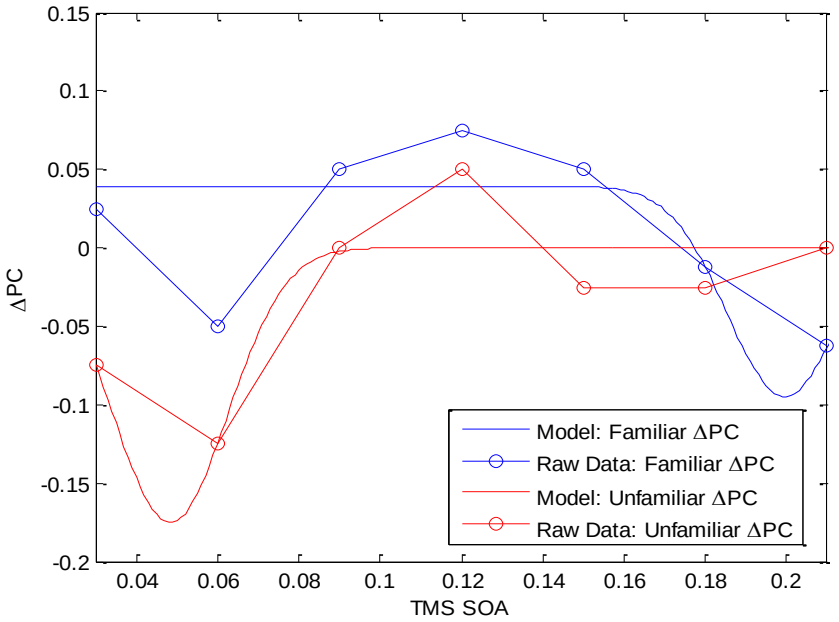

Participant 15						**Participant 16**					
Familiar	a_1	b_1	c_1	***x0***	***Adjusted r^2***	**Familiar**	a_1	b_1	c_1	***x0***	***Adjusted r^2***
	-0.083768	0.12	0.038938	0.0087677	0.1185		-0.134	0.19951	0.020002	0.039267	-0.1389
Unfamiliar	a_1	b_1	c_1	***x0***	***Adjusted r^2***	**Unfamiliar**	a_1	b_1	c_1	***x0***	***Adjusted r^2***
	-0.16026	0.02843	0.0051115	-0.0041667	-0.2708		-0.175	0.048403	0.019993	1.0153e-010	0.7079

References

Ahissar, M., & Hochstein, S. (2004). The reverse hierarchy theory of visual perceptual learning. *Trends in Cognitive Sciences*, 8, 457-464.

Albers, A. M., Kok, P., Toni, I., Dijkerman, H. C., & de Lange, F. P. (2013). Shared representations for working memory and mental imagery in early visual cortex. *Current Biology*, 23, 1427-1431.

Alink, A., Schwiedrzik, C. M., Kohler, A., Singer, W., & Muckli, L. (2010). Stimulus predictability reduces responses in primary visual cortex. *Journal of Neuroscience*, 30, 2960-2966.

Allen, C. P. G. (2012). Probing visual consciousness with transcranial magnetic stimulation. PhD Thesis, Cardiff University.

Allen, C. P. G., Sumner, P., & Chambers, C. D. (2014). The timing and neuroanatomy of conscious vision as revealed by TMS-induced blindsight. *Journal of Cognitive Neuroscience*, *26*, 1507-1518.

Amassian, V. E., Cracco, R. Q., Maccabee, P. J., Cracco, J. B., Rudell, A., & Eberle, L. (1989). Suppression of visual perception by magnetic coil stimulation of human occipital cortex. *Electroencephalography and Clinical Neurophysiology: Evoked Potentials Section*, 74, 458-462.

Angelucci, A., & Bullier, J. (2003). Reaching beyond the classical receptive field of V1 neurons: horizontal or feedback axons?. *Journal of Physiology-Paris*, *97*, 141-154.

Angelucci, A., Levitt, J. B., & Lund, J. S. (2002). Anatomical origins of the classical receptive field and modulatory surround field of single neurons in macaque visual cortical area V1. *Progress in brain research*, *136*, 373-388.

Bar, M. (2003). A cortical mechanism for triggering top-down facilitation in visual object recognition. *Journal of Cognitive Neuroscience*, 15, 600-609.

Bar, M., Kassam, K. S., Ghuman, A. S., Boshyan, Schmid, Dale, Hämäläinen, Bestmann, S., Ruff, C. C., Blakemore, C., Driver, J., & Thilo, K. V. (2007). Spatial attention changes excitability of human visual cortex to direct stimulation. *Current Biology*, 17, 134-139.

Bor, D., & Seth, A. K. (2012). Consciousness and the prefrontal parietal network: insights from attention, working memory, and chunking. *Frontiers in Psychology*, 10.3389/fpsyg.2012.00063

Bowers, J. S., & Davis, C. J. (2012). Bayesian just-so stories in psychology and neuroscience. *Psychological Bulletin*, 138, 389—414.

Bullier, J., & Nowak, L. G. (1995). Parallel versus serial processing: new vistas on the distributed organization of the visual system. *Current Opinion in Neurobiology*, 5, 497-503.

Caffier, P. P., Erdmann, U., & Ullsperger, P. (2005). The spontaneous eye-blink as sleepiness indicator in patients with obstructive sleep apnoea syndrome-a pilot study. *Sleep medicine*, *6*, 155-162.

Camprodon, J. A., Zohary, E., Brodbeck, V., & Pascual-Leone, A. (2010). Two phases of V1 activity for visual recognition of natural images. *Journal of Cognitive Neuroscience*, *22*, 1262-1269.

Cattaneo, Z., Bona, S., & Silvanto, J. (2012). Cross-adaptation combined with TMS reveals a functional overlap between vision and imagery in the early visual cortex. *NeuroImage*, 5, 3015-3020.

Cavada, C., Compañy, T., Tejedor, J., Cruz-Rizzolo, R. J., & Reinoso-Suárez, F. (2000). The anatomical connections of the macaque monkey orbitofrontal cortex. A review. *Cerebral Cortex*, 10, 220-242.

Chambers, C. D., & Mattingley, J. B. (2005). Neurodisruption of selective attention: insights and implications. *Trends in Cognitive Sciences*, 9, 542-550.

Chambers, C. D., Allen, C. P., Maizey, L., & Williams, M. A. (2013). Is delayed foveal feedback critical for extra-foveal perception? *Cortex*, 49, 327-335.

Chen, C. M., Lakatos, P., Shah, A. S., Mehta, A. D., Givre, S. J., Javitt, D. C., & Schroeder, C. E. (2006). Functional anatomy and interaction of fast and slow visual pathways in macaque monkeys. *Cerebral Cortex*, 17, 1561-1569.

Chiang, T. C., Lu, R. B., Hsieh, S., Chang, Y. H., & Yang, Y. K. (2014). Stimulation in the Dorsolateral Prefrontal Cortex Changes Subjective Evaluation of Percepts. *PLoS One,* e106943.

Clark, A. (2013). Whatever next? Predictive brains, situated agents, and the future of cognitive science. *Behavioral and Brain Sciences*, 36, 181-204.

Corthout, E., Uttl, B., Juan, C. H., Hallett, M., & Cowey, A. (2000). Suppression of vision by transcranial magnetic stimulation: a third mechanism. *Neuroreport*, 11, 2345-2349.

Corwin, J. (1994). On measuring discrimination and response bias: Unequal numbers of targets and distractors and two classes of distractors. *Neuropsychology*, 8, 110 – 117.

De Graaf, T. A., & Sack, A. T. (2011). Null results in TMS: from absence of evidence to evidence of absence. *Neuroscience & Biobehavioral Reviews*, 35, 871-877.

de Graaf, T. A., Cornelsen, S., Jacobs, C., & Sack, A. T. (2011). TMS effects on subjective and objective measures of vision: Stimulation intensity and pre-versus post-stimulus masking. *Consciousness and Cognition*, *20*, 1244-1255.

de Graaf, T. A., De Jong, M. C., Goebel, R., Van Ee, R., & Sack, A. T. (2011). On the functional relevance of frontal cortex for passive and voluntarily controlled bistable vision. *Cerebral Cortex*, 21, 2322-2331.

de Graaf, T. A., Goebel, R., & Sack, A. T. (2012). Feedforward and quick recurrent processes in early visual cortex revealed by TMS? *NeuroImage*, 61, 651-659.

de Graaf, T. A., Koivisto, M., Jacobs, C., & Sack, A. T. (2014). The chronometry of visual perception: review of occipital TMS masking studies. *Neuroscience & Biobehavioral Reviews,* 45, 295-304.

de Graaf, T. A., Koivisto, M., Jacobs, C., & Sack, A. T. (2014). The chronometry of visual
Desimone, R. (1996). Neural mechanisms for visual memory and their role in attention. *Proceedings of the National Academy of Sciences*, 93, 13494-13499.

Desimone, R., & Duncan, J. (1995). Neural mechanisms of selective visual attention. *Annual Review of Neuroscience*, 18, 193-222.

Di Lollo, V., Enns, J. T., & Rensink, R. A. (2000). Competition for consciousness among visual events: the psychophysics of re-entrant visual processes. *Journal of Experimental Psychology: General*, *129*, 481 – 507.

Dienes, Z. (2011). Bayesian versus orthodox statistics: Which side are you on? *Perspectives on Psychological Science*, 6, 274-290.

Dugué, L., Marque, P., & VanRullen, R. (2011). The phase of ongoing oscillations mediates the causal relation between brain excitation and visual perception. *Journal of Neuroscience*, 31, 11889-11893.

Edwards, A. L. (1951). Balanced latin-square designs in psychological research. *The American Journal of Psychology*, *64*, 598-603.

Feldman, H., & Friston, K. J. (2010). Attention, uncertainty, and free-energy. *Frontiers in Human Neuroscience*, 4.

Felleman, D. J., & Van Essen, D. C. (1991). Distributed hierarchical processing in the primate cerebral cortex. *Cerebral Cortex)*,*1*, 1-47.

Feredoes, E., Heinen, K., Weiskopf, N., Ruff, C., & Driver, J. (2011). Causal evidence for frontal involvement in memory target maintenance by posterior brain areas during distracter interference of visual working memory. *Proceedings of the National Academy of Sciences*, 108, 17510-17515.

Fletcher, P. C., Anderson, J. M., Shanks, D. R., Honey, R., Carpenter, T. A., Donovan, T. & Bullmore, E. T. (2001). Responses of human frontal cortex to surprising events are predicted by formal associative learning theory. *Nature Neuroscience*, 4, 1043 – 1048.

Foxe, J. J., & Simpson, G. V. (2002). Flow of activation from V1 to frontal cortex in humans. *Experimental Brain Research*, 142, 139-150.

Franca, M., Koch, G., Mochizuki, H., Huang, Y. Z., & Rothwell, J. C. (2006). Effects of theta burst stimulation protocols on phosphene threshold. *Clinical Neurophysiology*, 117, 1808-1813.

Freeman, T. C., Champion, R. A., & Warren, P. A. (2010). A Bayesian model of perceived head-centered velocity during smooth pursuit eye movement. *Current Biology*, 20, 757-762.

Fregni, F., Boggio, P. S., Nitsche, M., Bermpohl, F., Antal, A., Feredoes, E., ... & Pascual-Leone, A. (2005). Anodal transcranial direct current stimulation of prefrontal cortex enhances working memory.*Experimental Brain Research*, 166, 23-30.

Friston, K. (2005). A theory of cortical responses. *Philosophical Transactions of the Royal Society of London B: Biological Sciences*, 360, 815-836.

Gibson, J. J., & Radner, M. (1937). Adaptation, after-effect and contrast in the perception of tilted lines. I. Quantitative studies. *Journal of Experimental Psychology*, 20, 453 – 467/

Grosbras, M. H., & Paus, T. (2002). Transcranial magnetic stimulation of the human frontal eye field: effects on visual perception and attention. *Journal of Cognitive Neuroscience*, 14, 1109-1120.

Grotheer, M., Hermann, P., Vidnyánszky, Z., & Kovács, G. (2014). Repetition probability effects for inverted faces. *NeuroImage*, 102, 416-423.

Hanks, T. D., Ditterich, J., & Shadlen, M. N. (2006). Microstimulation of macaque area LIP affects decision-making in a motion discrimination task. *Nature Neuroscience*, 9, 682 – 689.

Hawkins, D. M. (2004). The problem of overfitting. *Journal of Chemical Information and Computer Sciences*, *44*, 1-12.

Heekeren, H. R., Marrett, S., & Ungerleider, L. G. (2008). The neural systems that mediate human perceptual decision making. *Nature Reviews Neuroscience*, 9, 467 – 479.

Heekeren, H. R., Marrett, S., Bandettini, P. A., & Ungerleider, L. G. (2004). A general mechanism for perceptual decision-making in the human brain. *Nature,* 431, 859 – 862.

Heekeren, H. R., Marrett, S., Ruff, D. A., Bandettini, P. A., & Ungerleider, L. G. (2006). Involvement of human left dorsolateral prefrontal cortex in perceptual decision making is independent of response modality. *Proceedings of the National Academy of Sciences*, 103, 10023-10028.

Heinen, K., Jolij, J., & Lamme, V.A.F. (2005). Figure-ground segregation requires two distinct periods of activity in V1: a transcranial magnetic stimulation study. *Neuroreport,* 16, 1483 – 1487.

Huang, D., Liang, H., Xue, L., Wang, M., Hu, Q., & Chen, Y. (2017). The time course of attention modulation elicited by spatial uncertainty.*Vision Research*, *138*, 50-58.

Hubel, D. H., & Wiesel, T. N. (1962). Receptive fields, binocular interaction and functional architecture in the cat's visual cortex. *The Journal of Physiology*, *160*, 106-154.

Hupe, J. M., James, A. C., Girard, P., Lomber, S. G., Payne, B. R., & Bullier, J. (2001). Feedback connections act on the early part of the responses in monkey visual cortex. *Journal of Neurophysiology*, 85, 134-145.

Hupé, J. M., James, A. C., Payne, B. R., & Lomber, S. G. (1998). Cortical feedback improves discrimination between figure and background by V1, V2 and V3 neurons. *Nature*, 394, 784 – 787.

Hurme, M., Koivisto, M., Revonsuo, A., & Railo, H. (2017). Early processing in primary visual cortex is necessary for conscious and unconscious vision while late processing is necessary only for conscious vision in neurologically healthy humans. *NeuroImage*, 150, 230-238.

Imamoglu, F., Kahnt, T., Koch, C., & Haynes, J. D. (2012). Changes in functional connectivity support conscious object recognition. *Neuroimage*, 63, 1909-1917.

Jacobs, C., de Graaf, T. A., & Sack, A. T. (2014). Two distinct neural mechanisms in early visual cortex determine subsequent visual processing. *Cortex*, 59, 1-11.

Juan, C. H., & Walsh, V. (2003). Feedback to V1: a reverse hierarchy in vision. *Experimental brain research*, 150, 259-263.

Kafaligonul, H., Breitmeyer, B. G., & Öğmen, H. (2015). Feedforward and feedback processes in vision. *Frontiers in psychology*, 6.

Kalla, R., Muggleton, N. G., Cowey, A., & Walsh, V. (2009). Human dorsolateral prefrontal cortex is involved in visual search for conjunctions but not features: a theta TMS study. *Cortex*, 45, 1085-1090.

Kammer, T. (2007). Masking visual stimuli by transcranial magnetic stimulation. *Psychological research*, *71*, 659-666.

Kammer, T., & Nusseck, H. G. (1998). Are recognition deficits following occipital lobe TMS explained by raised detection thresholds? *Neuropsychologia*, 36, 1161-1166.

Kammer, T., Beck, S., Erb, M., & Grodd, W. (2001). The influence of current direction on phosphene thresholds evoked by transcranial magnetic stimulation. *Clinical Neurophysiology*, *112*, 2015-2021.

Kammer, T., Puls, K., Strasburger, H., Hill, N. J., & Wichmann, F. A. (2005). A3B2Transcranial magnetic stimulation in the visual system. I. The psychophysics of visual suppression. *Experimental Brain Research*, 160, 118-128.

Kastner, S., Demmer, I., & Ziemann, U. (1998). Transient visual field defects induced by transcranial magnetic stimulation over human occipital pole. *Experimental Brain Research*, 118, 19-26.

Kastner, S., Pinsk, M. A., De Weerd, P., Desimone, R., & Ungerleider, L. G. (1999). Increased activity in human visual cortex during directed attention in the absence of visual stimulation. *Neuron*, 22, 751-761.

Klemen, J., & Chambers, C. D. (2012). Current perspectives and methods in studying neural mechanisms of multisensory interactions. *Neuroscience & Biobehavioral Reviews*, 36, 111-133.

Koivisto, M., Kastrati, G., & Revonsuo, A. (2014). Recurrent processing enhances visual awareness but is not necessary for fast categorization of natural scenes. *Journal of Cognitive Neuroscience*, 26, 223-231.

Koivisto, M., Lähteenmäki, M., Kaasinen, V., Parkkola, R., & Railo, H. (2014). Overlapping activity periods in early visual cortex and posterior intraparietal area in conscious visual shape perception: a TMS study. *NeuroImage*, 84, 765-774.

Koivisto, M., Mäntylä, T., & Silvanto, J. (2010). The role of early visual cortex (V1/V2) in conscious and unconscious visual perception. *Neuroimage*, 51, 828-834.

Kok, P., Brouwer, G. J., van Gerven, M. A., & de Lange, F. P. (2013). Prior expectations bias sensory representations in visual cortex. *Journal of Neuroscience*, 33, 16275-16284.

Kok, P., Failing, M. F., & de Lange, F. P. (2014). Prior expectations evoke stimulus templates in the primary visual cortex. *Journal of Cognitive Neuroscience*, 26, 1546-1554.

Kok, P., Rahnev, D., Jehee, J. F., Lau, H. C., & de Lange, F. P. (2011). Attention reverses the effect of prediction in silencing sensory signals. *Cerebral Cortex*, 22, 2197-2206.

Kveraga, K., Boshyan, J., & Bar, M. (2007). Magnocellular projections as the trigger of top-down facilitation in recognition. *Journal of Neuroscience*, 27, 13232-13240.

Lamme, V. A. F. (2006). Towards a true neural stance on consciousness. *Trends in Cognitive Sciences*, 10, 494-501.

Lamme, V. A., & Roelfsema, P. R. (2000). The distinct modes of vision offered by feedforward and recurrent processing. *Trends in Neurosciences*, 23, 571-579.

Lau, H. C., & Passingham, R. E. (2006). Relative blindsight in normal observers and the neural correlate of visual consciousness. *Proceedings of the National Academy of Sciences of the U.S.A.,* 103, 18763 – 18768.

Levitt, H. C. (1971). Transformed up-down methods in psychoacoustics. *The Journal of the Acoustical Society of America*, 49(2B), 467-477.

Luck, S. J., Chelazzi, L., Hillyard, S. A., & Desimone, R. (1997). Neural mechanisms of spatial selective attention in areas V1, V2, and V4 of macaque visual cortex. *Journal of Neurophysiology*, 77, 24-42.

Macmillan, N. A. & Creelman, C. D. (1991). Detection Theory: A User's Guide. Cambridge University Press, New York.

Maizey, L., Allen, C. P., Dervinis, M., Verbruggen, F., Varnava, A., Kozlov, M., ./., & Chambers, C. D. (2013). Comparative incidence rates of mild adverse effects to transcranial magnetic stimulation. *Clinical Neurophysiology*,*124*, 536-544.

Marinkovic, Schacter, Rosen & Halgren, E. (2006). Top-down facilitation of visual recognition. *Proceedings of the National Academy of Sciences of the United States of America*, 103, 449-454.

Maunsell, J. H., Nealey, T. A., & DePriest, D. D. (1990). Magnocellular and parvocellular contributions to responses in the middle temporal visual area (MT) of the macaque monkey. *Journal of Neuroscience*, 10, 3323-3334.

Merigan, W. H., & Maunsell, J. H. (1993). How parallel are the primate visual pathways?.*Annual Review of Neuroscience*, 16, 369-402.

Moore, T., & Armstrong, K. M. (2003). Selective gating of visual signals by microstimulation of frontal cortex. *Nature*, 421*,* 370 – 373.

Mundy, M. E., Downing, P. E., Honey, R. C., Singh, K. D., Graham, K. S., & Dwyer, D. M. (2014). Brain correlates of experience-dependent changes in stimulus discrimination based on the amount and schedule of exposure. *PloS One*, 9, e101011.

Nobre, A. C., Coull, J. T., Frith, C. D., & Mesulam, M. M. (1999). Orbitofrontal cortex is activated during breaches of expectation in tasks of visual attention. *Nature Neuroscience*, *2*, 11-12.

O'Shea, J., Muggleton, N. G., Cowey, A., & Walsh, V. (2004). Timing of target discrimination in human frontal eye fields. *Journal of Cognitive Neuroscience, 16,* 1060-1067.

Pascual-Leone, A., & Walsh, V. (2001). Fast backprojections from the motion to the primary visual area necessary for visual awareness. *Science*, 292, 510-512.

Paulus, W., Korinth, S., Wischer, S., & Tergau, F. (1999). Differential inhibition of chromatic and achromatic perception by transcranial magnetic stimulation of the human visual cortex. *Neuroreport*, *10*, 1245-1248.

Pearce, J. M., & Hall, G. (1980). A model for Pavlovian learning: variations in the effectiveness of conditioned but not of unconditioned stimuli. *Psychological Review*, 87, 532- 552.

Philiastides, M. G., Auksztulewicz, R., Heekeren, H. R., & Blankenburg, F. (2011). Causal role of dorsolateral prefrontal cortex in human perceptual decision making. *Current Biology*, *21*, 980-983.

Posner, M. I. (1980). Orienting of attention. *Quarterly Journal of Experimental Psychology*, 32, 3-25.

Posner, M. I., Snyder, C. R., & Davidson, B. J. (1980). Attention and the detection of signals. *Journal of Experimental Psychology: General*, 109, 160 – 174.

Rahnev, D. A., Maniscalco, B., Luber, B., Lau, H., & Lisanby, S. H. (2012). Direct injection of noise to the visual cortex decreases accuracy but increases decision confidence. *Journal of Neurophysiology*, 107, 1556-1563.

Rahnev, D., Koizumi, A., McCurdy, L. Y., D'Esposito, M., & Lau, H. (2015). Confidence leak in perceptual decision making. *Psychological Science*, 26, 1664-1680.

Rao, R. P., & Ballard, D. H. (1999). Predictive coding in the visual cortex: a functional interpretation of some extra-classical receptive-field effects. *Nature Neuroscience*, 2, 79-87.

Renzi, C., Schiavi, S., Carbon, C. C., Vecchi, T., Silvanto, J., & Cattaneo, Z. (2013). Processing of featural and configural aspects of faces is lateralized in dorsolateral prefrontal cortex: a TMS study. *Neuroimage*, 74, 45-51.

Rescorla, R.A. & Wagner, A.R. (1972). *A theory of Pavlovian conditioning: Variations in the effectiveness of reinforcement and nonreinforcement*, Classical Conditioning II, A.H. Black & W.F. Prokasy, Eds., pp.64–99. Appleton-Century-Crofts.

Ro, T., Breitmeyer, B., Burton, P., Singhal, N. S., & Lane, D. (2003). Feedback contributions to visual awareness in human occipital cortex. *Current Biology*, 13, 1038-1041.

Rouder, J. N., Speckman, P. L., Sun, D., Morey, R. D., & Iverson, G. (2009). Bayesian t tests for accepting and rejecting the null hypothesis. *Psychonomic Bulletin & Review*, 16(2), 225-237.

Rounis, E., Maniscalco, B., Rothwell, J. C., Passingham, R. E., & Lau, H. (2010). Theta-burst transcranial magnetic stimulation to the prefrontal cortex impairs metacognitive visual awareness. *Cognitive Neuroscience*, *1*, 165-175.

Ruff, C. C., Bestmann, S., Blankenburg, F., Bjoertomt, O., Josephs, O., Weiskopf, N., Deichmann, R. & Driver, J. (2007). Distinct causal influences of parietal versus frontal areas on human visual cortex: evidence from concurrent TMS–fMRI. *Cerebral Cortex*, 18, 817-827.

Ruff, C. C., Blankenburg, F., Bjoertomt, O., Bestmann, S., Freeman, E., Haynes, J. D., Rees, G., Josephs, O., Deichmann, R. & Driver, J. (2006). Concurrent TMS-fMRI and psychophysics reveal frontal influences on human retinotopic visual cortex. *Current Biology*, 16, 1479-1488.

Ruff, C. C., Blankenburg, F., Bjoertomt, O., Bestmann, S., Weiskopf, N., & Driver, J. (2009). Hemispheric differences in frontal and parietal influences on human occipital cortex: direct confirmation with concurrent TMS–fMRI. *Journal of Cognitive Neuroscience*, 21, 1146-1161.

Rusconi, E., Dervinis, M., Verbruggen, F., & Chambers, C. D. (2013). Critical time course of right frontoparietal involvement in mental number space. *Journal of Cognitive Neuroscience*, 25, 465-483.

Salminen-Vaparanta, N., Noreika, V., Revonsuo, A., Koivisto, M., & Vanni, S. (2012). Is selective primary visual cortex stimulation achievable with TMS? *Human Brain Mapping*, 33, 652-665.

Salzman, C. D., Britten, K. H., & Newsome, W. T. (1990). Cortical microstimulation influences perceptual judgements of motion direction. *Nature*, 346, 174 – 177.

Salzman, C. D., Murasugi, C. M., Britten, K. H., & Newsome, W. T. (1992). Microstimulation in visual area MT: effects on direction discrimination performance. *Journal of Neuroscience*, 12, 2331-2355.

Schmolesky, M. T., Wang, Y., Hanes, D. P., Thompson, K. G., Leutgeb, S., Schall, J. D., & Leventhal, A. G. (1998). Signal timing across the macaque visual system. *Journal of Neurophysiology*, 79, 3272-3278.

Shapley, R. (1990). Visual sensitivity and parallel retinocortical channels. *Annual Review of Psychology*, 41, 635-658.

Sherman, M. T., Kanai, R., Seth, A. K., & VanRullen, R. (2016). Rhythmic influence of top–down perceptual priors in the phase of prestimulus occipital alpha oscillations. *Journal of Ccognitive Neuroscience*. 1318 – 1330.

Sherman, M. T., Seth, A. K., Barrett, A. B., & Kanai, R. (2015). Prior expectations facilitate metacognition for perceptual decision. *Consciousness and Cognition*, 35, 53-65.

Silvanto, J., Lavie, N., & Walsh, V. (2005). Double dissociation of V1 and V5/MT activity in visual awareness. *Cerebral Cortex*, 15, 1736-1741.

Silvanto, J., Muggleton, N. G., Cowey, A., & Walsh, V. (2007). Neural adaptation reveals state-dependent effects of transcranial magnetic stimulation. *European Journal of Neuroscience*, *25*, 1874 – 1881.

Silvanto, J., Muggleton, N., & Walsh, V. (2008). State-dependency in brain stimulation studies of perception and cognition. *Trends in Cognitive Sciences*, 12, 447-454.

Snodgrass, J. G., & Corwin, J. (1988). Pragmatics of Measuring Recognition Memory: Applications to Dementia and Amnesia. *Journal of Experimental Psychology: General*, 117, 34 – 50.

Spratling, M. W. (2008). Reconciling predictive coding and biased competition models of cortical function. *Frontiers in Computational Neuroscience*, *2*.

Stevens, L. K., McGraw, P. V., Ledgeway, T., & Schluppeck, D. (2009). Temporal characteristics of global motion processing revealed by transcranial magnetic stimulation. *European Journal of Neuroscience*, 30, 2415-2426.

Stokes, M. G., Barker, A. T., Dervinis, M., Verbruggen, F., Maizey, L., Adams, R. C., & Chambers, C. D. (2013). Biophysical determinants of transcranial magnetic stimulation: effects of excitability and depth of targeted area. *Journal of Neurophysiology*, 109, 437-444.

Summerfield, C., & Egner, T. (2009). Expectation (and attention) in visual cognition. *Trends in cognitive sciences*, *13*(9), 403-409

Summerfield, C., Trittschuh, E. H., Monti, J. M., Mesulam, M. M., & Egner, T. (2008). Neural repetition suppression reflects fulfilled perceptual expectations. *Nature Neuroscience*, 11, 1004-1006.

Sumner, P. (2006). Inhibition versus attentional momentum in cortical and collicular mechanisms of IOR. *Cognitive Neuropsychology*, 23, 1035-1048.

Sumner, P., Adamjee, T., & Mollon, J. D. (2002). Signals invisible to the collicular and magnocellular pathways can capture visual attention. *Current Biology*, 12, 1312-1316.

Sumner, P., Nachev, P., Vora, N., Husain, M., & Kennard, C. (2004). Distinct cortical and collicular mechanisms of inhibition of return revealed with S cone stimuli. *Current Biology*, 14, 2259-2263.

Super, H., Spekreijse, H., & Lamme, V.A.F (2001). Two distinct modes of sensory processing observed in monkey primary visual cortex (V1). *Nature Neuroscience,* 4, 304 – 310.

Swensson, R. G. (1972). The elusive tradeoff: Speed vs accuracy in visual discrimination tasks. *Perception & Psychophysics*, 12, 16-32.

Tapia, E., & Beck, D. M. (2014). Probing feedforward and feedback contributions to awareness with visual masking and transcranial magnetic stimulation. *Frontiers in Psychology*, 10.3389/fpsyg.2014.01173

Thielscher, A., Reichenbach, A., Uğurbil, K., & Uludağ, K. (2009). The cortical site of visual suppression by transcranial magnetic stimulation. *Cerebral cortex*, *20*, 328-338.

Tootell, R. B., Hamilton, S. L., & Switkes, E. (1988). Functional anatomy of macaque striate cortex. IV. Contrast and magno-parvo streams. *Journal of Neuroscience* , 8, 1594-1609.

Trapp, S., Lepsien, J., Kotz, S. A., & Bar, M. (2016). Prior probability modulates anticipatory activity in category-specific areas. *Cognitive, Affective, & Behavioral Neuroscience*, 16, 135-144.

Tremblay, S., Larochelle-Brunet, F., Lafleur, L. P., El Mouderrib, S., Lepage, J. F., & Théoret, H. (2016). Systematic assessment of duration and intensity of anodal transcranial direct current stimulation on primary motor cortex excitability. *European Journal of Neuroscience*, 44, 2184-2190.

Turatto, M., Sandrini, M., & Miniussi, C. (2004). The role of the right dorsolateral prefrontal cortex in visual change awareness. *Neuroreport*, *15*, 2549-2552.

Varnava, A., Stokes, M. G., & Chambers, C. D. (2011). Reliability of the 'observation of movement'method for determining motor threshold using transcranial magnetic stimulation. *Journal of Neuroscience Methods*, *201*, 327-332.

Vernet, M., Brem, A. K., Farzan, F., & Pascual-Leone, A. (2015). Synchronous and opposite roles of the parietal and prefrontal cortices in bistable perception: A double-coil TMS–EEG study. *Cortex*, 64, 78-88.

Vetter, P., Grosbras, M. H., & Muckli, L. (2013). TMS over V5 disrupts motion prediction. *Cerebral Cortex*, 25, 1052 – 1059.

Walsh, V., & Cowey, A. (2000). Transcranial magnetic stimulation and cognitive neuroscience. *Nature Reviews. Neuroscience*, 1, 73 – 79.

Wassermann, E. M. (1998). Risk and safety of repetitive transcranial magnetic stimulation: report and suggested guidelines from the International Workshop on the Safety of Repetitive Transcranial Magnetic Stimulation, June 5–7, 1996. *Electroencephalography and Clinical Neurophysiology*, *108*, 1-16.

Wiggs, C. L., & Martin, A. (1998). Properties and mechanisms of perceptual priming. *Current Opinion in Neurobiology*, 8, 227-233.

Wokke, M. E., Sligte, I. G., Steven Scholte, H., & Lamme, V. A. F. (2012). Two critical periods in early visual cortex during figure–ground segregation. *Brain and Behavior*, 2, 763-777.

Yeshurun, Y., & Carrasco, M. (1998). Attention improves or impairs visual performance by enhancing spatial resolution. *Nature*, 396, 72 – 75.